United States
Environmental
Protection
Agency

Office of Air Quality
Planning and Standards
Research Triangle Park, NC 27711

EPA-450/4-90-006E
APRIL 1990

AIR

EPA

URBAN AIRSHED MODEL STUDY OF FIVE CITIES

A Low-Cost Application of the Urban Airshed Model to the New York Metropolitan Area and the City of St. Louis

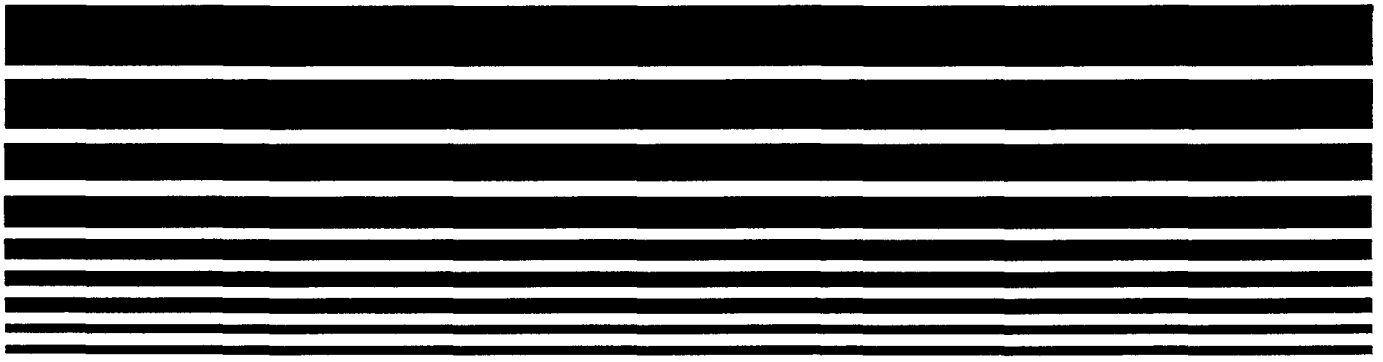

EPA-450/4-90-006E

URBAN AIRSHED MODEL STUDY OF FIVE CITIES

A Low-Cost Application of the Urban Airshed Model to the New York Metropolitan Area and the City of St. Louis

By

Ralph E. Morris
Thomas C. Myers
Henry Hogo
Lyle R. Chinkin
Lu Ann Gardner
Robert G. Johnson

Systems Applications, Inc.
101 Lucas Valley Road
San Rafael, CA 94903

EPA Project Officers:

John C. Chamberlin, Office of Policy Planning and Evaluation
Richard D. Scheffe, Office of Air Quality Planning and Standards

OFFICE OF AIR QUALITY PLANNING AND STANDARDS

U. S. ENVIRONMENTAL PROTECTION AGENCY

RESEARCH TRIANGLE PARK, NC 27711

APRIL 1990

Disclaimer

This material has been funded wholly or in part by the United States Environmental Protection Agency. It has been subject to the agency's review, and it has been approved for publication as an EPA document. Mention of trade names or commercial products does not constitute endorsement or recommendation for use.

Contents

Acknowledgments i

List of Figures iv

List of Tables viii

1 INTRODUCTION 1

Background 1
Comparison of EKMA and UAM 1
PLANR Use of UAM 2
EKMA Uses 4
Study Objectives 5
Study Approach 5

2 DESCRIPTION OF THE CB-IV VERSION OF THE URBAN AIRSHED MODEL (UAM(CB-IV)) 8

Use of the Smolarkiewicz Algorithm to Solve the Advection Equation 9
Use of the CB-IV to Solve Photochemistry 11

3 PREPARATION OF UAM INPUTS FOR NEW YORK AND ST. LOUIS 23

UAM Input Requirements 24
Wind Field Preparation Procedure 25
New York Application 26
St. Louis Application 38
Projection of Initial and Boundary Conditions to 1995 42

4 EMISSIONS INVENTORY DEVELOPMENT 48

Introduction 48
Definition of Emissions Scenarios 48

Overview of the Methodology Used for Generating Emission Inputs 50

Results 63

5 ANALYSIS OF THE URBAN AIRSHED MODELING RESULTS 119

Model Performance Evaluation 119

Analysis of UAM Results for New York 127

Analysis of UAM Results for St. Louis 133

References 214

Appendix A: Protocol Document for Urban Airshed and EKMA Modeling in the New York Metropolitan Area

Appendix B: Protocol Document for Urban Airshed and EKMA Modeling in the St. Louis Metropolitan Area

Appendix C: Episode Selection for St. Louis UAM Modeling

Appendix D: Isopleths of Hourly Ozone Concentrations (pphm) and Hourly Ozone Concentration Differences (ppb) Between Scenarios for the New York Application of the UAM on the Afternoon of 8 August 1980

Appendix E: Isopleths of Hourly Ozone Concentrations (pphm) and Hourly Ozone Concentration Differences (ppb) Between Scenarios for the St. Louis Application of the UAM on the Afternoon of 13 July 1976

Figures

2-1	NO, NO_2 and O_3 concentrations for Example 2	15
2-2	OH concentrations and HO_2 concentrations for Example 1	16
2-3	OH concentrations and HO_2 concentrations for Example 2	18
2-4	C_2O_3 concentrations for Example 1	19
2-5	C_2O_3 concentrations for Example 2	20
2-6	NO_3 concentrations and N_2O_5 concentrations for Example 1	21
3-1	OMNYMAP UAM modeling domain and location of surface and upper-air meteorological observation sites	30
3-2	The St. Louis area with locations of the RAPS surface stations and 4 x 4 km modeling grid superimposed	41
4-1	Flowchart for projection of 1985 emissions to 1995	53
4-2	Spatial distribution of 1995 NO_x emissions from elevated point sources for the New York study region	64
4-3	Spatial distribution of 1995 ROG emissions from elevated point sources for the New York study region	65
4-4	Spatial distribution of 1995 NO_x emissions from elevated point sources for the St. Louis study region	66
4-5	Spatial distribution of 1995 ROG emissions from elevated point sources for the St. Louis study region	67
4-6	Spatial distribution of total 1995 NO_x emissions from low level sources for scenario 1 for the New York study region	69
4-7	Spatial distribution of total 1995 ROG emissions from low level sources for scenario 1 for the New York study region	70

4-8 Spatial distribution of total 1995 NO_x emissions from low level sources for scenario 1 for the St. Louis study region 70

4-9 Spatial distribution of total 1995 ROG emissions from low level sources for scenario 1 for the St. Louis study region 71

5-1 Locations of ozone monitors within the New York modeling domain 138

5-2 Isopleths of predicted maximum daily ozone concentrations with superimposed observations for the New York region on 8 August 1980 139

5-3 Time series of predicted and observed hourly ozone concentrations at all sites in the New York modeling domain 140

5-4 Statistical performance measures and time series of predicted and observed hourly averaged ozone concentrations averaged over four sites in southern Connecticut 148

5-5a Scatterplot of predicted versus observed hourly ozone concentrations for New York region on 8 August 1980 149

5-5b Residual analysis of observed minus predicted hourly ozone concentrations for New York region on 8 August 1980 150

5-6a Scatterplot of predicted versus observed maximum daily ozone concentrations for 8 August 1980 151

5-6b Residual analysis of observed minus predicted maximum daily ozone concentrations for 8 August 1980 152

5-7 The St. Louis modeling domain showing the location of the RAPS ozone monitors 153

5-8 Isopleths of predicted maximum daily ozone concentrations with superimposed maximum daily observations for the St. Louis region on 13 July 1976 154

5-9 Time series of predicted and observed hourly ozone concentrations at all sites in the St. Louis modeling domain 155

5-10a Scatterplot of predicted versus observed hourly ozone concentrations for St. Louis region on 13 July 1976 161

5-10b Residual analysis of observed minus predicted hourly ozone concentrations for St. Louis region on 13 July 1976 162

5-11a Scatterplot of predicted versus observed maximum daily ozone concentrations for 13 July 1976 163

5-11b Residual analysis of observed minus predicted maximum daily ozone concentrations for 13 July 1976 164

5-12a Percent contribution of boundary and emitted hydrocarbon tracer, 8 August 1980 165

5-12b Percent contribution of boundary and emitted NO_x tracer, 8 August 1980 177

5-13 Maximum daily ozone concentrations for scenario 1 on 8 August 1980 189

5-14 Maximum daily ozone concentrations for scenario 2 on 8 August 1980 190

5-15 Differences in maximum daily ozone concentrations between scenario 1 and scenario 2 191

5-16 Maximum daily ozone concentrations for scenario 3 for 8 August 1980 192

5-17 Differences in maximum daily ozone concentrations between scenario 2 and scenario 3 193

5-18 Maximum daily ozone concentrations for scenario 4 for 8 August 1980 194

5-19 Differences in maximum daily ozone concentrations between scenario 1 and scenario 4 195

5-20 Maximum daily ozone concentrations for scenario 1 on 13 July 1976 196

5-21 Maximum daily ozone concentrations for scenario 2 on 13 July 1976 197

5-22 Differences in maximum daily ozone concentrations between scenario 1 and scenario 2 198

5-23 Maximum daily ozone concentrations for scenario 5 on 13 July 1976 199

5-24 Maximum daily ozone concentrations for scenario 7 on 13 July 1976 200

5-25 Differences in maximum daily ozone concentrations between scenario 2 and scenario 5 201

5-26 Differences in maximum daily ozone concentrations between scenario 2 and scenario 7 202

5-27 Maximum daily ozone concentrations for scenario 8 on 13 July 1976 203

5-28 Differences in maximum daily ozone concentrations between scenario 1 and scenario 8 204

5-29 Maximum daily ozone concentrations for SIP scenario A on 13 July 1976 205

5-30 Maximum daily ozone concentrations for SIP scenario B on 13 July 1976 206

5-31 Differences in maximum daily ozone concentrations between scenario 1 and SIP scenario A 207

5-32 Differences in maximum daily ozone concentrations between scenario 1 and SIP scenario B 208

Tables

2-1	The Carbon Bond Mechanism-IV	12
3-1	Comparison of average wind speeds and wind directions used in the OMNYMAP study and those used in this study	32
3-2	Respeciation of initial concentrations and emissions of hydrocarbons	33
3-3	Respeciation of boundary concentrations of hydrocarbons	34
3-4	Comparison of 1980 and 1995 mixed-layer southwestern boundary conditions used in this study and the mixed-layer southwestern boundary conditions used in the OMNYMAP 1988 Scope Base Case for 8 August 1980	37
3-5	Surface roughness and deposition factors based on studies by Argonne National Laboratories	39
3-6	Comparison of circa '78 and current surface roughness and vegetation factors	43
3-7	Initial and boundary condition projection factors (St. Louis)	45
3-8	Initial and boundary condition projection factors (New York)	45
3-9	Background concentrations for Carbon-Bond-IV species	47
4-1	NAPAP area source category codes	73
4-2	NAPAP area source codes and monthly and weekly allocation parameters	76

4-3	Relationship between cost pods, source categories, and source classification codes	80
4-4a	Carbon monoxide emissions for New York and St. Louis CMSA	91
4-4b	VOC emissions for New York and St. Louis CMSA	93
4-5	Exhaust and evaporative emission separation factors for 1985 NAPAP	95
4-6	I/M applicability by county	96
4-7	Multiplicative factors for adjusting 1985 NAPAP annual emissions to 1985 episode day conditions and for converting from MOBILE3 to MOBILE3.9	97
4-8	Factors to multiply by exhaust VOC tons to obtain 1985 uncontrolled refueling VOC tons for episode day conditions	99
4-9	Factors to increase 1985 exhaust VOC to account for unmeasured aldehydes	100
4-10	Growth factors for motor vehicle emissions	100
4-11	1995:1985 emission factor ratios for fleet turnover and RVP effects for episode day conditions and inventory scenarios 1 and 8	101
4-12	1995:1985 emission factor ratios for fleet turnover and RVP effects for episode day conditions and inventory scenario 2	102
4-13	1995:1985 emission factor ratios for fleet turnover and RVP effects for episode day conditions and inventory scenario 5	103
4-14	1995:1985 emission factor ratios for fleet turnover and RVP effects for episode day conditions and inventory scenario 7	104
4-15	1995:1985 emission factor ratios for fleet turnover and RVP effects for episode day conditions and inventory scenarios 1 and 4	105
4-16	1995:1985 emission factor ratios for fleet turnover and RVP effects for episode day conditions and inventory scenario 2	106
4-17	1995:1985 emission factor ratios for fleet turnover and RVP effects for episode day conditions and inventory scenario 3	107

4-18 1995:1985 emission factor ratios for fleet turnover and RVP effects for episode day conditions and inventory scenario 5 108

4-19 Adjustment factors to account for fuel composition effects (oxygen and distillation, but not RVP) for St. Louis scenario 3 109

4-20 Adjustment factors to account for fuel composition effects (oxygen and distillation, but not RVP) for St. Louis scenario 5 110

4-21 Adjustment factors to account for fuel composition effects (oxygen and distillation, but not RVP) for St. Louis scenario 7 111

4-22 Adjustment factors to account for fuel composition effects (oxygen and distillation, but not RVP) for New York scenario 3 112

4-23 Relationship between NAPAP area source category codes and area source types used for gridding purposes 113

4-24 Speciation of evaporative VOC emissions by weight percent of VOC 116

4-25 Speciation of exhaust VOC emissions by weight percent of VOC into CB-IV species 117

4-26 Total and on-road motor-vehicle-related emissions of ROG, CO, and NO_x by scenario 118

5-1 Ozone monitoring sites within the New York modeling domain 209

5-2 UAM model performance for 8 August 1980 hourly ozone concentrations (comparison of application of the UAM (CB-IV) in this study and application of the UAM (CB-II) in the OMNYMAP studies) 210

5-3 UAM model performance for 13 July 1980 hourly ozone concentrations (comparison of application of the UAM (CB-IV) in this study and application of the UAM (CB-II) in the St. Louis Ozone Modeling Project) 211

5-4 Summary of region-wide total emission rates, hydrocarbon-to-NO_x ratios, and percent differences for the 1995 scenarios 1 and 2 by scenario 212

5-5 Comparison of predicted peak ozone, percent change in peak ozone, and VOC emissions between scenarios 1 and 2 and all other 1995 emissions scenarios 213

1 INTRODUCTION

BACKGROUND

Reducing ozone concentrations to levels below the National Ambient Air Quality Standard (NAAQS) has proven to be far more difficult than was thought when the Clean Air Act was passed and amended. The level of ozone precursor emissions remains too high; thus historical emission reductions have been too small or have been required of the wrong sources, or both. Determining the actions needed to improve ozone air quality entails confronting complex scientific, engineering, economic, and political questions.

A plethora of technical explanations have been offered for failure to attain the ozone standard; several can be traced to perceived weaknesses in the attainment planning process (Federal Register, 1987; OTA, 1988a,b,c) and to incomplete understanding or recognition of the anthropogenic and natural factors that cause elevated tropospheric ozone levels (Science, 1988). The EPA, after lengthy consideration, has described a comprehensive policy that proposes major changes in the planning process (Federal Register, 1987). These changes include (1) improvements in modeling practices and (2) requirements for improving the emissions, air quality, and meteorological data bases to support improved modeling practices. The EPA is now evaluating public comments on the proposed policy.

COMPARISON OF EKMA AND UAM

The EPA recommends that states use the Urban Airshed Model (UAM), a three-dimensional photochemical grid model, for ozone modeling applications (EPA, 1986). As an alternative approach, the Empirical Kinetics Modeling Approach (EKMA) has been accepted by the EPA for demonstrating attainment for most State Implementation Plan (SIP) activities (Federal Register, 1987). The primary difference between the UAM and the EKMA stems from the trajectory nature of the EKMA versus the grid nature of the UAM. It is now generally recognized that the UAM incorporates a more complete description of the physical processes that govern ozone formation in urban areas than does the EKMA (Seinfeld, 1988a). The UAM also has a proven ability to reliably reproduce the magnitude and pattern of ozone concentrations in urban areas under meteorological conditions associated with ozone concentrations that exceed the ozone NAAQS (Seinfeld, 1988a, 1988b; Burton, 1988).

EKMA treats the atmospheric chemistry of a single parcel of air as representative of one trajectory reaching an observed ozone maximum and uses the Carbon-Bond Mechanism (CBM-IV) to describe ozone formation (Gery, Whitten, and Killus, 1988 and references cited therein). The EKMA calculation begins at 0800 LST with a specified initial loading of precursors (initial conditions), and more emissions are added each hour on the basis of county-wide emission averages using default reactivities for the VOC emissions for each class of compounds used in CBM-IV. The UAM divides an urban area into grid cells, and simulates the spatially (both horizontally and vertically) varying transport, diffusion, chemical transformation, deposition, and emissions distribution within the urban area by solving the physical governing equations for these processes; the UAM also uses the CBM-IV mechanism. The UAM is usually initiated a day or more before the ozone episode to minimize the effect of initial conditions, and the different reactivities of the VOC emission sources are explicitly treated. Whenever possible, the boundaries of the modeling region are chosen in a manner that reduces the effects of boundary values on ozone concentrations within the region being modeled.

The EKMA modeling approach has been more widely used in the past because it is simpler to apply. Reluctance to use the UAM has been based on the perception that it requires technical skills and computer resources that are too costly and that data requirements are too intensive. This view has prevailed despite the fact that the UAM has been installed and run on enhanced IBM-compatible personal computers (PCs). When examined side by side, the input requirements of the UAM and EKMA--winds, mixing heights, emissions, etc.--are somewhat similar; they differ primarily in the fact that the UAM requires gridded fields of input parameters and more extensive emissions data (Seinfeld, 1988a).

PLANR Use of UAM

Most of the cost of applying the UAM is attributed to the practice of conducting an extensive UAM performance evaluation, which in turn entails many diagnostic simulations. This evaluation enables us to understand why the UAM performs as it does for each application and, if deemed necessary, to take actions to improve model performance. Historically, it has been expected that the UAM will calculate hourly ozone concentrations to within approximately 15 to 20 percent of the observed peak value (Seinfeld, 1988a; Burton, 1988). This high level of performance achieved by the UAM far exceeds the expectations and requirements of any other EPA-recommended model (EPA, 1986), including EKMA, which cannot in the strict sense be evaluated (Seinfeld, 1988). More recent applications of the UAM to the Los Angeles basin have used routinely available meteorological data and predicted observed ozone levels with a high degree of skill (Seinfeld, 1988a; Hogo, Mahoney, and Yocke, 1988). A recent application of the UAM to the New York metropolitan area carried out by the state of New York used simple inputs (constant wind fields and mixing depths) (Rao, 1987). Model performance results in this application were adequate and appear to offer a much more robust method for calculating emission control requirements and planning for attainment of the ozone NAAQS than can be expected from EKMA.

This use of the UAM, which relies on routinely available data and reduces the requirement for strict model performance evaluations, offers a practical air quality assessment tool that air quality managers can use to identify emission control strategies that demonstrate attainment of the ozone NAAQS. This Practice-for-Low-cost-Airshed-application-for-Nonattainment-Regions (PLANR) use of the UAM could be exercised with almost the same quantity and quality of inputs as required by EKMA, and the overall application cost would be substantially reduced. The possible exception is the emissions inventory, which, in the PLANR UAM application, should still contain spatially (horizontally and vertically) and temporally varying emissions that account for the differing reactivities of VOC emissions. However, local agencies generally have emissions inventories at hand, and UAM input inventories can be readily estimated from existing national emissions inventories (e.g., the National Acid Precipitation Program (NAPAP) 1980 and 1985 inventories). In addition, estimates of the emission controls required to achieve attainment of the ozone NAAQS require knowledge of current emission rates.

The PLANR use of the UAM may not be appropriate for use in all nonattainment regions. When attainment is perceived to be imminent, improved methods for using EKMA may be adequate. In other more complex situations, such as the Los Angeles basin, complex meteorological conditions, emissions distribution, and severity of the ozone attainment problem probably require a more detailed application of the UAM. Similar requirements are also envisioned for the Houston area, the lower Lake Michigan area, portions of the northeastern United States, and other areas in California. This Practice-of-Airshed-application-in-Complex-Regions (PACR) use of the UAM would involve more extensive model performance requirements and hence more diagnostic simulations and a resultant increase in costs. However, even for a complex nonattainment region, the PLANR UAM approach would probably be a more comprehensive and reliable method than EKMA for estimating control requirements needed to achieve ozone attainment.

This report presents the application of the UAM to the New York metropolitan area and the city of St. Louis. In a strict sense these two UAM applications are not true PLANR uses of the UAM because (1) the episodes studied made use of UAM inputs prepared in previous modeling studies, (2) the preparation of the UAM model inputs made use of nonroutine meteorological (St. Louis) or air quality (New York) observations, and (3) due to larger amounts of transported pollutants and complex land-sea meteorology, the New York region is not a PLANR region. In Phase II of the Five Cities Project, we will conduct true PLANR applications of UAM for the cities of Atlanta, Dallas-Fort Worth, and Philadelphia. In addition, we will repeat the St. Louis analysis using routinely available data.

Although the New York and St. Louis applications cannot be considered true PLANR uses of the UAM, this report represents the first demonstration of several features of the PLANR use of the UAM since (1) the UAM inputs were prepared according to PLANR objective procedures and used any available meteorological and air quality

data; (2) emissions inputs for the 1995 scenarios were developed from the 1985 NAPAP county emissions inventory; and (3) no attempt was made to adjust the UAM inputs to improve model performance; only one simulation was performed for the model performance evaluation.

EKMA Uses

The EKMA can be extremely valuable for calculating the relative reactivities of different species, or for estimating emission control requirements for regions that have a well-defined urban core and trajectory to the location of the observed ozone maximum. Examples of EKMA use are the studies by the EPA (1987a) and Whitten (1988) that investigated the possible impacts on urban-ozone formation from use of ethanol-blended gasoline fuels.

The use of petroleum-based fuels in the transportation sector represents a major contribution to both CO and the ozone air quality problem. Several studies have suggested oxygenated fuels as replacements for conventional gasoline fuels. The use of ethanol (or methanol) blends offers environmental benefits due to reduced levels of CO emissions; however, their increased volatility has the potential to hinder ozone attainment. The two studies that used EKMA to estimate the effects of ethanol-blended fuels on urban ozone formation indicated that whether the use of ethanol-blended fuels ultimately degrades, improves, or has no effect on ozone air quality depends on the reactivity of the emissions (including CO) that result from their use relative to the reactivity of emissions from the use of conventional gasoline fuels.

Increases in ozone caused by enhanced evaporative emissions of VOCs from the ethanol blends may be offset by reductions in tailpipe CO emissions. The studies indicated that when the average default reactivity was used in the EKMA (an approach that does not require knowledge of the composition of the evaporative emissions but that probably overstates the reactivity and therefore the ozone-formation potential) for the ethanol blends, increases in urban ozone concentrations were usually calculated. In one study that attempted to explicitly treat the reactivity of the emissions resulting from the use of ethanol-blended fuels (Whitten, 1988), there was a net decrease in urban ozone concentrations compared to conventional gasoline fuels. However, the reactivity of the ethanol emissions may have been underestimated, and the use of a region-wide average emission rate and other simplifications in the EKMA may affect calculations of the effects of ethanol blending.

The UAM can examine more than just the explicit chemistry of the evaporative automotive emissions affected by the use of ethanol-blended fuels. For example, the UAM can treat the different reactivities, timing, and locations of the mobile evaporative and exhaust emissions, but the simple EKMA cannot. The possibility that such subtleties as emissions timing and location can significantly affect the results of the EKMA-based study may be remote; however, it has been calculated that ethanol-blended fuels can produce small net decreases in ozone predicted by

EKMA when the differing reactivities are taken into account. Furthermore, the small net decreases and increases in ozone predicted by EKMA when the model uses the default reactivity assumption need to be addressed through use of the UAM, which can account for such subtleties in emission characteristics and distributions.

STUDY OBJECTIVES

The EPA has funded the Five Cities UAM Modeling Project to address the PLANR application of the UAM and to examine the effects of ethanol-blended fuels on urban ozone formation. The five main objectives of the Five Cities study are as follows:

1. Demonstrate the Practice-for-Low-cost-Airshed-application-for-Non-attainment-Regions (PLANR) use of the UAM for air quality planning;

2. Determine the effects of ethanol-blended fuels and alternative Reid Vapor Pressure (RVP) values for fuels on ozone concentrations in a number of urban areas, and compare UAM results with those obtained with EKMA;

3. Investigate and clarify the effects of VOC reactivity potential in emission control strategy evaluations;

4. Demonstrate the PLANR use of the UAM for SIP control strategy evaluations, and compare the results with those obtained through use of the EKMA modeling approach; and

5. Transfer the UAM modeling data bases and application technology to the states for use in future SIPs.

This report documents the first phase of the Five Cities Project, which involves using modified PLANR procedures for applying the UAM to two urban areas: the New York metropolitan area and St. Louis. However, as noted previously, since these two applications did use nonroutine data, they are not true PLANR applications.

STUDY APPROACH

To meet the extreme time constraints imposed on the first phase of the Five Cities Project, use of the PLANR procedures for applying UAM to New York and St. Louis will rely on existing historical UAM inputs. The New York application of the UAM will adapt one of the inputs prepared by the New York Department of Environmental Conservation that span the hours 0400 to 2000 LST on 8 August 1980 (Rao, 1987). The St. Louis application of the UAM will adapt one episode of UAM inputs from the St. Louis ozone modeling project (Schere and Shreffler, 1982; Cole et al., 1983).

Phase one of the Five Cities Project will be accomplished by carrying out the following tasks:

1. Acquire the existing UAM inputs for the New York metropolitan area on 8 August 1980 and several UAM inputs from the St. Louis modeling project. Select a St. Louis UAM input episode for further analysis.

2. Improve the existing UAM inputs to incorporate more recent techniques in developing meteorological inputs for the UAM. Extend the UAM modeling periods to minimize the effects of initial conditions.

3. Adapt the existing emissions inventory and air quality inputs, which were derived for the CB-II chemical mechanisms, to the new UAM(CB-IV).

4. Carry out a limited performance evaluation using the improved UAM inputs, the adapted existing inventories, and the UAM(CB-IV).

5. Develop techniques for converting the 1985 NAPAP annual county emissions inventory to the UAM formats. This effort will involve adjustment to the episodic period, inclusion of source-category-specific diurnal variation and speciation, inclusion of running loss emissions, projection of the emission inventory to 1995, and adjustment of the mobile emissions inventory to account for the effects of temperature, differing RVP fuel values, and ethanol-blended fuels. In addition, at least one SIP emission control strategy inventory will be developed for St. Louis.

6. Use the PLANR procedures for preparing inputs for the UAM and exercise the UAM(CB-IV) for New York and St. Louis for at least four emission scenarios reflecting differing RVP fuel values and ethanol blends and for at least one St. Louis SIP control strategy.

7. Deliver and install on the State of New York's computer system a compiled version of the UAM(CB-IV) and all modeling input files used in the PLANR application of the UAM to the New York modeling region. Provide copies of these input files to the EPA's Office of Air Quality Planning and Standards (OAQPS) Source Receptor Analysis Branch (SRB).

8. Prepare a draft report documenting the effects of VOC reactivity on urban-ozone formation.

This report documents Tasks 1 through 6 of Phase I of the Five Cities UAM Modeling Project. The UAM (CB-IV) was delivered and installed on the New York State Department of Environmental Conservation computer system (Task 7) in October, 1988. Section 2 describes the CB-IV version of the UAM; Section 3 discusses preparation of UAM inputs for New York and St. Louis; Section 4 describes development of the emissions inventory; Section 5 presents an analysis of the UAM modeling results.

The procedures to be followed for the application of the UAM to New York and St. Louis have been outlined in two modeling protocol documents. These two documents, presented in Appendixes A and B, form the basis of the UAM modeling study described in this report. The analysis contained in this report deviates slightly from the protocol documents (Appendixes A and B) in that no EKMA analysis is presented. The EKMA analysis has been omitted because the UAM modeling analysis was conducted for a future year (1995), whereas EKMA requires the use of historical observations (measured 0600-0900 VOC and NO_x concentrations and maximum daily observed ozone concentrations). Thus, results of the UAM and EKMA could not be compared under Phase 1 of the Five Cities UAM Modeling Project.

2 DESCRIPTION OF THE CB-IV VERSION OF THE URBAN AIRSHED MODEL (UAM(CB-IV))

The Urban Airshed Model (UAM) is a three-dimensional grid model designed to calculate the concentrations of both inert and chemically reactive pollutants by simulating the various physical and chemical processes that take place in the atmosphere. The basis of the UAM is the atmospheric diffusion or species continuity equation. This equation represents a mass balance in which all of the relevant emissions, transport, diffusion, chemical reaction, and removal processes are expressed in mathematical terms. Based on the grid concept, the model is generally employed to simulate an 8- to 72-hour period during which episodic meteorological conditions persist.

Because the model can resolve both spatial and temporal features of the concentration field, it is well suited to the analysis of future control strategies and their effects on air quality in various parts of the modeling region. This analysis is accomplished by first replicating a historical ozone episode. Model inputs are prepared on the basis of observed meteorological, emission, and air quality data for a particular day or days. The model is then evaluated with these inputs to determine its "performance." Evaluation of the model is necessary before the modeled episode can be used as the basis for future air quality predictions. Once the model inputs have been evaluated and determined to perform within prescribed levels, the emission inventory can be changed to replicate possible future emission scenarios (e.g., future base case conditions and the effects of alternative emission control strategies). The model simulation is then re-run with the forecasted emissions, resulting in hourly ozone patterns likely to occur in similar future meteorological/emission configurations.

The UAM is the only air quality model recommended by the EPA for photochemical or reactive pollutant modeling applications involving entire urban areas (EPA, 1986). The EPA guidelines refer to the 1978-1980 version of the UAM, which contains the Carbon-Bond Mechanism-Version II (CB-II) (Whitten, Killus, and Hogo, 1980) for chemical transformation and uses the Sharp and Smooth Transport Algorithm (SHASTA) (Boris and Book, 1973) for advection. The formulation of the 1978-1980 UAM is discussed in Ames et al. (1985). Over the last 10 years there have been improvements to the UAM. The two most significant updates to the latest 1988 version of the UAM, the UAM (CB-IV), are as follows:

1. Incorporation of the latest version of the Carbon-Bond Mechanism, the CB-IV (Gery, Whitten, and Killus,1988)

2. Use of the Smolarkiewicz algorithm for advection (Smolarkiewicz, 1983)

These two features are discussed in the following subsections.

USE OF THE SMOLARKIEWICZ ALGORITHM TO SOLVE THE ADVECTION EQUATION

Grid-based air quality simulation models require a numerical approximation of the horizontal advection terms in the species conservation equations. The 1978-1980 version of the Urban Airshed Model (UAM) utilizes a variant of the Sharp and Smooth Transport Algorithm (SHASTA) originally formulated by Boris and Book (1973). Conceptually, the SHASTA scheme can be divided into two steps: (1) a second-order "transport" step, which introduces significant numerical diffusion; and (2) a fourth-order "anti-diffusion" step, which removes a portion of the diffusion introduced by the transport step. SHASTA is exercised in a "time-split" sense, i.e., advection calculations for each horizontal direction are carried out separately within a given time step.

In the original SHASTA formulation, a "flux limitation" constrains the anti-diffusion step so that it does not by itself produce maxima or minima in the advected field. Killus and co-workers (1977) replaced the SHASTA "flux limitation" constraint with the imposition of an arbitrary positive minimum on the advected field, an artifice that prevents negative concentrations but precludes conservation of mass. They demonstrated that "non-flux-limited, non-mass-conservative" SHASTA displayed accuracy superior to both standard SHASTA and to the Price et al. (1966) advection scheme utilized in the original UAM. Thus, non-flux-limited, non-mass-conservative SHASTA was adopted for the UAM. We refer to this advection scheme as "UAM-SHASTA" in the following discussion.

Although UAM-SHASTA is economical and has produced credible UAM results in a variety of applications, its behavior can be undesirable in certain situations. Even with the "anti-diffusion" operator, UAM-SHASTA can be highly diffusive. A portion of this numerical diffusion is velocity-independent; if the wind velocity at a given point is zero, UAM-SHASTA will produce a spurious advective change in the species concentration at that point. Killus et al. (1977) show that UAM-SHASTA is most accurate when the Courant number $u\ \Delta t/\Delta x = 0.5$. If the Courant number exceeds 0.5, the scheme is unstable; as the Courant number decreases from 0.5, the accuracy of the scheme deteriorates.

In the current UAM, Δt is determined so that the Courant number is 0.5 for the maximum value of u or v in the three-dimensional input wind field. In regions of complex terrain, wind speeds can vary between, say, 1 and 10 m s^{-1} within a UAM

domain at a given time; in this situation, inaccuracies in the simulation of horizontal transport can be expected in low-wind subregions. This behavior motivated investigation of a possible replacement for UAM-SHASTA.

Since 1977 there have been many comparative studies of advection schemes. Examples of such studies relevant to the UAM are those of Schere (1983), Chock and Dunker (1983), Chock (1985), and Smolarkiewicz (1983). In each of these studies, an idealized scalar function (a cone, block, ellipse, or cosine wave) representative of a concentration distribution is advected by a rotating wind field (constant angular velocity). The rotating wind field implies a range of Courant numbers, depending on radial distance from the center of the domain. The degree to which the attributes of the idealized function (total mass, peak value, mean value, and gradients) are preserved indicates the accuracy of the scheme.

The above studies show that a number of advection schemes are more accurate than UAM-SHASTA, as measured by the idealized tests. The specific requirements of the UAM narrow the selection of candidate schemes. First, it is important that the scheme be positive definite, i.e., that it not result in negative concentrations. Second, the scheme should utilize forward time differencing to minimize storage requirements and to insure compatibility with chemical mechanism numerics. Third, the ability of an advection scheme to represent the magnitudes and locations of peak concentrations is of major importance in regulatory applications. Fourth, to handle complex airflows, the scheme should display relatively uniform accuracy over a wide range of Courant numbers.

Further review indicated that the advection scheme developed by Smolarkiewicz (1983) may represent the best combination of accuracy and economy. The Smolarkiewicz scheme is conceptually similar to SHASTA, in that a highly diffusive transport step is followed by an anti-diffusive correction step. The transport step is essentially the well-known "upstream" finite-difference scheme. The correction step involves a second exercise of the upstream finite difference scheme, substituting the anti-diffusive velocity for the actual velocity. The Smolarkiewicz scheme is positive definite and forward in time, and can be utilized in either a time-split or multi-dimensional mode. Smolarkiewicz demonstrated the scheme to be superior in both accuracy and economy to the multidimensional generalization of SHASTA formulated by Zalesak (1979). (Note that Schere (1983) shows the Zalesak scheme to be more accurate than UAM-SHASTA.)

Our investigations of UAM applications to Kern County, California (Whitten et al., 1985) and the Los Angeles area (Hogo, Mahoney, and Yocke, 1988) found the SHASTA algorithm to be inaccurate in that a "pseudo" buildup of mass occurred (as much as 10 percent within the first hour of simulation). When the Smolarkiewicz algorithm was incorporated into the UAM and tested with the same input data, the "pseudo" buildup did not occur. Thus, the Smolarkiewicz algorithm has been implemented in the UAM (CB-IV) because it is accurate, positive definite, forward in time, and economical.

USE OF THE CB-IV TO SOLVE PHOTOCHEMISTRY

The latest version of the Carbon-Bond Mechanism (CBM-IV) and associated computer subroutines needed to solve time-dependent chemistry have been implemented in the UAM (CB-IV). Table 2-1 lists the full CBM-IV chemical mechanism. For a complete description of the CBM-IV, the reader is referred to Gery, Whitten, and Killus (1988).

As with any new merger of chemistry into a large air quality simulation model (AQSM), the predictive capabilities and solution speed of the new computer code required optimization and evaluation. This process is even more pertinent at present because the recent generation of gas-phase chemical kinetics mechanisms (CAL, RADM, and the CBM-IV) are larger than previous mechanisms and therefore require significantly more computing time. Using internal resources, Systems Applications, Inc. implemented the CBM-IV in the Urban Airshed Model. There are some minor differences between Table 2-1 and implementation of the CB-IV in the UAM. For example, isoprene was not a species in the UAM applied in this report since it is not an important species in urban photochemistry of Los Angeles and can be accurately modeled using other species in the CB-IV. However, isoprene is to be included in the UAM (CB-IV) in the future. In addition, specifically for this project, ethanol (ETOH) was added as a species. The ethanol reaction is:

$$\text{ETOH} + \text{OH} \rightarrow \text{ALD2} + \text{HO}_2 \text{ with a rate constant of } 4{,}300 \ \frac{1}{\text{ppm-min}} \ .$$

Both numerical and chemical improvements were made to the CB-IV representation so that computational speed could be increased, and solution uncertainty diminished.

Evaluations such as those discussed here should be performed during implementation of all new mechanisms because of the conflicting constraints of high computing costs for large AQSMs and somewhat limited accuracy of faster solution techniques. These constraints result in an operational tradeoff between the time required to perform chemistry calculations and the accuracy of the predicted concentrations. For any given mechanism and solution technique, either speed or accuracy is inevitably sacrificed. However, when we implemented the CBM-IV in the UAM, we were able to slightly modify the solution technique to minimize the need for a tradeoff between speed and accuracy. In some cases, we were able to improve computer solution time without loss of solution accuracy, and in others, we actually improved the chemistry representation and thus obtained more accurate concentrations. We next consider each of these solution algorithms individually.

TABLE 2-1. The Carbon Bond Mechanism-IV.*

Number	Reaction[1]	Reaction Rate Data: Pre-factor ($ppm^{-n}min^{-1}$)	Temp. Factor exp((-E/R)/T)	Rate Constant @ 298K k_{298} ($ppm^{-n}min^{-1}$)
1)	NO2 -hν1-> NO + O			see notes
2)	O -----> O3	8.383 E+04	*EXP(1175/T)	4.323 E+06
3)	O3 + NO -----> NO2	2.643 E+03	*EXP(- 1370/T)	2.664 E+01
4)	O + NO2 -----> NO	1.375 E+04		1.375 E+04
5)	O + NO2 -----> NO3	2.303 E+02	*EXP(687/T)	2.309 E+03
6)	O + NO -----> NO2	3.233 E+02	*EXP(602/T)	2.438 E+03
7)	O3 + NO2 -----> NO3	1.760 E+02	*EXP(- 2450/T)	4.731 E-02
8)	O3 -hν1-> O	5.300 E-02		5.300 E-02×k_1
9)	O3 -hν4-> O1D			see notes
10)	O1D -----> O	1.147 E+05	*EXP(390/T)	4.246 E+05
11)	O1D + H2O -----> 2.00OH	3.260		3.260
12)	O3 + OH -----> HO2	2.344 E+03	*EXP(- 940/T)	1.000 E+02
13)	O3 + HO2 -----> OH	2.100 E+01	*EXP(- 580/T)	2.999
14)	NO3 -hν1-> 0.89NO2 + 0.890 + 0.11NO	3.390 E+01		3.390 E+01×k_1
15)	NO3 + NO -----> 2.00NO2	1.909 E+04	*EXP(250/T)	4.416 E+04
16)	NO3 + NO2 -----> NO + NO2	3.660 E+01	*EXP(- 1230/T)	5.901 E-01
17)	NO3 + NO2 -----> N2O5	7.849 E+02	*EXP(256/T)	1.853 E+03
18)	N2O5 + H2O -----> 2.00HNO3	1.900 E-06		1.900 E-06
19)	N2O5 -----> NO3 + NO2	2.110 E+16	*EXP(-10897/T)	2.776
20)	NO + NO -----> 2.00NO2	2.600 E-05	*EXP(530/T)	1.539 E-04
21)	NO + NO2 + H2O -----> 2.00HONO	1.600 E-11		1.600 E-11
22)	OH + NO -----> HONO	6.554 E+02	*EXP(806/T)	9.799 E+03
23)	HONO -hν1-> OH + NO	1.975 E-01		1.975 E-01×k_1
24)	OH + HONO -----> NO2	9.770 E+03		9.770 E+03
25)	HONO + HONO -----> NO + NO2	1.500 E-05		1.500 E-05
26)	OH + NO2 -----> HNO3	1.537 E+03	*EXP(713/T)	1.682 E+04
27)	OH + HNO3 -----> NO3	7.600	*EXP(1000/T)	2.179 E+02
28)	HO2 + NO -----> OH + NO2	5.482 E+03	*EXP(240/T)	1.227 E+04
29)	HO2 + NO2 -----> PNA	1.640 E+02	*EXP(749/T)	2.025 E+03
30)	PNA -----> HO2 + NO2	2.876 E+15	*EXP(-10121/T)	5.115
31)	OH + PNA -----> NO2	1.909 E+03	*EXP(380/T)	6.833 E+03
32)	HO2 + HO2 -----> H2O2	8.739 E+01	*EXP(1150/T)	4.144 E+03
33)	HO2 + HO2 + H2O -----> H2O2	7.690 E-10	*EXP(5800/T)	2.181 E-01
34)	H2O2 -hν3-> 2.00OH	2.550 E-01		2.550 E-01×k_{39}
35)	OH + H2O2 -----> HO2	4.720 E+03	*EXP(- 187/T)	2.520 E+03
36)	OH + CO -----> HO2	3.220 E+02		3.220 E+02
37)	FORM + OH -----> HO2 + CO	1.500 E+04		1.500 E+04
38)	FORM -hν2-> CO + 2.00HO2			see notes
39)	FORM -hν3-> CO			see notes
40)	FORM + O -----> OH + HO2 + CO	4.302 E+04	*EXP(- 1550/T)	2.370 E+02
41)	FORM + NO3 -----> HNO3 + HO2 + CO	9.300 E-01		9.300 E-01
42)	ALD2 + O -----> C2O3 + OH	1.739 E+04	*EXP(- 986/T)	6.360 E+02
43)	ALD2 + OH -----> C2O3	1.037 E+04	*EXP(250/T)	2.400 E+04
44)	ALD2 + NO3 -----> C2O3 + HNO3	3.700		3.700
45)	ALD2 -hν6-> FORM + XO2 + CO + 2.00HO2			see notes
46)	C2O3 + NO -----> NO2 + XO2 + FORM + HO2	7.915 E+03	*EXP(250/T)	1.831 E+04
47)	C2O3 + NO2 -----> PAN	1.180 E-04	*EXP(5500/T)	1.223 E+04
48)	PAN -----> C2O3 + NO2	5.616 E+18	*EXP(-14000/T)	2.220 E-02
49)	C2O3 + C2O3 -----> 2.00FORM + 2.00XO2 + 2.00HO2	3.700 E+03		3.700 E+03
50)	C2O3 + HO2 -----> 0.79FORM + 0.79XO2 + 0.79HO2 + 0.79OH	9.600 E+03		9.600 E+03
51)	OH -----> XO2 + FORM + HO2	6.521 E+03	*EXP(- 1710/T)	2.100 E+01

(Continued)

*As currently implemented in the UAM (CB-IV), isoprene is not explicitly treated as a separate species, and ethanol has been added to the CB-IV.

TABLE 2-1 Concluded.

Number	Reaction[1]	Reaction Rate Data: Pre-factor ($ppm^{-n}min^{-1}$)	Temp. Factor exp((-E/R)/T)	Rate Constant @ 298K k_{298} ($ppm^{-n}min^{-1}$)
52)	PAR + OH -----> 0.87XO2 + 0.13XO2N + 0.11HO2 + 0.11ALD2 + 0.76ROR - 0.11PAR	1.203 E+03		1.203 E+03
53)	ROR -----> 1.10ALD2 + 0.96XO2 + 0.94HO2 + 0.04XO2N + 0.02ROR - 2.10PAR	6.250 E+16	*EXP(- 8000/T)	1.371 E+05
54)	ROR -----> HO2	9.545 E+04		9.545 E+04
55)	ROR + NO2 ----->	2.200 E+04		2.200 E+04
56)	O + OLE -----> 0.63ALD2 + 0.38HO2 + 0.28XO2 + 0.30CO + 0.20FORM + 0.02XO2N + 0.22PAR + 0.20OH	1.756 E+04	*EXP(- 324/T)	5.920 E+03
57)	OH + OLE -----> FORM + ALD2 + XO2 + HO2 - PAR	7.740 E+03	*EXP(504/T)	4.200 E+04
58)	O3 + OLE -----> 0.50ALD2 + 0.74FORM + 0.33CO + 0.44HO2 + 0.22XO2 + 0.10OH - PAR	2.104 E+01	*EXP(- 2105/T)	1.800 E-02
59)	NO3 + OLE -----> 0.91XO2 + FORM + ALD2 + 0.09XO2N + NO2 - PAR	1.135 E+01		1.135 E+01
60)	O + ETH -----> FORM + 0.70XO2 + CO + 1.70HO2 + 0.30OH	1.540 E+04	*EXP(- 792/T)	1.080 E+03
61)	OH + ETH -----> XO2 + 1.56FORM + HO2 + 0.22ALD2	3.000 E+03	*EXP(411/T)	1.192 E+04
62)	O3 + ETH -----> FORM + 0.42CO + 0.12HO2	1.856 E+01	*EXP(- 2633/T)	2.700 E-03
63)	OH + TOL -----> 0.08XO2 + 0.36CRES + 0.44HO2 + 0.56TO2	3.106 E+03	*EXP(322/T)	9.150 E+03
64)	TO2 + NO -----> 0.90NO2 + 0.90HO2 + 0.90OPEN	1.200 E+04		1.200 E+04
65)	TO2 -----> CRES + HO2	2.500 E+02		2.500 E+02
66)	OH + CRES -----> 0.40CRO + 0.60XO2 + 0.60HO2 + 0.30OPEN	6.100 E+04		6.100 E+04
67)	CRES + NO3 -----> CRO + HNO3	3.250 E+04		3.250 E+04
68)	CRO + NO2 ----->	2.000 E+04		2.000 E+04
69)	OPEN -h ν2-> C2O3 + HO2 + CO	9.040		9.040 $\times k_{38}$
70)	OPEN + OH -----> XO2 + 2.00CO + 2.00HO2 + C2O3 + FORM	4.400 E+04		4.400 E+04
71)	OPEN + O3 -----> 0.03ALD2 + 0.62C2O3 + 0.70FORM + 0.03XO2 + 0.69CO + 0.08OH + 0.76HO2 + 0.20MGLY	8.030 E-02	*EXP(- 500/T)	1.500 E-02
72)	OH + XYL -----> 0.70HO2 + 0.50XO2 + 0.20CRES + 0.80MGLY + 1.10PAR + 0.30TO2	2.453 E+04	*EXP(116/T)	3.620 E+04
73)	OH + MGLY -----> XO2 + C2O3	2.600 E+04		2.600 E+04
74)	MGLY -h ν2-> C2O3 + HO2 + CO	9.640		9.640 $\times k_{38}$
75)	O + ISOP -----> 0.60HO2 + 0.80ALD2 + 0.55OLE + 0.50XO2 + 0.50CO + 0.45ETH + 0.90PAR	2.700 E+04		2.700 E+04
76)	OH + ISOP -----> XO2 + FORM + 0.67HO2 + 0.40MGLY + 0.20C2O3 + 1.00ETH + 0.20ALD2 + 0.13XO2N	1.420 E+05		1.420 E+05
77)	O3 + ISOP -----> FORM + 0.40ALD2 + 0.55ETH + 0.20MGLY + 0.10PAR + 0.06CO + 0.44HO2 + 0.10OH	1.800 E-02		1.800 E-02
78)	NO3 + ISOP -----> XO2N	4.700 E+02		4.700 E+02
79)	XO2 + NO -----> NO2	1.200 E+04		1.200 E+04
80)	XO2 + XO2 ----->	2.550 E+01	*EXP(1300/T)	2.000 E+03
81)	XO2N + NO ----->	1.000 E+03		1.000 E+03

87048r 11
88097
88151

Uncertainty in the Chemistry Solution Routine

In most AQSMs, a number of new or updated chemistry solution techniques are currently being employed in conjunction with several chemical mechanisms. The solution techniques include those used in the EPA Regional Oxidant Model (ROM), the UAM, various versions of the California Air Resources Board's UAM, the SAI Regional Oxidant Model (the RTM-III), and the Regional Acid Deposition Model (RADM). Some new algorithms have also been suggested, but have not yet been employed for atmospheric photochemical systems. Most people outside the modeling field consider only the mechanism, assuming that the same mechanism implemented with two different techniques should give identical predictions. Although this is the ideal, it is not the case. For a number of years, we have advocated comparison of individual techniques, both with each other and with a reasonably accurate standard solution method such as that of Gear. Comparisons with the Gear routine were performed for implementation of the CBM-IV in the UAM and should be performed for all solution schemes currently implemented in complex chemistry AQSMs. To our knowledge, this is rarely done (or at least rarely reported).

In the current implementation of the CBM-IV, we utilized a modified Crank-Nicholson algorithm for the simultaneous solution of the differential equations that represent each species. Because this algorithm utilizes both the rate of change for each species and a Jacobian matrix relating the changes in each species to all others, the technique can be slow under certain conditions. However, it was chosen because, when combined with our steady-state approximations, it calculates concentrations of non-steady-state species that are very similar to those of the Gear algorithm (some typical results of single-cell simulations with diurnally varying light are shown for a few non-steady-state species in Figures 2-1 and 2-2). Thus, we have sacrificed some speed for more accurate predictions (at least in relation to Gear), but as discussed later, we have devised some methods for regaining speed without the loss of accuracy.

Further research is required to implement more efficient numerical integration schemes for complex chemical mechanisms, such as the CB-IV, that will provide computational speed as well accuracy that are comparable to Gear's. This research should consider investigation into the speed and accuracy of as many solution packages as possible in an effort to (1) identify the state of the science regarding speed and uncertainty, (2) establish testing standards, and (3) weed out solution packages that do not respond well in the rather unique environment of diurnally varying atmospheric chemistry solutions. At the least, we should verify that all the major AQSMs can predict nearly the same results (similar to those of Gear) for simple and representative atmospheric tests. Most of the codes are in the public domain and need not be tested in an Eulerian model. For the CBM-IV implementation, for instance, we used a trajectory model with five-layer vertical resolution and a base in an Eulerian emissions grid for much of the comparison work (this work could even be performed with a single box model). Establishing, performing, and reporting such a set of tests for other solution packages is in the best interest of the general photochemical kinetics modeling community.

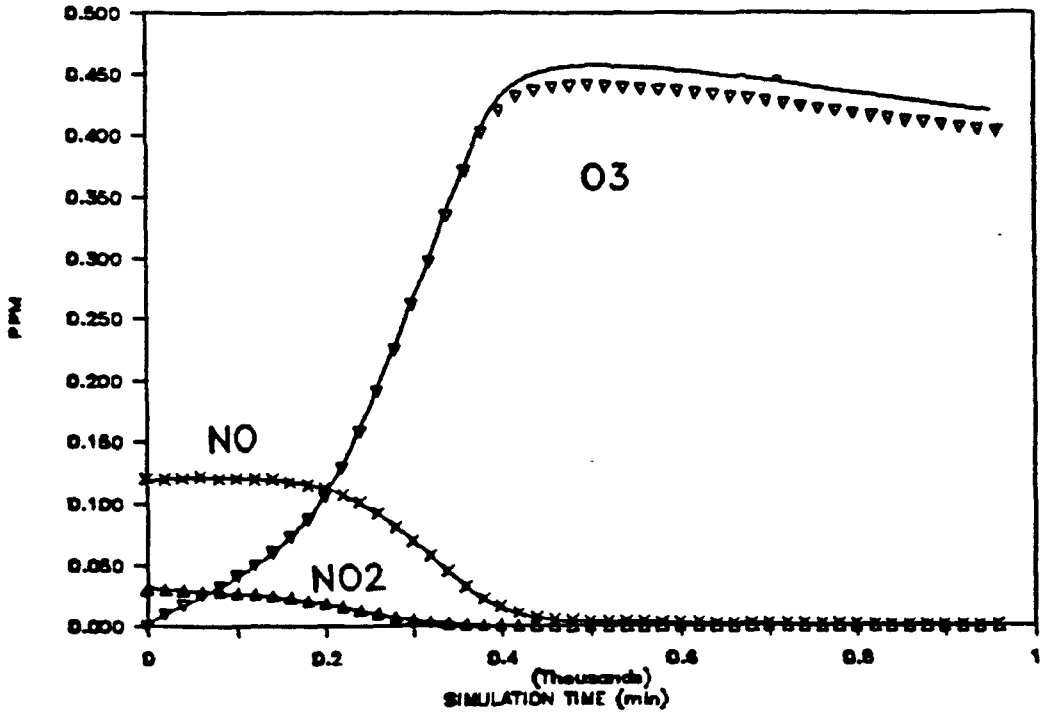

FIGURE 2-1. NO, NO_2 and O_3 concentrations for Example 2 (sunset is at 680 minutes); lines are Gear simulation results and symbols are Crank-Nicholson predictions.

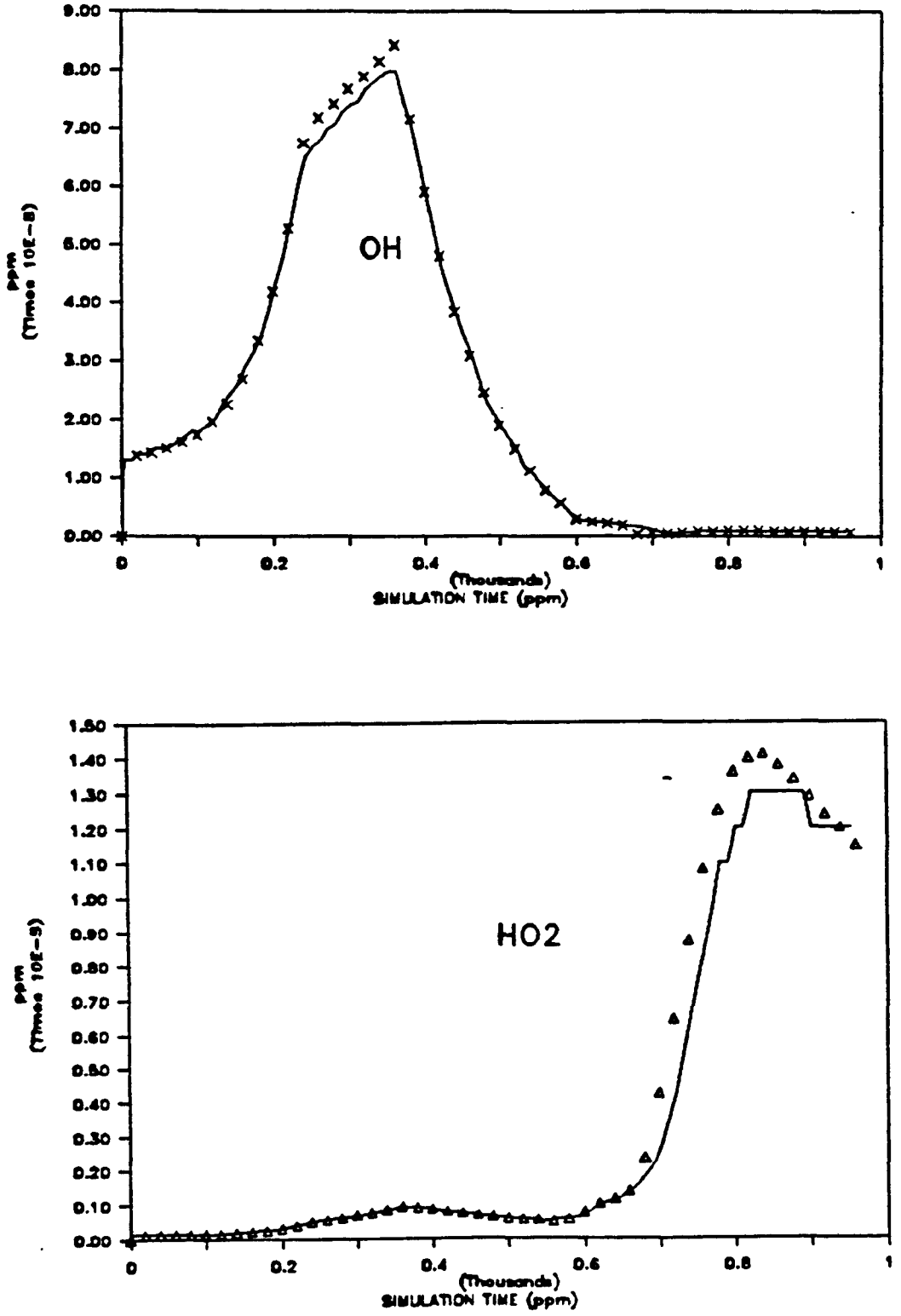

FIGURE 2-2. OH concentrations (top) and HO_2 concentrations (bottom) for Example 1 (sunset is at 680 minutes); lines are Gear simulation results and symbols are Crank-Nicholson predictions.

Implementation of Speed Enhancement Procedures

Related to the solution algorithms are the approximations used to represent the chemical features of a mechanism and, concurrently, to enhance the solution speed. An explicit mechanistic representation of a chemical mechanism, which assumes few or no steady-state approximations, provides a solution that most accurately accounts for the mass of each species (provided numerical errors do not arise because of the large range of concentration variation between species); however, this technique may be computationally slower than is necessary. The speed of a photochemical solution can be improved in a number of ways without sacrificing accuracy. As noted, implementation of appropriate steady-state approximations is probably the best known. We have successfully utilized steady-state approximations in the Carbon-Bond chemistry solution packages, and see no reason why at least a moderate set of such calculations cannot be performed in all models requiring some improvements in speed.

Recently, an algorithm that solves high-order steady-state relationships has been successfully formulated. In this way, the fourth- and sometimes fifth-order algebraic solutions for the OH, C_2O_3, and HO_2 radical species can be rapidly derived. Results of our steady-state and Gear predictions are shown in Figures 2-3 through 2-6 for the conditions of the earlier non-steady-state examples. Since these simulations were 24-hour tests with diurnally varying sunlight, the performance is shown to be good for all parts of the day. We caution, however, that steady-state approximations can be misleadingly simple. Some aspects of their use, such as numerical roundoff errors and mass balance considerations, must be investigated carefully to ensure confidence in implementation. As noted, we pay particular attention to comparisons with the Gear predictions, proceeding through a number of different test cases at each logical step of a steady-state approximation.

This type of analysis has recently led us toward another potential enhancement in mechanism representation. One of the most difficult and potentially stiff chemistry loops is the NO_2-NO_3-N_2O_5-HNO_3 cycle in which the intermediate species (NO_3 and N_2O_5) are potential steady-state species (especially during the day), whereas NO_2 and HNO_3 are necessarily non-steady-state compounds because of their high concentrations. Under certain nighttime conditions, however, NO_3 and N_2O_5 concentrations can be relatively large, thus eliminating the possibility of steady-state treatment. The dilemma is that steady-state representation tends to cause nitrogen mass to be artificially lost, while non-steady-state representation is still stiff in many circumstances. We have recently tested a technique that allows us to move between state and steady-state representations with the inclusion of only one additional non-steady-state species, which is represented by the species NXOY. This technique ensures nitrogen mass balance, but allows steady-state representation when it is preferable. Recent test results have been compared to those of Gear for these conditions (note that one of the earlier figures has rather high ozone concentrations at

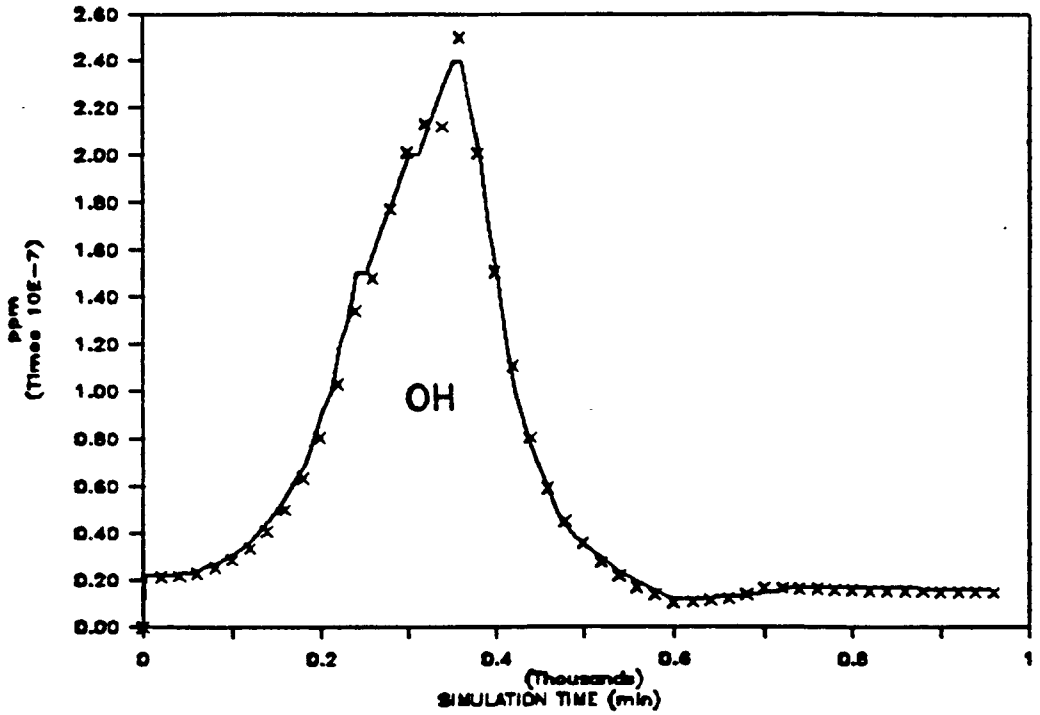

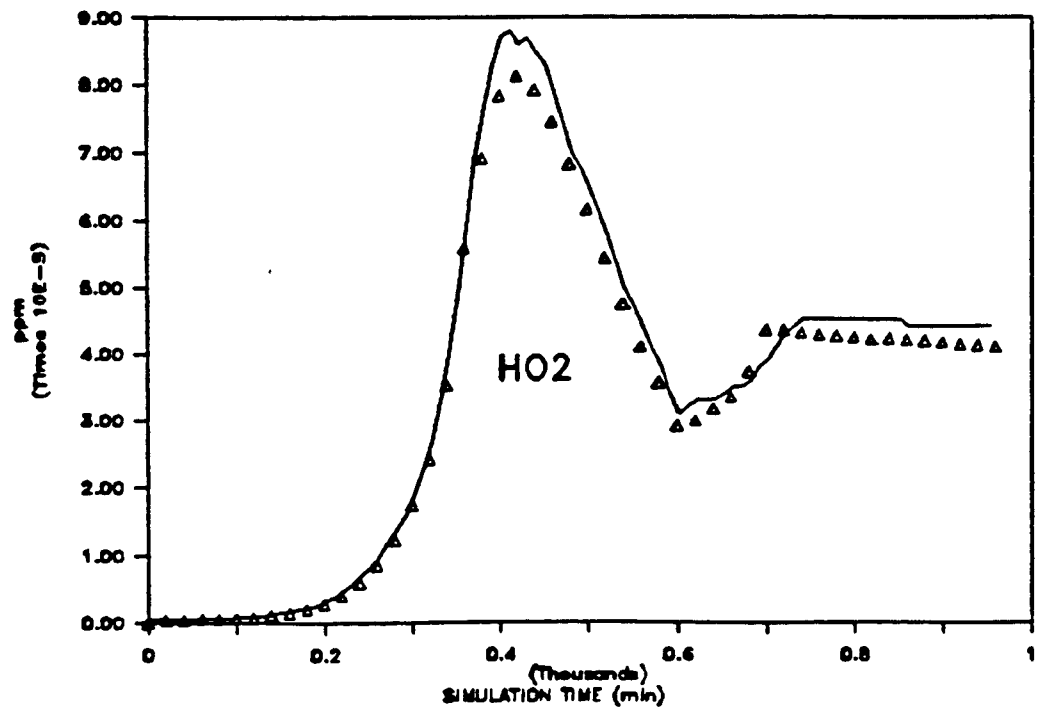

FIGURE 2-3. OH concentrations (top) and HO_2 concentrations (bottom) for Example 2 (sunset is at 680 minutes); lines are Gear simulation results and symbols are Crank-Nicholson predictions.

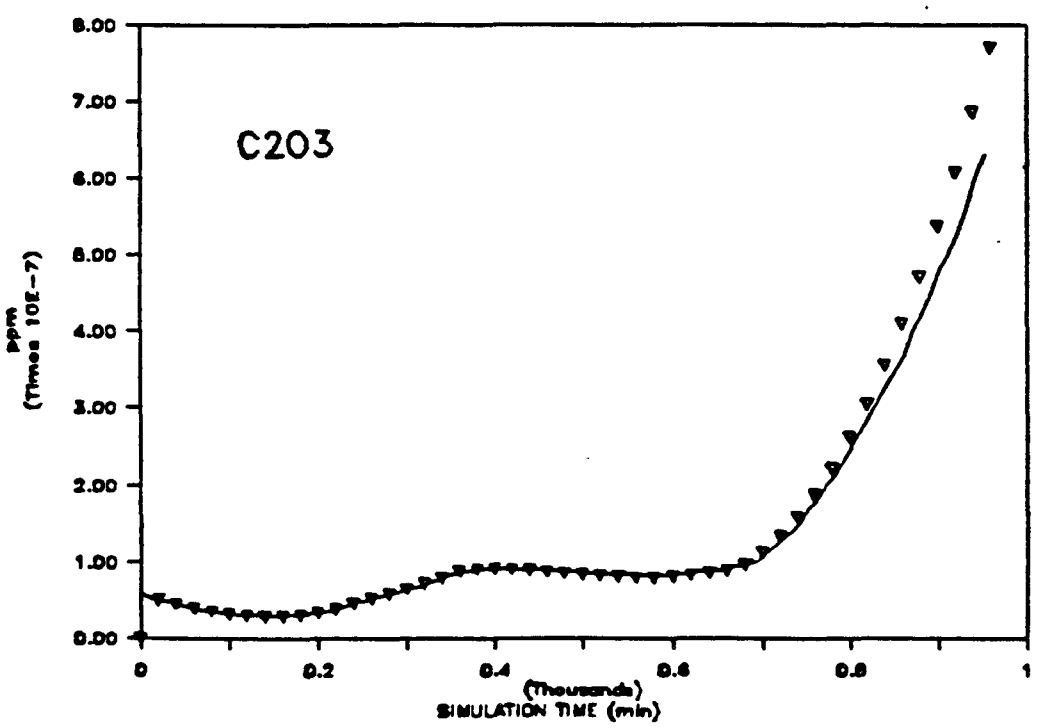

FIGURE 2-4. C_2O_3 concentrations for Example 1 (sunset is at 680 minutes); lines are Gear simulation results and symbols are Crank-Nicholson predictions.

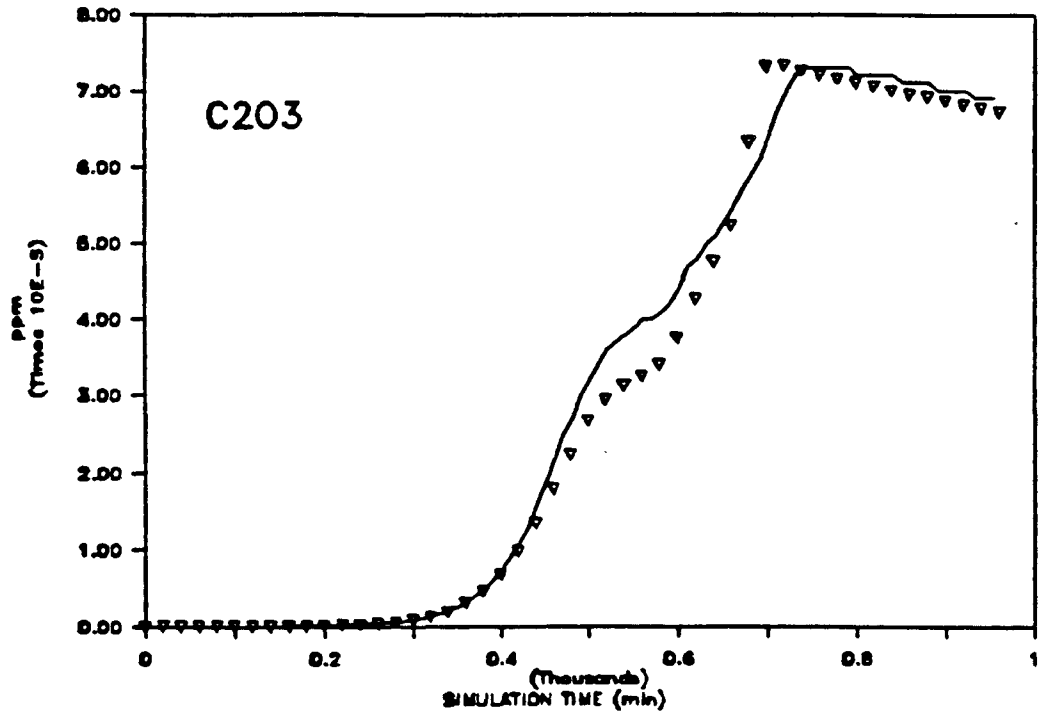

FIGURE 2-5. C_2O_3 concentrations for Example 2 (sunset is at 680 minutes); lines are Gear simulation results and symbols are Crank-Nicholson predictions.

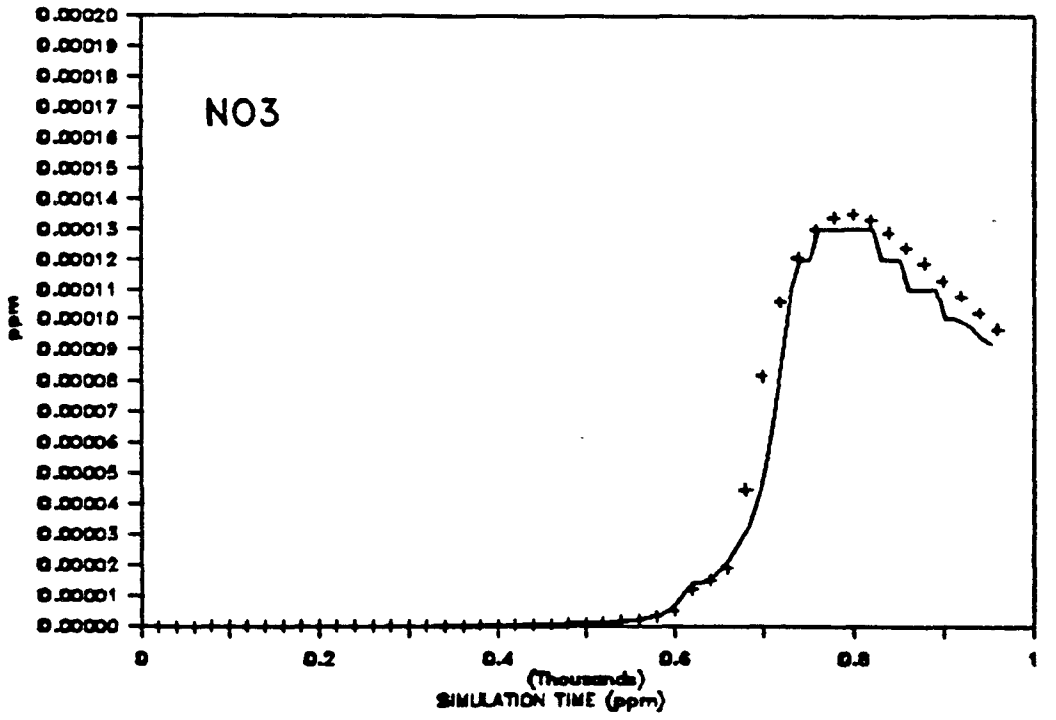

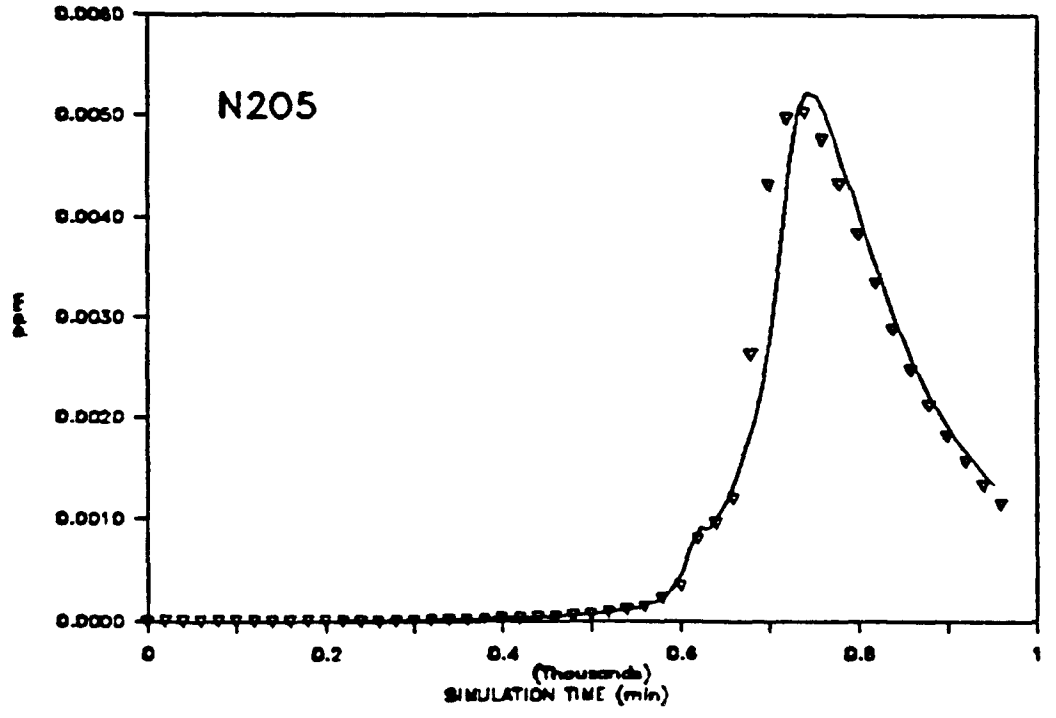

FIGURE 2-6. NO_3 concentrations (top) and N_2O_5 concentrations (bottom) for Example 1 (sunset is at 680 minutes); lines are Gear simulation results and symbols are Crank-Nicholson predictions.

sunset) and are shown in Figure 2-7. We are now considering this technique for the SO_2 oxidation cycle, which will be better served with a "guaranteed" sulfur balance.

Photolysis Rate Calculations

There are fundamental differences in the representations of photolysis rate expressions in CB-II and CB-IV. In the CB-II all photolysis reaction rates are calculated via a direct porportionality relationship with the NO_2 photolysis reaction rate. However, other photolysis reactions (e.g., ozone, formaldehyde, and higher aldehyde photolysis rates) are activated at spectrums of ultraviolet radiation different from those of NO_2. Thus CB-IV requires separate photolysis reaction rates for NO_2, formaldehyde, higher aldehydes, and ozone. Thus, on the basis of the input NO_2 photolysis rate, the UAM (CB-IV) calculates the solar zenith angle required to produce the NO_2 photolysis rates and then calculates the photolysis rates for the other photolytic reactions on the basis of the intensity of the solar radiation.

3 PREPARATION OF UAM INPUTS FOR NEW YORK AND ST. LOUIS

An important component of the PLANR use of the UAM is consistency in the procedures used to prepare model inputs. Procedures to be followed in preparing UAM inputs with limited data availability must be developed and clearly stated. When there is a lack of data, there must be recommended procedures to be used. The preprocessor programs supplied with the 1978-1980 version of the UAM rely on intensive measurement program; data are interpolated from these measurements to obtain gridded fields of input parameters required by the UAM. Over the last 10 years, many of these programs have been outdated. More recent applications of the UAM have prepared input files using only routinely available meteorological and air quality data (Hogo, Mahoney, and Yocke, 1988). However, the procedures used for input preparation have been developed on a case-by-case basis and are tailored to data availability.

In this section we discuss how the meteorological, air quality, and terrain inputs were prepared for the New York and St. Louis UAM modeling episodes. However, time constraints did not permit identification of ozone episodes or development of additional modeling data bases for this project. Instead, ozone episodes that had been previously modeled for St. Louis and New York were used for this study. When data from the original studies were deemed suitable for the current application, they were used without change. However, changes and additions to the data were made to allow use of the Carbon-Bond-IV Mechanism, to extend the time span of the simulations, to alter the definition of the modeling grid, and to improve the quality of the input data using current input preparation procedures.

Although this study makes use of previously developed UAM inputs as a basis for the New York and St. Louis modeling data bases, the general procedures should be viewed as a starting point for development of a consistent UAM input preparation methodology for the PLANR use of the UAM. The reader is again cautioned that these two applications of UAM are not true PLANR uses because of the use of nonroutine data. Moreover, for New York in particular, this study has indicated the area is not amenable to PLANR because of the large amounts of transported pollutants and the complex land-sea meteorology.

UAM INPUT REQUIREMENTS

The following 13 input files are required for UAM modeling analyses:

DIFFBREAK — This file contains the daytime mixing height or nighttime inversion height for each column of cells at the beginning and end of each hour of the simulation.

REGIONTOP — This file contains the height of each column of cells at the beginning and end of each hour of the simulation. If this height is greater than the mixing height, the cell or cells above the mixing height are assumed to be within an inversion.

WIND — This file contains the x and y components of the wind velocity for every grid cell for each hour of the simulation. Also the maximum wind speed for the entire grid and average wind speeds at each boundary for each hour are included in this file.

METSCALARS — This file contains the hourly values of the meteorological parameters that do not vary spatially. These scalars are the NO_2 photolysis rate constant, the concentration of water vapor, the temperature gradient above and below the inversion base, the atmospheric pressure, and the exposure class.

AIRQUALITY — This file contains the initial concentrations of each species for each grid cell at the start of the simulation.

BOUNDARY — This file contains the location of the modeling region boundaries. This file also contains the concentration of each species that is used as the boundary condition along each boundary segment at each vertical level.

TOPCONC — This file contains the concentration of each species for the area above the modeling region. These concentrations are the boundary conditions for vertical integration.

TEMPERATUR — This file contains the hourly temperature for each surface layer grid cell.

EMISSIONS — This file contains the ground-level emissions of NO, NO_2, seven carbon-bond categories, and CO for each grid square for each hour of the simulation.

PTSOURCE — This file contains the point source information, including the stack height, temperature and flow rate, the plume rise, the grid cell into which the emissions are emitted, and the emissions rates for NO, NO_2, seven carbon-bond categories, and CO for each point source for each hour.

TERRAIN This file contains the value of the surface roughness and deposition factor for each grid square.

CHEMPARAM This file contains information regarding the chemical species to be simulated including reaction rate constants, upper and lower bounds, activation energy, and reference temperature.

SIMCONTROL This file contains the simulation control information such as the time of the simulation, file option information, default information, and information on integration and chemistry time steps.

WIND FIELD PREPARATION PROCEDURE

One of the most important UAM inputs is the wind field. A key component in the PLANR use of the UAM will be use of a new diagnostic wind model developed by Systems Applications, Inc. for the U.S. Environmental Protection Agency. This model was originally developed to simulate airflow over data-sparse regions of complex terrain (Morris et al., 1987, 1988).

Hourly gridded wind fields were generated for St. Louis (13 July 1976) and New York (07 - 08 August 1980) using the Systems Applications' Diagnostic Wind Model (Douglas and Kessler, 1988). This model incorporates local surface and upper-air observations, where available, and provides some information on terrain-induced airflow in regions where local observations are unavailable. The diagnostic wind model is formulated in terrain-parallel coordinates. Generation of a wind field using the diagnostic wind model is a two-step procedure.

In Step 1, a domain-mean wind, which is obtained from a representative upper-air observation, is adjusted for terrain effects. These include the kinematic effects of terrain (the lifting and acceleration of the airflow over terrain obstacles), thermodynamically generated slope flows, and blocking effects. Step 1 produces a spatially varying gridded field of u and v for each vertical layer within the model domain.

In Step 2, observational information is added to the Step 1 (u,v) field. An objective analysis procedure is applied in which the observations are utilized within a user-specified radius of influence while the Step 1 (u,v) field dominates in subregions where observations are unavailable. The objective analysis procedure consists of the following four substeps: (1) interpolation, (2) smoothing of the analyzed field, (3) computation of a vertical-velocity field, and (4) minimization of the three-dimensional divergence. The following modified inverse-distance-squared weighting scheme (Ross and Smith, 1986) is used for the interpolation:

$$(u,v)' = \{\mathrm{sum}_k[r_k^{-2}(u_o,v_o)_k] + R^{-2}(u,v)_1\}/\{\mathrm{sum}_k r_k^{-2} + R^{-2}\}$$

where $(u_o,v_o)_k$ denotes an observed wind at station k, r_k is the distance from station k to a given grid point, $(u,v)_1$ is the Step 1 wind field at this grid point, and $(u,v)'$ is the updated wind vector. The parameter R controls the relative influence of the observations and the Step 1 wind field.

Following the interpolation, a five-point smoother is applied to the analyzed wind field to reduce discontinuities that may result from the interpolation. An initial vertical velocity, W', is calculated from $(u,v)'$ by integrating the incompressible conservation-of-mass equation. It has been noted (Godden and Lurmann, 1983) that vertical velocities obtained from an objectively anlayzed field may be unrealistically large near the top of the domain. In the diagnostic wind model, W' is modified using a procedure suggested by O'Brien (1970):

$$W_2(Z) = W'(Z) - (Z/Z_{top})W'_{top} \quad .$$

Here Z is height in terrain-following coordinates, and Z_{top} is the height of the model top. Note that W_2 is zero at the top of the model.

After the vertical velocity profile is adjusted, it is necessary to adjust the objective analysis product $(u,v)'$ so that it is mass-consistent with W_2. An iterative adjustment of the horizontal (u,v) field is performed to minimize the three-dimensional divergence within each layer. The adjusted horizontal wind field $(u,v)_2$ is the final product of the diagnostic model.

For both the New York and St. Louis applications of the UAM, the diagnostic wind model was exercised with 13 to 14 vertical levels using available meteorological measurements. These wind fields were then vertically averaged to the vertical five-layer configuration used in these UAM applications.

NEW YORK APPLICATION

In the following subsections we describe UAM input preparation for the New York modeling episode.

New York Modeling Domain and Period

An ozone episode simulated in the original OMNYMAP (Oxidant Modeling in the New York Metropolitan Area Program) study by the State of New York Department of Environmental Conservation (NYDEC) (Rao, 1987) was used as the starting point for the New York simulation in this study. This episode (8 August 1980) was simulated originally from 0400 to 2000 LST. Because it is important in any photochemical modeling application that initial conditions do not greatly influence the peak calculated concentration, the simulations performed as part of this project began at noon on 7 August. A tracer simulation showed that with this starting time, the simulation was not influenced by initial concentrations after 0600 LST on 8 August. A two-day simulation of the New York modeling region also allowed investigation of the effects

of slower-reacting hydrocarbon species, such as those produced by ethanol-blended fuels, on peak ozone concentrations. Inputs were created for the hours preceding 0400 LST on 8 August and 7 August.

The modeling was performed on the original OMNYMAP (Rao, 1987) modeling grid, which consists of 31 by 25 grid cells with a horizontal dimension of 8 km, covering an area 248 by 200 km. The location of this grid and its relation to other northeastern states is presented in Figure 3-1. It covers parts of New Jersey, New York, and Connecticut. The grid is located in UTM zone 18, with the origin set at 520,000. m Easting and 446,000. m Northing.

The original vertical structure of the UAM in the OMNYMAP study contained four vertical cells that were constrained to three below and one above the hourly mixing height. Vertical layers above the mixing height that are allowed to become very thick during certain simulation hours may result in inadequate vertical resolution. Under certain conditions, especially during nighttime hours when mixing heights are low, pollutants from large point sources that are emitted aloft may be artificially dispersed in such thick layers. Also, with thick layers, the wind speed and direction, and vertical and horizontal shear above the mixing height may not be appropriately resolved. To adequately resolve the vertical structure, modeling with as many as eight vertical layers might be desirable but might also be computationally impractical. To provide a balance between practicality and appropriate vertical resolution, we used a new vertical grid structure consisting of five vertical cells, with two below and three above the hourly mixing height. The heights of the vertical layers varied in thickness spatially and temporally depending on the hourly mixing height field. The minimum thickness of the lower cells was 50 m, and the minimum thickness of the upper cells was 150 m.

Much of the data used in the previous OMNYMAP application of UAM for 8 August was used "as is" in this application. However, certain of the files (e.g., WINDS and BOUNDARY) were recreated using new techniques, and one new file (TERRAIN) was added. In the original OMNYMAP application, spatially constant default deposition and surface roughness parameters were used in place of spatially varying parameters. The new TERRAIN file contains updated spatially varying parameters based on land use data. Because of the changes in the vertical layer structure for the new UAM modeling, those files affected by this change were also recreated.

The procedures for preparing each of the input files for the New York application are described below. Some data files for New York were taken from the previous OMNYMAP application. However, in order to begin the simulation at 1200 LST on 7 August 1980, data files were created for 7 August. In addition, some data files for 8 August were revised.

Meteorological Inputs

DIFFBREAK

Mixing heights for 8 August were retained from the OMNYMAP application. Mixing heights for 7 August were derived from the soundings at John F. Kennedy (JFK) Airport and Albany using an objective method described by Kelley (1981). The mixing heights varied hourly but were spatially constant for 7 and 8 August.

For the time period from 1200 LST on 7 August to 0400 LST on 8 August, new data were prepared. Twice-daily soundings at Albany, New York, and JFK Airport provided information on the vertical structure of the atmosphere in the modeling region. Surface temperatures at Albany and La Guardia were needed to determine the temporal variation of the mixing heights. Mixing heights were determined from these data using a computerized analysis method described by Kelley (1981). Data for the time period after the last sounding on the 7th were set to the same value as at 0400 LST on the 8th. DIFFBREAK values are listed below:

Date	Time (EST)	Height of DIFFBREAK (meters)
7 August	1200	1700.
	1300	1700.
	1600	1700.
	1700	1380.
	1800	1080.
	1900	800.
	2000	610.
	2100	430.
	2200	360.
	2300	345.
8 August	0000	345.
	0600	345.
	0700	375.
	0800	405.
	0900	450.
	1000	540.
	1100	700.
	1200	1020.
	1300	1400.
	1400	1400.
	1500	1400.
	1600	1400.
	1700	1170.
	1800	940.
	1900	710.
	2000	710.

REGIONTOP

The top of the modeling region was set to a constant value of 1500 meters above ground level. This value is 100 meters above the maximum mixing height on 8 August. Specifying a higher value may result in articifical dilution of emissions from elevated point sources. If a temporally varying region top is used that rises with the mixing height, as was used in the OMNYMAP study, emissions from elevated point sources whose plume rise exceeds the region top may be lost from the modeling domain.

METSCALARS

METSCALARS data for 8 August were left mostly unchanged from those used in the OMNYMAP study. Radiation factors were recalculated for the Carbon-Bond IV Mechanism by using the procedures described by Schere and Demerjian (1977) and actinic flux data collected by Bass and co-workers (1980) (see Gery, Whitten, and Killus, 1988). A few values of the temperature gradient below the inversion were altered from values greater than -.01 degrees K/meter to -.01 degrees K/meter to make them more consistent with the high radiation intensity found at the same time. Other METSCALARS data were created for 7 August by using data from the corresponding hour on the 8th. Gaps in the data (i.e., 2000 to 0400) were filled in by linearly interpolating the data on either side of the gap. The exposure class, however, was not interpolated, but rather was set to -2 for these nighttime hours.

TEMPERATUR

Surface temperature data from the OMNYMAP application were used for 8 August 1980. Data for corresponding hours of 8 August were used for 7 August. Missing hours were linearly interpolated.

WIND

Three surface stations within the New York modeling domain provided hourly observations of wind speed and wind direction for the 7 and 8 August modeling period. The stations located at La Guardia Airport in New York City and at Bridgeport and Hartford in Connecticut are plotted in Figure 3-1. Twice-daily upper-air observations were available from radiosondes located at JFK Airport in New York City and Albany, New York. The upper-air observations were vertically interpolated to the diagnostic wind model layers and temporally interpolated so that data were available for each hourly analysis. The diagnostic wind model was exercised using 14 vertical layers with interfaces at 0, 50, 100, 150, 200, 300, 400, 500, 600, 750, 900, 1050, 1200, 1350, and 1500 m agl. A maximum radius of influence of 40 km was used at the surface, and 150 km was used aloft. The weighting parameter for the terrain effects was specified as 20 km.

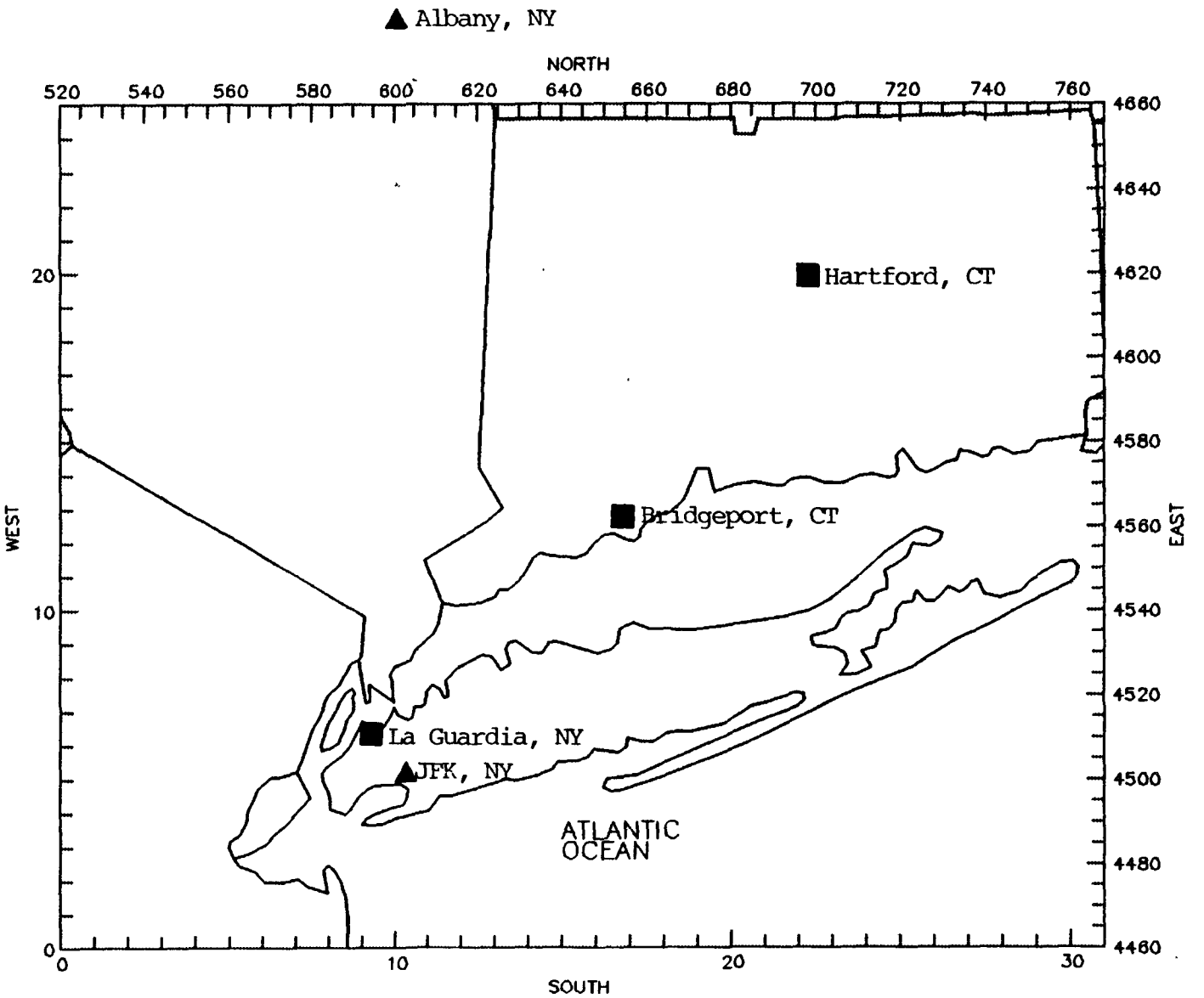

FIGURE 3-1. OMNYMAP UAM modeling domain and location of surface (■) and upper-air (▲) meteorological observation sites.

The diagnostic wind model fields were interpolated to the four UAM layers and the O'Brien-Cressman vertical-velocity-adjustment procedure was applied to reduce the vertical velocity at the top of the modeling domain.

Table 3-1 compares the wind fields for 8 August 1980 used in this study and those used in the OMNYMAP study. The OMNYMAP study used horizontally and vertically spatially constant winds. The average mixed-layer and aloft-layer winds used in this study are displayed in Table 3-1, along with the variability (i.e., maximum and minimum wind speeds and directions). In this study, these wind fields have a more westerly wind component in the afternoon of 8 August, which results in the highest ozone concentrations being located in the middle of Long Island Sound rather than along the southern coast of Connecticut as predicted in the OMNYMAP study.

Air Quality Inputs

The UAM requires specification of hourly values of initial and boundary concentrations for each species in the CB-IV mechanism.

AIRQUALITY

No hydrocarbon measurements and very few NO_x measurements were available at 1200 on 7 August 1980. A tracer simulation revealed that initial pollutants were transported out of the modeling region by 0600 on 8 August. Therefore initial concentrations would not influence the formation of ozone on that date. Given the time constraints and lack of representative observations, initial conditions data from the OMNYMAP study (0400; 8/8/80) were used to initialize the model on 7 August. The OMNYMAP hydrocarbon species were resplit for the Carbon-Bond-IV Mechanism as shown in Table 3-2.

BOUNDARY

Boundary conditions near the south, west and north boundaries were determined from station measurements in the neighborhood of these boundaries. The eastern boundary and the eastern portions of the south and north boundaries were assigned relatively clean values. Hydrocarbon species were split for the Carbon-Bond-IV Mechanism as shown in Table 3-3. Concentrations on the lateral boundaries of the modeling region are of considerable importance to the model results and were based on measurements when available. For NO2, NO, and ozone, measurements within and near the boundaries of the OMNYMAP region were available from the Storage and Retrieval Of Aerometric Data (SAROAD) base. In addition, hydrocarbon measurements for several sites in New Jersey and New York were available from the NECRMP study

TABLE 3-1. Comparison of average wind speeds and wind directions used in the OMNYMAP study and those used in this study. (Note: this study uses spatially varying winds; values in parentheses denote maximum and minimum values.)

	OMNYMAP Study		This Study			
			Mixed Layers		Layers Aloft	
Hour	Wind Speed (m/s)	Wind Direction	Wind Speed (m/s)	Wind Direction	Wind Speed (m/s)	Wind Direction
1	NA	NA	3.5 (0.5:4.7)	309 (9:263)	6.9 (4.9:9.7)	312 (301:318)
2	NA	NA	3.6 (1.8:4.6)	310 (264:338)	6.9 (4.8:9.8)	314 (305:320)
3	NA	NA	3.3 (1.6:4.4)	303 (260:332)	6.9 (4.6:9.8)	314 (306:320)
4	3.5	227	3.4 (1.6:4.4)	299 (260:325)	7.0 (4.5:9.9)	315 (308:320)
5	3.7	236	3.8 (2.3:4.7)	301 (265:324)	7.2 (4.8:10.1)	316 (310:323)
6	3.8	241	3.8 (2.1:4.7)	312 (270:334)	7.4 (4.9:10.2)	320 (315:327)
7	3.2	244	4.1 (2.4:5.1)	310 (271:326)	7.6 (5.2:10.3)	321 (316:330)
8	3.7	231	5.0 (3.2:5.7)	312 (278:328)	7.7 (6.2:10.2)	318 (313:325)
9	3.8	232	3.9 (2.3:5.0)	315 (275:331)	7.1 (5.4:9.6)	316 (310:320)
10	4.0	237	3.8 (2.2:5.0)	319 (280:335)	6.8 (5.4:9.4)	314 (310:318)
11	4.6	238	2.7 (1.4:4.1)	271 (225:304)	6.0 (3.8:8.9)	304 (290:314)
12	5.3	233	3.0 (1.6:4.2)	283 (238:323)	5.9 (4.3:8.7)	302 (293:314)
13	4.8	235	3.7 (2.7:4.6)	274 (236:308)	5.8 (4.6:8.6)	296 (282:309)
14	5.1	236	4.8 (3.6:5.8)	247 (224:277)	5.7 (4.2:8.4)	283 (259:297)
15	5.6	236	4.5 (3.9:5.0)	266 (239:286)	5.7 (4.2:8.4)	285 (274:296)
16	4.5	234	3.6 (2.8:4.3)	261 (234:296)	5.3 (4.0:8.1)	280 (268:295)
17	5.1	245	4.1 (3.5:4.5)	258 (238:274)	5.4 (4.1:8.1)	274 (263:285)
18	4.5	239	3.5 (2.8:4.2)	259 (234:284)	5.2 (3.9:8.0)	259 (235:284)
19	4.8	224	4.0 (3.4:4.6)	267 (240:286)	5.4 (4.1:8.2)	267 (251:281)
20	NA	NA	4.4 (3.6:5.1)	265 (250:280)	5.5 (4.3:8.2)	268 (252:282)

TABLE 3-2. Respeciation of initial concentrations and emissions of hydrocarbons.

CBM-IV Species	As a Function of CBM-II Species
OLE	OLE
PAR	PAR - ARO * 0.432 - ARO * 2 * 0.568
TOL	ARO * 0.432
XYL	ARO * 0.568
FORM	CARB * 0.288
ALD2	CARB * 0.712
ETH	ETH
CRES	1×10^{-6} ppm
MGLY	1×10^{-6} ppm
OPEN	1×10^{-6} ppm

TABLE 3-3. Respeciation of boundary concentrations of hydrocarbons.

CBM-IV Species	As a Function of CBM-II Species
OLE	RHC * 0.027/2
PAR	RHC * 0.685
TOL	RHC * 0.058/7
XYL	RHC * 0.036/8
FORM	RHC * 0.096
ALD2	RHC * 0.051/2
ETH	RHC * 0.047/2
CRES	1 X 10^{-6} ppm
MGLY	1 X 10^{-6} ppm
OPEN	1 X 10^{-6} ppm

where RHC = 2 * ETH + 2 * OLE + PAR + CARB + 6 * ARO.

(PEDCo Environmental, Inc., 1980). In utilizing these measurements, the boundary of the modeling domain was divided into three sectors:

The Southwest sector - the southern half of the west boundary and the western half of the south boundary.

The Northwest sector - the northern half of the west boundary and the western half of the north boundary.

The East sector - the remainder of the region boundary, including the eastern halves of the north and south boundaries and the east boundary.

The Southwest sector is the most important in the New York simulation since it is more frequently an inflow boundary than are the other boundaries. Also, the concentrations that occur near this boundary are higher than those that occur near the other sectors, probably because of the presence of several major metropolitan areas upwind. The East sector is the least important since it is seldom an inflow boundary on either 7 or 8 August.

In the portion of the region below the height of the mixing height, the values of the species were based on average surface measurements near the appropriate sector, as described below. The concentrations above the height of the mixing height were set to the values in the TOPCONC file, which is discussed later in this section.

NO_2 and NO surface concentrations in the Southwest sector were based on measurements at Flemington, Phillipsburg, New Brunswick, and Monmouth, NJ. For each hour of the day, each cell in the sector was set to the average of the measurements at these sites. This resulted in boundary NO_x concentrations of approximately 60 ppb at night and 30 ppb during the day for the southwest corner of the modeling domain. Similarly, ozone was set to the average of measurements at Flemington, Trenton, Monmouth, and Plainfield, NJ. Hydrocarbon measurements in New Brunswick, Linden, Newark, and Bayonne, NJ show rather severe fluctuations during the course of the modeled days, and therefore the boundary values for HC were not assigned hourly values based on these measurements. Instead, an estimate of the daily average at these stations during daytime (650 ppbc) was used. Since all of these stations show somewhat elevated hydrocarbon values during nighttime hours, 1,050 ppbc was used after sunset. Considerably higher values for hydrocarbons could possibly be justified at some hours based on the measured values; however, these boundary concentrations are quite high already, and higher values could cause excessive amounts of material to be transported into the region. Surface hydrocarbon measurements tend to overestimate the mixed-layer average hydrocarbon concentrations represented by the boundary conditions. Therefore, the very highest hydrocarbon measurements were not deemed appropriate and consequently not used in prescription of the boundary conditions.

Table 3-4 compares southwest corner (10 grid cells in the east and north direction from the southwest corner) mixed-layer average VOC and NO_x boundary conditions for the OMNYMAP 1988 Scope Base Case and this study's 1980 and 1995 boundary conditions. The OMNYMAP 1988 boundary conditions were obtained from the base year (1980) boundary conditions by reducing the VOC and NO_x boundary concentrations by 40 and 20 percent, respectively. Thus, the OMNYMAP 1980 VOC boundary conditions for the Southwest region were approximately twice that used in this study. During the early morning (before 7:00 a.m.) this study used slightly higher NO_x boundary conditions than those used in the 1980 OMNYMAP UAM simulations. However, after around 9:00 a.m., the 1980 OMNYMAP NO_x boundary conditions were about the same as those used in this study.

For the Northwest sector, NO and NO_2 at each hour were based on measurements at Syracuse, NY and Hartford, CT. Ozone for this sector was assigned hour by hour based on measurements at Poughkeepsie and Syracuse, NY and Hartford and Litchfield, CT. No hydrocarbon measurements were available in the vicinity of the Northwest sector of the boundary, so the hydrocarbon values on this boundary were taken to be two-thirds of the values in the Southwest sector (based on the relative magnitude of the NO_x measurements near the two sectors). Thus, 200 ppbc was used in the daytime, and 333 ppbc was used at night.

In the East sector, which is bounded by ocean and is almost always an outflow boundary, constant values were used for the entire run. Ozone was set to the clean value of 40 ppb, and NO_2 and NO were set to 6 ppb and 3 ppb, respectively. Hydrocarbons were set to 30 ppb. Tracer runs show that the model results will not be significantly affected by concentrations in this sector of the boundary.

TOPCONC

Concentrations at the top of the modeling region were set to clean values based on aircraft spiral measurements taken in New Jersey on the modeled days. Concentrations at the top of the modeling region were revised for the entire span of the run because of the change in values in the REGIONTOP file from the values used in the OMNYMAP study. Although the fixed top of the region and the divergence minimization technique utilizied in preparing the wind field virtually eliminate the effects of the top boundary concentrations on model results, it was still appropriate to use the lower concentration values typically found at 1500 meters. Aircraft spirals in New York City on 7 and 8 August from the NECRMP study show very low values for NO_x at 1500 meters, sometimes less than 1 ppb but usually nearer 10 ppb. Therefore, 9 ppb was used for the top boundary concentration of NO_x, split two-thirds NO_2 and one-third NO. Ozone measurements in the spirals hovered a little above 5 pphm; hence we retained the value of 5.6 pphm for the ozone top boundary concentration. No hydrocarbon measurements were available from the spirals, so the OMNYMAP hydrocarbon value of 28 ppbC was retained. This hydrocarbon value was resplit according to the formula in Table 3-3 to obtain Carbon-Bond-IV species.

TABLE 3-4. Comparison of 1980 and 1995 mixed-layer southwestern boundary conditions used in this study and the mixed-layer southwestern boundary conditions used in the OMNYMAP 1988 Scope Base Case for 8 August 1980.

	VOC Boundary Conditions (ppbc)			NO_x Boundary Conditions (ppb)		
	OMNYMAP 1988 Scope	This Study		OMNYMAP 1988 Scope	This Study	
Hour	Base Case	1980	1995	Base Case	1980	1995
1	NA	1,051	646	NA	50	38
2	NA	1,051	646	NA	48	29
3	NA	1,051	646	NA	50	30
4	1,239	1,051	646	25	52	31
5	1,224	1,051	646	27	60	36
6	1,163	1,051	646	37	80	48
7	967	1,051	646	30	62	37
8	904	1,051	646	35	72	43
9	811	631	394	34	58	35
10	999	631	394	37	42	25
11	946	631	394	38	34	20
12	1,006	631	394	38	32	19
13	1,067	631	394	30	26	16
14	1,127	631	394	35	36	22
15	1,119	631	394	30	44	26
16	1,158	631	394	33	42	25
17	1,188	631	394	30	42	25
18	1,369	631	394	29	46	28
19	976	631	394	30	64	38
20	NA	1,051	646	NA	62	37

Terrain Inputs

TERRAIN

Dominant land use in each grid cell of the New York modeling region was estimated from USGS 1:250000 scale maps. Cells were categorized as urban, deciduous forest, agricultural or range land, or water. Surface roughness and vegetation factors were derived from the values given by a recent Argonne National Laboratory study listed in Table 3-5.

Existing Emissions Data

An emissions inventory for the UAM(CB-IV) was obtained from the emissions inventory used for the OMNYMAP application of the UAM(CB-II) for the 1988 SCOPE base case. Hydrocarbon species from the OMNYMAP application were resplit according to the formulas given in Table 3-2. The 1980 OMNYMAP emissions inventory was not available in time to be used in the model evaluation exercise; therefore, the OMNYMAP 1988 Scope Base Case inventory had to be used in the model evaluation study. The 1988 inventory contained approximately 32 and 14 percent less VOC and NO_x emissions, respectively.

ST. LOUIS APPLICATION

Time constraints did not permit identification of a new episode for St. Louis PLANR use of the UAM. Instead, an episode was chosen from the 20 St. Louis ozone episodes prepared by the EPA as part of the St. Louis Ozone Modeling Project (Schere and Shreffler, 1982; Cole et al., 1983). A preliminary analysis of these 20 St. Louis UAM episodes identified four possible candidate days for this project. On the basis of objective selection requirements discussed in Appendix C, the 13 July 1976 ozone episode day was selected for application of the UAM (CB-IV).

Many of the data files for St. Louis were taken from the previous EPA application (Schere and Shreffler, 1982). Tracer runs had shown that significant initial material was still retained within the region at mid-morning if the simulation was begun at 0300 LST. We therefore decided to push the beginning of the run back to 0000 hours. In order to begin the simulation at 0000 hours on 13 July 1976, data from 0500-0600 LST were used for prior hours. Information on individual data files follows.

TABLE 3-5. Surface roughness and deposition factors based on studies by Argonne National Laboratories.

Land Use Category	Surface Roughness (meters)	Deposition Factor
Urban	3.00	0.2
Agricultural	0.25	0.5
Range	0.05	0.4
Deciduous Forest	1.00	0.4
Coniferous Forest including wetland	1.00	0.3
Mixed Forest	1.00	0.3
Water	0.0001	0.03
Barren land	0.002	0.2
Nonforest Wetlands	0.15	0.3
Mixed Agricultural and range	0.10	0.5
Rocky (low shrubs)	0.10	0.3

Meteorological and Surface Characteristics Files

DIFFBREAK

Values in this file remain unchanged from the previous EPA application. The procedures used to generate mixing heights are described in Schere and Shreffler (1982).

REGIONTOP

The top of the modeling region was set to a constant value of 1600 meters for the entire run. This is a higher region top than that used in the previous EPA study and thus will (1) retain more emitted pollutants (such as from elevated point sources) within the modeling region, and (2) reduce the influence of the boundary top concentrations on model results.

METSCALARS

Values established in the EPA application were retained with the exception of the NO_2 photolysis rates (radfactor) and temperature gradient above the mixing height (tgradabove). Radiation factors were recalculated for the Carbon-Bond-IV Mechanism according to the procedures developed by Schere and Demerjian (1977). Temperature gradients above the inversion base included positive values characteristic of the gradient within the inversion. Because of the new definition of the top of the modeling region, positive values of this gradient were reduced to zero to better reflect the new averaging depth.

TEMPERATUR

Surface temperature data from the EPA application were used.

WIND

A dense surface monitoring network from the RAPS network consisting of 25 stations provided hourly observations of wind speed and wind direction for the 13 July 1976 simulation. The locations of the surface stations are shown in Figure 3-2. A radiosonde located just north of the eastern boundary of the domain provided hourly upper-air observations with approximately 100 m vertical resolution. These observations were vertically averaged within the diagnostic wind model layers. The diagnostic model was exercised using 13 vertical layers with interfaces at 0, 50, 100, 150, 200, 300, 400, 500, 600, 800, 1000, 1200, 1400, and 1600 m agl. A maximum radius of influence of 20 km was used in the surface layer, and 200 km was used aloft. The weighting parameter for the terrain effects was 10 km.

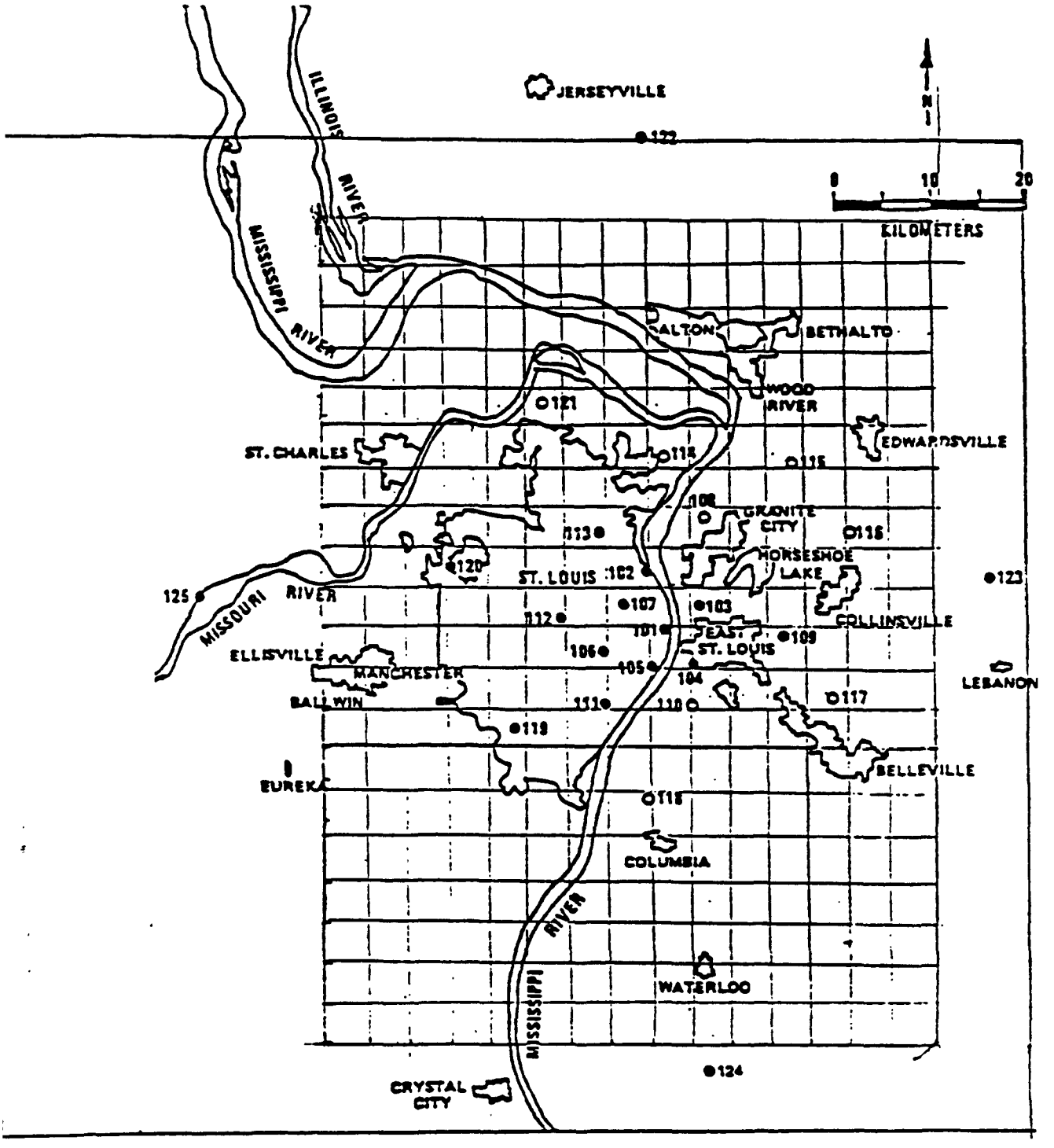

FIGURE 3-2. The St. Louis area with locations of the RAPS surface stations and 4 x 4 km modeling grid superimposed. (Source: Cole et al., 1983)

Postprocessing of the model output consisted of interpolating the diagnostic wind model fields to the five spatially and temporally varying UAM layers.

Initial and Boundary Concentration Files

AIRQUALITY, BOUNDARY, and TOPCONC

Hydrocarbon species from the EPA UAM application were resplit according to the formula given in Tables 3-2 and 3-3.

Terrain Inputs

TERRAIN

Surface roughness and vegetation factors from the EPA UAM application were scaled to make them agree with the recent Argonne National Laboratory measurements. The relative values used in older studies are compared with the Argonne recommendations in Table 3-6. Since the magnitudes of the surface roughness values are comparable, the change made was to set a minimum value of 0.0001 m. The deposition factors differ considerably and were therefore recalculated as follows. First a minimum of 0.03 was set. Values in the range 0.03 to 0.2 were left unchanged. For values greater than 0.2, the value was recalculated by the equation

$$\text{new value} = \frac{(\text{old value} - 0.2)}{(1.0 - 0.2)} * (0.5 - 0.2) + 0.2$$

Existing Emissions Files

EMISSIONS and PTSOURCE

Hydrocarbon species from the EPA application were resplit according to the formula given in Table 3-2. Other values were used without change.

PROJECTION OF INITIAL AND BOUNDARY CONDITIONS TO 1995

For the purposes of future year (1995) modeling, adjustments in initial and boundary concentrations were projected to occur in proportion to estimated changes in air quality from the original modeled year (1976 for St. Louis and 1980 for New York) to the 1995 emissions. Since more than one basic emission inventory was involved, it was not possible to simply apply the ratio of emissions totals in 1995 to the totals in

TABLE 3-6. Comparison of circa '78 and current surface roughness and vegetation factors.

Land Use Category	Circa '78 Roughness (m)	Argonne Lab. Study Roughness (m)[a]
Water	0.00001	0.0001
Brush	0.2	0.1[b]
Forest	2.8	1.0
Populated	1.75	--
Densely populated	3.2	3.0

Land Use Category	Circa '78 Vegetation Factor	Argonne Lab Study Vegetation Factor[a]
Water	0.0	0.03
Brush	1.0	0.5[b]
Forest	1.5	0.4
Populated	0.5	--
Densely populated	0.2	0.2

a Hogo et al. (1987)

b Value is for mixed agricultural and range land.

the original emission inventories. First of all there are several scenarios in 1995 with differing emissions totals. Second, the original inventories and the 1985 inventories (from which the 1995 inventories are projected) are based on different raw data. Third, the 1995 inventories include estimates of running losses, whereas the earlier inventories do not. Fourth, the New York 1980 inventory was not available. To address these discrepancies, we elected to use the following procedures.

Consensus among all EPA participants was to use only one set of initial and boundary conditions for all 1995 emission scenarios. For New York this is an especially important factor limiting the results because the effects of changes in emissions of the different emission scenarios were not reflected in the long-range transport of pollutants, which have a major impact on the area's air quality. The 1995 initial and boundary conditions were to be compatible with the 1995 scenario #1 emissions (see Section 4). To avoid making a faulty projection based on the intercomparison of disparate emissions inventories, a projection factor from 1976 (or 1980 for New York) to 1995 was estimated by a two-step process. The first step was to develop projection factors from 1976 (or 1980 for New York) to 1985 based on changes in measured air quality from the national air quality trends for VOC, NO_x and CO (EPA, 1985b). The second step was to develop another set of projection factors from 1985 to 1995. For NO_x and CO the second projection factor from 1985 to 1995 was based on the ratio of the 1995 (scenario #1) emission totals to the 1985 NAPAP emissions inventory totals. Because the 1995 inventory includes running losses of hydrocarbons and the 1985 inventory does not, simply using the ratio of the hydrocarbon totals in the two inventories is not an appropriate means of obtaining the projection factor for this species. Instead, VOC projection factors were obtained from E. H. Pechan and Associates (Pechan, 1988) that were developed by the Bureau of Economic Analysis. These factors indicated an approximate VOC emission change consisting of 35 percent and 25 percent reductions in hydrocarbon for New York and St. Louis, respectively. These factors are appropriate for boundary conditions in New York since projected emission changes in cities upwind of New York are similar to those in New York, according to E. H. Pechan and Associates (1988). The resulting factors are tabulated in Tables 3-7 and 3-8 (Pechan, 1988).

These reductions were not applied to the entire concentration to obtain the 1995 levels. Instead, a global background value considered not to be due to emissions was first subtracted and the projection factor applied to the remainder. The background value was then added back to obtain the 1995 concentration. The following formula describes the projection, where N is the new concentration (1995), F is the net reduction factor from Tables 3-7 or 3-8, O is the old concentration (1976 or 1980), and B is the background value:

$$N = F*(O - B) + B \quad .$$

If a value of O was less than B, then N was set equal to O.

TABLE 3-7. Initial and boundary condition projection factors (St. Louis).

Species	Reduction (1976 to 1985) (percent)	Reduction (1985 to 1995) (percent)	Net Reduction (percent)
VOC	12	25	34
NOx	3	24	26
CO	22	54	64

TABLE 3-8. Initial and boundary condition projection factors (New York).

Species	Reduction (1980 to 1985) (percent)	Reduction (1985 to 1995) (percent)	Net Reduction (percent)
VOC	8	35	40
NOx	3	39	41
CO	12	52	58

Background values for each species were estimated from several sources. Tropospheric ozone estimates by Logan (1985) indicate that 40 ppb is a reasonable background in mid-summer. Fehsenfeld and co-workers (1988) have published values for NO_x at several locations around the world. A typical NO_x value for the continental United States is 0.5 ppb, which was then split two-thirds into NO_2 and one-third into NO. Brimblecombe (1986) reports a hydrocarbon value of 25 ppbC near forests. Given this value as a natural lower bound of hydrocarbon, this 25 ppbC was then resplit according to Table 5 of the "User's Guide for Executing OZIPM-4 with CBM-IV or Optional Mechanisms" (Hogo and Gery, 1988). For CO, an average mid-latitude value appears to be about 0.18 ppm (Peters and Chameides, 1980). Values used for background for each Carbon-Bond-IV species are listed in Table 3-9.

TABLE 3-9. Background concentrations for Carbon-Bond-IV species.

Species	Concentration (ppb)
NO	0.17
NO2	0.33
O3	40.
OLE	0.425
PAR	12.5
TOL	0.15
XYL	0.018
FORM	1.75
ALD2	0.925
ETH	0.425
CRES	0.01
MGLY	0.01
OPEN	0.01
PNA	0.01
NXOY	0.01
PAN	0.01
CO	180.
HONO	0.01
H2O2	0.01
HNO3	0.01
MEOH	0.1
ETOH	0.1

4 EMISSIONS INVENTORY DEVELOPMENT

INTRODUCTION

The Urban Airshed Model requires that emissions data be input in a specific and detailed format. These requirements are more rigorous than those typical of inventories used for planning purposes or trends analysis. For example, total emissions for entire states or EPA regions may be sufficient for tracking overall trends in emissions. Photochemical modeling, however, requires a spatially disaggregated, temporally allocated, and chemically speciated emissions inventory. Meeting these more rigorous requirements entails the collection of additional emissions-related information such as population distribution data.

In this study we used the 1985 NAPAP Emisions Inventory as the base year from which all future-year emissions scenarios were developed (Zimmerman et al., 1988). The future year selected for use in this study is 1995. The 1985 NAPAP Emissions Inventory consists of annual county-wide area source emissions including mobile sources and annual emissions for large point sources, along with stack parameters (i.e., stack height, diameter, flow rate, and temperature). The methods used to spatially disaggregate county-wide area source emissions throughout the modeling domain and the procedure used to temporally adjust annual emission rates to reflect conditions on a typical summer weekday are discussed in detail later in this section.

The stationary source emissions for the 1995 scenario year were projected from 1985 NAPAP emissions by utilizing growth factors by source category available from an EPA study by E. H. Pechan and Associates, Inc. (1988). The growth factors used in this study are discussed in greater detail later. Mobile source emissions were prepared by using scaling factors provided by EPA's Office of Mobile Sources (OMS) specifically for each scenario to be analyzed and are presented at length later in this section.

DEFINITION OF EMISSIONS SCENARIOS

Several emissions inventories were used to verify the UAM and assess the effects of alternative fuel use and SIP control strategies. The following list describes each of the emissions inventories developed for use in this study.

1985 NAPAP--gridding of 1985 NAPAP inventory for CB4 species, as is, to the modeling domain.

1995 base case--this inventory is based on the 1985 NAPAP county inventory. Stationary source emissions are projected to 1995 by using emission adjustment factors obtained from E. H. Pechan and associates (1988), who estimated emission adjustments between 1985 and 1995 based on growth estimates obtained from the Bureau of Economic Analysis (BEA). Mobile source emissions were projected from values provided by OMS.

1995 Emissions Scenarios--these inventories reflect changes in VOC, NO_x, and CO due to assumptions of future changes in mobile source emission rates such as changes in RVP and use of ethanol-blended fuels. Many possible combinations of fuel blends and RVP were considered before we selected the following emissions scenarios for development and eventual model simulation.

For New York:*

Scenario #1--1995 base case with mobile emissions at current RVP values (11.5 psi) with running losses.

Scenario #2--1995 case with mobile emissions at low RVP values (9.0 psi) with running losses.

Scenario #3--1995 case with 100 percent market penetration of a 10 percent ethanol blend at low RVP values with a 1 psi exemption (10.0 psi) with running losses.

Scenario #4--1995 case at current RVP values without running losses.

For St. Louis:*

Scenario #1--1995 base case with mobile emissions at current RVP values (10.0 psi) with running losses.

Scenario #2--1995 case with mobile emissions at low RVP values (7.8 psi) with running losses.

Scenario #5--1995 case with 50 percent market penetration of a 10 percent ethanol blend at low RVP values with a 1 psi exemption (8.8 psi) with running losses.

---

* Time constraints and the need to analyze several alternative emission scenarios precluded our performing Scenarios 3 and 4 for St. Louis, and the SIP scenarios and Scenarios 6 and 7 for New York.

Scenario #6--1995 case with 100 percent market penetration of an ethyl tertiary butyl (ETBE) blended fuel with a 2 percent oxygen content at low RVP values (7.8 psi) with running losses.

Scenario #7--1995 case with mobile emissions at current RVP values (10 psi) with higher estimates of running losses. These higher running loss emissions were 2.24, 2.02, and 1.58 times higher than the running loss emissions in Scenario #1 for, respectively; the light duty gas vehicles, light duty gas trucks, and heavy duty gas trucks source categories.

SIP Scenario A--1995 case with mobile emissions at low RVP values with running losses and enhanced I/M (23 percent reduction of on-road motor vehicle exhaust VOC emissions), and reduction of non-mobile-source VOC emissions to achieve an overall VOC reduction of 40 percent from Scenario 1. NO_x and CO emissions specified were the same as those in Scenario #1.

SIP Scenario B--1995 case with an overall VOC reduction of 40 percent from Scenario 1, where the most reactive species of hydrocarbons are reduced first. Reactivity of the individual CB-IV hydrocarbon species was ranked by the rate constant used in its reaction with the hydroxyl (OH) as follows (CB-IV species and OH rate constant ppmC/min at 298°K):

OLE	21,000
FORM	15,000
ALD2	12,000
ETH	5,960
XYL	4,525
ETOH	2,550
TOL	1,307
PAR	1,203

For each grid cell, up to 80 percent of an individual hydrocarbon species can be reduced, and this reduction is accomplished according to the above ordering until a 40 percent VOC reduction in that grid cell is reached.

OVERVIEW OF THE METHODOLOGY USED FOR GENERATING EMISSION INPUTS

The 1985 NAPAP Emissions Inventory contains annual emissions rates from point and area sources, with area sources compiled on a county-wide basis. To support UAM applications in this study, many refinements of the 1985 NAPAP inventory were required. Listed below are some of the most important activities undertaken to make the 1985 NAPAP emissions inventory compatible for use in the UAM.

Annual emissions were resolved to hourly values for a typical summer weekday;

County-level area source emissions were spatially allocated to grid cells;

Mobile source emissions were recalculated by using EPA procedures based on updated MOBILE 3.9 estimates;

Refueling emissions were removed from the 1985 NAPAP stationary source inventory and recalculated according to methodologies supplied by EPA;

Mobile source running losses were calculated by using EPA procedures based on RVP, ambient temperatures, and exhaust emissions, and were added to the mobile source inventory;

VOC emissions were assigned to photochemical reactivity classes; and

NO_x emissions were speciated into NO and NO_2.

To create the various emissions inventories needed to simulate the desired scenarios, sets of temporal, spatial, and pollutant species allocation factors were developed and applied to the annual data contained in the 1985 NAPAP Emissions Inventory. Development of the allocation factors and the approach taken to apply them to the annual data are discussed next.

Temporal Allocation

Temporal allocation of the 1985 NAPAP emissions data was accomplished by applying seasonal, daily, and hourly fractions to the annual emissions totals to generate hourly emissions values for a typical summer weekday.

For point sources, the 1985 NAPAP emissions data included process-specific temporal allocation factors; accordingly, the temporal allocation of point sources was based on the factors supplied in the inventory.

For most area source categories, temporal allocation factors were derived from monthly, daily, and hourly cycle information used in a recent application of the UAM in the South Coast Air Basin region of California (Hogo, Mahoney, and Yocke, 1988). Table 4-1 lists the area source categories used in the 1985 NAPAP data base. For those source categories for which no information was available, engineering judgment was employed to determine temporal allocation factors. For many source categories, summer weekday emissions are considerably different from values calculated by using a simple annual average emission rate. Mobile source emissions were adjusted to reflect the episodic temperature conditions by applying adjustment factors provided by the EPA. Table 4-2 shows the monthly and weekly variations assigned to area source categories. On-road motor vehicles were assigned a double-peaked diurnal profile. Annual emissions were adjusted to episode levels by using VMT as an activity indicator. For the reader's convenience, all tables are located at the end of this section.

Projection of Stationary Point and Area Source Emissions to 1995

As part of the UAM modeling effort, it was necessary to project a 1995 emissions inventory from the 1985 NAPAP Emissions Inventory. Projections were made for both point and area sources for VOC, NO_x, and CO emissions. Figure 4-1 presents a flowchart of the projection process; the procedures used are described below.

The growth factors used to project the 1985 NAPAP emissions to 1995 were determined from emission projections developed for the EPA by E. H. Pechan & Associates (1988), who used BEA estimates of economic growth. The emission projections were grouped by "cost pod," assuming only current EPA emissions control policy. The "cost pods" represent emission controls of similar cost and were used as part of an economic analysis carried out for the EPA and unrelated to this study. For this study, it was necessary to pair the "cost pods" with the NAPAP source categories for both area and point sources. The resulting pairings are shown in Table 4-3. The growth factors used in this study were determined by calculating the ratio of the projected 1995 emissions and the base-year 1985 emissions by "cost pod." The resulting growth factors by pollutant for CO and VOC are shown in Table 4-4. Based on the projection factors from E. H. Pechan and Associates, NO_x emissions from 1995 were assumed to be the same as for 1985. In the data base provided to Systems Applications, there were some "cost pods" for which no base-year or projected emissions estimates were provided. For those cases, after consulting with Pechan and Associates, we made the assumption that the emissions would remain the same between 1985 and 1995. In addition, there were numerous point source categories in the 1985 NAPAP Emissions Inventory which had not been assigned to "cost pods" by E. H. Pechan & Associates. We assigned these point source categories to "cost pods" based upon similarity of source categories, using engineering judgment.

The 1995 inventory was generated by computer. We used programs developed by Systems Applications that read each source description in the inventory and matched its Source Classification Code (SCC) or NAPAP area source category with a corresponding "cost pod." The corresponding growth factors for the "cost pod" were then retrieved and used to scale the 1985 NAPAP emissions to project the 1995 emissions.

Projection of 1985 Mobile Source Emissions to Base Year 1995

Mobile source emissions were projected to 1995 levels using methodology and data provided by EPA's Office of Mobile Sources (OMS). First, the total on-road motor vehicle VOC emissions were divided into exhaust and evaporative emissions according to the separation factors contained in Table 4-5, which are based on MOBILE3 simulations and use the same inputs as those used in the development of the 1985 NAPAP inventory. These factors are given by vehicle type (light-duty gasoline vehicle, light-duty gasoline truck, heavy-duty gasoline vehicle, and heavy-duty diesel

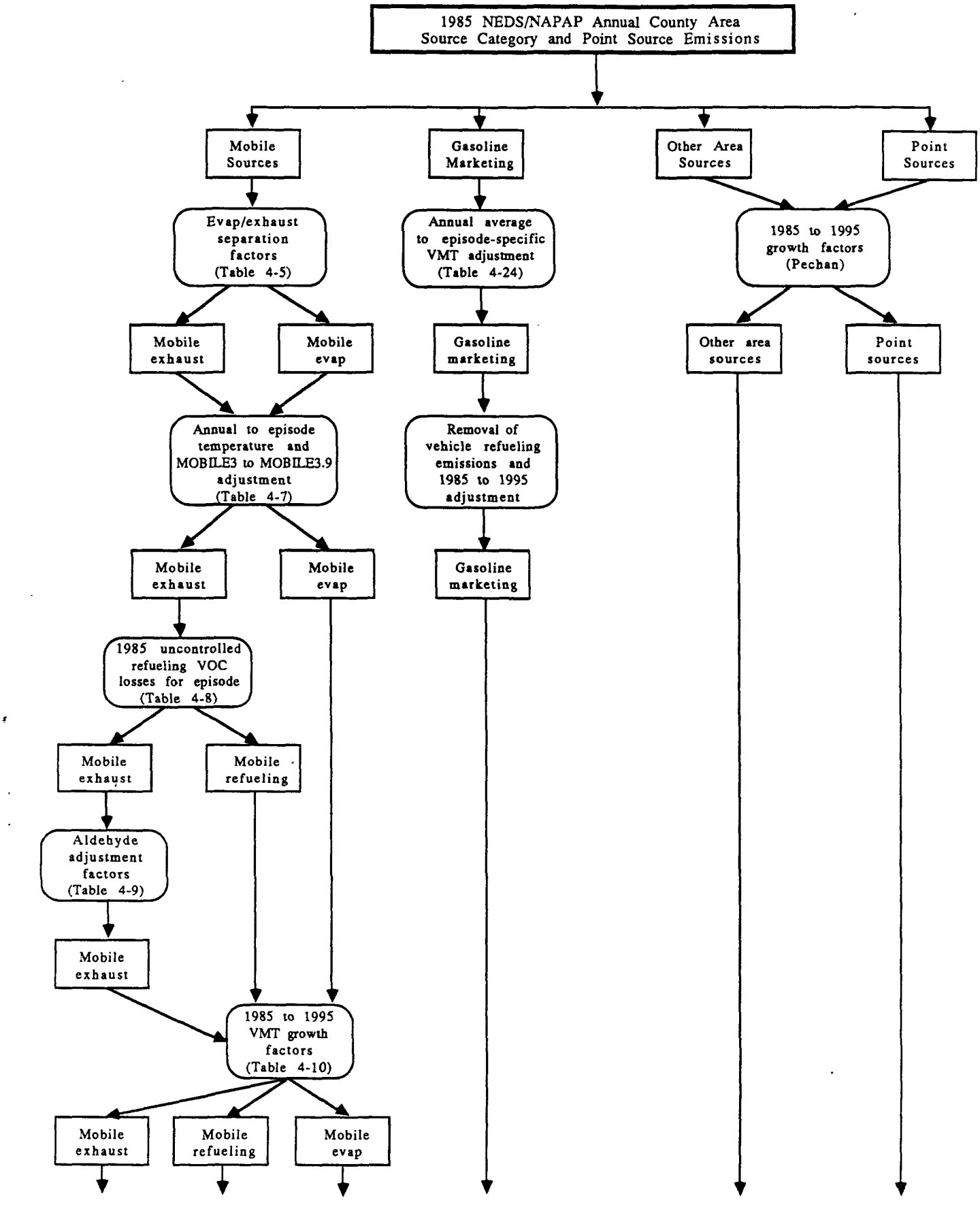

FIGURE 4-1. Flowchart for projection of 1985 emissions to 1995.

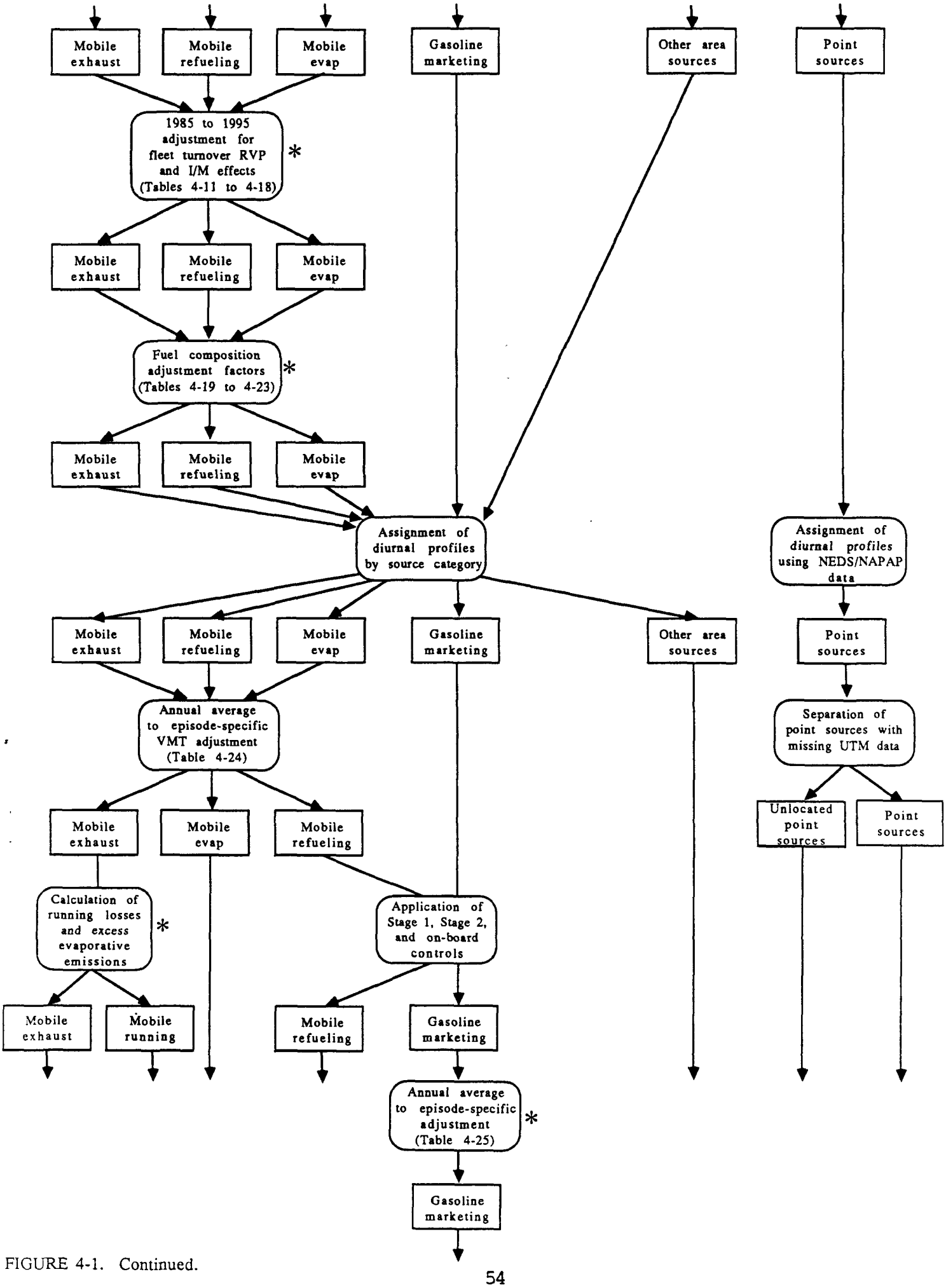

FIGURE 4-1. Continued.

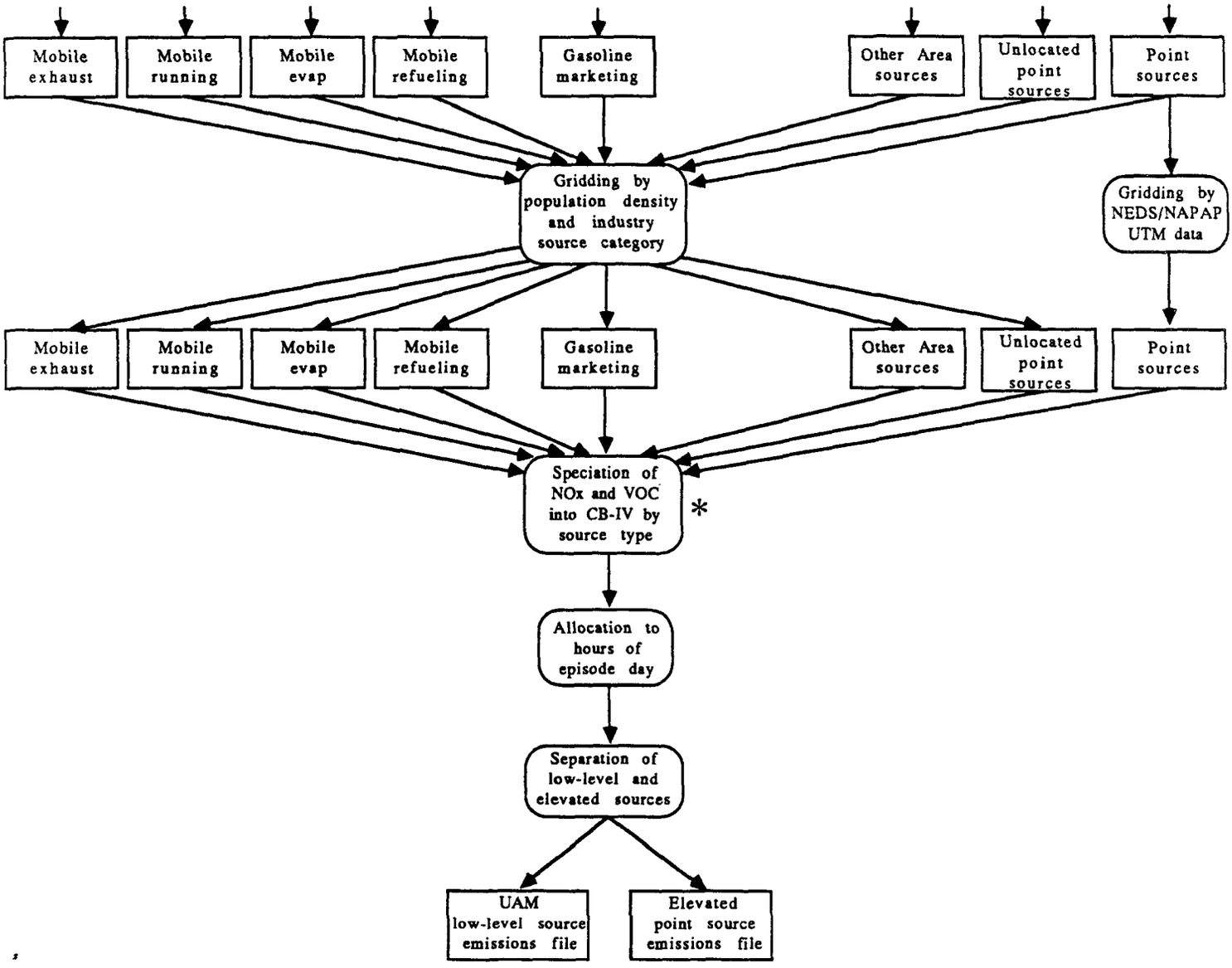

* Denotes . scenario-specific adjustments.

FIGURE 4-1. Concluded.

vehicle) and road class (urban, rural, and limited access) for counties with and without I/M programs in the two study regions. A list of I/M applicability by county appears in Table 4-6.

The resulting exhaust (VOC, CO, and NO_x) emissions and evaporative VOC emissions were adjusted from the MOBILE3-based values used in the 1985 NAPAP inventory to values consistent with MOBILE 3.9 using the multiplicative factors contained in Table 4-7. These factors adjust for the fuel RVP of the emissions scenario (currently at 11.5 psi for New York and 10.0 psi for St. Louis), and the episodic temperature.

Uncontrolled refueling losses for 1985 were calculated by multiplying the exhaust VOC emissions by the factors given in Table 4-8. The multiplicative factors in Table 4-9 were then used to increase exhaust VOC emissions for each vehicle type to account for the presence of aldehydes that were not counted completely in the FID reading.

The resulting 1985 exhaust, evaporative, and refueling emissions were projected to 1995 levels using the methodology described below. First, the emissions by vehicle type for each county were multiplied by the appropriate factor from Table 4-10 to reflect the expected growth in VMT between 1985 and 1995. Emissions of the three pollutants (VOC, CO, and NO_x) were then scaled by scenario-specific factors that account for fleet turnover and fuel RVP effects between 1985 and 1995. The factors for each scenario appear in Tables 4-11 through 4-17.

The multiplicative factors in Tables 4-18 through 4-20, which are also scenario-specific, were used to account for the effect of oxygenate in the fuel (in the form of ethanol or ETBE) on emissions of VOC, CO, and NO_x. Note that of the scenarios modeled, only scenarios 3, 5, and 6, which specify use of ethanol blends or ETBE, require application of these factors.

The 1995 emissions were then converted from an annually averaged daily rate to an episode-specific daily rate based on the portion of annual VMT occurring on the episode day. The fractions used were derived from 1985 weekday VMT levels for the state of California. These data, presented in Table 4-21, include both urban and rural VMT and were thus considered indicative of a typical mix of road classes such as that present in the New York or St. Louis study regions.

All of the scenarios, except scenario 4, also required calculation of additional VOC emissions due to running losses and excess evaporative emissions that are not included in the 1985 NAPAP inventory. In this calculation the exhaust VOC emissions were multiplied by a scenario-specific fraction. The numerator of this fraction consists of the sum of two terms: the running loss and the excess evaporative emissions, both in grams per mile. The first term, running losses, is dependent on temperature, fuel RVP, and the average speed of travel associated with each road class. The excess evaporative emissions depend on vehicle type and fuel RVP.

Running losses and excess evaporative emissions for heavy-duty diesel vehicles were assumed to be zero. The denominator of the fraction depends on vehicle type, road class, fuel RVP, and I/M applicability; equations and tables provided by OMS were used to calculate these fractions on an hourly basis using hourly averaged episode-day temperature data for the region. The hourly fractions were multiplied by the portion of the exhaust VOC emissions inventory occurring in each hour of the episode day, which was determined by applying a double-peaked diurnal profile of on-road motor vehicle emissions.

Finally, losses from both truck unloading at service stations and spillage and vapor displacement occurring during vehicle refueling were adjusted to include the effects of Stage 1 and Stage 2 gasoline marketing controls. The 1985 gasoline marketing VOC emissions for each county were converted from an annual average to an episode-specific level using the fraction of annual VMT occurring on the episode day (Table 4-21). The gasoline marketing emissions were then scaled using factors provided by OMS to remove refueling losses and adjust for projected decreases in gasoline consumption. Gasoline marketing emissions for all counties in Missouri and New Jersey and I/M counties in New York were adjusted by a factor that included Stage 1 controls of 48 percent on unloading losses, Stage 2 controls of 74 percent on breathing and emptying losses, and an on-board coverage of 20 percent. A different factor was used for counties in Connecticut and Illinois and non-I/M counties in New York to exclude any benefit from Stage 2 controls. The resulting gasoline marketing inventory was then adjusted to scenario-specific levels using the appropriate factors from Table 4-22. The hourly vehicle refueling losses were also scaled to reflect 92 percent control of 20 percent of sales due to the 20 percent on-board coverage.

Spatial Allocation of Emissions

Point source records in the 1985 NAPAP Emissions Inventory contain locational information that allows straightforward assignment to grid cells. Area sources are scattered sources of air pollution, such as cars and home heaters, that emit small quantities of air pollutants individually but potentially significant quantities in the aggregate. Since the UAM requires a gridded emissions input, the county totals were spread out (gridded) throughout the county by grid squares. Area source emissions are typically allocated from counties to individual grid cells using spatial allocation factors, which are fractional multipliers that assign a portion of each county's emissions to a particular grid cell. Generally, since the subcounty distribution of emissions is unknown, emissions are apportioned on the basis of the known distribution of some surrogate indicator. Approximately 80 point sources in the St. Louis region had incomplete or missing locational information. These points were treated as low-level sources and their emissions were distributed as area source emissions associated with commercial or industrial activities. Development and application of the spatial allocation factors used in this study are described in this section.

Generally, area source emissions are prepared on a county-wide basis using throughput or quantity-type data from a variety of informational sources and emissions factors published by the EPA (EPA AP-42). This procedure results in a relatively high degree of certainty in county total emissions but does not assign the emissions to any sub-county regions.

The most straightforward means to apportion county emission totals to sub-county regions is to distribute them evenly over the entire county. Although this is the simplest method, smoothing of the emissions data defeats the benefits of a sophisticated grid model such as the UAM. In a more accurate allocation scheme, the emissions sources are divided into several classes that can be associated with parameters for which the distribution is known, such as population, and allocated accordingly. The more accurate of these approaches was used in this study; emissions were allocated using several different factors, depending on the source type.

The following steps are necessary to apportion county-wide area source emissions to grid cells:

Assign area source categories to classes with surrogate allocation parameters having known distributions.

Determine the fractional area of each county within the modeling domain.

Determine the fraction of the county-wide total emissions within the modeling domain.

Develop procedures to combine emissions for grid cells overlying more than one county.

Develop an emission grid.

Perform quality assurance checks to insure the accuracy of the results.

The application of these steps is described in greater detail below.

Methodology

This subsection describes the efforts undertaken to develop a gridded emission inventory suitable for use as input to the UAM. A computer program "EMGRID" was developed especially for this project.

STEP 1: Assign area source categories to classes with surrogate allocation parameters having known distributions.

Throughout this section there are references to area source category and area source type. These terms are distinct and non-interchangeable. The source category refers to the 109 different categories of emission sources that are included in the 1985 NAPAP Emissions Inventory. The source type refers to a grouping of the source categories, employing engineering judgment to determine similarities between emissions source categories. The source types used were:

Type 1: Emissions associated with population distribution

Type 2: Emissions associated with commercial or industrial activities

Type 3: Emissions associated with off-highway activities

Type 4: Emissions associated with agricultural or rural activities

Table 4-23 shows the pairing between area source category and area source type. (Note that the area source category information was retained during the gridding process for later chemical speciation.)

STEP 2: Determine the fractional area of each county within the modeling domain.

As noted earlier, the starting point for the gridding process was the 1985 NAPAP area source emissions data, which contains county-wide emissions for 109 area source categories. The computer program EMGRID was developed with the capability to overlay county boundaries onto any grid system desired. Using EMGRID, we determined the fractional area of each county within the modeling domain.

STEP 3: Determine the fraction of the county-wide total emissions within the modeling domain.

Emissions of Types 1, 2, and 4 (discussed earlier) were apportioned according to the percentage of population within each county in the modeling domain. Emissions of Type 3 were apportioned according to the amount of each county's area that lay within the modeling domain. For example, a county might have 40 percent of its area but 60 percent of its population within the modeling domain. In this case, 60 percent of the Types 1, 2, and 4 emissions for that county and 40 percent of the Type 3 emissions would be retained for gridding purposes.

STEP 4: Develop procedures to combine emissions for grid cells overlying more than one county.

Since most county boundaries are irregular in shape, it is likely that many grid squares in a modeling region will overly more than one county. Particular care was taken in apportioning emissions in these cases. An apportioning scheme was developed to account for the difference between the four source types described

above; the scheme was applied when a grid cell overlay more than one county. The apportioning of these grid cells was performed as follows: (1) for area source categories of Types 1, 2, or 4 emissions, each county's population-weighted emissions and emissions related to commerce, industry, or agriculture were summed over the grid cell; and (2) for area source categories of Type 3 emissions, each county's emissions were apportioned on the basis of the fraction of the cell that fell within the county and were summed accordingly.

STEP 5: Develop an emissions grid using the scheme designed in the steps above.

Type 1: Emissions associated with population distribution

Type 1 emissions are those most commonly associated with population density, that is, emissions that result from everyday activities, such as residential fuel combustion or motor vehicle usage. These emissions were apportioned on the basis of population density. For example, if a grid cell contained 5 percent of the county's population, it was allocated 5 percent of the Type 1 emissions. For those counties that were only partially contained within the modeling region, the fraction used was based on the portion of the county's population in the modeling domain. If 60 percent of the population of Sample County (total population 100,000) was in the modeling domain, the modeling domain population would be 60,000; if one of the grid cells contained 6,000 Sample County residents, that grid cell would be allocated 10 percent of the modeling portion of the county's total Type 1 emissions (or 6 percent of its actual total Type 1 emissions).

Type 2: Emissions associated with commercial or industrial activities

Allocation of Type 2 emissions is not as straightforward as the allocation of Type 1 emissions. Type 2 emissions are associated with commercial and industrial activities, which usually occur near or in heavily urbanized cities or population centers, but are not directly proportional to population density. Areas of very high population density have little space remaining for industrial activities, and areas of moderate to low population density may include some combination of industrial and commercial activities. Additionally, factories that are large enough to be located away from cities are usually large enough to be treated as point sources, and they are handled separately. The approach taken in this study was to identify a subset of grid cells as "commercial/industrial" and to divide each county's Type 2 emissions evenly among this subset of cells. As a result, if Sample County had 10 commercial/industrial grid cells, each cell would be allocated one-tenth of the total Type 2 emissions for the county.

The method for designating commercial/industrial grid cells was based upon the fraction of the county population within the grid cell. After careful examination of the

urban areas of the region being modeled, it was determined that if an individual grid cell contained more than 2 percent of a county's population, it would be designated as a commercial/industrial grid cell.

Type 3: Emissions associated with off-highway activities

Type 3 emissions include two distinctly different source categories of emissions called "Off Highway" emissions. For rural counties, these emissions would result primarily from agricultural equipment. For urban and suburban counties, they would result from construction and industrial equipment. These emissions were apportioned equally over all grid cells in the county. For grid cells containing more than one county, area-weighted emissions were computed and summed over the grid cell.

Type 4: Emissions associated with agricultural or rural activities

Several of the area source categories in the 1985 NAPAP Emissions Inventory are identified as rural or agricultural, as Table 4-23 shows. Examples of this type of emission source include vehicles traveling on rural roads and activities related to agriculture and forestry. Emissions from these source categories were apportioned according to inverse population density. That is, more Type 4 emissions were allocated to grid cells with the lowest populations.

STEP 6: Perform quality assurance checks to insure the accuracy of the results.

The spatial allocation scheme described above is quite complex. In order to insure that a proper accounting of all emissions was performed, the EMGRID program was developed with the capability to perform internal quality assurance checks. One of these checks involves printing summary emissions tables prior to and following gridding. The gridding program automatically highlights any discrepancies.

Chemical Speciation

The UAM requires further refinement of VOC and NO_x emissions beyond spatial and temporal distribution. NO_x emissions must be divided into NO and NO_2, and VOC emissions must be categorized according to photochemical reactivity class. Literature concerning specific NO/NO_2 splits for different source types is sparse. However, on the basis of similar UAM applications in other urban areas and on EPA guidance, an overall NO/NO_2 split of 90 percent/10 percent was used for all source types in this study. VOC emissions were divided into photochemical reactivity class by source type for area sources and by Source Classification Code (SCC) for point sources, using the recently released "Air Emissions Species Manual--Vol. 1: VOC Species Profiles" (EPA 1988).

Special treatment was required for the speciation of evaporative and exhaust VOC emissions from mobile and refueling sources for the different modeling scenarios. There are very little data on the exact composition of these emissions. One method of obtaining a higher RVP fuel is to add butane to the fuel mixture. Some previous modeling studies have assumed that the excess evaporative emissions from the higher RVP fuels are all butane (Whitten, 1988); however, this approach may underestimate the reactivity of the extra evaporative emissions produced by a higher RVP fuel. The use of the speciation tables from the EPA speciation manual (EPA, 1988) for evaporative emissions would incorrectly characterize the composition of the different RVP fuels. In this study the speciation of evaporative emissions into their basic hydrocarbon classes followed the EPA/OMS guidelines as listed in Table 4-24. The further speciation of these basic hydrocarbon classes into the CB-IV mechanism species followed the procedures given in the speciation manual with some allowances, as described below. The speciation of exhaust emissions for the gasoline fuel scenarios followed the speciation manual, but some interpretation of the data was necessary and, where appropriate, ethanol or ETBE emissions were accounted for.

The speciation manual (EPA, 1988) lumps propane and propylene into one class (propane) because the two species cannot be distinguished in the measurement process. The combined propylene + propane species is assumed to be 100 percent propane for evaporative emissions and 100 percent propylene for exhaust emissions. Similarly, to speciate the aromatic species, the manual combines benzene and cyclohexane for both the evaporative and exhaust emissions. It was assumed that the combined benzene + cyclohexane species emissions were split 50/50 between benzene and cyclohexane for both evaporative and exhaust emissions.

Additional allowances in the VOC speciation were made for the ethanol blend-scenarios. In addition to the changes in evaporative emissions given in Table 4-24, the ethanol blends will also slightly modify the composition of the exhaust emissions given in the speciation manual. For the 10 percent ethanol blend scenarios, it was assumed that 2 percent by weight of the exhaust VOC emissions were ethanol, with the remainder of the exhaust emissions speciated according to the manual with the allowances discussed above. In addition, information provided by EPA/OMS indicated that exhaust emissions for the ethanol blend had three times the acetaldehyde emissions of gasoline. For the ETBE scenario it was assumed that 2 percent by weight of the exhaust VOC emissions was ETBE, and the remainder of the exhaust VOC emissions was speciated according to the procedures given in the speciation manual. Table 4-25 shows the resultant speciation of the exhaust VOC emissions into the CB-IV species used by the UAM. On the basis of its molecular structure, the ETBE was speciated into 4 PARs and 1 ALD2.

RESULTS

Figures 4-2 and 4-3 show the spatial distribution of 1995 NO_x and VOC emissions from elevated point sources for the New York study region; Figures 4-4 and 4-5 present the same information for St. Louis. Emissions from elevated sources did not change with scenario, with the exceptions of SIP Scenarios A and B. NO_x and VOC emissions from all low-level sources, including on-road motor vehicles, for New York scenario 1 are shown in Figures 4-6 and 4-7. Figures 4-8 and 4-9 show low-level source NO_x and VOC emissions for St. Louis scenario 1. Table 4-26 contains total and on-road motor-vehicle-related emissions of VOC, CO, and NO_x by scenario for both the New York and St. Louis study regions.

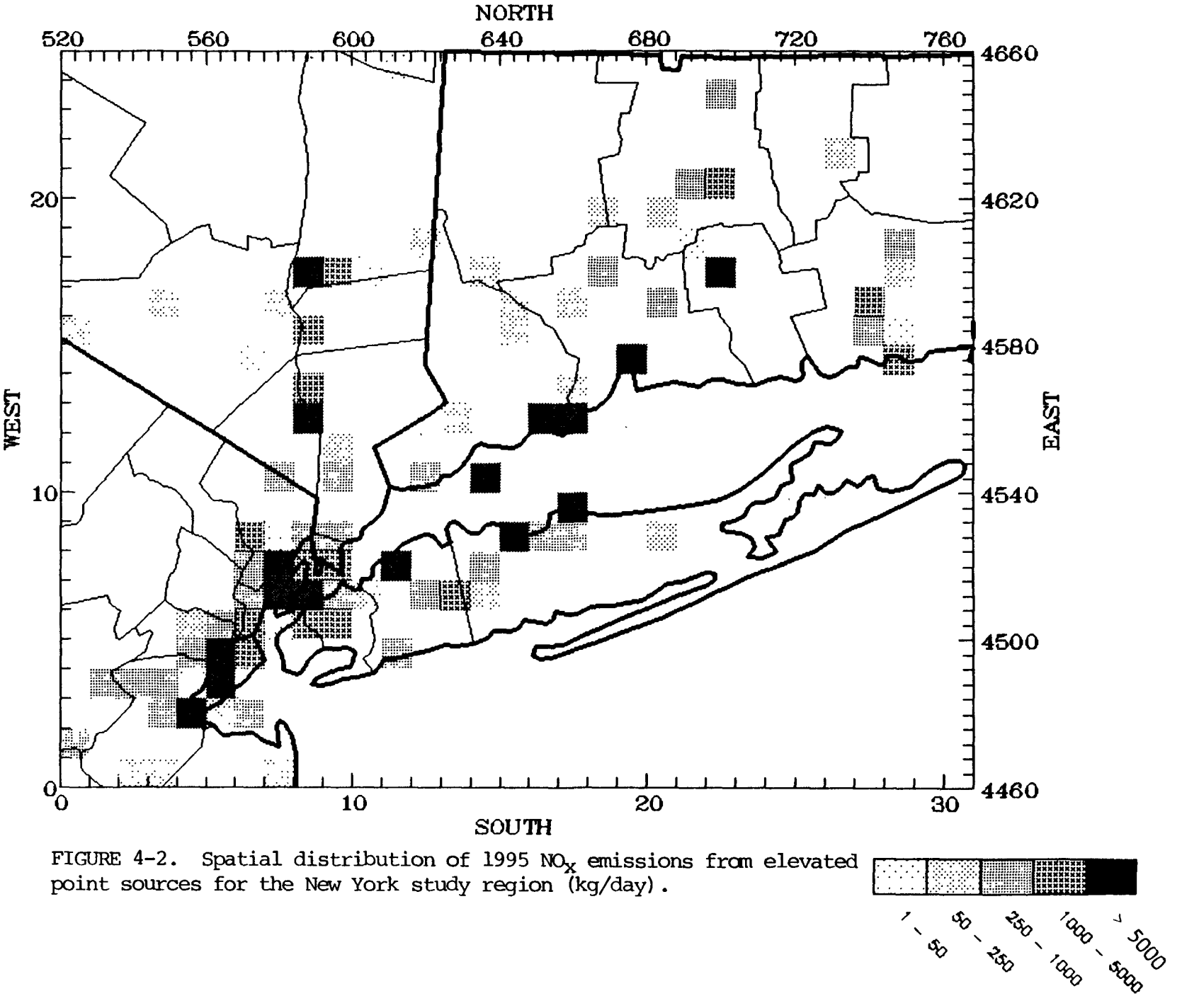

FIGURE 4-2. Spatial distribution of 1995 NO_x emissions from elevated point sources for the New York study region (kg/day).

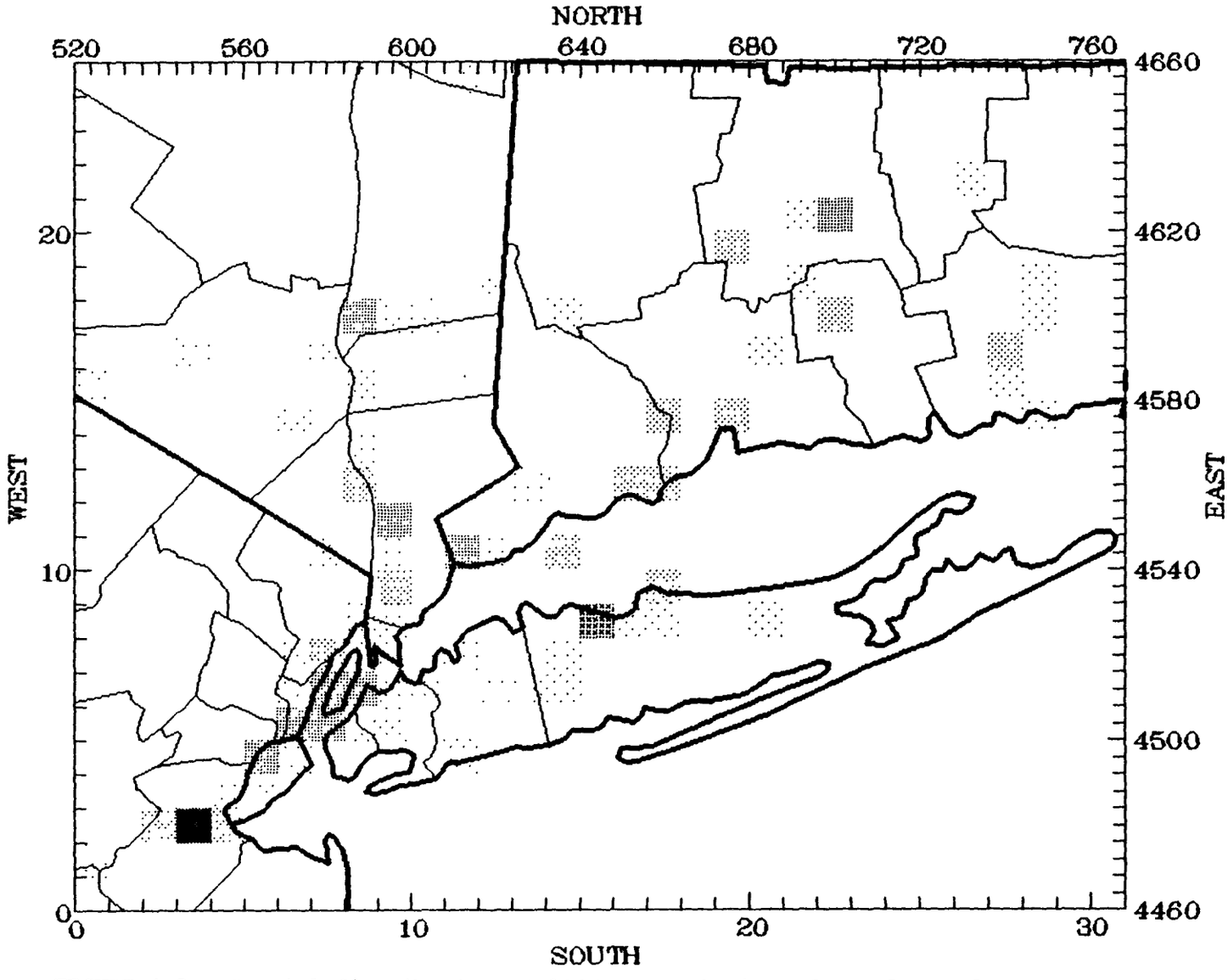

FIGURE 4-3. Spatial distribution of 1995 VOC emissions from elevated point sources for the New York study region (kg/day).

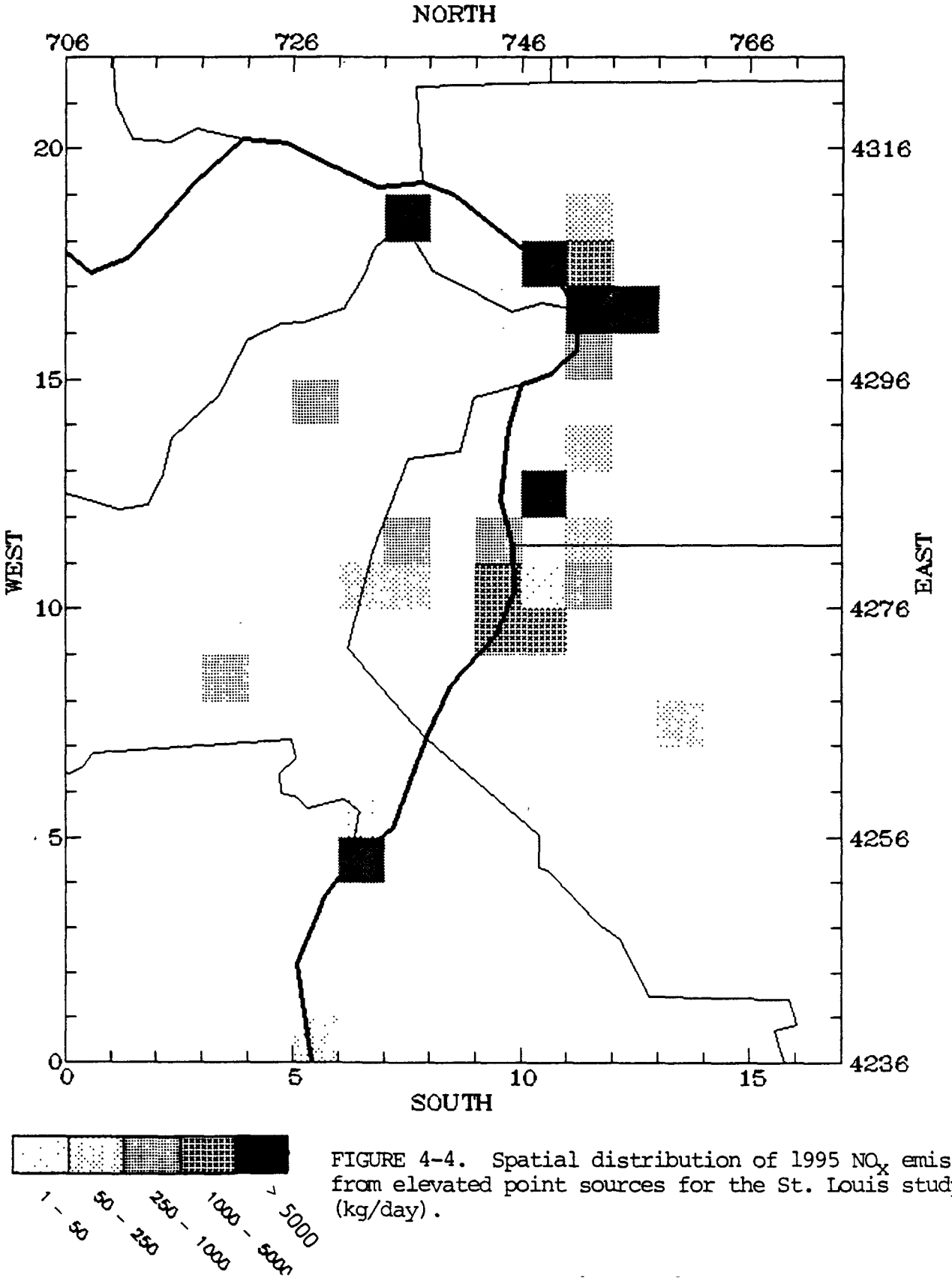

FIGURE 4-4. Spatial distribution of 1995 NO_x emissions from elevated point sources for the St. Louis study region (kg/day).

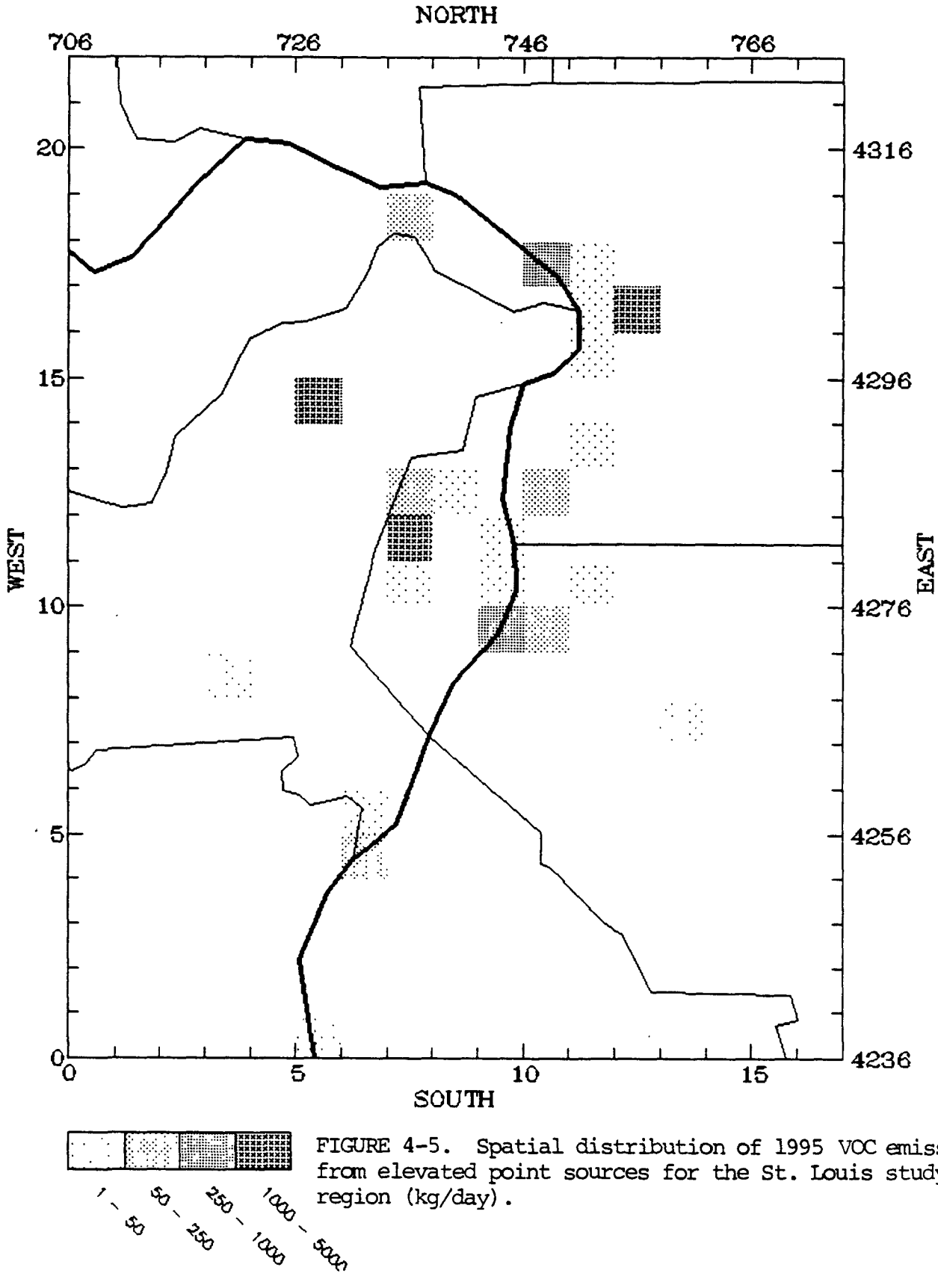

FIGURE 4-5. Spatial distribution of 1995 VOC emissions from elevated point sources for the St. Louis study region (kg/day).

emissions from all low-level sources, including on-road motor vehicles, for New York scenario 1 are shown in Figures 4-6 and 4-7. Figures 4-8 and 4-9 show low-level source NO_x and VOC emissions for St. Louis scenario 1. Table 4-29 contains total and on-road motor-vehicle-related emissions of VOC, CO, and NO_x by scenario for both the New York and St. Louis study regions.

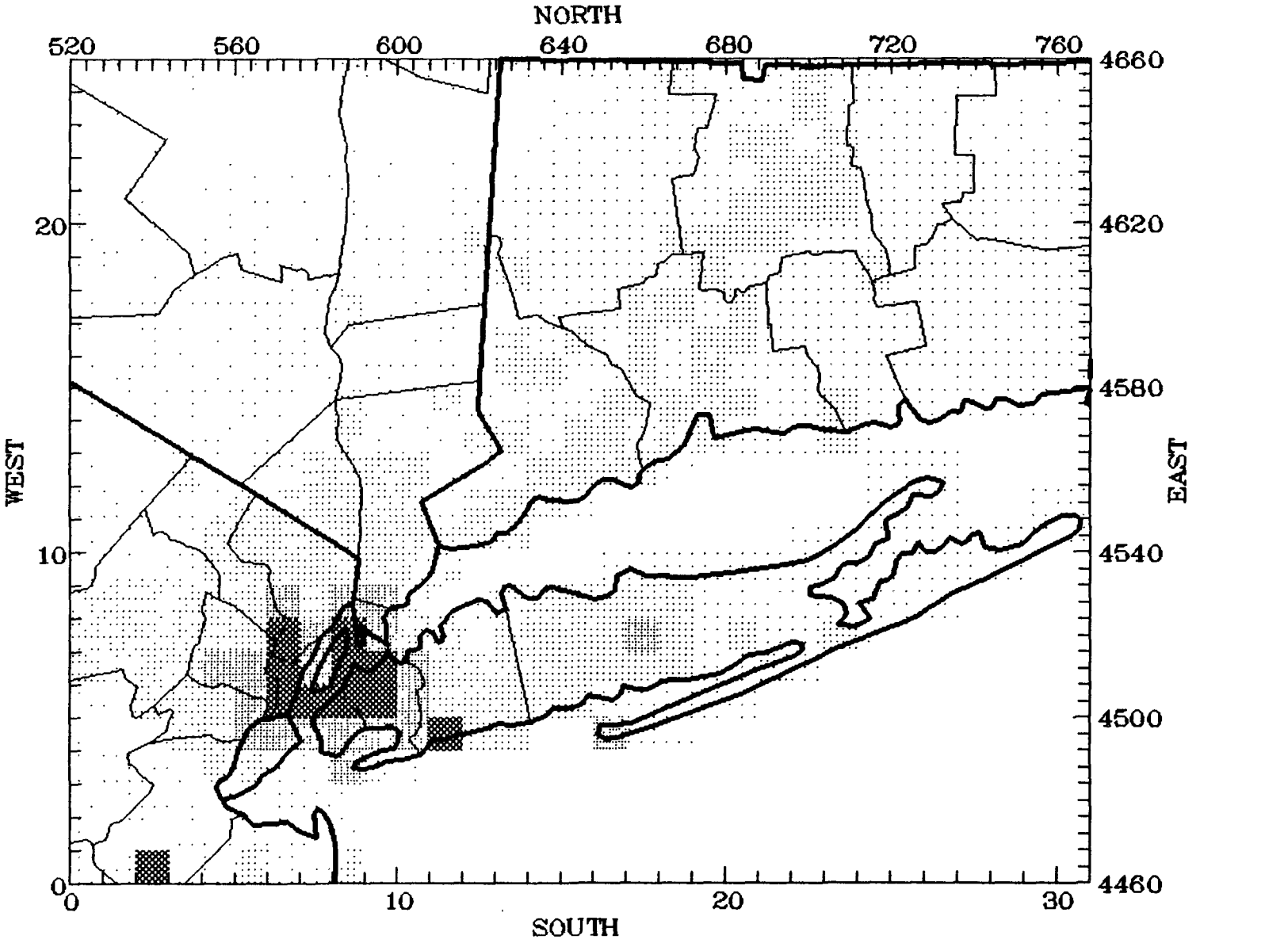

FIGURE 4-6. Spatial distribution of total 1995 NO_x emissions from low level sources for Scenario 1 for the New York study region (kg/day).

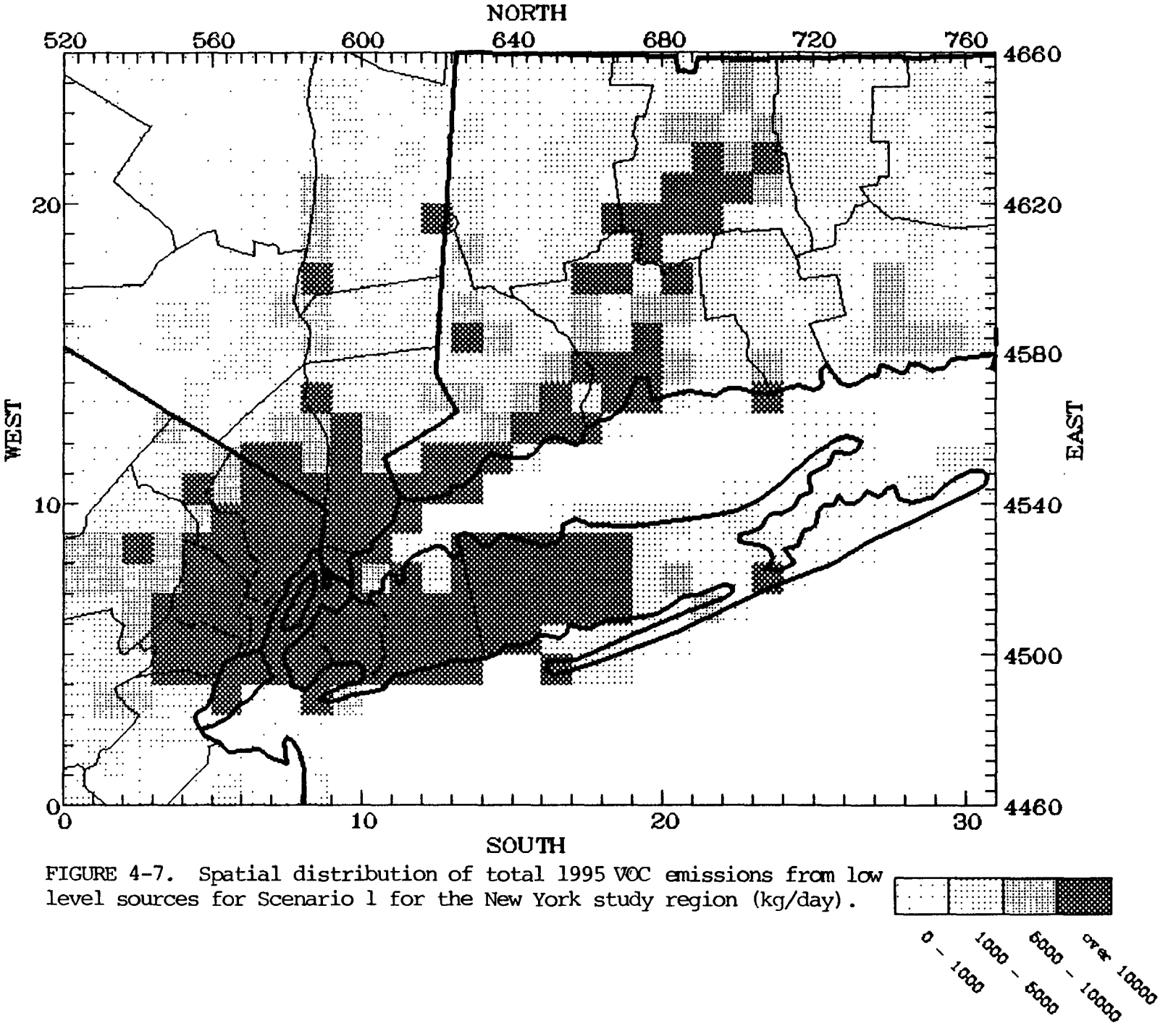

FIGURE 4-7. Spatial distribution of total 1995 VOC emissions from low level sources for Scenario 1 for the New York study region (kg/day).

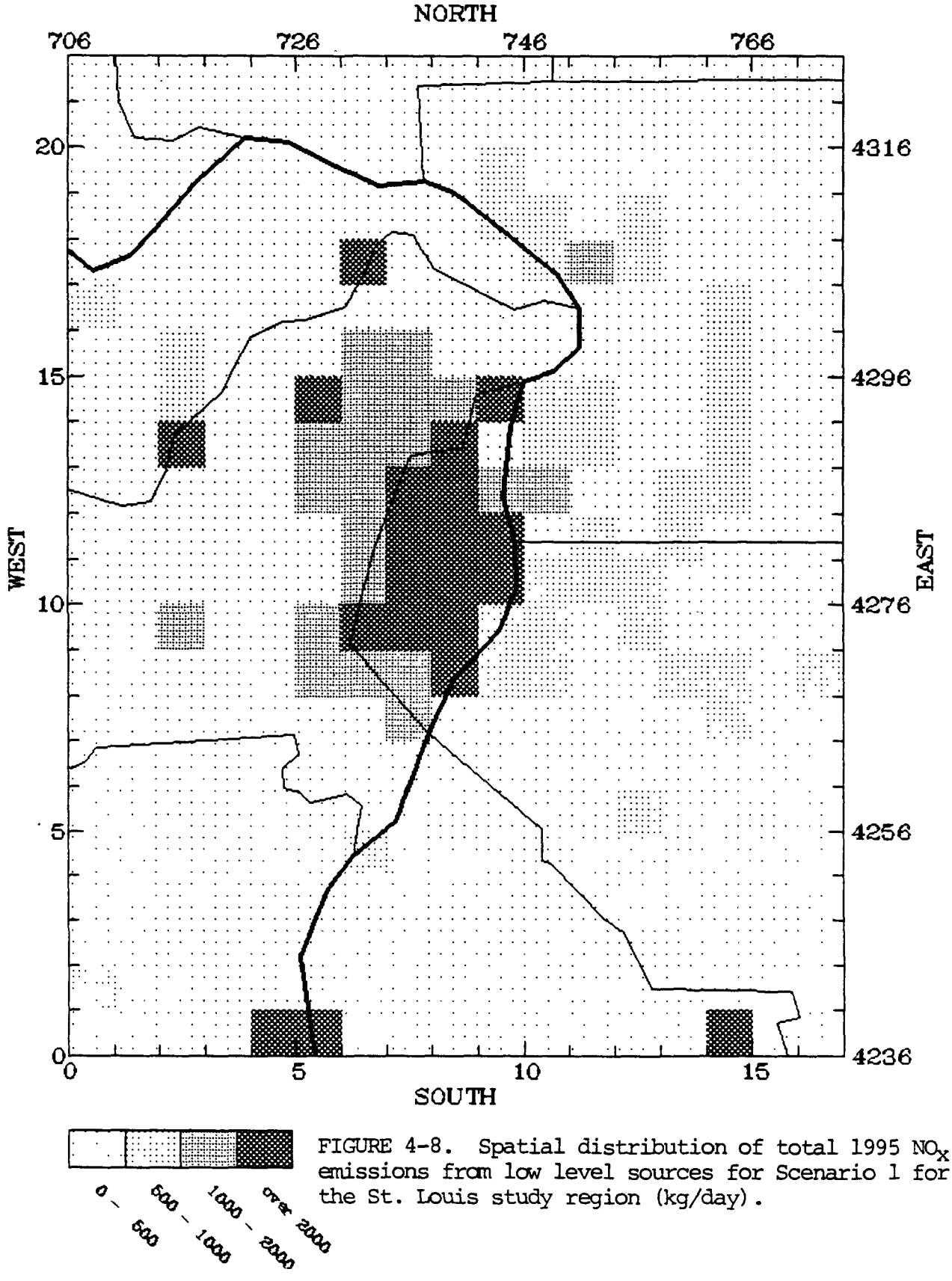

FIGURE 4-8. Spatial distribution of total 1995 NO_x emissions from low level sources for Scenario 1 for the St. Louis study region (kg/day).

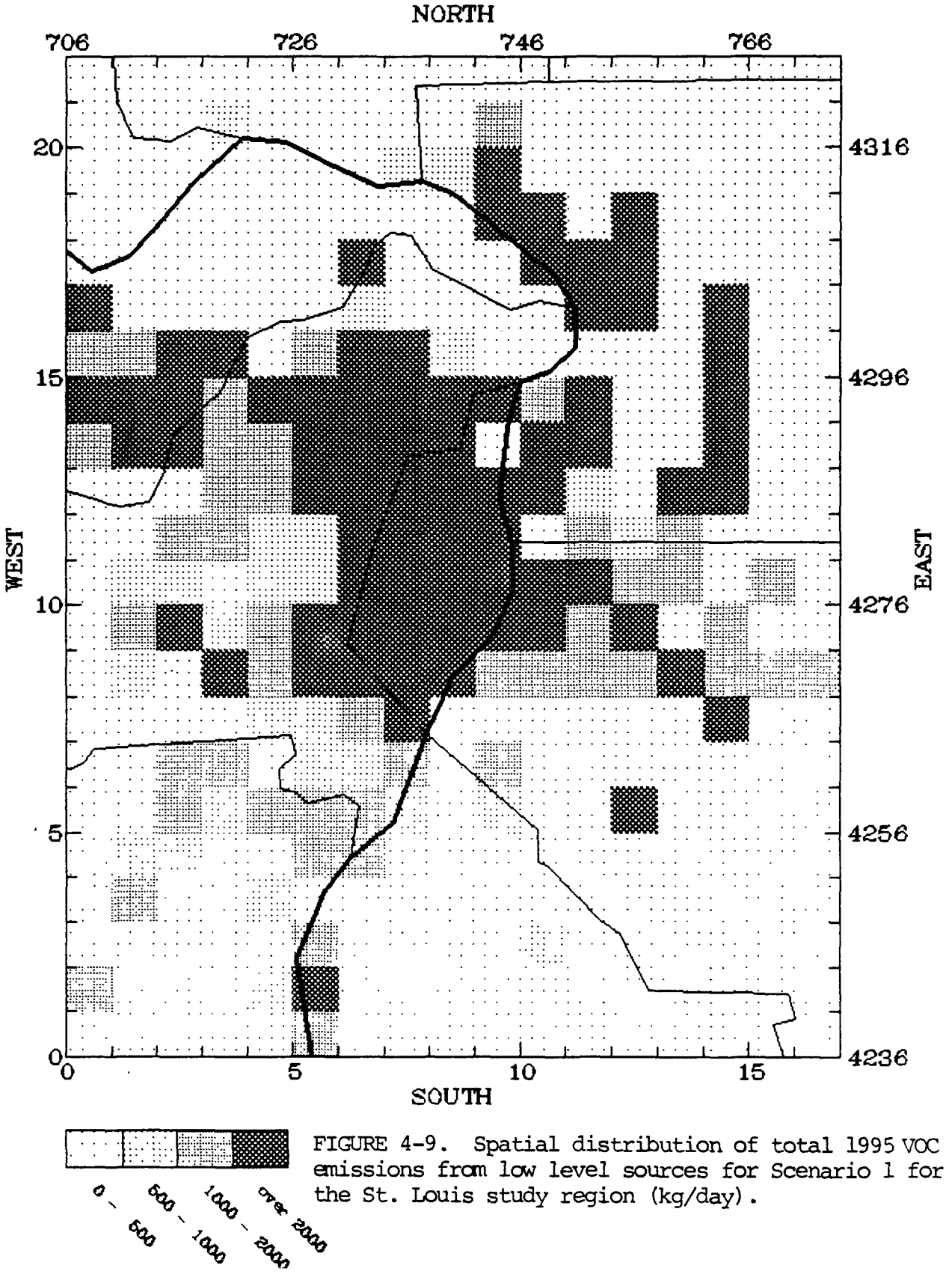

FIGURE 4-9. Spatial distribution of total 1995 VOC emissions from low level sources for Scenario 1 for the St. Louis study region (kg/day).

88151

TABLE 4-1. NAPAP area source category codes.

Source Category Code	Category Description
1	Residential Fuel - Anthracite Coal
2	Residential Fuel - Bituminous Coal
3	Residential Fuel - Distillate Oil
4	Residential Fuel - Residual Oil
5	Residential Fuel - Natural Gas
6	Residential Fuel - Wood
7	Commercial/Institutional Fuel - Anthracite Coal
8	Commercial/Institutional Fuel - Bituminous Coal
9	Commercial/Institutional Fuel - Distillate Oil
10	Commercial/Institutional Fuel - Residual Oil
11	Commercial/Institutional Fuel - Natural Gas
12	Commercial/Institutional Fuel - Wood
13	Industrial Fuel - Anthracite Coal
14	Industrial Fuel - Bituminous Coal
15	Industrial Fuel - Coke
16	Industrial Fuel - Distillate Oil
17	Industrial Fuel - Residual Oil
18	Industrial Fuel - Natural Gas
19	Industrial Fuel - Wood
20	Industrial Fuel - Process Gas
21	On-Site Incineration - Residential
22	On-Site Incineration - Industrial
23	On-site Incineration - Commercial/Institutional
24	Open Burning - Residential
25	Open Burning - Industrial
26	Open Burning - Commercial/Institutional
27	Light Duty Gasoline Vehicles - Limited Access Roads
28	Light Duty Gasoline Vehicles - Rural Roads
29	Light Duty Gasoline Vehicles - Suburban Roads
30	Light Duty Gasoline Vehicles - Urban Roads
31	Medium Duty Gasoline Vehicles - Limited Access Roads
32	Medium Duty Gasoline Vehicles - Rural Roads
33	Medium Duty Gasoline Vehicles - Suburban Roads
34	Medium Duty Gasoline Vehicles - Urban Roads
35	Heavy Duty Gasoline Vehicles - Limited Access Roads
36	Heavy Duty Gasoline Vehicles - Rural Roads
37	Heavy Duty Gasoline Vehicles - Suburban Roads
38	Heavy Duty Gasoline Vehicles - Urban Roads
39	Off Highway Gasoline Vehicles
40	Heavy Duty Diesel Vehicles - Limited Access Roads

continued

TABLE 4-1. (continued) NAPAP area source category codes.

Source Category Code	Category Description
41	Heavy Duty Diesel Vehicles - Rural Roads
42	Heavy Duty Diesel Vehicles - Suburban Roads
43	Heavy Duty Diesel Vehicles - Urban Roads
44	Off Highway Diesel Vehicles
45	Railroad Locomotives
46	Aircraft LTOs - Military
47	Aircraft LTOs - Civil
48	Aircraft LTOs - Commercial
49	Vessels - Coal
50	Vessels - Diesel Oil
51	Vessels - Residual Oil
52	Vessels - Gasoline
53†	Solvents Purchased (not used)
54	Gasoline Marketed
55	Unpaved Road Travel
56	Unpaved Airstrip LTOs
57	(Not used)
58	(Not used)
59	(Not used)
60	Forest Wild Fires
61	Managed Burning - Prescribed
62	Agricultural Field Burning
63	Frost control - Orchard Heaters
64	Structural Fires
65	(Not used)
66	Ammonia Emissions - Light duty Gasoline Vehicles
67	Ammonia Emissions - Heavy Duty Gasoline Vehicles
68	Ammonia Emissions - Heavy Duty Diesel Vehicles
69§	Livestock Waste Management - Turkeys
70§	Livestock Waste Management - Sheep
71§	Livestock Waste Management - Beef Cattle
72§	Livestock Waste Management - Dairy Cattle
73§	Livestock Waste Management - Swine
74§	Livestock Waste Management - Broilers
75§	Livestock Waste Management - Other Chickens
76†	Anhydrous Ammonia Fertilizer Application
77	Beef Cattle Feed Lots
78	Degreasing
79	Dry Cleaning
80	Graphic Arts/Printing

continued

TABLE 4-1. (concluded) NAPAP area source category codes.

Source Category Code	Category Description
81	Rubber and Plastics Manufacture
82	Architectural Coatings
83	Auto body Repair
84	Motor Vehicle Manufacture
85	Paper Coating
86	Fabricated Metals
87	Machinery Manufacture
88	Furniture Manufacture
89	Flatwood Products
90	Other Transportation Equipment Manufacture
91	Electrical Equipment Manufacture
92	Shipbuilding and Repairing
93	Miscellaneous Industrial Manufacture
94**	(Not used)
95**	Miscellaneous Solvent Use
96	(Not used)
97	(Not used)
98	(Not used)
99	(Not used)
100	Publicly Owned Treatment Works (POTWs)
101	Cutback Asphalt Paving Operation
102	Fugitives from Synthetic Organic Chemical Manufacture
103	Bulk Terminal and Bulk Plants
104	Fugitives from Petroleum Refinery Operations
105	Process Emissions from Bakeries
106	Process Emissions from Pharmaceutical Manufacture
107	Process Emissions from Synthetic Fibers Manufacture
108	Crude Oil and Natural Gas Production Fields
109	Hazardous Waste Treatment, Storage, and Disposal Facilities (TSDFs)

† SCC 53 is disaggregated into process categories 78 to 95.
§ These categories formerly referred to as "manure field application."
** Formerly "miscellaneous industrial solvent use" (94) and "miscellaneous nonindustrial solvent use" (95); now combined into one category.

TABLE 4-2. NAPAP area source codes and monthly and weekly allocation parameters.

NAPAP Area Source Code	Days Per Week	Monthly Fractions											
		Jan	Feb	Mar	Apr	May	June	July	Aug	Sep	Oct	Nov	Dec
1	7	0.178	0.178	0.143	0.107	0.036	0.036	0.036	0.036	0.036	0.036	0.036	0.143
2	7	0.178	0.178	0.143	0.107	0.036	0.036	0.036	0.036	0.036	0.036	0.036	0.143
3	7	0.178	0.178	0.143	0.107	0.036	0.036	0.036	0.036	0.036	0.036	0.036	0.143
4	7	0.178	0.178	0.143	0.107	0.036	0.036	0.036	0.036	0.036	0.036	0.036	0.143
5	7	0.200	0.200	0.100	0.100	0.000	0.000	0.000	0.000	0.000	0.100	0.100	0.200
6	7	0.178	0.178	0.143	0.107	0.036	0.036	0.036	0.036	0.036	0.036	0.036	0.143
7	7	0.178	0.178	0.143	0.107	0.036	0.036	0.036	0.036	0.036	0.036	0.036	0.143
8	7	0.178	0.178	0.143	0.107	0.036	0.036	0.036	0.036	0.036	0.036	0.036	0.143
9	7	0.178	0.178	0.143	0.107	0.036	0.036	0.036	0.036	0.036	0.036	0.036	0.143
10	7	0.178	0.178	0.143	0.107	0.036	0.036	0.036	0.036	0.036	0.036	0.036	0.143
11	2	0.178	0.178	0.143	0.107	0.036	0.036	0.036	0.036	0.036	0.036	0.036	0.143
12	7	0.178	0.178	0.143	0.107	0.036	0.036	0.036	0.036	0.036	0.036	0.036	0.143
13	7	0.178	0.178	0.143	0.107	0.036	0.036	0.036	0.036	0.036	0.036	0.036	0.143
14	7	0.178	0.178	0.143	0.107	0.036	0.036	0.036	0.036	0.036	0.036	0.036	0.143
15	7	0.178	0.178	0.143	0.107	0.036	0.036	0.036	0.036	0.036	0.036	0.036	0.143
16	7	0.178	0.178	0.143	0.107	0.036	0.036	0.036	0.036	0.036	0.036	0.036	0.143
17	7	0.178	0.178	0.143	0.107	0.036	0.036	0.036	0.036	0.036	0.036	0.036	0.143
18	2	0.178	0.178	0.143	0.107	0.036	0.036	0.036	0.036	0.036	0.036	0.036	0.143
19	7	0.178	0.178	0.143	0.107	0.036	0.036	0.036	0.036	0.036	0.036	0.036	0.143
20	2	0.178	0.178	0.143	0.107	0.036	0.036	0.036	0.036	0.036	0.036	0.036	0.143
21	7	0.039	0.065	0.065	0.039	0.039	0.130	0.130	0.104	0.104	0.130	0.104	0.052
22	7	0.039	0.065	0.065	0.039	0.039	0.130	0.130	0.104	0.104	0.130	0.104	0.052
23	7	0.039	0.065	0.065	0.039	0.039	0.130	0.130	0.104	0.104	0.130	0.104	0.052
24	7	0.039	0.065	0.065	0.039	0.039	0.130	0.130	0.104	0.104	0.130	0.104	0.052
25	7	0.039	0.065	0.065	0.039	0.039	0.130	0.130	0.104	0.104	0.130	0.104	0.052
26	7	0.039	0.065	0.065	0.039	0.039	0.130	0.130	0.104	0.104	0.130	0.104	0.052

TABLE 4-2. NAPAP area source codes and monthly and weekly allocation parameters (continued)

NAPAP Area Source Code	Days Per Week	Monthly Fractions											
		Jan	Feb	Mar	Apr	May	June	July	Aug	Sep	Oct	Nov	Dec
39	1	0.013	0.027	0.040	0.067	0.133	0.133	0.133	0.133	0.133	0.107	0.067	0.013
44	7	0.083	0.083	0.083	0.083	0.083	0.083	0.083	0.083	0.083	0.083	0.083	0.083
45	7	0.083	0.083	0.083	0.083	0.083	0.083	0.083	0.083	0.083	0.083	0.083	0.083
46	7	0.083	0.083	0.083	0.083	0.083	0.083	0.083	0.083	0.083	0.083	0.083	0.083
47	7	0.083	0.083	0.083	0.083	0.083	0.083	0.083	0.083	0.083	0.083	0.083	0.083
48	7	0.083	0.083	0.083	0.083	0.083	0.083	0.083	0.083	0.083	0.083	0.083	0.083
49	7	0.178	0.178	0.143	0.107	0.036	0.036	0.036	0.036	0.036	0.036	0.036	0.143
50	7	0.083	0.083	0.083	0.083	0.083	0.083	0.083	0.083	0.083	0.083	0.083	0.083
51	7	0.083	0.083	0.083	0.083	0.083	0.083	0.083	0.083	0.083	0.083	0.083	0.083
52	7	0.083	0.083	0.083	0.083	0.083	0.083	0.083	0.083	0.083	0.083	0.083	0.083
53	5	0.100	0.100	0.100	0.100	0.100	0.100	0.100	0.100	0.100	0.100	0.000	0.000
54	7	0.083	0.083	0.083	0.083	0.083	0.083	0.083	0.083	0.083	0.083	0.083	0.083
55	7	0.083	0.083	0.083	0.083	0.083	0.083	0.083	0.083	0.083	0.083	0.083	0.083
56	7	0.083	0.083	0.083	0.083	0.083	0.083	0.083	0.083	0.083	0.083	0.083	0.083
57	5	0.083	0.083	0.083	0.083	0.083	0.083	0.083	0.083	0.083	0.083	0.083	0.083
58	7	0.061	0.073	0.098	0.122	0.098	0.073	0.061	0.061	0.073	0.122	0.098	0.061
59	7	0.061	0.073	0.098	0.122	0.098	0.073	0.061	0.061	0.073	0.122	0.098	0.061
60	7	0.000	0.000	0.015	0.074	0.147	0.147	0.147	0.147	0.147	0.147	0.029	0.000
61	7	0.000	0.000	0.167	0.333	0.333	0.000	0.000	0.000	0.000	0.000	0.000	0.167
62	7	0.039	0.065	0.065	0.039	0.039	0.130	0.130	0.104	0.104	0.130	0.104	0.052
63	7	0.333	0.167	0.000	0.000	0.000	0.000	0.000	0.000	0.000	0.000	0.167	0.333
64	7	0.083	0.083	0.083	0.083	0.083	0.083	0.083	0.083	0.083	0.083	0.083	0.083
66	5	0.079	0.079	0.082	0.083	0.084	0.084	0.085	0.087	0.085	0.084	0.084	0.084
67	5	0.079	0.079	0.082	0.083	0.084	0.084	0.085	0.087	0.085	0.084	0.084	0.084
68	5	0.079	0.079	0.082	0.083	0.084	0.084	0.085	0.087	0.085	0.084	0.084	0.084
69	7	0.083	0.083	0.083	0.083	0.083	0.083	0.083	0.083	0.083	0.083	0.083	0.083

TABLE 4-2. NAPAP area source codes and monthly and weekly allocation parameters (continued)

NAPAP Area Source Code	Days Per Week	Monthly Fractions											
		Jan	Feb	Mar	Apr	May	June	July	Aug	Sep	Oct	Nov	Dec
70	7	0.083	0.083	0.083	0.083	0.083	0.083	0.083	0.083	0.083	0.083	0.083	0.083
71	7	0.083	0.083	0.083	0.083	0.083	0.083	0.083	0.083	0.083	0.083	0.083	0.083
72	7	0.083	0.083	0.083	0.083	0.083	0.083	0.083	0.083	0.083	0.083	0.083	0.083
73	7	0.083	0.083	0.083	0.083	0.083	0.083	0.083	0.083	0.083	0.083	0.083	0.083
74	7	0.083	0.083	0.083	0.083	0.083	0.083	0.083	0.083	0.083	0.083	0.083	0.083
75	7	0.083	0.083	0.083	0.083	0.083	0.083	0.083	0.083	0.083	0.083	0.083	0.083
76	7	0.061	0.073	0.098	0.122	0.098	0.073	0.061	0.061	0.073	0.122	0.098	0.061
77	7	0.083	0.083	0.083	0.083	0.083	0.083	0.083	0.083	0.083	0.083	0.083	0.083
78	5	0.083	0.083	0.083	0.083	0.083	0.083	0.083	0.083	0.083	0.083	0.083	0.083
79	6	0.083	0.083	0.083	0.083	0.083	0.083	0.083	0.083	0.083	0.083	0.083	0.083
80	5	0.100	0.100	0.100	0.100	0.100	0.100	0.100	0.100	0.100	0.100	0.000	0.000
81	5	0.100	0.100	0.100	0.100	0.100	0.100	0.100	0.100	0.100	0.100	0.000	0.000
82	7	0.060	0.060	0.090	0.090	0.100	0.100	0.100	0.100	0.090	0.080	0.070	0.060
83	5	0.083	0.083	0.083	0.083	0.083	0.083	0.083	0.083	0.083	0.083	0.083	0.083
84	5	0.100	0.100	0.100	0.100	0.100	0.100	0.100	0.100	0.100	0.100	0.000	0.000
85	5	0.083	0.083	0.083	0.083	0.083	0.083	0.083	0.083	0.083	0.083	0.083	0.083
86	7	0.083	0.083	0.083	0.083	0.083	0.083	0.083	0.083	0.083	0.083	0.083	0.083
87	5	0.100	0.100	0.100	0.100	0.100	0.100	0.100	0.100	0.100	0.100	0.000	0.000
88	5	0.083	0.083	0.083	0.083	0.083	0.083	0.083	0.083	0.083	0.083	0.083	0.083
89	5	0.100	0.100	0.100	0.100	0.100	0.100	0.100	0.100	0.100	0.100	0.000	0.000
90	5	0.100	0.100	0.100	0.100	0.100	0.100	0.100	0.100	0.100	0.100	0.000	0.000
91	5	0.100	0.100	0.100	0.100	0.100	0.100	0.100	0.100	0.100	0.100	0.000	0.000
92	5	0.100	0.100	0.100	0.100	0.100	0.100	0.100	0.100	0.100	0.100	0.000	0.000
93	5	0.100	0.100	0.100	0.100	0.100	0.100	0.100	0.100	0.100	0.100	0.000	0.000
95	5	0.100	0.100	0.100	0.100	0.100	0.100	0.100	0.100	0.100	0.100	0.000	0.000

TABLE 4-2. NAPAP area source codes and monthly and weekly allocation parameters (concluded).

NAPAP Area Source Code	Days Per Week	Monthly Fractions											
		Jan	Feb	Mar	Apr	May	June	July	Aug	Sep	Oct	Nov	Dec
100	7	0.083	0.083	0.083	0.083	0.083	0.083	0.083	0.083	0.083	0.083	0.083	0.083
101	7	0.032	0.043	0.064	0.085	0.106	0.106	0.106	0.106	0.106	0.106	0.085	0.053
102	7	0.083	0.083	0.083	0.083	0.083	0.083	0.083	0.083	0.083	0.083	0.083	0.083
103	7	0.083	0.083	0.083	0.083	0.083	0.083	0.083	0.083	0.083	0.083	0.083	0.083
104	7	0.083	0.083	0.083	0.083	0.083	0.083	0.083	0.083	0.083	0.083	0.083	0.083
105	7	0.083	0.083	0.083	0.083	0.083	0.083	0.083	0.083	0.083	0.083	0.083	0.083
106	5	0.100	0.100	0.100	0.100	0.100	0.100	0.100	0.100	0.100	0.100	0.000	0.000
107	5	0.100	0.100	0.100	0.100	0.100	0.100	0.100	0.100	0.100	0.100	0.000	0.000
108	7	0.083	0.083	0.083	0.083	0.083	0.083	0.083	0.083	0.083	0.083	0.083	0.083
109	7	0.083	0.083	0.083	0.083	0.083	0.083	0.083	0.083	0.083	0.083	0.083	0.083

TABLE 4-3. Relationship between cost pods, source categories, and source classification codes (SCC). (Source: E. H. Pechan & Associates, 1988).

Source Category	Pod #	SCC
0 - Combustion	0	1------
	0	2------
	0	1
	0	2
	0	3
	0	4
	0	5
	0	6
	0	7
	0	8
	0	9
	0	10
	0	11
	0	12
	0	13
	0	14
	0	15
	0	16
	0	17
	0	18
	0	19
	0	20
1 - Solvent metal cleaning	1	40100201
	1	40100202
	1	40100203
	1	40100204
	1	40100205
	1	40100206
	1	40100297
	1	40100299
	1	40100306
2 - Printing and publishing	2	40200912
	2	40201199
	2	40200920
	2	41200921
	2	40500101
	2	40500201
	2	40500211
	2	40500212
	2	40500301

88151 3

TABLE 4-3 (continued) Relationship between cost pods, source categories, and source classification codes (SCC). (Source: E. H. Pechan & Associates, 1988).

Source Category	Pod #	SCC
	2	40500303
	2	40500304
	2	40500305
	2	40500311
	2	40500312
	2	40500401
	2	40500411
	2	40500412
	2	40500501
	2	40500510
	2	40500511
	2	40500512
	2	40500513
	2	40500598
	2	40500599
	2	40500701
3 - Dry cleaning	3	40100101
	3	40100102
	3	40100103
	3	40100104
	3	40100199
4 - Fixed roof crude tanks	4	40300102
	4	40300104
	4	40300105
	4	40300107
	4	40300150
	4	40300152
	4	40300198
	4	40300199
	4	40301010
	4	40301011
	4	40301012
	4	40301013
	4	40301015
	4	40301019
	4	40301021
	4	40301097
	4	40301099

TABLE 4-3 (continued) Relationship between cost pods, source categories, and source classification codes (SCC). (Source: E. H. Pechan & Associates, 1988).

Source Category	Pod #	SCC
5 - Fixed roof gasoline tanks	5	40300101
	5	40300103
	5	40301001
	5	40301002
	5	40301003
	5	40301004
	5	40301007
	5	40301008
	5	40301009
	5	40400101
	5	40400102
	5	40400107
	5	40400108
	5	40400202
	5	40400205
6 - Floating roof crude tanks	6	40300203
	6	40300204
	6	40301109
	6	40301110
	6	40301132
	6	40301197
	6	40301198
	6	40301199
7 - Floating roof gasoline tanks	7	40300201
	7	40300202
	7	40301101
	7	40301102
	7	40301103
	7	40301104
	7	40301105
	7	40301107
	7	40301108
	7	40400110
	7	40400111
	7	40400115
	7	40400116
	7	40400117

TABLE 4-3 (continued) Relationship between cost pods, source categories, and source classification codes (SCC). (Source: E. H. Pechan & Associates, 1988).

Source Category	Pod #	SCC
	7	40400207
	7	40400210
8 - Bulk terminals-splash loading	8	40600136
9 - Bulk terminals vapor balanced	9	40600141
10 - Bulk terminals-submerged loading	10	40600126
	10	40600131
	10	103
11 - Stage I	11	40600301
	11	40600302
	11	40600306
	11	40600307
12 - Stage II	12	40600401
	12	40600402
	12	40600403
15 - Ethylene oxide manufacture	15	30117401
16 - Phenol Manufacture	16	30120201
17 - Terephthalic acid manufacture	17	30100103
	17	30103101
	17	30112099
	17	30113205
	17	30113299
18 - Acrylonitrile manufacture	18	30125405
19 - SOCMI fugitives	19	30100509
	19	30199999
	19	30113799
	19	30103499
	19	30106099
	19	30106008
	19	30116799
	19	30100902
	19	30100999
	19	30100901
	19	30180001
	19	30183001
	19	30188801
	19	102
	19	106

88151 3

TABLE 4-3 (continued) Relationship between cost pods, source categories, and source classification codes (SCC). (Source: E. H. Pechan & Associates, 1988).

Source Category	Pod #	SCC
20 - Petroleum refinery fugitives	20	30600801
	20	30600802
	20	30600803
	20	30600804
	20	30600805
	20	30600806
	20	30600807
	20	30600811
	20	30600812
	20	30600813
	20	30600814
	20	30600815
	20	30600816
	20	30600817
	20	30600818
	20	30600819
	20	30600820
	20	30600821
	20	30600822
	20	30688801
	20	30688802
	20	30688803
	20	30688804
	20	30688805
	20	104
21 - Cellulose acetate manufacture	21	30102401
	21	30102410
	21	30102415
	21	30102499
	21	30102501
	21	30102505
	21	107
22 - Styrene-butadiene rubber manufacture	22	30102601
	22	30102608
	22	30102609
	22	30102615
	22	30102699
23 - Polypropylene manufacture	23	30101802

TABLE 4-3 (continued) Relationship between cost pods, source categories, and source classification codes (SCC). (Source: E. H. Pechan & Associates, 1988).

Source Category	Pod #	SCC
24 - Polyethylene manufacture	24	30101807
	24	30101812
	24	30101817
	24	30101892
	24	30101899
25 - Ethylene manufacture	25	30119701
	25	30119705
	25	30119799
	25	30125801
	25	30125810
	25	30125815
	25	30125899
26 - Pet. ref. wastewater treatment	26	30182001
	26	30600503
	26	30600504
27 - Pet. ref. vacuum distillation	27	30600201
	27	30600301
	27	30600602
	27	30600603
28 - Vegetable oil manufacture	28	30201901
	28	30201902
	28	30201903
	28	30201911
	28	30201914
29 - Paint and varnish manufacture	29	30101401
	29	30101499
	29	30101503
	29	30101599
	29	30102001
	29	30102099
30 - Rubber tire manufacture	30	30800104
	30	30800105
	30	30800199
31 - Green tire spray	31	30800106
32 - Carbon black manufacture	32	30100504
33 - Automobile surface coating	33	40200101
	33	40201620
	33	40200110
	33	40200401
	33	40200501
	33	40200510
	33	40200601

TABLE 4-3 (continued) Relationship between cost pods, source categories, and source classification codes (SCC). (Source: E. H. Pechan & Associates, 1988).

Source Category	Pod #	SCC
	33	40200610
	33	40200901
	33	40200998
	33	40201601
	33	40201606
	33	40201631
34 - Beverage can surface coating	34	40200301
	34	40201724
	34	40201705
	34	40200310
	34	40200801
	34	40200802
	34	40200803
	34	40200810
	34	40201702
	34	40201721
	34	40201722
	34	40201723
	34	40201725
	34	40201726
	34	40201727
	34	40201728
	34	40201731
	34	40201736
	34	40201799
35 - General surface coating	35	40200410
	35	40201901
	35	40202106
	35	40202108
	35	40202109
	35	40202199
36 - Paper surface coating	36	40200701
	36	40200706
	36	40200710
	36	40201301
	36	40201399
37 - Miscellaneous surface coating	37	40200902
	37	40200903
	37	40200904

TABLE 4-3 (continued) Relationship between cost pods, source categories, and source classification codes (SCC). (Source: E. H. Pechan & Associates, 1988).

Source Category	Pod #	SCC
	37	40200905
	37	40200906
	37	40200907
	37	40200909
	37	40200910
	37	40200914
	37	40200915
	37	40200917
	37	40200918
	37	40200919
	37	40200922
	37	40200923
	37	40200924
	37	40200925
	37	40201101
	37	40201103
	37	40201406
	37	40201801
	37	40201806
	37	40201899
	37	40202001
	37	40202201
	37	40202501
	37	40202531
	37	40202599
	37	40288801
	37	40299998
	37	40299999
40 - Paper surface coating	40	85
41 - Degreasing	41	78
42 - Dry cleaning	42	79
43 - Printing/publishing	43	80
44 - Rubber & plastics	44	81
45 - Miscellaneous	45	83
	45	84
	45	86
	45	87
	45	88
	45	89
	45	90

88151 3

TABLE 4-3 (continued) Relationship between cost pods, source categories, and source classification codes (SCC). (Source: E. H. Pechan & Associates, 1988).

Source Category	Pod #	SCC
	45	91
	45	92
	45	93
	45	94
	45	95
46 - Stage I	46	54
47 - Stage II	47	54
48 - Architectural surface coating	48	82
50 - Coke ovens - door and topside leaks	50	30300302
	50	30300314
51 - Coke oven by-product plants	51	30300315
52 - Aircraft surface coating	52	40202401
	52	40202406
	52	40202499
53 - Whiskey fermentation - aging	53	30201003
54 - Charcoal manufacturing	54	30100601
	54	30100603
55 - Vessel loading: petroleum liquids	55	40600231
	55	40600232
	55	40600233
	55	40600234
	55	40600235
	55	40600236
	55	40600237
	55	40600238
	55	40600239
	55	40600240
60 - Light duty gasoline vehicles	60	27
	60	28
	60	29
	60	30
61 - Light duty gasoline trucks	61	31
	61	32
	61	33
	61	34
62 - Heavy duty gasoline vehicles	62	35
	62	36
	62	37
	62	38

TABLE 4-3 (continued) Relationship between cost pods, source categories, and source classification codes (SCC). (Source: E. H. Pechan & Associates, 1988).

Source Category	Pod #	SCC
63 - Heavy duty diesel vehicles	63	40
	63	41
	63	42
	63	43
64 - Off highway vehicles	64	39
	64	44
	64	55
65 - Railroads	65	45
66 - Burning and fires	66	24
	66	25
	66	26
	66	60
	66	61
	66	62
	66	64
67 - Area source incineration	67	21
	67	50100101
	67	22
	67	23
68 - Aircraft and marine vessels	68	46
	68	47
	68	48
	68	49
	68	50
	68	51
	68	52
	68	56
70 - TSDFs	70	109
71 - Bakeries	71	105
72 - Cutback Asphalt	72	101
73 - POTWs	73	100
90 - Other	90	63
	90	30510199
	90	30501402
	90	30502001
	90	66
	90	67
	90	68
	90	69
	90	70

TABLE 4-3 (concluded) Relationship between cost pods, source categories, and source classification codes (SCC). (Source: E. H. Pechan & Associates, 1988).

Source Category	Pod #	SCC
	90	71
	90	72
	90	73
	90	74
	90	75
	90	76
	90	77
	90	108

88151 3

TABLE 4-4a. Carbon monoxide emissions for New York CMSA assuming continuation of current EPA policy. (Source: E. H. Pechan & Associates, 1988).

Pod No.	1985 NEDS Emissions	1995 Projected Base Emissions	1995/1985 Ratio
0	15002	15002	1.000
12	704	704	1.000
15	2235	2235	1.000
16	1031	1031	1.000
60	1002244	583115	0.582
61	160258	122453	0.764
62	172701	52813	0.306
63	26047	18216	0.699
80	128048	139016	1.086
90	391321	424843	1.086

TABLE 4-4a. (concluded) Carbon monoxide emissions for St. Louis CMSA assuming continuation of current EPA policy. (Source: E. H. Pechan & Associates, 1988).

Pod No.	1985 NEDS Emissions	1995 Projected Base Emissions	1995/1985 Ratio
0	19204	19204	1.000
11	18992	18992	1.000
12	3864	3864	1.000
15	1050	1050	1.000
17	4069	4069	1.000
23	246	246	1.000
60	208366	121229	0.582
61	65017	49680	0.764
62	29925	9152	0.306
63	6261	4378	0.699
80	30062	32637	1.086
90	81123	88072	1.086

TABLE 4-4b. VOC emissions for New York CMSA assuming continuation of current EPA policy. (Source: E. H. Pechan & Associates, 1988).

Pod No.	1985 NEDS Emissions	1995 Projected Base Emissions	1995/1985 Ratio
0	4147	5659	1.365
1	52	42	0.808
2	2109	449	0.213
4	193	150	0.777
5	247	288	1.166
6	29	14	0.483
7	1477	2516	1.703
19	252	299	1.187
21	12	13	1.083
23	77	78	1.013
24	142	144	1.014
25	32	35	1.094
29	71	76	1.070
33	1765	262	0.148
34	2057	1855	0.902
35	1017	1864	1.833
36	12	1	0.083
37	3417	1464	0.428
40	3173	3950	1.245
41	41217	53263	1.292
42	27451	32776	1.194
43	15892	18977	1.194
44	11920	5255	0.441
45	91382	118894	1.301
46	1556	1383	0.889
47	33314	44418	1.333
48	43703	56859	1.301
49	92824	120768	1.301
60	227311	141082	0.621
61	36193	28240	0.780
62	17305	7094	0.410
63	9492	6360	0.670
64	25774	36508	1.416
65	7443	10276	1.381
66	16836	16836	1.000
67	8231	10656	1.295
68	9996	14724	1.473
70	105446	136596	1.295
71	4198	5552	1.323
72	14403	0	0.000
73	1906	2469	1.295
90	23460	23756	1.013

TABLE 4-4b. (concluded) VOC emissions for St. Louis CMSA assuming continuation of current EPA policy. (Source: E. H. Pechan & Associates, 1988).

Pod No.	1985 NEDS Emissions	1995 Projected Base Emissions	1995/1985 Ratio
0	1131	1441	1.274
1	501	310	0.619
2	4322	2329	0.539
4	480	10	0.021
5	1491	71	0.048
6	2081	246	0.118
7	2957	322	0.109
19	184	256	1.391
21	95	95	1.000
23	80	90	1.125
24	909	132	0.145
25	769	679	0.883
29	3099	11	0.004
33	2	3	1.500
34	8530	1401	0.164
35	2250	1600	0.711
36	83	22	0.265
37	334	244	0.731
40	423	546	1.291
41	5746	7412	1.290
42	3853	4508	1.170
43	2231	2610	1.170
44	1673	722	0.432
45	12826	16546	1.290
46	226	273	1.208
47	7256	8779	1.210
48	6134	7913	1.290
49	13029	16808	1.290
55	1742	211	0.121
60	38862	23617	0.608
61	13121	9887	0.754
62	3086	1265	0.410
63	2274	1524	0.670
64	5348	6846	1.280
65	2603	3332	1.280
66	2596	2596	1.000
67	2890	3728	1.290
68	2882	3689	1.280
70	14392	18566	1.290
71	512	737	1.439
72	1966	0	0.000
73	260	366	1.408
90	10148	5199	0.512

TABLE 4-5. Exhaust and evaporative emission separation factors for 1985 NAPAP (tons of VOC).

		Road Class		
		Urban	Rural	Limited Access
St Louis (Counties with I/M)				
LDV	Exh.	0.682	0.504	0.460
	Evap.	0.318	0.496	0.540
LDT	Exh.	0.700	0.523	0.477
	Evap.	0.300	0.477	0.523
HDGV	Exh.	0.432	0.223	0.187
	Evap.	0.568	0.777	0.813
HDDV	Exh.	1.000	1.000	1.000
	Evap.	0.000	0.000	0.000
St. Louis (Counties without I/M)				
LDV	Exh.	0.707	0.533	0.489
	Evap.	0.293	0.467	0.511
LDT	Exh.	0.722	0.548	0.503
	Evap.	0.278	0.452	0.497
HDGV	Exh.	0.432	0.223	0.187
	Evap.	0.568	0.777	0.813
HDDV	Exh.	1.000	1.000	1.000
	Evap.	0.000	0.000	0.000
New York (Counties with I/M)				
LDV	Exh.	0.66	0.479	0.436
	Evap.	0.340	0.521	0.564
LDT	Exh.	0.677	0.495	0.450
	Evap.	0.323	0.505	0.550
HDGV	Exh.	0.435	0.226	0.189
	Evap.	0.565	0.774	0.811
HDDV	Exh.	1.000	1.000	1.000
	Evap.	0.000	0.000	0.000
New York (Counties without I/M)				
LDV	Exh.	0.712	0.54	0.679
	Evap.	0.288	0.460	0.321
LDT	Exh.	0.727	0.565	0.554
	Evap.	0.273	0.435	0.446
HDGV	Exh.	0.435	0.794	0.226
	Evap.	0.565	0.206	0.774
HDDV	Exh.	1.000	1.000	1.000
	Evap.	0.000	0.000	0.000

88151 7

TABLE 4-6. I/M applicability by county.

I/M	No I/M
New York region:	
All CT counties	Columbia, NY
All NJ counties	Dutchess, NY
Bronx, NY	Orange, NY
Kings, NY	Putram, NY
Nassau, NY	Sullivan, NY
New York, NY	Ulster, NY
Queens, NY	
Richmond, NY	
Rockland, NY	
Suffolk, NY	
Westchester, NY	
St. Louis region:	
Madison, Il	Calhoun, IL
St. Clair, IL	Greene, IL
Jefferson, MO	Jersey, IL
St. Charles, MO	Macoupin, IL
St. Louis, MO	Monroe, IL
	Randolph, IL
	Lincoln, MO

TABLE 4-7. Multiplicative factors for adjusting 1985 NAPAP annual emissions to 1985 episode day conditions and for converting from MOBILE3 to MOBILE3.9 (RVP equal to ASTM limit).

		Road Class		
		Urban	Rural	Limited Access
St Louis (10.0 RVP) (Counties with I/M)				
LDV	Exh. VOC	0.861	0.862	0.866
	Evap. VOC	1.230	1.230	1.230
	CO	0.844	0.887	0.910
	NOx	0.771	0.780	0.785
LDT	Exh. VOC	0.873	0.874	0.876
	Evap. VOC	1.050	1.050	1.050
	CO	0.938	0.941	0.948
	NOx	0.800	0.727	0.805
HDGV	Exh. VOC	0.986	0.991	0.989
	Evap. VOC	0.950	0.950	0.950
	CO	1.150	1.150	1.150
	NOx	0.858	0.858	0.858
HDDV	Exh. VOC	1.00	1.00	1.00
	Evap. VOC	NA	NA	NA
	CO	1.00	1.00	1.00
	NOx	1.00	1.00	1.00
St. Louis (10.0 RVP) (Counties without I/M)				
LDV	Exh. VOC	0.865	0.861	0.862
	Evap. VOC	1.230	1.230	1.230
	CO	0.886	0.891	0.912
	NOx	0.767	0.784	0.782
LDT	Exh. VOC	0.893	0.891	0.888
	Evap. VOC	1.050	1.050	1.050
	CO	0.958	0.956	0.959
	NOx	0.798	0.807	0.806
HDGV	Exh. VOC	0.986	0.991	0.989
	Evap. VOC	0.950	0.950	0.950
	CO	1.150	1.150	1.150
	NOx	0.858	0.858	0.858
HDDV	Exh. VOC	1.00	1.00	1.00
	Evap. VOC	NA	NA	NA
	CO	1.00	1.00	1.00
	NOx	1.00	1.00	1.00

88151 7

TABLE 4-7. (Continued). Multiplicative factors for adjusting 1985 NAPAP annual emissions to 1985 episode day conditions and for converting from MOBILE3 to MOBILE3.9 (RVP equal to ASTM limit).

		Road Class		
		Urban	Rural	Limited Access
New York (11.5 RVP) (Counties with I/M)				
LDV	Exh. VOC	0.855	0.848	0.852
	Evap. VOC	1.480	1.480	1.480
	CO	0.869	0.874	0.902
	NOx	0.736	0.748	0.748
LDT	Exh. VOC	0.886	0.880	0.880
	Evap. VOC	1.210	1.210	1.210
	CO	0.971	0.969	0.973
	NOx	0.767	0.777	0.776
HDGV	Exh. VOC	0.992	0.995	1.000
	Evap. VOC	1.020	1.020	1.020
	CO	1.190	1.190	1.190
	NOx	0.835	0.835	0.834
HDDV	Exh. VOC	1.00	1.00	1.00
	Evap. VOC	NA	NA	NA
	CO	1.00	1.00	1.00
	NOx	1.00	1.00	1.00
New York (11.5 RVP) (Counties without I/M)				
LDV	Exh. VOC	0.862	0.858	0.857
	Evap. VOC	1.480	1.480	1.480
	CO	0.900	0.904	0.927
	NOx	0.733	0.749	0.749
LDT	Exh. VOC	0.889	0.885	0.886
	Evap. VOC	1.210	1.210	1.210
	CO	0.979	0.976	0.978
	NOx	0.767	0.775	0.774
HDGV	Exh. VOC	0.995	0.966	1.000
	Evap. VOC	1.020	1.020	1.070
	CO	1.190	1.190	1.190
	NOx	0.835	0.834	0.834
HDDV	Exh. VOC	1.00	1.00	1.00
	Evap. VOC	NA	NA	NA
	CO	1.00	1.00	1.00
	NOx	1.00	1.00	1.00

88151 7

TABLE 4-8. Factors to multiply by exhaust VOC tons (after adjustment using Table 2) to obtain 1985 uncontrolled refueling VOC tons for episode day conditions.

	Road Class		
	Urban	Rural	Limited Access
St Louis (10.0 RVP (Counties with I/M)			
LDV	0.138	0.29	0.345
LDT	0.096	0.206	0.245
HDGV	0.106	0.280	0.351
HDDV	0.000	0.000	0.000
St. Louis (10.0 RVP) (Counties without I/M)			
LDV	0.122	0.259	0.308
LDT	0.078	0.168	0.202
HDGV	0.106	0.280	0.351
HDDV	0.000	0.000	0.000
New York (11.5) (Counties with I/M)			
LDV	0.180	0.382	0.453
LDT	0.113	0.244	0.293
HDGV	0.120	0.315	0.393
HDDV	0.000	0.000	0.000
New York (11.5 RVP) (Counties without I/M)			
LDV	0.140	0.296	0.354
LDT	0.089	0.192	0.195
HDGV	0.120	0.315	0.393
HDDV	0.000	0.000	0.000

88151 7

TABLE 4-9. Factors to increase 1985 exhaust VOC to account for unmeasured aldehydes.

	All Road Classes 1985
LDV	1.0116
LDT	1.0116
HDGV	1.0116
HDDV	1.0420

TABLE 4-10. Growth factors for motor vehicle emissions.

	All Road Classes	
	Annual	1995:1985
LDV	1.9%	1.207
LDT	2.1%	1.231
HDGV	0.1%	1.010
HDDV	2.9%	1.331

88151 7

TABLE 4-11. 1995:1985 emission factor ratios for fleet turnover and RVP effects for episode day conditions and inventory scenarios 1 and 7.

City: St. Louis — Gasohol RVP: NA
Gasoline RVP: 10.0 — Gasohol Market Share: 0%

		Road Class		
		Urban	Rural	Limited Access
(Counties with I/M)				
LDV	Exh. VOC	0.367	0.360	0.333
	Evap. VOC	0.493	0.493	0.493
	Refuel VOC	0.759	0.759	0.759
	CO	0.339	0.319	0.255
	NOx	0.583	0.473	0.456
LDT	Exh. VOC	0.387	0.364	0.337
	Evap. VOC	0.470	0.470	0.470
	Refuel VOC	0.811	0.811	0.811
	CO	0.330	0.301	0.249
	NOx	0.596	0.520	0.520
HDGV	Exh. VOC	0.456	0.454	0.454
	Evap. VOC	0.337	0.337	0.337
	Refuel VOC	0.852	0.852	0.852
	CO	0.243	0.243	0.243
	NOx	0.853	0.855	0.854
HDDV	Exh. VOC	0.630	0.630	0.628
	Evap. VOC	NA	NA	NA
	Refuel VOC	NA	NA	NA
	CO	0.819	0.817	0.818
	NOx	0.613	0.613	0.613
(Counties without I/M)				
LDV	Exh. VOC	0.487	0.482	0.447
	Evap. VOC	0.493	0.493	0.493
	Refuel VOC	0.759	0.759	0.759
	CO	0.477	0.450	0.362
	NOx	0.631	0.508	0.490
LDT	Exh. VOC	0.555	0.523	0.486
	Evap. VOC	0.470	0.470	0.470
	Refuel VOC	0.811	0.811	0.811
	CO	0.518	0.477	0.398
	NOx	0.651	0.563	0.563
HDGV	Exh. VOC	0.456	0.454	0.454
	Evap. VOC	0.337	0.337	0.337
	Refuel VOC	0.852	0.852	0.852
	CO	0.243	0.243	0.243
	NOx	0.853	0.855	0.854
HDDV	Exh. VOC	0.630	0.630	0.628
	Evap. VOC	NA	NA	NA
	Refuel VOC	NA	NA	NA
	CO	0.819	0.817	0.818
	NOx	0.613	0.613	0.613

TABLE 4-12. 1995:1985 emission factor ratios for fleet turnover and RVP effects for episode day conditions and inventory scenario 2.

City: St. Louis
Gasoline RVP: 7.8
Gasohol RVP: NA
Gasohol Market Share: 0%

		Road Class		
		Urban	Rural	Limited Access
(Counties with I/M)				
LDV	Exh. VOC	0.338	0.330	0.298
	Evap. VOC	0.236	0.236	0.236
	Refuel VOC	0.586	0.586	0.586
	CO	0.283	0.265	0.213
	NOx	0.583	0.473	0.456
LDT	Exh. VOC	0.365	0.344	0.319
	Evap. VOC	0.274	0.274	0.274
	Refuel VOC	0.649	0.649	0.649
	CO	0.293	0.266	0.221
	NOx	0.596	0.520	0.520
HDGV	Exh. VOC	0.441	0.440	0.443
	Evap. VOC	0.209	0.209	0.209
	Refuel VOC	0.672	0.672	0.672
	CO	0.233	0.233	0.233
	NOx	0.853	0.855	0.854
HDDV	Exh. VOC	0.630	0.630	0.628
	Evap. VOC	NA	NA	NA
	Refuel VOC	NA	NA	NA
	CO	0.819	0.817	0.818
	NOx	0.613	0.613	0.613
(Counties without I/M)				
LDV	Exh. VOC	0.445	0.438	0.404
	Evap. VOC	0.236	0.236	0.236
	Refuel VOC	0.586	0.586	0.586
	CO	0.399	0.376	0.303
	NOx	0.631	0.508	0.490
LDT	Exh. VOC	0.523	0.491	0.449
	Evap. VOC	0.274	0.274	0.274
	Refuel VOC	0.649	0.649	0.649
	CO	0.461	0.424	0.355
	NOx	0.651	0.563	0.563
HDGV	Exh. VOC	0.441	0.440	0.443
	Evap. VOC	0.209	0.209	0.209
	Refuel VOC	0.672	0.672	0.672
	CO	0.233	0.233	0.233
	NOx	0.853	0.855	0.854
HDDV	Exh. VOC	0.630	0.630	0.628
	Evap. VOC	NA	NA	NA
	Refuel VOC	NA	NA	NA
	CO	0.819	0.817	0.818
	NOx	0.613	0.613	0.613

TABLE 4-13. 1995:1985 emission factor ratios for fleet turnover and RVP effects for episode day conditions and inventory scenario 5.

City: St. Louis
Gasoline RVP: 7.8
Gasohol RVP: 8.8
Gasohol Market Share: 50%

		Road Class		
		Urban	Rural	Limited Access
(Counties with I/M)				
LDV	Exh. VOC	0.348	0.340	0.310
	Evap. VOC	0.271	0.271	0.271
	Refuel VOC	0.621	0.621	0.621
	CO	0.298	0.279	0.224
	NOx	0.583	0.473	0.456
LDT	Exh. VOC	0.370	0.349	0.325
	Evap. VOC	0.307	0.307	0.307
	Refuel VOC	0.676	0.676	0.676
	CO	0.303	0.276	0.229
	NOx	0.596	0.520	0.520
HDGV	Exh. VOC	0.444	0.445	0.443
	Evap. VOC	0.231	0.231	0.231
	Refuel VOC	0.705	0.705	0.705
	CO	0.236	0.236	0.236
	NOx	0.853	0.855	0.854
HDDV	Exh. VOC	0.630	0.630	0.628
	Evap. VOC	NA	NA	NA
	Refuel VOC	NA	NA	NA
	CO	0.819	0.817	0.818
	NOx	0.613	0.613	0.613
(Counties without I/M)				
LDV	Exh. VOC	0.458	0.455	0.415
	Evap. VOC	0.271	0.271	0.271
	Refuel VOC	0.621	0.621	0.621
	CO	0.420	0.396	0.319
	NOx	0.631	0.508	0.490
LDT	Exh. VOC	0.532	0.500	0.464
	Evap. VOC	0.307	0.307	0.307
	Refuel VOC	0.676	0.676	0.676
	CO	0.476	0.439	0.366
	NOx	0.651	0.563	0.563
HDGV	Exh. VOC	0.444	0.445	0.443
	Evap. VOC	0.231	0.231	0.231
	Refuel VOC	0.705	0.705	0.705
	CO	0.236	0.236	0.236
	NOx	0.853	0.855	0.854
HDDV	Exh. VOC	0.630	0.630	0.628
	Evap. VOC	NA	NA	NA
	Refuel VOC	NA	NA	NA
	CO	0.819	0.817	0.818
	NOx	0.613	0.613	0.613

TABLE 4-14. 1995:1985 emission factor ratios for fleet turnover and RVP effects for episode day conditions and inventory scenario 6.

City: St. Louis
Fuel Type: 100% sales of ETBE blend at 2% oxygen level
RVP: 7.8

		Road Class		
		Urban	Rural	Limited Access
(Counties with I/M)				
LDV	Exh. VOC	0.338	0.330	0.298
	Evap. VOC	0.236	0.236	0.236
	Refuel VOC	0.586	0.586	0.586
	CO	0.283	0.265	0.213
	NOx	0.583	0.473	0.456
LDT	Exh. VOC	0.365	0.344	0.319
	Evap. VOC	0.274	0.274	0.274
	Refuel VOC	0.649	0.649	0.649
	CO	0.293	0.266	0.221
	NOx	0.596	0.520	0.520
HDGV	Exh. VOC	0.441	0.440	0.443
	Evap. VOC	0.209	0.209	0.209
	Refuel VOC	0.672	0.672	0.672
	CO	0.233	0.233	0.233
	NOx	0.853	0.855	0.854
HDDV	Exh. VOC	0.630	0.630	0.628
	Evap. VOC	NA	NA	NA
	Refuel VOC	NA	NA	NA
	CO	0.819	0.817	0.818
	NOx	0.613	0.613	0.613
(Counties without I/M)				
LDV	Exh. VOC	0.445	0.438	0.404
	Evap. VOC	0.236	0.236	0.236
	Refuel VOC	0.586	0.586	0.586
	CO	0.399	0.376	0.303
	NOx	0.631	0.508	0.490
LDT	Exh. VOC	0.523	0.491	0.449
	Evap. VOC	0.274	0.274	0.274
	Refuel VOC	0.649	0.649	0.649
	CO	0.461	0.424	0.355
	NOx	0.651	0.563	0.563
HDGV	Exh. VOC	0.441	0.440	0.443
	Evap. VOC	0.209	0.209	0.209
	Refuel VOC	0.672	0.672	0.672
	CO	0.233	0.233	0.233
	NOx	0.853	0.855	0.854
HDDV	Exh. VOC	0.630	0.630	0.628
	Evap. VOC	NA	NA	NA
	Refuel VOC	NA	NA	NA
	CO	0.819	0.817	0.818
	NOx	0.613	0.613	0.613

TABLE 4-15. 1995:1985 emission factor ratios for fleet turnover and RVP effects for episode day conditions and inventory scenarios 1 and 4.

City: New York
Gasoline RVP: 11.5
Gasohol RVP: NA
Gasohol Market Share: 0%

		Road Class		
		Urban	Rural	Limited Access
(Counties with I/M)				
LDV	Exh. VOC	0.407	0.404	0.360
	Evap. VOC	0.491	0.491	0.491
	Refuel VOC	0.735	0.735	0.735
	CO	0.437	0.416	0.337
	NOx	0.568	0.459	0.444
LDT	Exh. VOC	0.414	0.392	0.367
	Evap. VOC	0.421	0.421	0.421
	Refuel VOC	0.791	0.791	0.791
	CO	0.423	0.397	0.333
	NOx	0.583	0.508	0.512
HDGV	Exh. VOC	0.456	0.455	0.455
	Evap. VOC	0.341	0.341	0.341
	Refuel VOC	0.843	0.843	0.843
	CO	0.239	0.239	0.239
	NOx	0.827	0.829	0.828
HDDV	Exh. VOC	0.630	0.630	0.628
	Evap. VOC	NA	NA	NA
	Refuel VOC	NA	NA	NA
	CO	0.819	0.817	0.818
	NOx	0.613	0.613	0.613
(Counties without I/M)				
LDV	Exh. VOC	0.486	0.478	0.438
	Evap. VOC	0.533	0.533	0.533
	Refuel VOC	0.735	0.735	0.735
	CO	0.464	0.438	0.352
	NOx	0.617	0.495	0.477
LDT	Exh. VOC	0.559	0.527	0.489
	Evap. VOC	0.486	0.486	0.486
	Refuel VOC	0.791	0.791	0.791
	CO	0.514	0.475	0.396
	NOx	0.636	0.552	0.552
HDGV	Exh. VOC	0.456	0.435	0.435
	Evap. VOC	0.341	0.341	0.341
	Refuel VOC	0.843	0.843	0.843
	CO	0.239	0.239	0.239
	NOx	0.827	0.829	0.828
HDDV	Exh. VOC	0.630	0.630	0.628
	Evap. VOC	NA	NA	NA
	Refuel VOC	NA	NA	NA
	CO	0.819	0.817	0.818
	NOx	0.613	0.613	0.613

TABLE 4-16. 1995:1985 emission factor ratios for fleet turnover and RVP effects for episode day conditions and inventory scenario 2.

City: New York
Gasoline RVP: 9.0
Gasohol RVP: NA
Gasohol Market Share: 0%

		Road Class		
		Urban	Rural	Limited Access
(Counties with I/M)				
LDV	Exh. VOC	0.370	0.371	0.333
	Evap. VOC	0.172	0.172	0.172
	Refuel VOC	0.559	0.559	0.559
	CO	0.364	0.348	0.282
	NOx	0.568	0.459	0.444
LDT	Exh. VOC	0.388	0.369	0.340
	Evap. VOC	0.194	0.194	0.194
	Refuel VOC	0.628	0.628	0.628
	CO	0.375	0.351	0.294
	NOx	0.583	0.508	0.512
HDGV	Exh. VOC	0.441	0.441	0.438
	Evap. VOC	0.198	0.198	0.198
	Refuel VOC	0.657	0.657	0.657
	CO	0.229	0.229	0.229
	NOx	0.827	0.829	0.828
HDDV	Exh. VOC	0.630	0.630	0.628
	Evap. VOC	NA	NA	NA
	Refuel VOC	NA	NA	NA
	CO	0.819	0.817	0.818
	NOx	0.613	0.613	0.613
(Counties without I/M)				
LDV	Exh. VOC	0.444	0.435	0.406
	Evap. VOC	0.201	0.201	0.201
	Refuel VOC	0.559	0.559	0.559
	CO	0.388	0.366	0.295
	NOx	0.617	0.495	0.477
LDT	Exh. VOC	0.526	0.496	0.462
	Evap. VOC	0.249	0.249	0.249
	Refuel VOC	0.628	0.628	0.628
	CO	0.459	0.423	0.354
	NOx	0.636	0.552	0.552
HDGV	Exh. VOC	0.441	0.441	0.438
	Evap. VOC	0.198	0.198	0.198
	Refuel VOC	0.657	0.657	0.657
	CO	0.229	0.229	0.229
	NOx	0.827	0.829	0.828
HDDV	Exh. VOC	0.630	0.630	0.628
	Evap. VOC	NA	NA	NA
	Refuel VOC	NA	NA	NA
	CO	0.819	0.817	0.818
	NOx	0.613	0.613	0.613

TABLE 4-17. 1995:1985 emission factor ratios for fleet turnover and RVP effects for episode day conditions and inventory scenario 3.

City: New York
Gasoline RVP: 9.0

Gasohol RVP: 10.0
Gasohol Market Share: 100%

		Road Class		
		Urban	Rural	Limited Access
(Counties with I/M)				
LDV	Exh. VOC	0.386	0.382	0.347
	Evap. VOC	0.254	0.254	0.254
	Refuel VOC	0.647	0.647	0.647
	CO	0.394	0.375	0.303
	NOx	0.568	0.459	0.444
LDT	Exh. VOC	0.398	0.381	0.354
	Evap. VOC	0.255	0.255	0.255
	Refuel VOC	0.698	0.698	0.698
	CO	0.394	0.369	0.310
	NOx	0.583	0.509	0.511
HDGV	Exh. VOC	0.448	0.446	0.444
	Evap. VOC	0.239	0.239	0.239
	Refuel VOC	0.743	0.743	0.743
	CO	0.233	0.233	0.233
	NOx	0.827	0.829	0.828
HDDV	Exh. VOC	0.630	0.630	0.628
	Evap. VOC	NA	NA	NA
	Refuel VOC	NA	NA	NA
	CO	0.819	0.817	0.818
	NOx	0.613	0.613	0.613
(Counties without I/M)				
LDV	Exh. VOC	0.453	0.443	0.406
	Evap. VOC	0.243	0.243	0.243
	Refuel VOC	0.618	0.618	0.618
	CO	0.406	0.383	0.309
	NOx	0.617	0.495	0.477
LDT	Exh. VOC	0.532	0.504	0.468
	Evap. VOC	0.285	0.285	0.285
	Refuel VOC	0.651	0.651	0.651
	CO	0.472	0.435	0.364
	NOx	0.636	0.552	0.552
HDGV	Exh. VOC	0.444	0.446	0.444
	Evap. VOC	0.219	0.219	0.219
	Refuel VOC	0.714	0.714	0.714
	CO	0.449	0.229	0.232
	NOx	0.701	0.829	0.828
HDDV	Exh. VOC	0.630	0.630	0.628
	Evap. VOC	NA	NA	NA
	Refuel VOC	NA	NA	NA
	CO	0.819	0.817	0.818
	NOx	0.613	0.613	0.613

TABLE 4-18. Adjustment factors to account for fuel composition effects (oxygen and distillation, but not RVP) for St. Louis scenario 5.

City: St. Louis
Scenarios: 50% gasohol sales (scenario 5)

		Road Class		
		Urban	Rural	Limited Access
(Counties with I/M)				
LDV	Exh. VOC	0.969	0.967	0.967
	Evap. VOC	1.033	1.033	1.033
	CO	0.883	0.889	0.882
	NOx	1.038	1.037	1.037
LDT	Exh. VOC	0.948	0.949	0.949
	Evap. VOC	1.052	1.052	1.052
	CO	0.860	0.861	0.862
	NOx	1.029	1.029	1.029
HDGV	Exh. VOC	0.946	0.946	0.946
	Evap. VOC	1.076	1.076	1.076
	CO	0.858	0.858	0.858
	NOx	1.020	1.020	1.020
HDDV	Exh. VOC	1.000	1.000	1.000
	Evap. VOC	NA	NA	NA
	CO	1.000	1.000	1.000
	NOx	1.000	1.000	1.000
(Counties without I/M)				
LDV	Exh. VOC	0.965	0.966	0.965
	Evap. VOC	1.033	1.033	1.033
	CO	0.881	0.882	0.881
	NOx	1.038	1.038	1.038
LDT	Exh. VOC	0.948	0.949	0.949
	Evap. VOC	1.052	1.052	1.052
	CO	0.859	0.861	0.861
	NOx	1.030	1.029	1.029
HDGV	Exh. VOC	0.946	0.946	0.946
	Evap. VOC	1.073	1.073	1.073
	CO	0.858	0.858	0.858
	NOx	1.020	1.020	1.020
HDDV	Exh. VOC	1.000	1.000	1.000
	Evap. VOC	NA	NA	NA
	CO	1.000	1.000	1.000
	NOx	1.000	1.000	1.000

TABLE 4-19. Adjustment factors to account for fuel composition effects (oxygen and distillation, but not RVP) for St. Louis scenario 6.

City: St. Louis
Scenarios: 100% ETBE blend sales (scenario 6)

		Road Class		
		Urban	Rural	Limited Access
(Counties with I/M)				
LDV	Exh. VOC	0.963	0.963	0.963
	Evap. VOC	1.035	1.035	1.035
	CO	0.873	0.873	0.872
	NOx	1.041	1.041	1.041
LDT	Exh. VOC	0.944	0.945	0.945
	Evap. VOC	1.044	1.044	1.044
	CO	0.848	0.850	0.850
	NOx	1.032	1.032	1.031
HDGV	Exh. VOC	0.941	0.941	0.941
	Evap. VOC	1.053	1.053	1.053
	CO	0.846	0.846	0.846
	NOx	1.022	1.022	1.022
HDDV	Exh. VOC	1.000	1.000	1.000
	Evap. VOC	NA	NA	NA
	CO	1.000	1.000	1.000
	NOx	1.000	1.000	1.000
(Counties without I/M)				
LDV	Exh. VOC	0.962	0.963	0.962
	Evap. VOC	1.035	1.035	1.035
	CO	0.871	0.872	0.871
	NOx	1.041	1.041	1.041
LDT	Exh. VOC	0.943	0.945	0.945
	Evap. VOC	1.044	1.044	1.044
	CO	0.847	0.849	0.849
	NOx	1.033	1.032	1.032
HDGV	Exh. VOC	0.941	0.941	0.941
	Evap. VOC	1.053	1.053	1.053
	CO	0.846	0.846	0.846
	NOx	1.022	1.022	1.022
HDDV	Exh. VOC	1.000	1.000	1.000
	Evap. VOC	NA	NA	NA
	CO	1.000	1.000	1.000
	NOx	1.000	1.000	1.000

TABLE 4-20. Adjustment factors to account for fuel composition effects (oxygen and distillation, but not RVP) for New York scenario 3.

City: New York
Scenarios: 100% gasohol sales (scenario 3)

		Road Class		
		Urban	Rural	Limited Access
(Counties with I/M)				
LDV	Exh. VOC	0.932	0.933	0.933
	Evap. VOC	1.050	1.050	1.050
	CO	0.766	0.768	0.766
	NOx	1.075	1.074	1.074
LDT	Exh. VOC	0.898	0.900	0.900
	Evap. VOC	1.092	1.092	1.092
	CO	0.720	0.724	0.725
	NOx	1.059	1.058	1.057
HDGV	Exh. VOC	0.891	0.891	0.892
	Evap. VOC	1.144	1.144	1.144
	CO	0.716	0.716	0.716
	NOx	1.039	1.039	1.039
HDDV	Exh. VOC	1.000	1.000	1.000
	Evap. VOC	NA	NA	NA
	CO	1.000	1.000	1.000
	NOx	1.000	1.000	1.000
(Counties without I/M)				
LDV	Exh. VOC	0.930	0.931	0.931
	Evap. VOC	1.050	1.050	1.050
	CO	0.762	0.763	0.762
	NOx	1.075	1.075	1.074
LDT	Exh. VOC	0.895	0.897	0.897
	Evap. VOC	1.092	1.092	1.092
	CO	0.716	0.720	0.721
	NOx	1.060	1.059	1.058
HDGV	Exh. VOC	0.891	0.891	0.892
	Evap. VOC	1.144	1.144	1.144
	CO	0.716	0.716	0.716
	NOx	1.039	1.039	1.039
HDDV	Exh. VOC	1.000	1.000	1.000
	Evap. VOC	NA	NA	NA
	CO	1.000	1.000	1.000
	NOx	1.000	1.000	1.000

TABLE 4-21. California state highway system estimated VMT for 1985 weekday travel. (Source: California Department of Transportation, 1987).

Month	VMT (billion miles)	Fraction of Annual Total
January	5.83	0.075
February	5.97	0.077
March	6.13	0.079
April	6.50	0.084
May	6.52	0.084
June	6.77	0.087
July	6.94	0.089
August	7.28	0.094
September	6.71	0.086
October	6.42	0.082
November	6.40	0.082
December	6.36	0.082
TOTAL	77.83	

TABLE 4-22. Gasoline marketing emission adjustment factors for RVP and fuel type (EPA, OMS, 1988).

RVP	Gasoline	100% Gasohol	100% ETBE Blend	50% Gasohol
11.5	1.15	not needed	not needed	not needed
10.0	1.0	0.958	not needed	not needed
9.0	0.9	not needed	0.953	not needed
8.8	not needed	not needed	not needed	not needed
8.4	not needed	not needed	not needed	0.812
7.8	0.78	not needed	0.826	not needed

TABLE 4-23. Relationship between NAPAP area source category codes and area source types used for gridding purposes.

Source Category Code	Source Type*	Category Description
1	1	Residential Fuel - Anthracite Coal
2	1	Residential Fuel - Bituminous Coal
3	1	Residential Fuel - Distillate Oil
4	1	Residential Fuel - Residual Oil
5	1	Residential Fuel - Natural Gas
6	1	Residential Fuel - Wood
7	2	Commercial/Institutional Fuel - Anthracite Coal
8	2	Commercial/Institutional Fuel - Bituminous Coal
9	2	Commercial/Institutional Fuel - Distillate Oil
10	2	Commercial/Institutional Fuel - Residual Oil
11	2	Commercial/Institutional Fuel - Natural Gas
12	2	Commercial/Institutional Fuel - Wood
13	2	Industrial Fuel - Anthracite Coal
14	2	Industrial Fuel - Bituminous Coal
15	2	Industrial Fuel - Coke
16	2	Industrial Fuel - Distillate Oil
17	2	Industrial Fuel - Residual Oil
18	2	Industrial Fuel - Natural Gas
19	2	Industrial Fuel - Wood
20	2	Industrial Fuel - Process Gas
21	1	On-Site Incineration - Residential
22	2	On-Site Incineration - Industrial
23	2	On-site Incineration - Commercial/Institutional
24	1	Open Burning - Residential
25	2	Open Burning - Industrial
26	2	Open Burning - Commercial/Institutional
27	2	Light Duty Gasoline Vehicles - Limited Access Roads
28	4	Light Duty Gasoline Vehicles - Rural Roads
29	1	Light Duty Gasoline Vehicles - Suburban Roads
30	1	Light Duty Gasoline Vehicles - Urban Roads
31	2	Medium Duty Gasoline Vehicles - Limited Access Roads
32	4	Medium Duty Gasoline Vehicles - Rural Roads
33	1	Medium Duty Gasoline Vehicles - Suburban Roads
34	1	Medium Duty Gasoline Vehicles - Urban Roads
35	2	Heavy Duty Gasoline Vehicles - Limited Access Roads
36	4	Heavy Duty Gasoline Vehicles - Rural Roads
37	1	Heavy Duty Gasoline Vehicles - Suburban Roads
38	1	Heavy Duty Gasoline Vehicles - Urban Roads
39	3	Off Highway Gasoline Vehicles
40	2	Heavy Duty Diesel Vehicles - Limited Access Roads

continued

TABLE 4-23. (continued) Relationship between NAPAP area source category codes and area source types used for gridding purposes.

Source Category Code	Source Type*	Category Description
41	4	Heavy Duty Diesel Vehicles - Rural Roads
42	1	Heavy Duty Diesel Vehicles - Suburban Roads
43	1	Heavy Duty Diesel Vehicles - Urban Roads
44	3	Off Highway Diesel Vehicles
45	2	Railroad Locomotives
46	0	Aircraft LTOs - Military
47	0	Aircraft LTOs - Civil
48	0	Aircraft LTOs - Commercial
49	0	Vessels - Coal
50	0	Vessels - Diesel Oil
51	0	Vessels - Residual Oil
52	0	Vessels - Gasoline
53†	0	Solvents Purchased (not used)
54	1	Gasoline Marketed
55	4	Unpaved Road Travel
56	4	Unpaved Airstrip LTOs
57	0	(Not used)
58	0	(Not used)
59	0	(Not used)
60	4	Forest Wild Fires
61	4	Managed Burning - Prescribed
62	4	Agricultural Field Burning
63	4	Frost control - Orchard Heaters
64	1	Structural Fires
65	0	(Not used)
66	1	Ammonia Emissions - Light duty Gasoline Vehicles
67	1	Ammonia Emissions - Heavy Duty Gasoline Vehicles
68	1	Ammonia Emissions - Heavy Duty Diesel Vehicles
69§	4	Livestock Waste Management - Turkeys
70§	4	Livestock Waste Management - Sheep
71§	4	Livestock Waste Management - Beef Cattle
72§	4	Livestock Waste Management - Dairy Cattle
73§	4	Livestock Waste Management - Swine
74§	4	Livestock Waste Management - Broilers
75§	4	Livestock Waste Management - Other Chickens
76†	4	Anhydrous Ammonia Fertilizer Application
77	4	Beef Cattle Feed Lots
78	2	Degreasing
79	2	Dry Cleaning
80	2	Graphic Arts/Printing

continued

TABLE 4-23. (concluded) Relationship between NAPAP area source category codes and area source types used for gridding purposes.

Source Category Code	Source Type*	Category Description
81	2	Rubber and Plastics Manufacture
82	1	Architectural Coatings
83	2	Auto body Repair
84	2	Motor Vehicle Manufacture
85	2	Paper Coating
86	2	Fabricated Metals
87	2	Machinery Manufacture
88	2	Furniture Manufacture
89	2	Flatwood Products
90	2	Other Transportation Equipment Manufacture
91	2	Electrical Equipment Manufacture
92	2	Shipbuilding and Repairing
93	2	Miscellaneous Industrial Manufacture
94**	0	(Not used)
95**	1	Miscellaneous Solvent Use
96	0	(Not used)
97	0	(Not used)
98	0	(Not used)
99	0	(Not used)
100	2	Publicly Owned Treatment Works (POTWs)
101	2	Cutback Asphalt Paving Operation
102	2	Fugitives from Synthetic Organic Chemical Manufacture
103	2	Bulk Terminal and Bulk Plants
104	2	Fugitives from Petroleum Refinery Operations
105	2	Process Emissions from Bakeries
106	2	Process Emissions from Pharmaceutical Manufacture
107	2	Process Emissions from Synthetic Fibers Manufacture
108	4	Crude Oil and Natural Gas Production Fields
109	2	Hazardous Waste Treatment, Storage, and Disposal Facilities (TSDFs)

Notes:

* Source type:

1 - Population
2 - Commercial industrial
3 - Off-highway
4 - Rural
0 - Not used

† SCC 53 is disaggregated into process categories 78 to 95.
§ These categories formerly referred to as "manure field application."
** Formerly "miscellaneous industrial solvent use" (94) and "miscellaneous nonindustrial solvent use" (95); now combined into one category.

TABLE 4-24. Speciation of evaporative VOC emissions by weight percent of VOC (Source: EPA/OMS, 1988).

	Gasoline RVP				Ethanol Blend RVP		ETBE Blend RVP	
	11.5	10.0	9.0	7.8	10.0	8.8	9.0	7.8
Paraffins (total)	70	67	64	60	57	55	58	54
n-butane	27	24	21	17	14	12	15	11
Isobutane	6	6	6	6	6	6	6	6
n-pentane	4	4	4	4	4	4	4	4
Isopentane	13	13	13	13	13	13	13	13
Other paraffins[1]	20	20	20	20	20	20	20	20
Olefins[1,2]	13	15	17	20	13	14	15	18
Aromatics[1,3]	17	18	19	20	15	16	17	18
Ethanol	0	0	0	0	15	15	0	0
ETBE	0	0	0	0	0	0	10	10

[1] Within other paraffins, olefins, and aromatics, speciated with the same relative weights as given in the speciation manual (EPA, 1988).

[2] Speciation manual combines propylene (propene) and propane and lists it as propane; assumed it was 100 percent propane.

[3] Speciation manual combines benzene and cyclohexane, speciated as half each compound.

TABLE 4-25. Speciation of exhaust VOC emissions by weight percent of VOC into CB-IV species.

CB-IV Species	Gasoline RVP				Ethanol Blend RVP/Market Share		ETBE Blend RVP (100% Market Share)
	11.5	10.0	9.0	7.8	10.0/100%	8.8/50%	7.8
OLE	3	3	3	3	4	4	4
PAR	53	53	53	53	51	52	53
TOL	11	11	11	11	11	11	11
XYL	20	20	20	20	19	19	19
FORM	1	1	1	1	1	1	1
ALD2	2	2	2	2	3	3	3
ETH	10	10	10	10	10	10	10
MEOH	0	0	0	0	0	0	0
ETOH	0	0	0	0	2	1	0

TABLE 4-26. Total and on-road motor-vehicle-related emissions of VOC, CO, and NO_x by scenario.

Scenario	VOC (TPD)		CO (TPD)		NO_x (TPD)	
	On-Road Motor-Vehicle-Related*	Total	On-Road Motor-Vehicle-Related*	Total	On-Road Motor-Vehicle-Related*	Total
New York						
Scenario 1	2247.4	4429.5	1834.0	3546.5	532.8	1181.4
Scenario 2	1162.9	3343.6	1586.0	3298.2	534.4	1182.9
Scenario 3	1314.6	3495.8	1296.4	2762.6	560.1	1208.5
Scenario 4	779.2	2959.6	1834.0	3546.5	533.0	1181.5
St. Louis						
Scenario 1	258.6	676.3	274.1	591.9	101.8	349.7
Scenario 2	157.8	575.4	237.4	555.2	101.8	349.7
Scenario 5	167.8	585.5	219.0	523.0	103.9	352.0
Scenario 6	150.2	567.9	207.9	510.7	104.1	352.2
Scenario 7	431.3	849.2	274.1	591.9	101.8	349.7
SIP Scenario A	150.5	404.3	274.1	591.9	101.8	349.7
SIP Scenario B	NA	405.0	274.1	591.9	101.8	349.7

* Includes on-road motor-vehicle exhaust, evaporative, running losses, refueling, and gasoline marketing emissions.

5 ANALYSIS OF THE URBAN AIRSHED MODELING RESULTS

In this section we present the results of exercising the UAM(CB-IV) for the New York and St. Louis episodes using various emission scenarios. These emission scenarios consist of a base year inventory, several inventories for 1995 reflecting the effects of changes in mobile VOC and CO emissions due to different fuel RVP and ethanol blends, and SIP control strategies for St. Louis. In the following discussion, we present ozone concentrations in parts per hundred million (pphm) and differences in ozone concentrations in parts per billion (ppb). Note that for the ozone NAAQS .12 ppm = 12.0 pphm = 120 ppb. To have confidence in model results, it is desirable to first evaluate the model by using a meteorological base year emissions inventory and concurrent ozone observations to compare model results with measurements.

MODEL PERFORMANCE EVALUATION

A major effort in past UAM applications was devoted to the many diagnostic simulations required to achieve strict model performance standards. One of the key components of the UAM PLANR application is a relaxation of these strict model performance evaluation requirements. Thus the goal of the UAM PLANR application is to achieve a satisfactory level of performance involving as few diagnostic simulations as possible. However, the model must show some skill in predicting observations to promote confidence in its ability to correctly respond to changes in inputs, such as alternative emission scenarios.

Model performance evaluation can be divided into two categories: statistical and diagnostic. In the statistical evaluation, model predictions are compared with observations to see how well model results agree with observations. In a diagnostic evaluation, the goal is to determine why the model predicts what it does. Diagnostic evaluation generally involves many simulations in which the input data vary to provide insight into the reasons for the model's predictions. Although diagnostic evaluations are important, time and resource constraints allowed only a statistical evaluation of the UAM to be carried out as part of this project.

For the PLANR use of the UAM(CB-IV) for New York and St. Louis described herein, only one evaluation simulation was carried out. Model inputs were prepared according to the objective techniques described in Section 3, and the model was exercised using the best estimate of a meteorological base year inventory. For St. Louis, the

emission inventory used in the model evaluation was derived from the emission inventory used in the St. Louis ozone modeling project (Schere and Shreffler, 1982; Cole et al., 1983) and was for the year 1976. For the New York metropolitan area, the emission inventory used in the model evaluation was derived from the 1988 SCOPE Base Case inventory used in the OMNYMAP project (Rao, 1987) and was for the year 1988. Both inventories had to be converted from CB-II to CB-IV species. The uncertainties introduced by not using proper CB-IV speciation methodologies and the 1988 year inventory for the New York evaluations are unknown. Model predictions were compared with observations, and, given the uncertainties noted, the model exhibited sufficient skill in predicting observations that no diagnostic simulations were deemed necessary to improve model performance.

The fairly good level of model performance noted in these two UAM applications using the PLANR procedures may be due in part to the fact that both episodes were modeled and evaluated in a previous simulation involving the CB-II version of the UAM and that both applications made use of nonroutine data. Thus it is possible that future UAM PLANR applications may require some diagnostic simulations to improve model performance.

In the following discussions of model performance evaluation, we focus on three aspects of the model's ability to replicate observations:

1. Accuracy in predicting the peak observation. The peak observation will be compared with the peak prediction that occurs anywhere within the modeling domain (unmatched by time and location). Traditionally, it has been a UAM performance goal that the peak predicted value be within 30 percent and in the general location of the peak observed value unmatched by time or location. Traditionally, model performance has been considered to be good if the maximum ozone concentration is matched to within 15 percent. In addition, the peak prediction at the location of the peak observation will be compared with the maximum observation (matched by location but not time).

2. Accuracy in predicting hourly ozone concentrations. Hourly predicted and observed ozone concentrations will be paired together, matched by time and location, to reveal whether the model replicates the diurnal and spatial variability noted in the observations. Model results will be examined to determine whether the model exhibits any systematic bias in predicting observations.

3. Accuracy in predicting maximum daily observations throughout the modeling domain. Model results will be examined to determine whether the model predicts the observed spatial patterns of the maximum daily ozone observations. Exceptional model performance will be indicated if the model predicts all of the observed maximum daily ozone observations within 30 percent matched by location but not by time.

The focus has been on accuracy because, if desired, it can be accounted for in the development and adoption of control strategies.

Although there are many statistical measures that can be used to evaluate model performance (Fox, 1981, 1984; Dennis, Downton, and Keil, 1983), only a few key statistical measures are discussed for the two paired data sets of predictions and observations: hourly ozone concentrations matched by time and location and maximum daily ozone concentrations matched by location only. Other statistical measures of model performance are presented in figures and tables. Since statistical performance measures alone do not always provide a clear picture of model performance, we also present several qualitative measures of model performance. These measures include time series of predicted and observed hourly ozone concentrations at each monitoring site and spatial maps containing isopleths of predicted maximum daily ozone concentrations, with the maximum daily observation superimposed at the location of the observation.

The key statistical performance measures to be presented for the two paired data sets are as follows:

Average Observed

Average Predicted

Bias = Averge Observed - Average Predicted

Absolute Average Gross Error

Correlation Coefficient

Comparison of the average observed and predicted hourly ozone concentrations provides an indication of how well the model is reproducing the observations on average. A zero bias indicates that the model is underpredicting to the same degree that it is overpredicting. The absolute average gross error measures how well the hourly model predictions match the observations in an absolute sense. If the bias is approximately equal in magnitude to the absolute average gross error, then the model is systematically over- or underpredicting. The correlation coefficient, when applied to the hourly ozone concentration pairs, provides insight into how well the model can reproduce the diurnal and spatial variability of the observations. Perfect model performance, which is nearly impossible to attain because of the stochastic nature of the atmosphere and the differences in what the predictions and observations represent, would be a bias and absolute average gross error of zero and a correlation coefficient of one.

The correlation coefficient between the predicted and observed maximum daily ozone concentration pairs indicates how well the model replicates the spatial pattern of the maximum daily ozone observations. Before we present a comparison of the predicted and observed hourly ozone concentrations, it should be noted that there are fundamental differences in what the observed and predicted ozone values represent.

Model predictions are for a grid cell average and represent a volumetric average for a volume ranging from approximately 2 to 100 cubic kilometers. The observations, on the other hand, are representative of a point and may be subject to sub-grid-scale influences. Of particular importance for ozone measurements is the possibility that NO_x sources located near the ozone monitor may cause a local titration of the observed ozone concentration that is not reflected in the grid cell ensemble concentration.

Evaluation of the New York Application of the UAM(CB-IV)

The New York modeling episode spanned the period beginning at 1200 LST on 7 August 1980 and ending at 2000 LST on 8 August 1980. The sole purpose of initializing the model at noon on 7 August was to eliminate the effects of initial conditions on ozone and ozone precursor concentrations on 8 August. Thus we limit our evaluation discussion for the New York episode to model predictions for 8 August 1980.

Within the New York modeling domain there were 32 ozone monitoring sites. The site names and four-character identifiers are listed in Table 5-1, while the locations of the monitors are shown in Figure 5-1. Of the 32 sites, two (LIND and MIDS) did not collect any ozone observations on 8 August, and another (MORR) lay inside a boundary cell that is not modeled by the UAM. Thus 29 observation sites remained for model evaluation. (For the reader's convenience, all figures and tables are located at the end of this section.)

Figure 5-2 displays isopleths of the predicted maximum daily ozone concentrations on 8 August 1980. Also shown in Figure 5-2 are the maximum daily observed ozone concentrations at all sites superimposed over the predicted isopleths. The peak observed ozone of 24.6 pphm occurred at Stratford, CT (STRF), while the peak prediction of 23.5 pphm occurred approximately 30 km to the east-southeast of STRF in the Long Island Sound between Long Island, NY and the coast of Connecticut. The model predicts the peak observed ozone concentration within 4 percent, unmatched by time or location. Since there are no ozone monitors in the vicinity of the predicted peak ozone concentration, it is uncertain whether the ozone peak actually occurred over the Long Island Sound.

Examination of the predicted and observed maximum daily ozone concentrations away from the peak observation at STRF reveals that the model tends to overpredict the maximum daily ozone concentrations throughout the region (Figure 5-2). This tendency toward overprediction of the afternoon ozone concentrations is also illustrated in the time series plots of predicted and observed hourly ozone concentrations at all sites presented in Figure 5-3. The maximum daily ozone concentration predicted by the model typically occurs 1 to 3 hours later in the afternoon than does the observed maximum. The model predicts a maximum daily ozone concentration of

21.4 pphm (underprediction by 13 percent) at STRF 3 hours later (4:00 p.m.) than the occurrence of the observed peak. However, there is some doubt whether the STRF observations are representative of the large-scale ozone buildup observed in southern Connecticut. In fact, at an ozone monitor in Bridgeport, CT (BRPT), less than 8 km from STRF, the observed maximum daily ozone is 17 pphm, whereas the predicted maximum daily ozone concentration is 20 pphm, an 18 percent overprediction at this site. Clearly, the model cannot resolve such sharp spatial concentration gradients in the observations using an 8-km grid spacing.

A more representative measure of the observed ozone buildup over southern Connecticut would be to combine the four ozone monitors, STRF, BRPT, Derby (DRBY), and New Haven (NHVN), that lie within a few grid cells of each other. When the hourly observations from these four sites are averaged and compared with the corresponding average predictions, we see that the model is better at predicting the ensemble spatially averaged observed ozone than a point measurement (Figure 5-4). The model overpredicts the observed maximum daily ozone averaged for the four sites in southern Connecticut by about 27 percent, matched by time and location. The maximum observed and maximum predicted ozone concentrations both occur at the same time of the day (2:00 p.m.).

The maximum predicted ozone concentrations at all other sites are within a factor of two except at three sites (HEMP, MAMA, and POUG). This discrepancy may be due to ozone titration from local sources at these sites. The HEMP site is the only site with concurrent NO_x measurements, and observed NO_x concentrations are high (10 pphm). Thus overprediction of ozone at the HEMP site can be attributed to local NO_x emissions. Unfortunately, there are no concurrent NO_x measurements at the other two sites, where significant overprediction occurs.

Figures 5-5 and 5-6 display scatterplots, residual analysis, and some statistical measures for all hourly ozone concentrations (matched by time and location) and for the maximum daily ozone concentrations (matched by location but not time). Over all hours (Figure 5-5a) the predictions and observations correlate well, with a correlation coefficient of 0.80. However, as illustrated in the time series analysis and maximum daily ozone isopleths in Figures 5-2 and 5-3, the model tends to overpredict observations, on average, by approximately 3.1 pphm (51 percent). The absolute average gross error is 3.8 pphm (62 percent), approximately the same as the bias, which indicates that the model is systematically overpredicting the observations.

The model, on average, tends to overpredict by 5.4 pphm (45 percent) the maximum daily ozone concentrations at each site (Figure 5-6). The absolute average gross error is 5.6 pphm (47 percent), again indicating a systematic overprediction. The model does show some skill in replicating the spatial distribution of the observed maximum daily ozone concentrations, with a correlation coefficient of 0.58 between predicted and observed maximum daily ozone concentrations matched in location but not in time.

Comparison of UAM(CB-IV) Model Performance for New York with Performance in a Previous Study

The 8 August 1980 episode was modeled with the CB-II version of the UAM by the New York State Department of Environmental Conservation (NYSDEC) as part of the Oxidant Modeling in the New York Metropolitan Area Program (OMNYMAP). As discussed in Section 3, the OMNYMAP UAM(CB-II) inputs formed a starting point for the inputs prepared for the UAM(CB-IV) for this study. The principal differences between this study and the OMNYMAP UAM evaluation of 8 August 1980 are: (1) this study used the latest version of the UAM, which includes the chemistry of the CB-IV and an improved advection algorithm; (2) in this study the modeling period was extended by beginning the simulation at noon on 7 August compared to starting at 4:00 a.m. on 8 August in the OMNYMAP study; (3) this study used a diagnostic wind model, whereas the OMNYMAP study used constant wind fields; however, the bulk flow direction remains similar; (4) in this study the region top was held constant at 1500 m, whereas a rising region top was used in the OMNYMAP study; (5) this study used slightly lower boundary conditions on the southwestern inflow boundary; and (6) this study used a 1988 emissions inventory whereas the OMNYMAP study used a 1980 inventory.

Table 5-2 compares some key statistical performance measures for application of the UAM(CB-IV) in this study and the OMNYMAP application of the UAM(CB-II) for 8 August 1980. As seen in Table 5-2, the OMNYMAP application of the UAM(CB-II) also tended to overpredict observations.

The OMNYMAP application of the UAM tended to produce a double ozone peak: one centered over the Connecticut coastline and one located over the New Jersey coastline. The ozone peak over New Jersey predicted by the UAM in the OMNYMAP study is not supported by the observations (see sites EORG, BAYO, and PLFD in Figure 5-3). It is suspected that this predicted ozone peak may have been caused by prescription of higher boundary condition concentrations near the southwest corner of the modeling domain. In this study the UAM did not predict an ozone peak over New Jersey. In general, however, the UAM model performance in this study was comparable to the performance in the OMNYMAP study. Any differences may be attributable to this study's use of a 1988 emissions inventory, which contains approximately 32 and 14 percent less VOC and NO_x emissions, respectively.

The UAM(CB-IV) application has shown some skill in predicting observed ozone concentrations for 8 August 1980 in the New York metropolitan area. There is a general tendency to overpredict the maximum afternoon observed ozone concentration. However, the peak observed ozone concentration is replicated within 4 percent unmatched by time and location, and within 13 percent when matched by location but not time. Overall model performance could most likely be improved by using a 1980 emissions inventory and/or finer model resolution and/or by lowering the boundary conditions or other uncertain inputs that would in turn lower the predicted afternoon

peak ozone concentrations throughout the modeling region. However, this procedure may also result in less agreement with the observed peak ozone value. The single evaluation simulation of the UAM(CB-IV) indicates that the model displays sufficient skill in replicating observations and will provide a useful and credible tool for analysis of the formation of elevated ozone episodes in the New York metropolitan area.

Evaluation of the St. Louis Application of the UAM(CB-IV)

The St. Louis modeling episode spanned the period from midnight to 1900 LST on 13 July 1976. This modeling episode was an extension of a previous UAM(CB-II) modeling episode performed as part of the St. Louis modeling project (Cole et al., 1983; Schere and Shreffler, 1982), in which the model was exercised from 0400 to 1800 LST. The purpose of extending the episode the extra four hours in this study was to minimize the effects of initial conditions on the afternoon peak predicted ozone concentrations.

The St. Louis modeling period coincided with the Regional Air Pollution Study (RAPS); thus there was a fairly dense network of 21 ozone monitors within and around the city of St. Louis. On 13 July 1976, seven of the monitors did not measure afternoon ozone concentrations; 14 monitoring sites provided sufficient data for conducting a model performance evaluation. Figure 5-7 shows the spatial distribution of the ozone monitoring network; sites 102, 104, 105, 111, 115, 118, and 121 are the seven sites with no afternoon ozone observations.

Figure 5-8 shows isopleths of the predicted maximum daily ozone concentrations with the maximum daily observations superimposed. The peak observation is 22.2 pphm and occurs at hour 16, while the peak prediction anywhere in the modeling domain is 24.2 pphm (within 9 percent of the peak observation) and also occurs at hour 16, approximately 10 km to the southwest (upwind) of the observation.

The time series of predicted and observed ozone concentrations for all the sites within the St. Louis modeling domain are shown in Figure 5-9. The model exhibits very good agreement at almost all sites. At the location of the observed peak ozone concentration (site 114), the model appears to replicate the rise of the observations in the morning until around 1000 LST, when a shoulder appears in the time series of predicted concentrations. This shoulder is most probably due to a wind shift in the input wind field. Despite the shoulder, the model reproduces the observed peak at site 114 within 1 percent (22.2 pphm observed versus 21.9 pphm predicted), although the modeled peak occurs two hours later than the observed peak. The peak observed ozone concentration at each site is replicated by the model within 30 percent at all sites except site 108. At site 108 the model predicts a sharp spike for peak ozone that is not supported by observations.

Figure 5-10 contains a scatterplot, residual analysis, and some statistical measures comparing the hourly predicted and observed ozone concentrations for all hours of 13

July 1976. Except for a tendency to overpredict the extremely low nighttime ozone observations, the model exhibits no systematic bias in predicting the hourly observed ozone concentrations. The bias between the predicted and observed ozone concentrations is -0.9 pphm, yielding an average overprediction of approximately 14 percent. The gross absolute error is 1.7 pphm (28 percent), which indicates that the model is not systematically over- or underpredicting. The predicted hourly ozone concentrations correlate extremely well with the observations, with a correlation coefficient of 0.92.

A scatterplot and statistical measures for the predicted and observed maximum daily ozone concentrations, matched by location but not time, are given in Figure 5-11. Again the model exhibits substantial skill in replicating the observed maximum daily ozone concentrations with a bias of only 1.0 pphm (6 percent) and an absolute average gross error of only 2.4 pphm (16 percent). The spatial distribution of the observed maximum daily ozone concentrations is also reproduced by the model, with a correlation coefficient of 0.68.

Comparison of UAM(CB-IV) Model Performance for St. Louis with Performance in a Previous Study

The 13 July 1976 episode was one of the 20 early ozone episodes from RAPS used to evaluate an early version of the UAM and other urban-scale photochemical air quality simulation models in the early 1980s (Schere and Shreffler, 1982). Table 5-3 displays several key statistical performance measures for the 13 July 1976 St. Louis modeling episode discussed in this study using the UAM(CB-IV) and from the previous study using the UAM(CB-II). In general, the bias and correlation coefficients for both the UAM(CB-IV) and UAM(CB-II) applications to St. Louis on 13 July indicate quite good model performance (bias in magnitude is less than 1 pphm, and correlation coefficients are greater than 0.9). However, the UAM(CB-IV) predictions of peak observed ozone concentrations in this study are substantially better than those produced by the UAM(CB-II) in the previous study. Comparison of the peak predicted ozone concentrations anywhere within the modeling domain with the peak observed ozone concentrations (unmatched by time or location) reveals that the UAM(CB-IV) overpredicted by 9 percent, whereas the UAM(CB-II) underpredicted by 22 percent. The UAM(CB-IV) predicted the observed peak ozone at the monitoring site (matched by location but not time) to within 2 percent, whereas the UAM(CB-II) underpredicted the maximum observed ozone concentration at the site by 25 percent.

The UAM(CB-IV) model performance for the St. Louis region is quite good by any measure. The improvement in model performance over the past application of the UAM(CB-II) may be due to improvements in the treatment of chemistry and advection in the model, and improvements in the wind fields. However, this improvement in model performance tends to indicate that the UAM(CB-IV), using the PLANR input preparation procedures, does produce significantly better modeling results than those obtained with the earlier version of the UAM and its preprocessor programs.

ANALYSIS OF UAM RESULTS FOR NEW YORK

The UAM(CB-IV) was exercised for four separate future year emission sensitivity scenarios reflecting VOC emissions changes resulting from use of different fuel RVP, use of ethanol-blended fuels, and running loss mobile emissions. These four emission scenarios for New York can be summarized as follows:

Scenario 1: 1995 emission rates at current RVP values (11.5 psi) with running losses,

Scenario 2: 1995 emission rates at low RVP values (9.0 psi) with running losses,

Scenario 3: 1995 emission rates with a 100 percent market penetration of a 10 percent ethanol-blended fuel at the low RVP values with a 1 psi exemption (10.0 psi) with running losses, and

Scenario 4: 1995 emission rates at current RVP values (11.5 psi) with no running losses.

All four of the 1995 emission scenarios were exercised using the same initial and boundary conditions (i.e., the changes in the 1995 emission scenarios were not reflected in the boundary conditions). Thus the changes in the 1995 emissions have to be viewed as local changes in the emissions inventory within the New York modeling domain. The changes in emissions are not reflected in regions upwind of the New York metropolitan area. It is even more important that the reader bear in mind that the results do not reflect changes from regional and/or national policies (e.g., reducing RVP on a regional basis). This study treated the lower RVP as occurring only in the study area.

The four 1995 emission scenarios described above are designed to address the following issues:

Fuel RVP. The EPA is considering regulations to require lower fuel RVP to reduce evaporative VOC emissions from mobile and gas refueling sources. Note that limitations in our modeling capabilities precluded our examining at this time the impact of regional (i.e., Northeast Corridor) lowering of RVP. Results of scenarios 1 and 2 do not reflect the likely "real-world" policy, nor does comparison of them provide definitive results.

Ethanol-blended fuels. The use of ethanol blends in gasoline-powered vehicles results in significant reductions in exhaust CO emissions but some increases in exhaust NO_x and evaporative VOC emissions. At this time it is unclear whether the increase in ozone concentrations due to the increases in VOC emissions will be counteracted by the reductions in ozone due to the reductions

in CO emissions. Comparison of scenarios 2 and 3 allows us to assess the potential benefits or disbenefits of ethanol-blended fuels regarding ozone concentrations.

Running losses. The term "running losses" refers to VOC emissions that occur during the operation of the vehicle that have not been accounted for in past mobile source emission inventories. These VOC emissions have only recently been estimated and have not been rigorously treated in any previous ozone modeling analysis. Comparison of scenarios 1 and 4 allows us to estimate the effects of running loss emissions on urban ozone concentrations.

Previous UAM studies of the New York modeling domain have reported a high degree of sensitivity of peak ozone predictions to initial and boundary conditions (Rao, 1987; Rao and Sistla, 1987). Rao and Sistla examined the sensitivity of the UAM to emissions, initial concentrations, and boundary conditions by exercising the UAM with and without the influences of these components. Although their sensitivity analysis was performed for a different episode than the one studied here, the general meteorological conditions, boundary conditions, and model predictions were similar. The overall conclusion reached by Rao and Sistla was that initial and boundary conditions contributed approximately 70 to 90 percent of the maximum ozone concentrations in the New York metropolitan area for the episode studied.

In light of the importance of initial and boundary conditions in the work reported by Rao and Sistla, it was decided to perform a weighted tracer simulation for the New York modeling episode. The weighted tracer simulation gives an indication of the relative influences of initial conditions, boundary conditions, and emissions on VOC and NO_x concentrations in the regions of elevated ozone predictions. Since the weighted tracer simulation will provide insight into the UAM results for the 1995 emission scenarios, it is discussed next.

Tracer Simulation for New York

In a weighted tracer simulation, the UAM is run in an inert mode (i.e., no chemistry or deposition) with seven different "colored tracers" (species) representing the effects of initial conditions, lateral boundary conditions (four colors, one for each face), boundary top conditions, and emissions. Each colored tracer represents the different contributors to VOC concentrations within the modeling domain. The magnitudes of the initial and boundary conditions and emission rates correspond to the actual VOC initial and boundary conditions and emissions for the 1995 modeling scenario 1. Similarly, seven other colored tracers are set up for the NO_x species, resulting in a UAM 14-species weighted tracer simulation.

Note that the weighted tracer simulation cannot be used for a secondary species such as ozone. Also, colored tracers cannot exactly apportion the source (initial condition, boundary condition, or emissions) of a pollutant concentration at a given grid

cell and time since the inert tracer simulation neglects deposition and chemical transformation. However, the simulation can, in a general sense, provide an estimate of the relative importance of the contribution of initial concentrations, boundary conditions, and emissions to pollutant concentrations.

Figure 5-12a displays the percent contribution of the hydrocarbon boundary conditions and emissions to the total hydrocarbon concentrations for hours 1200 LST through 1700 LST on 8 August 1980. Upwind of New York City, boundary conditions are the predominant contributor to modeled hydrocarbon concentrations. From New York City to the location of the peak predicted ozone concentration, which the calculations locate in the middle of Long Island Sound late in the afternoon, boundary conditions and emissions contribute about equally to the modeled atmospheric concentrations of hydrocarbons. Downwind of the location of the peak modeled ozone concentration, boundary conditions contribute approximately 40 percent, and emissions about 60 percent to the total modeled hydrocarbon concentrations. Away from the predicted elevated ozone cloud that stretches from New York City over the Long Island Sound, boundary conditions tend to contribute more than emissions to the predicted hydrocarbon concentrations. Initial conditions do not contribute at all to the atmospheric concentrations on 8 August.

The percent contribution of boundary conditions and emissions to calculated ambient NO_x concentrations on the afternoon of 8 August is presented in Figure 5-12b. Boundary NO_x concentrations contribute approximately 40 percent to ambient NO_x concentrations in the regions of highest predicted ozone concentrations, with NO_x emissions contributing the remainder. As has been noted for the hydrocarbons, away from the predicted peak ozone cloud, NO_x concentrations are more influenced by boundary conditions than by emissions within the modeling domain.

New York 1995 Emission Scenarios

Interpretation of the effects of the different 1995 emission scenarios on ozone concentrations must include the influences of boundary conditions. Since boundary conditions are estimated to contribute about half of the hydrocarbon concentrations in the region of elevated ozone concentrations, and boundary conditions remained unchanged for all 1995 emission scenarios, then the effectiveness of VOC emission reductions on ambient ozone concentrations would be much less than if the boundary conditions also reflected the changes in the alternative emission inventories.

Table 5-4 summarizes the hydrocarbon, nitrogen oxides, and carbon monoxide emission rates for the 1995 emission inventories. Also tabulated are VOC-to-NO_x ratio, estimated from the inventory, for each scenario. Of particular note is that the VOC-to-NO_x ratio for the 1995 scenario 1 base case emissions inventory is 10.8 compared to current urban emission inventory VOC-to-NO_x ratios that usually range from 3 to 6. Since NO_x reacts away into secondary products faster than VOC species do, urban ambient measurements of VOC-to-NO_x ratios are higher (the national average is

around 10, and a three-year average (1983-1985) for New York City is around 12). Reductions of VOC emissions are less effective in reducing ozone at high VOC-to-NO_x ratios than at lower VOC-to-NO_x ratios. The 1988 Scope Base Case and 1985 NAPAP emission inventories have lower VOC-to-NO_x ratios, 3.4 and 4.8, respectively, than those exhibited by the 1995 scenario 1 base case. The projection of the emissions from the 1985 NAPAP inventory to the 1995 inventory without running losses (scenario 4) results in a VOC-to-NO_x ratio of 7.2. This increase in the VOC-to-NO_x ratio is primarily due to the increases in evaporative VOC emissions resulting from the change from Mobile-3 to Mobile-3.9 emissions. Mobile-3.9 accounts for increases in evaporative emissions due to increases in temperature and RVP. The addition of running loss VOC emissions to the inventory, which adds an additional 50 percent VOC to the scenario 4 inventory, results in a 50 percent increase in the VOC-to-NO_x ratio, from 7.2 to 10.8 in the 1995 base case inventory at current RVP (scenario 1).

Exercising the UAM(CB-IV) for the four 1995 emission scenarios generates gridded fields of hourly concentrations for 22 species at 5 vertical levels for the 32-hour simulation. The following discussion is accompanied by isopleth maps of the maximum daily ozone concentrations and hourly ozone concentrations in the afternoon of 8 August. In addition, difference plots of maximum daily and hourly ozone concentrations between scenarios are presented, where appropriate.

Effects of Lower RVP

As seen in Table 5-4, the effect of lowering the RVP of gasoline fuel in New York from the current value of 11.5 to 9.0 results in a 24 percent reduction in VOC emissions. Although these VOC reductions are mainly lower reactive hydrocarbons (butane and pentane), there are also some reductions in more reactive species such as olefins and xylenes.

Figures 5-13 and 5-14 show isopleth maps of maximum daily ozone concentrations for the current RVP (scenario 1) and low RVP (scenario 2), respectively. Isopleths of afternoon hourly ozone concentrations for scenarios 1 and 2 are presented in Appendixes D-1 and D-2. Qualitatively, the effect of lower RVP on ambient ozone concentrations is very small. The calculated highest ozone concentration of 17.4 pphm is similar for both scenarios. The highest ozone concentration for scenario 2 is calculated to be located somewhat further downwind of the city (Figures 5-13 and 5-14). Further evidence of the similarity of results is observed in the difference plots between scenario 1 and scenario 2 for the maximum daily ozone and afternoon hourly ozone concentrations shown in Figure 5-15 and Appendix D-3. Immediately downwind of New York City, the area with the largest fraction of mobile emissions, there is a region of decreased maximum ozone concentrations due to lower RVP stretching across Long Island. The maximum decrease is approximately 1.4 ppb. However, further downwind at the end of Long Island, there is a region of slight increases in

the maximum daily ozone concentrations due to the lower RVP. Although the increases and decreases in the ozone concentrations are low, maximum values of approximately 1.5 ppb, the observation that a reduction in VOC emissions results in an increase in the maximum daily ozone concentration in some regions is somewhat surprising. This topic is discussed further later in this section.

Although the highest ozone concentrations are the same for the current and low RVP scenarios, the low RVP scenario produces lower ozone concentrations earlier in the day (see Appendixes D-1, D-2, and D-3). Thus the lower RVP may help reduce the number of people-hours exposed to ozone concentrations in excess of the NAAQS. It is important to remember that, given the large VOC reductions, the apparent lack of change in ambient ozone is confounded by the analysis's failure to account for the effects of changes in fuel RVP on the long-range transport of pollutants (i.e., boundary conditions).

Effects of Ethanol-Blended Fuels

Figures 5-16 and 5-17 display, respectively, isopleths of the maximum daily ozone concentrations predicted for the 1995 ethanol-blend scenario (scenario 3) and the difference in maximum daily ozone concentrations between scenario 3 and scenario 2. (similar figures for the afternoon hourly ozone concentrations are given in Appendixes D-4 and D-5). There is a very slight increase in the maximum daily ozone concentrations, with a maximum increase of less than 1 ppb. Downwind of New York City, CO concentrations decrease about 2 to 4 percent, while there are slight increases in hydrocarbon and NO_x concentrations. Examination of the differences in hourly ozone concentrations between the ethanol-blend scenario (scenario 3) and the low RVP scenario (scenario 2) (Appendix D-5) reveals that the effects of ethanol blends on hourly ozone concentrations are very small, with ozone increases or decreases always less than 1 ppb.

Effects of Running Losses

The maximum daily ozone isopleth concentrations for the current RVP scenario without running losses (scenario 4) and differences with the scenario with running losses at current RVP (scenario 1) are shown in Figures 5-18 and 5-19, respectively (the corresponding figures for afternoon hourly ozone concentrations are given in Appendixes D-6 and D-7). Despite a 33 percent reduction in VOC emissions, there is only a slight (up to 2 ppb) reduction in the maximum daily ozone concentrations. As was noted for the low RVP scenario, further downwind from the region of elevated ozone, there is a slight increase in ozone for the scenario with running losses. However, it appears that including running loss VOC emissions will result in significant increases in hourly ozone concentrations earlier in the day (see Appendix D-7). Between the hours of 1200 to 1300, running loss VOC emissions increase ozone concentrations in some regions by as much as 20 ppb (2.0 pphm).

Preliminary Analysis of the New York 1995 Emission Scenarios

Table 5-5 summarizes the VOC emission reductions and the predicted changes in the highest ozone concentrations for the four 1995 emission scenario simulations for New York. The most striking feature of these simulations is the insensitivity of the highest ozone concentration to the VOC emission reductions. However, this insensitivity is not surprising when one considers the effects of the boundary conditions, the high VOC-to-NO_x ratio in the 1995 emission inventories, and the fact that a higher percentage of less reactive hydrocarbon species (paraffins) is part of the VOC emission reductions than is in the normal distribution of the inventory.

The southwestern boundary conditions (the most prominent inflow boundary) have (molar) VOC-to-NO_x ratios that vary from approximately 30 to 70. Given this VOC-to-NO_x ratio; the estimate from the tracer simulation that approximately half of the hydrocarbons and NO_x concentrations at the location of the maximum ozone concentrations come from the boundary conditions; and the fact that NO_x reacts away faster than VOC, the effective atmospheric VOC-to-NO_x ratio would be greater than about 20. Thus the largest VOC emissions reduction, a 33 percent VOC reduction from scenario 1 to scenario 4, would only lower the effective atmospheric VOC-to-NO_x ratio by about 2 units (from a value greater than 20 to a value greater than 18). Usually the atmospheric VOC-to-NO_x ratio must be below approximately 15 before the beneficial effects of hydrocarbon reductions on ozone concentrations can be realized.

Calculated VOC-to-NO_x ratios tend to be higher than those estimated above because the effects of chemical transformation and deposition of NO_x are included. The 6:00 to 9:00 a.m. LST VOC-to-NO_x ratios range from 8 to 15 at sites in New York City to approximately 20 on the Connecticut-New York coastline border (WPLN and GWCH) and up to 16 to 40 for the sites around the location of the peak ozone (STRF) on the Connecticut coastline.

Although the effects of the boundary conditions and high VOC-to-NO_x ratios in the 1995 emission inventories can explain the small reductions in ozone concentrations due to VOC emission reductions; they do not, by themselves, explain the slight ozone increases further downwind of New York City at the end of Long Island and in northeastern Connecticut that are associated with the lowering of VOC emissions in scenarios 2 and 4. Comparisons of predicted concentrations in the afternoon for scenarios 1 and 4 reveal that scenario 4 contains about 10 percent higher NO_x concentrations in this region. This higher NO_x concentration is almost exactly compensated by lower peroxyacyl nitrate (PAN) and nitric acid concentrations, which may explain the slight increases in ozone concentrations far downwind of New York City in scenarios 2 and 4. The reductions in VOC emissions in New York City, noted in scenarios 2 and 4, result in a decrease in the generation of radical concentrations immediately downwind of New York City. These decreases in radical concentrations

result in a decrease in the rate of ozone formation (as indicated by the lower ozone concentrations earlier in the day) and in the rate of transformation of NO_x to PAN and nitric acid. Further downwind, there is still an abundance of hydrocarbon concentrations; however, NO_x levels are low near the eastern end of Long Island (less than 1 ppb). Since less of the NO_x has been transformed to PAN in the VOC emission reduction scenarios, there is more NO_x available for ozone formation. At these high VOC-to-NO_x ratios, small increases in NO_x concentrations result in increases in ozone.

Another possible explanation for the predicted increases in ozone in VOC emission reduction scenarios 2 and 4 compared to scenario 1 is the ozone reaction with olefins and toluene VOC species. At lower VOC concentrations there is less depletion of ozone due to its reaction with olefins and toluene, resulting in slightly higher ozone concentrations. Although these explanations appear plausible, time constraints did not allow thorough investigation into the causes of these phenomena; thus further study is needed.

ANALYSIS OF UAM RESULTS FOR ST. LOUIS

The UAM(CB-IV) was exercised for the St. Louis episode for seven 1995 emission scenarios--five reflecting the changes in mobile sources due to differences in fuels, and two VOC reduction scenarios corresponding to State Implementation Plan (SIP) control strategies. These 1995 emission scenarios are summarized as follows:*

Scenario 1: 1995 emission rates at current RVP values (10.0 psi) with running losses,

Scenario 2: 1995 emission rates at low RVP values (7.8 psi) with running losses,

Scenario 5: 1995 emission rates with a 50 percent market penetration of a 10 percent ethanol-blended fuel at low RVP values with a 1 psi exemption (8.8 psi) with running losses,

Scenario 6: 1995 emission rates with a 100 percent market penetration of oxygenated fuel with enough ethyl butyl tertiary ether (ETBE) to produce a fuel with a 2 percent oxygen content with running losses (note that a 10 percent ethanol blend results in a fuel with a 3.7 percent oxygen content),

---

* Time constraints and the need to analyze several alternative emission scenarios precluded our performing Scenarios 3 and 4 for St. Louis, and the SIP scenarios and Scenarios 6 and 7 for New York.

Scenario 7: 1995 emission rates at current RVP values (10.0 psi) with a high estimate of running losses,

SIP scenario A: 1995 emission rates at low RVP (7.8 psi) with enhanced I/M and other non-mobile-source VOC emissions reduced uniformly to result in a 40 percent VOC reduction from scenario 1, with the same CO and NO_x emissions as in scenario 1, and

SIP scenario B: 1995 emission rates with a 40 percent VOC reduction from scenario 1, where the most reactive species of hydrocarbons are first reduced up to 80 percent in each grid cell to obtain the 40 percent total VOC reduction.

These 1995 emission scenarios are designed to address the following issues:

Fuel RVP. As in the New York scenarios, comparison of scenarios 1 and 2 will allow us to estimate the effects of lower fuel RVP on urban ozone concentrations,

Alternative fuels. Two types of alternative fuel scenarios will be simulated for St. Louis: a 50 percent market penetration of a 10 percent ethanol-blend and a 100 percent market penetration of an ETBE blend. Unlike ethanol blends, ETBE does not increase evaporative VOC emissions and thus may produce more benefits regarding ozone reductions than will an ethanol blend.

Running losses. There is considerable uncertainty in running loss emission rates. The 1995 UAM simulations for New York and St. Louis have used a best guess of running losses obtained from an EPA OMS analysis of running loss emissions from 12 cars. Running loss emissions may be higher or lower than the best guess estimate. A higher estimate of running losses is used in scenario 7. Comparison of scenarios 7 and 1 allows us to estimate the effects of the uncertainty in running loss emissions on ozone concentrations.

SIP control strategies. The two SIP scenarios represent two different ways of obtaining a 40 percent VOC emissions reduction from scenario 1. The main difference in the two SIP scenarios is that in SIP scenario B, the most reactive hydrocarbon species are targeted for reduction first. Comparison of the ozone reductions obtained in SIP scenarios A and B with those in scenario 1 allows us to estimate the importance of including hydrocarbon reactivity in SIP control strategies.

Effects of Lower RVP

Figures 5-20 and 5-21, respectively, display isopleths of the maximum daily ozone concentrations for the current RVP (scenario 1) and low RVP (scenario 2) scenarios. Isopleth plots of afternoon hourly ozone concentrations for scenarios 1 and 2 are

given in Appendixes E-1 and E-2. The difference plots of maximum daily ozone and afternoon ozone concentrations between scenario 1 and scenario 2 are illustrated in Figure 5-22 and Appendix E-3. Despite the lower net VOC emissions reduction due to lower RVP than was noted in the corresponding New York case (15 percent reduction versus 24 percent reduction), ozone concentrations are reduced to a greater extent in St. Louis (up to 5 ppb at the location of the peak). As Table 5-5 shows, the highest ozone concentration is reduced over 3 percent due to the 15 percent VOC reduction. The maximum decrease in the afternoon hourly ozone concentrations due to the lower RVP is approximately 6 ppb (see Appendix E-3).

Effects of Alternative Fuels

Isopleths of maximum daily ozone predictions for the ethanol-blend scenario (scenario 5) and ETBE blend scenario (scenario 6) are shown in Figures 5-23 and 5-24, respectively. The corresponding difference plots for these two scenarios versus scenario 2 are given in Figures 5-25 and 5-26. Similar isopleth plots of afternoon hourly ozone concentrations for scenarios 5 and 6, and difference plots for these two scenarios versus scenario 2 are given in Appendixes E-4 through E-7. When compared to the low RVP scenario, the use of a 50 percent market penetration of a 10 percent ethanol-blended fuel with the 1 psi exemption results in no increase in the highest ozone concentration (Table 5-5) and a slight increase in the maximum daily ozone concentrations (less than 1 ppb) downwind of the location of the highest ozone concentration (see Figure 5-25). In the early afternoon (1200-1400) any increases in hourly ozone concentrations are compensated by an equal decrease (Appendix E-6). Later in the afternoon there are more increases due to the ethanol blend although these increases in hourly ozone concentrations are always very small (less than 1 ppb).

As Figure 5-26 shows, the use of an ETBE blend results in a larger benefit (decrease of 0.8 ppb) than disbenefit (increase of 0.6 ppb) in the changes in maximum daily ozone concentrations when compared to the low RVP scenario. The highest ozone concentration is reduced by 1 ppb (Table 5-5). Further evidence of the benefits of using an ETBE blend for reducing ozone concentrations can be seen in the difference plots of hourly ozone concentrations in Appendix E-7. Maximum decreases in hourly ozone concentrations resulting from use of an ETBE blend always exceed any increases.

Effects of Running Losses

Assuming a higher estimate of running loss emissions (scenario 7) results in an increase in the maximum ozone concentration by as much as 7 ppb (Figures 5-27 and 5-28 and Appendixes E-8 and E-9). The predicted regional maximum ozone concentration increases by about 5 ppb (3 percent) due to the 26 percent increase in VOC

emissions when compared to the high RVP scenario (Table 5-5). Clearly, more data must be collected to provide a better estimate of the amount and speciation of running loss emissions.

SIP Control Strategies

The two SIP control strategies (SIP A and B) represent a 40 percent VOC reduction from scenario 1. However, they differ in the method of VOC reduction. In SIP scenario A, the 40 percent VOC reduction is obtained by switching to a low RVP fuel and including an enhanced I/M program. This results in a 15 percent reduction in VOC emissions from scenario 1. The remainder of the 25 percent VOC reduction is obtained by uniformly reducing VOC emissions from nonmobile area sources and point sources. Under SIP scenario B, the 40 percent VOC reduction from scenario 1 is obtained by reducing the most reactive VOC species first (up to 80 percent for each species in each grid cell). The same NO_x and CO emissions used in scenario 1 are used in SIP scenarios A and B.

Figures 5-29 and 5-30 show isopleths of maximum daily ozone concentrations for SIP scenarios A and B, respectively. Corresponding isopleths of afternoon hourly ozone concentrations for the SIP scenarios are given in Appendixes E-10 and E-11. Difference plots between maximum daily and afternoon hourly ozone concentrations for the SIP scenarios and scenario 1 are shown in Figures 5-31 and 5-32 and in Appendixes E-12 and E-13.

The 40 percent reduction in SIP scenario A results in a 10 percent reduction in the highest ozone concentration (Table 5-5). However, in targeting the most reactive VOC species for reduction first (SIP scenario B), the 40 percent VOC reduction results in an 18 percent reduction in the highest ozone concentration. In fact, under SIP scenario A, the region is still experiencing an exceedance of the ozone NAAQS (i.e., the highest ozone, 14 pphm, is greater than the NAAQS of 12 pphm). However, under SIP scenario B the region does not experience an exceedance of the ozone NAAQS (i.e., the highest ozone, 12 pphm, is not greater than the ozone NAAQS).

The differences in hourly ozone concentrations for the SIP scenarios and scenario 1 (Appendixes E-12 and E-13) suggest that targeting the most reactive VOC species for reduction first is approximately twice as effective at reducing ozone concentrations as are the usual VOC emission reduction strategies.

Preliminary Analysis of the St. Louis 1995 Emission Scenarios

Without the large influences of the boundary conditions and the high VOC-to-NO_x ratios that complicate the New York UAM application, VOC emission reductions are much more effective in lowering ozone concentrations for the St. Louis UAM simulations. A measure of the efficiency in ozone reduction as a function of VOC emission reductions can be obtained for a given scenario by deriving a ratio of the percentage change between the predicted highest ozone concentration from scenario 1 to the

percentage VOC emission reductions from scenario 1. As Table 5-5 indicates, these VOC reduction efficiency values range from 0.20 to 0.25 for almost all of the emission scenarios (e.g., a 10 percent VOC emission reduction results in approximately a 2 to 2.5 percent reduction in the peak ozone). The exception is SIP scenario B, which has a VOC reduction efficiency value of almost double that of all the other emission scenarios. Thus targeting the most reactive hydrocarbon species for emission reductions is expected to be twice as effective at reducing ozone concentrations as the usual across-the-board VOC reductions. It appears reasonable that the reverse of this result is also true, i.e., reducing the less reactive hydrocarbon species will not have as beneficial an effect in reducing ozone concentrations. Clearly, hydrocarbon reactivity should be taken into account to the extent possible in analyzing VOC emission control strategies.

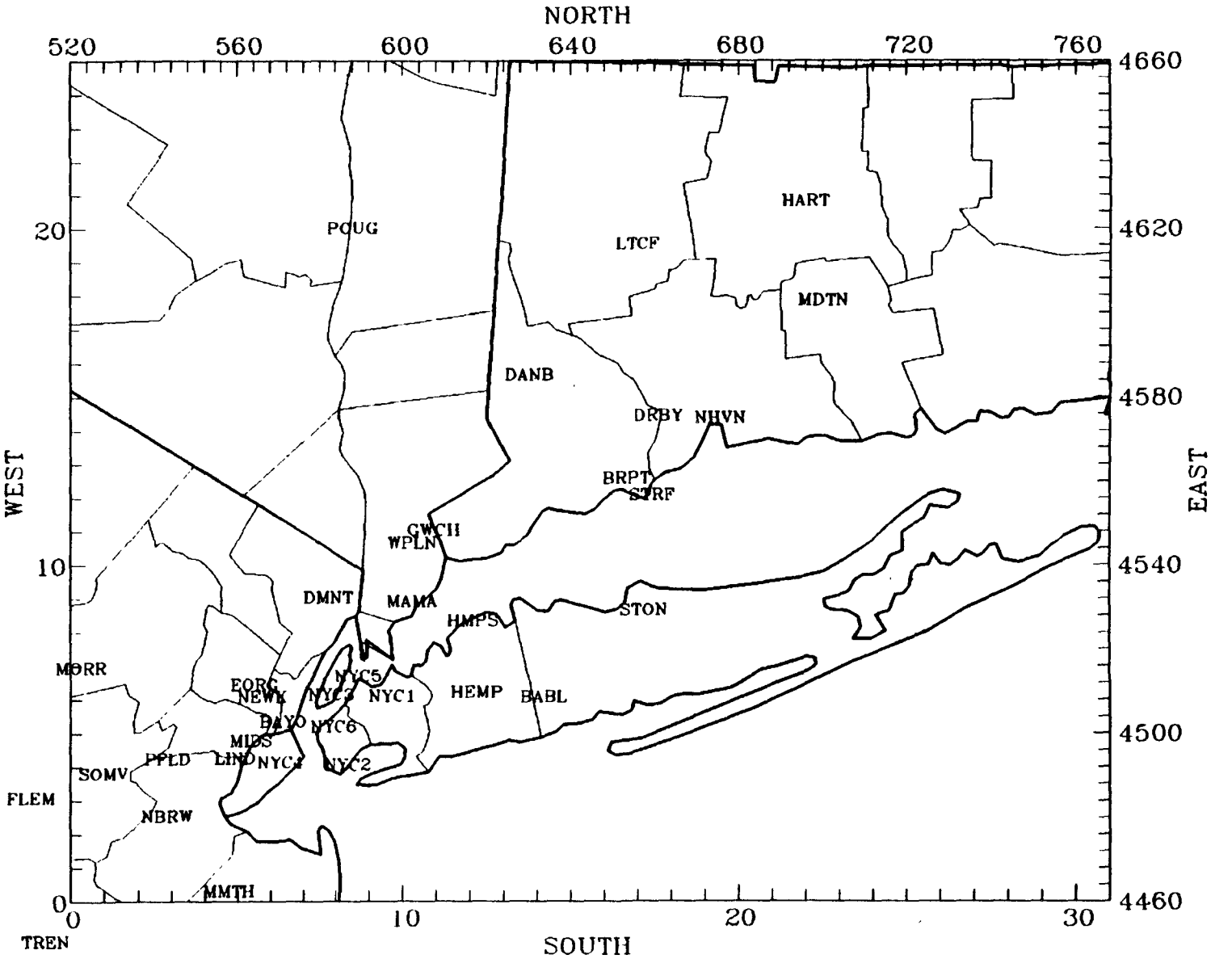

FIGURE 5-1. Locations of ozone monitors within the New York modeling domain.

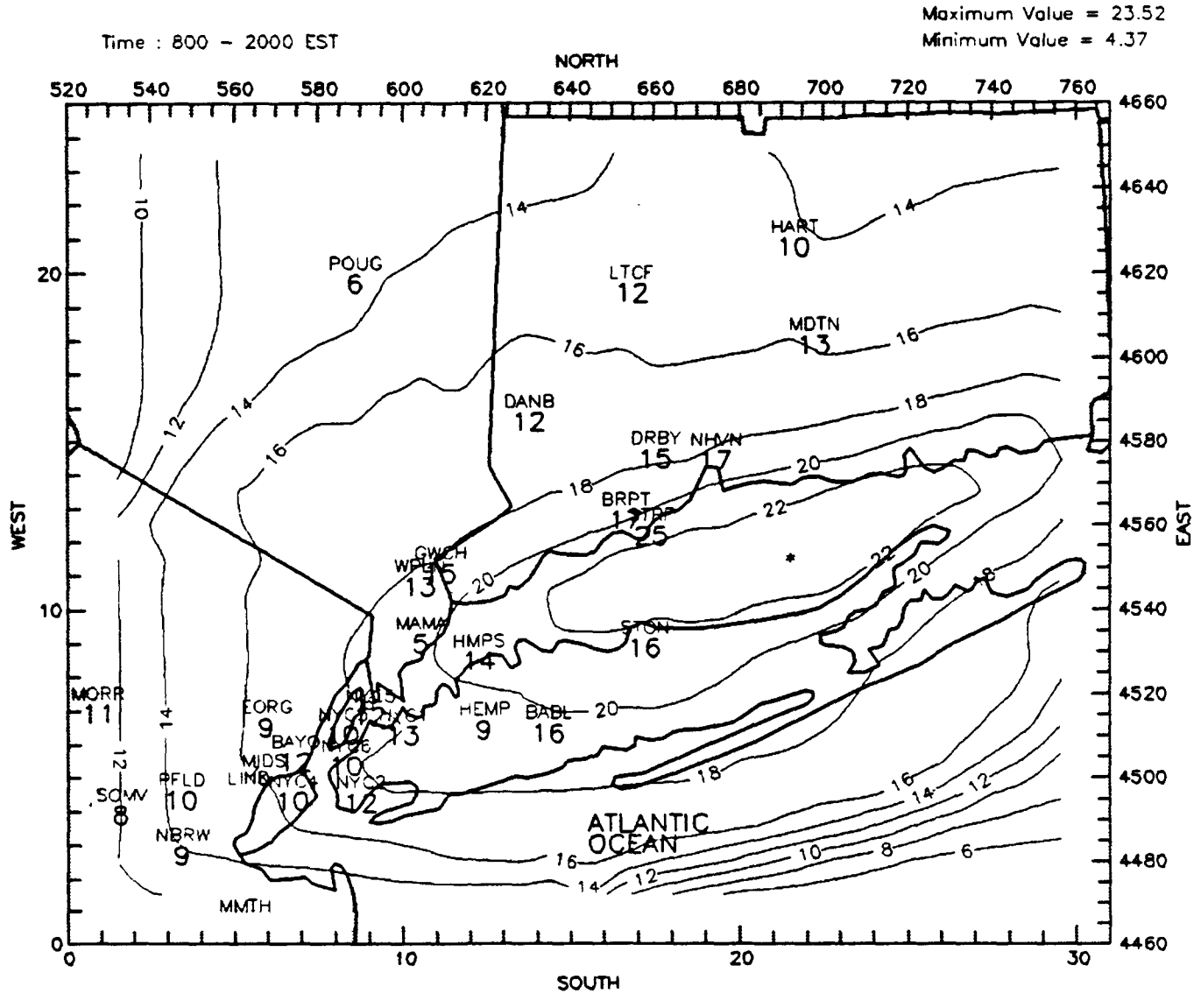

Maximum Ozone Concentration
Evaluation 1
Aug 8, 1980 (pphm)

FIGURE 5-2. Isopleths of predicted maximum daily ozone concentrations (pphm) with superimposed observations for the New York region on 8 August 1980. (* denotes location of maximum concentration value.)

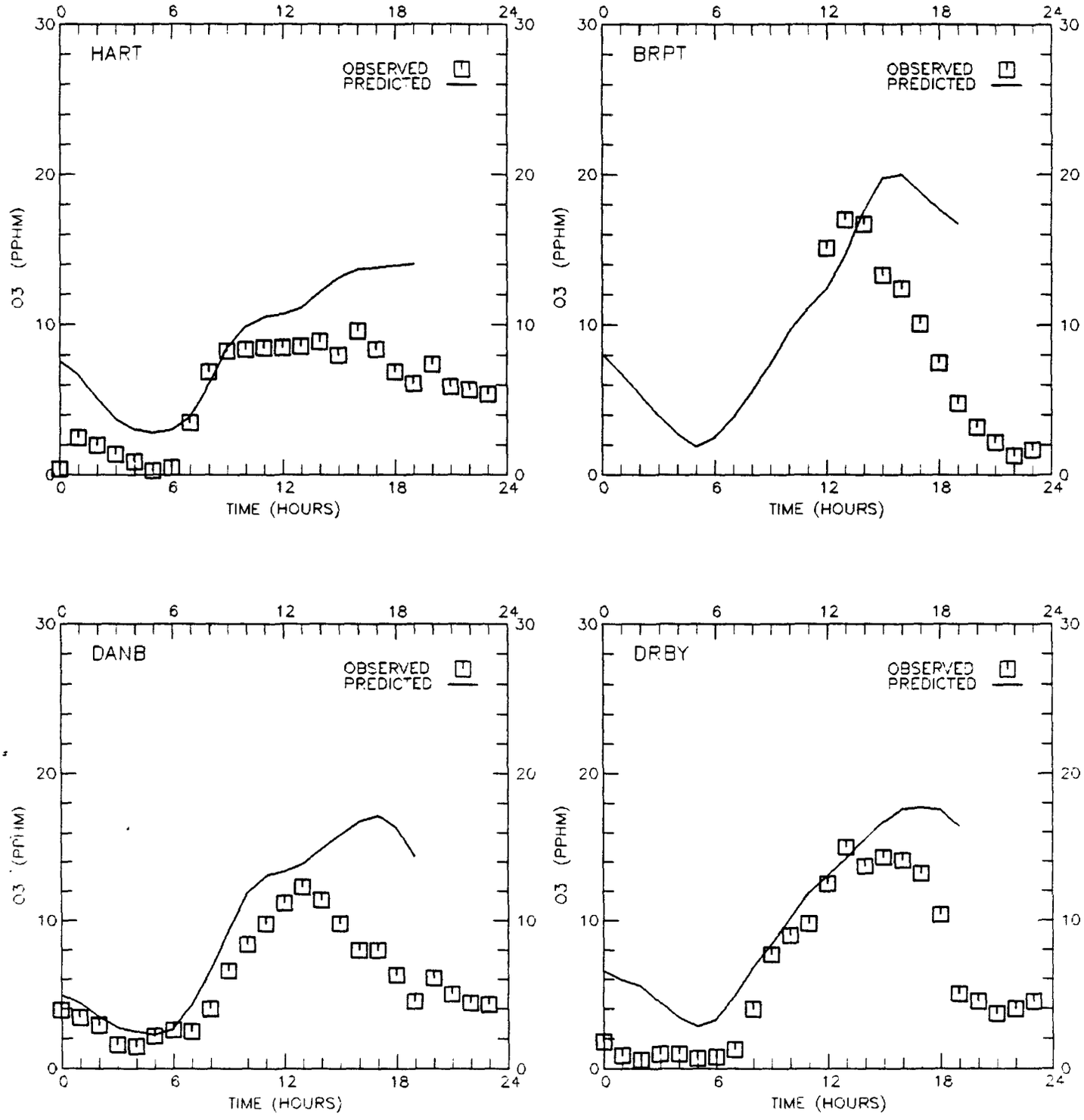

New York - 8/8/80 - O3 - EVALUATION RUN

FIGURE 5-3. Time series of predicted and observed hourly ozone concentrations at all sites in the New York modeling domain.

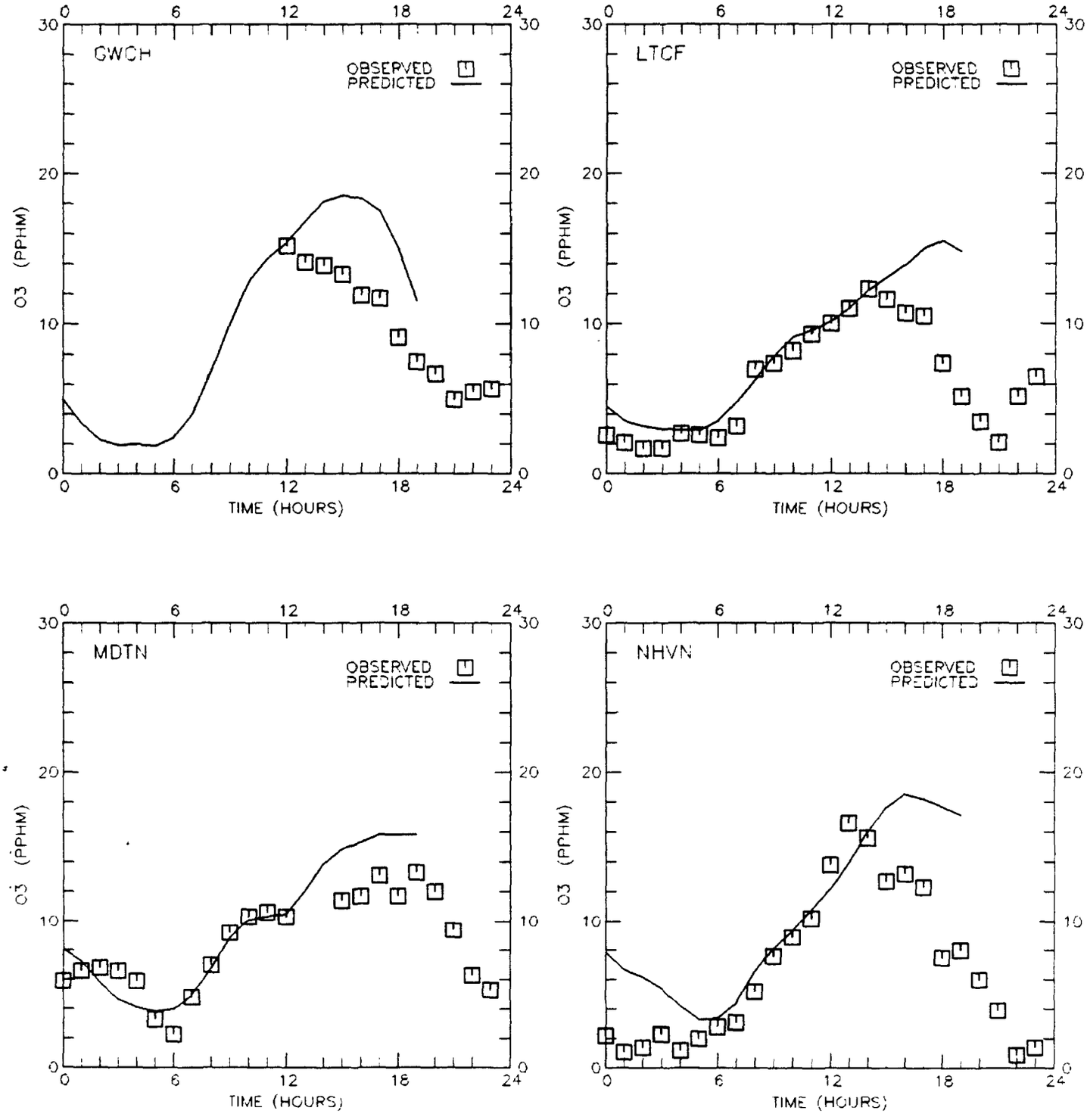

New York – 8/8/80 – O3 – EVALUATION RUN

FIGURE 5-3. Continued.

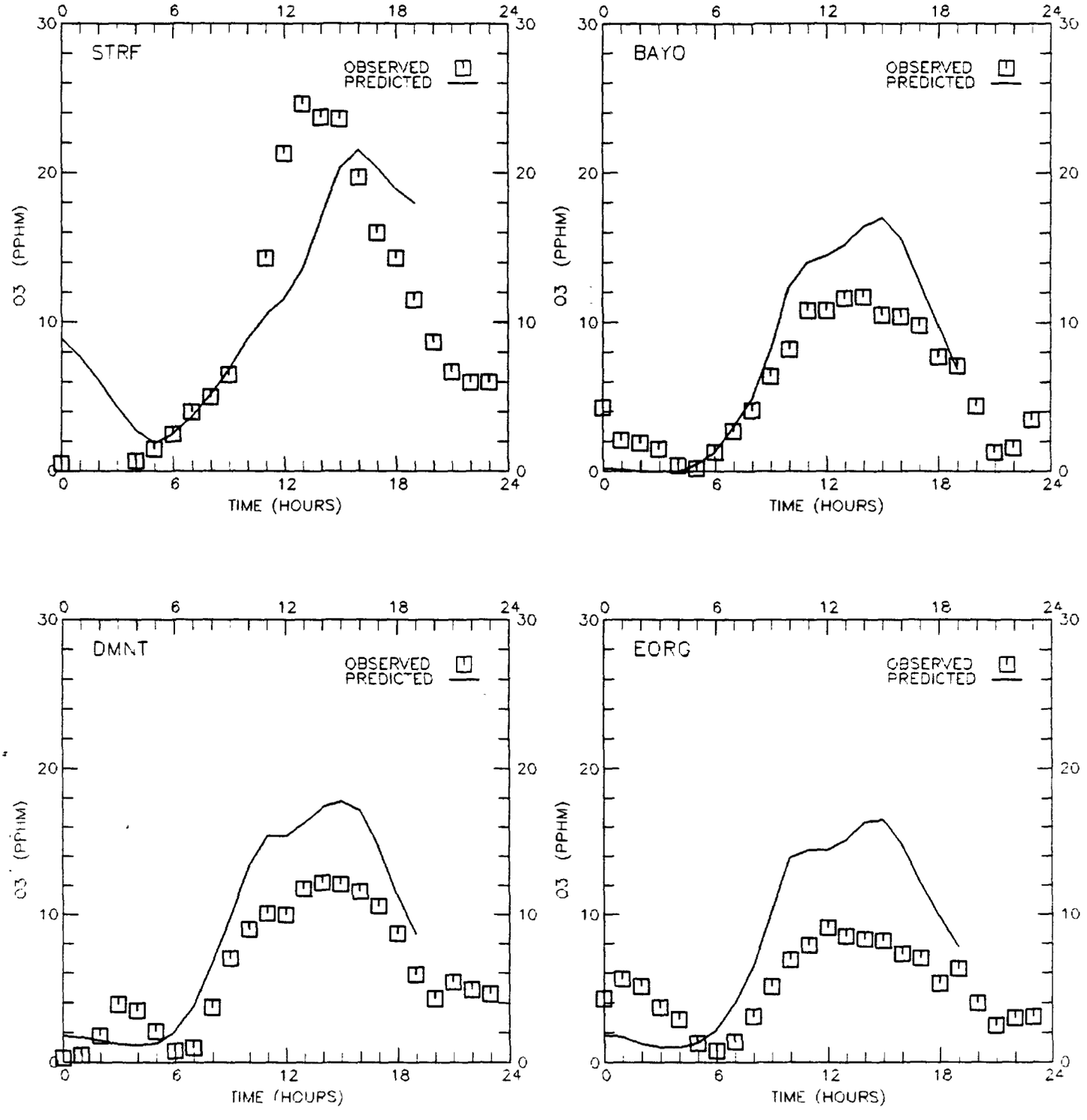

New York – 8/8/80 – O3 – EVALUATION RUN

FIGURE 5-3. Continued.

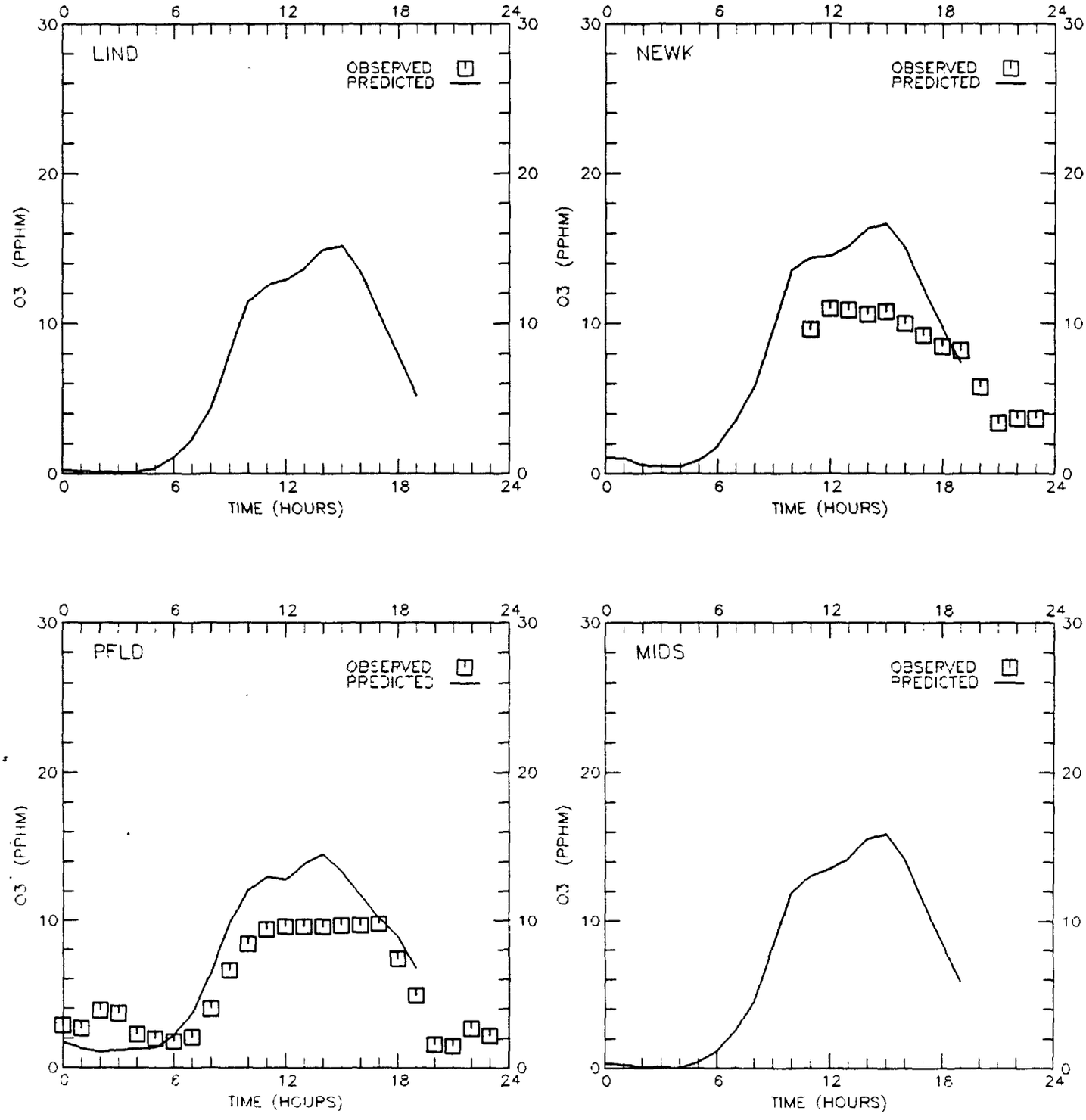

New York – 8/8/80 – O3 – EVALUATION RUN

FIGURE 5-3. Continued.

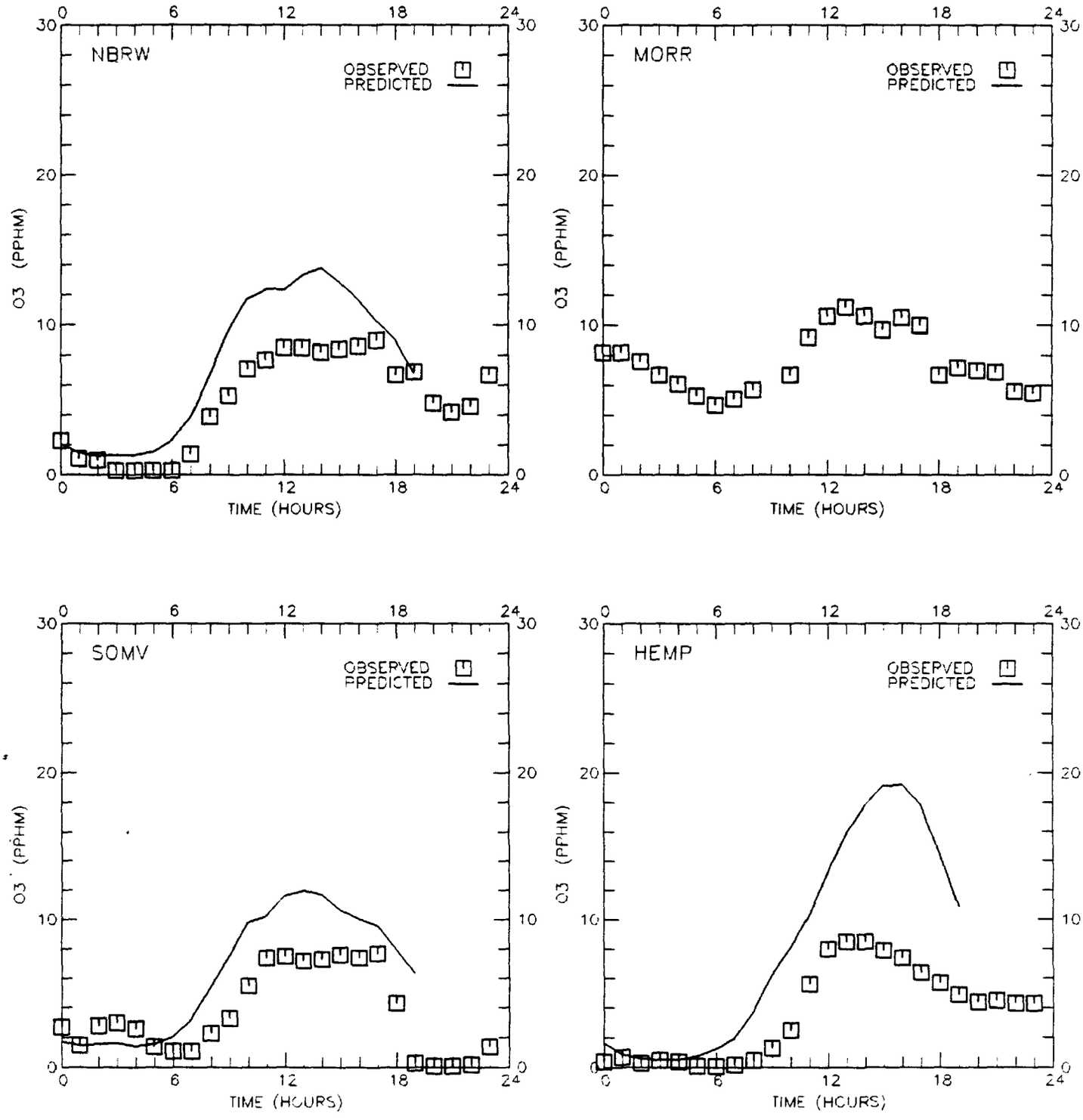

New York – 8/8/80 – O3 – EVALUATION RUN

FIGURE 5-3. Continued.

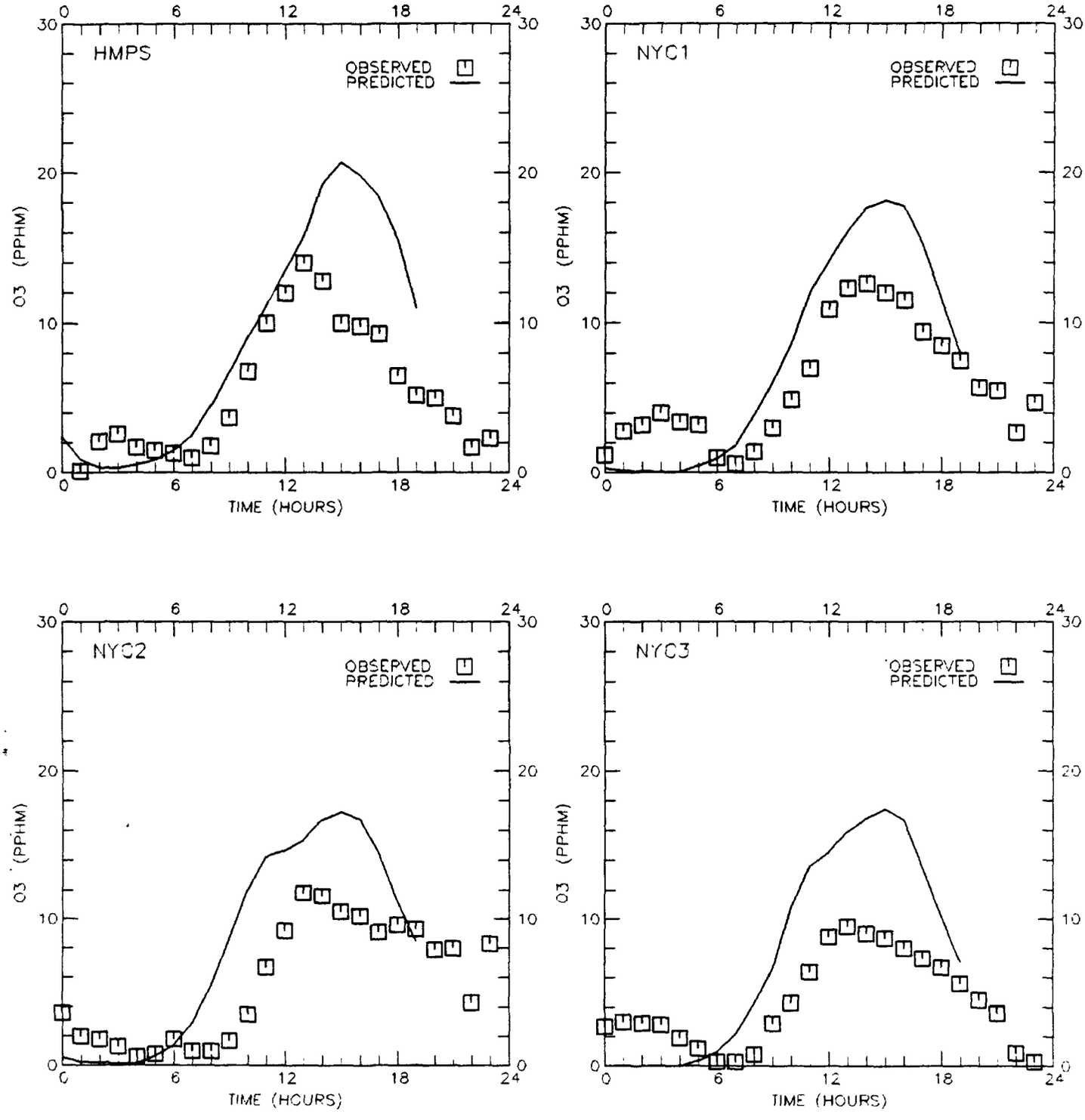

New York – 8/8/80 – O3 – EVALUATION RUN

FIGURE 5-3. Continued.

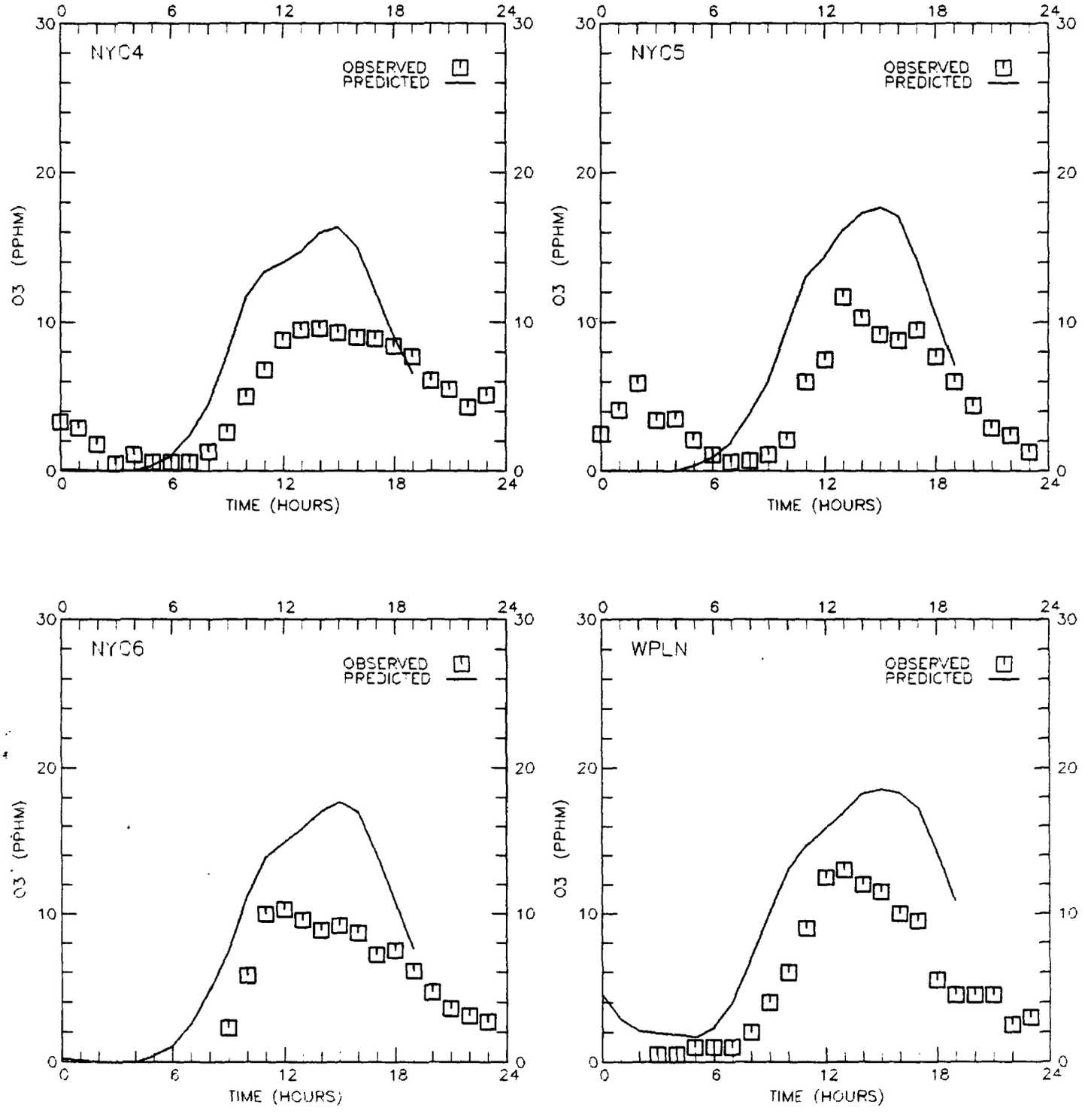

New York – 8/8/80 – O3 – EVALUATION RUN

FIGURE 5-3. Continued.

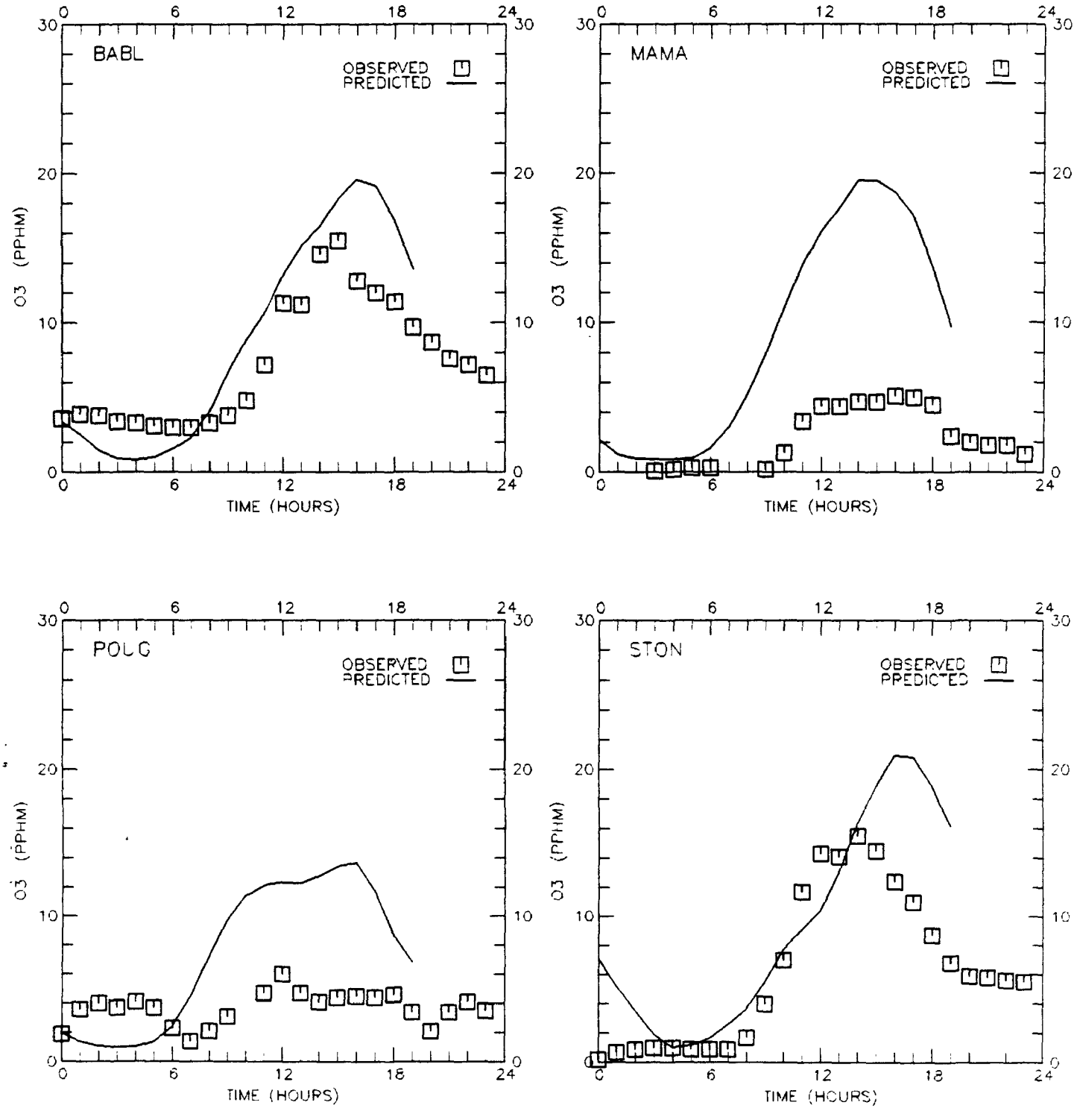

New York – 8/8/80 – O3 – EVALUATION RUN

FIGURE 5-3. Concluded.

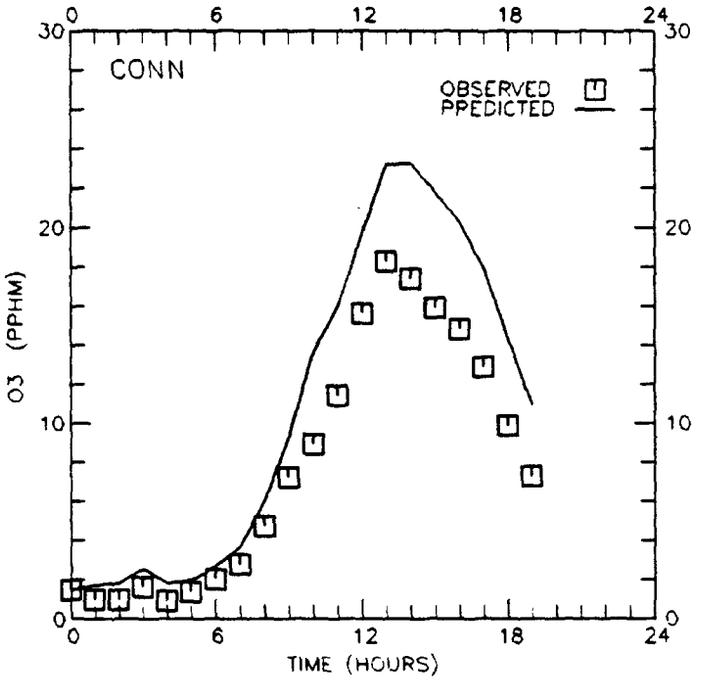

Average Observed = 7.9

Average Predicted = 10.7

Bias = -2.8

Correlation Coefficient = 0.996

Peak Predicted/Peak Observed = 1.27
(at hour 13)

FIGURE 5-4. Statistical performance measures and time series of predicted and observed hourly averaged ozone concentrations averaged over four sites (STRF, BRPT, DRBY, and NHVN) in southern Connecticut.

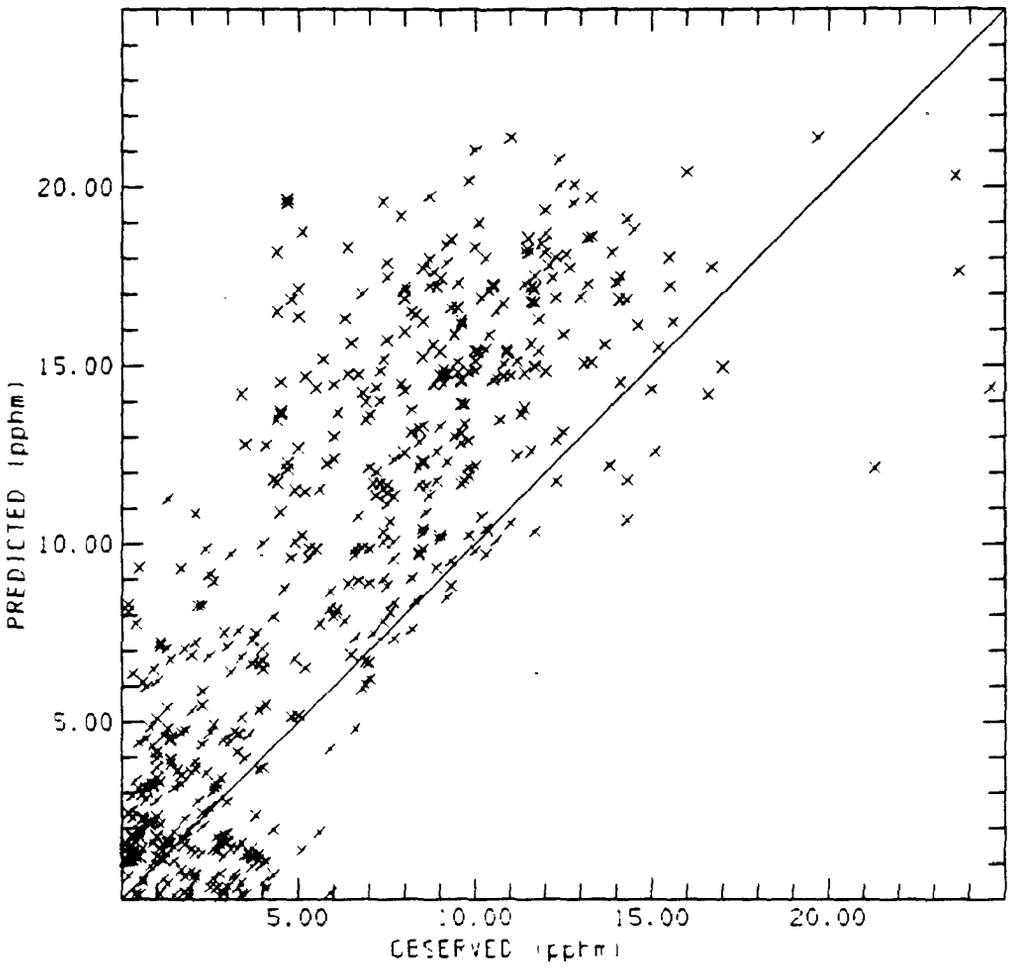

MOMENTS OF THE PROBABILITY DENSITY FUNCTION

	OBSERVED	PREDICTED
AVERAGE	6.15970	9.28025
STANDARD DEVIATION	4.48305	6.17426
SKEWNESS	0.70407	0.04050
KURTOSIS	0.40520	-1.35550
OTHER MEASURES		
MEDIAN	5.60000	9.70000
UPPER QUARTILE	9.30000	14.77000
LOWER QUARTILE	2.20000	3.16000
MINIMUM VALUE	0.10000	0.08000
MAXIMUM VALUE	24.60000	21.37000

SKILL OF PREDICTION PARAMETERS

CORRELATION COEFFICIENT OF PREDICTED VERSUS OBSERVED 0.800
THE BOUNDS OF THE CORRELATION AT THE CONFIDENCE LEVEL OF 0.950 ARE
LOW BOUND 0.767 HIGH BOUND 0.829
RATIO OF OVER TO UNDER PREDICTIONS 4.200
PERCENT OF OVER PREDICTIONS GREATER THAN 200 PERCENT OF THE OBSERVED 30.192
PERCENT OF UNDER PREDICTIONS LESS THAN 50 PERCENT OF THE OBSERVED 9.808

FIGURE 5-5a. Scatterplot of predicted versus observed hourly ozone concentrations (matched by time and locations) for New York region on 8 August 1980 (N = 520).

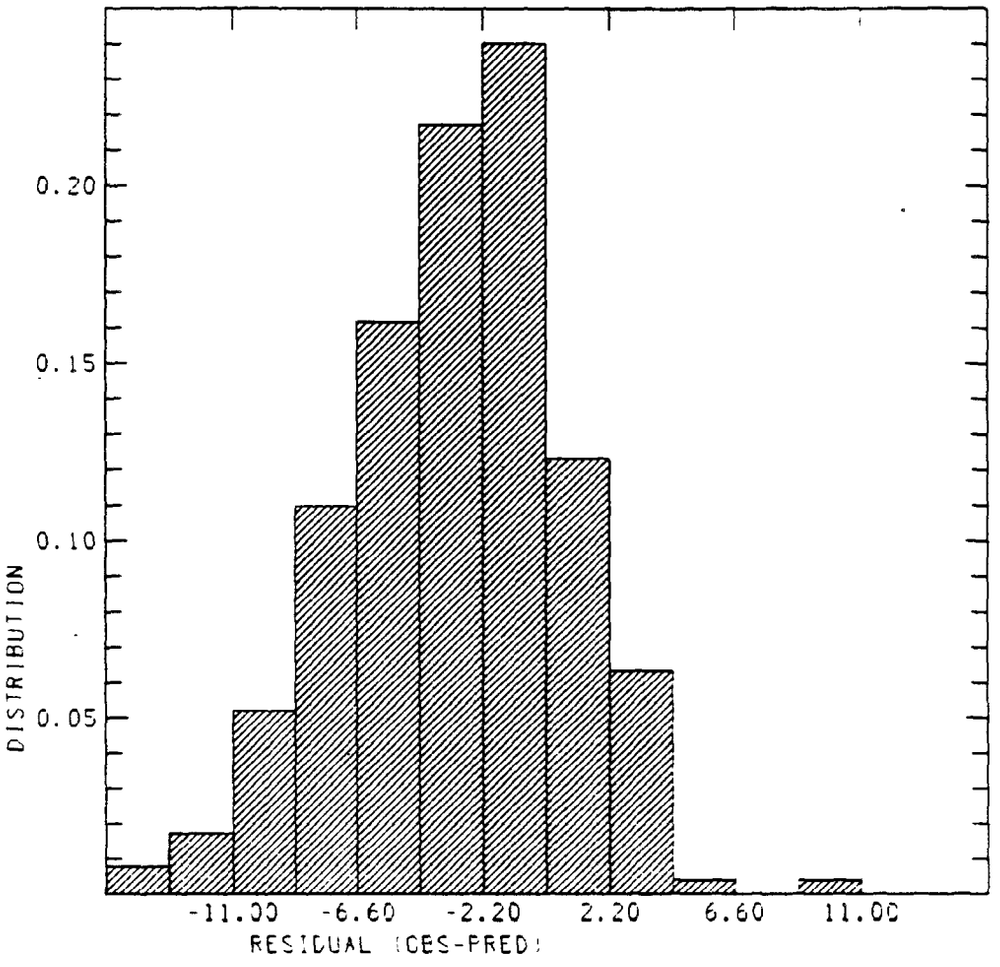

THE BINSIZE EQUALS 2.200

RESIDUAL ANALYSIS

AVERAGE	-3.12072
STANDARD DEVIATION	3.73333
SKEWNESS	-0.22626
KURTOSIS	0.18046
OTHER MEASURES	
MEDIAN	-2.78000
UPPER QUARTILE	-0.47000
LOWER QUARTILE	-5.61000
MINIMUM VALUE	-14.96000
MAXIMUM VALUE	10.21000

BIAS CONFIDENCE INTERVAL
AT THE 0.0500 LEVEL
LOWER BOUND -3.6722
UPPER BOUND -2.5692

STD RESIDUAL CONFIDENCE INTERVAL
AT THE 0.0500 LEVEL
LOWER BOUND 12.6228
UPPER BOUND 15.4829

THE MEASURES OF GROSS ERROR
THE ROOT MEAN SQUARE ERROR IS 4.86
THE AVERAGE ABSOLUTE ERROR IS 3.84

VARIOUS MEASURES OF RELATIVE VARIABILITY
OBSERVATION COEFFICIENT OF VARIATION
0.7278
RESIDUAL COEFFICIENT OF VARIATION
0.6061
RATIO OF RESIDUAL TO OBSERVED ST. DEV.
0.8328

FIGURE 5-5b. Residual analysis of observed minus predicted hourly ozone concentrations for New York region on 8 August 1980 (N = 520).

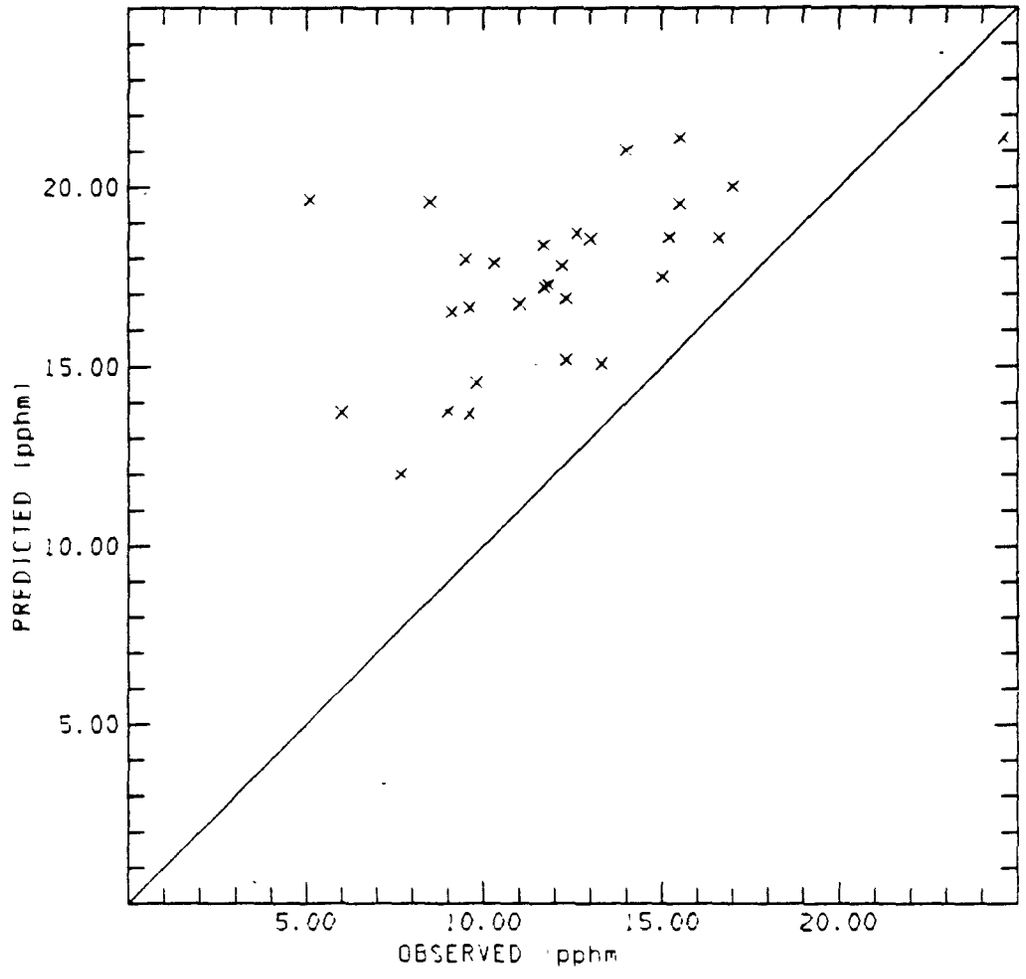

MOMENTS OF THE PROBABILITY DENSITY FUNCTION

	OBSERVED	PREDICTED
AVERAGE	12.05171	17.43653
STANDARD DEVIATION	3.84678	2.41584
SKEWNESS	0.93123	-0.34467
KURTOSIS	1.85087	-0.65029
OTHER MEASURES		
MEDIAN	11.70000	17.48000
UPPER QUARTILE	13.30000	18.59000
LOWER QUARTILE	9.50000	15.16000
MINIMUM VALUE	5.10000	12.01000
MAXIMUM VALUE	24.60000	21.37000

SKILL OF PREDICTION PARAMETERS

CORRELATION COEFFICIENT OF PREDICTED VERSUS OBSERVED 0.576
THE BOUNDS OF THE CORRELATION AT THE CONFIDENCE LEVEL OF 0.050 ARE
LOW BOUND 0.266 HIGH BOUND 0.778
RATIO OF OVER TO UNDER PREDICTIONS 28.000
PERCENT OF OVER PREDICTIONS GREATER THAN 200 PERCENT OF THE OBSERVED 10.345
PERCENT OF UNDER PREDICTIONS LESS THAN 50 PERCENT OF THE OBSERVED 0.000

FIGURE 5-6a. Scatterplot of predicted versus observed maximum daily ozone concentrations (matched by location but not time) for 8 August 1980 (N = 29).

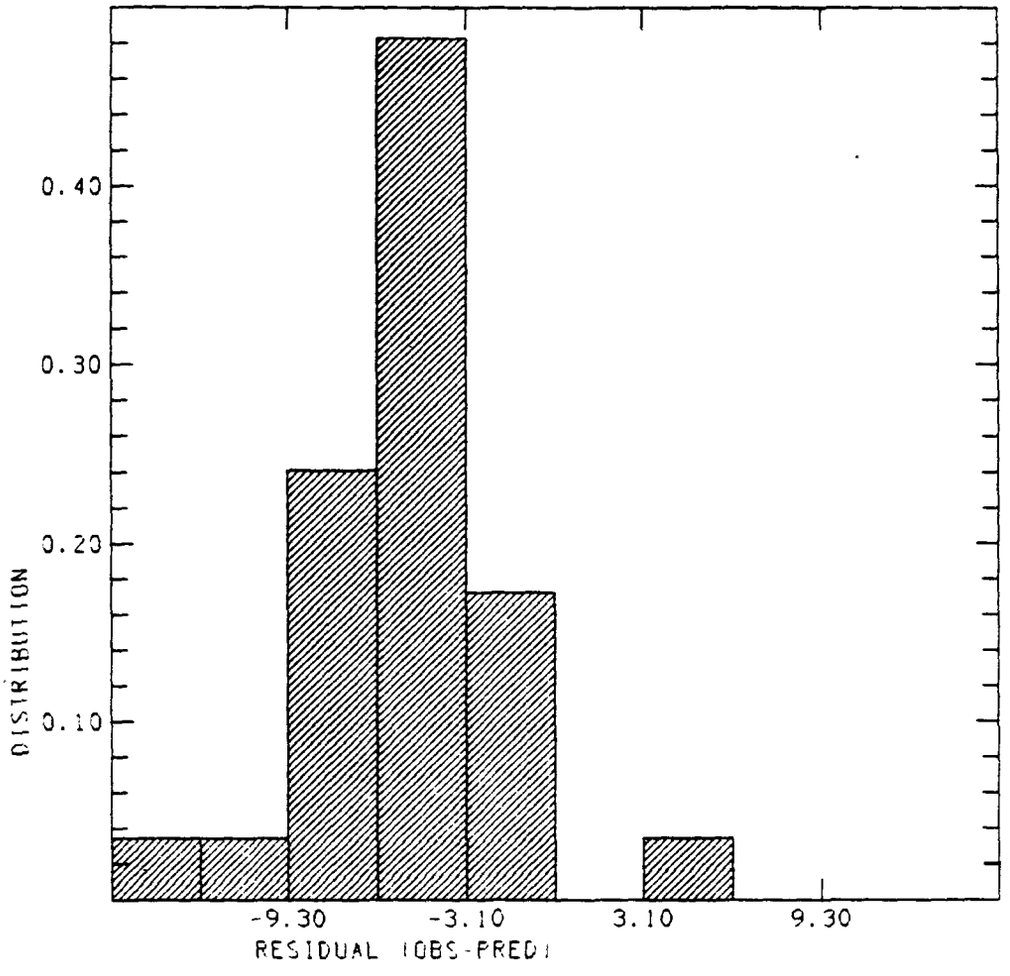

THE BINSIZE EQUALS 3.100

RESIDUAL ANALYSIS

AVERAGE	-5.38483
STANDARD DEVIATION	3.15023
SKEWNESS	-0.25710
KURTOSIS	2.01413
OTHER MEASURES	
MEDIAN	-5.56000
UPPER QUARTILE	-4.10000
LOWER QUARTILE	-7.02000
MINIMUM VALUE	-14.56000
MAXIMUM VALUE	3.24000

BIAS CONFIDENCE INTERVAL
AT THE 0.0500 LEVEL
LOWER BOUND -6.8184
UPPER BOUND -3.9513

STD RESIDUAL CONFIDENCE INTERVAL
AT THE 0.0500 LEVEL
LOWER BOUND 6.7631
UPPER BOUND 16.2557

THE MEASURES OF GROSS ERROR
THE ROOT MEAN SQUARE ERROR IS 6.21
THE AVERAGE ABSOLUTE ERROR IS 5.61

VARIOUS MEASURES OF RELATIVE VARIABILITY
OBSERVATION COEFFICIENT OF VARIATION
0.3192
RESIDUAL COEFFICIENT OF VARIATION
0.2614
RATIO OF RESIDUAL TO OBSERVED ST. DEV.
0.8189

FIGURE 5-6b. Residual analysis of observed minus predicted maximum daily ozone concentrations for 8 August 1980 (N = 29).

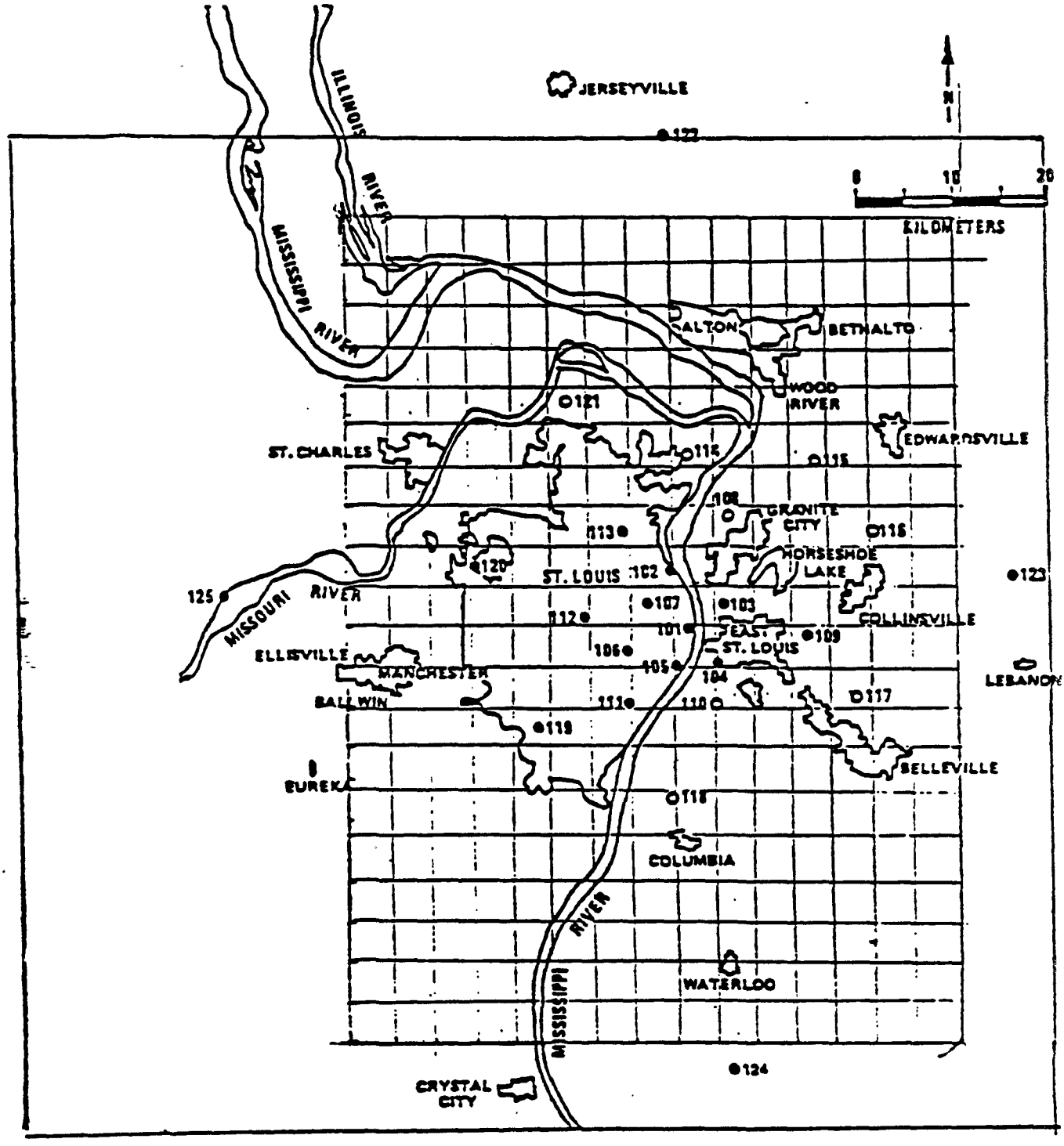

FIGURE 5-7. The St. Louis modeling domain showing the location of the RAPS ozone monitors. (Source: Cole et al., 1983)

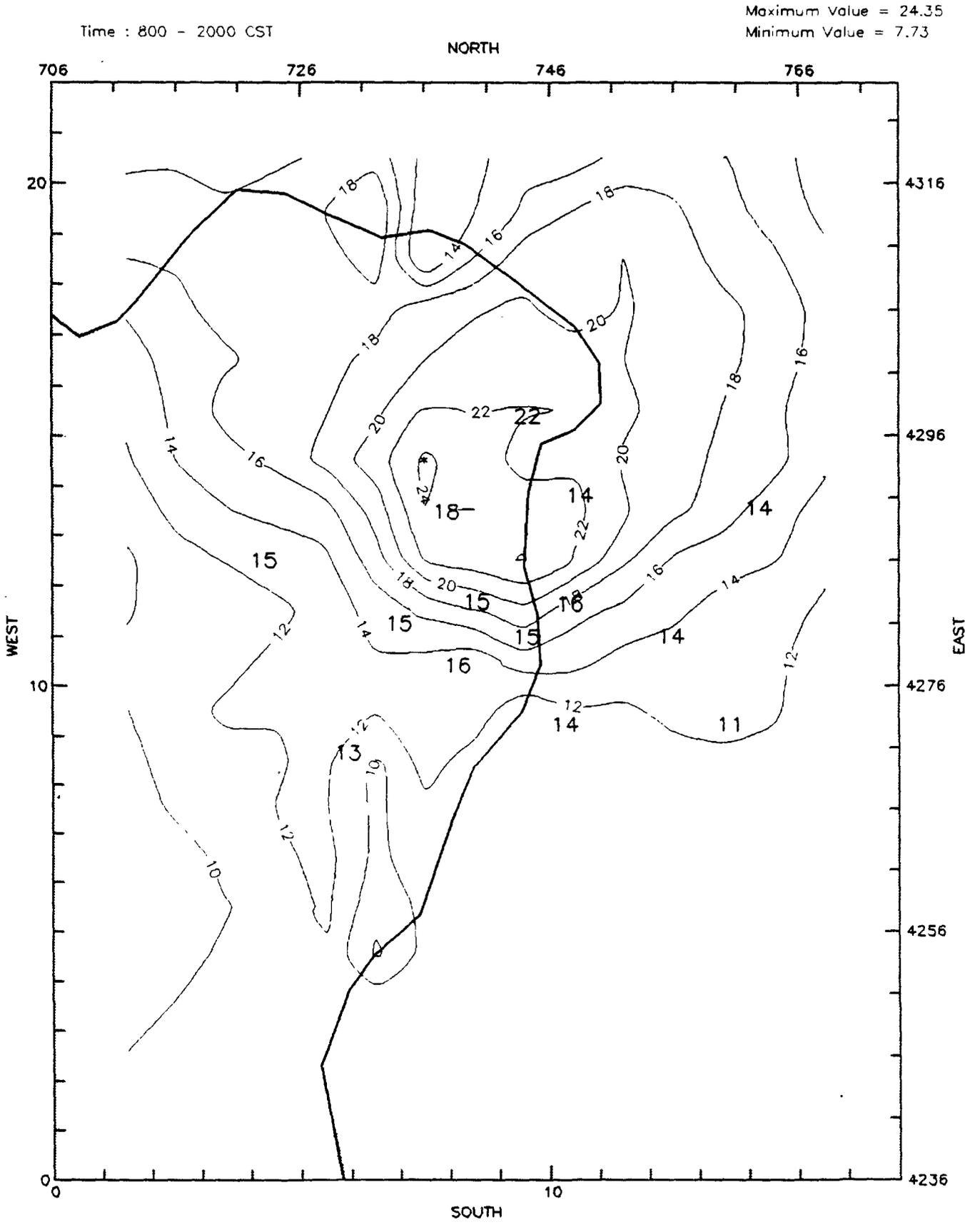

FIGURE 5-8. Isopleths of predicted maximum daily ozone concentrations (pphm) with superimposed maximum daily observations for the St. Louis region on 13 July 1976. (* denotes location of maximum concentration value.)

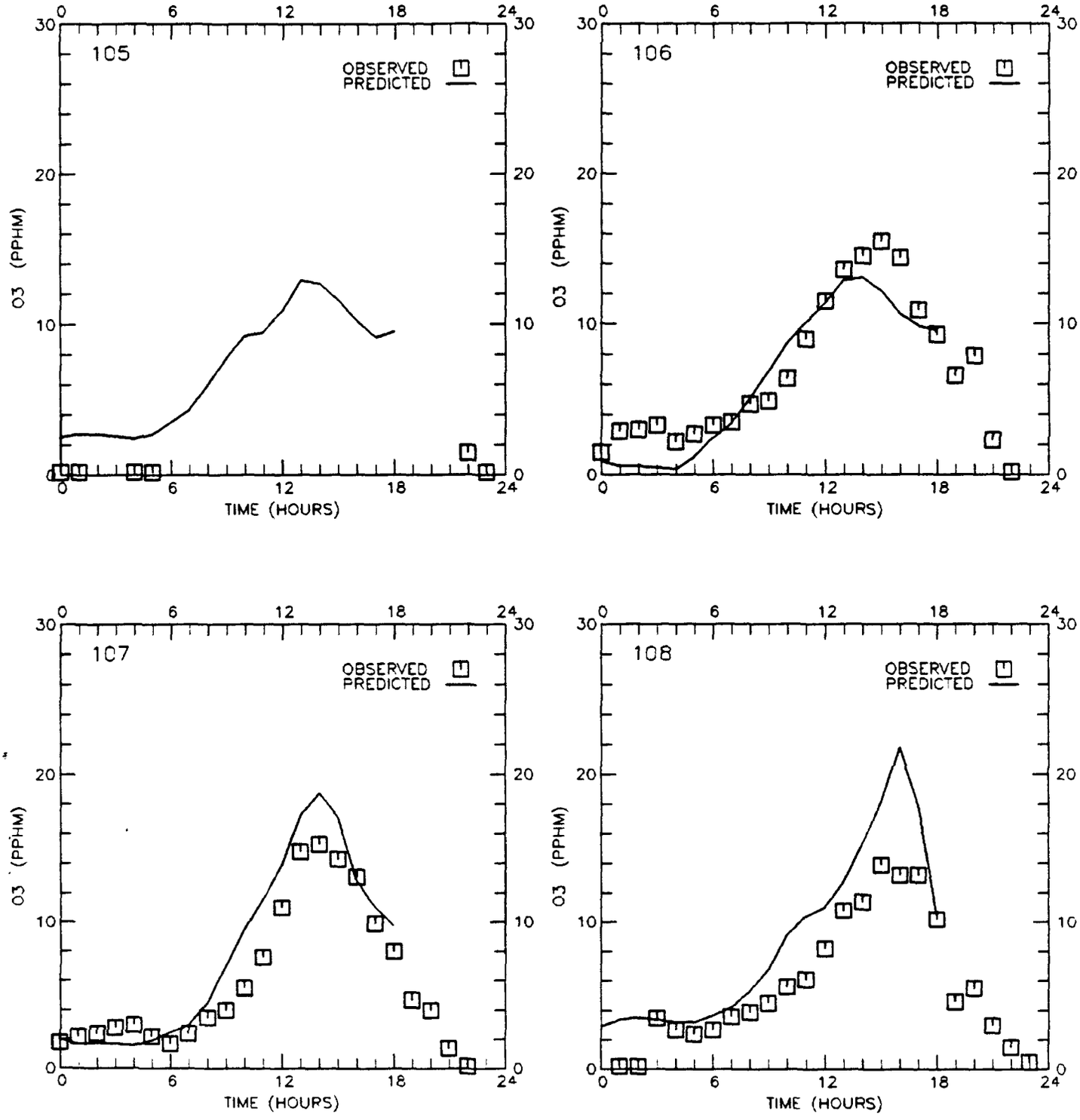

ST. LOUIS - 7/13/76 - O3 - EVALUATION RUN

FIGURE 5-9. Time series of predicted and observed hourly ozone concentrations at all sites in the St. Louis modeling domain.

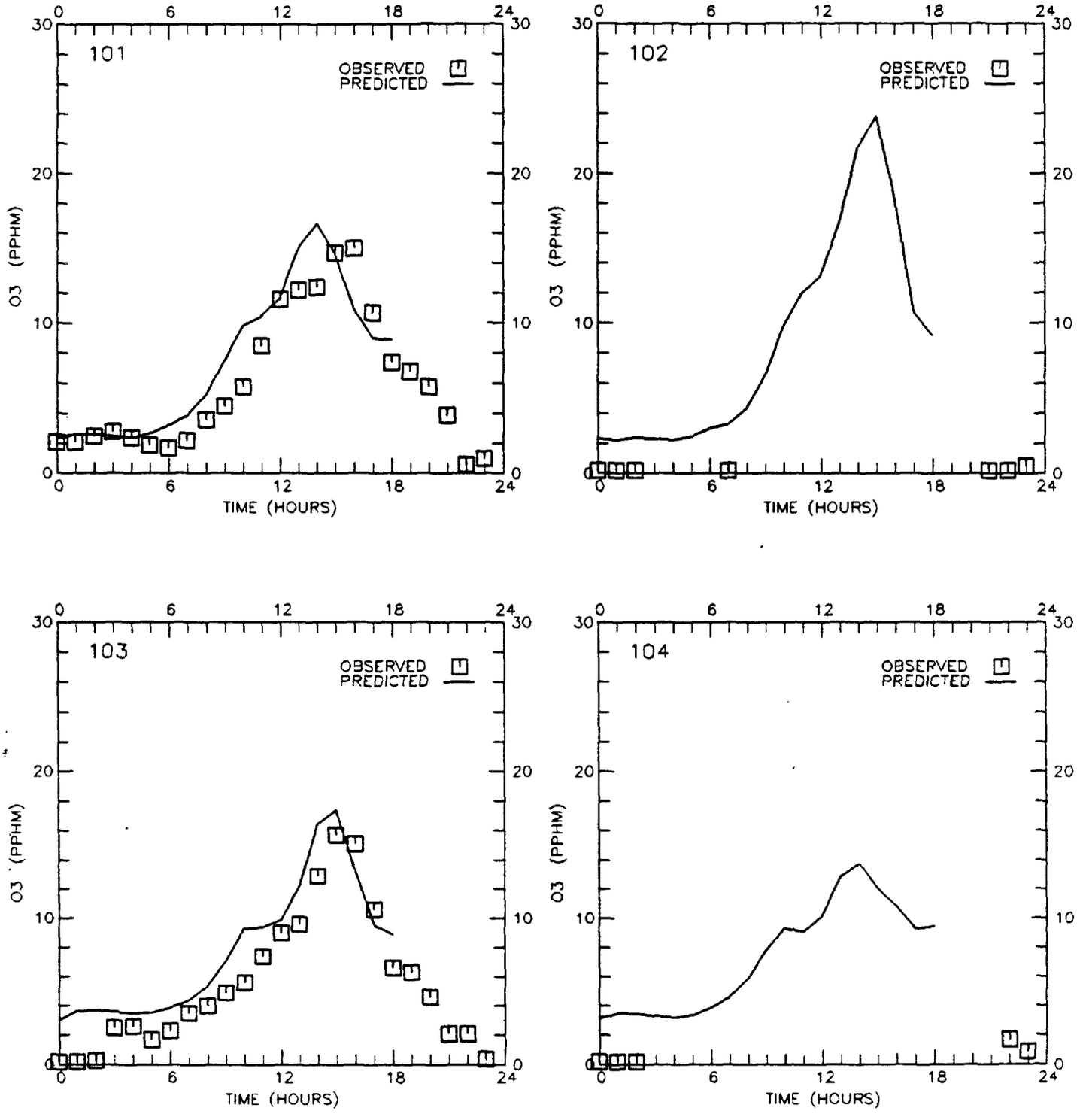

ST. LOUIS - 7/13/76 - O3 - EVALUATION RUN

FIGURE 5-9. Continued.

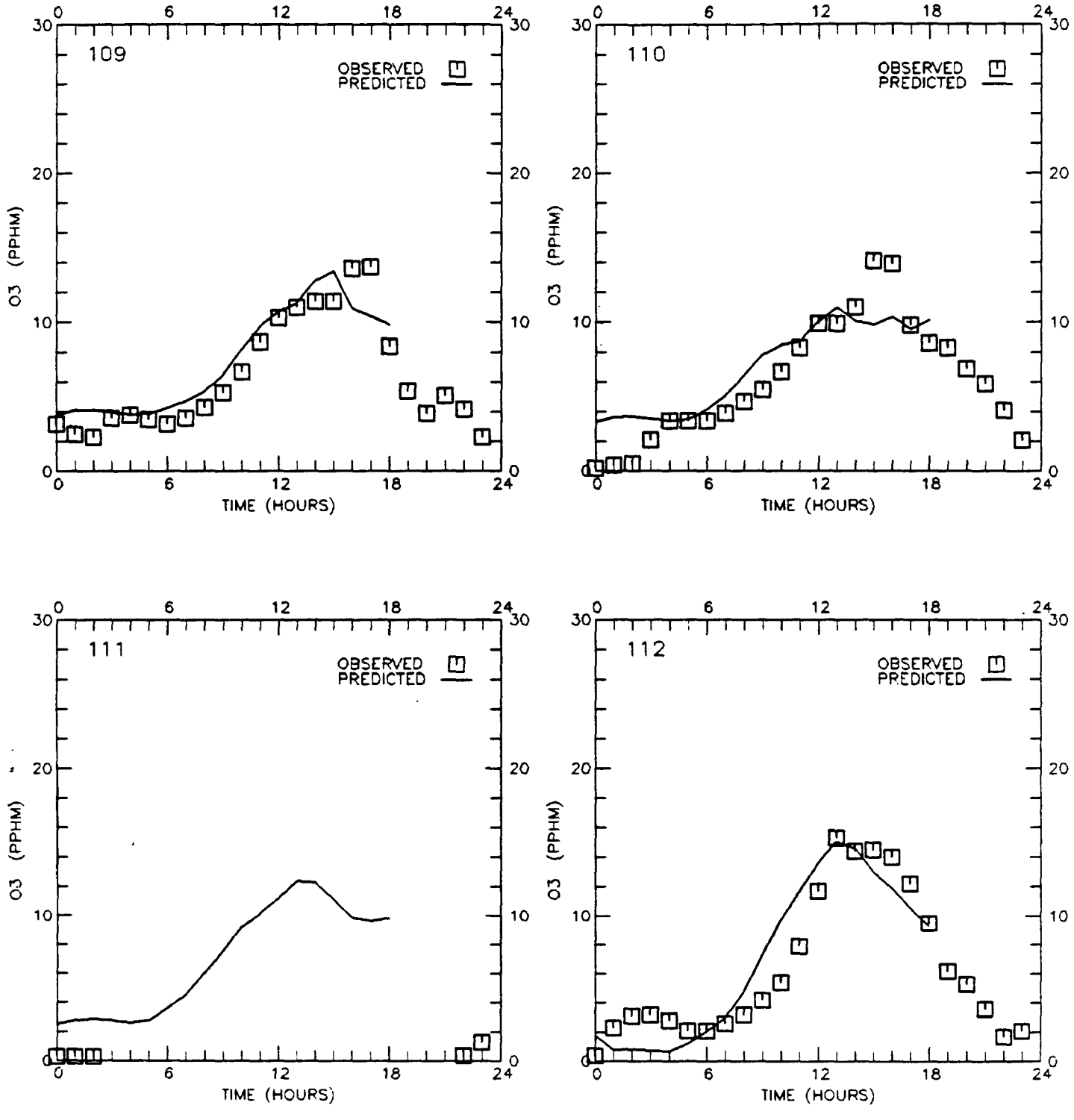

ST. LOUIS – 7/13/76 – O3 – EVALUATION RUN

FIGURE 5-9. Continued.

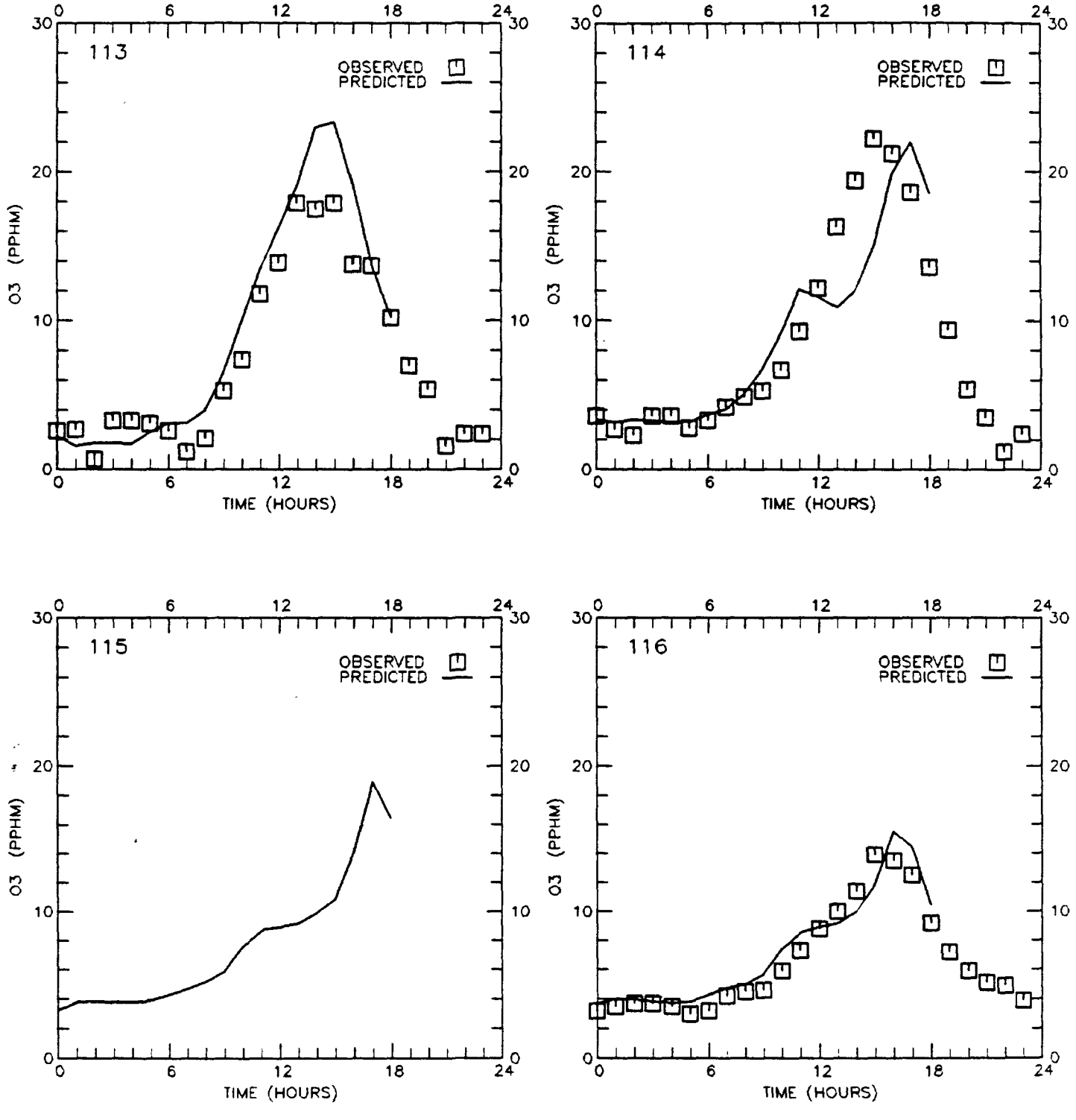

ST. LOUIS - 7/13/76 - O3 - EVALUATION RUN

FIGURE 5-9. Continued.

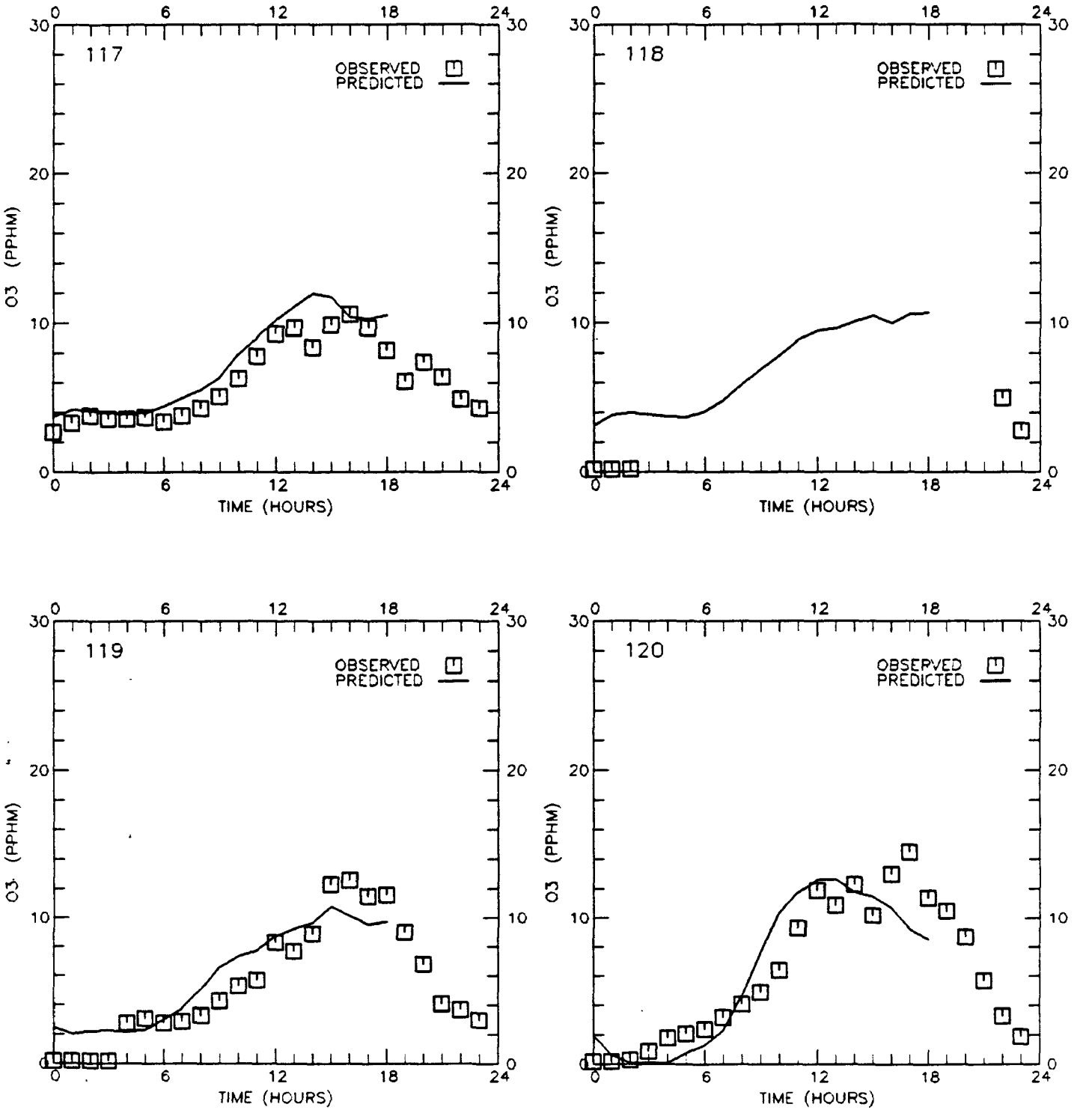

ST. LOUIS - 7/13/76 - O3 - EVALUATION RUN

FIGURE 5-9. Continued.

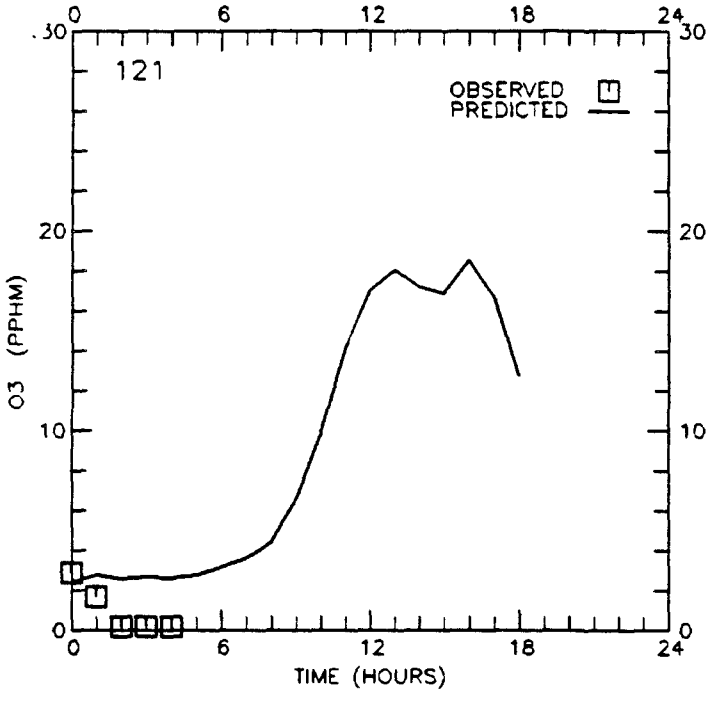

ST. LOJIS – 7/13/76 – 03 – EVALUATION RUN

FIGURE 5-9. Concluded.

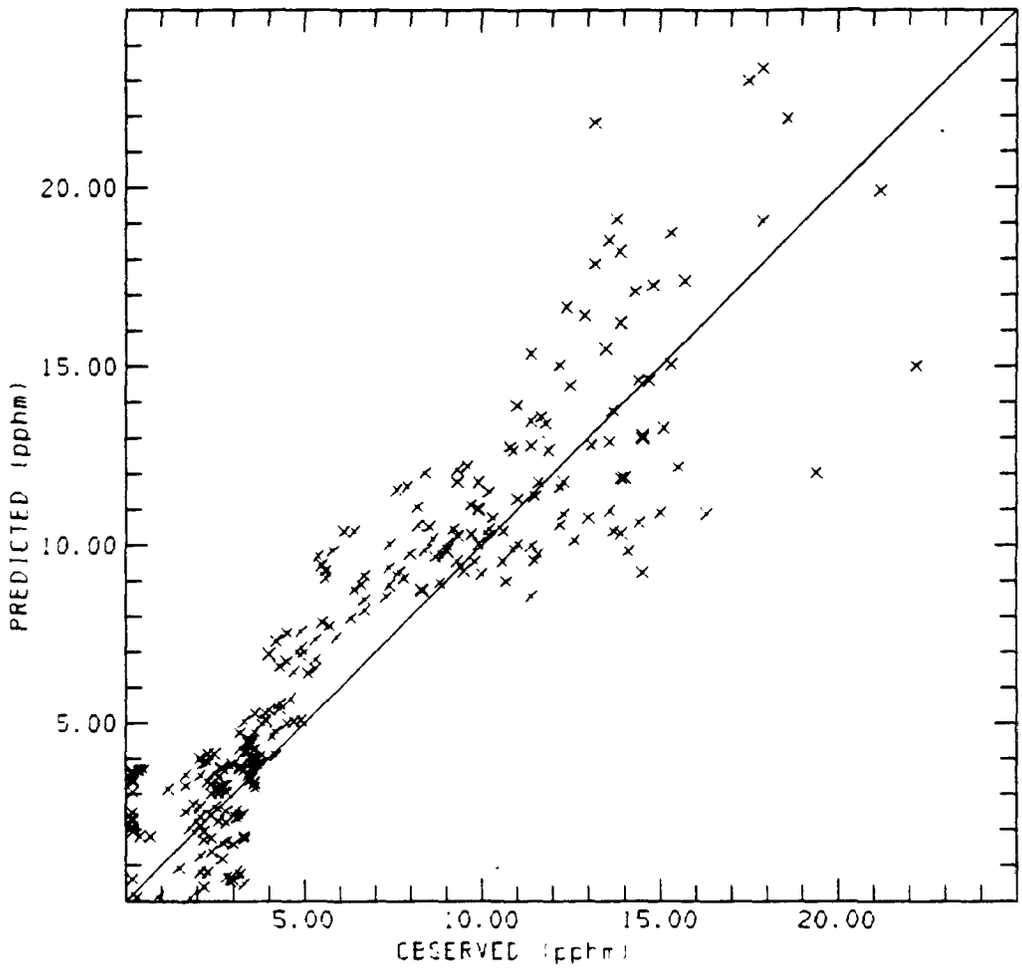

MOMENTS OF THE PROBABILITY DENSITY FUNCTION

	OBSERVED	PREDICTED
AVERAGE	6.77843	7.51675
STANDARD DEVIATION	4.85895	4.99583
SKEWNESS	0.68694	0.69536
KURTOSIS	-0.47257	-0.01638
OTHER MEASURES		
MEDIAN	4.90000	6.79000
UPPER QUARTILE	10.60000	10.57000
LOWER QUARTILE	2.90000	3.42000
MINIMUM VALUE	0.20000	0.11000
MAXIMUM VALUE	22.20000	23.37000

SKILL OF PREDICTION PARAMETERS

CORRELATION COEFFICIENT OF PREDICTED VERSUS OBSERVED 0.914
THE BOUNDS OF THE CORRELATION AT THE CONFIDENCE LEVEL OF 0.950 ARE
LOW BOUND 0.891 HIGH BOUND 0.932
RATIO OF OVER TO UNDER PREDICTIONS 2.442
PERCENT OF OVER PREDICTIONS
GREATER THAN 200 PERCENT OF THE
OBSERVED 6.792
PERCENT OF UNDER PREDICTIONS
LESS THAN 50 PERCENT OF THE
OBSERVED 4.906

FIGURE 5-10a. Scatterplot of predicted versus observed hourly ozone concentrations (matched by time and locations) for St. Louis region on 13 July 1976 (N = 265).

88151

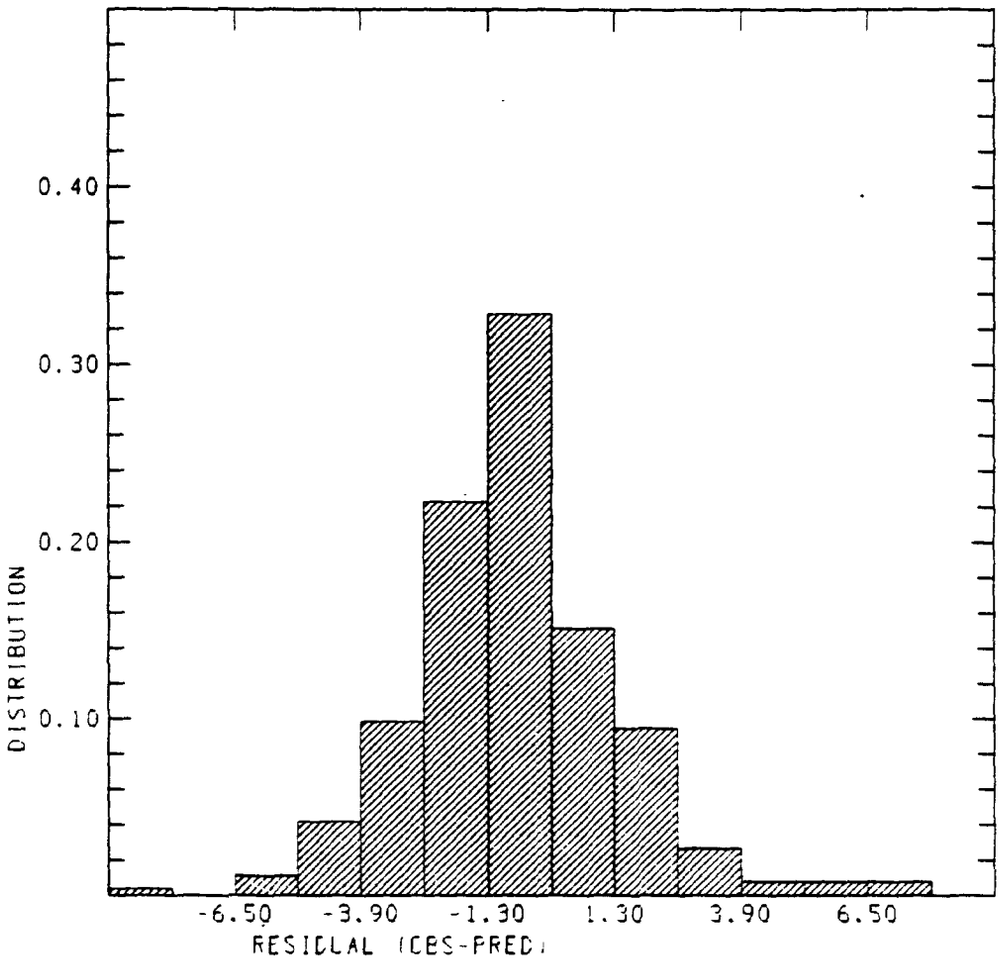

THE BINSIZE EQUALS 1.300

RESIDUAL ANALYSIS

AVERAGE	-0.73835
STANDARD DEVIATION	2.05125
SKEWNESS	0.40933
KURTOSIS	2.00005
OTHER MEASURES	
MEDIAN	-0.88000
UPPER QUARTILE	0.25000
LOWER QUARTILE	-1.92000
MINIMUM VALUE	-8.62000
MAXIMUM VALUE	7.36000

BIAS CONFIDENCE INTERVAL
AT THE 0.0500 LEVEL
LOWER BOUND -1.4451
UPPER BOUND -0.0316

STD RESIDUAL CONFIDENCE INTERVAL
AT THE 0.0500 LEVEL
LOWER BOUND 3.6681
UPPER BOUND 4.8841

THE MEASURES OF GROSS ERROR
THE ROOT MEAN SQUARE ERROR IS 2.18
THE AVERAGE ABSOLUTE ERROR IS 1.67

VARIOUS MEASURES OF RELATIVE VARIABILITY
OBSERVATION COEFFICIENT OF VARIATION
0.7168
RESIDUAL COEFFICIENT OF VARIATION
0.3026
RATIO OF RESIDUAL TO OBSERVED ST. DEV.
0.4222

FIGURE 5-10b. Residual analysis of observed minus predicted hourly ozone concentrations for St. Louis region on 13 July 1976 (N = 265).

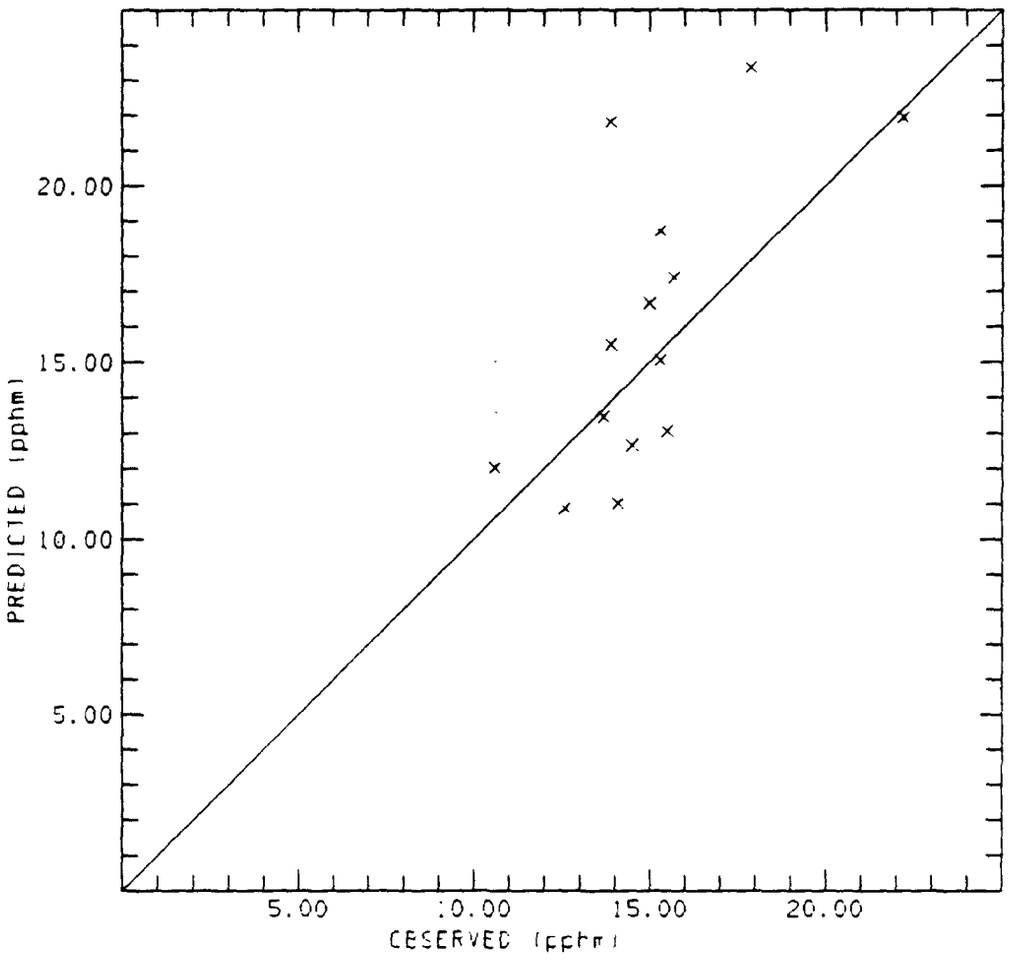

MOMENTS OF THE PROBABILITY DENSITY FUNCTION

	OBSERVED	PREDICTED
AVERAGE	15.01427	15.96999
STANDARD DEVIATION	2.65243	4.18404
SKEWNESS	1.10826	0.43840
KURTOSIS	1.55511	-1.30929
OTHER MEASURES		
MEDIAN	14.50000	15.06000
UPPER QUARTILE	15.30000	17.39000
LOWER QUARTILE	13.70000	12.62000
MINIMUM VALUE	10.60000	10.87000
MAXIMUM VALUE	22.20000	23.37000

SKILL OF PREDICTION PARAMETERS

CORRELATION COEFFICIENT OF PREDICTED VERSUS OBSERVED 0.676
THE BOUNDS OF THE CORRELATION AT THE CONFIDENCE LEVEL OF 0.950 ARE
LOW BOUND 0.227 HIGH BOUND 0.888
RATIO OF OVER TO UNDER PREDICTIONS 1.000
PERCENT OF OVER PREDICTIONS
GREATER THAN 200 PERCENT OF THE OBSERVED 0.000
PERCENT OF UNDER PREDICTIONS
LESS THAN 50 PERCENT OF THE OBSERVED 0.000

FIGURE 5-11a. Scatterplot of predicted versus observed maximum daily ozone concentrations (matched by location but not time) for 13 July 1976 (N = 14).

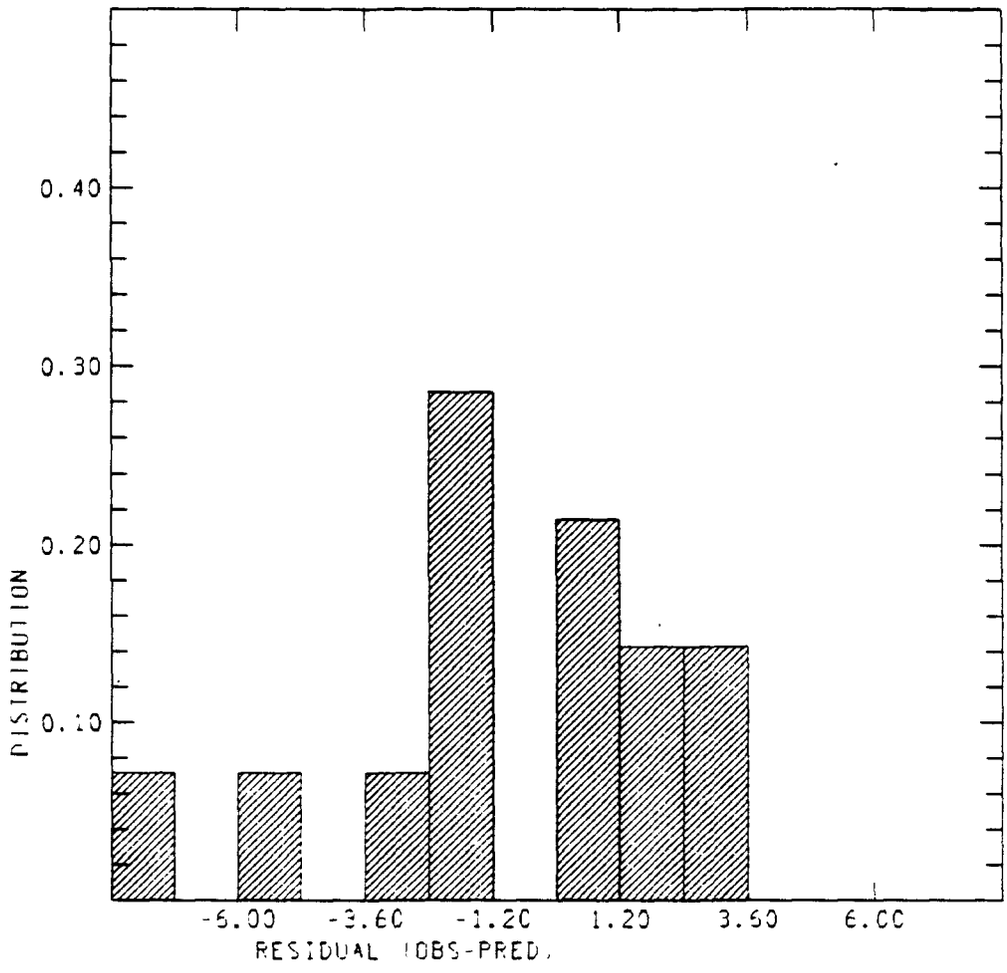

THE BINSIZE EQUALS 1.200

RESIDUAL ANALYSIS

AVERAGE	-0.95571
STANDARD DEVIATION	3.08663
SKEWNESS	-0.71570
KURTOSIS	-0.38413
OTHER MEASURES	
MEDIAN	-1.42000
UPPER QUARTILE	0.26000
LOWER QUARTILE	-3.43000
MINIMUM VALUE	-7.92000
MAXIMUM VALUE	3.08000

BIAS CONFIDENCE INTERVAL
AT THE 0.0500 LEVEL
LOWER BOUND -3.2883
UPPER BOUND 1.3769

STD RESIDUAL CONFIDENCE INTERVAL
AT THE 0.0500 LEVEL
LOWER BOUND 5.6337
UPPER BOUND 20.3216

THE MEASURES OF GROSS ERROR
THE ROOT MEAN SQUARE ERROR IS 3.12
THE AVERAGE ABSOLUTE ERROR IS 2.36

VARIOUS MEASURES OF RELATIVE VARIABILITY
OBSERVATION COEFFICIENT OF VARIATION
0.1767
RESIDUAL COEFFICIENT OF VARIATION
0.2056
RATIO OF RESIDUAL TO OBSERVED ST. DEV.
1.1637

FIGURE 5-11b. Residual analysis of observed minus predicted maximum daily ozone concentrations for 13 July 1976 (N = 14).

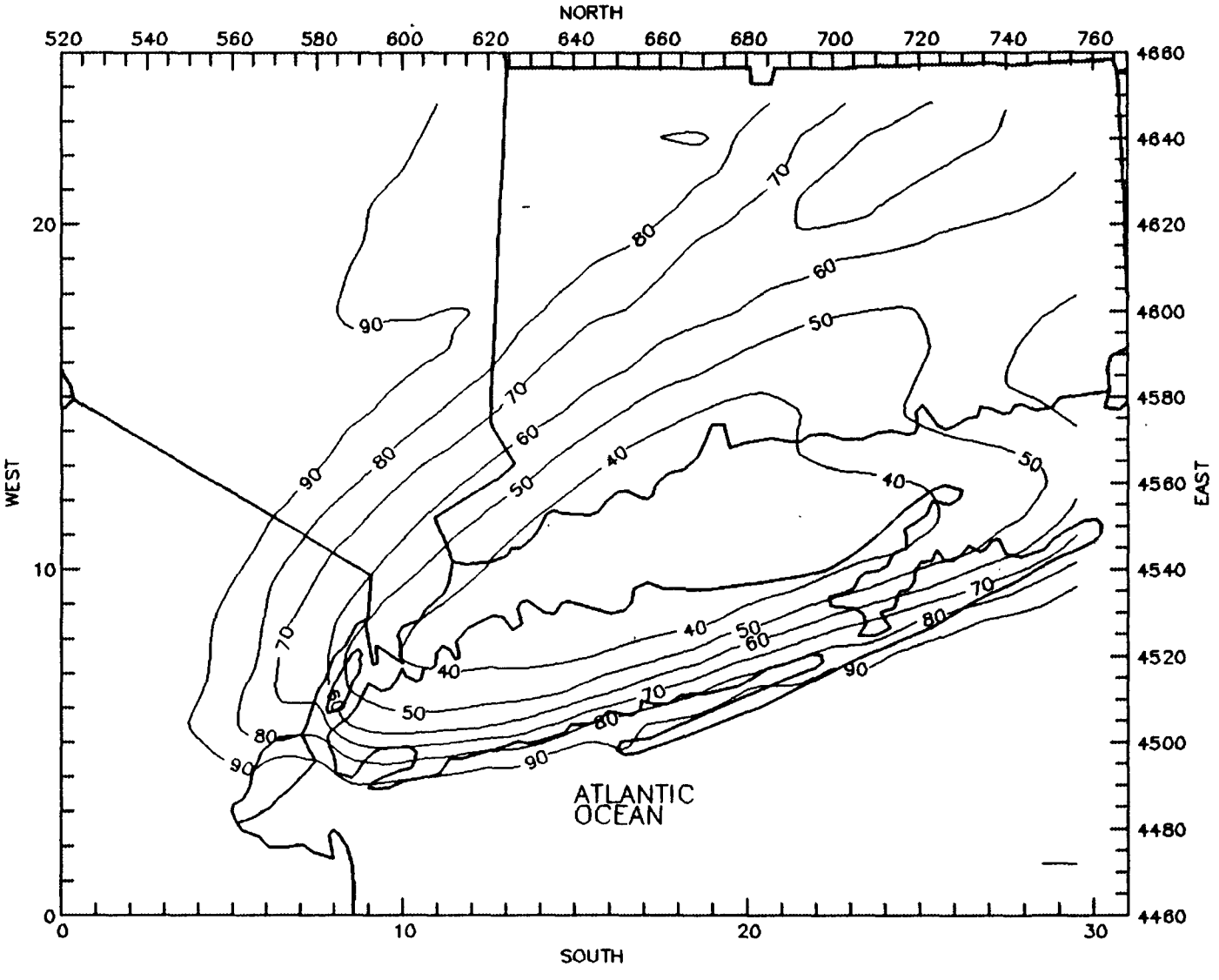

FIGURE 5-12a. Percent contribution of boundary hydrocarbon tracer at 1200 EST, 8 August 1980.

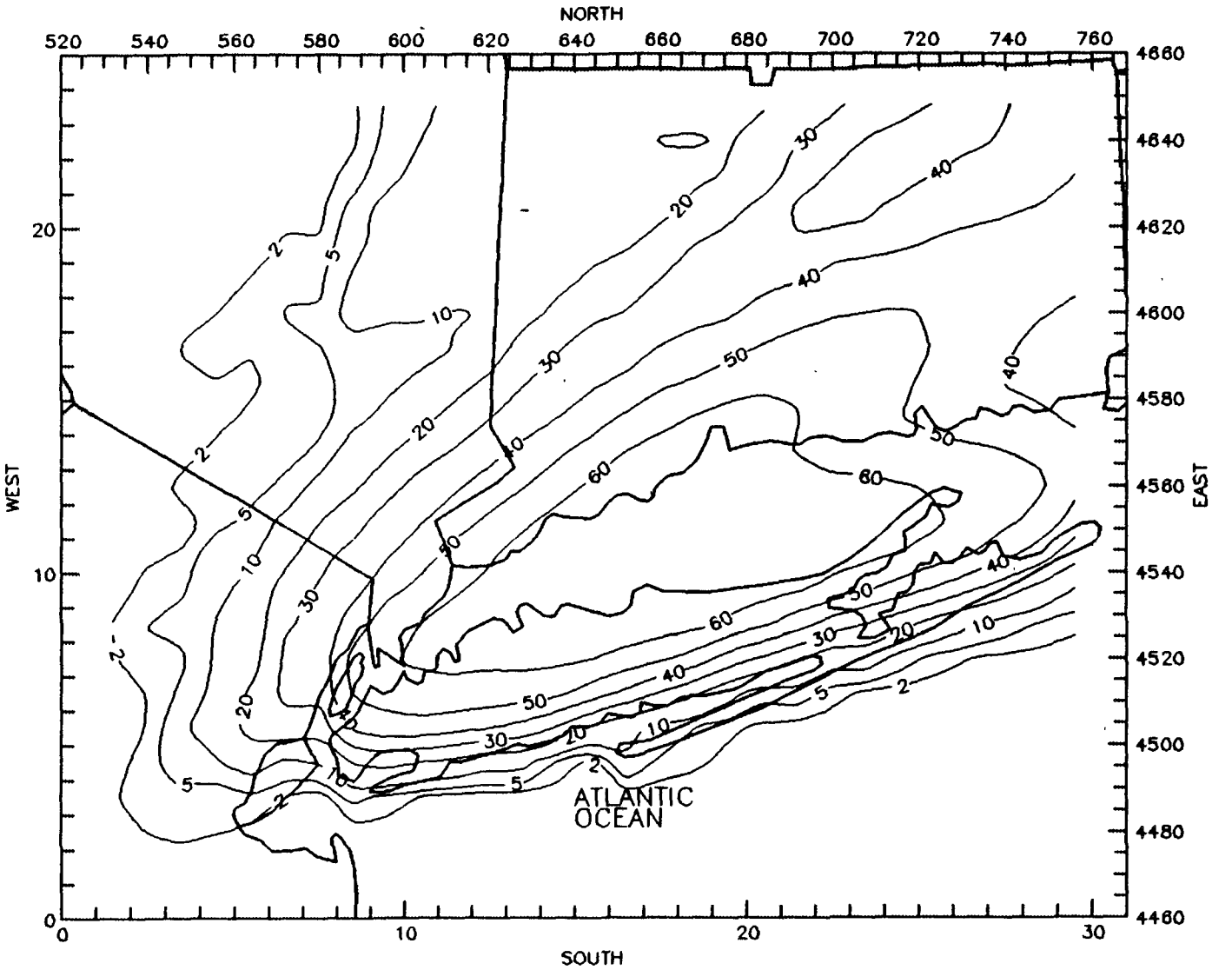

FIGURE 5-12a. Percent contribution of emitted hydrocarbon tracer at 1200 EST, 8 August 1980.

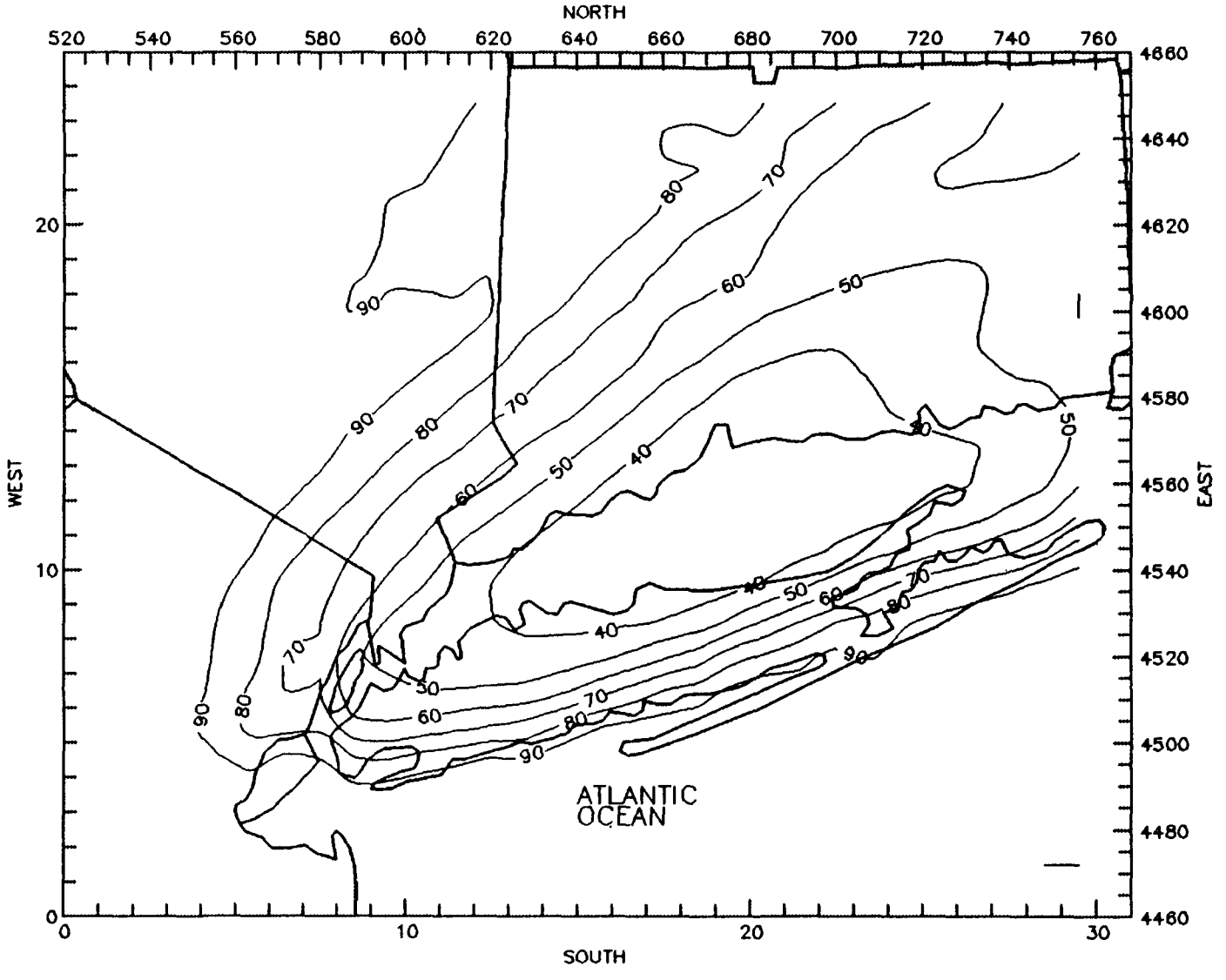

FIGURE 5-12a. Percent contribution of boundary hydrocarbon tracer at 1300 EST, 8 August 1980.

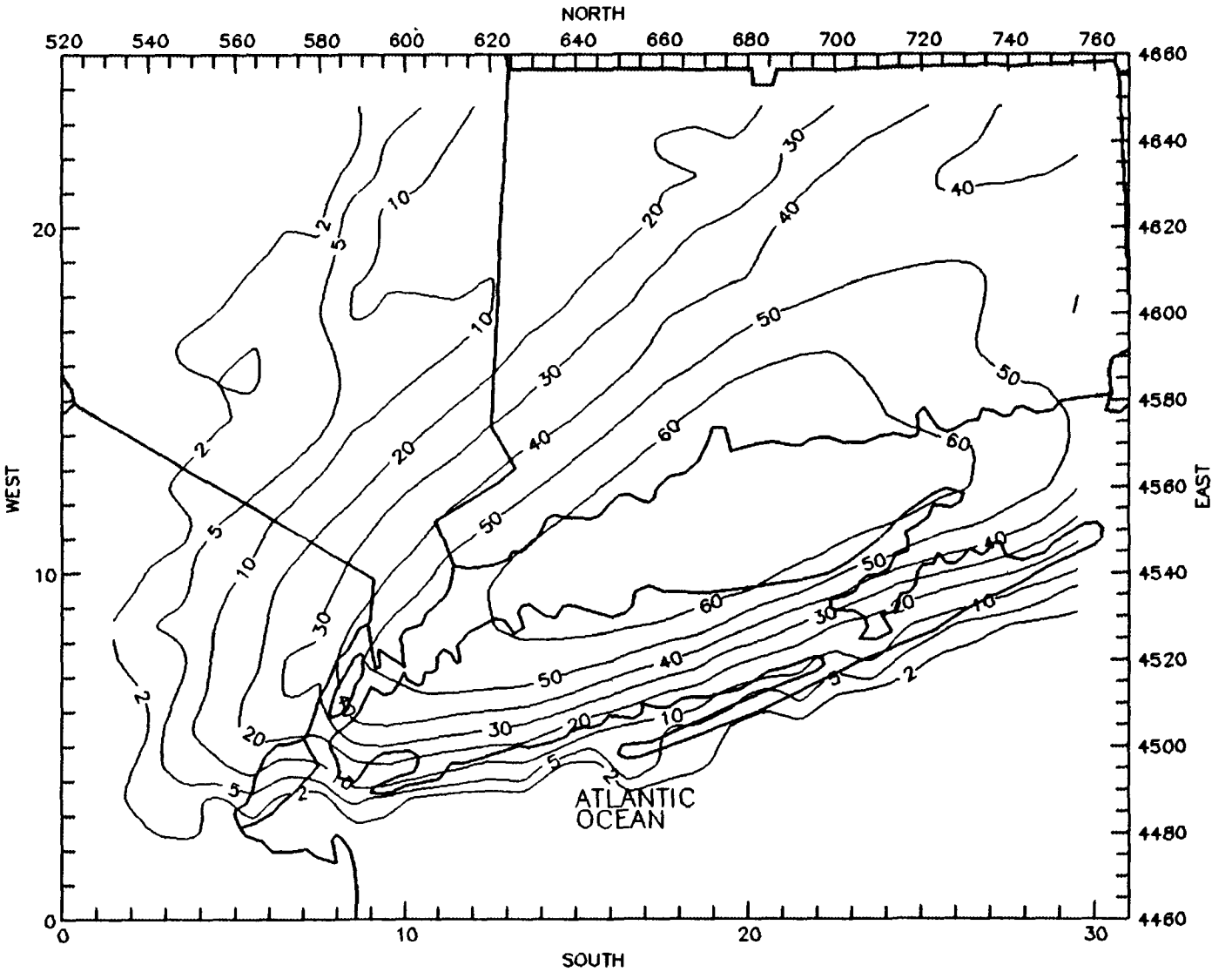

FIGURE 5-12a. Percent contribution of emitted hydrocarbon tracer at 1300 EST, 8 August 1980.

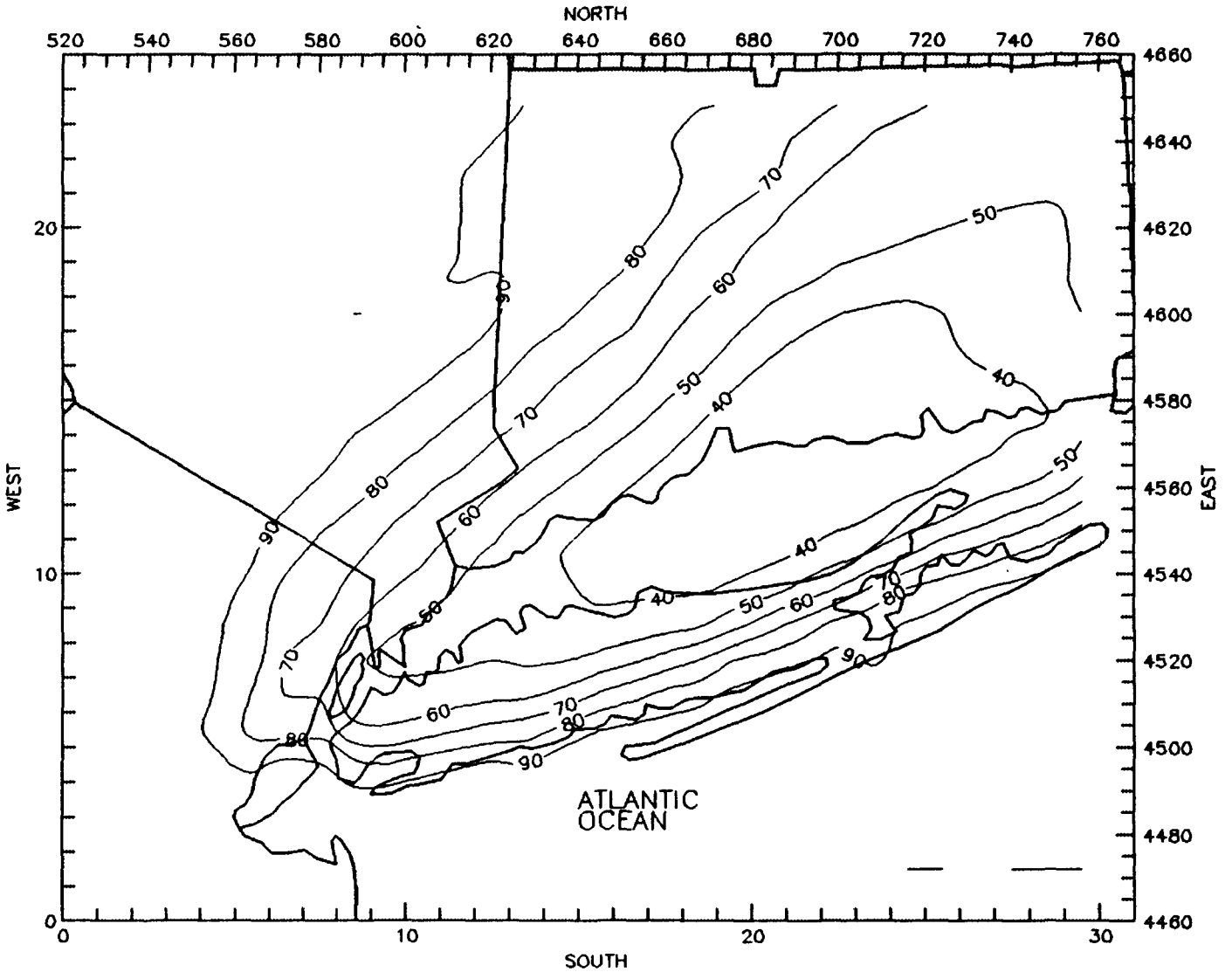

FIGURE 5-12a. Percent contribution of boundary hydrocarbon tracer at 1400 EST, 8 August 1980.

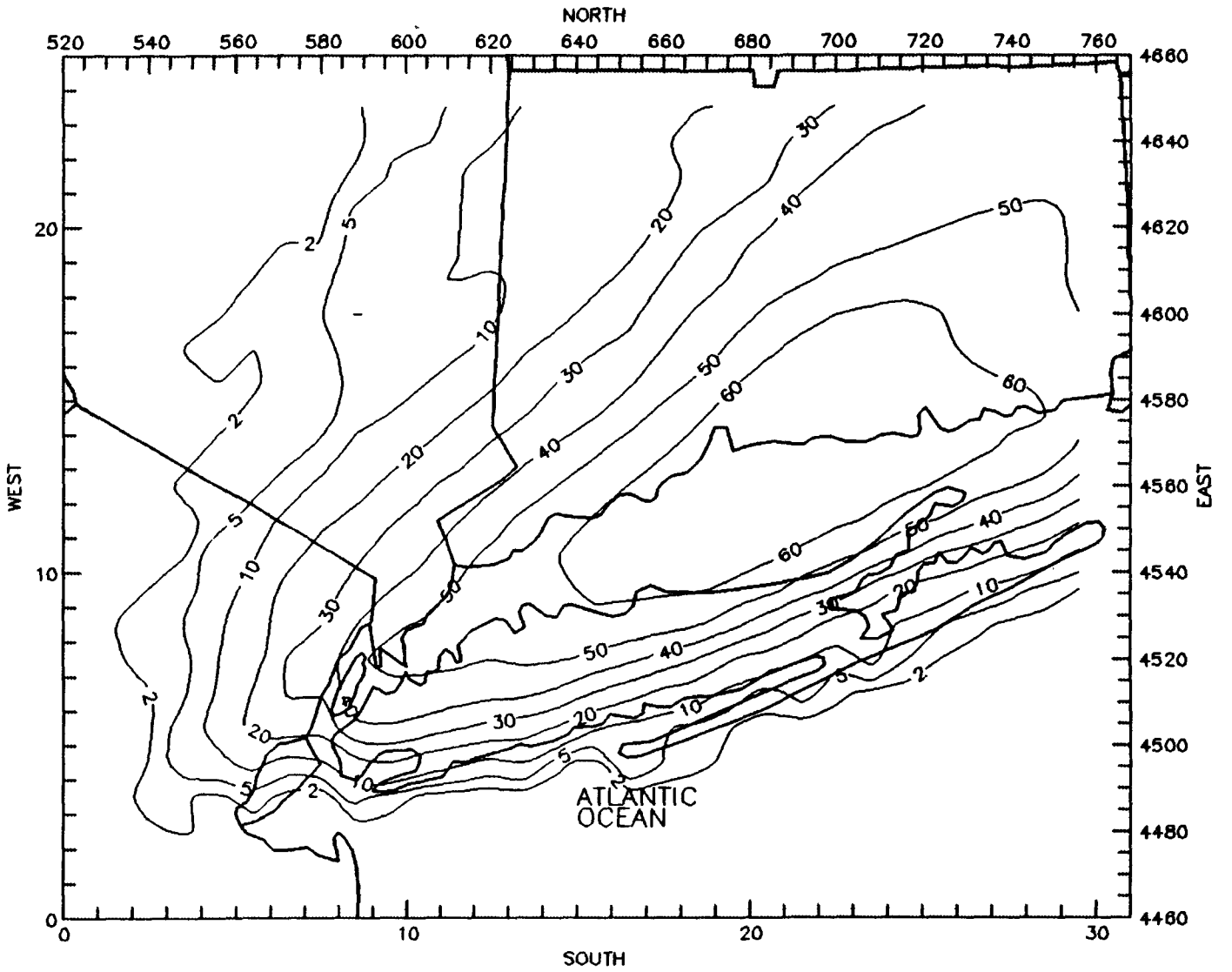

FIGURE 5-12a. Percent contribution of emitted hydrocarbon tracer at 1400 EST, 8 August 1980.

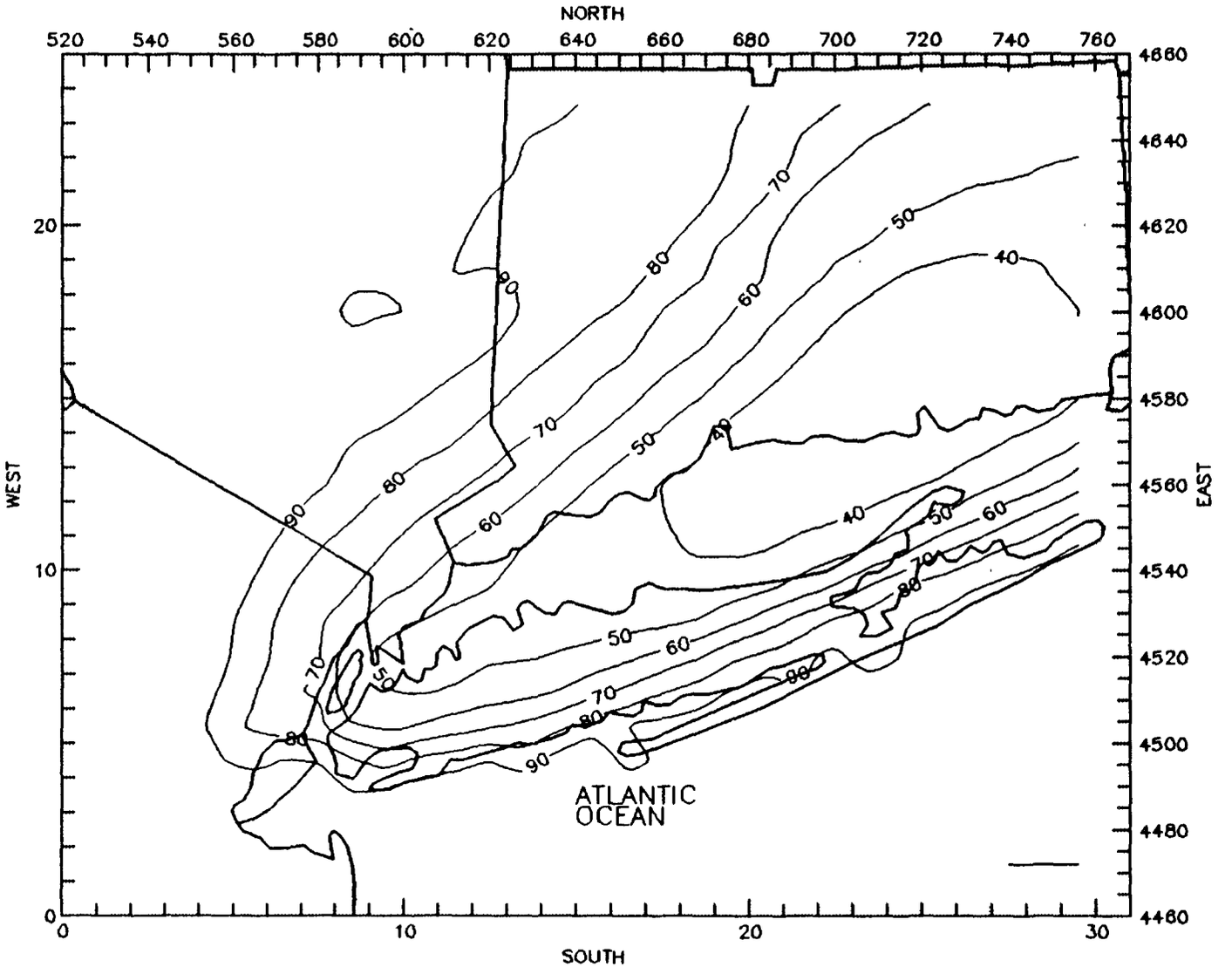

FIGURE 5-12a. Percent contribution of boundary hydrocarbon tracer at 1500 EST, 8 August 1980.

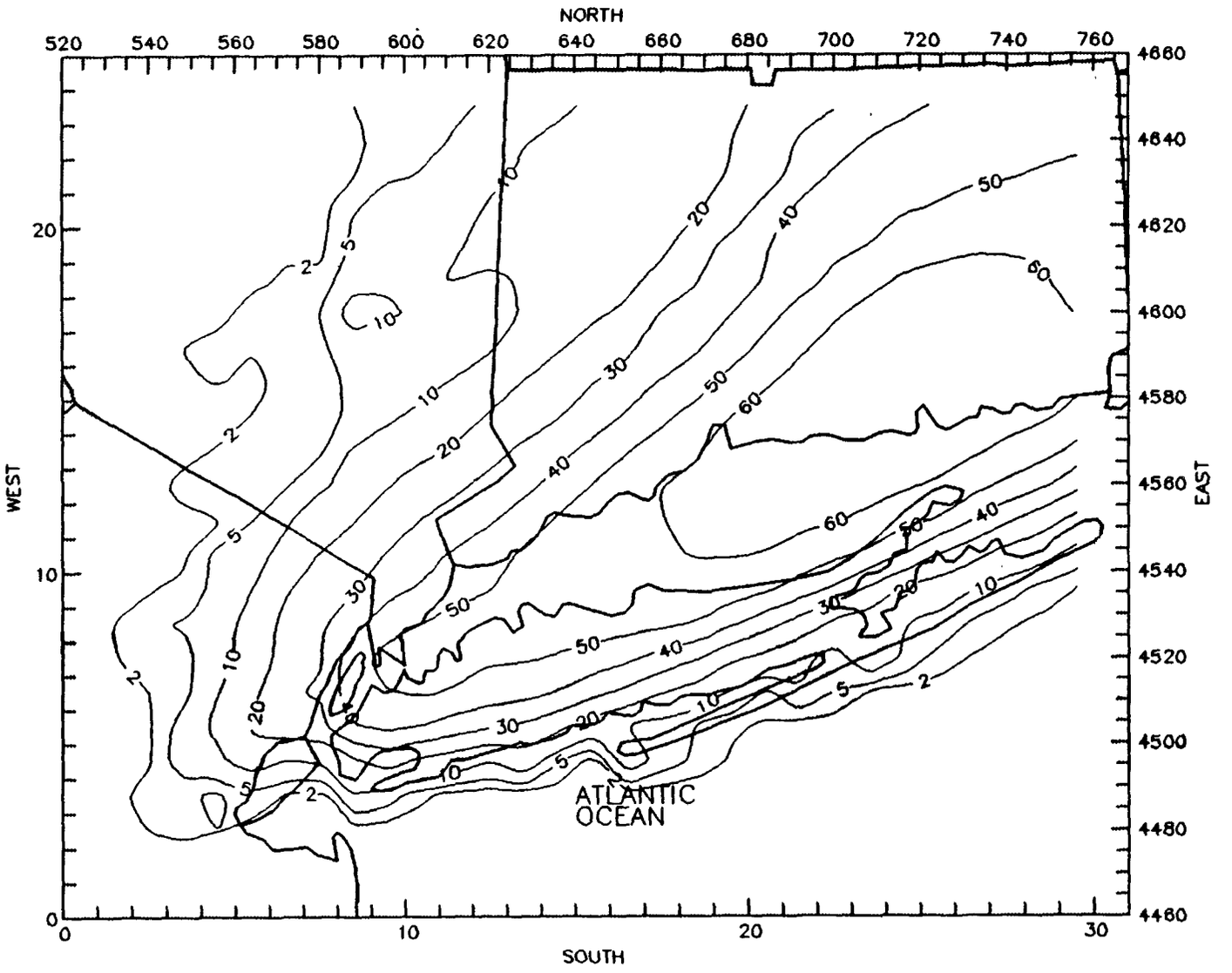

FIGURE 5-12a. Percent contribution of emitted hydrocarbon tracer at 1500 EST, 8 August 1980.

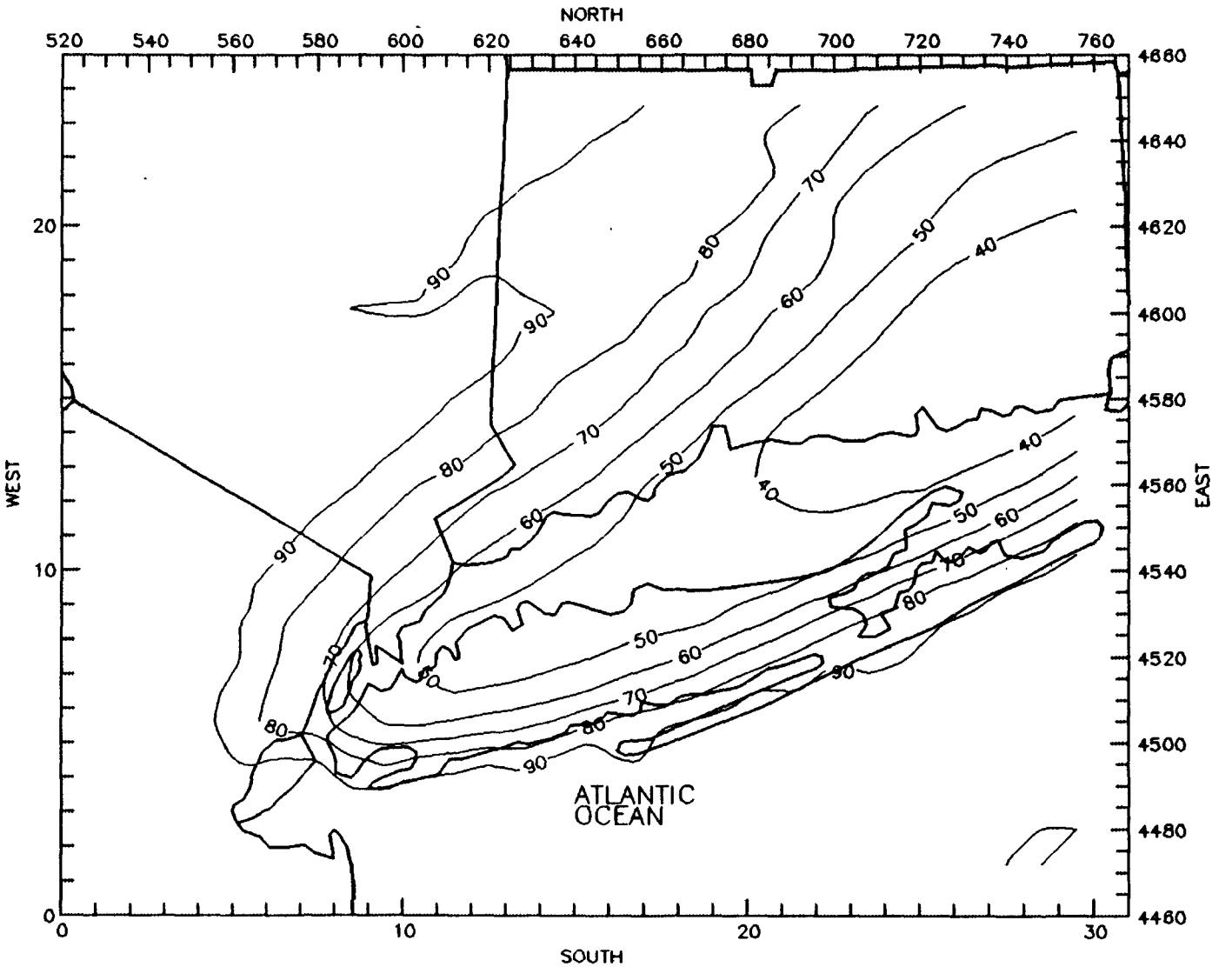

FIGURE 5-12a. Percent contribution of boundary hydrocarbon tracer at 1600 EST, 8 August 1980.

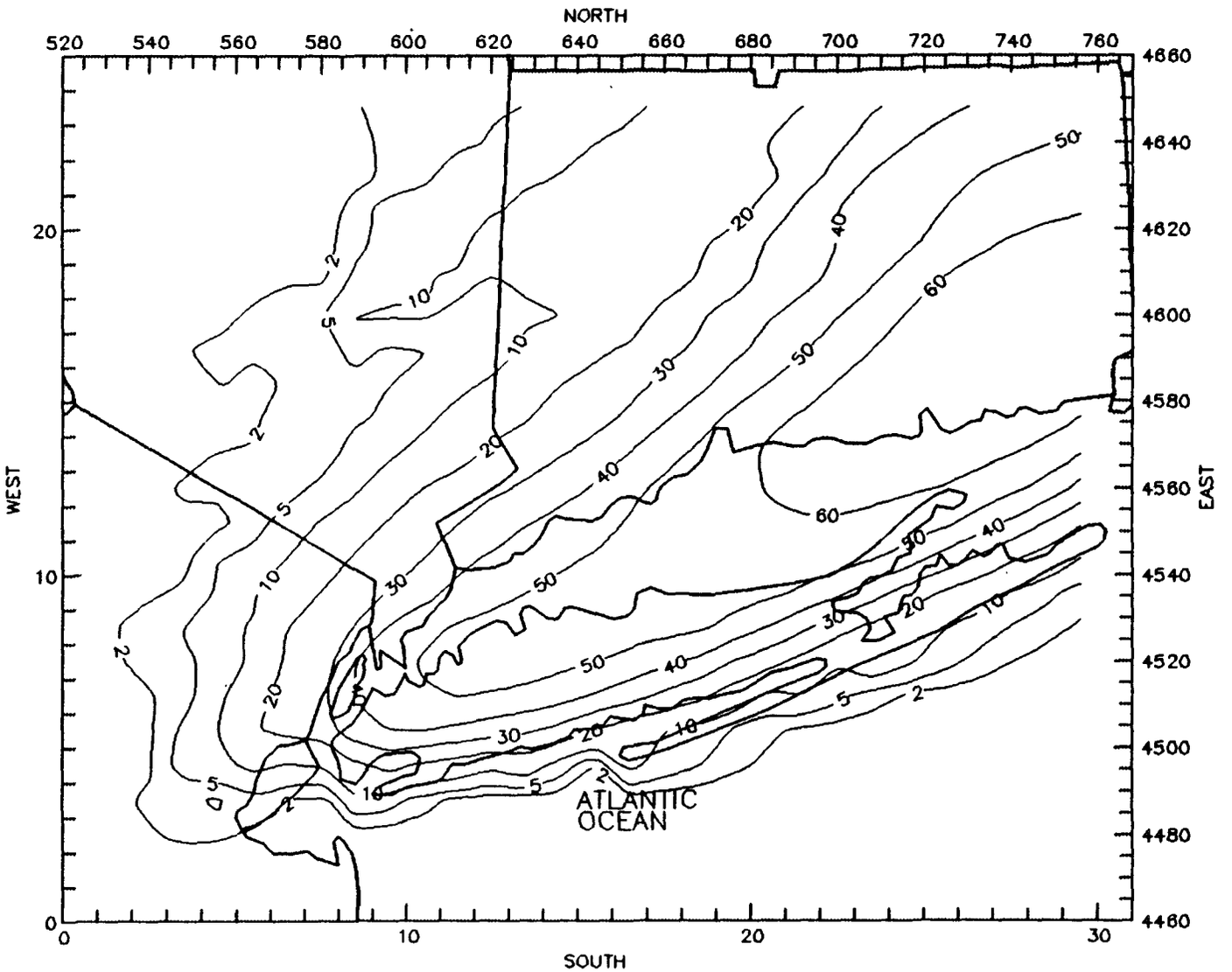

FIGURE 5-12a. Percent contribution of emitted hydrocarbon tracer at 1600 EST, 8 August 1980.

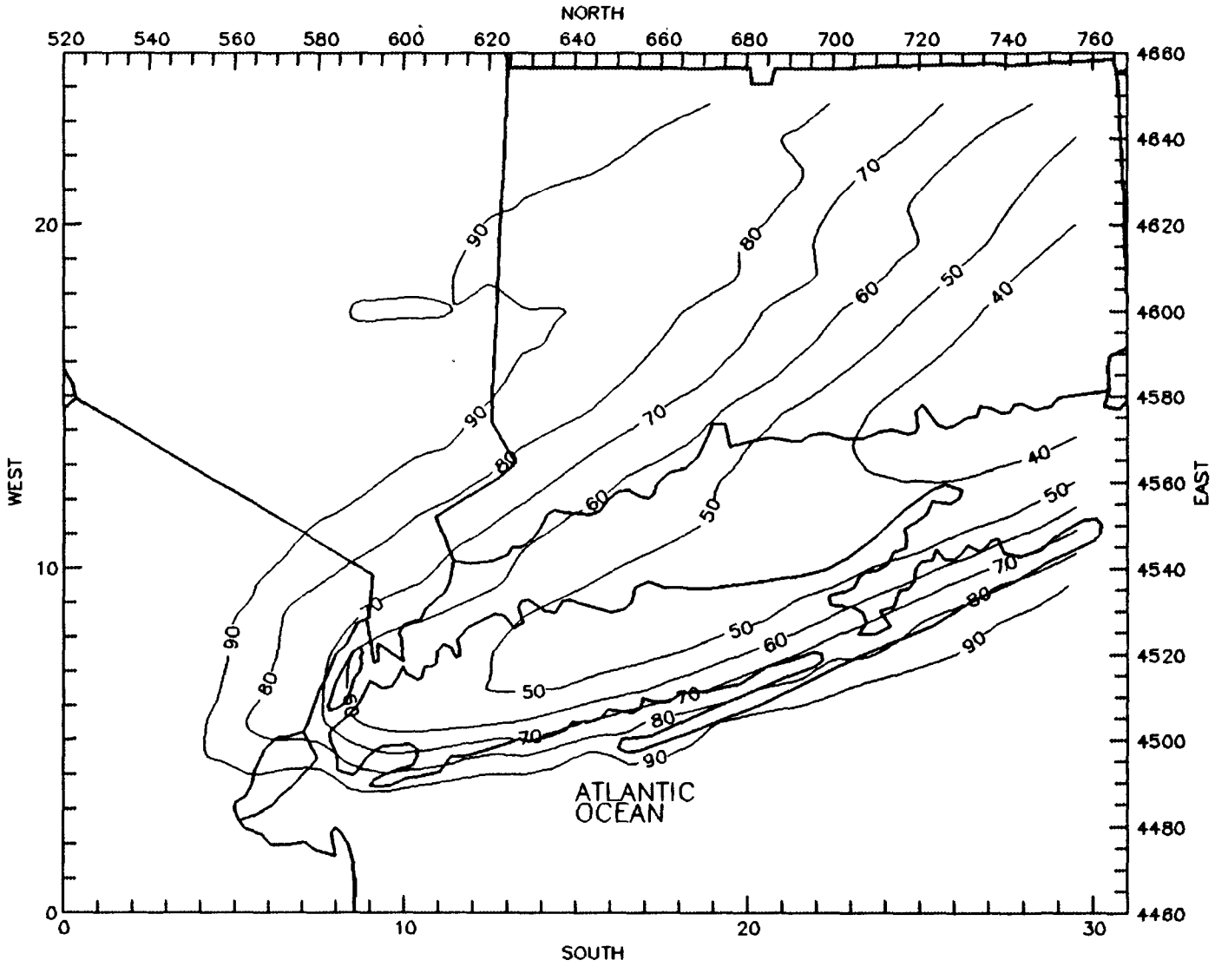

FIGURE 5-12a. Percent contribution of boundary hydrocarbon tracer at 1700 EST, 8 August 1980.

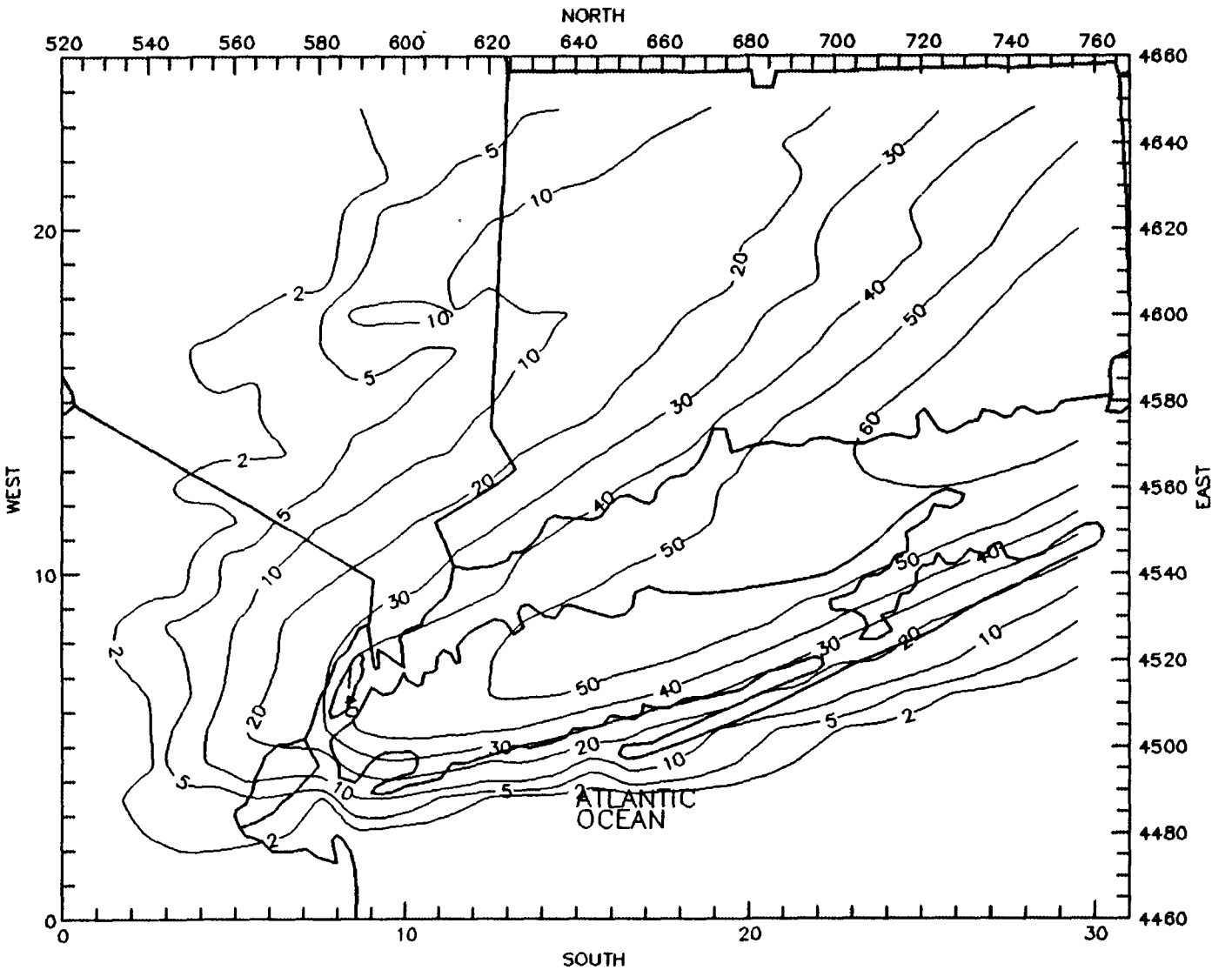

FIGURE 5-12a. Percent contribution of emitted hydrocarbon tracer at 1700 EST, 8 August 1980.

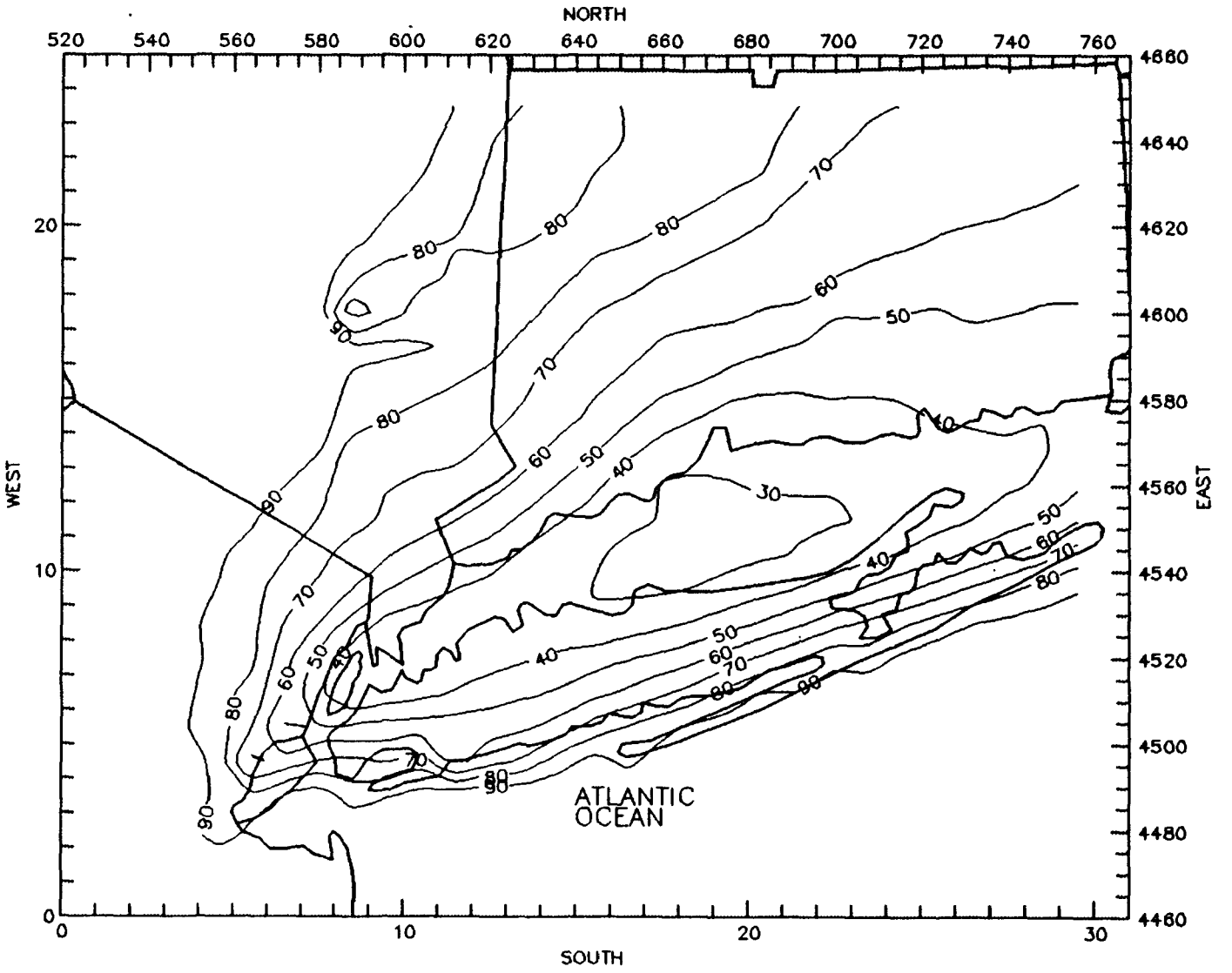

FIGURE 5-12b. Percent contribution of boundary NOx tracer at 1200 EST, 8 August 1980.

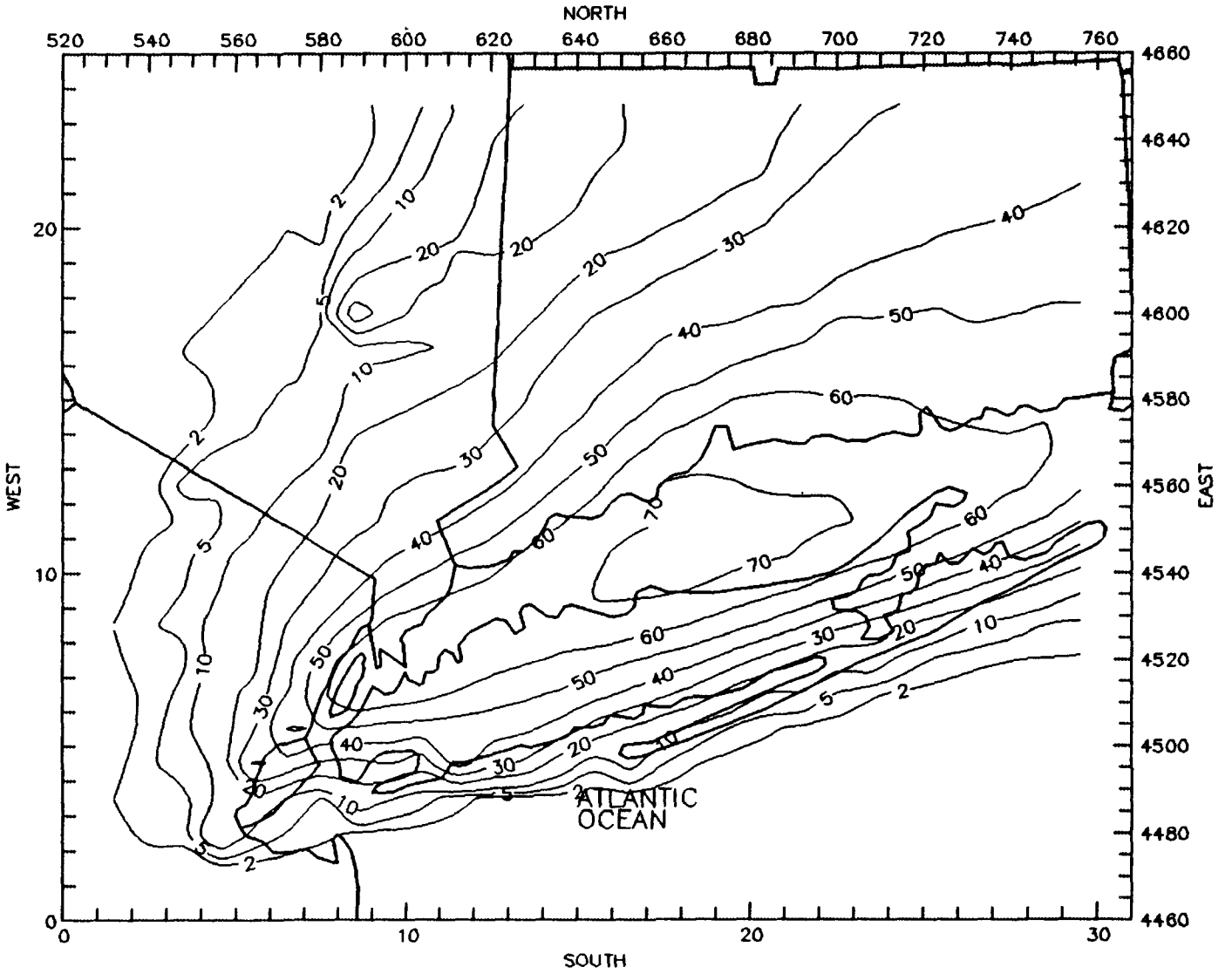

FIGURE 5-12b. Percent contribution of emitted NOx tracer at 1200 EST, 8 August 1980.

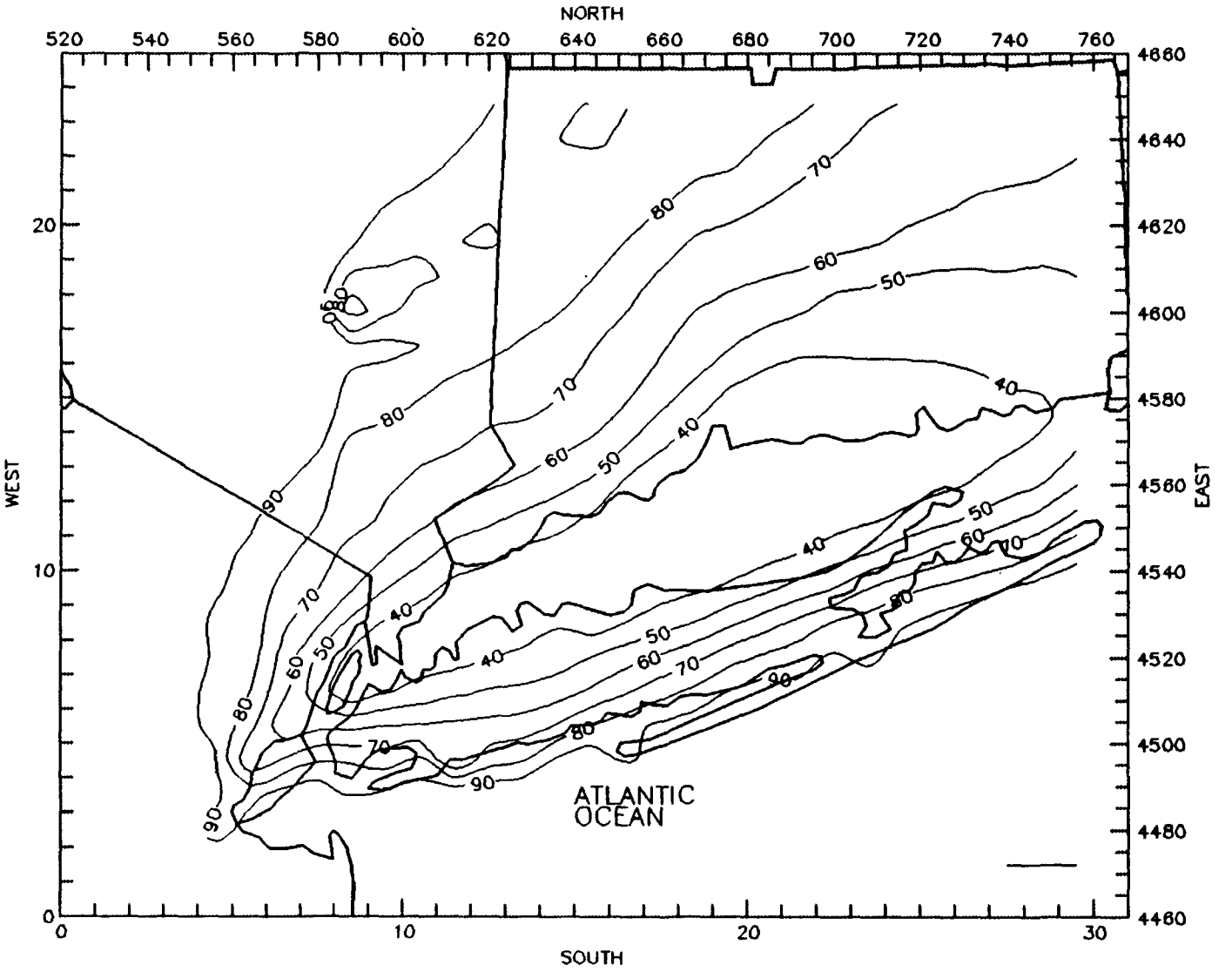

FIGURE 5-12b. Percent contribution of boundary NOx tracer at 1300 EST, 8 August 1980

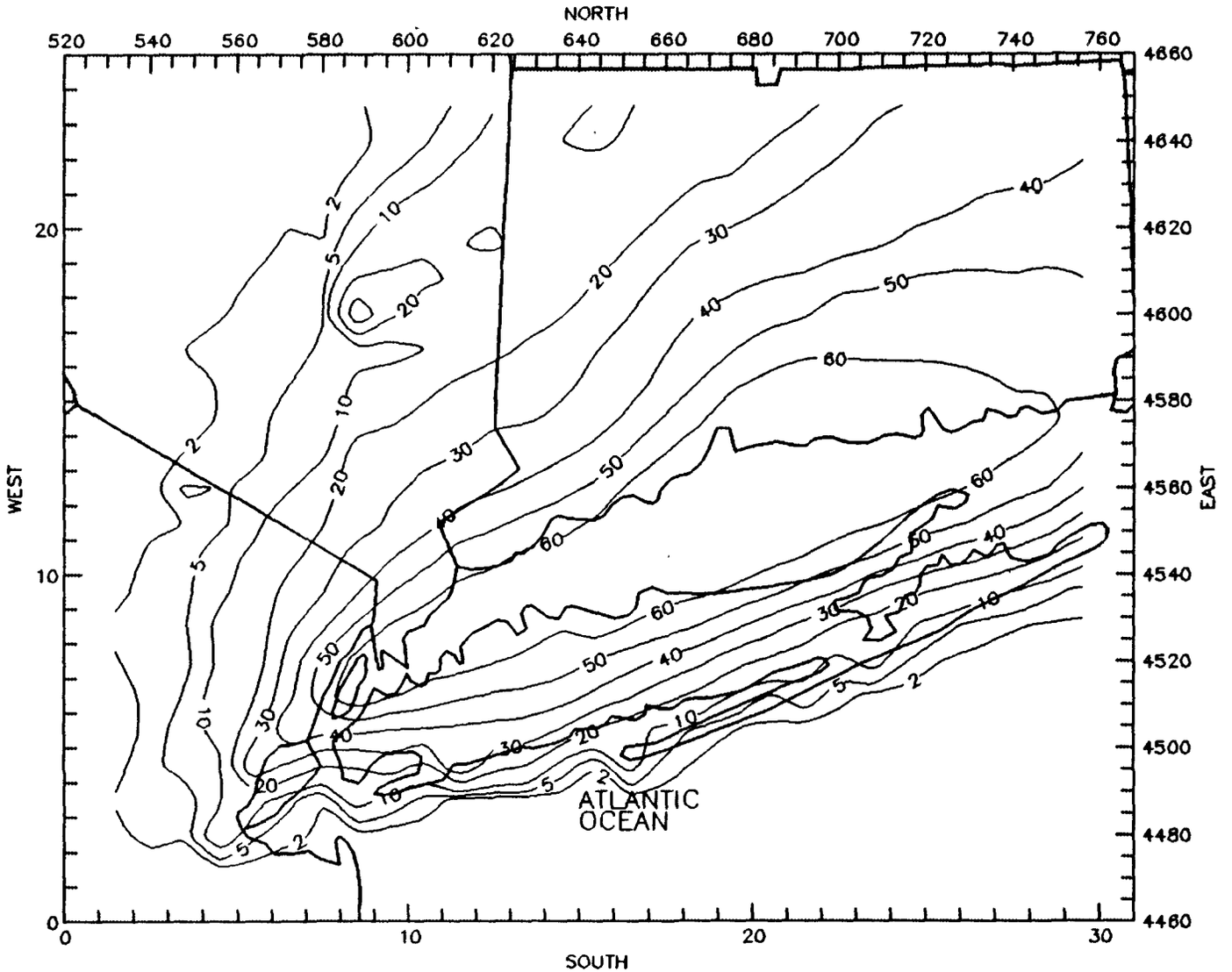

180

FIGURE 5-12b. Percent contribution of emitted NOx tracer at 1300 EST, 8 August 1980.

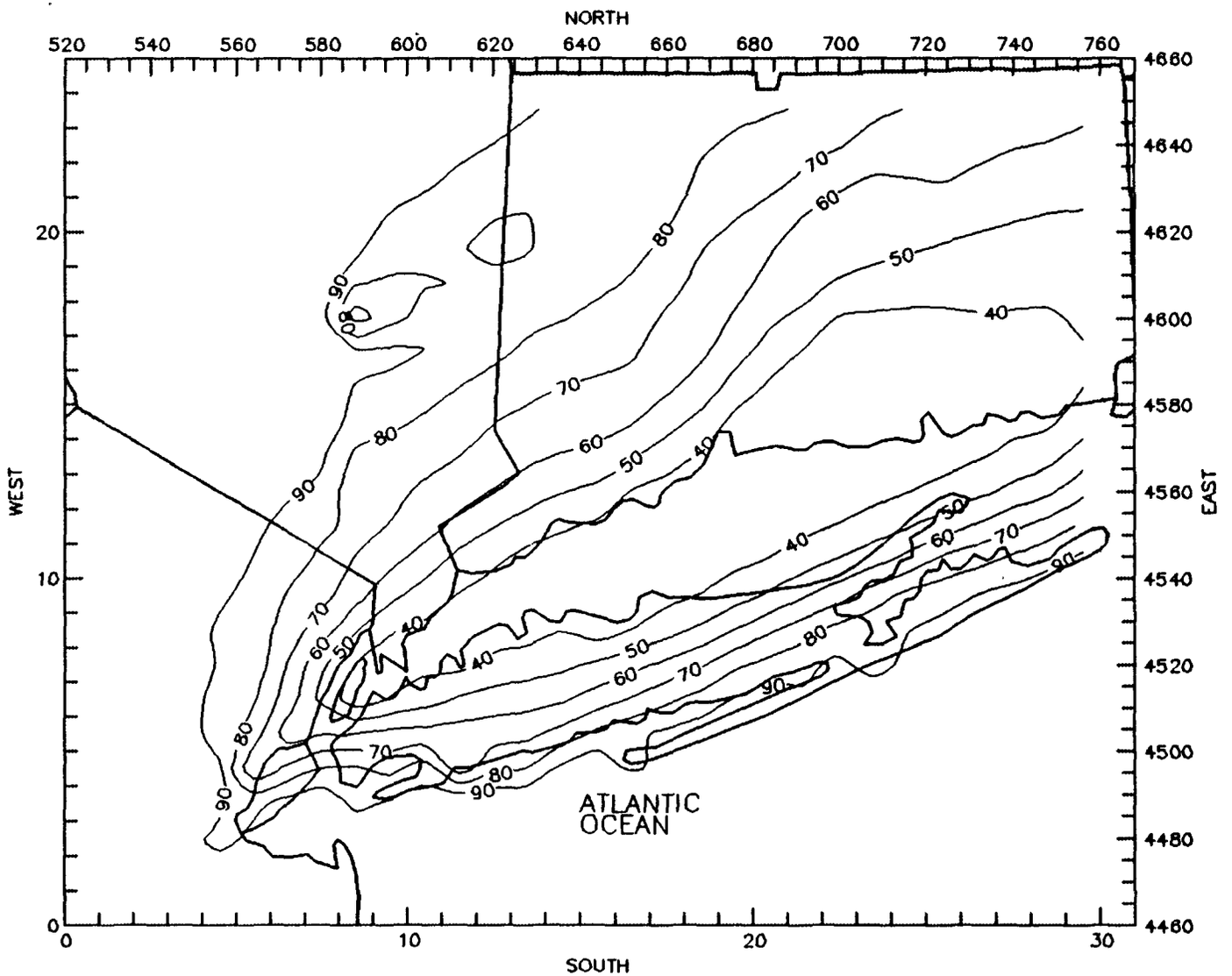

FIGURE 5-12b. Percent contribution of boundary NOx tracer at 1400 EST, 8 August 1980.

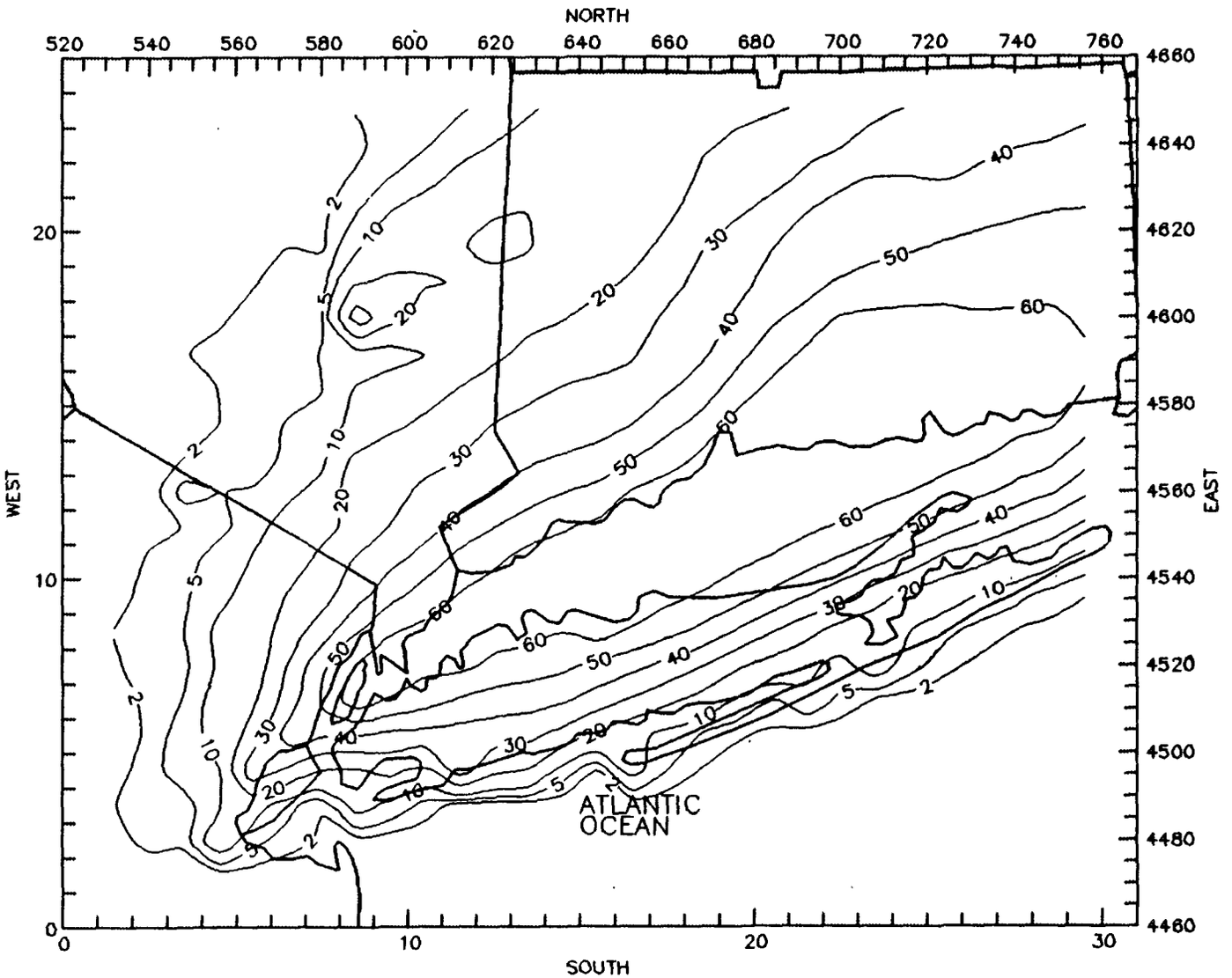

FIGURE 5-12b. Percent contribution of emitted NOx tracer at 1400 EST, 8 August 1980.

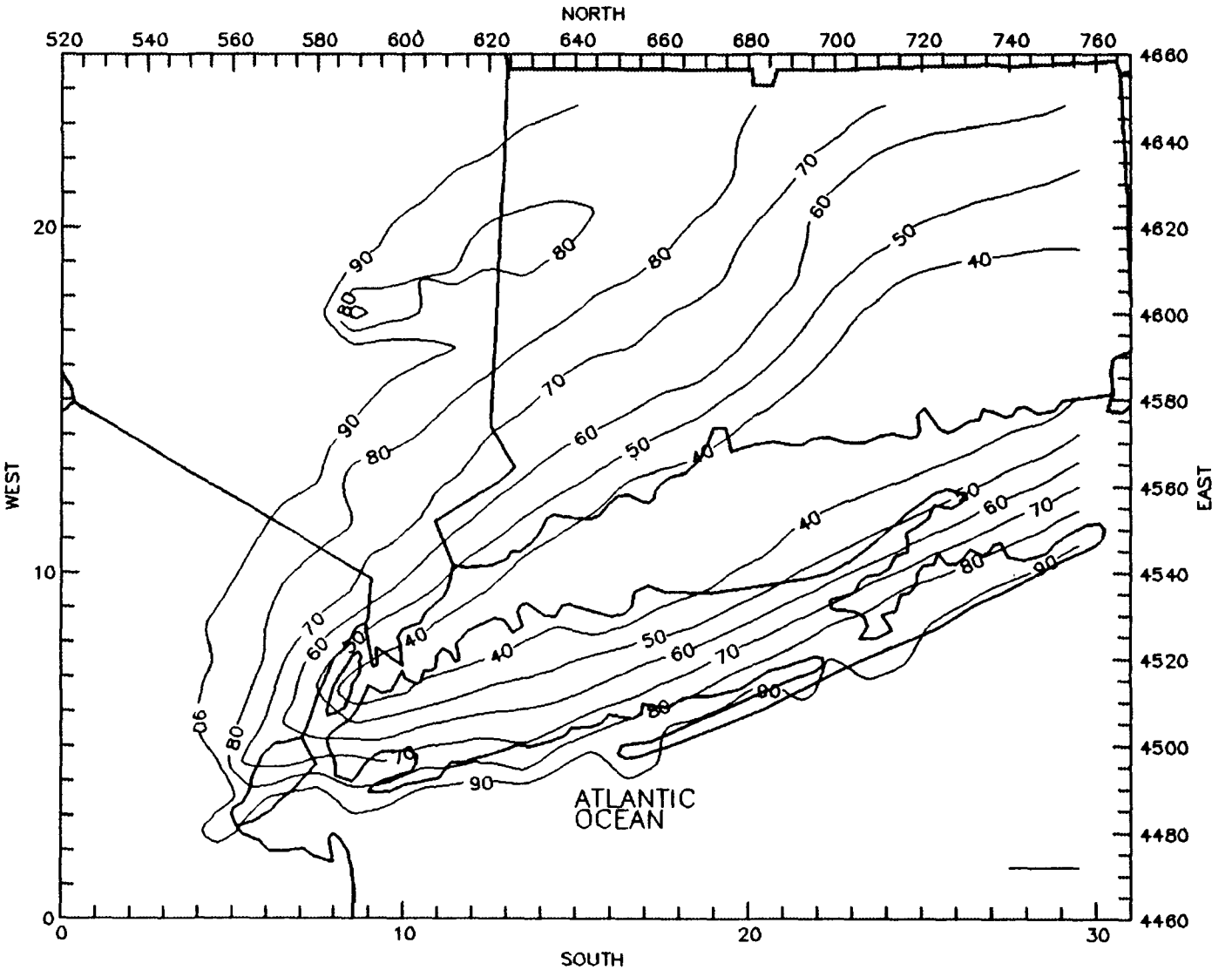

FIGURE 5-12b. Percent contribution of boundary NOx tracer at 1500 EST, 8 August 1980

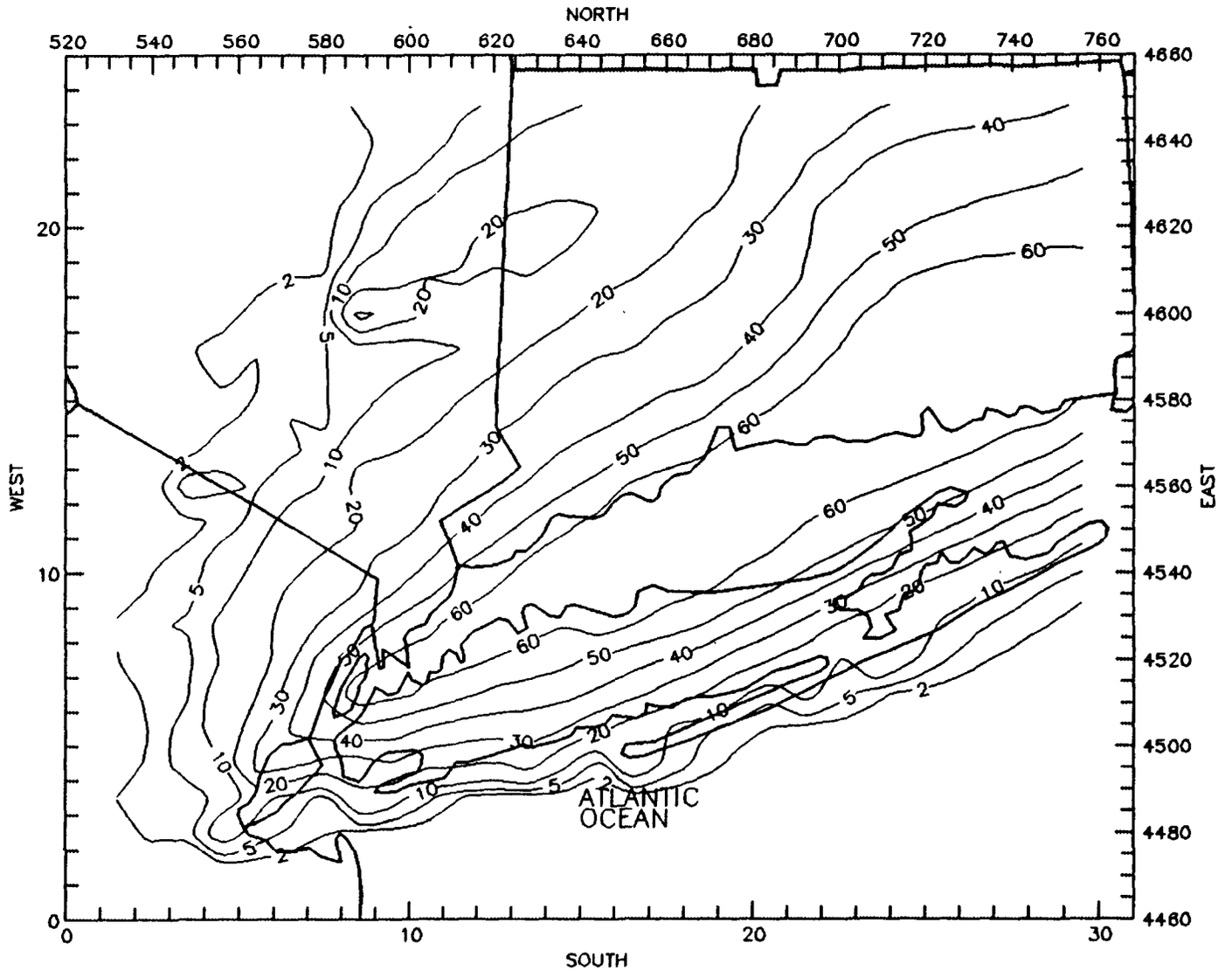

FIGURE 5-12b. Percent contribution of emitted NOx tracer at 1500 EST, 8 August 1980.

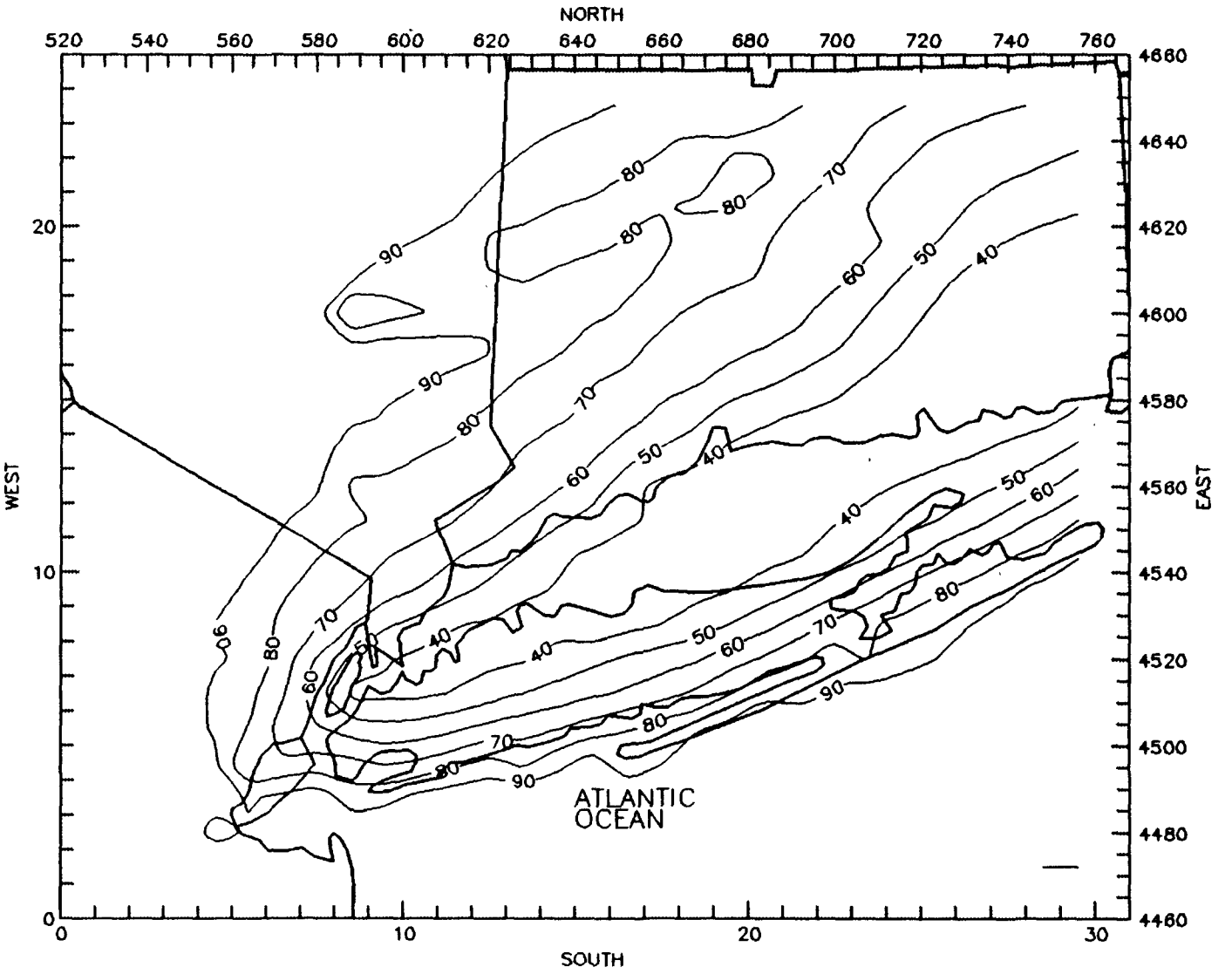

FIGURE 5-12b. Percent contribution of boundary NOx tracer at 1600 EST, 8 August 1980.

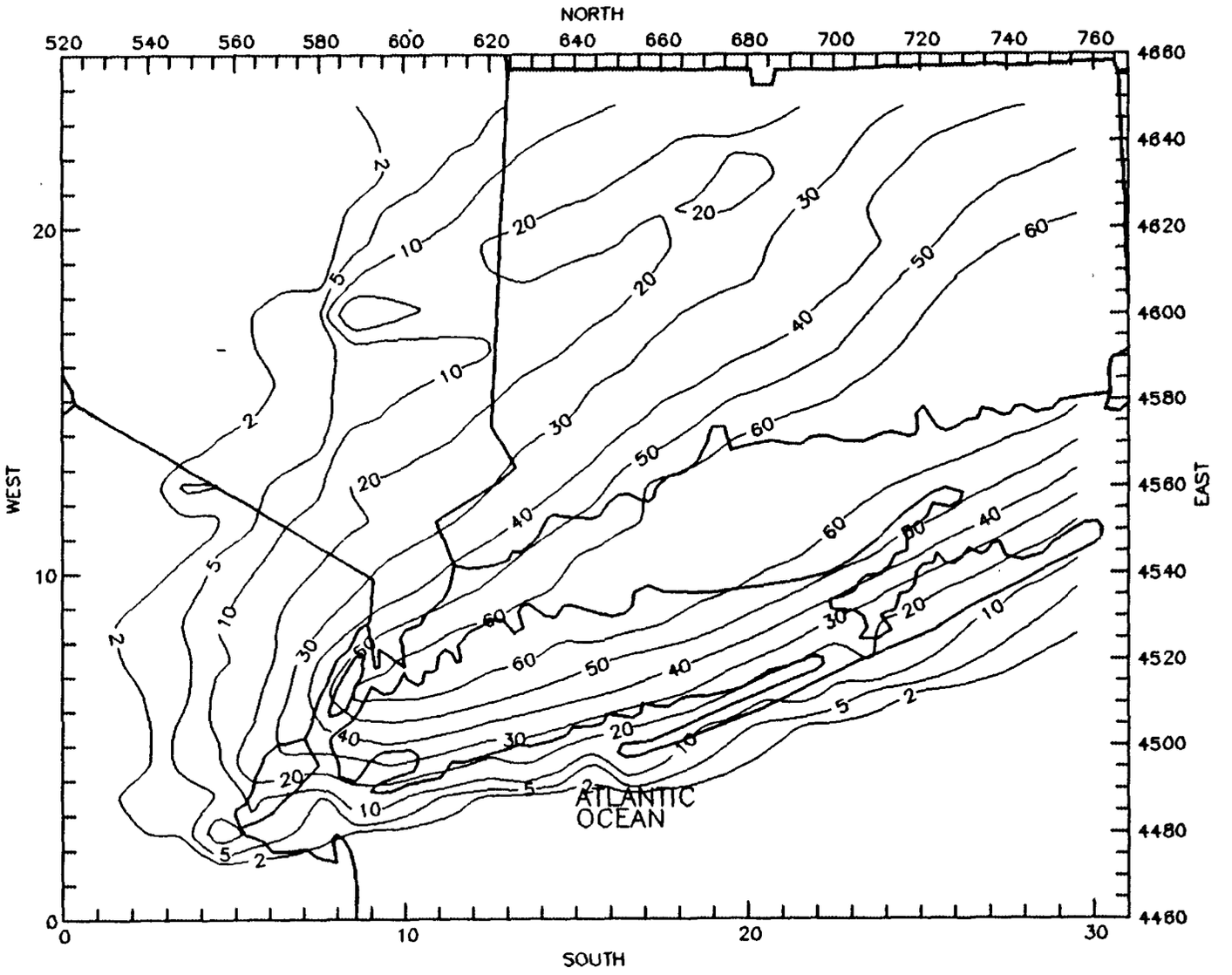

FIGURE 5-12b. Percent contribution of emitted NO_x tracer at 1600 EST, 8 August 1980.

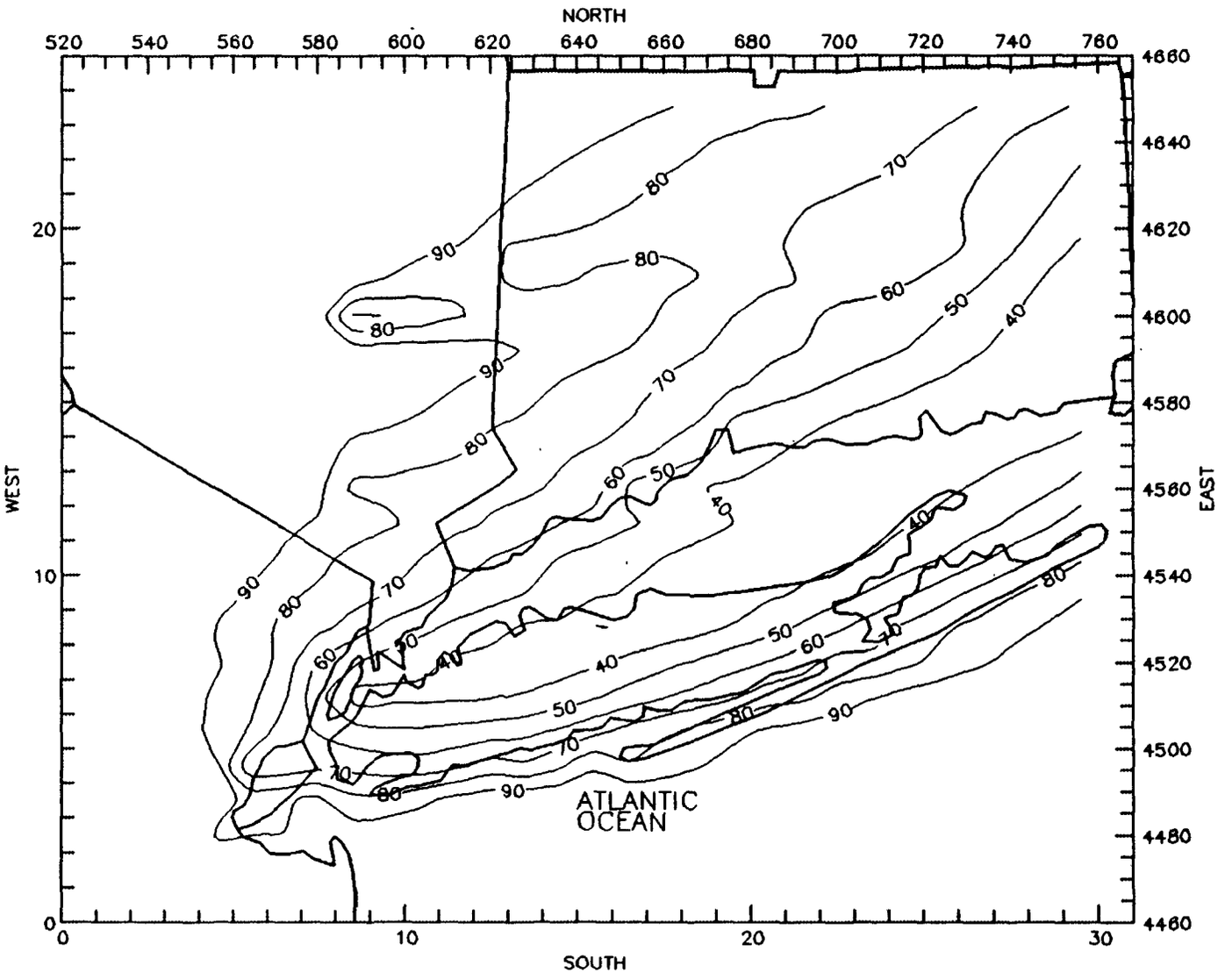

FIGURE 5-12b. Percent contribution of boundary NOx tracer at 1700 EST, 8 August 1980

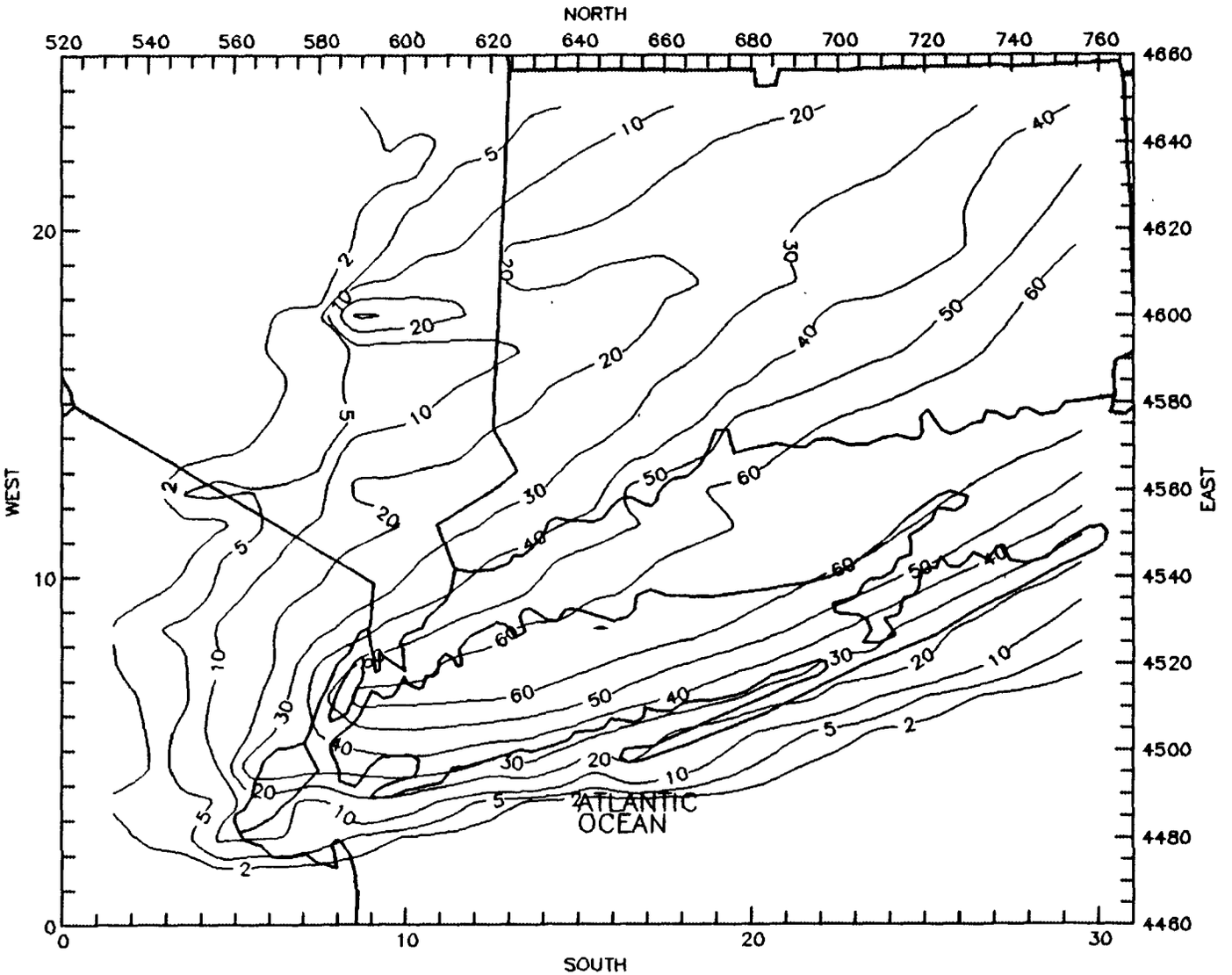

FIGURE 5-12b. Percent contribution of emitted NO_x tracer at 1700 EST, 8 August 1980.

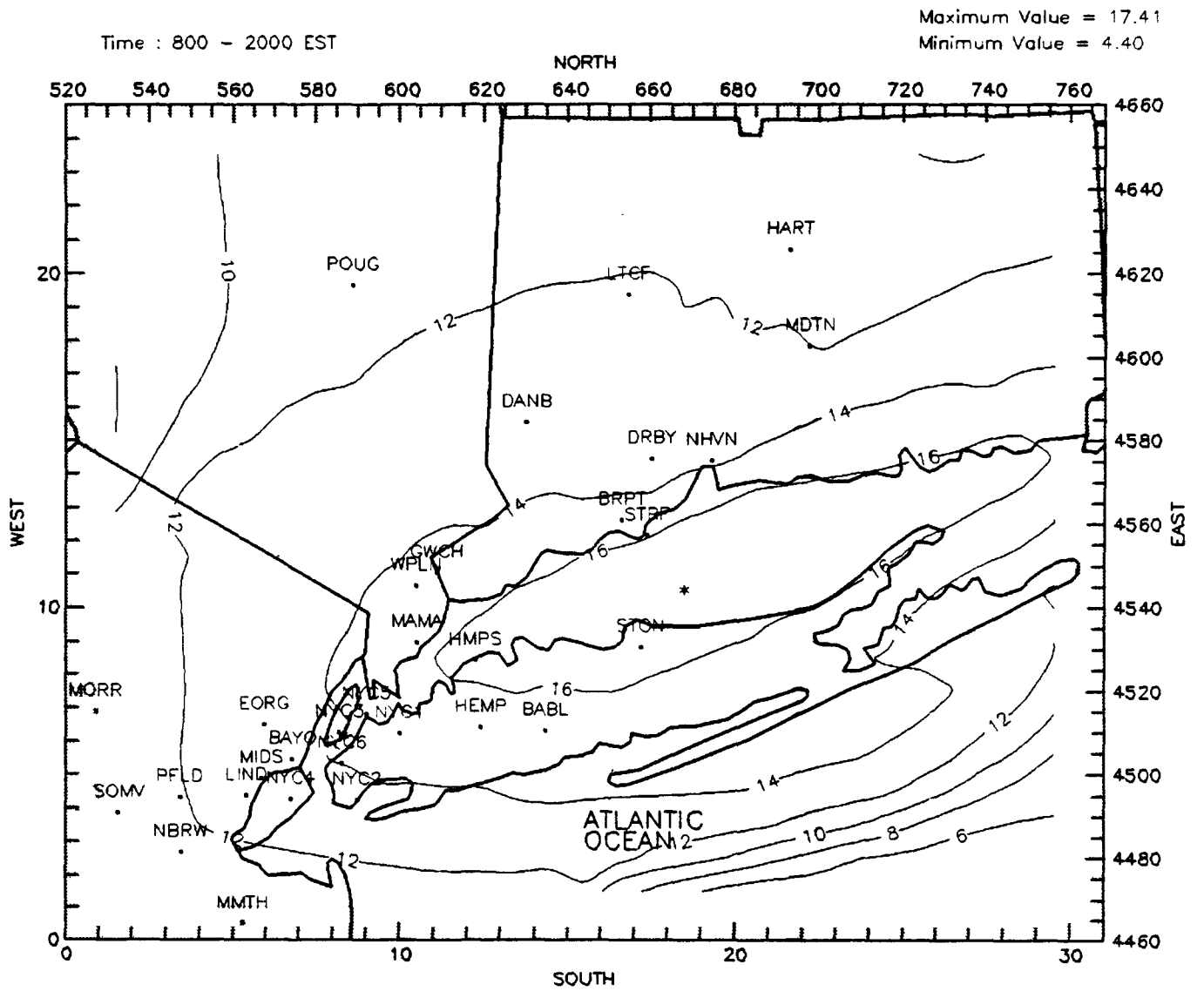

FIGURE 5-13. Maximum daily ozone concentrations (pphm) for scenario 1 on 8 August 1980. (* denotes location of maximum concentration value)

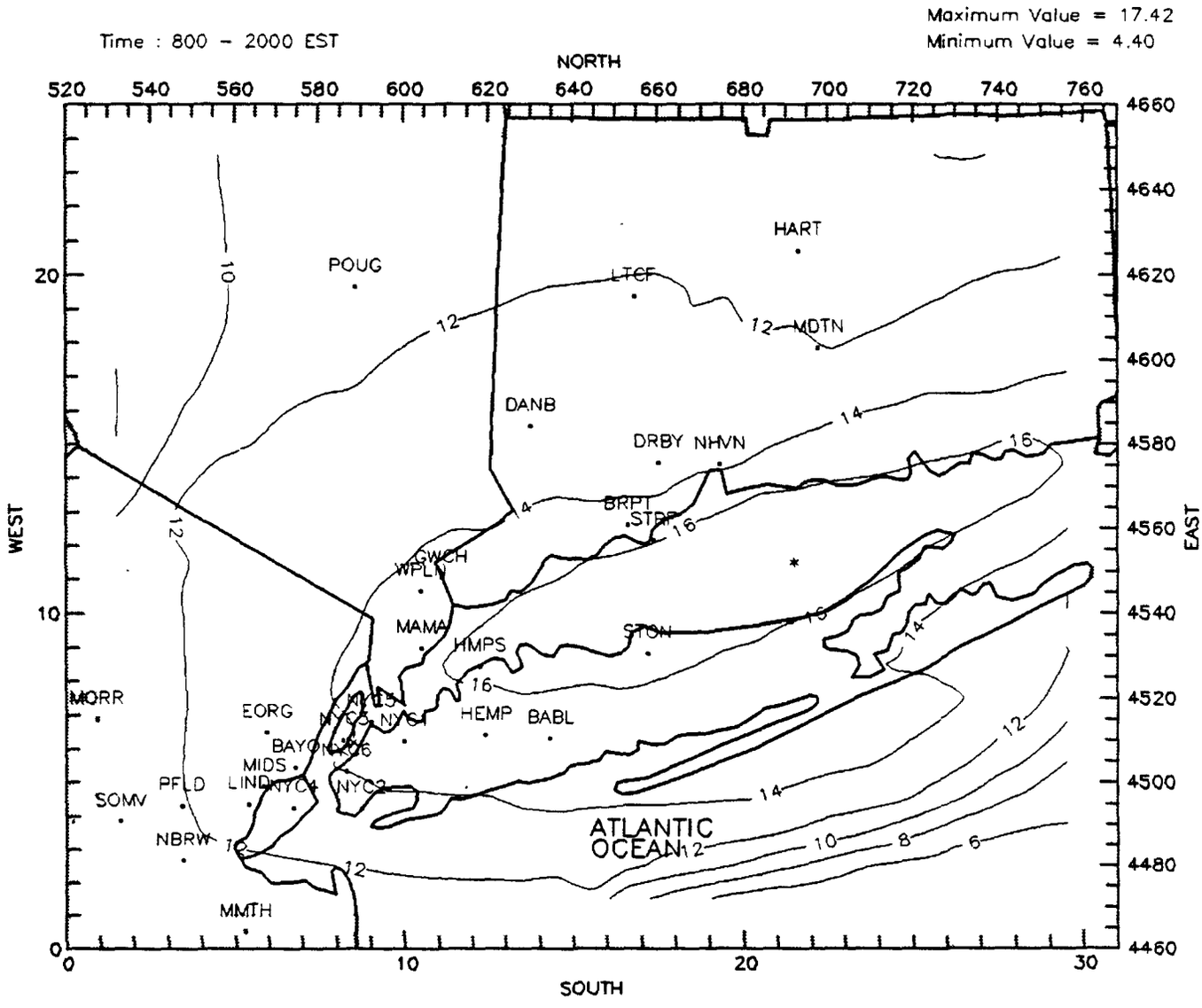

FIGURE 5-14. Maximum daily ozone concentrations (pphm) for scenario 2 on 8 August 1980. (* denotes location of maximum concentration value)

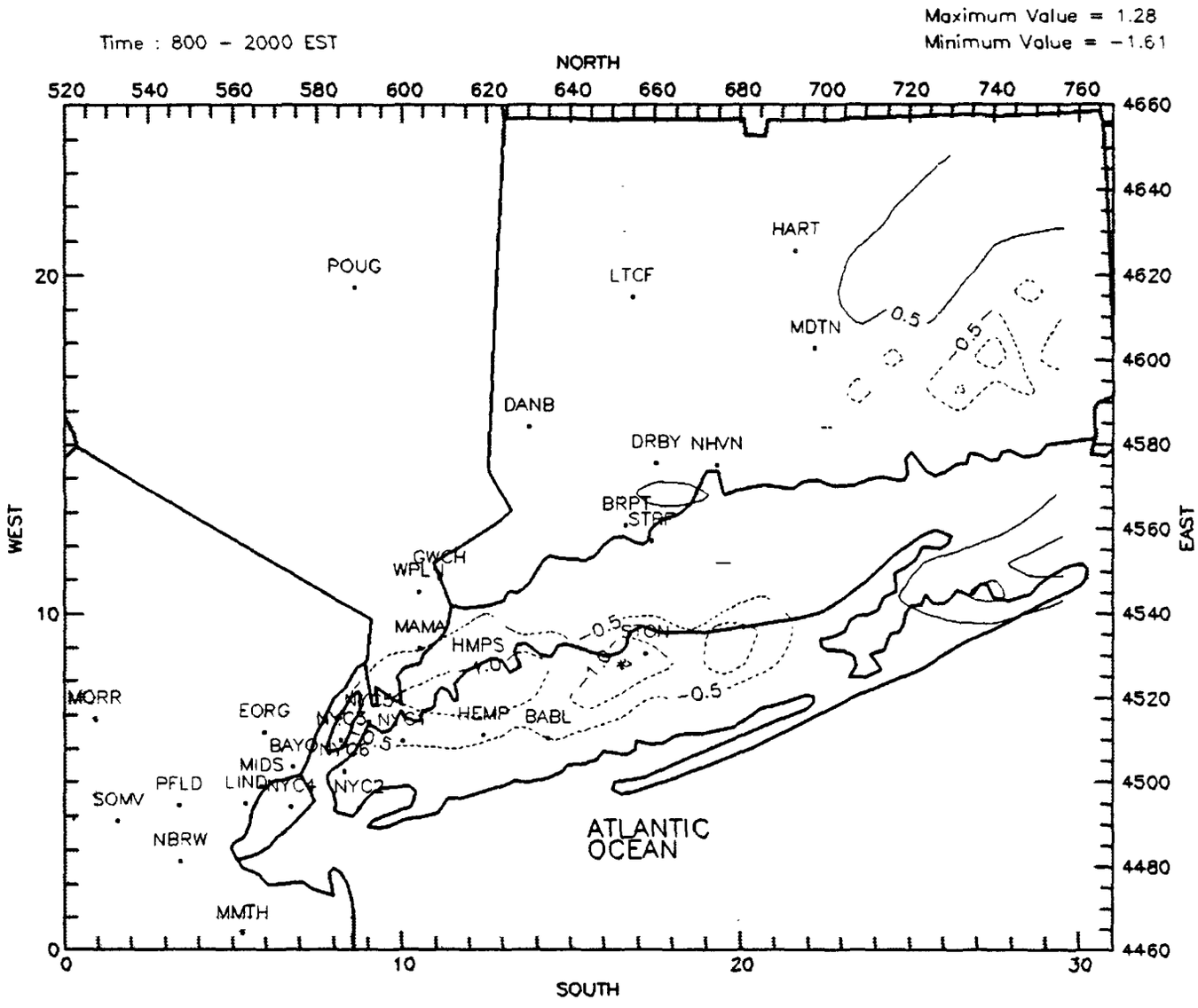

FIGURE 5-15. Differences in maximum daily ozone concentrations (ppb) between scenario 1 and scenario 2. (* denotes location of maximum ozone decrease)

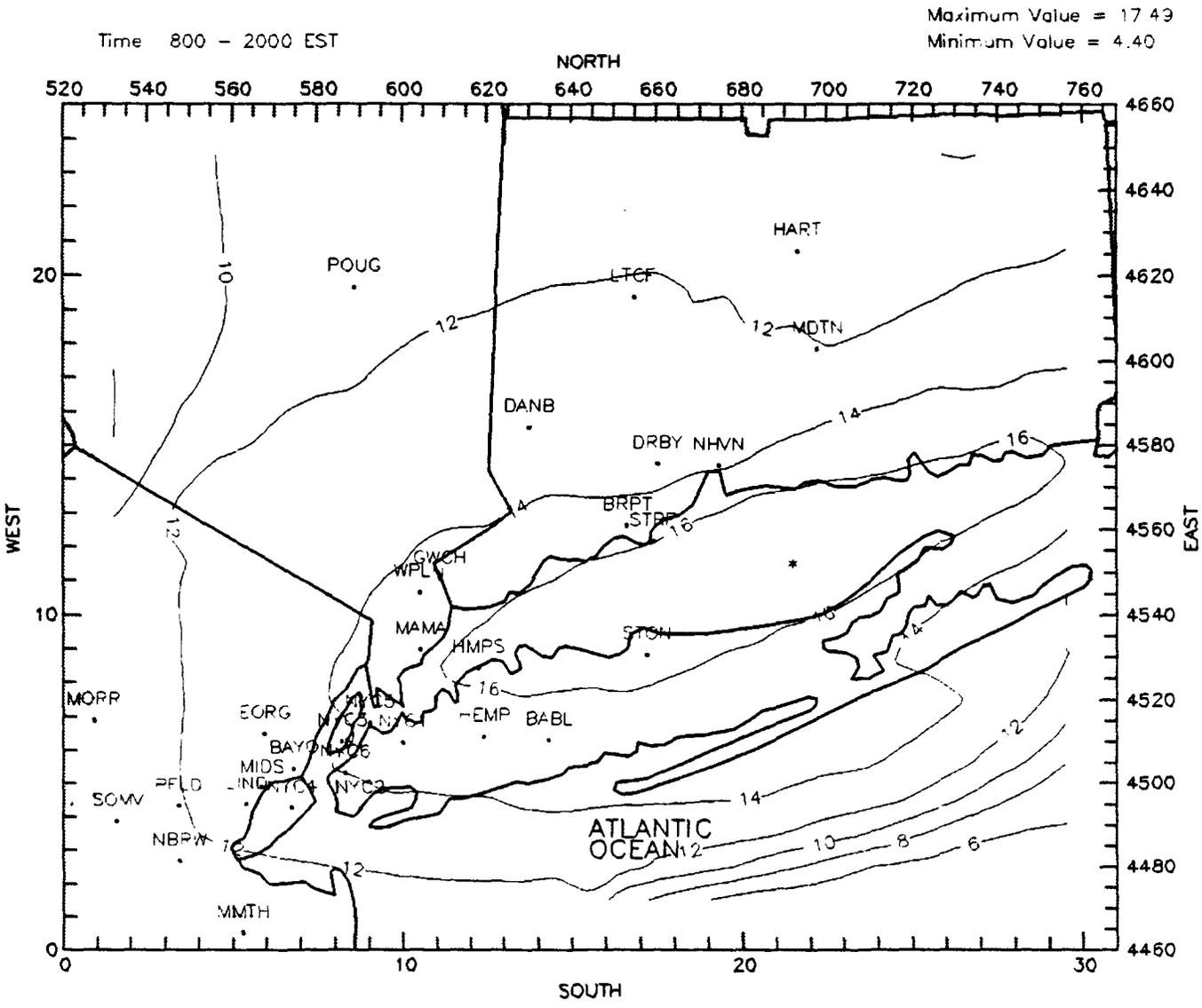

FIGURE 5-16. Maximum daily ozone concentrations (pphm) for scenario 3 for 8 August 1980. (* denotes location of maximum concentration value.)

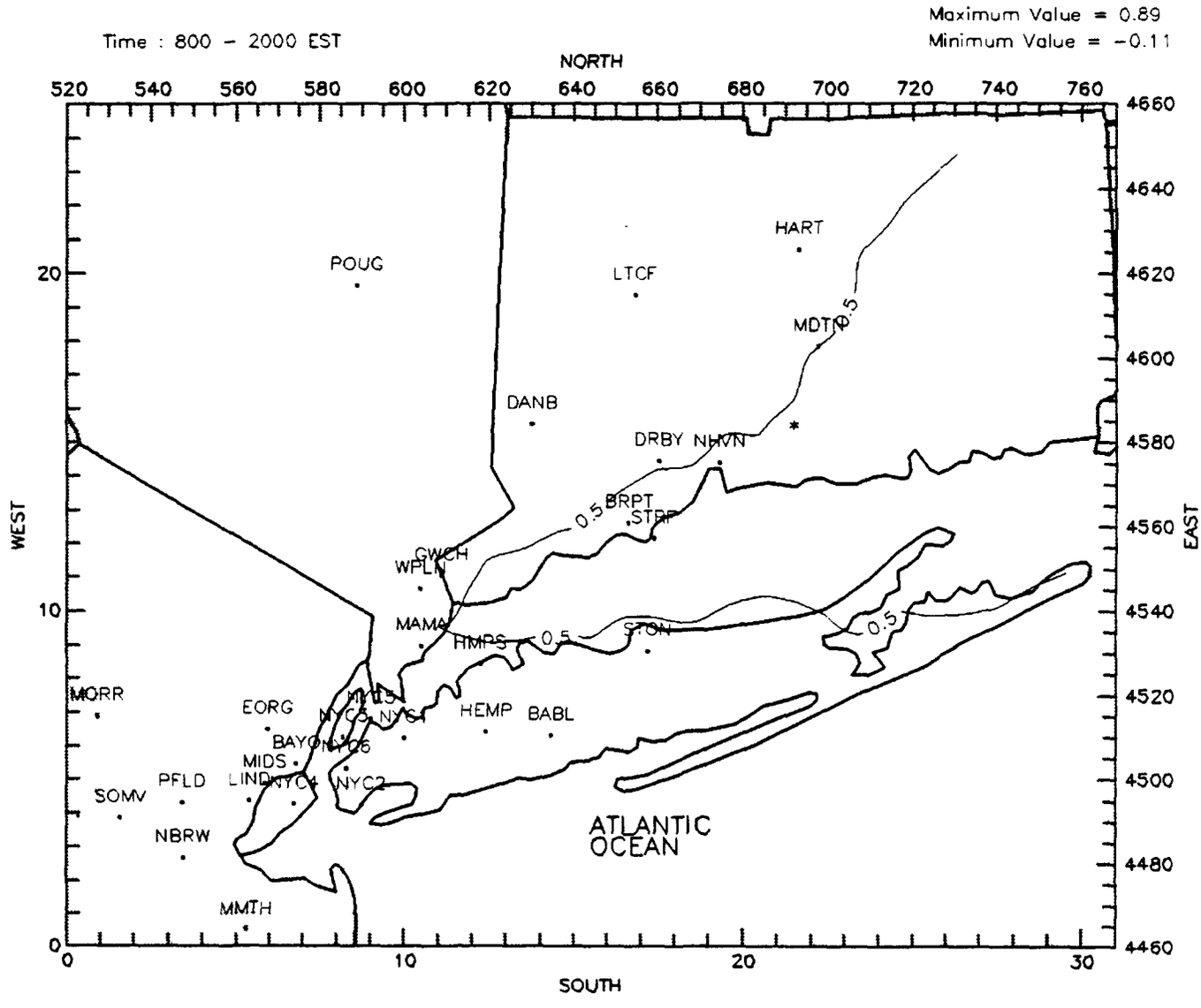

FIGURE 5-17. Differences in maximum daily ozone concentrations (ppb) between scenario 2 and scenario 3. (* denotes location of maximum ozone decrease.)

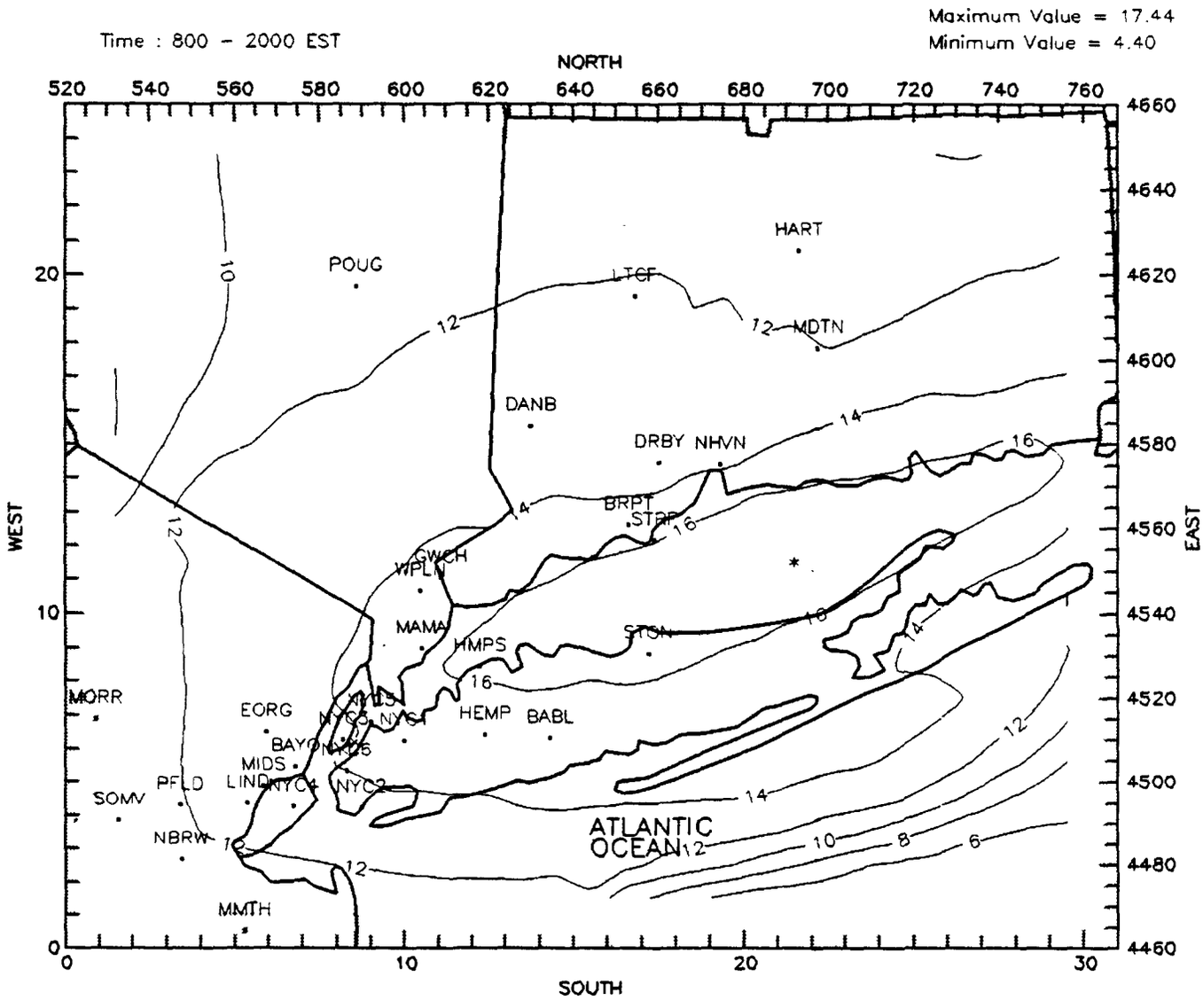

FIGURE 5-18. Maximum daily ozone concentrations (pphm) for scenario 4 for 8 August 1980. (* denotes location of maximum concentration value)

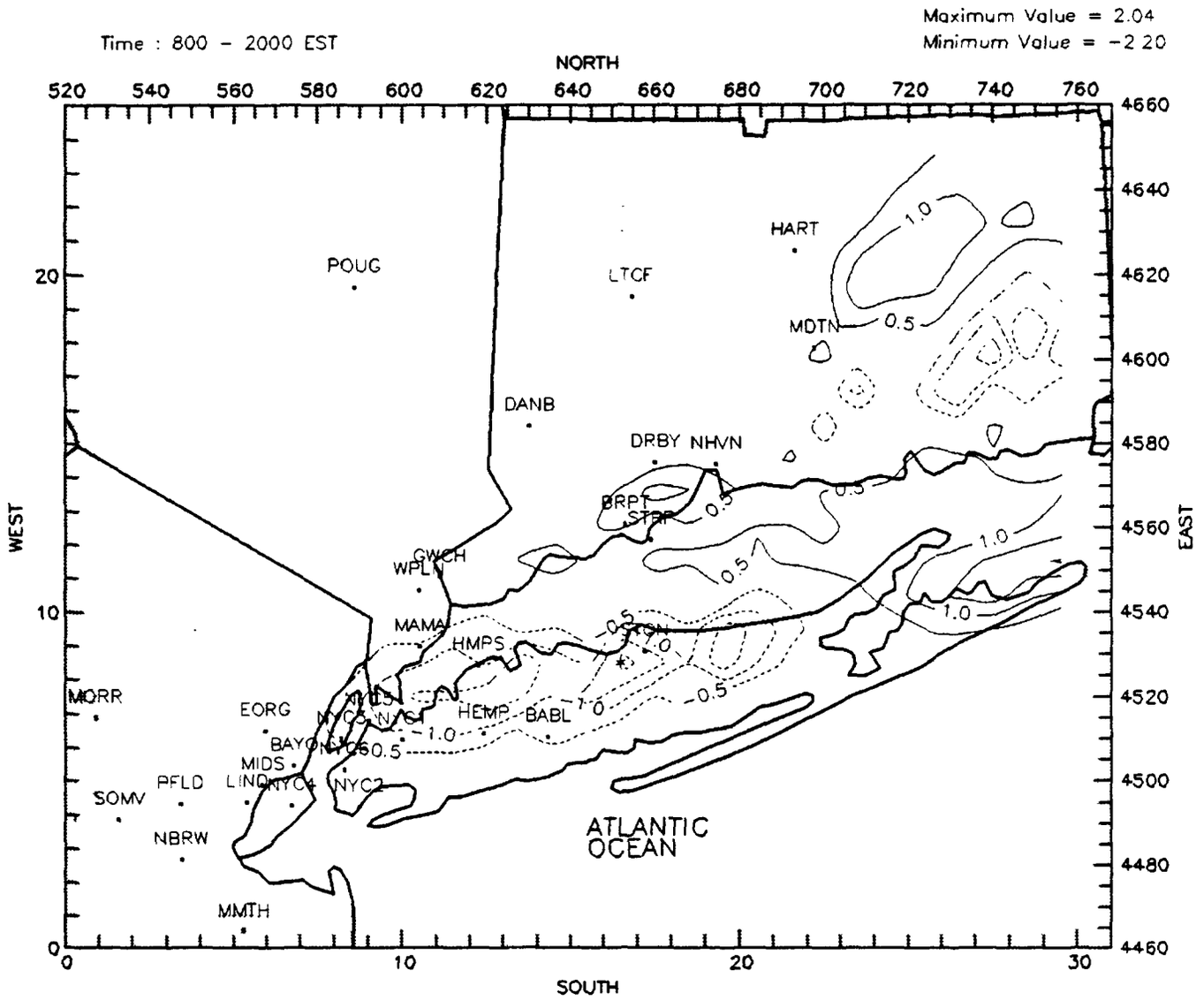

FIGURE 5-19. Differences in maximum daily ozone concentrations (ppb) between scenario 1 and scenario 4. (* denotes location of maximum ozone decrease.)

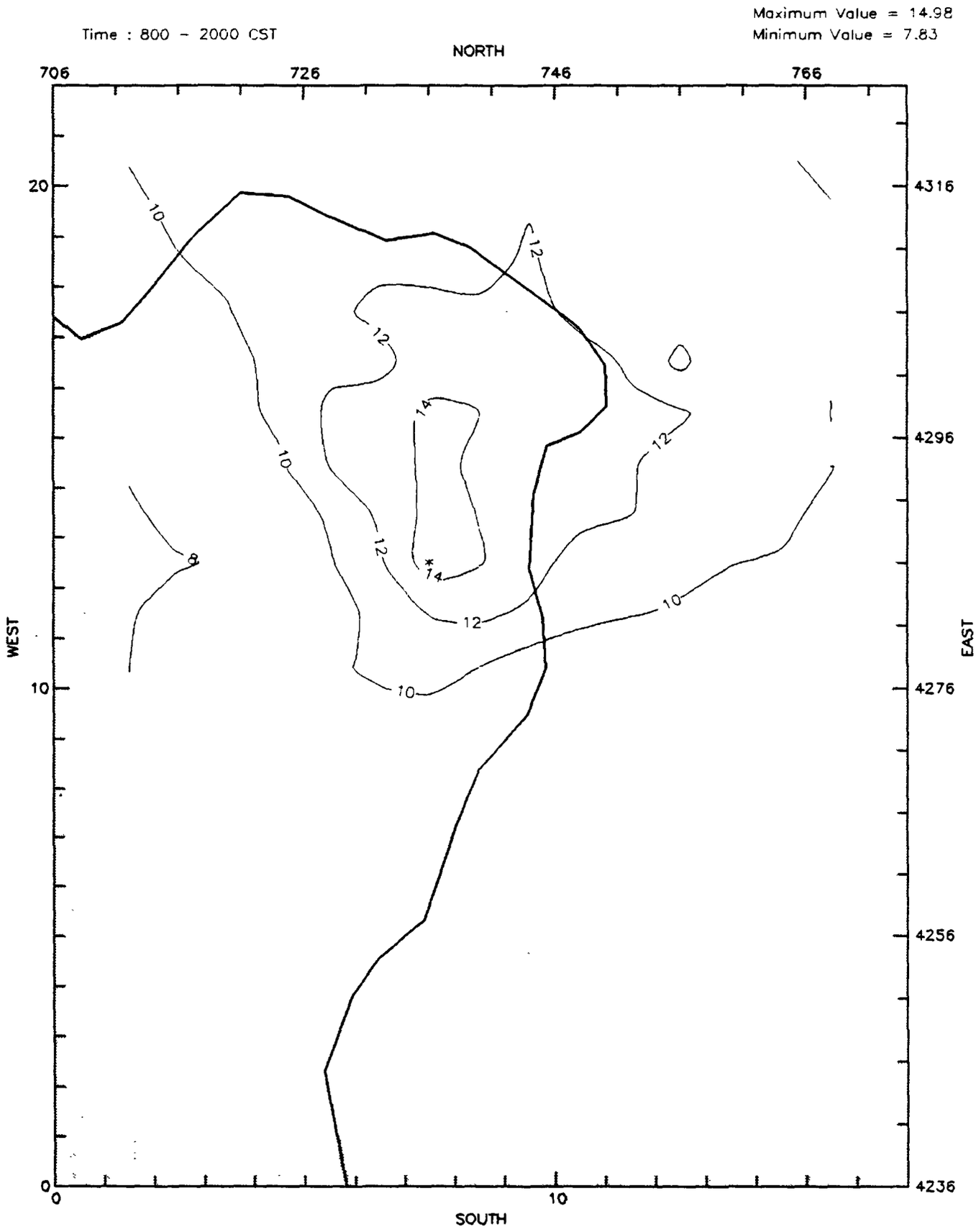

FIGURE 5-20. Maximum daily ozone concentrations (pphm) for scenario 1 on 13 July 1976. (* denotes location of maximum concentration value)

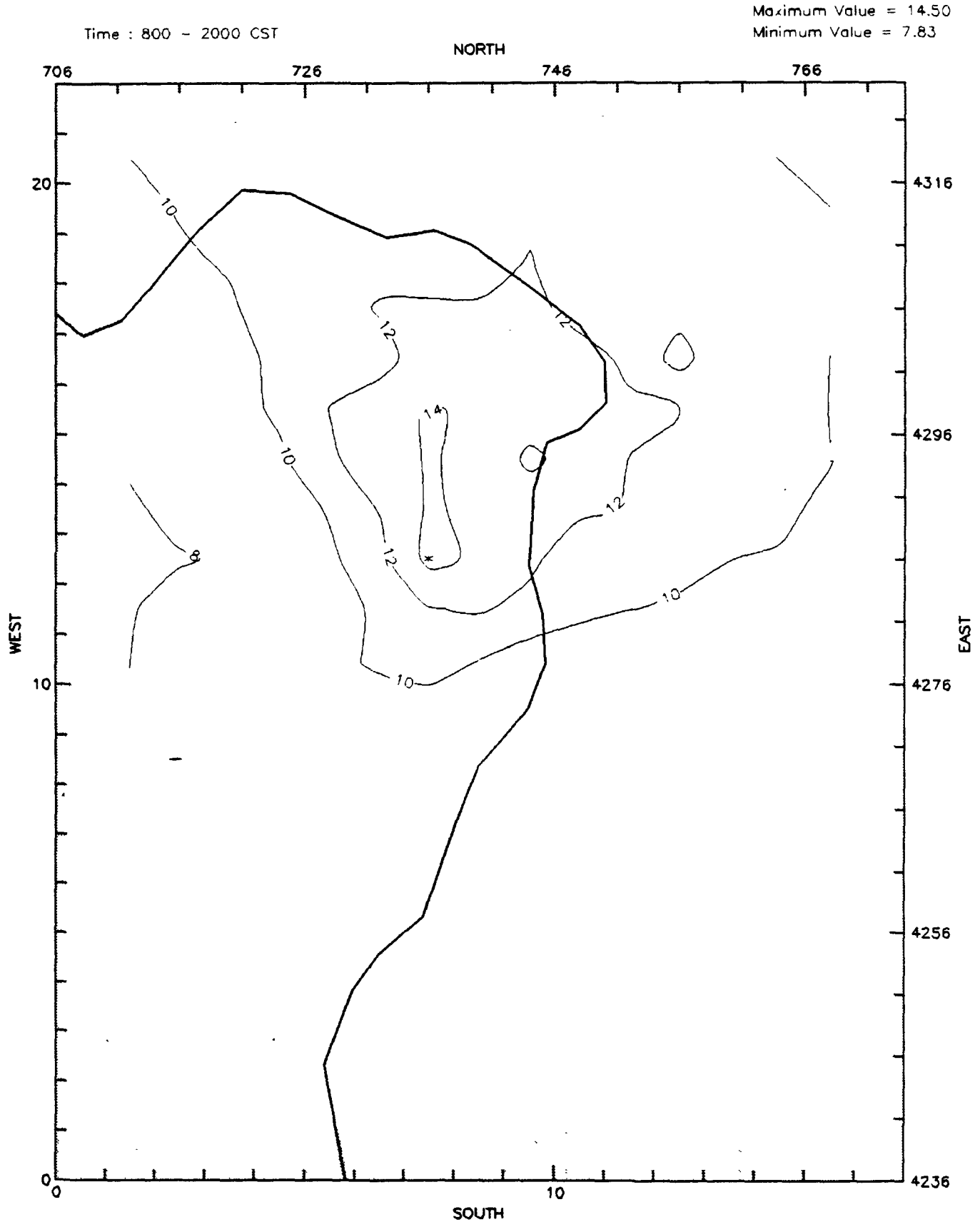

FIGURE 5-21. Maximum daily ozone concentrations (pphm) for scenario 2 on 13 July 1976. (* denotes location of maximum concentration value)

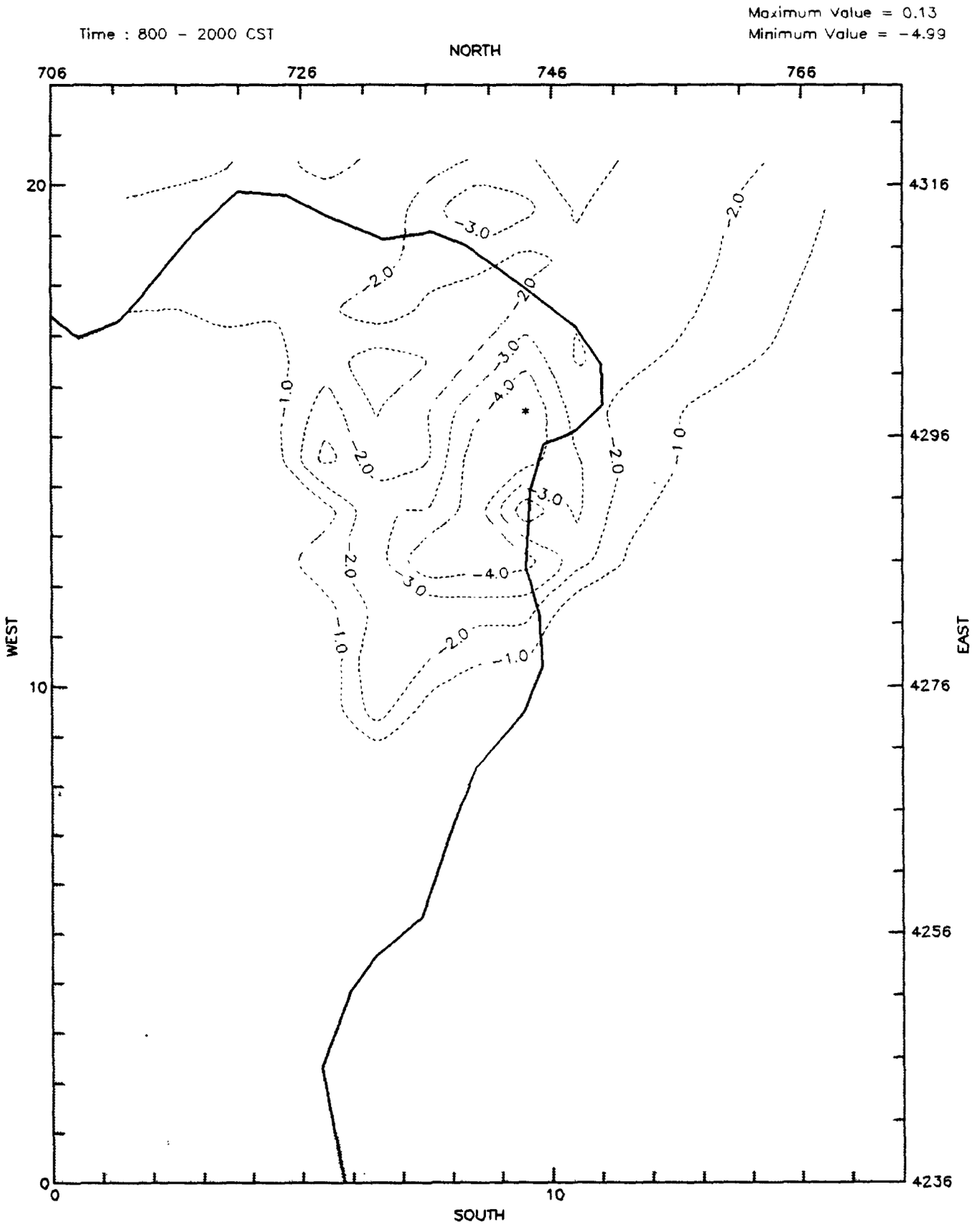

FIGURE 5-22. Differences in maximum daily ozone concentrations (ppb) between scenario 1 and scenario 2. (* denotes location of maximum ozone decrease.)

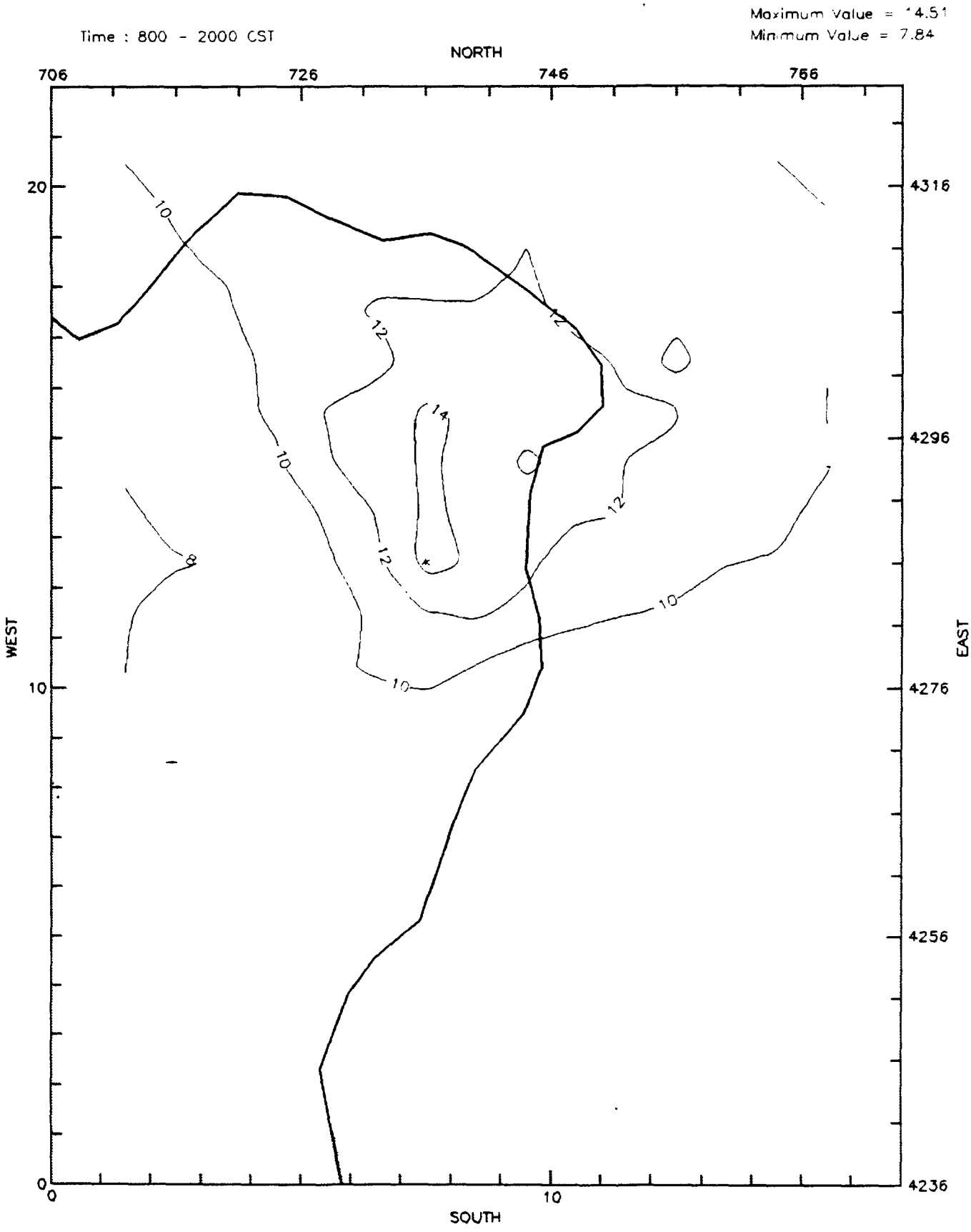

FIGURE 5-23. Maximum daily ozone concentrations (pphm) for scenario 5 on 13 July 1976. (* denotes location of maximum concentration value.)

88151

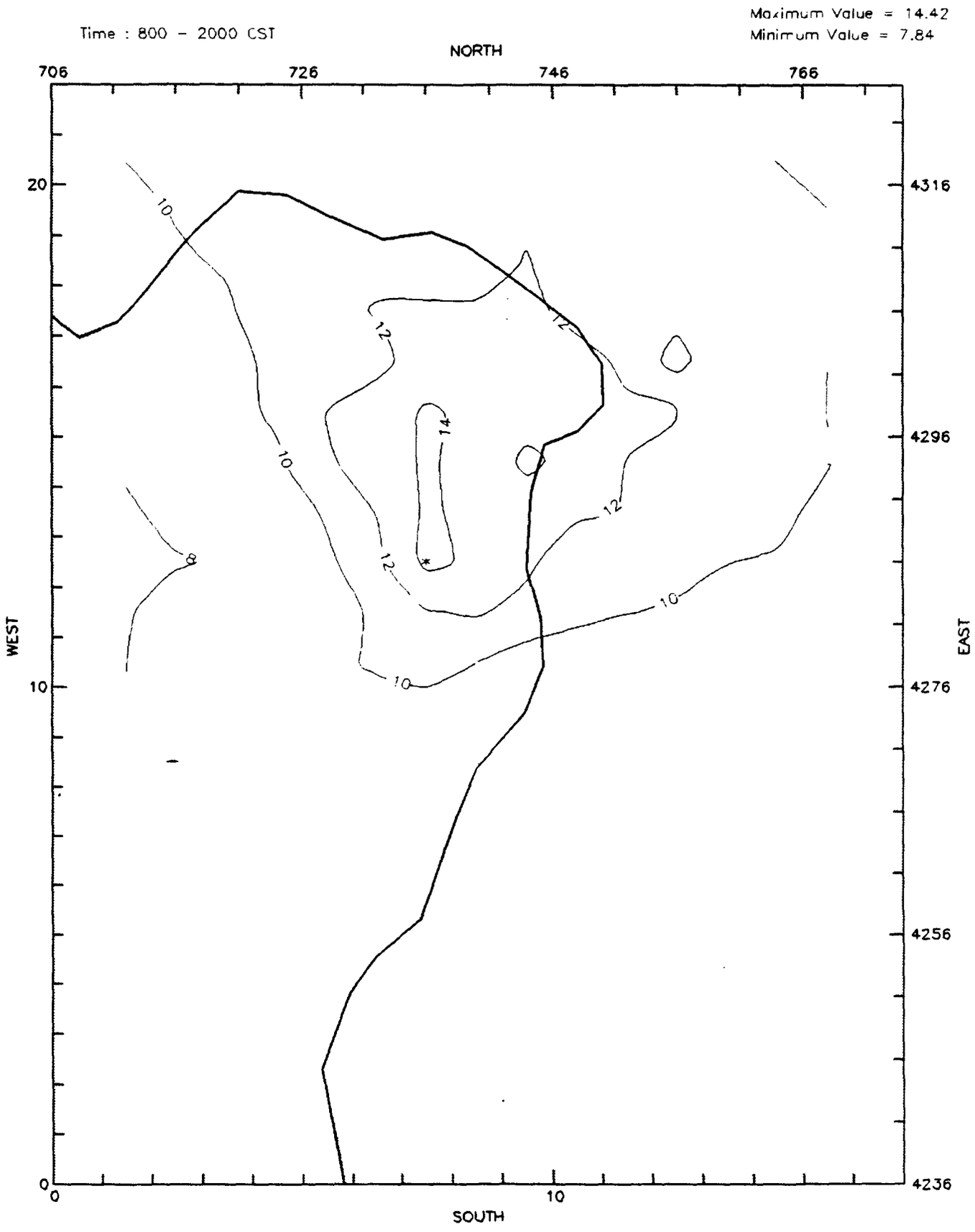

FIGURE 5-24. Maximum daily ozone concentrations (pphm) for scenario 6 on 13 July 1976. (* denotes location of maximum concentration value.)

88151

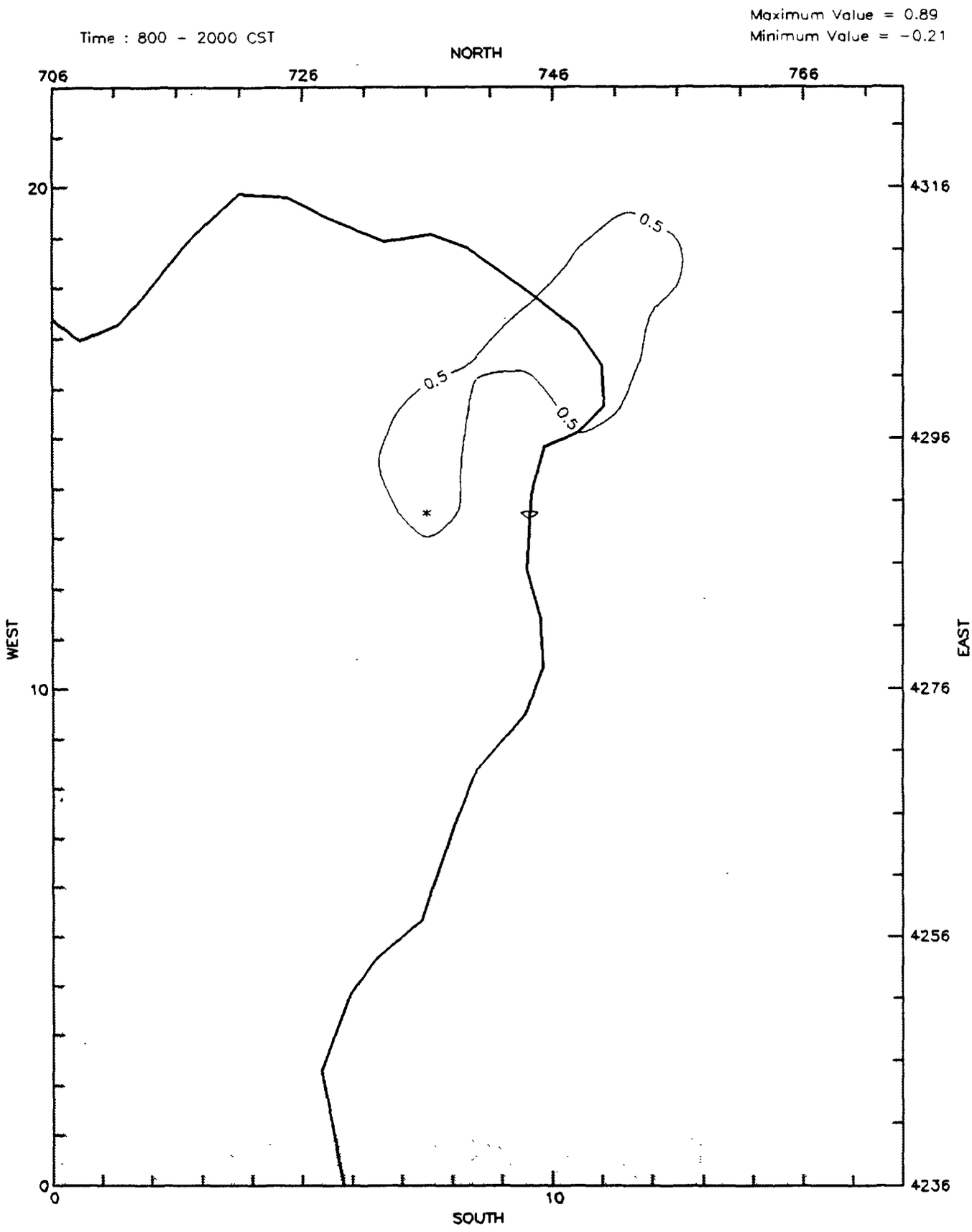

FIGURE 5-25. Differences in maximum daily ozone concentrations (ppb) between scenario 2 and scenario 5. (* denotes location of maximum ozone increase.)

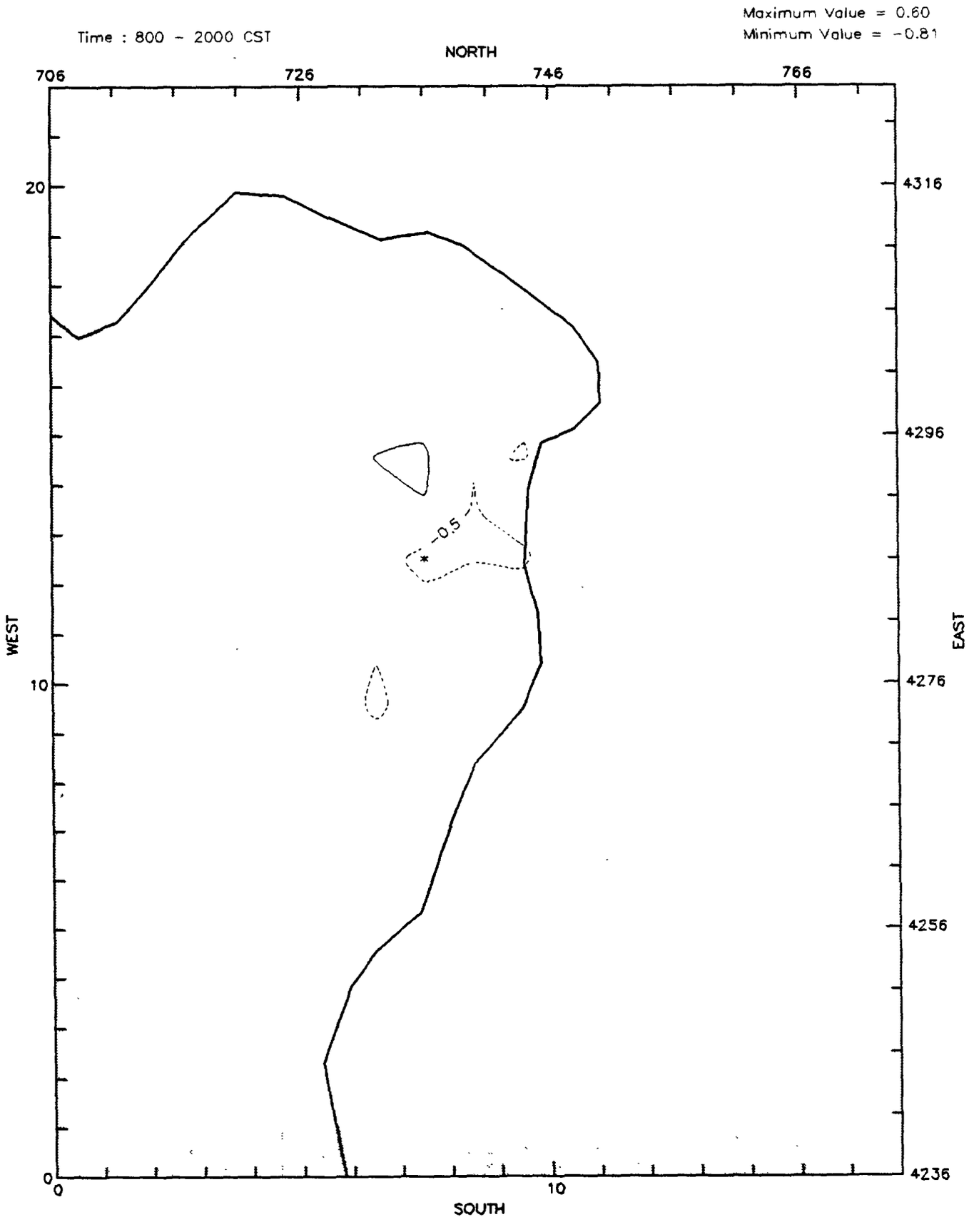

FIGURE 5-26. Differences in maximum daily ozone concentrations (ppb) between scenario 2 and scenario 6. (* denotes location of maximum ozone decrease.)

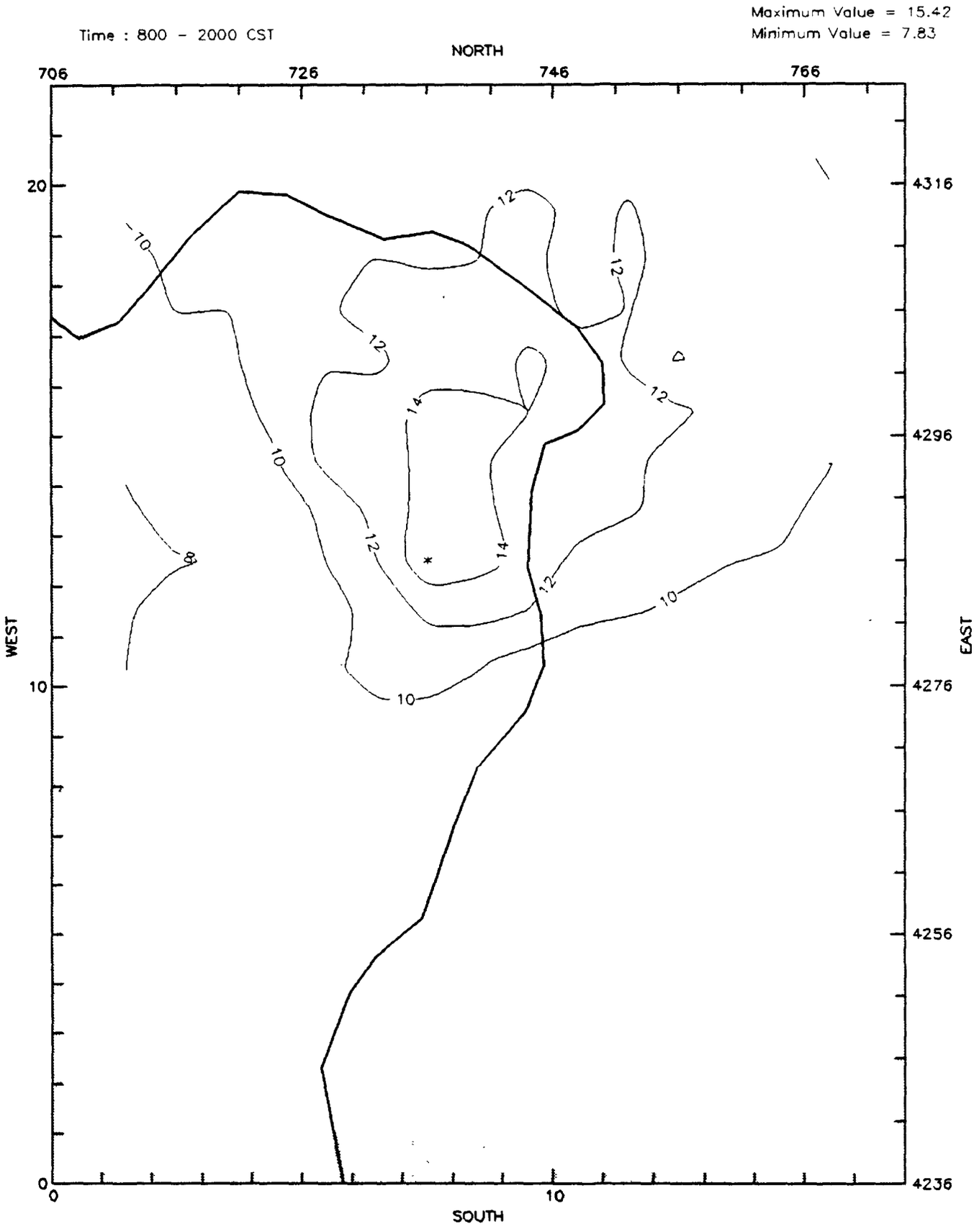

FIGURE 5-27. Maximum daily ozone concentrations (pphm) for scenario 7 on 13 July 1976. (* denotes location of maximum concentration value)

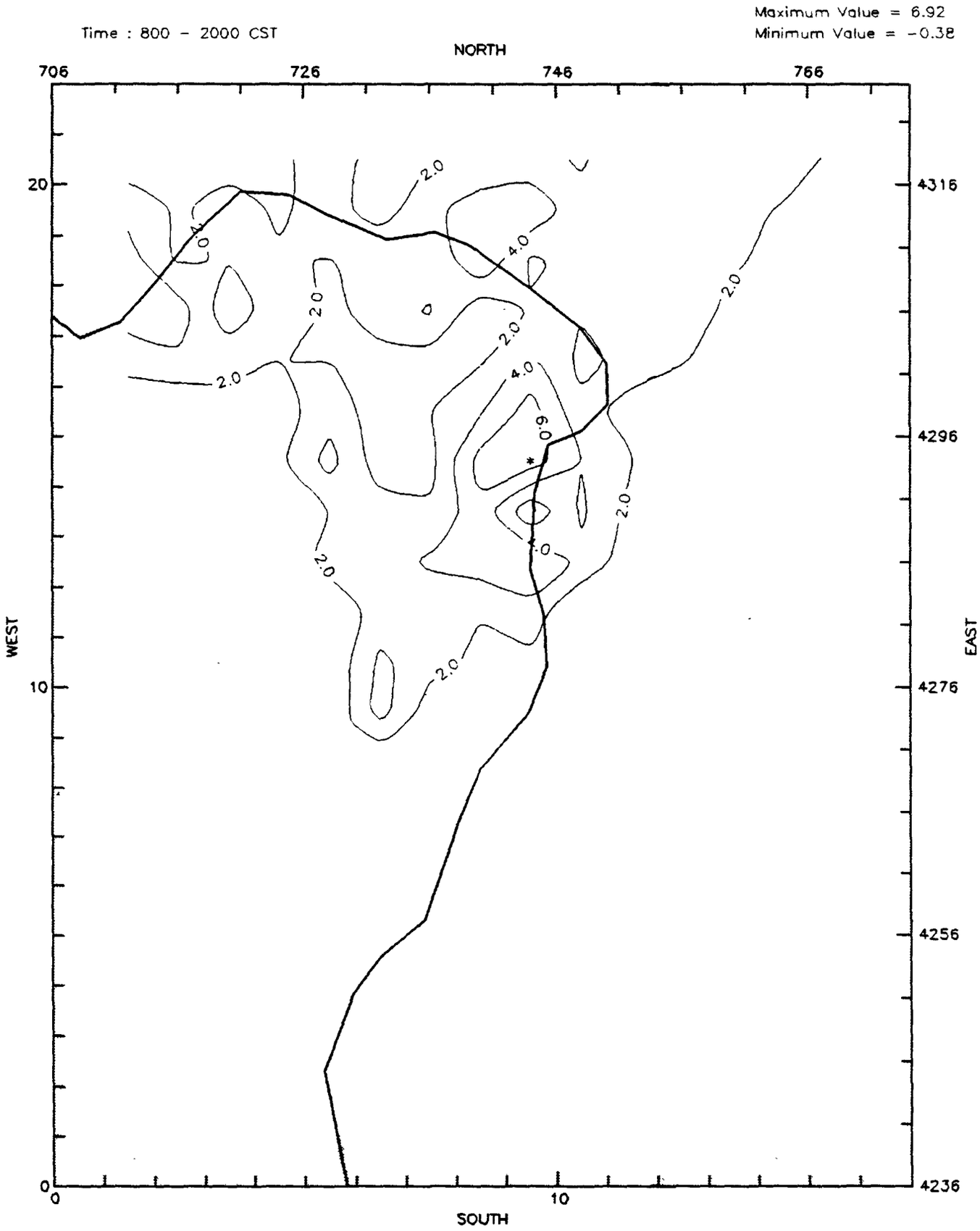

FIGURE 5-28. Differences in maximum daily ozone concentrations (ppb) between scenario 1 and scenario 7. (* denotes location of maximum ozone increase.)

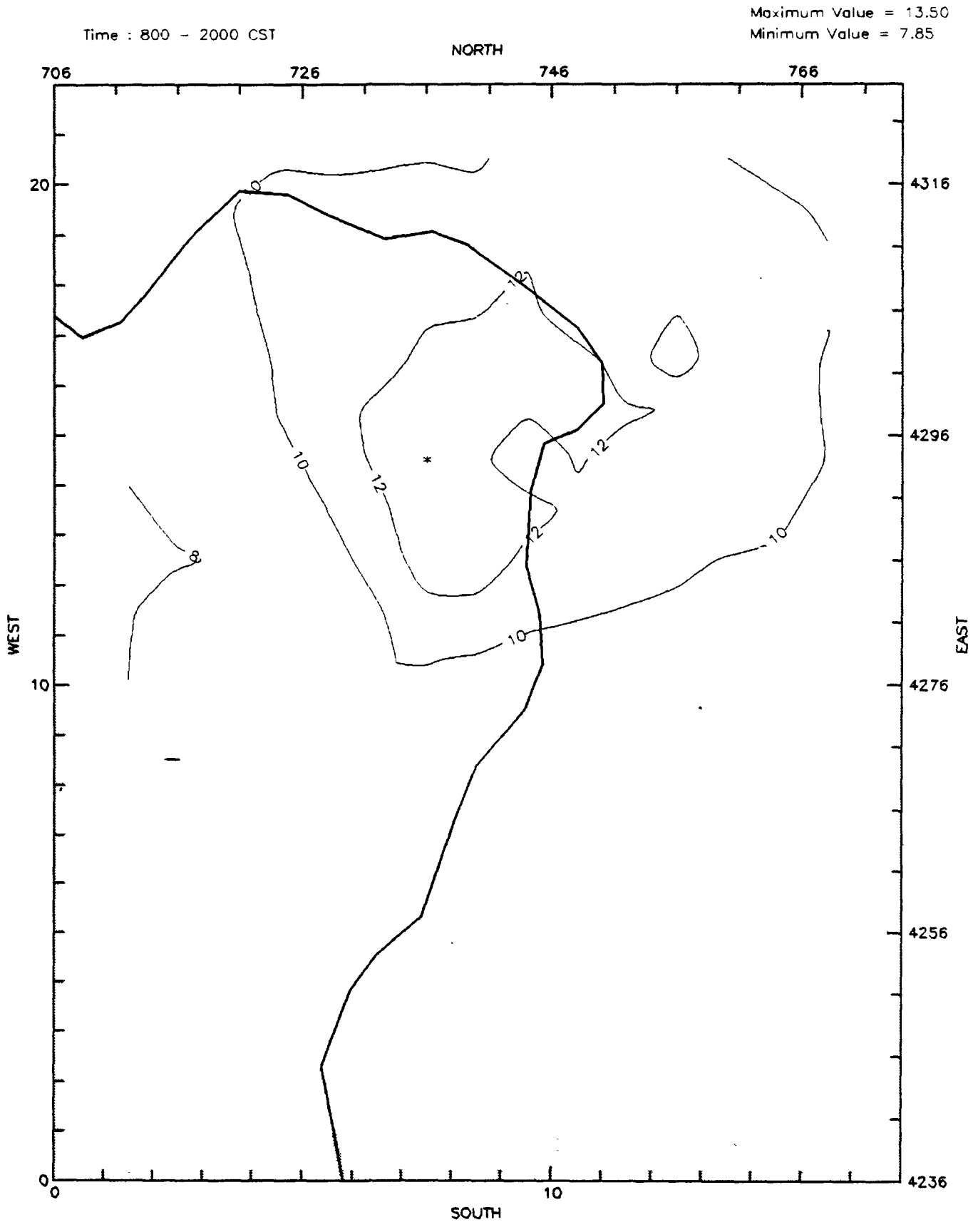

FIGURE 5-29. Maximum daily ozone concentrations (pphm) for SIP scenario A on 13 July 1976. (* denotes location of maximum concentration value)

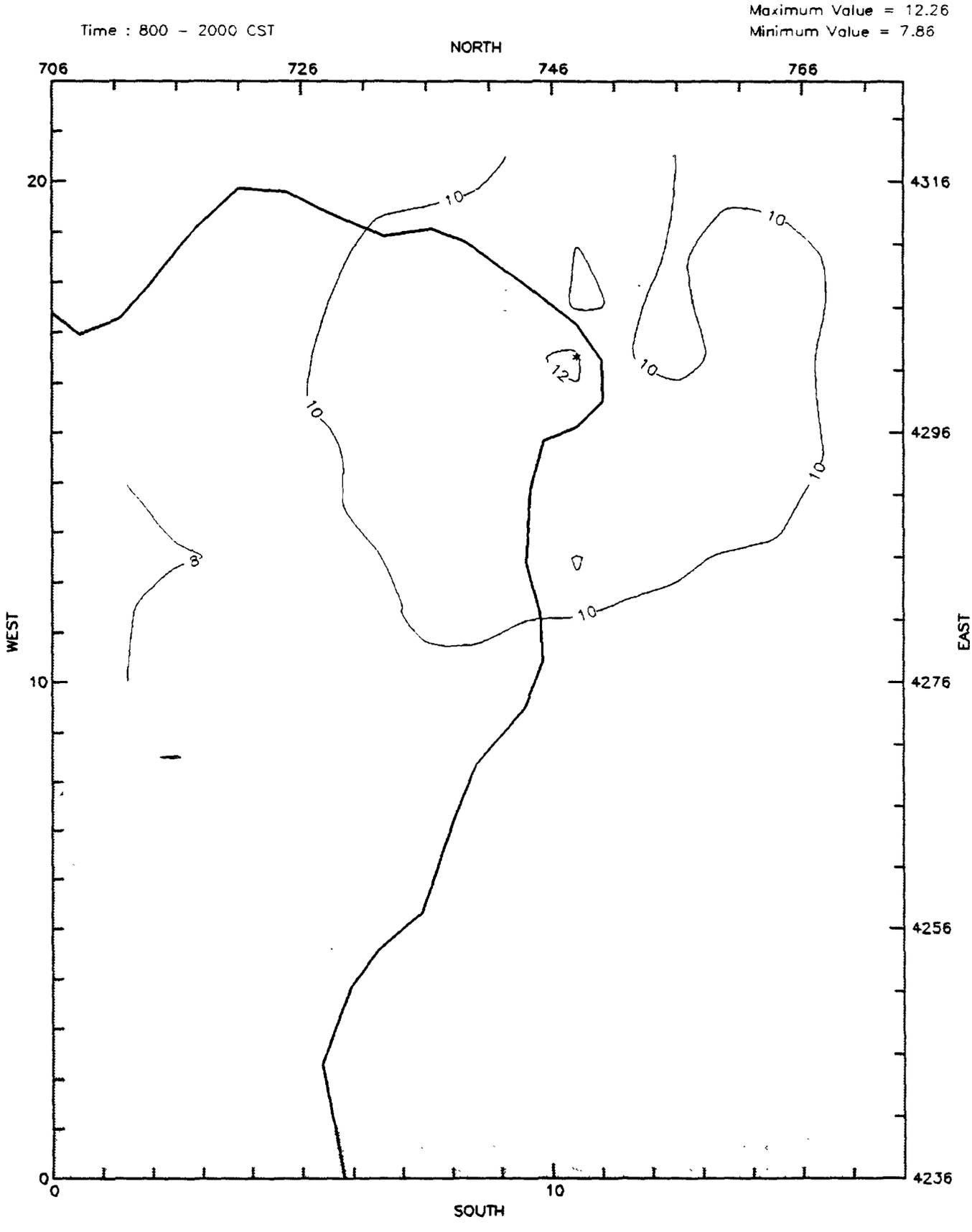

FIGURE 5-30. Maximum daily ozone concentrations (pphm) for SIP scenario B on 13 July 1976. (* denotes location of maximum concentration value)

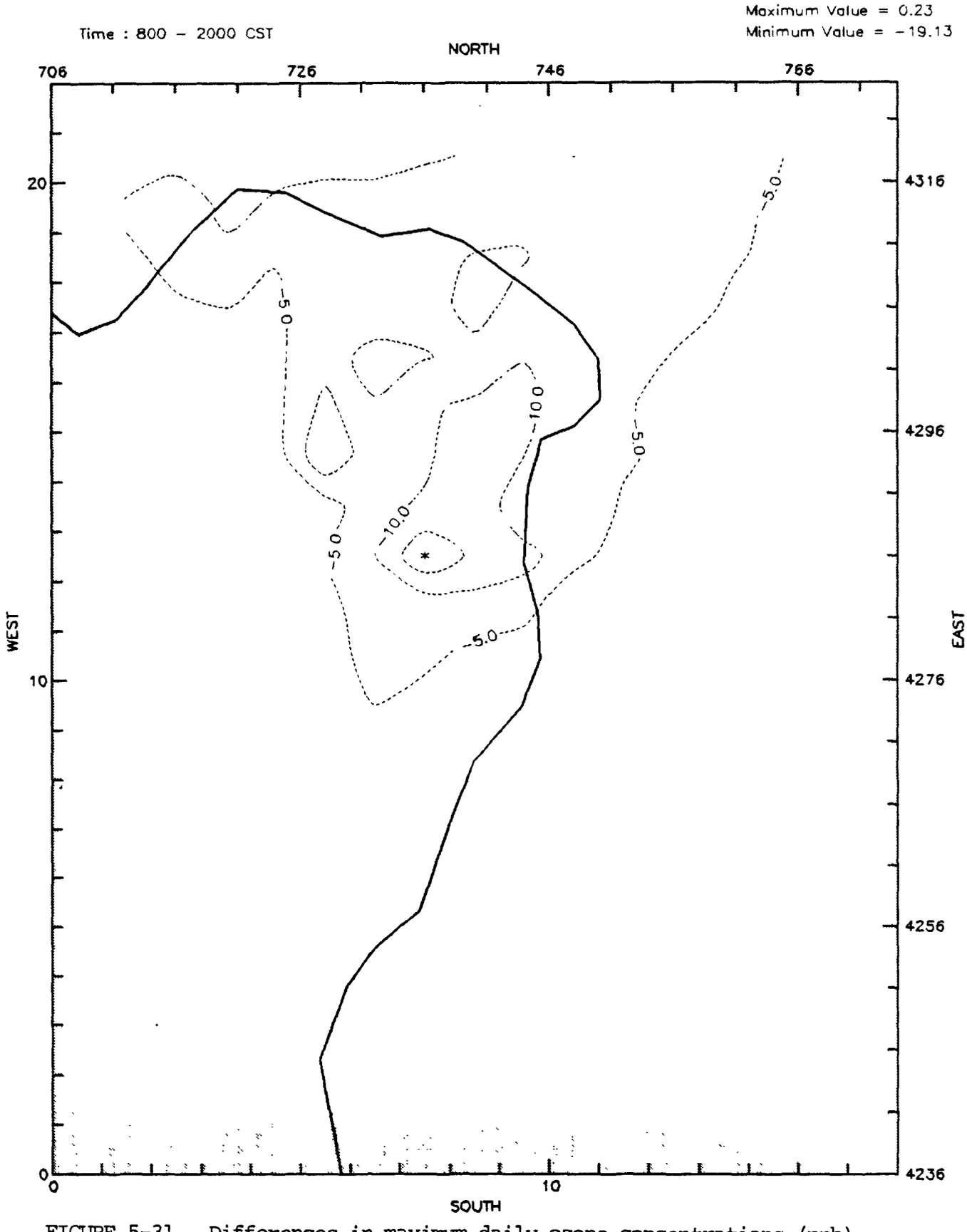

FIGURE 5-31. Differences in maximum daily ozone concentrations (ppb) between scenario 1 and SIP scenario A. (* denotes location of maximum ozone decrease.)

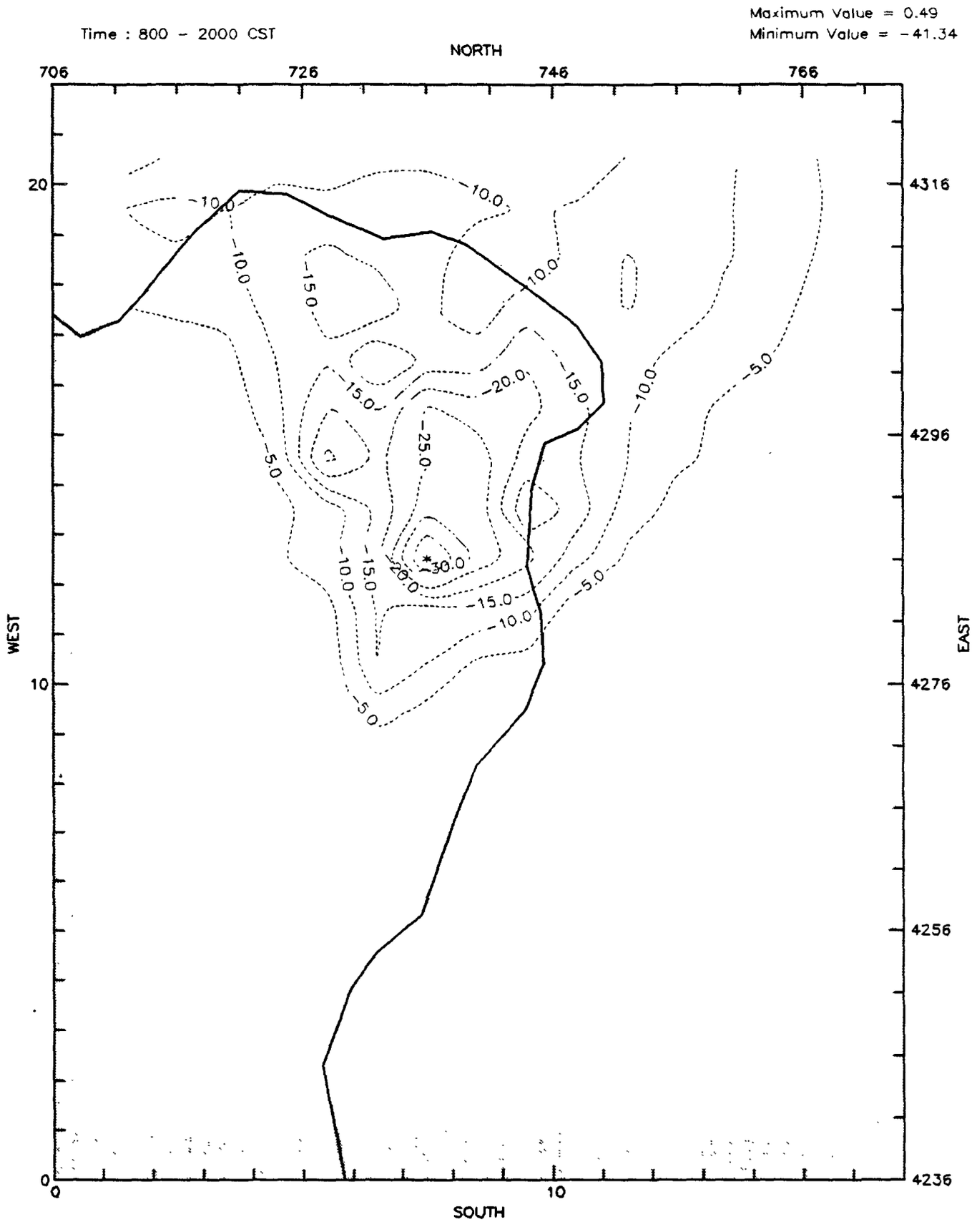

FIGURE 5-32. Differences in maximum daily ozone concentrations (ppb) between scenario 1 and SIP scenario B. (* denotes location of maximum ozone decrease.)

TABLE 5-1. Ozone monitoring sites within the New York modeling domain.

Site Name	Four-Letter Identifier
Hartford CT	HART
Bridgeport CT	BRPT
Danbury CT	DANB
Derby CT	DRBY
Greenwich CT	GWCH
Litchfield CT	LTCF
Middletown CT	MDTN
New Haven CT	NHVN
Stratford CT	STRF
Bayonne NJ	BAYO
Dumont NJ	DMNT
East Orange NJ	EORG
Linden NJ	LIND
Newark NJ	NEWK
Plainfield NJ	PLFD
Middlesex County NJ	MIDS
New Brunswick NJ	NBRW
Morris County NJ	MORR
Somerville NJ	SOMV
Hempstead Park NY	HEMP
Hempstead NY	HMPS
NYC Queens College NY	NYC1
NYC Kings NY	NYC2
NYC 2nd Avenue NY	NYC3
NYC Richmond NY	NYC4
NYC Woolsey NY	NYC5
NYC PS 321 NY	NYC6
White Plains NY	WPLN
Babylon NY	BABL
Mamaroneck NY	MAMA
Poughkeepsie NY	POUG
Stonybrook NY	STON

TABLE 5-2. UAM model performance for 8 August 1980 hourly ozone concentrations (comparison of application of the UAM (CB-IV) in this study and application of the UAM (CB-II) in the OMNYMAP studies).

Performance Measure	This Study UAM (CB-IV)	OMNYMAP Study UAM (CB-II)
Number of pairs	520	408
Average observed (pphm)	6.1	7.0
Average predicted (pphm)	9.3	11.7
Bias (pphm)	-3.1	-4.7
Average percent overprediction	51%	67%
Absolute average gross error (pphm)	3.8	5.0
Gross error percent difference	62%	71%
Root mean squared error (pphm)	4.9	6.8
Correlation coefficient	0.800	0.739
Peak observed (pphm)	24.6	24.6
Peak predicted (pphm) (unmatched by time or location)	23.5	26.3
Percent agreement of peak (unmatched by time or location)	4%	7%
Peak predicted (pphm) (matched by location but not time)	21.4	-23
Percent agreement of peak (matched by location but not time	13%	-7%

88151 9

TABLE 5-3. UAM model performance for 13 July 1980 hourly ozone concentrations (comparison of application of the UAM (CB-IV) in this study and application of the UAM (CB-II) in the St. Louis Ozone Modeling Project).

Performance Measure	This Study UAM (CB-IV)	St. Louis Ozone Modeling Project UAM (CB-II)
Number of pairs	265	184
Average observed (pphm)	6.8	8.3
Average predicted (pphm)	7.5	7.4
Bias (pphm)	-0.7	0.9
Average percent difference	11%	11%
Average absolute gross error (pphm)	1.7	N/A
Gross error percent difference	25%	N/A
Root mean squared error	2.2	1.8
Correlation coefficient	0.91	0.95
Peak observed (pphm)	22.3	22.3
Peak predicted (pphm) (unmatched by time or location)	24.2	17.4
Percent agreement of peak (unmatched by time or location)	9%	22%
Peak predicted (pphm) (matched by location but not time)	21.9	16.8
Percent agreement of peak (matched by location but not time)	2%	25%

88151 9

TABLE 5-4. Summary of region-wide total emission rates, VOC-to-NO_x ratios, and percent differences with the 1995 scenarios 1 and 2 for the 1995 emission scenarios.

Scenario*	VOC			CO			NO_x			VOC-to-NO_x Ratio
	Total (tons/day)	Percent Change from Scenario 1	Percent Change from Scenario 2	Total (tons/day)	Percent Change from Scenario 1	Percent Change from Scenario 2	Total (tons/day)	Percent Change from Scenario 1	Percent Change from Scenario 2	
New York										
Scenario 1	4429	-	+32	3547	-	+8	1181	-	0	10.8
Scenario 2	3344	-24	-	3298	-7	-	1183	0	-	8.1
Scenario 3	3496	-21	+5	2763	-22	-16	1209	+2	+2	8.3
Scenario 4	2960	-33	-11	3547	0	+8	1182	0	0	7.2
St. Louis										
Scenario 1	676	-	+18	592	-	+7	350	-	0	5.6
Scenario 2	575	-15	-	555	-6	-	350	0	-	4.7
Scenario 5	586	-13	+2	523	-12	-6	352	+1	+1	4.8
Scenario 6	568	-16	-1	511	-14	-8	352	+1	+1	4.6
Scenario 7	849	+26	+48	592	0	+7	350	0	0	7.0
SIP Scenario A	404	-40	-30	592	0	+7	350	0	0	3.3
SIP Scenario B	405	-40	-30	592	0	+7	350	0	0	3.3

* See text for elaboration of scenarios (pages 49-50).

TABLE 5-5. Comparison of predicted peak ozone, percent change in peak ozone, and VOC emissions between scenarios 1 and 2 and all other 1995 emission scenarios.

Scenario*	Highest Ozone Concentration (pphm)	Percent Change of Highest Ozone with Scenario 1	Percent Change of VOC Emissions with Scenario 1	Percent Change of Highest Ozone with Scenario 2	Percent Change of VOC Emissions with Scenario 2
New York†					
Scenario 1 (current RVP)	17.4	0	0	0	+32
Scenario 2 (low RVP)	17.4	0	-24	0	0
Scenario 3 (low RVP with ethanol)	17.5	+0.5	-21	+0.5	+5
Scenario 4 (current RVP with no running losses)	17.4	0	-33	0	-11
St. Louis					
Scenario 1 (current RVP)	15.0	0	0	+7.0	+18
Scenario 2 (low RVP)	14.5	-3.1	-15	0	0
Scenario 5 (low RVP with ethanol)	14.5	-3.1	-13	0	+2
Scenario 6 (low RVP with ETBE)	14.4	-3.8	-16	-0.2	-1
Scenario 7 (current RVP with high running losses)	15.4	+2.7	+26	+6.2	+48
SIP Scenario A (40% VOC reduction)	13.5	-10.0	-40	-6.9	-30
SIP Scenario B (40% VOC reduction based on reactivity)	12.3	-18.7	-40	-15.7	-30

* See text for elaboration of scenarios (pages 49-50).

† The analysis did not consider the effects of changes in emissions of the different emission scenarios on the long-range transport of pollutants (i.e., boundary conditions). This contributes heavily to the apparent insensitivity of the ozone peak to large changes in the VOC inventory for the New York applications. The reader is referred to the text for further explanation (pages 132-133).

References

Ames, J., T. C. Myers, L. E. Reid, D. C. Whitney, S. H. Golding, S. R. Hayes, and S. D. Reynolds. 1985. "SAI Airshed Model Operations Manuals, Volume I--User's Manual and Volume II--Systems Manual." U.S. Environmental Protection Agency, Research Triangle Park, North Carolina (EPA-600/8-85-007a,b).

Bass, A. M., L. C. Glasgow, C. Miller, J. P. Jesson, and D. L. Filken. 1980. Planet Space Sci., 28:675.

Boris, J. P., and D. L. Book. 1973. Flux-corrected transport: I. SHASTA, a fluid transport algorithm that works. J. Comp. Phys., 11:38-69.

Brimblecombe, P. 1986. Air Composition and Chemistry. Cambridge University Press.

Burton, C. S. 1988. Comments on "Ozone Air Quality Models." J. Air Pollut. Control Assoc., 38(9):1119-1128.

Chock, D. P., and A. M. Dunker. 1983. A comparison of numerical methods for solving the advection equation. Atmos. Environ., 17:11-24.

Chock, D. P. 1985. A comparison of numerical methods for solving the advection equation--II. Atmos. Environ., 19:571-586.

Cole, H. S., D. E. Layland, G. K. Moss, and C. F. Newberry. 1983. "The St. Louis Ozone Modeling Project." U.S. Environmental Protection Agency, Research Triangle Park, NC (EPA-450/4-83-019).

Dennis, R. L., M. W. Downton, and R. S. Keil. 1983. "Evaluation of Performance Measures for an Urban Photochemical Model." U.S. Environmental Protection Agency (EPA-450/4-83-021).

Douglas, S., and R. Kessler. 1988. "User's Guide to the Diagnostic Wind Model. Version 1.0." Systems Applications, Inc., San Rafael, California.

EPA. 1980. "Northeast Corridor Regional Modeling Project Continuous Nonmethane Organic Compound Data Collection." U.S. Environmental Protection Agency, Research Triangle Park, North Carolina (EPA-450/4-80-034).

EPA. 1985a. "Compilation of Air Pollutant Emission Factors. Volume I: Stationary Point and Area Sources." U.S. Environmental Protection Agency, Research Triangle Park, North Carolina (AP-42).

EPA. 1985b. "National Air Quality and Emissions Trends Report, 1985." U.S. Environmental Protection Agency, Research Triangle Park, North Carolina (EPA-450/4-87-001).

EPA. 1986. "Guideline on Air Quality Models (Revised)." U.S. Environmental Protection Agency, Research Triangle Park, North Carolina (EPA-450/2-78-027R).

EPA. 1987a. "Control of Gasoline Volatility and Evaporative Hydrocarbon Emissions from New Motor Vehicles." U.S. Environmental Protection Agency.

EPA. 1987b. "Guideline for Use of City-Specific EKMA in Preparing Post-1987 Ozone SIP's." U.S. Environmental Protection Agency.

EPA. 1988. Office of Mobile Sources, personal communication.

EPA. 1988. "Air Emissions Species Manual. Volume I: Volatile Organic Compound Species Profiles." U.S. Environmental Protection Agency, Research Triangle Park, North Carolina (EPA-450/2-88-003a).

Federal Register. 1987. "State Implementation Plans; Approval of Post-1987 Ozone and Carbon Monoxide Plan Revisions for Areas Not Attaining the National Ambient Air Quality Standards; Notice." Federal Register, Vol. 52, No. 226 (November 24, 1987).

Fehsenfeld, F. C., D. D. Parrisch, and D. W. Fahey. 1988. "The Measurement of NO_x in the Non-Urban Troposphere," in Tropospheric Ozone, I. Isaksen, ed. (D. Reidel Publishing Company).

Fox, D. 1981. Judging air quality model performance. Bull. Am. Meteorol. Soc., 62(5):599-609.

Fox, D. G. 1984. Uncertainty in air quality modeling. Bull. Am. Meteorol. Soc., 65:27-36.

Gery, M. W., G. Z. Whitten, and J. P. Killus. 1988. "Development and Testing of the CBM-IV for Urban and Regional Modeling." Systems Applications, Inc., San Rafael, California (SYSAPP-88/002).

Godden, D., and F. Lurmann. 1983. "Development of the PLMSTAR Model and Its Application to Ozone Episode Conditions in the South Coast Air Basin." Environmental Research & Technology, Inc., Westlake Village, California (ERT P-A702-200).

Hogo, H., L. A. Mahoney, and M. A. Yocke. 1988. "Draft Air Quality Management Plan 1988 Revision. Draft Appendix V-R. Urban Airshed Model Performance Evaluation for 5-7 June 1985." Systems Applications, Inc., San Rafael, California (SYSAPP-88/138).

Hogo, H., and M. W. Gery. 1988. "User's Guide for Executing OZIPM-4 with CBM-IV or Optional Mechanisms. Vol. I. Description of the Ozone Isopleth Plotting Package, Version 4." Systems Applications, Inc., San Rafael, California (SYSAPP-88/001).

Hogo, H., and M. W. Gery. 1988. "Guidelines for Using OZIPM-4 with CBM-IV or Optional Mechanisms, Volume 1: Description of the Ozone Isopleth Plotting Package, Version 4." Systems Applications, Inc., San Rafael, California (SYSAPP-88/001).

Hogo, H., L. A. Mahoney, M. A. Yocke, and C. S. Burton. 1987. "Proposed UAM Modeling Protocol to Assess Ozone Air Quality in the South Coast Air Basin." Systems Applications, Inc., San Rafael, California (SYSAPP-88/107).

Kelley, R. F. 1981. "User's Manual for Mixing Height Computer Program." U.S. Environmental Protection Agency, Research Triangle Park, North Carolina (EPA-450/4-81-022).

Killus, J. P., J. P. Meyer, D. R. Durran, G. E. Anderson, T. N. Jerskey, S. D. Reynolds, and J. Ames. 1977. "Continued Research in Mesoscale Air Pollution Simulation Modeling--Vol. V: Refinements in Numerical Analysis, Transport, Chemistry, and Pollutant Removal." Systems Applications, Inc., San Rafael, California (EF77-142R).

Logan, J. A. 1985. Tropospheric ozone: seasonal behaviour, trends, and anthropogenic influence. J. Geophys. Res., 90:10463-10468.

Morris, R. E., R. C. Kessler, S. G. Douglas, and K. R. Styles. 1987. "Rocky Mountain Acid Deposition Model Assessment: Evaluation of Mesoscale Models for Use in Complex Terrain." U.S. Environmental Protection Agency (EPA-600/3-87-013; NTIS PB87-180584-AS).

Morris, R. E., R. C. Kessler, S. G. Douglas, K. R. Styles, and G. E. Moore. 1988. "Rocky Mountain Acid Deposition Model Assessment Acid Rain Mountain Mesoscale Model (ARM3)." Systems Applications, Inc., San Rafael, California (SYSAPP-88/152).

O'Brien, J. J. 1970. A note on the vertical structure of the eddy exchange coefficient in the planetary boundary layer. J. Atmos. Sci., 27:1213-1215.

OTA. 1988a. "Urban Ozone and the Clean Air Act: Problems and Proposals for Change." Office of Technology Assessment, Washington, D.C.

OTA. 1988b. "Ozone and the Clean Air Act: Summary of OTA Workshop with State and Local Air Pollution Control Agency Officials." Office of Technology Assessment, Washington, D.C.

OTA. 1988c. "Ozone and the Clean Air Act: A Summary of OTA Workshops on Congressional Options to Address Nonattainment of the Ozone Standard." Office of Technology Assessment, Washington, D.C.

Pechan, E. H., and Associates. 1988. "National Assessment of VOC, CO, and NO_x Emissions and Costs for Attainment of the Ozone and CO Standards" (in preparation).

Pedco. 1980. "Northeast Corridor Regional Modeling Project (NECRMP)." U.S. Environmental Protection Agency (EPA-450/4-80-034).

Peters, L. K., and W. L. Chameides. 1980. "Methane and Carbon Monoxide in the Troposphere," in Advances in Environmental Science and Engineering, Volume 3, Pfaffin and Ziegler, eds. (Gordon and Breach Science Publishers), pp. 100-149.

Price, H. S., R. S. Varga, and J. E. Warren. 1966. Applications of oscillation matrices to diffusion and convection equations. J. Math. Phys., 45:301-311.

Rao, S. T. 1987. "Application of the Urban Airshed Model to the New York Metropolitan Area." U.S. Environmental Protection Agency, Research Triangle Park, North Carolina (EPA-450/4-87-011).

Rao, S. T., and G. Sistla. 1987. "Sensitivity Analysis of the Urban Airshed Model." Air Pollution Control Association Conference on the Scientific & Technical Issues Facing the Post-1987 Ozone Control Strategies. Hartford, Connecticut (16-19 November).

Ross, D. G., and I. Smith. 1986. "Diagnostic Wind Field Modeling for Complex Terrain--Testing and Evaluation." Centre for Applied Mathematical Modeling, Chisholm Institute of Technology (CAMM Report No. 5/86).

Schere, K. L. 1983. An evaluation of several numerical advection schemes. Atmos. Environ., 17:1897-1907.

Schere, K. L., and K. L. Demerjian. 1977. "Calculation of Selected Photolytic Rate Constants over a Diurnal Range. A Computer Algorithm." U.S. Environmental Protection Agency, Research Triangle Park, North Carolina (EPA-600/4-77-015).

Schere, K. L., and J. H. Shreffler. 1982. "Final Evaluation of Urban-Scale Photochemical Air Quality Simulation Models." Environmental Sciences Research Laboratory, U.S. Environmental Protection Agency, Research Triangle Park, North Carolina (EPA-600/3-82-094).

Science. 1988. Rural and urban ozone. Editorial in Science, 241(4873):1569.

Seinfeld, J. H. 1988a. Ozone air quality models. A critical review. J. Air Pollut. Control Assoc., 38(5):616.

Seinfeld, J. H. 1988b. Closing remarks. J. Air Pollut. Control Assoc., 38(8):1136-1137.

Shareef, G. S., W. A. Butler, L. A. Bravo, and M. B. Stockton. 1988. "Air Emissions Species Manual. Volume I. Volatile Organic Compound Species Profiles." U.S. Environmental Protection Agency, Research Triangle Park, North Carolina (EPA-450/2-88-003a).

Smolarkiewicz, P. K. 1983. A simple positive definite advection scheme with small implicit diffusion. Monthly Weather Review, 111:479-486.

Whitten, G. Z. 1988. "Evaluation of the Impact of Ethanol/Gasoline Blends on Urban Ozone Formation." Systems Applications, Inc., San Rafael, California (SYSAPP-88/029).

Whitten, G. Z., J. P. Killus, and H. Hogo. 1980. "Modeling of Simulated Photochemical Smog with Kinetic Mechanisms. Volume 1. Final Report." Systems Applications, Inc., San Rafael, California (EPA-600/3-80-028a).

Whitten, G. Z., T. C. Meyers, C. Daly, L. R. Chinkin, S. D. Reynolds, N. M. Yonkow, and B. Austin. 1985. "Application of the Urban Airshed Model to Kern County." Systems Applications, Inc., San Rafael, California (SYSAPP-85/200).

Zalesak, S. T. 1979. Fully multi-dimensional flux-corrected transport algorithms for fluids. J. Comput. Phys., 31:335-362.

Zimmerman, D., W. Tax, M. Smith, J. Demmy, and R. Battye. 1988. "Anthropogenic Emissions Data for the 1985 NAPAP Inventory." U.S. Environmental Protection Agency, Washington, D.C. (EPA-600/7-88-022).

Appendix A

PROTOCOL DOCUMENT FOR URBAN AIRSHED AND EKMA MODELING IN THE NEW YORK METROPOLITAN AREA

Final Report

PROTOCOL DOCUMENT FOR URBAN AIRSHED AND EKMA MODELING IN THE NEW YORK METROPOLITAN AREA

SYSAPP-88/149

September 1988

Prepared for

Mr. John Chamberlin

U.S. Environmental Protection Agency
Office of Policy Planning and Evaluation
Washington, DC 20460

and

Mr. Richard Scheffe

U.S. Environmental Protection Agency
Office of Air Quality Planning and Standards
Research Triangle Park, NC 27711

Prepared by

Systems Applications, Inc.
101 Lucas Valley Road
San Rafael, CA 94903
(415)-472-4011

D9510 88136r1

1 INTRODUCTION

BACKGROUND

Four offices of the U.S. Environmental Protection Agency are involved in a joint EPA-sponsored research study to investigate urban ozone air quality in a number of U.S. cities. The offices involved are the following: Office of Air Quality Planning and Standards (OAQPS), Office of Research and Development (ORD), Office of Mobile Sources (OMS), and the Office of Policy, Planning and Evaluation (OPPE). The urban areas to be studied include New York, St. Louis, Philadelphia, Dallas, and Atlanta. A photochemical modeling analysis will be conducted in each of these urban areas. This protocol addresses the New York application in particular.

Over 60 urban areas in the United States have failed to meet the legislated deadline (31 December 1987) for ozone attainment. Possible reasons for this include one or more of the following: the failure to actually reduce emissions or enforce emission control requirements, the underestimation of actual urban hydrocarbon emissions, and/or reliance on overly simplistic modeling approaches for calculating emission control requirements. In the past, many air quality planners have relied on the EKMA procedure (Empirical Kinetics Modeling Approach) to provide control requirements for ozone attainment purposes. The EKMA procedure uses a trajectory model (OZIPM) to simulate ozone formation of an observed design value concentration at a downwind monitor. An ozone isopleth diagram is created (from multiple simulations) that depicts ozone concentrations as a function of initial NO_x and VOC concentration. The diagram can be used to equate emission control requirements to the required percentage change between the observed ozone design value isopleth and the isopleth of the National Ambient Air Quality Standard (NAAQS) (0.12 ppm).

An approach to estimating the effectiveness of alternative ozone attainment strategies uses grid models such as the Urban Airshed Model (UAM). The UAM numerically simulates the effects of emissions, interurban transport of ozone and precursors, advection, diffusion, chemistry, and surface removal processes on pollutant concentrations in a three-dimensional grid covering an urban area. The UAM has been applied in a number of urban areas across the United States, Europe, and the Far East but there has been a reluctance by some air quality planners to use the model in other urban areas mainly because of the time and costs involved in collecting input data and undertaking extensive performance evaluations. However, depending on the complexity of the ozone problem of the urban area and the particular needs of the

air quality planners, extensive data bases and model evaluations may not be necessary for an application of UAM. Indeed, no other air quality model currently in use is subject to this level of performance evaluation. Moreover, even a "simplified" or less stringent application of UAM appears desirable because it incorporates a reasonably complete mathematical treatment of the physical and chemical processes believed to govern ozone formation. Furthermore, because this treatment appears to be capable of reliably reproducing peak ozone concentrations and ozone concentrations under episode conditions, the UAM provides more useful air quality planning information than does EKMA (Seinfeld, 1988; Burton, 1988). As one aspect of this study, the application of UAM will follow the simplified approach for the five urban areas to demonstrate and test the utility of such an approach for air quality planning purposes and future applications in other urban areas.

In recent years, air quality regulators have found it increasingly difficult to identify additional urban hydrocarbon emissions that can be controlled in an effort to reduce ozone concentrations. Yet at the same time there has been interest in using renewable fuels such as ethanol, which increase the evaporative emissions from light duty vehicles while reducing exhaust CO emissions. Automobiles can be operated without modification using 10 percent ethanol blended into gasoline. Substantial utilization of ethanol can reduce the need for imported oil, the trade deficit, and farm subsidies, but concern over increased evaporative emissions has hindered its widespread use, especially in nonattainment areas. A recent EKMA modeling study of ethanol-blended gasoline in seven urban areas showed a near balance in ozone increases due to increased evaporative volatile organic compound (VOC) emissions and ozone decreases from reduced exhaust emissions of carbon monoxide (CO). When the chemistry of the evaporative emissions was explicitly treated in the model, the results always showed a net reduction in ozone associated with the use of ethanol blends (Whitten, 1988). The results of this study have been questioned by the EPA (Emison, 1988).

Because there is considerable interest nationwide in the potential benefits from the expanded use of ethanol as an automotive fuel, more studies are needed to support or refute the findings of the initial EKMA study. Such studies will provide guidance for other urban areas. The current effort will use the Urban Airshed Model and EKMA to examine the effects of using ethanol fuels in the five urban areas. A comparison of results will be performed to test the reliability of EKMA for such evaluations. In addition to the ethanol emission sensitivity work, the effects of VOC reactivity in control strategy evaluation will be examined, and future year control strategy simulations will be performed for the five urban areas.

The version of the UAM used in this project (UAM CBM-IV) contains several improvements: (1) a new chemical mechanism of ozone formation that is further extended here to treat ethanol and methanol explicitly; (2) a new numerical integration scheme for horizontal advection and transport; and (3) revised estimates of dry deposition.

STUDY OBJECTIVES

The five key objectives to be accomplished in the overall 5-city study are as follows:

1. Demonstrate the simplified, limited-data application of UAM for air quality planning;

2. Determine the effects of Reid vapor pressure (RVP) and ethanol-blended gasoline on urban ozone concentrations in a number of urban areas, and compare UAM results with those obtained with EKMA;

3. Investigate and clarify the effects of VOC reactivity potential in emission control strategy evaluation;

4. Perform SIP control strategy simulations with UAM and EKMA for air quality planning and comparison of the two modeling approaches (this will be performed by the New York Department of Environmental Conservation (NYDEC) after acquisition of the modeling data base).

5. Transfer the UAM modeling data bases and application technology to the 5 states and EPA.

PURPOSE OF THE STUDY PROTOCOL

This protocol is intended to serve as the basis for the performance and successful completion of a photochemical modeling analysis of the New York metropolitan area (separate protocols will be prepared for each of the 5 urban areas in the overall study). The purpose of this protocol is to describe the methodologies to be followed throughout the study. It should be viewed as a set of general guidelines that provide focus, consistency, and a basis for consensus for all parties involved in the study. It will be reviewed and approved by all participants at the beginning of the study.

At this time, some portions of the modeling analysis have not been finalized in this document (e.g., the specific emission sensitivity scenarios). For those items that have not been finalized, we provide lists of options that may be followed. For some items, it will be up to the study participants to choose from the list of options as the study evolves.

OVERVIEW OF THE STUDY

The ozone air quality study in the New York metropolitan area comprises the following tasks:

1. Prepare a protocol document (this document) that describes the background, purpose, and objectives of the study, and the procedures to be followed in the remainder of the study. A draft protocol will be prepared and sent to all participants for consensus and approval before the bulk of the technical work is initiated.

2. Prepare future base year and ethanol-use sensitivity inventories for the application of UAM for New York that will use the latest version of the model containing the Carbon-Bond IV chemical mechanism. (Because of time constraints, an existing episode created by the state of New York in the OMNYMAP [Oxidant Modeling in the New York Metropolitan Area Project] study will be used.) The future year inventories will be prepared for 1995 and will be projected from the existing 1985 NAPAP inventory.

3. Perform an EKMA analysis for the New York area, following the 1987 EPA modeling guidelines, using the future year base case and ethanol-use sensitivity inventories.

4. Perform an application of UAM for the future year base case and ethanol-use scenarios. Examine the results and compare with those obtained in the EKMA analysis.

5. Prepare an interim report that will summarize the ethanol sensitivity studies for EKMA and UAM, and provide an overview of the current understanding of the factors that influence the effectiveness of precursor control, such as VOC reactivity, NO_x emissions character, timing, and spatial emission source distribution.

6. Deliver and install a compiled copy of the CBM-IV version of UAM, and all modeling input files used in the UAM application on the State of New York's computer system. Provide copies of these input files to the OAQPS Source Receptor Analysis Branch.

2 UAM MODELING METHODOLOGY

This section of the protocol provides details of the Urban Airshed Model (UAM) application in the New York area including input preparation procedures, base case simulations, and preparation of future year emission scenario inventories. The results of these simulations will be compared to the results of the EKMA modeling described in Section 3 of this protocol.

UAM INPUT PREPARATION PROCEDURES

Time constraints do not permit identification of ozone episodes or development of additional modeling data bases for this project. Instead, an ozone episode simulated in the original OMNYMAP study by NYDEC (Rao, 1987) will be used in this study. This episode (8 August 1980) was simulated from 0400 to 2000 LST. Because it is important in any photochemical modeling application that initial conditions do not greatly influence the peak calculated concentration, the simulations performed as part of this project should begin on 7 August. A two-day simulation for the New York modeling region will also allow investigation into the effects of slower reacting hydrocarbon species, such as those produced by ethanol blended fuels, on peak ozone concentrations. Inputs will be created for the hours preceding 0400 LST on 8 August and 7 August.

The latest version of the UAM containing the Carbon-Bond IV (CBM-IV) chemical mechanism (Gery et al., 1988) will be applied in this study. To ensure that the modeling data base for 8 August received from NYDEC has been properly transferred and converted to our in-house computer system, the base case simulation performed by NYDEC will be re-run using the Carbon-Bond II version of UAM. All subsequent modeling will involve the CBM-IV version of UAM.

UAM Modeling Grid Specification

The modeling will be performed on the original OMNYMAP (Rao, 1987) modeling grid, which consists of 31 by 25 grid cells with a horizontal dimension of 8 km, covering an area 248 by 200 km. The location of this grid and its relation to other northeastern states is presented in Figure 2-1. It covers parts of New Jersey, New York, and Connecticut. The grid is located in UTM zone 18 with the origin set at 520,000 m Easting and 4,460,000 m Northing.

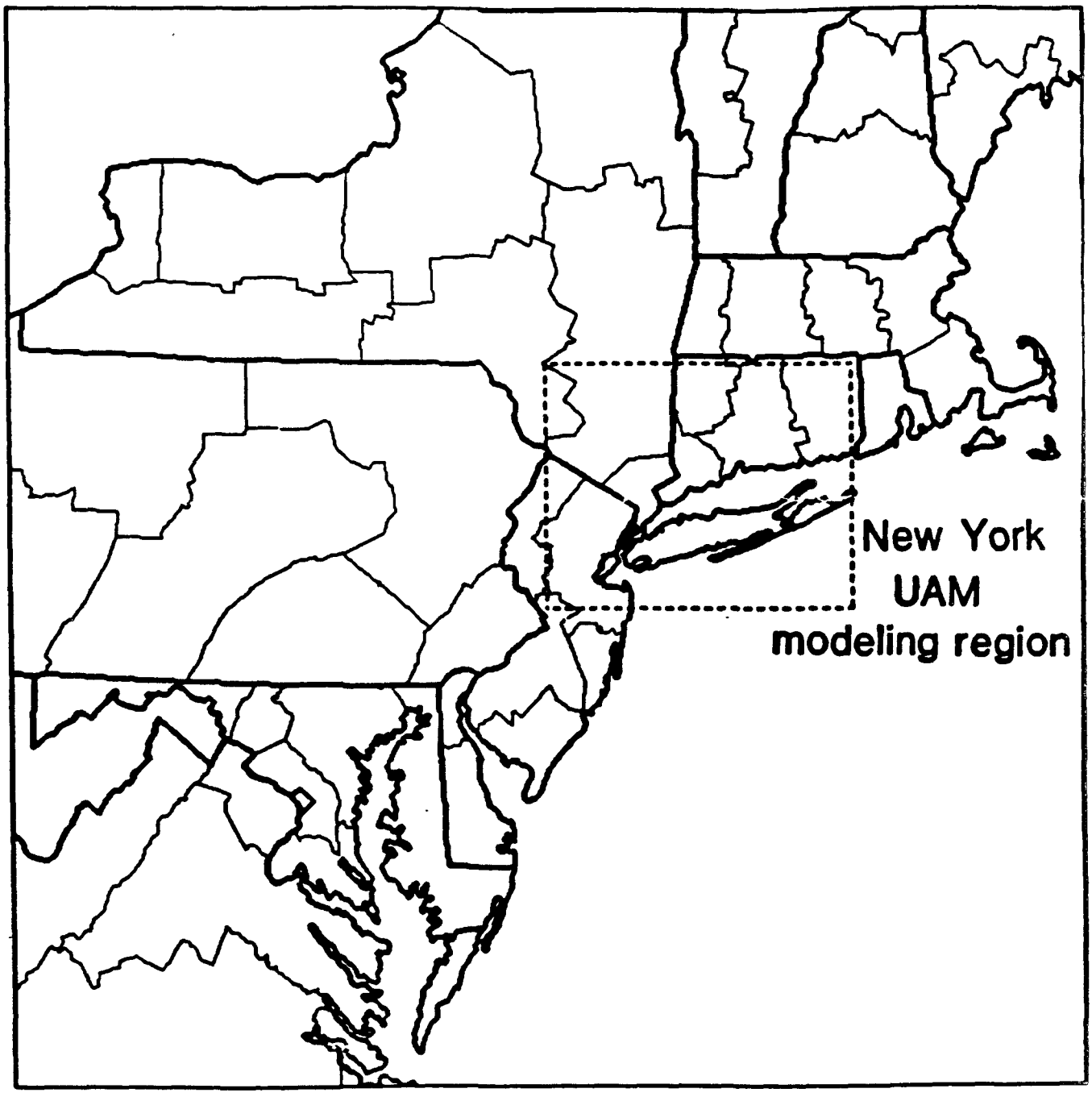

FIGURE 2-1. Geographical location of the New York metropolitan area UAM modeling region (intrastate boundaries denote AQCR's).

The original vertical structure of the OMNYMAP study contained 4 vertical cells that were constrained to 3 below and 1 above the hourly mixing height. Vertical layers above the mixing height that are allowed to become very thick during certain simulation hours may result in inadequate vertical resolution. Under certain conditions, especially during nighttime hours when mixing heights are low, pollutants from large point sources that are emitted aloft may be artificially dispersed in such thick layers. Also, with thick layers, the wind speed and direction, and vertical and horizontal shear above the mixing height may not be appropriately resolved. To appropriately resolve the vertical structure, modeling with as many as 8 vertical layers might be desirable but might also be computationally impractical. To provide a balance between practicality and appropriate vertical resolution, we recommend a new vertical grid structure consisting of 5 vertical cells, with 2 below and 3 above the hourly mixing height. The heights of the vertical layers will vary in thickness spatially and temporally depending on the hourly mixing height field. The minimum height of the lower cells is to be 50 m, and the maximum height of the upper cells, 150 m.

The following 13 input files are required for UAM modeling analyses:

DIFFBREAK — This file contains the daytime mixing height or nighttime inversion height for each column of cells at the beginning and end of each hour of the simulation.

REGIONTOP — This file contains the height of each column of cells at the beginning and end of each hour of the simulation. If this height is greater than the mixing height, the cell or cells above the mixing height are assumed to be within an inversion.

WIND — This file contains the x and y components of the wind velocity for every grid cell for each hour of the simulation. Also the maximum wind speed for the entire grid and average wind speeds at each boundary for each hour are included in this file.

METSCALARS — This file contains the hourly values of the meteorological parameters that do not vary spatially. These scalars are the NO_2 photolysis rate constant, the concentration of water vapor, the temperature gradient above and below the inversion base, the atmospheric pressure, and the exposure class.

AIRQUALITY — This file contains the initial concentrations of each species for each grid cell at the start of the simulation.

BOUNDARY — This file contains the location of the modeling region boundaries. This file also contains the concentration of each species that is used as the boundary condition along each boundary segment at each vertical level.

TOPCONC — This file contains the concentration of each species for the area above the modeling region. These concentrations are the boundary conditions for vertical integration.

TEMPERATURE — This file contains the hourly temperature for each surface layer grid cell.

EMISSIONS — This file contains the ground-level emissions of NO, NO_2, seven carbon bond categories, and CO for each grid square for each hour of the simulation.

PTSOURCE — This file contains the point source information, including the stack height, temperature and flow rate, the plume rise, the grid cell into which the emissions are emitted, and the emissions rates for NO, NO_2, seven carbon bond categories, and CO for each point source for each hour.

TERRAIN — This file contains the value of the surface roughness and deposition factor for each grid square.

CHEMPARAM — This file contains information regarding the chemical species to be simulated including reaction rate constants, upper and lower bounds, activation energy, and reference temperature.

SIMCONTROL — This file contains the simulation control information such as the time of the simulation, file option information, default information, and information on integration and chemistry time steps.

The majority of the input files used in the previous OMNYMAP application of UAM for 8 August will be used "as is" in this application. However, certain of the files (e.g., WINDS) will be recreated using new techniques, and one new file (TERRAIN) will be added. In the original OMNYMAP application, spatially constant default deposition and surface roughness parameters were used in place of spatially varying parameters. The new TERRAIN file will contain updated spatially varying parameters based on land use data. Because of the recommended changes in the vertical layer structure for the new UAM modeling, those files affected by this change will also be recreated.

The recommended procedures for preparing each of the above input files for the New York application are summarized in the following subsections.

DIFFBREAK - The upper air sounding data collected at the John F. Kennedy airport will be examined to provide estimates of daytime hourly mixing heights for those hours preceding 0400 LST. The methodology followed in arriving at spatially constant, temporally varying mixing heights for 7 August and the

nighttime hours of 8 August will be the same as that used in the original OMNYMAP work (i.e., following procedures developed by Benkley and Schulman, 1979; Garret, 1987).

REGIONTOP - The original OMNYMAP application used a temporally varying height for the top of the region ranging from 1000 m to 1500 m. During the nighttime hours, with a 1000 m region top, emissions from large point sources may have plume rises above this level and will not be emitted into the modeling region. Lowering the region top during the evening hours of 7 August causes artificial dispersion of pollutants out of the top level of the modeling region that are lost from the modeling domain. To avoid these potential problems, we recommend setting the top of the region at a fixed level of 1500 m for all hours of the simulation.

WIND - The wind fields created for the original OMNYMAP application were temporally varying, spatially constant, based on observed surface and upper air data. In the new application, we are recommending using a wind model along with the measured data to derive new wind fields that are both temporally and spatially varying. Hourly wind speed and direction data will be used along with the Hybrid Diagnostic Wind Model (HDWM) (Douglas and Kessler, 1988; Morris et al., 1987) to create new three-dimensional modeling wind fields.

METSCALARS - Meteorological data collected in the modeling region will be used to complete this file for those hours preceding 0400 LST on 8 August. The spatially constant, temporally varying parameters include estimates for NO_2 photolysis rate, water concentration, exposure class, atmospheric pressure, and temperature gradients above and below the mixing height.

AIRQUALITY - The species initial concentration field, the AIRQUALITY file, will be created by using air quality data collected at monitors in the modeling domain. The values will correspond to the specific initial hour of the simulation, which is not known at this time. The upper-layer initial field will use values specified in the TOPCONC file. The AIRQUALITY file will be updated with the new CBM-IV species.

BOUNDARY - Hourly boundary conditions will be specified based on observed air quality data at monitors both near and outside the inflow boundaries. The flow regime of 7-8 August is dominated by southwest transport; therefore, the critical inflow boundaries will be the southern and western boundaries. Boundary conditions above the mixing height will use the values specified in the TOPCONC file. The new CBM-IV species will be added to the BOUNDARY file for the CBM-IV simulations.

TOPCONC - The original concentrations specified at the top of the modeling region were based on air quality data derived from aircraft spirals. This data will be examined to determine whether the values specified for 0400 LST can be used

for the preceding hours for 8 August and 7 August. CBM-IV species will be added to this file before the UAM CBM-IV is exercised.

TEMPERATURE - The TEMPERATURE file contains gridded hourly surface temperature information for the modeling region. This file is used in the UAM for those chemical reactions that are temperature-dependent. Gridded temperature fields for hours preceding 0400 LST on 8 August will be derived from observed data collected at National Weather Service and other local air quality monitoring network sites. The Poisson interpolation method is used in the UAM system for processing temperature observations. The Poisson method is a distance-weighted interpolation scheme that is most accurate when a reasonable estimate is made of the initial field. A set of "pseudo" stations may have to be used at the edges of the domain or where there are data gaps (e.g., over the ocean) in the modeling region to ensure a good initial estimate.

EMISSIONS - The original inventory used in the OMNYMAP exercise containing information on the CBM-II species will be updated to correspond to a CBM-IV inventory. This will be accomplished by splitting total aromatics (ARO) into the new CBM-IV species toluene (TOL) and xylene (XYL), and splitting total carbonyls (CARB) into the new CBM-IV species formaldehyde (FORM) and other aldehydes (ALD2). The splitting factors for the new CBM-IV species will be taken from the recently published EKMA guidelines for CBM-IV (Hogo and Gery, 1988). This 1980 base year CBM-IV inventory is needed for a new 1980 CBM-IV base case simulation to ensure that the changes made to all of the other input files have been correctly implemented. The methodology for creating the future year emission scenario inventories is presented in the next section.

PTSOURCE - The CBM-II input file containing point source information will be updated for the 1980 CBM-IV base case simulation following the procedure performed for the low level emissions. Methodology for deriving the future year base case and emission scenario point source files is presented in the next section.

TERRAIN - This file will be added to the OMNYMAP modeling data base. It will contain surface roughness and deposition information as a function of land use (no terrain height information). The land use data for the OMNYMAP modeling region will be derived from data obtained from the U.S. Geological Survey. The deposition values as a function of land use are derived from studies performed by the Argonne National Laboratory (Sheih et al., 1986). These values are summarized in Table 2-1.

CHEMPARAM - The CHEMPARAM file contains information regarding (1) the species to be modeled by the UAM; (2) upper and lower bounds on numerical and steady-state calculations along with species "resistance" to dry deposition; and (3) the rate constants for the photochemical reactions. Before the CBM-IV

TABLE 2-1. Surface roughness and deposition factors based on studies by Argonne National Laboratories.

Land Use Category	Surface Roughness (meters)	Deposition Factor
Urban	3.00	0.2
Agricultural	0.25	0.5
Range	0.05	0.4
Deciduous Forest	1.00	0.4
Coniferous Forest including wetland	1.00	0.3
Mixed Forest	1.00	0.3
Water	0.0001	0.03
Barren land	0.002	0.2
Nonforest Wetlands	0.15	0.3
Mixed Agricultural and range	0.10	0.5
Rocky (low shrubs)	0.10	0.3

1980 base case simulation is performed, the CHEMPARAM file will be updated to correspond to the new species simulated with the new mechanism.

SIMCONTROL - The SIMCONTROL file controls the actual simulation parameters of the UAM run (i.e., simulation time period, minimum time steps, output time intervals). At this time it is not known when the simulation will be initiated; however, all other information contained in the file will not change from one simulation to another.

Assessment of Model Performance for the Base Case

After the modeling inputs have been finalized and rendered consistent with UAM CBM-IV requirements for the 1980 base case simulation, a new base case simulation will be run. As noted, it is not certain at this time when the simulation will be initiated; however, the simulation will be run to 2000 LST on 8 August. Before using the updated modeling data base in any future year emission scenario simulations, it is essential that at least a limited assessment of model performance be undertaken, even in this low-cost, simplified UAM application. The model's ability to predict the level and spatial orientation of the observed ozone field will be assessed by comparing the UAM-calculated concentrations with the measured data.

We will compute a limited set of model performance statistics that summarize error, bias, and the model's ability to calculate the peak ozone concentration. In this application, no specific performance criteria will be established, and no strict performance evaluation will be undertaken. However, if the modeling system shows very poor performance, we may undertake one (or more as time allows) diagnostic simulation(s) to identify a range of alternatives for improving model performance. For example, a diagnostic simulation may involve changes to the three-dimensional wind field (within the range of the uncertainty of the data used to prepare the field) if spatial alignment problems occur in the base case simulation. Future year emission scenario simulations using the CBM-IV modeling data base will be performed only after there is agreement from participating technical representatives that performance in the base case is adequate.

Future Year Emission Inventory Development

Improved Urban Airshed Model performance is achieved when emissions data in a very specific and detailed format is available. UAM requires a spatially disaggregated and temporally allocated emissions inventory. Performance is improved if a chemically speciated emissions inventory is obtained, although speciation could be achieved by using default speciation profiles, as is customarily done with EKMA. Meeting these requirements often entails the collection of additional emissions-related information such as population distribution and industrial activity data.

In this study we will be using the 1985 NAPAP (National Acid Precipitation Assessment Program) Emissions Inventory as the base year from which all future year emission scenarios will be developed. The future year selected for use in this study is 1995. The 1985 NAPAP Emissions Inventory consists of annual county-wide area source emissions (including mobile sources), and annual emissions for large point sources along with stack parameters (i.e., stack height, diameter, flow rate, and temperature). The county-wide area source emissions will be disaggregated onto the gridded modeling domain using the gridded population distribution. Source categories will be classified as related to the population distribution, inversely related to the population distribution, or not related at all to population, and gridded accordingly. The annual emission rates will be adjusted for each source category to summer weekday emissions by using scaling factors based upon typical values of monthly throughputs and weekday factors. Likewise, hourly variations in emissions will be based upon typical diurnal activity levels for each source category.

The stationary source emissions for the 1995 scenario year will be projected from 1985 NAPAP emissions by utilizing growth factors by source category available from an EPA-sponsored study (Pechan, 1988). Mobile source emissions will be prepared using scaling factors provided by the EPA Office of Mobile Sources specifically for each scenario to be analyzed.

Several emissions inventories will be used for the limited performance evaluation of the UAM and assessment of the effects of alternative fuel use and SIP control strategies. The following list describes each of the emission scenarios:

CBM-II 1980 case - the inventory used for the past UAM/CBM-II applications.

CBM-IV 1980 case - a modified version of the CBM-II met case for CBM-IV species. This inventory will be used to verify that the UAM/CBM-IV is operating properly and predicts ozone patterns comparable to those predicted by the UAM/CBM-II. This inventory is valid for 1980. The creation of this inventory was described in the input preparation section above.

1985 NAPAP - gridding of 1985 NAPAP inventory for CBM-IV species, as is, to the modeling domain.

1995 base case - this inventory is based on the 1985 NAPAP county inventory. Stationary source emissions are projected to 1995 using growth factors from Pechan (1988). Mobile source emissions will be based on values provided by OMS reflecting fleet turnover and present fuel properties. The emission scenarios will correspond to different assumptions in the mobile source emissions.

1995 Emission Scenarios - these inventories will reflect changes in VOC, NO_x, and CO due to assumptions of future changes in mobile source emission rates

such as changes in Reid vapor pressure (RVP) and use of ethanol-blended fuels. For New York, EPA/OPPE has defined 6 separate emission scenarios as follows:

Scenario #1 - 1995 base case with mobile emissions at current RVP values (11.5 psi) with running losses

Scenario #2 - 1995 base case with mobile emissions at low RVP values (9.0 psi) with running losses

Scenario #3 - 1995 base case with 100 percent ethanol penetration* and 10 percent ethanol blend at low RVP (10.0 psi) plus 1 psi exemption with running losses

Scenario #4 - 1995 base case with mobile emissions at current RVP values (11.5 psi) without running losses

Scenario #5 - 1995 base case with 50 percent ethanol penetration at low RVP (9.0 psi) plus 1 psi exemption with running losses

Scenario #6 - 1995 base case with current RVP and running losses using alternative speciation methodology

Emission Scenario Simulations

On the basis of emission scenario options outlined in the previous section, a subset will be chosen for UAM modeling. In addition to changes in the input emissions files, the initial condition (AIRQUALITY) and boundary condition (BOUNDARY) files will be changed to reflect general estimates of future year air quality. Estimates for initial conditions will be changed (increased/decreased) to reflect changes in the emission inventory for the New York metropolitan area from 1980 to 1995 based on projected growth and anticipated future emission controls. To calculate a future year estimate, the urban background estimate will first be subtracted from the actual meteorological base year concentration for 1980. The resulting concentration will be changed in proportion to changes in emissions. The background will then be added to this concentration to arrive at a future year estimate. Similarly, on the basis of emission changes in upwind areas (for this episode, New Jersey), the upwind inflow boundary conditions will be changed to reflect forecasted changes in emissions

---

* In this context, "penetration" is defined as the change from one type of fuel to another. A 50 percent ethanol penetration scenario is one in which 50 percent of fuel used in vehicles is converted from gasoline to an ethanol-blended fuel.

between 1980 and 1995. Only one set of future year initial and boundary conditions will be selected and used for all modeling pertaining to a given future year. We will not use multiple sets that reflect specific differences in emissions between scenarios.

The results of the UAM simulations will be presented in the form of ozone difference plots. These plots are created by subtracting the calculated ozone concentration of the future year base case (for each grid cell, for each hour) from the concentration obtained in the emission sensitivity simulations. This results in hourly isopleth maps that show both the magnitude and spatial extent of differences in ozone concentrations due to changes in emissions. Changes in calculated peak ozone will also be summarized in tabular format.

3 EKMA MODELING METHODOLOGY

BACKGROUND

A recent study used the simple photochemical modeling approach known as EKMA (Empirical Kinetics Modeling Approach) to investigate the possible impacts on urban ozone formation from the use of ethanol-blended gasoline fuels (Whitten, 1988). The study addressed the comparative reactivities of the relevant ozone precursor emissions affected by the use of ethanol blends. Atmospheric conditions were varied to represent those found in seven cities. The key finding of the study was a near balance between ozone increases from enhanced evaporative emissions of VOC and ozone decreases from reduced exhaust emissions of CO. This was the first study to consider mitigation of ozone VOC precursors through CO reductions. When the chemistry of the individual evaporative emissions species was explicitly treated in the model, the results always showed a net reduction in ozone associated with the use of ethanol blends. However, the U.S. EPA recommends simplified treatment of reactivity in the EKMA, whereby the reactivity of all VOC emissions species is treated as being equal to the reactivity of overall average VOC. While this simplified treatment overestimates the reactivity of the increased evaporative emissions, the EKMA modeling results indicated small net reductions in ozone formation from the use of ethanol blends in some cases, and in others the simplified reactivity assumption showed a small net increase in ozone. Although the existing EKMA model can explicitly treat the chemistry of evaporative automotive emissions, the simplified treatment of reactivity is more consistent with the overall simplified philosophy embodied in regulatory applications of EKMA.

The negative or positive direction of the small ozone impacts derived from the simplified treatment of VOC reactivity and the size of the ozone reductions derived from the explicit chemical treatment of the affected emissions appear to depend on the mobile-related fraction of total VOC and the ratio of CO emissions to VOC emissions. Areas with low mobile-related VOC fractions and high CO-to-VOC ratios are expected to show the largest net ozone reductions if ethanol fuels are used because, under these conditions, the overall ambient increases in VOC will be smaller, and the decreases in ambient CO concentrations will be larger. However, it is important to increase the confidence in the preliminary EKMA analyses thus far carried out. Further UAM and EKMA evaluations are thus warranted, and will be carried out as a part of this study.

The study by Whitten (1988) used EKMA episodes previously set up for 1982 SIP calculations plus CO estimates based on the CO-to-VOC ratios in the NEDS data base. Also, RVP changes and volatility increases due to ethanol blends were estimated from a 1987 RVP impact study by the EPA. Since the release of the Whitten study, new emissions guidelines for alternate fuels have been released by the EPA (29 January 1988). Therefore, new EKMA simulations, which use the new EPA guidelines for alternate fuels, and are appropriate to 1995 projections in New York, are needed.

COMPARISON OF EKMA AND UAM

Some factors regarding changes in mobile-related emissions cannot be addressed with the EKMA. These factors can be treated by UAM. For example, the diurnal timing and location of evaporative emissions are not always equal to those of exhaust emissions. The UAM is capable of treating cold-start, hot-soak, highway-cruising and congested-traffic emissions separately depending on local data for hourly temperatures, spatially resolved traffic counts, average speeds, and vehicle miles traveled. Alternatively, EKMA uses constant grams per mile emissions based on data from standard federal trip and mileage test procedures (FTP) and estimates of local automobile populations.

The principal differences between EKMA and UAM stem from the trajectory nature of EKMA versus the grid nature of UAM. EKMA treats the atmospheric chemistry of a single parcel of air as representative of one reaching an observed ozone maximum. The model simulation begins at 0800 hours with an initial loading of precursors, and more emissions are added each hour on the basis of county-wide emission averages. The UAM treats gridded points throughout the urban region (resolved both horizontally and vertically) for a day or more preceding an ozone episode. Precursors are emitted and move about within the gridded model region according to the physical equations governing wind flow, dispersion, and surface deposition. The secondary pollutants (such as ozone) are formed in both models on the basis of atmospheric chemistry. Hence EKMA provides information at one point in time and space on the basis of a few hours' highly averaged information, whereas UAM provides information at all points in time and space on the basis of a day or more of highly resolved information.

It is possible that the UAM will provide results that are significantly different from those of the EKMA-based study because of UAM's ability to treat spatially varying emissions. However, this discussion illustrates the vast differences in complexity and sophistication between the EKMA and UAM models and the potential for somewhat different results.

PURPOSE OF ANALYSIS

The purpose of using EKMA to simulate the same scenarios as those simulated by UAM is threefold. The first is to use the UAM to support or refute the EKMA results

obtained in the previous study on the effects of ethanol fuel use on urban ozone concentrations in seven U.S. cities (Whitten, 1988).

The second purpose of the EKMA simulations is to estimate the uncertainties involved in using a trajectory model like EKMA to examine the effects of different emission scenarios such as alternative fuel use. Even though the changes in the observed maximum ozone may be in agreement for both models, the different reactivities, source configurations, and three-dimensional structure of the UAM may result in the UAM predicting new hot spots of high ozone concentrations occurring outside of the EKMA trajectory.

The third purpose of the EKMA simulations is to study the effects of reactivity of VOC emissions on ozone formation. EKMA's use of the default and actual reactivity of the emission scenarios will provide insight into the uncertainties produced by these assumptions.

EKMA MODELING METHODOLOGY

Two sets of EKMA calculations will be made for each UAM scenario. The first will be performed in strict accordance with EPA guidelines for using EKMA for post-1987 State Implementation Plans (SIPs) (Hogo and Gery, 1988). The UAM modeling period will be viewed as a "design day" in setting up the OZIPM simulation. However, in keeping with EKMA guidance, none of the UAM inputs will be used for creating the EKMA inputs. County total emissions of NO_x, VOC, CO, and other species (corrected for season and MOBILE 3.9) will be used for each emissions scenario. The VOC emissions will be speciated using the default EKMA reactivity. For the ethanol-blended fuel cases, these emissions will have higher total VOC and lower CO emissions and will not account for the lower reactivity of ethanol-blended fuels.

The second set of EKMA simulations will be performed in the same manner as the first set, but the county VOC emissions will be speciated according to the source-specific speciation profiles for the emission scenario in question. Thus for the ethanol fuel cases, there will be a higher VOC emissions rate, but these simulations will take into account the lower reactivity of emissions from ethanol-blended fuels.

References

Benkley, C. W., and L. L. Schulman. 1979. Estimating hourly mixing depths from historical meteorological data. J. Appl. Meteorol., 18:772.

Burton, C. S. 1988. Comments on "Ozone Air Quality Models." To be published in J. Air Pollut. Control Assoc.

Douglas, S., and R. Kessler. 1988. "User's Guide to the Diagnostic Wind Model. Version 1.0." Systems Applications, Inc., San Rafael, California.

Emison, G. A. 1988. Memo to William G. Laxton, EPA-OAQPS. May 1988.

Garrett, A. J. 1981. Comparison of observed mixed-layer depths to model estimates using observed temperatures and wind and MUS forecasts. J. Appl. Meteorol., 20:1277.

Gery, M. W., G. Z. Whitten, and J. P. Killus. 1988. "Development and Testing of the CBM-IV for Urban and Regional Modeling." Systems Applications, Inc., San Rafael, California (SYSAPP-88/002).

Hogo, H., and M. W. Gery. 1988. "Guidelines for Using OZIPM-4 with CBM-IV or Optional Mechanisms, Volume 1: Description of the Ozone Isopleth Plotting Package, Version 4." Systems Applications, Inc., San Rafael, California (SYSAPP-88/001).

Morris, R. E., R. C. Kessler, S. G. Douglas, and K. R. Styles. 1987. "Rocky Mountain Acid Deposition Model Assessment: Evaluation of Mesoscale Models for Use in Complex Terrain." U.S. Environmental Protection Agency (EPA-600/3-87-013; NTIS PB87-180584-AS).

Pechan, E. H., and Associates. 1988. "National Assessment of VOC, CO, and NO_x Emissions and Costs for Attainment of the Ozone and CO Standards."

Rao, S. T. 1987. "Application of the Urban Airshed Model to the New York Metropolitan Area." Bureau of Air Research, Division of Air Resources, New York State Department of Environmental Conservation, Albany, New York (CA No. CX811945-01-0; EPA-450/4-87-011).

Seinfeld, J. H. 1988. Ozone air quality models. A critical review. J. Air Pollut. Control Assoc., 38(5):616.

Sheih, B. F., N. L. Wesely, and C. J. Walcek. 1986. "The Dry Deposition Module for Regional Acid Deposition Models." Argonne National Laboratories (DW89930060-01).

Whitten, G. Z. 1988. "Evaluation of the Impact of Ethanol/Gasoline Blends on Urban Ozone Formation." Systems Applications, Inc., San Rafael, California (SYSAPP-88/029.

Appendix B

PROTOCOL DOCUMENT FOR URBAN AIRSHED AND EKMA MODELING IN THE ST. LOUIS METROPOLITAN AREA

Final Report

PROTOCOL DOCUMENT FOR URBAN AIRSHED AND EKMA MODELING IN THE ST. LOUIS METROPOLITAN AREA

SYSAPP-88/150

September 1988

Prepared for

Mr. John Chamberlin

U.S. Environmental Protection Agency
Office of Policy Planning and Evaluation
Washington, DC 20460

and

Mr. Richard Scheffe

U.S. Environmental Protection Agency
Office of Air Quality Planning and Standards
Research Triangle Park, NC 27711

Prepared by

Systems Applications, Inc.
101 Lucas Valley Road
San Rafael, CA 94903
(415) 472-4011

D9510 88139r1

INTRODUCTION

BACKGROUND

Four offices of the U.S. Environmental Protection Agency are involved in a joint EPA-sponsored research study to investigate urban ozone air quality in a number of U.S. cities. The offices involved are the following: Office of Air Quality Planning and Standards (OAQPS), Office of Research and Development (ORD), Office of Mobile Sources (OMS), and the Office of Policy, Planning and Evaluation (OPPE). The urban areas to be studied include New York, St. Louis, Philadelphia, Dallas, and Atlanta. A photochemical modeling analysis will be conducted in each of these urban areas. This protocol addresses the St. Louis application in particular.

Over 60 urban areas in the United States have failed to meet the legislated deadline (31 December 1987) for ozone attainment. Possible reasons for this include one or more of the following: the failure to actually reduce emissions or enforce emission control requirements, the underestimation of actual urban hydrocarbon emissions, and/or reliance on overly simplistic modeling approaches for calculating emission control requirements. In the past, many air quality planners have relied on the EKMA procedure (Empirical Kinetics Modeling Approach) to provide control requirements for ozone attainment purposes. The EKMA procedure uses a trajectory model (OZIPM) to simulate ozone formation of an observed design value concentration at a downwind monitor. An ozone isopleth diagram is created (from multiple simulations) that depicts ozone concentrations as a function of initial NO_x and VOC concentration. The diagram can be used to equate emission control requirements to the required percentage change between the observed ozone design value isopleth and the isopleth of the National Ambient Air Quality Standard (NAAQS) (0.12 ppm).

An approach to estimating the effectiveness of alternative ozone attainment strategies uses grid models such as the Urban Airshed Model (UAM). The UAM numerically simulates the effects of emissions, interurban transport of ozone and precursors, advection, diffusion, chemistry, and surface removal processes on pollutant concentrations in a three-dimensional grid covering an urban area. The UAM has been applied in a number of urban areas across the United States, Europe, and the Far East, but some air quality planners have been reluctant to use the model in other urban areas mainly because of the time and costs involved in collecting input data and undertaking extensive performance evaluations. However, depending on the complexity of the ozone problem of the urban area and the particular needs of the air quality planners, extensive data bases and model evaluations may not be

necessary for an application of UAM. Indeed, no other air quality model currently in use is subject to this level of performance evaluation. Moreover, even a "simplified" or less stringent application of UAM appears desirable because it incorporates a reasonably complete mathematical treatment of the physical and chemical processes believed to govern ozone formation. Furthermore, because this treatment appears to be capable of reliably reproducing peak ozone concentrations and ozone concentrations under episode conditions, the UAM provides more useful air quality planning information than does EKMA (Seinfeld, 1988; Burton, 1988). As one aspect of this study, the application of UAM will follow the simplified approach for the five urban areas to demonstrate and test the utility of such an approach for air quality planning purposes and future applications in other urban areas.

In recent years, air quality regulators have found it increasingly difficult to identify additional urban hydrocarbon emissions that can be controlled in an effort to reduce ozone concentrations. Yet at the same time there has been interest in using renewable fuels such as ethanol, which increase the evaporative emissions from light duty vehicles while reducing exhaust CO emissions. Automobiles can be operated without modification using 10 percent ethanol blended into gasoline. Substantial utilization of ethanol can reduce the need for imported oil, the trade deficit, and farm subsidies, but concern over increased evaporative emissions has hindered its widespread use, especially in nonattainment areas. A recent EKMA modeling study of ethanol-blended gasoline in seven urban areas showed a near balance in ozone increases due to increased evaporative volatile organic compound (VOC) emissions and ozone decreases from reduced exhaust emissions of carbon monoxide (CO). When the chemistry of the evaporative emissions was explicitly treated in the model, the results always showed a net reduction in ozone associated with the use of ethanol blends (Whitten, 1988). The results of this study have been questioned recently by the EPA (Emison, 1988).

Because there is considerable interest nationwide in the potential benefits from the expanded use of ethanol as an automotive fuel, more studies are needed to support or refute the findings of the initial EKMA study. Such studies will provide guidance for other urban areas. The current effort will use the Urban Airshed Model and EKMA to examine the effects of using ethanol fuels in the five urban areas. A comparison of results will be performed to test the reliability of EKMA for such evaluations. In addition to the ethanol emission sensitivity work, the effects of VOC reactivity in control strategy evaluation will be examined, and future year control strategy simulations will be performed for the five urban areas.

The version of the UAM used in this project (UAM CBM-IV) contains several improvements: (1) a new chemical mechanism of ozone formation that is further extended here to treat ethanol and methanol explicitly; (2) a new numerical integration scheme for horizontal advection and transport; and (3) revised estimates of dry deposition.

STUDY OBJECTIVES

The five key objectives to be accomplished in the overall 5-city study are as follows:

1. Demonstrate the simplified, limited-data application of UAM for air quality planning;

2. Determine the effects of Reid vapor pressure (RVP) and ethanol blended gasoline on urban ozone concentrations in a number of urban areas, and compare UAM results with those obtained with EKMA;

3. Investigate and clarify the effects of VOC reactivity potential in emission control strategy evaluation;

4. Perform SIP control strategy simulations with UAM and EKMA for air quality planning and comparison of the two modeling approaches;

5. Transfer the UAM modeling data bases and application technology to the 5 states and EPA.

PURPOSE OF THE STUDY PROTOCOL

This protocol is intended to serve as the basis for the performance and successful completion of a photochemical modeling analysis of the St. Louis metropolitan area (separate protocols will be prepared for each of the 5 urban areas in the overall study). The purpose of this protocol is to describe the methodologies to be followed throughout the study. It should be viewed as a set of general guidelines that provide focus, consistency, and a basis for consensus for all parties involved in the study. It will be reviewed and approved by all participants at the beginning of the study.

At this time, some portions of the modeling analysis have not been finalized in this document (e.g., the specific emission sensitivity scenarios). For those items that have not been finalized, we provide lists of options that may be followed. For some items, it will be up to the study participants to choose from the list of options as the study evolves.

OVERVIEW OF THE STUDY

The ozone air quality study in the St. Louis metropolitan area comprises the following tasks:

1. Prepare a protocol document (this document) that describes the background, purpose, and objectives of the study, and the procedures to be followed in the remainder of the study. A draft protocol will be prepared and sent to all participants for consensus and approval before the bulk of the technical work is initiated.

2. Select a modeling episode from a set of four days simulated in a previous application of UAM using data collected during the Regional Air Pollution Study (RAPS) in 1975 and 1976.

3. Prepare future base year and ethanol-use sensitivity inventories for the application of UAM for St. Louis that will use the latest version of the model containing the Carbon-Bond IV chemical mechanism. The future year inventories will be prepared for 1995 and will be projected from the existing 1985 NAPAP inventory.

4. Perform an EKMA analysis for the St. Louis area, following the 1987 EPA modeling guidelines, using the future year base case and ethanol-use sensitivity inventories.

5. Perform an application of UAM for the future year base case and ethanol-use scenarios. Examine the results and compare with those obtained in the EKMA analysis.

6. Prepare an interim report that will summarize the ethanol sensitivity studies for EKMA and UAM, and provide an overview of the current understanding of the factors that influence the effectiveness of precursor control, such as VOC reactivity, NO_x emissions character, timing, and spatial emission source distribution.

7. Perform SIP control strategy simulations using both UAM and EKMA for air quality planning and comparison of the two modeling approaches.

2 UAM MODELING METHODOLOGY

This section of the protocol provides details of the Urban Airshed Model (UAM) application in the St. Louis area including episode selection, input preparation procedures, base case simulations, and preparation of future year emission scenario inventories. The results of these simulations will be compared to the results of the EKMA modeling described in Section 3 of this protocol.

EPISODE SELECTION

This section provides a summary of the procedures that will be used to select the ozone episode for the CBM-IV UAM modeling. Time constraints do not permit identification of new ozone episodes or development of additional modeling data bases for this project. Instead, an ozone episode day will be chosen from a set of episode days that were developed as part of the original St. Louis Ozone Modeling Project (EPA, 1983). These days are the following:

Thursday, May 22, 1975
Saturday, July 26, 1975
Tuesday, July 13, 1976
Friday, October 1, 1976

The following referenced reports will be used to perform the episode selection:

1. Regional Air Monitoring System Flow and Procedures Manual (Rockwell, 1977).

2. Final Evaluation of Urban-Scale Photochemical Air Quality Simulation Models (ESRL, 1982).

3. The St. Louis Ozone Modeling Project (EPA, 1983).

4. The Surface Ozone Record for the Regional Air Pollution Study, 1975-1976 (Atmospheric Environment, 1982).

Data bases containing hourly ozone concentrations are not available for review during the selection process. Some ozone data was plotted for selected stations in various reports; however, only peak ozone concentrations for these days are known.

Observed wind data used to create the original three-dimensional wind fields for UAM will be used to create interpolated surface wind fields with a distance-weighted interpolation algorithm. Surface wind fields will be created to determine the hourly flow patterns for each episode day. These surface wind fields will be used to track air parcels released at various times and locations to determine (a) the timing of the "flushing" of initial conditions from the modeling domain, (b) the general area of origin of material affecting peak observed ozone concentrations, and (c) the influence of boundary conditions on calculated ozone concentrations.

The episode will be selected on the basis of the following criteria:

High and widespread ozone concentrations
Minimal effects of boundary conditions
Organized transport conditions
No atypical meteorological conditions

The episode selection will be performed immediately following the completion of the protocol. The episode selection will be summarized in a technical memorandum and sent to all participating members for review.

UAM INPUT PREPARATION PROCEDURES

As summarized in the previous section, one of the modeling days formulated in the previous EPA UAM study will be used in this study. The latest version of the UAM containing the Carbon-Bond IV (CBM-IV) chemical mechanism (Gery et al., 1988) will be applied in this study. To ensure that the modeling data base for the episode selected has been properly converted on our in-house computer system, a base case simulation will be re-run using the Carbon-Bond II version of UAM. All subsequent modeling will involve the CBM-IV version of UAM.

UAM Modeling Grid Specification

The modeling will be performed on the original St. Louis modeling grid, which consists of 17 by 22 grid cells with a horizontal dimension of 4 km, covering an area 68 by 88 km. The modeling grid is depicted in Figure 2-1. It covers parts of Missouri and Illinois, encompassing the majority of the smaller, outlying urban areas surrounding metropolitan St. Louis. The grid is located in UTM zone 15 with the origin set at 706,000. m Easting and 4,326,000. m Northing.

The following 13 input files are required for UAM modeling analyses:

DIFFBREAK — This file contains the daytime mixing height or nighttime inversion height for each column of cells at the beginning and end of each hour of the simulation.

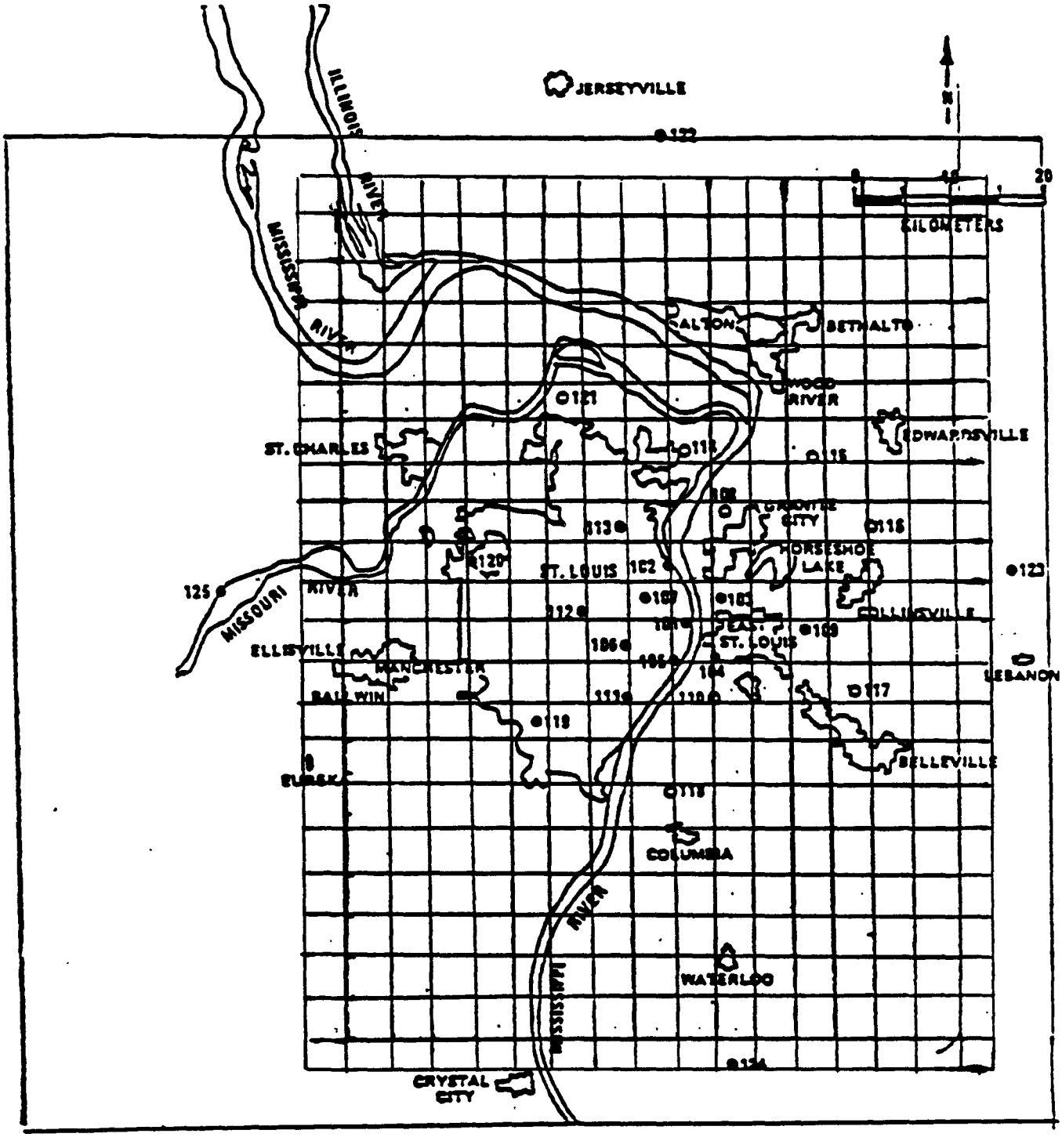

FIGURE 2-1. The St. Louis metropolitan area UAM modeling grid and RAPS station locations. (Grid cells are 4 x 4 km). (Source: EPA, 1983).

REGIONTOP	This file contains the height of each column of cells at the beginning and end of each hour of the simulation. If this height is greater than the mixing height, the cell or cells above the mixing height are assumed to be within an inversion.
WIND	This file contains the x and y components of the wind velocity for every grid cell for each hour of the simulation. Also the maximum wind speed for the entire grid and average wind speeds at each boundary for each hour are included in this file.
METSCALARS	This file contains the hourly values of the meteorological parameters that do not vary spatially. These scalars are the NO_2 photolysis rate constant, the concentration of water vapor, the temperature gradient above and below the inversion base, the atmospheric pressure, and the exposure class.
AIRQUALITY	This file contains the initial concentrations of each species for each grid cell at the start of the simulation.
BOUNDARY	This file contains the location of the modeling region boundaries. This file also contains the concentration of each species that is used as the boundary condition along each boundary segment at each vertical level.
TOPCONC	This file contains the concentration of each species for the area above the modeling region. These concentrations are the boundary conditions for vertical integration.
TEMPERATURE	This file contains the hourly temperature for each surface layer grid cell.
EMISSIONS	This file contains the ground-level emissions of NO, NO_2, seven carbon bond categories, and CO for each grid square for each hour of the simulation.
PTSOURCE	This file contains the point source information, including the stack height, temperature and flow rate, the plume rise, the grid cell into which the emissions are emitted, and the emissions rates for NO, NO_2, seven carbon bond categories, and CO for each point source for each hour.
TERRAIN	This file contains the value of the surface roughness and deposition factor for each grid square.

CHEMPARAM This file contains information regarding the chemical species to be simulated including reaction rate constants, upper and lower bounds, activation energy, and reference temperature.

SIMCONTROL This file contains the simulation control information such as the time of the simulation, file option information, default information, and information on integration and chemistry time steps.

The majority of the input files used in the previous St. Louis application of UAM will be used "as is" in this application. However, the WIND file will be recreated using a new technique, and other files affected by the change to CBM-IV will also be updated. The recommended procedures for preparing those files that will be changed in the St. Louis application are summarized in the following subsections.

REGIONTOP - The original St. Louis application used a temporally varying height for the top of the region that was situated 400 m above the hourly mixing height (DIFFBREAK) value. For the current study, we will use a constant value for the top of the region, tentatively chosen to be 1600 m. The final selection for the top of the region will be based on the maximum mixing height used in the modeling day selected.

WIND - The wind fields created for the original St. Louis application used the WINDSET preprocessor algorithm. The three-dimensional wind fields created for a number of the modeling days, however, did not always replicate the measured data well. In the new application, we recommend using a wind model along with the measured data to derive new wind fields in an attempt to avoid problems encountered in the past. Hourly wind speed and direction data will be used along with the Hybrid Diagnostic Wind Model (HDWM) (Douglas and Kessler, 1988; Morris et al., 1987) to create new three-dimensional modeling wind fields.

METSCALARS - The parameters contained in this file will be examined and reviewed to determine whether they are to be changed/updated. Available meteorological data collected in the modeling region will be used to complete this file for those parameters that are changed. The spatially constant, temporally varying parameters include estimates for NO_2 photolysis rate, water concentration, exposure class, atmospheric pressure, and temperature gradients above and below the mixing height. Because of changes in the CBM-IV chemistry, the NO_2 photolysis rate constants may need updating. Because of changes to the REGIONTOP file, the temperature gradients above the mixing height will have to be updated.

AIRQUALITY - The species initial concentration field, the AIRQUALITY file, will be created by using air quality data collected at monitors in the modeling

domain. The values will correspond to the specific initial hour of the simulation, which is not known at this time. The upper-layer initial field will use values specified in the TOPCONC file. The AIRQUALITY file will be updated with the new CBM-IV species.

BOUNDARY - The new CBM-IV species will be added to the BOUNDARY file for the CBM-IV simulations.

TOPCONC - New CBM-IV species will be added to this file before the UAM CBM-IV is exercised.

EMISSIONS - The original inventory used in the previous St. Louis application containing information on the CBM-II species will be updated to correspond to a CBM-IV inventory. This will be accomplished by splitting total aromatics (ARO) into the new CBM-IV species toluene (TOL) and xylene (XYL), and splitting total carbonyls (CARB) into the new CBM-IV species formaldehyde (FORM) and other aldehydes (ALD2). The splitting factors for the new CBM-IV species will be taken from the recently published EKMA guidelines for CBM-IV (Hogo and Gery, 1988). This new base year CBM-IV inventory is needed for a new CBM-IV base case simulation to ensure that the changes made to all of the other input files have been correctly implemented. The methodology for creating the future year emission scenario inventories is presented in the next section.

PTSOURCE - The CBM-II input file containing point source information will be updated for the new CBM-IV base case simulation following the procedure performed for the low level emissions. Methodology for deriving the future year base case and emission scenario point source files is presented in the next section.

TERRAIN - This file will be updated using land-use information. It will contain surface roughness and deposition information as a function of land use (no terrain height information). The deposition values as a function of land use are derived from studies performed by the Argonne National Laboratory (Sheih et al., 1986). These values are summarized in Table 2-1.

CHEMPARAM - The CHEMPARAM file contains information regarding (1) the species to be modeled by the UAM; (2) upper and lower bounds on numerical and steady-state calculations along with species "resistance" to dry deposition; and (3) the rate constants for the photochemical reactions. Before the CBM-IV base case simulation is performed, the CHEMPARAM file will be updated to correspond to the new species simulated with the new mechanism.

SIMCONTROL - The SIMCONTROL file controls the actual simulation parameters of the UAM run (i.e., simulation time period, minimum time steps, output time intervals). At this time it is not known when the simulation will be initiated;

TABLE 2-1. Surface roughness and deposition factors based on studies by Argonne National Laboratories.

Land Use Category	Surface Roughness (meters)	Deposition Factor
Urban	3.00	0.2
Agricultural	0.25	0.5
Range	0.05	0.4
Deciduous Forest	1.00	0.4
Coniferous Forest including wetland	1.00	0.3
Mixed Forest	1.00	0.3
Water	0.0001	0.03
Barren land	0.002	0.2
Nonforest Wetlands	0.15	0.3
Mixed Agricultural and range	0.10	0.5
Rocky (low shrubs)	0.10	0.3

however, all other information contained in the file will not change from one simulation to another.

Assessment of Model Performance for the Base Case

After the modeling inputs have been finalized and rendered consistent with UAM CBM-IV requirements, a new base case simulation will be run. Before using the updated modeling data base in any future year emission scenario simulations, it is essential that at least a limited assessment of model performance be undertaken, even in this low-cost, simplified UAM application. The model's ability to predict the level and spatial orientation of the observed ozone field will be assessed by comparing the UAM-calculated concentrations with the measured data.

If we can locate the observed hourly data, we will compute a limited set of model performance statistics that summarize error, bias, and the model's ability to calculate the peak ozone concentration. In this application, no specific performance criteria will be established, and no strict performance evaluation will be undertaken. However, if the modeling system shows very poor performance, we may undertake one (or more as time allows) diagnostic simulation(s) to identify a range of alternatives for improving model performance. For example, a diagnostic simulation may involve changes to the three-dimensional wind field (within the range of the uncertainty of the data used to prepare the field) if spatial alignment problems occur in the base case simulation. If necessary, these diagnostic simulations will only be undertaken after consultation with the project's technical representative. Future year emission scenario simulations using the CBM-IV modeling data base will be performed only after there is agreement from participating technical representatives that performance in the base case is adequate.

Future Year Emission Inventory Development

Improved Urban Airshed Model performance is achieved when emissions data in a very specific and detailed format is available. UAM requires a spatially disaggregated and temporally allocated emissions inventory. Performance is improved if a chemically speciated emissions inventory is obtained, although speciation could be achieved by using default speciation profiles, as is customarily done with EKMA. Meeting these requirements often entails the collection of additional emissions-related information such as population distribution and industrial activity data.

In this study we will be using the 1985 NAPAP (National Acid Precipitation Assessment Program) Emissions Inventory as the base year from which all future year emission scenarios will be developed. The future year selected for use in this study is 1995. The 1985 NAPAP Emissions Inventory consists of annual county-wide area source emissions (including mobile sources), and annual emissions for large point

sources along with stack parameters (i.e., stack height, diameter, flow rate, and temperature). The county-wide area source emissions will be disaggregated onto the gridded modeling domain using the gridded population distribution. Source categories will be classified as related to the population distribution, inversely related to the population distribution, or not related at all to population, and gridded accordingly. The annual emission rates will be adjusted for each source category to summer weekday emissions by using scaling factors based upon typical values of monthly throughputs and weekday factors. Likewise, hourly variations in emissions will be based upon typical diurnal activity levels for each source category.

The stationary source emissions for the 1995 scenario year will be projected from 1985 NAPAP emissions by utilizing growth factors by source category available from an EPA-sponsored study (Pechan, 1988). Mobile source emissions will be prepared using scaling factors provided by the EPA Office of Mobile Sources specifically for each scenario to be analyzed.

Several emissions inventories will be used for the limited performance evaluation of the UAM and assessment of the effects of alternative fuel use and SIP control strategies. The following list describes each of the emission scenarios:

CBM-II 1975 or 1976 case - the inventory used for the past UAM/CBM-II applications. This emissions scenario will be used to verify that the UAM inputs are set up correctly on the Systems Applications' computer. This inventory is valid for 1975 or 1976.

CBM-IV 1975 or 1976 case - a modified version of the CBM-II meteorological case for CBM-IV species. This inventory will be used to verify that the UAM/CBM-IV is operating properly and predicts ozone patterns comparable to those predicted by the UAM/CBM-II. This inventory is valid for 1975 or 1976. The creation of this inventory was described in the input preparation section above.

1985 NAPAP - gridding of 1985 NAPAP inventory for CBM-IV species, as is, to the modeling domain.

1995 base case - this inventory is based on the 1985 NAPAP county inventory. Stationary source emissions are projected to 1995 using growth factors from EPA (Pechan, 1988). Mobile source emissions will be based on values provided by OMS. The emission scenarios will correspond to different assumptions in the mobile source emissions.

1995 Emission Scenarios - these inventories will reflect changes in VOC, NO_x, and CO due to assumptions of future changes in mobile source emission rates such as changes in Reid vapor pressure (RVP) and use of ethanol blended fuels. For St. Louis, EPA/OPPE has defined 4 separate emission scenarios as follows:

Scenario #1 - 1995 base case with mobile emissions at current RVP values (11.5 psi) with running losses

Scenario #2 - 1995 base case with mobile emissions at low RVP values (9.0 psi) with running losses

Scenario #5 - 1995 base case with 50 percent ethanol penetration* and a 10 percent ethanol blend at low RVP (9.0 psi) plus 1 psi exemption with running losses

Scenario #7 - 1995 base case with 100 percent penetration and enough Ethyl Tertiary Butyl Ether (ETBE) to produce 2 percent oxygenated fuels with running losses

SIP Inventory Development

In addition to the ethanol blended fuels inventories prepared to determine ozone sensitivity information, an inventory reflecting SIP information for the St. Louis area will be prepared based on the 1985 NAPAP inventory. This inventory will be developed in consultation with representatives from the State of Missouri, the State of Illinois, EPA Region VII, and EPA OAQPS.

Emission Scenario Simulations

On the basis of emission scenario options outlined in the previous section, a subset will be chosen for UAM modeling. In addition to changes in the input emissions files, the initial condition (AIRQUALITY) and boundary condition (BOUNDARY) files will be changed to reflect general estimates of future year air quality. Estimates for initial conditions will be changed (increased/decreased) to reflect changes in the emission inventory for the St. Louis metropolitan area from 1975 to 1995 based on projected growth and anticipated future emission controls. To calculate a future year estimate, the urban background estimate will first be subtracted from the actual meteorological base year concentration for 1975 or 1976. The resulting concentration will be changed in proportion to changes in emissions. The background will then be added to this concentration to arrive at a future year estimate. Similarly, on the basis of emission changes in the St. Louis area, the upwind inflow boundary conditions will be changed to reflect forecasted changes in emissions between

---

* In this context, "penetration" is defined as the change from one type of fuel to another. A 50 percent ethanol penetration scenario is one in which 50 percent of fuel used in vehicles is converted from gasoline to an ethanol-blended fuel.

1975 and 1995. Only one set of future year initial and boundary conditions will be selected and used for all modeling pertaining to a given future year. We will not use multiple sets that reflect specific differences in emissions between scenarios.

The results of the UAM simulations will be presented in the form of ozone difference plots. These plots are created by subtracting the calculated ozone concentration of the future year base case (for each grid cell, for each hour) from the concentration obtained in the emission sensitivity simulations. This results in hourly isopleth maps that show both the magnitude and spatial extent of differences in ozone concentrations due to changes in emissions. Changes in calculated peak ozone will also be summarized in tabular format.

SIP Emission Scenario UAM Simulation

After a SIP modeling inventory has been prepared and approved by all affected participants, at least one future year SIP simulation will be undertaken. It is anticipated that the initial and boundary condition values may have to be changed to reflect the forecasted changes in the inventory from 1985 to some future year. Initial and boundary conditions will be changed in the same manner as described above for the future year ethanol sensitivity simulations. The results of this SIP simulation will be compared to results obtained with EKMA.

3 EKMA MODELING METHODOLOGY

BACKGROUND

A recent study used the simple photochemical modeling approach known as EKMA (Empirical Kinetics Modeling Approach) to investigate the possible impacts on urban ozone formation from the use of ethanol-blended gasoline fuels (Whitten, 1988). The study addressed the comparative reactivities of the relevant ozone precursor emissions affected by the use of ethanol blends. Atmospheric conditions were varied to represent those found in seven cities. The key finding of the study was a near balance between ozone increases from enhanced evaporative emissions of VOC and ozone decreases from reduced exhaust emissions of CO. This was the first study to consider mitigation of ozone VOC precursors through CO reductions. When the chemistry of the individual evaporative emissions species was explicitly treated in the model, the results always showed a net reduction in ozone associated with the use of ethanol blends. However, the U.S. EPA recommends simplified treatment of reactivity in the EKMA, whereby the reactivity of all VOC emissions species is treated as being equal to the reactivity of overall average VOC. While this simplified treatment overestimates the reactivity of the increased evaporative emissions, the EKMA modeling results indicated small net reductions in ozone formation from the use of ethanol blends in some cases, and in others the simplified reactivity assumption showed a small net increase in ozone. Although the existing EKMA model can explicitly treat the chemistry of evaporative automotive emissions, the simplified treatment of reactivity is more consistent with the overall simplified philosophy embodied in regulatory applications of EKMA.

The negative or positive direction of the small ozone impacts derived from the simplified treatment of VOC reactivity and the size of the ozone reductions derived from the explicit chemical treatment of the affected emissions appear to depend on the mobile-related fraction of total VOC and the ratio of CO emissions to VOC emissions. Areas with low mobile-related VOC fractions and high CO-to-VOC ratios are expected to show the largest net ozone reductions if ethanol fuels are used because, under these conditions, the overall ambient increases in VOC will be smaller, and the decreases in ambient CO concentrations will be larger. However, it is important to increase the confidence in the preliminary EKMA analyses thus far carried out. Further UAM and EKMA evaluations are thus warranted, and will be carried out as a part of this study.

The study by Whitten (1988) used EKMA episodes previously set up for 1982 SIP calculations plus CO estimates based on the CO-to-VOC ratios in the NEDS data base. Also, RVP changes and volatility increases due to ethanol blends were estimated from a 1987 RVP impact study by the EPA. Since the release of the Whitten study, new emissions guidelines for alternate fuels have been released by the EPA (29 January 1988). Therefore, new EKMA simulations, which use the new EPA guidelines for alternate fuels, and are appropriate to 1995 projections in St. Louis, are needed.

COMPARISON OF EKMA AND UAM

Some factors regarding changes in mobile-related emissions cannot be addressed with the EKMA. These factors can be treated by UAM. For example, the diurnal timing and location of evaporative emissions are not always equal to those of exhaust emissions. The UAM is capable of treating cold-start, hot-soak, highway-cruising and congested-traffic emissions separately depending on local data for hourly temperatures, spatially resolved traffic counts, average speeds, and vehicle miles traveled. Alternatively, EKMA uses constant grams per mile emissions based on data from standard federal trip and mileage test procedures (FTP) and estimates of local automobile populations.

The principal differences between EKMA and UAM stem from the trajectory nature of EKMA versus the grid nature of UAM. EKMA treats the atmospheric chemistry of a single parcel of air as representative of one reaching an observed ozone maximum. The model simulation begins at 0800 hours with an initial loading of precursors, and more emissions are added each hour on the basis of county-wide emission averages. The UAM treats gridded points throughout the urban region (resolved both horizontally and vertically) for a day or more preceding an ozone episode. Precursors are emitted and move about within the gridded model region according to the physical equations governing wind flow, dispersion, and surface deposition. The secondary pollutants (such as ozone) are formed in both models on the basis of atmospheric chemistry. Hence EKMA provides information at one point in time and space on the basis of a few hours' highly averaged information, whereas UAM provides information at all points in time and space on the basis of a day or more of highly resolved information.

It is possible that the UAM will provide results that are significantly different from those of the EKMA-based study because of UAM's ability to treat spatially varying emissions. However, this discussion illustrates the vast differences in complexity and sophistication between the EKMA and UAM models and the potential for somewhat different results.

PURPOSE OF ANALYSIS

The purpose of using EKMA to simulate the same scenarios as those simulated by UAM is threefold. The first is to use the UAM to support or refute the EKMA

results obtained in the previous study on the effects of ethanol fuel use on urban ozone concentrations in seven U.S. cities (Whitten, 1988).

The second purpose of the EKMA simulations is to estimate the uncertainties involved in using a trajectory model like EKMA to examine the effects of different emission scenarios such as alternative fuel use. Even though the changes in the observed maximum ozone may be in agreement for both models, the different reactivities, source configurations, and three-dimensional structure of the UAM may result in the UAM predicting new hot spots of high ozone concentrations occurring outside of the EKMA trajectory.

The third purpose of the EKMA simulations is to study the effects of reactivity of VOC emissions on ozone formation. EKMA's use of the default and actual reactivity of the emission scenarios will provide insight into the uncertainties produced by these assumptions.

EKMA MODELING METHODOLOGY

Two sets of EKMA calculations will be made for each UAM scenario. The first will be performed in strict accordance with EPA guidelines for using EKMA for post-1987 State Implementation Plans (SIPs) (Hogo and Gery, 1988). The UAM modeling period will be viewed as a "design day" in setting up the OZIPM simulation. However, in keeping with EKMA guidance, none of the UAM inputs will be used for creating the EKMA inputs. County total emissions of NO_x, VOC, CO, and other species (corrected for season and MOBILE 3.9) will be used for each emissions scenario. The VOC emissions will be speciated using the default EKMA reactivity. For the ethanol-blended fuel cases, these emissions will have higher total VOC and lower CO emissions and will not account for the lower reactivity of ethanol-blended fuels.

The second set of EKMA simulations will be performed in the same manner as the first set, but the county VOC emissions will be speciated according to the source-specific speciation profiles for the emission scenario in question. Thus for the ethanol fuel cases, there will be a higher VOC emissions rate, but these simulations will take into account the lower reactivity of emissions from ethanol-blended fuels.

SIP Emission Scenario EKMA Simulation

In addition to the ethanol fuel sensitivity simulation using EKMA, a SIP simulation will also be performed. Emission inventory information derived from the UAM gridded SIP inventory will be used to supply information for the application of EKMA. The results of this analysis will be compared to the information derived from the UAM SIP simulation for St. Louis.

References

Benkley, C. W., and L. L. Schulman. 1979. Estimating hourly mixing depths from historical meteorological data. J. Appl. Meteorol., 18:772.

Burton, C. S. 1988. Comments on "Ozone Air Quality Models." Submitted to J. Air Pollut. Control Assoc.

Cole, H. S., D. E. Layland, G. K. Moss, and C. F. Newberry. 1983. "The St. Louis Ozone Modeling Project." U.S. Environmental Protection Agency, Research Triangle Park, North Carolina (EPA-450/4-83-019).

Douglas, S., and R. Kessler. 1988. "User's Guide to the Diagnostic Wind Model. Version 1.0." Systems Applications, Inc., San Rafael, California.

Emison, G. A. 1988. Memo to William G. Laxton, EPA-OAQPS, May 1988.

Gery, M. W., G. Z. Whitten, and J. P. Killus. 1988. "Development and Testing of the CBM-IV for Urban and Regional Modeling." Systems Applications, Inc., San Rafael, California (SYSAPP-88/002).

Hogo, H., and M. W. Gery. 1988. "Guidelines for Using OZIPM-4 with CBM-IV or Optional Mechanisms, Volume 1: Description of the Ozone Isopleth Plotting Package, Version 4." Systems Applications, Inc., San Rafael, California (SYSAPP-88/001).

Morris, R. E., R. C. Kessler, S. G. Douglas, and K. R. Styles. 1987. "Rocky Mountain Acid Deposition Model Assessment: Evaluation of Mesoscale Models for Use in Complex Terrain." U.S. Environmental Protection Agency (EPA-600/3-87-013; NTIS PB87-180584-AS).

Pechan, E. H., and Associates. 1988. "National Assessment of VOC, CO, and NO_x Emissions and Costs for Attainment of the Ozone and CO Standards."

Rao, S. T. 1987. "Application of the Urban Airshed Model to the New York Metropolitan Area." Bureau of Air Research, Division of Air Resources, New York State Department of Environmental Conservation, Albany, New York (CA No. CX811945-01-0; EPA-450/4-87-011).

Seinfeld, J. H. 1988. Ozone air quality models. A critical review. J. Air Pollut. Control Assoc., 38(5):616.

Sheih, B. F., N. L. Wesely, and C. J. Walcek. 1986. "The Dry Deposition Module for Regional Acid Deposition Models." Argonne National Laboratories (DW89930060-01).

Whitten, G. Z. 1988. "Evaluation of the Impact of Ethanol/Gasoline Blends on Urban Ozone Formation." Systems Applications, Inc., San Rafael, California (SYSAPP-88/029.

Appendix C

EPISODE SELECTION FOR ST. LOUIS UAM MODELING

Appendix C

EPISODE SELECTION FOR ST. LOUIS UAM MODELING

INTRODUCTION

This appendix provides a summary of the procedures that were used to select an ozone episode for the CBM-IV UAM modeling of St. Louis for the EPA Five Cities modeling project. Time constraints did not permit identification of new ozone episodes or development of additional modeling data bases for this project. Instead, an ozone episode day was chosen from a set of four episode days that were developed as part of the original St. Louis Ozone Modeling Project (EPA, 1983). The modeling data bases for these days were obtained from EPA. The raw data from which the inputs were created were not available for review. The modeling days include the following:

Thursday, 22 May 1975

Saturday, 26 July 1975

Tuesday, 13 July 1976

Friday, 1 October 1976

The episode selection was based on the UAM input files and information that could be derived from the following reports:

1. Regional Air Monitoring System Flow and Procedures Manual (Rockwell, 1977).

2. Final Evaluation of Urban-Scale Photochemical Air Quality Simulation Models (ESRL, 1982).

3. The St. Louis Ozone Modeling Project (EPA, 1983).

4. The Surface Ozone Record for the Regional Air Pollution Study, 1975-1976 (Atmospheric Environment, 1982).

SELECTION METHODOLOGY

The episode-selection process in which candidate days are chosen for UAM modeling usually involves an intense review of all available meteorological and air quality data. Air quality data are examined to determine days with high and widespread ozone concentrations. Meteorological data are examined to determine the specific factors causing the high observed ozone (e.g., temperatures, winds, sky cover). Urban areas located in complex geographical locations may observe high ozone concentrations resulting from different meteorological mechanisms. For these locations, a number of episodes should be chosen to include all of the meteorological regimes that cause high ozone in the urban area. In this study, we were constrained to choosing only one modeling day, and only a limited amount of data were examined. Data bases containing hourly ozone concentrations were not available for review during the selection process. Some ozone data were plotted for selected stations in various reports; however, only peak ozone concentrations for these days are known. Table C-1 presents a summary of the meteorological and air quality parameters for the episode days.

TABLE C-1. Summary of meteorological and air quality parameters observed for selected days in St. Louis.

Date	WS (m/s)	WD (deg)	Temp (°C)	Solar (ly/min)	Max MH (m)	Max O_3 (pphm)
5/22/75	1.1	224	29	1.12	1504	19.5
7/26/75	1.0	139	26	0.98	1477	18.5
7/13/76	2.3	145	28	1.02	1853	22.3
10/1/76	0.6	222	22	0.78	527	24.6

The modeling episode was selected on the basis of the following criteria:

- High and widespread ozone concentrations
- Minimal effects of boundary conditions
- Organized transport conditions
- No atypical meteorological conditions

Because the 1 October 1976 day was an atypical ozone event that occurred outside the normal ozone season and was characterized by unusually low mixing heights, cool temperatures, and stagnation conditions, it was not considered further in the selection process. Although it is an interesting event, it is not reflective of a normal summertime ozone event in St. Louis.

Data from the remaining days were examined further to determine differences in the flow fields and effects of boundary and initial conditions on modeled concentrations. The wind files for each of the modeling days were used to track air parcels released at various times and locations to determine (1) the timing of the "flushing" of initial conditions from the modeling domain, (2) the general area of origin of material affecting peak observed ozone concentrations, and (3) the influence of boundary conditions on calculated ozone concentrations.

Three sets of surface air parcel trajectories were performed for each of the three modeling days. These trajectories include the following:

1. Forward trajectories starting at 0500 LST in the center of, and surrounding, the city of St. Louis. These trajectories were tracked until the end of the day or until they moved out of the modeling domain. They were released to determine the fate of the initial condition field in the center of the city.

2. A backward trajectory from the site and time of the observed ozone maximum. This trajectory was run to determine the general origin of the parcel affecting the monitor showing peak observed ozone concentrations.

3. Forward trajectories from the edges of the inflow boundaries starting at 0500 LST, with additional releases every two hours until 1900 LST. These trajectories were released to determine the extent and influence of the boundary conditions on the calculated ozone concentrations. The inflow boundaries were determined after examination of the plotted surface wind fields.

Figures C-1, C-2, and C-3 present these three types of trajectories, respectively, for 22 May 1975, 26 July 1975, and 13 July 1976.

Thursday, 22 May 1975

The relatively slow southwesterly flow on this day has transported the 0500 LST initial condition field north and east, and only the northern portions of the initial conditions have been transported out of the region by the time of the peak observed ozone (1500 LST). The peak observed ozone was measured at RAPS station 101, located in downtown St. Louis along the Mississippi River. The back trajectory shows the general origin of the parcel to be south of the city. Boundary conditions from the southern and western boundaries are not transported near the location of the peak observed ozone concentration.

Saturday, 26 July 1975

Because of the light southeasterly winds, the 0500 LST initial condition field for this day is transported northwestward and not flushed from the modeling region by the time of the observed peak (1500 LST). The peak observed ozone was measured at RAPS station 113, located just north of downtown St. Louis. The backward trajectory shows the origin of the parcel to be located near the southern edge of the St. Louis metropolitan area at 0500 LST. Inflow boundary conditions from the east and south do not influence the area of the observed peak ozone.

Tuesday, 13 July 1976

The relatively strong southerly flow on this day has transported a large portion of the 0500 LST initial condition field to the north and west, out of the modeling domain by the time of the observed peak ozone (1600 LST). Peak ozone was observed at RAPS station 114, located north of downtown St. Louis. The back trajectory shows that the parcel arriving at this station at the time of the peak originated just north of Belleville, Illinois. Because of higher wind speeds (compared to the other two days) for this day, the boundary conditions influence a larger portion of the modeling domain by the time of the peak; however, the area of the peak is free from the influence of boundary conditions.

Given the selection criteria and the results of the trajectory analysis, it appears that any of these three episodes would be suitable for UAM modeling. The 13 July 1976 day is attractive because it (1) has the largest observed ozone of the three days, (2) has well-organized transport conditions, and (3) is relatively free of the effects of initial conditions. However, the 13 July 1976 day also is the most influenced by boundary conditions of the three candidate days, although the boundary conditions do not appear to influence the region of maximum ozone concentrations. Stagnant meteorological conditions are prevalent on both 22 May and 26 July 1975. Initial conditions for both of the 1975 days may affect concentrations in the region of the maximum ozone concentrations. The 26 July day is a Saturday, when atypical emission characteristics exist. The 22 May day occurs fairly early in the ozone season; however, it appears to have meteorological conditions fairly typical of an ozone episode. Since the 13 July 1976 day contains the highest observed ozone of the candidate days, has well-organized transport conditions, and is minimally affected by initial and boundary conditions, it was chosen as the episode day for the PLANR use of the UAM (CB-IV) for St. Louis.

FIGURE 1

AIR PARCEL TRAJECTORIES FOR
ST. LOUIS FOR THURSDAY, MAY 22, 1975

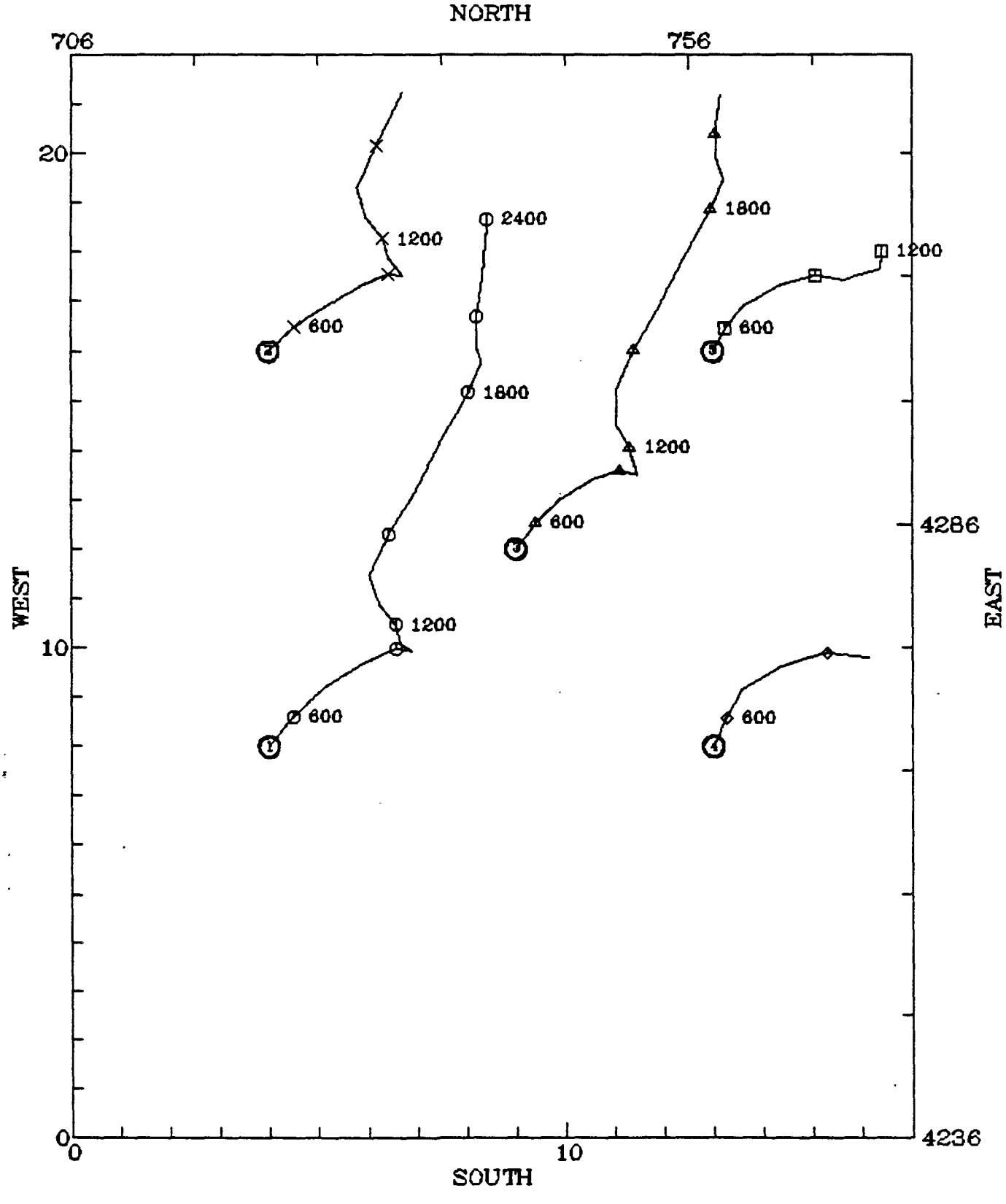

Initialized on

① 500 ON 5/22/75
② 500 ON 5/22/75
③ 500 ON 5/22/75
④ 500 ON 5/22/75
⑤ 500 ON 5/22/75

ST. LOUIS REGIONAL OZONE ANALYSIS
Forward Trajectories

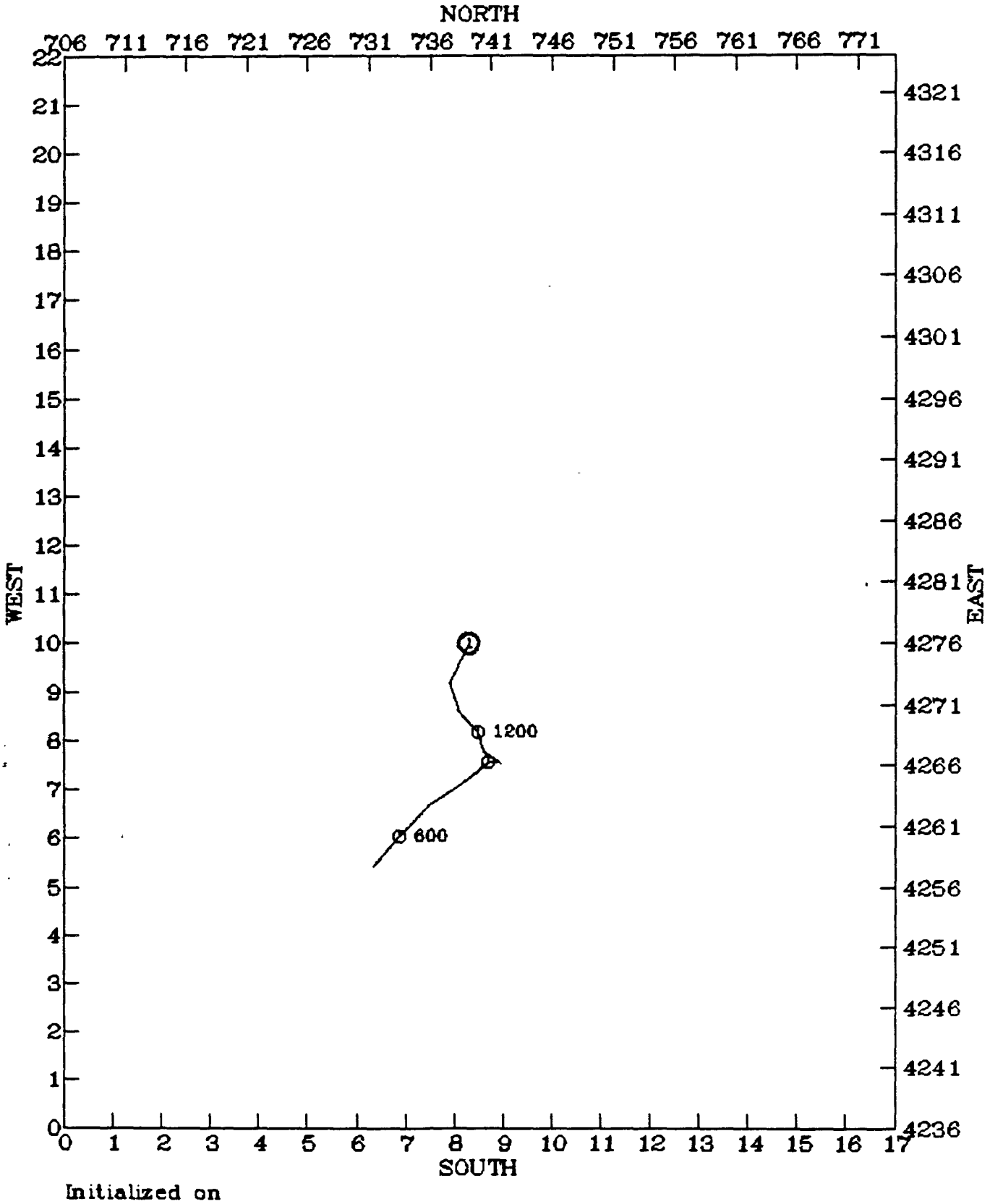

Initialized on

① 1500 ON 5/22/75

Backward Trajectories

ST. LOUIS REGIONAL OZONE ANALYSIS

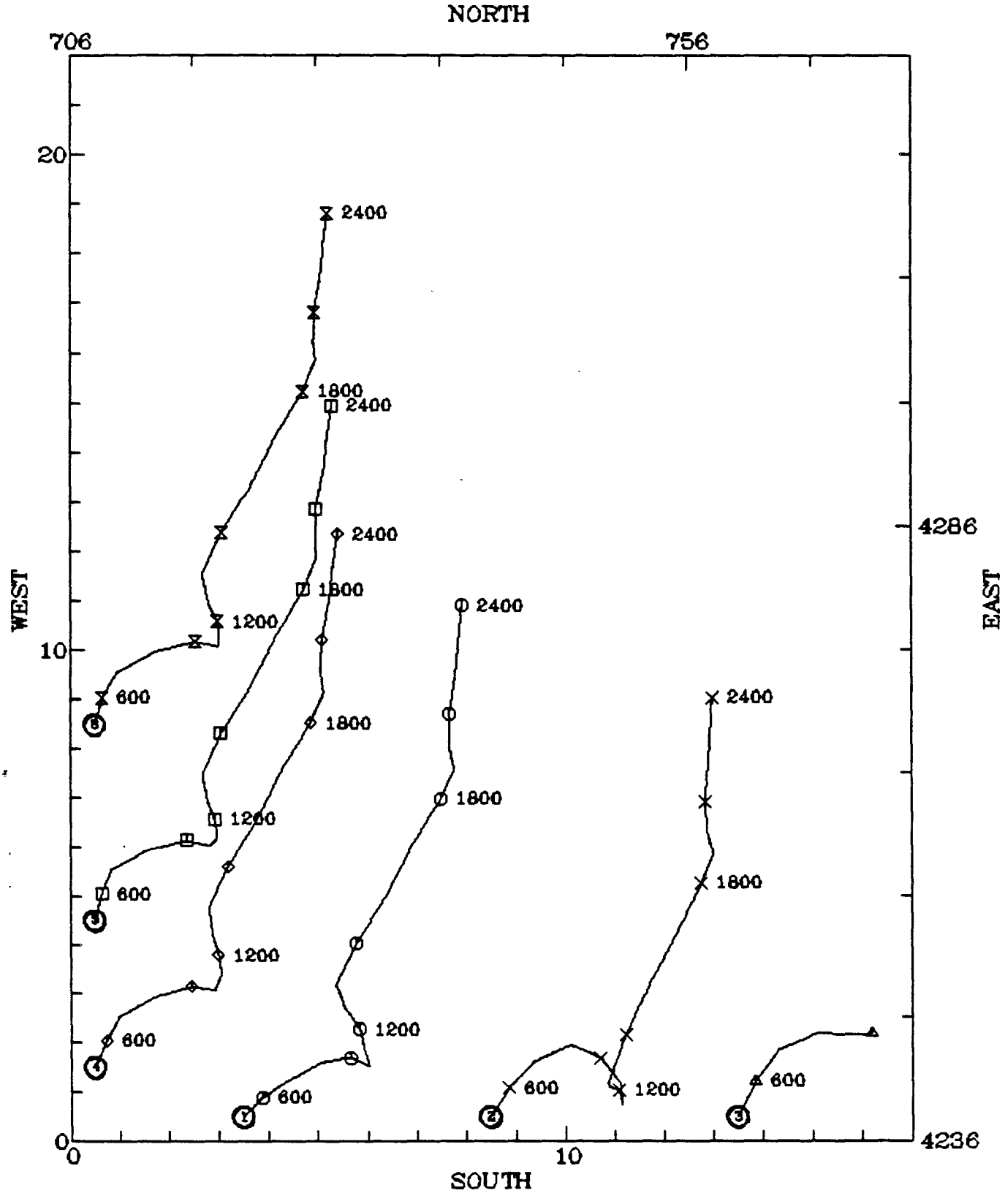

Initialized on

① 500 ON 5/22/75
② 500 ON 5/22/75
③ 500 ON 5/22/75
④ 500 ON 5/22/75
⑤ 500 ON 5/22/75
⑥ 500 ON 5/22/75

ST. LOUIS REGIONAL OZONE ANALYSIS
Forward Trajectories

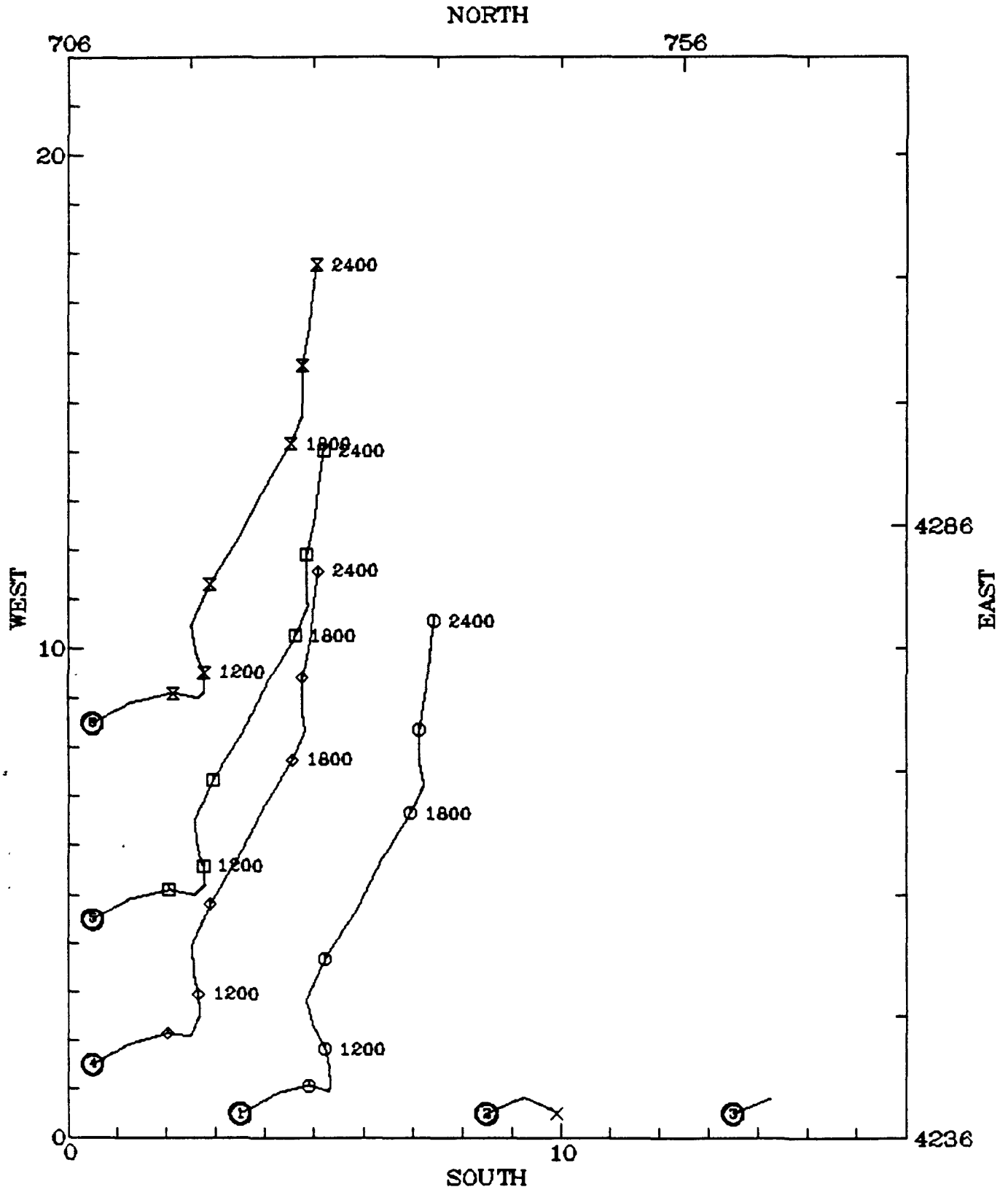

Initialized on

① 700 ON 5/22/75
② 700 ON 5/22/75
③ 700 ON 5/22/75
④ 700 ON 5/22/75
⑤ 700 ON 5/22/75
⑥ 700 ON 5/22/75

ST. LOUIS REGIONAL OZONE ANALYSIS
Forward Trajectories

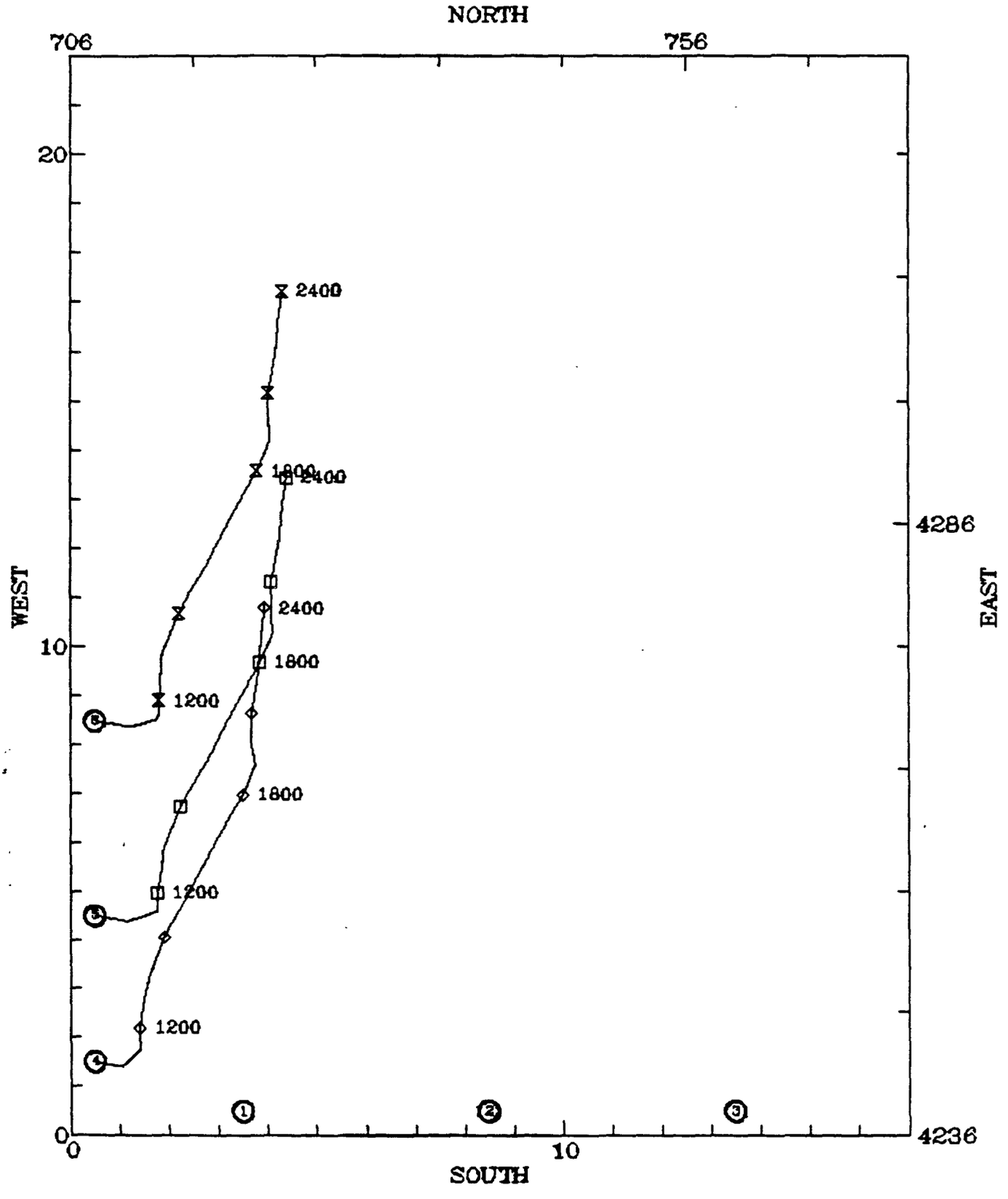

Initialized on

① 900 ON 5/22/75
② 900 ON 5/22/75
③ 900 ON 5/22/75
④ 900 ON 5/22/75
⑤ 900 ON 5/22/75
⑥ 900 ON 5/22/75

ST. LOUIS REGIONAL OZONE ANALYSIS
Forward Trajectories

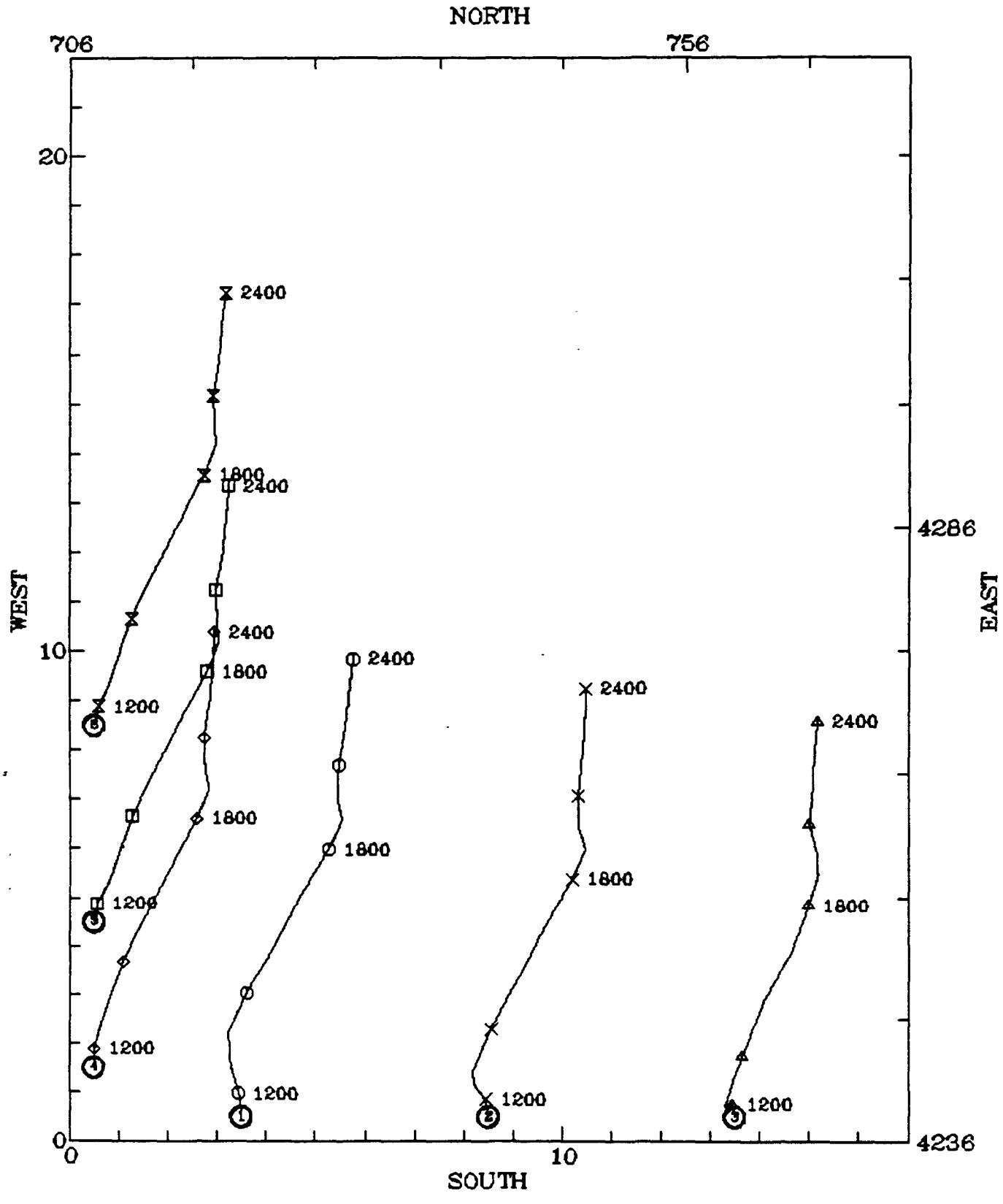

Initialized on

① 1100 ON 5/22/75
② 1100 ON 5/22/75
③ 1100 ON 5/22/75
④ 1100 ON 5/22/75
⑤ 1100 ON 5/22/75
⑥ 1100 ON 5/22/75

ST. LOUIS REGIONAL OZONE ANALYSIS
Forward Trajectories

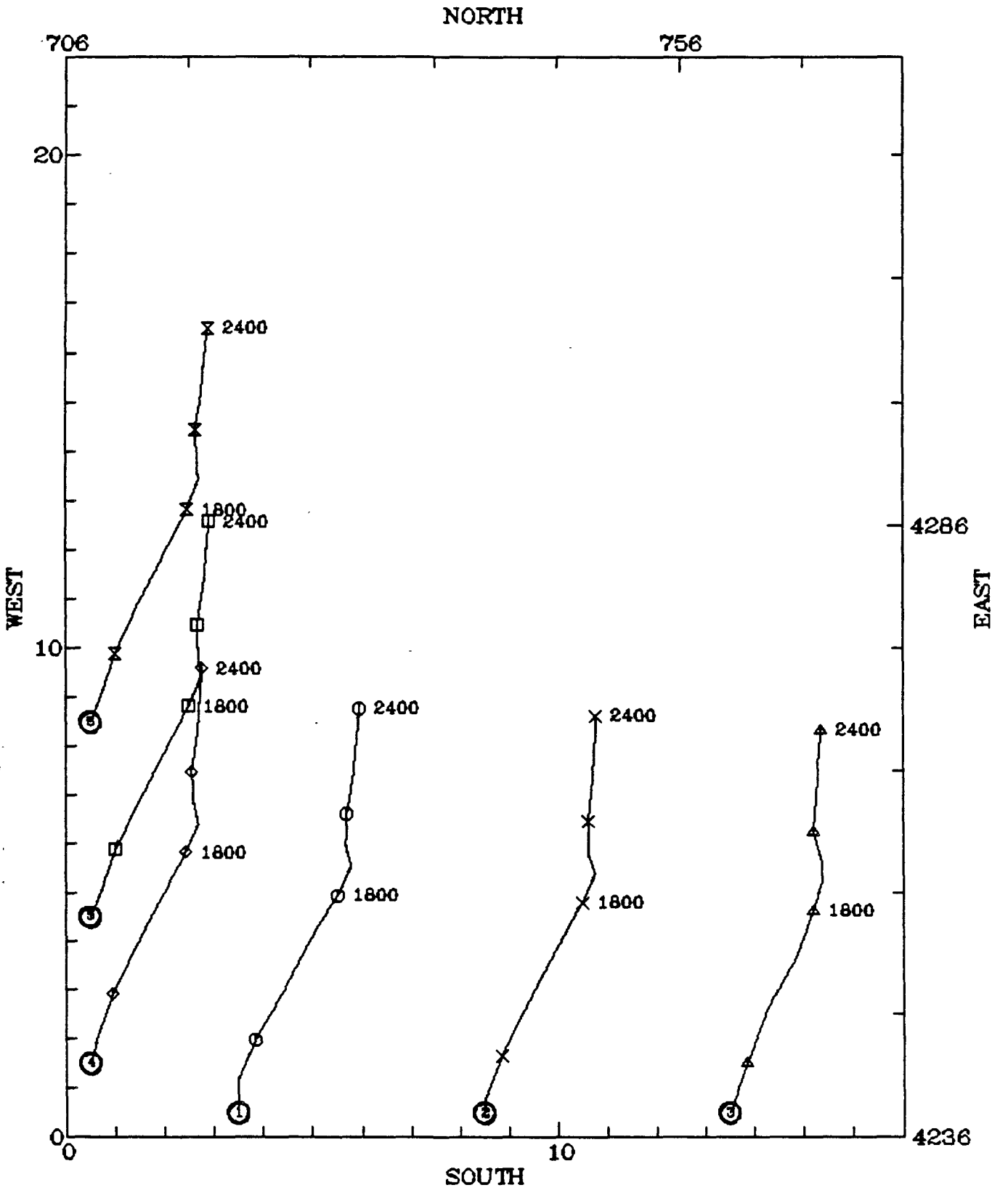

ST. LOUIS REGIONAL OZONE ANALYSIS
Forward Trajectories

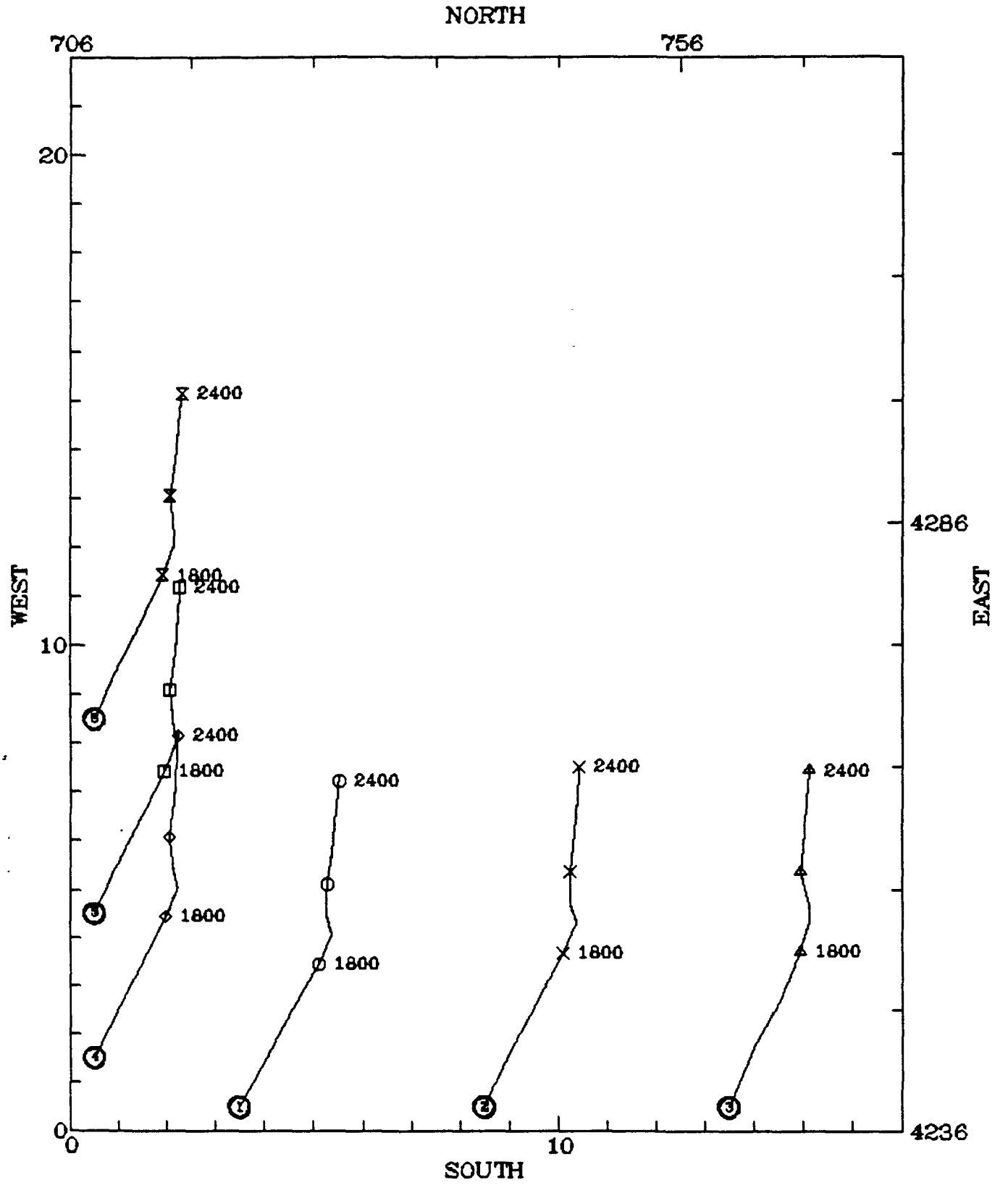

Initialized on

① 1500 ON 5/22/75
② 1500 ON 5/22/75
③ 1500 ON 5/22/75
④ 1500 ON 5/22/75
⑤ 1500 ON 5/22/75
⑥ 1500 ON 5/22/75

ST. LOUIS REGIONAL OZONE ANALYSIS
Forward Trajectories

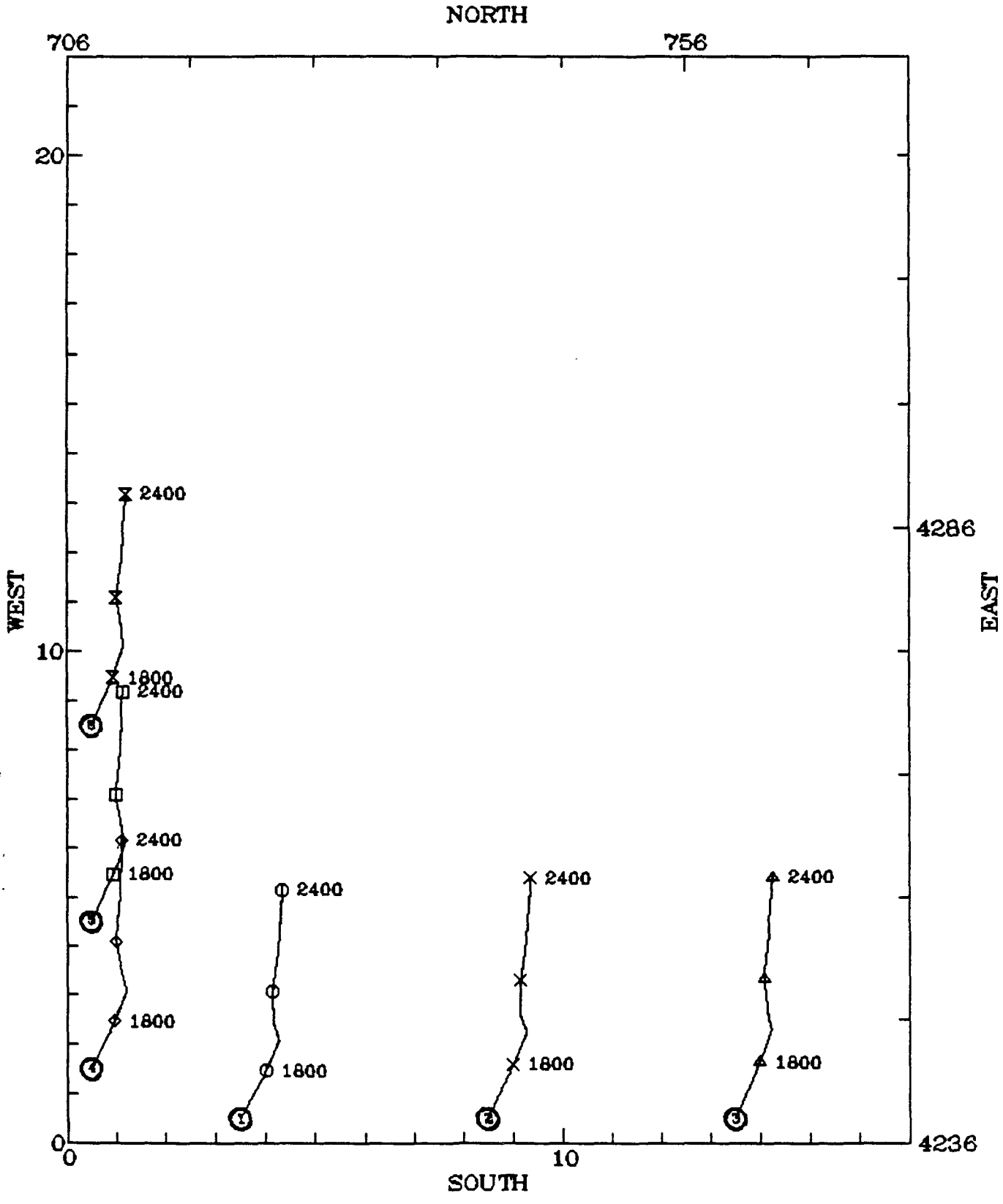

Initialized on

① 1700 ON 5/22/75
② 1700 ON 5/22/75
③ 1700 ON 5/22/75
④ 1700 ON 5/22/75
⑤ 1700 ON 5/22/75
⑥ 1700 ON 5/22/75

ST. LOUIS REGIONAL OZONE ANALYSIS
Forward Trajectories

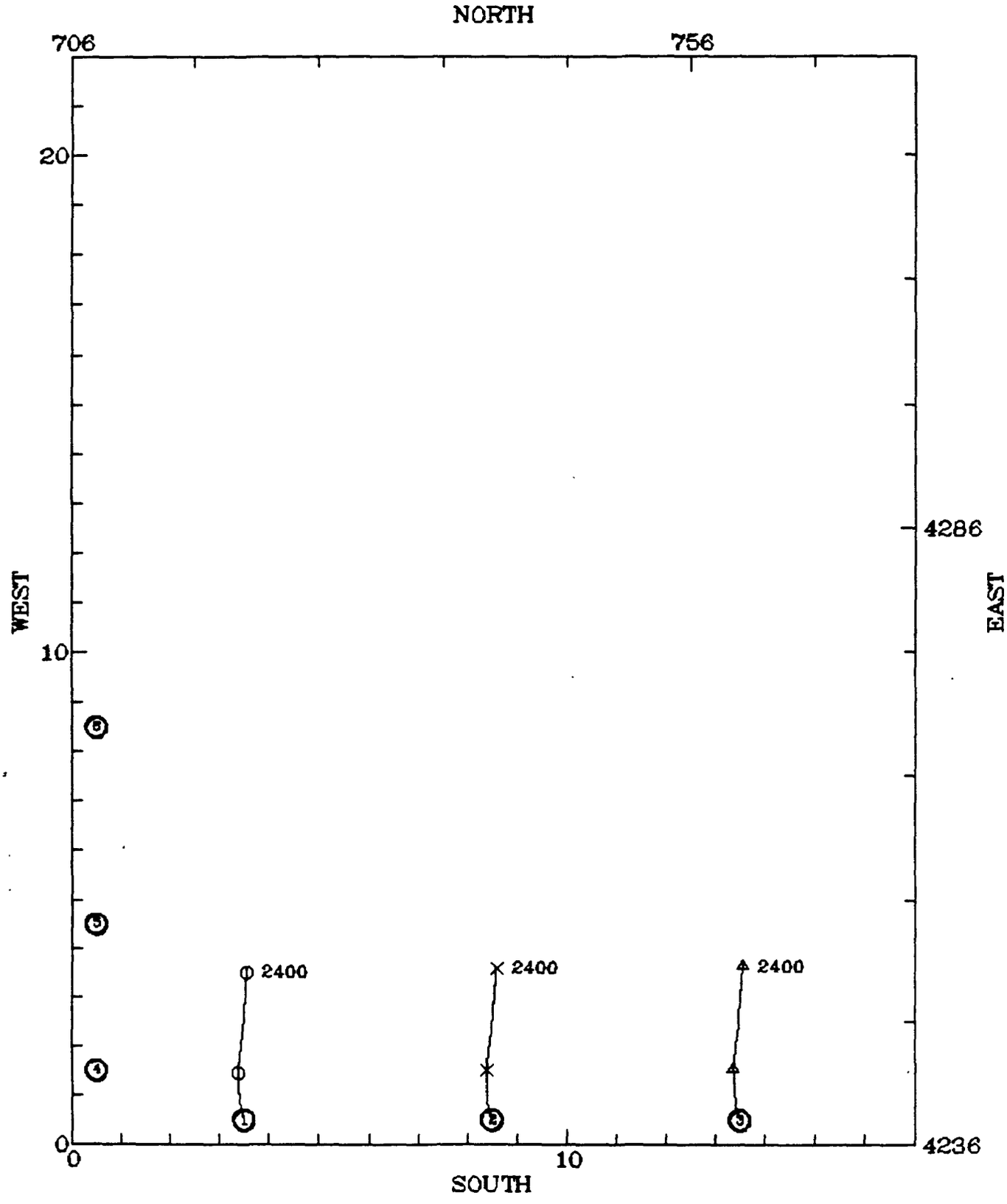

Initialized on

① 1900 ON 5/22/75
② 1900 ON 5/22/75
③ 1900 ON 5/22/75
④ 1900 ON 5/22/75
⑥ 1900 ON 5/22/75

ST. LOUIS REGIONAL OZONE ANALYSIS
Forward Trajectories

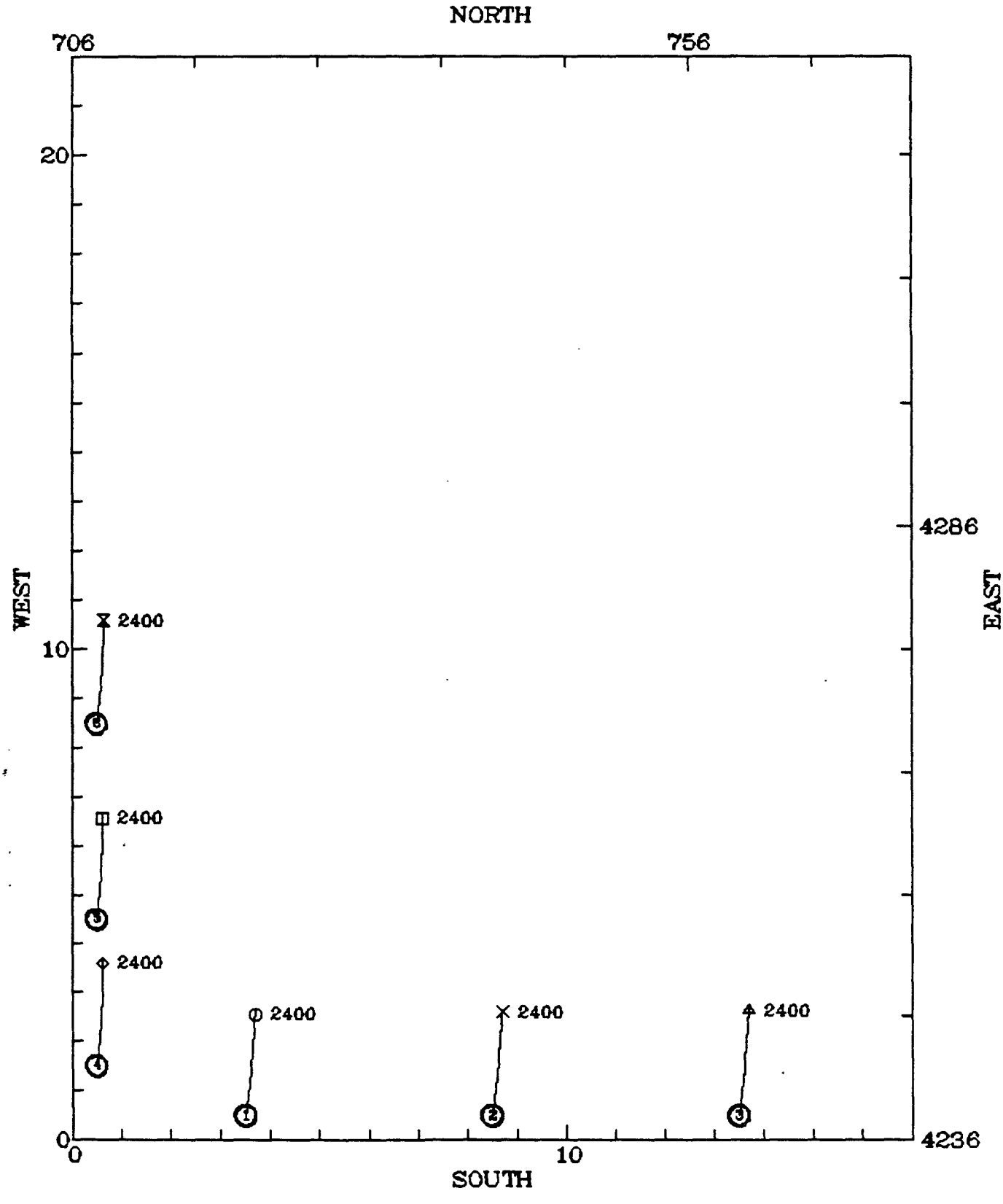

Initialized on

① 2100 ON 5/22/75
② 2100 ON 5/22/75
③ 2100 ON 5/22/75
④ 2100 ON 5/22/75
⑤ 2100 ON 5/22/75
⑥ 2100 ON 5/22/75

ST. LOUIS REGIONAL OZONE ANALYSIS
Forward Trajectories

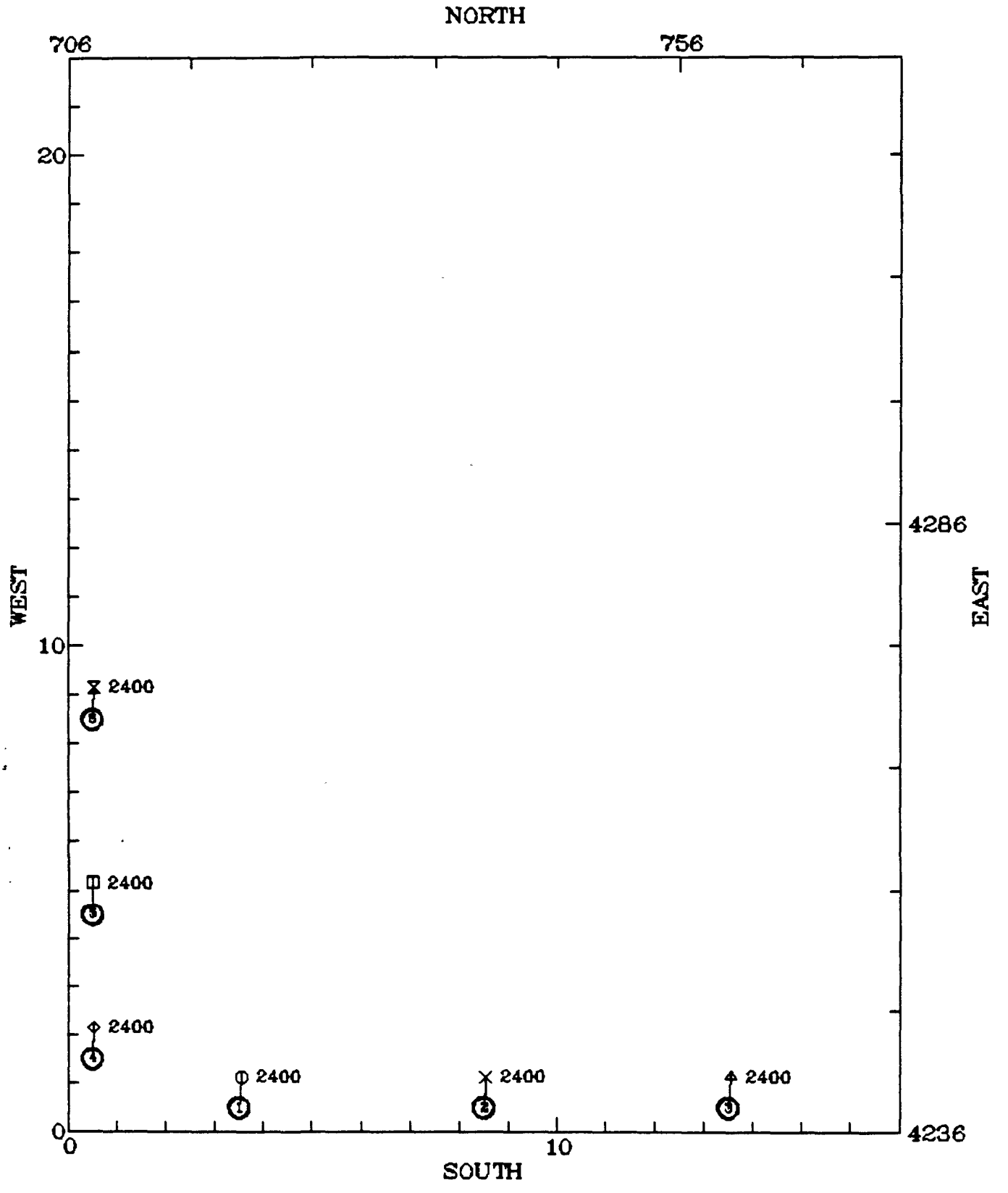

Initialized on

① 2300 ON 5/22/75
② 2300 ON 5/22/75
③ 2300 ON 5/22/75
④ 2300 ON 5/22/75
⑥ 2300 ON 5/22/75
⑧ 2300 ON 5/22/75

ST. LOUIS REGIONAL OZONE ANALYSIS
Forward Trajectories

FIGURE 2

AIR PARCEL TRAJECTORIES FOR
ST. LOUIS FOR SATURDAY, JULY 26, 1975

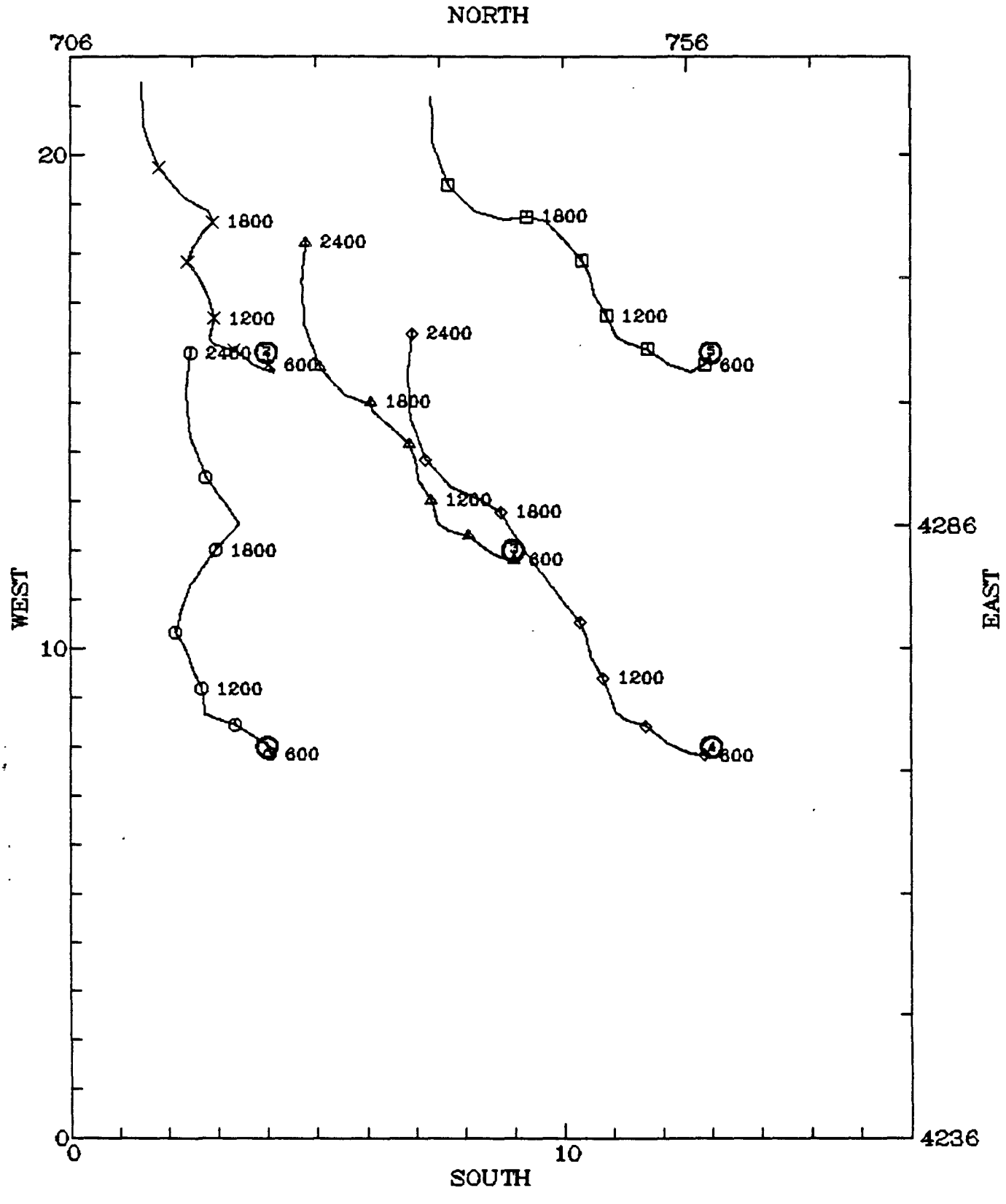

Initialized on

① 500 ON 7/26/75
② 500 ON 7/26/75
③ 500 ON 7/26/75
④ 500 ON 7/26/75
⑤ 500 ON 7/26/75

ST. LOUIS REGIONAL OZONE ANALYSIS
Forward Trajectories

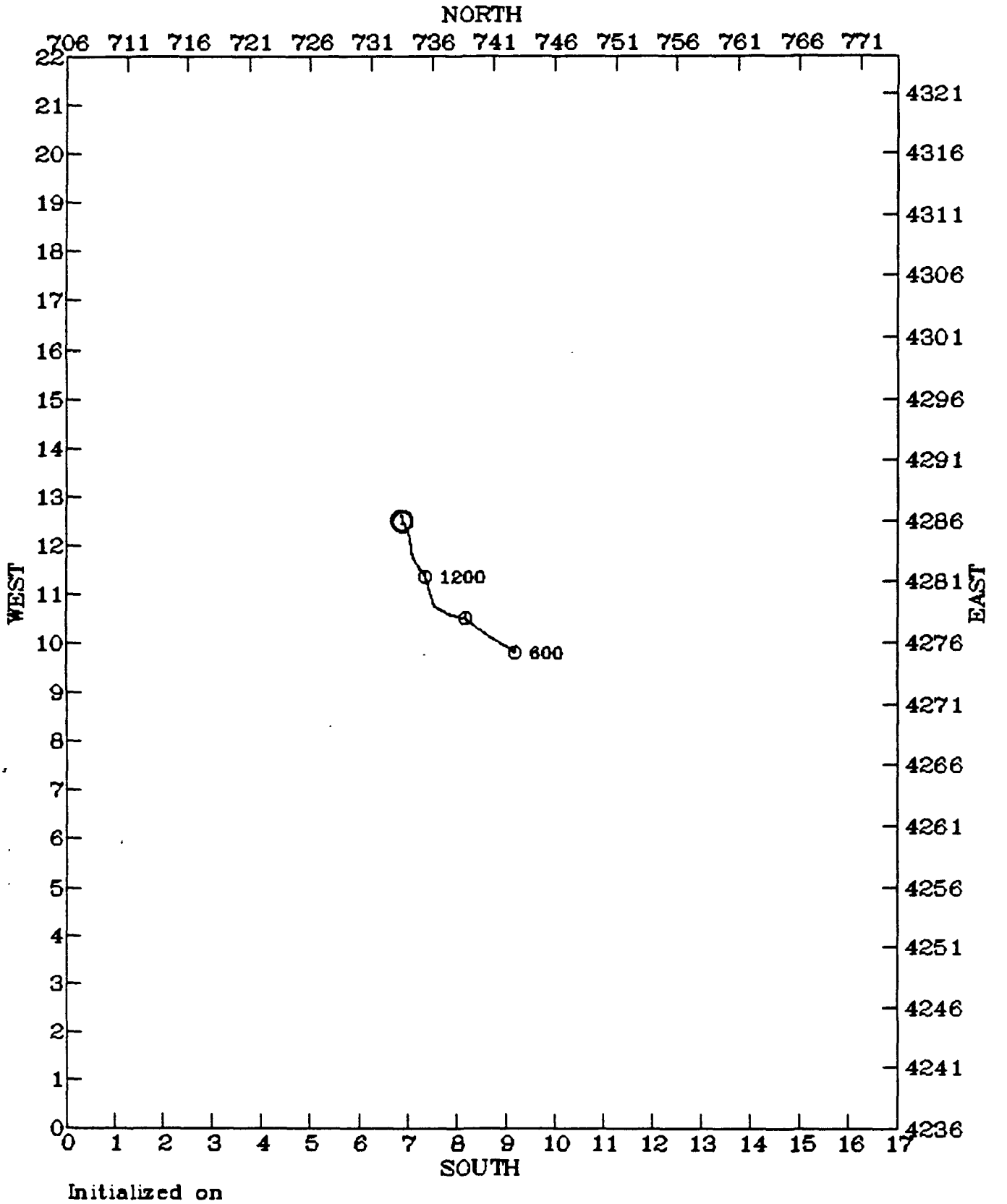

Initialized on

① 1500 ON 7/26/75

Backward Trajectories

ST. LOUIS REGIONAL OZONE ANALYSIS

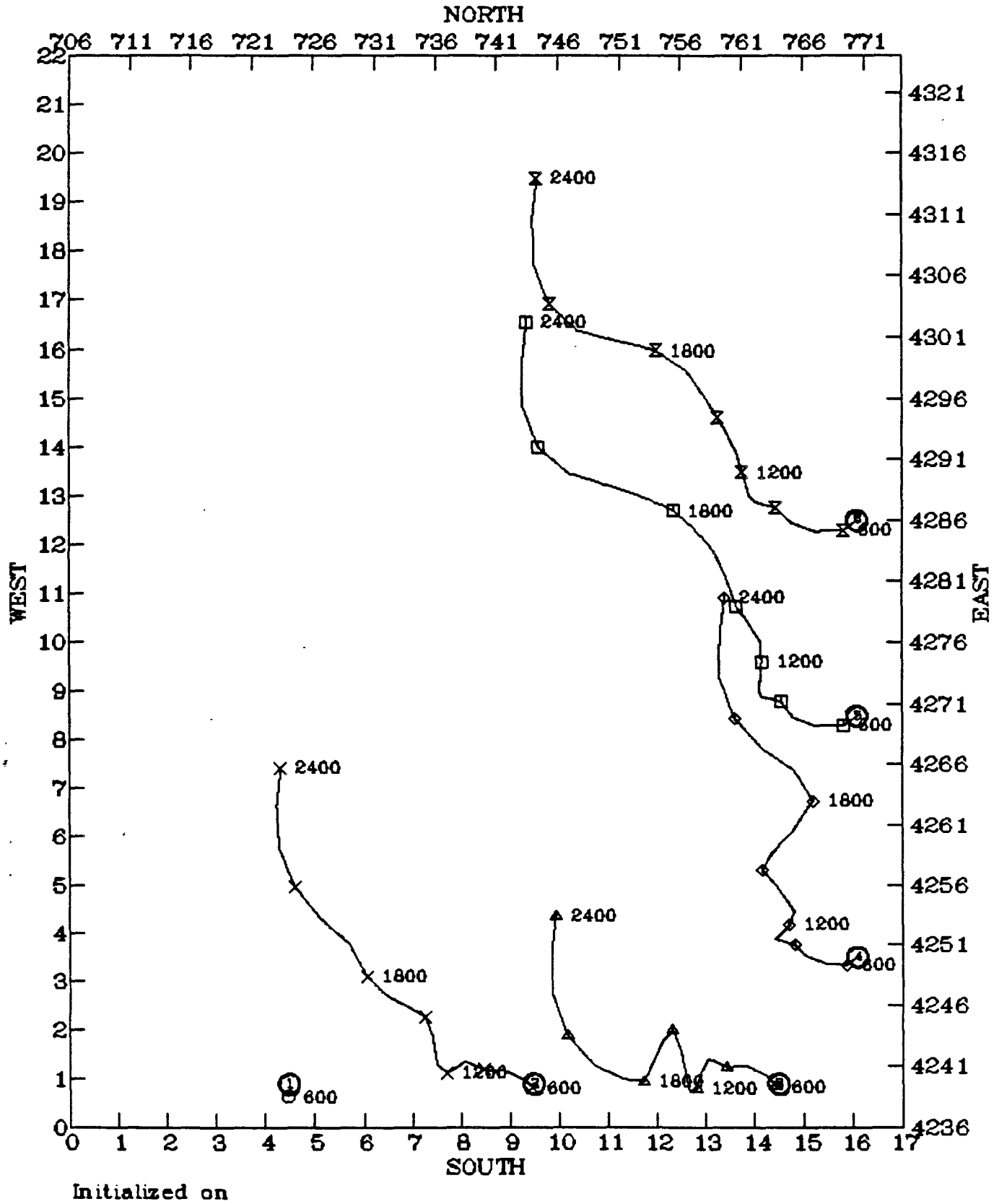

Initialized on

① 500 ON 7/26/75
② 500 ON 7/26/75
③ 500 ON 7/26/75
④ 500 ON 7/26/75
⑤ 500 ON 7/26/75
⑥ 500 ON 7/26/75

ST. LOUIS REGIONAL OZONE ANALYSIS
Forward Trajectories

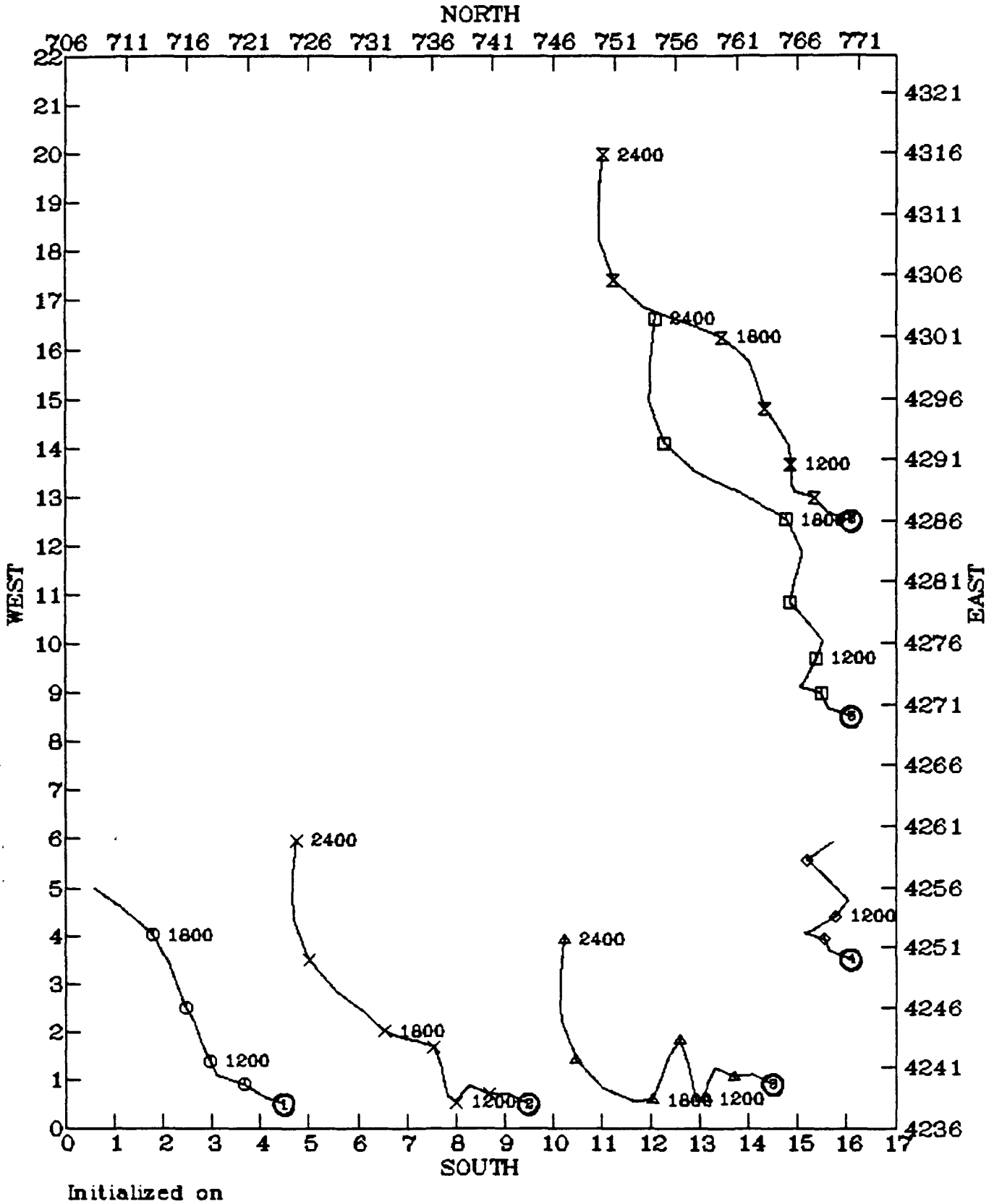

Initialized on

① 700 ON 7/26/75
② 700 ON 7/26/75
③ 700 ON 7/26/75
④ 700 ON 7/26/75
⑤ 700 ON 7/26/75
⑥ 700 ON 7/26/75

ST. LOUIS REGIONAL OZONE ANALYSIS
Forward Trajectories

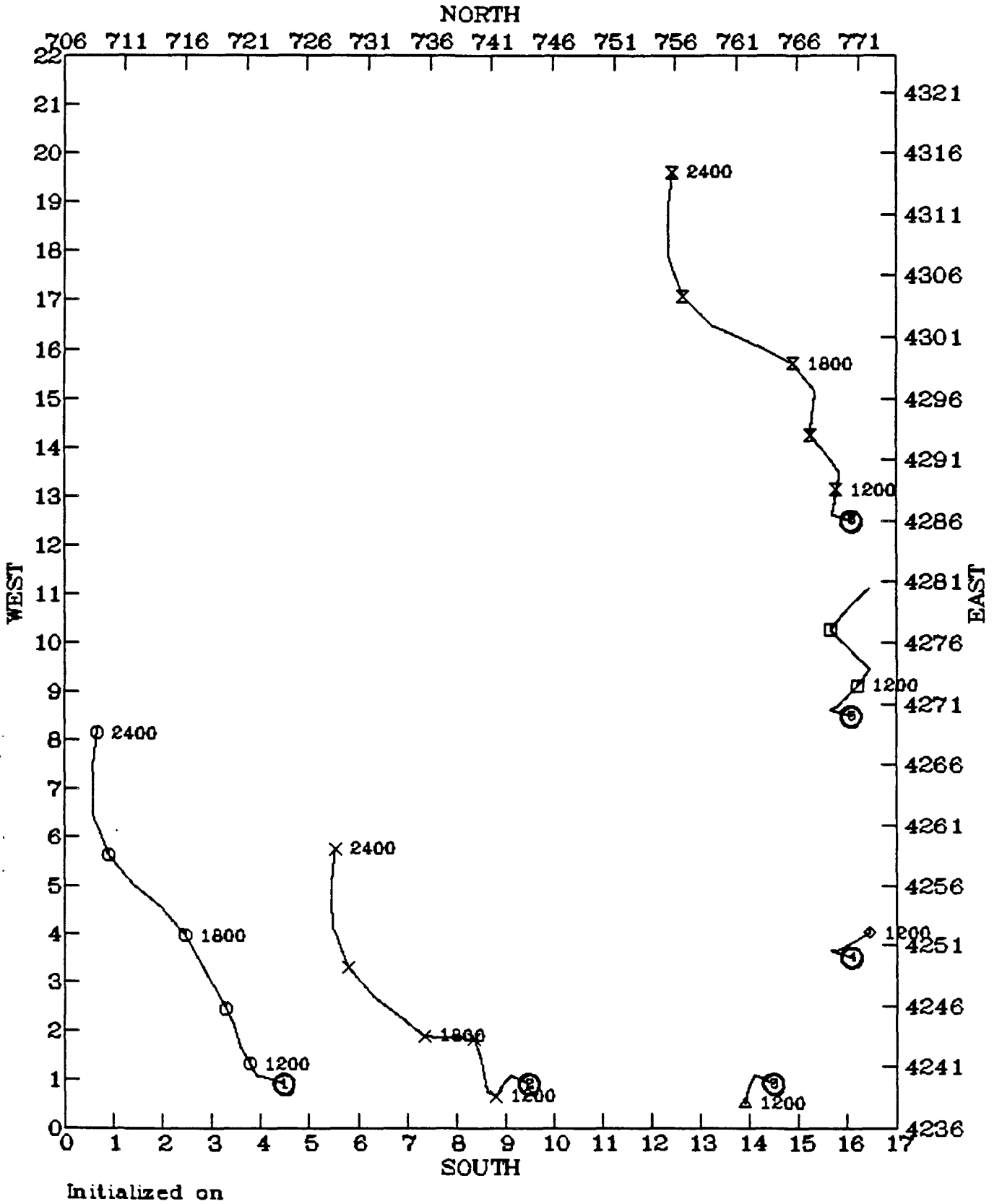

Initialized on

① 900 ON 7/26/75
② 900 ON 7/26/75
③ 900 ON 7/26/75
④ 900 ON 7/26/75
⑤ 900 ON 7/26/75
⑥ 900 ON 7/26/75

ST. LOUIS REGIONAL OZONE ANALYSIS
Forward Trajectories

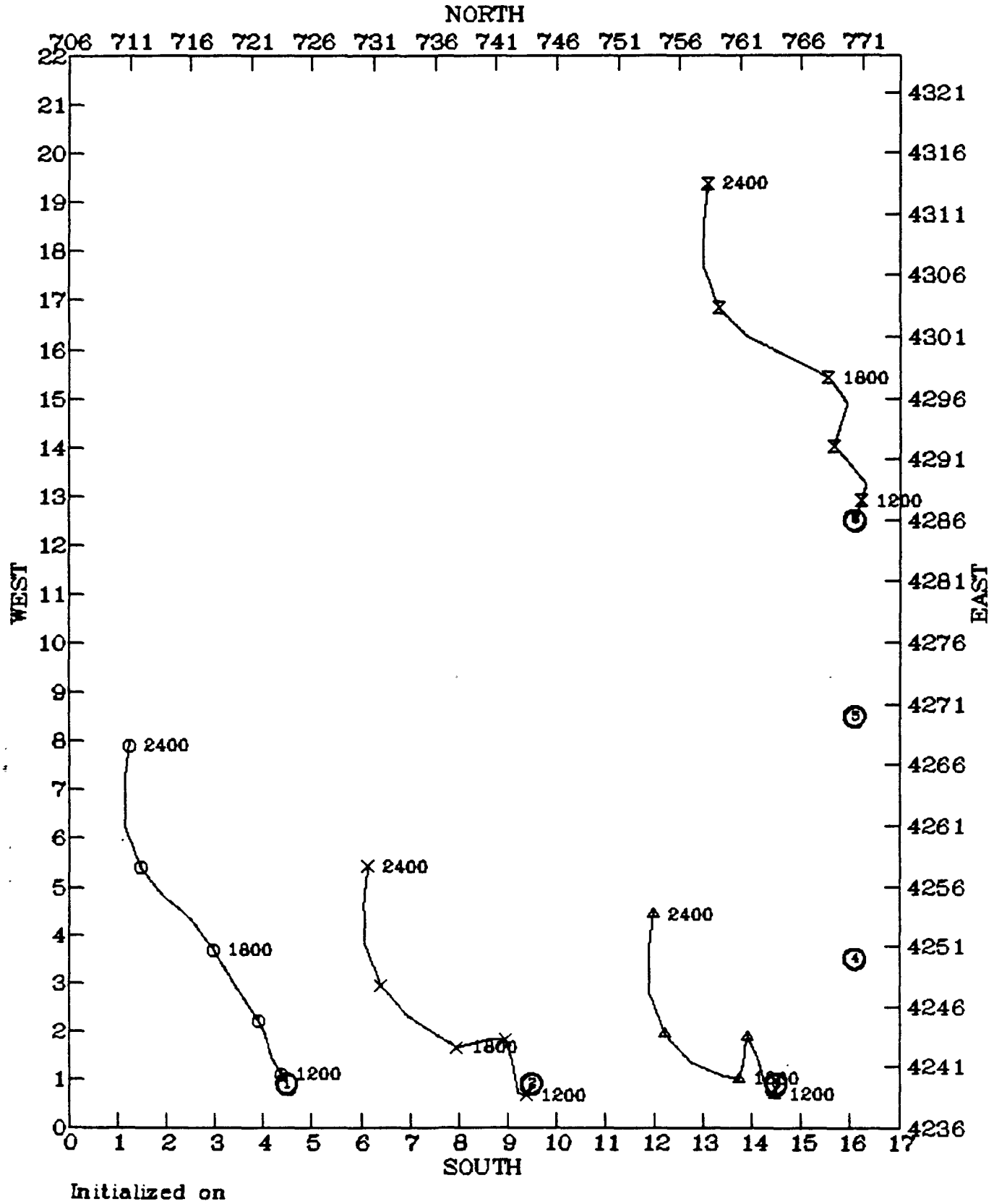

Initialized on

① 1100 ON 7/26/75
② 1100 ON 7/26/75
③ 1100 ON 7/26/75
④ 1100 ON 7/26/75
⑤ 1100 ON 7/26/75
⑥ 1100 ON 7/26/75

ST. LOUIS REGIONAL OZONE ANALYSIS
Forward Trajectories

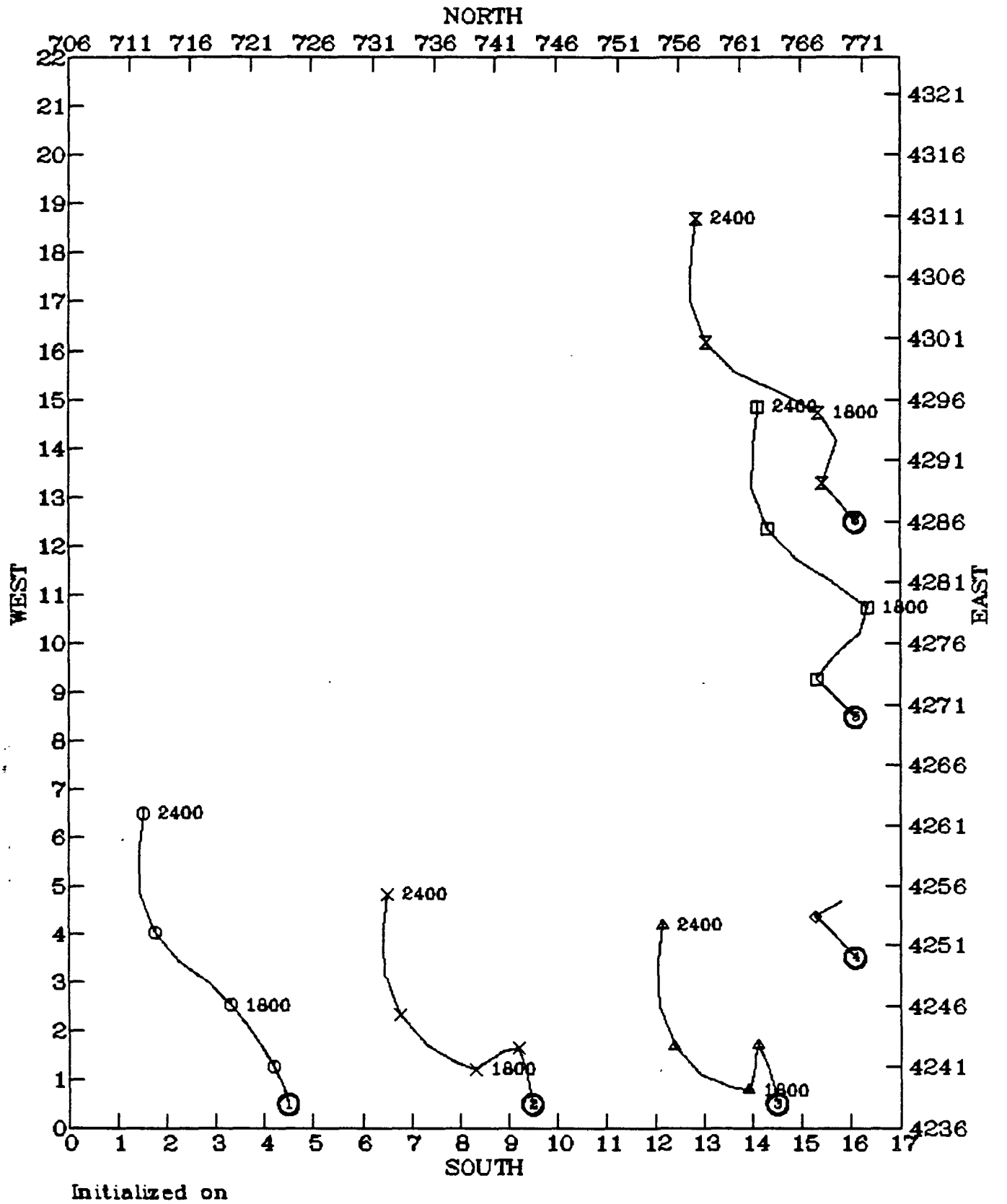

Initialized on

① 1300 ON 7/26/75
② 1300 ON 7/26/75
③ 1300 ON 7/26/75
④ 1300 ON 7/26/75
⑤ 1300 ON 7/26/75
⑥ 1300 ON 7/26/75

ST. LOUIS REGIONAL OZONE ANALYSIS
Forward Trajectories

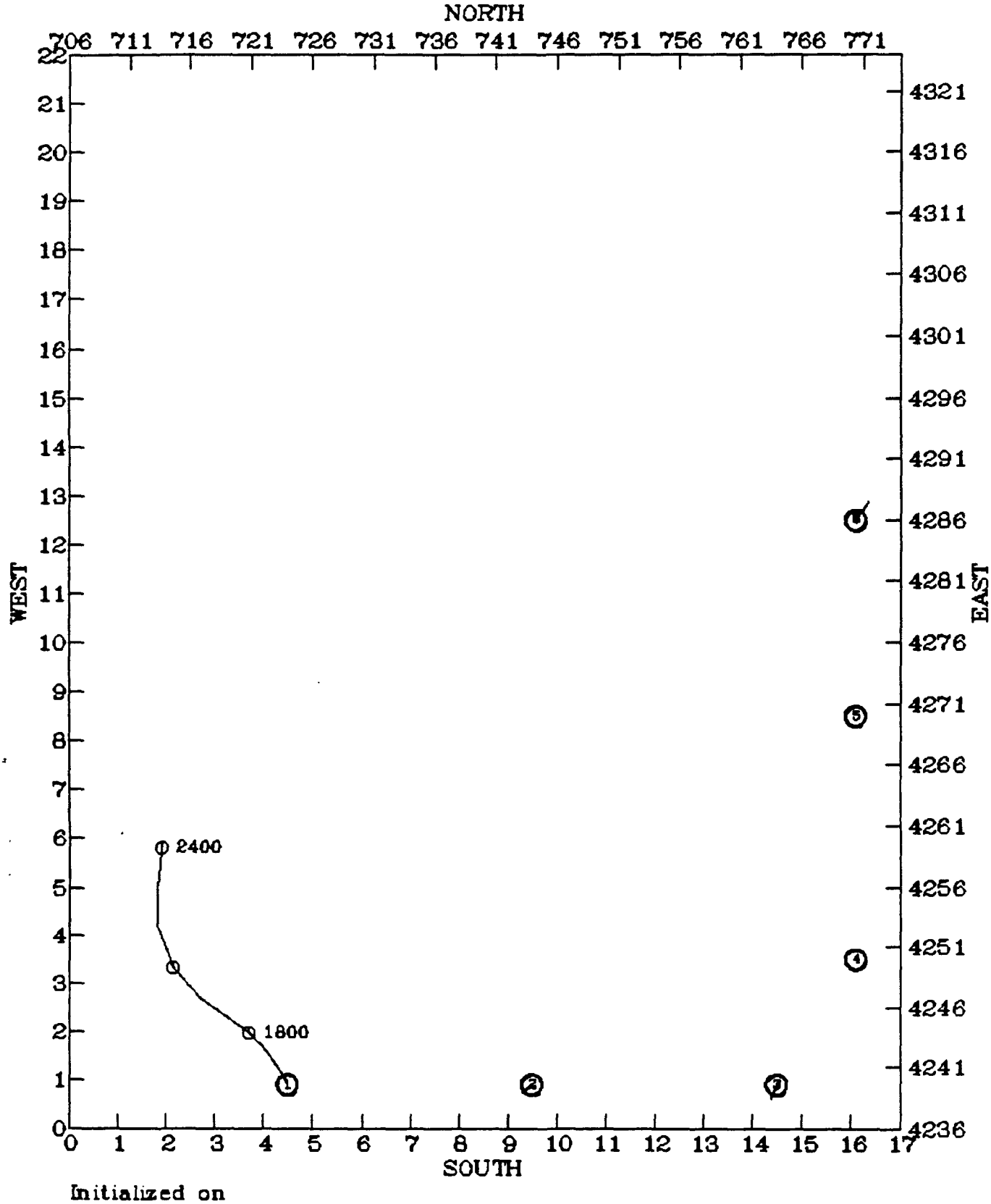

Initialized on

① 1500 ON 7/26/75
② 1500 ON 7/26/75
③ 1500 ON 7/26/75
④ 1500 ON 7/26/75
⑤ 1500 ON 7/26/75
⑥ 1500 ON 7/26/75

ST. LOUIS REGIONAL OZONE ANALYSIS
Forward Trajectories

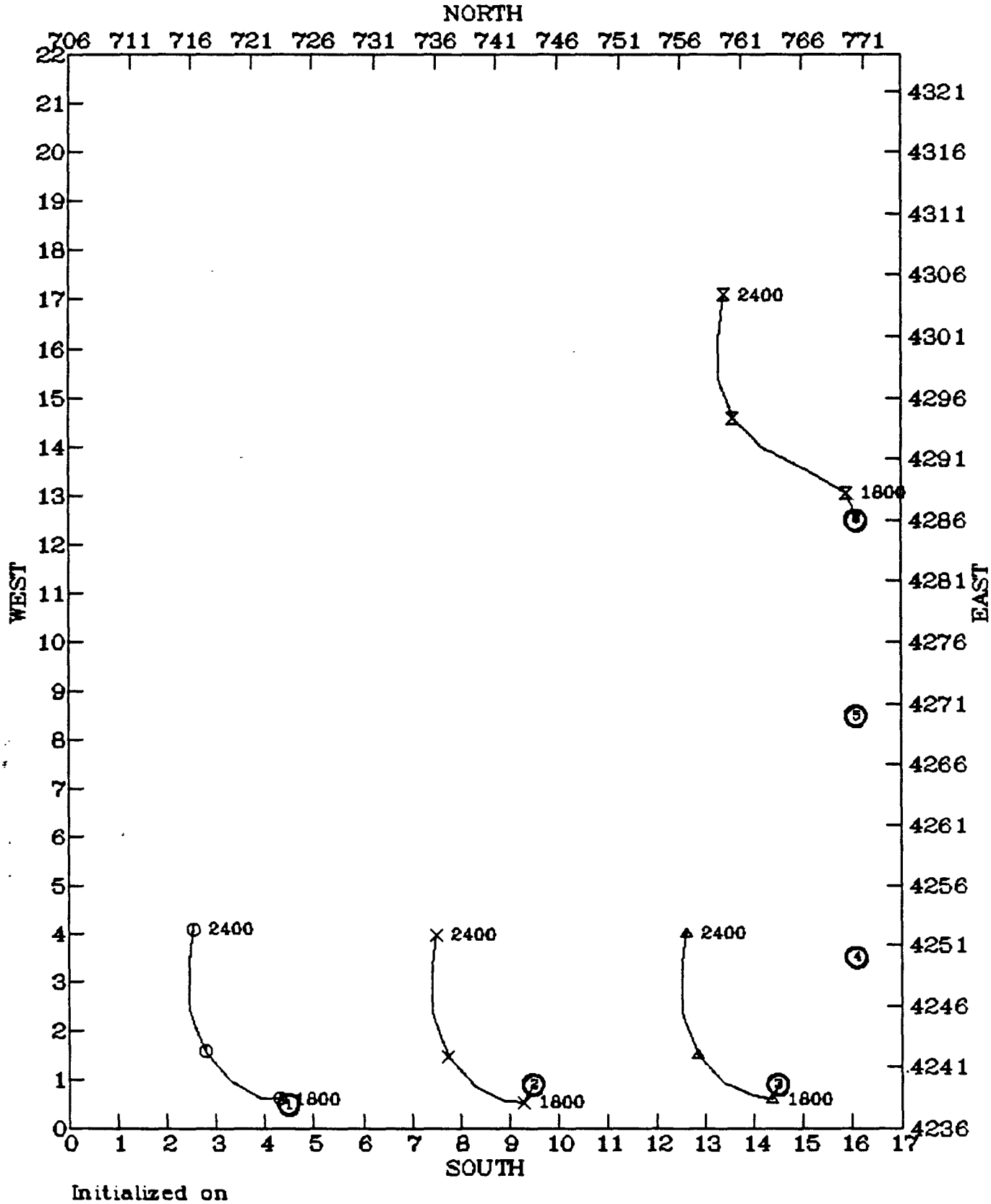

Initialized on

① 1700 ON 7/26/75
② 1700 ON 7/26/75
③ 1700 ON 7/26/75
④ 1700 ON 7/26/75
⑤ 1700 ON 7/26/75
⑥ 1700 ON 7/26/75

ST. LOUIS REGIONAL OZONE ANALYSIS
Forward Trajectories

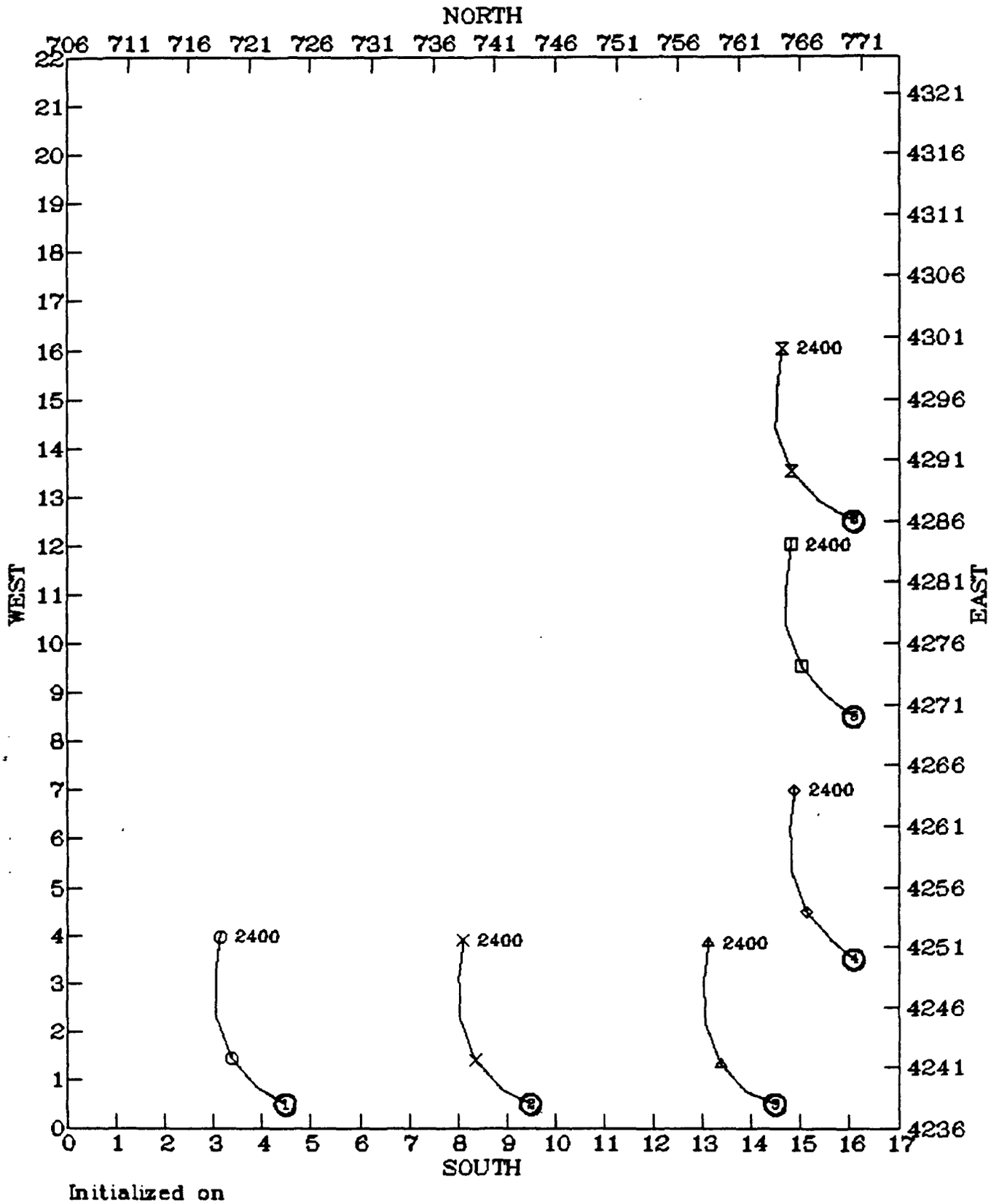

Initialized on

① 1900 ON 7/26/75
② 1900 ON 7/26/75
③ 1900 ON 7/26/75
④ 1900 ON 7/26/75
⑤ 1900 ON 7/26/75
⑥ 1900 ON 7/26/75

ST. LOUIS REGIONAL OZONE ANALYSIS
Forward Trajectories

FIGURE 3

AIR PARCEL TRAJECTORIES FOR
ST. LOUIS FOR TUESDAY, JULY 13, 1976

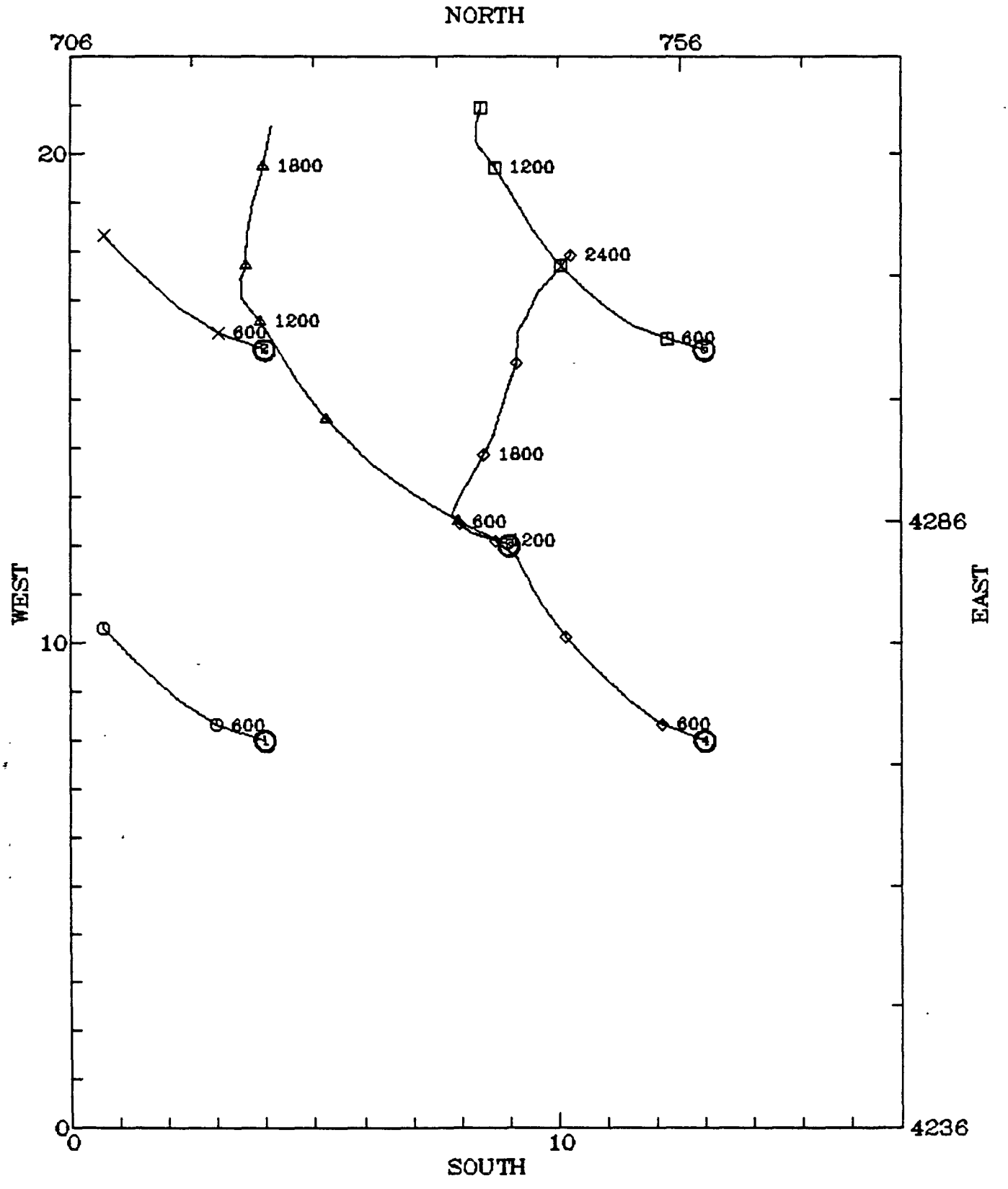

Initialized on

① 500 ON 7/13/76
② 500 ON 7/13/76
③ 500 ON 7/13/76
④ 500 ON 7/13/76
⑤ 500 ON 7/13/76

ST. LOUIS REGIONAL OZONE ANALYSIS
Forward Trajectories

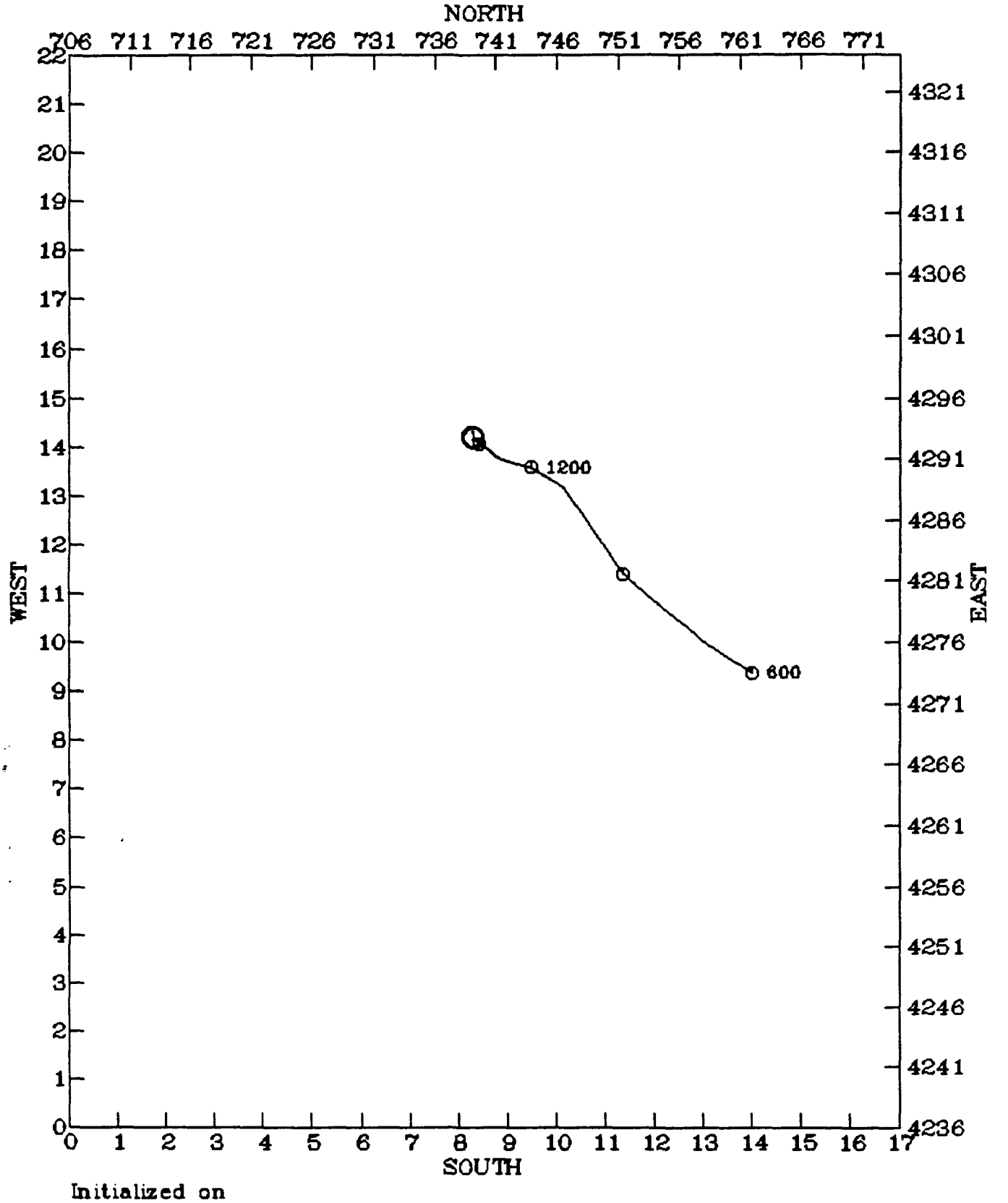

Initialized on

① 1600 ON 7/13/76

Backward Trajectories

ST. LOUIS REGIONAL OZONE ANALYSIS

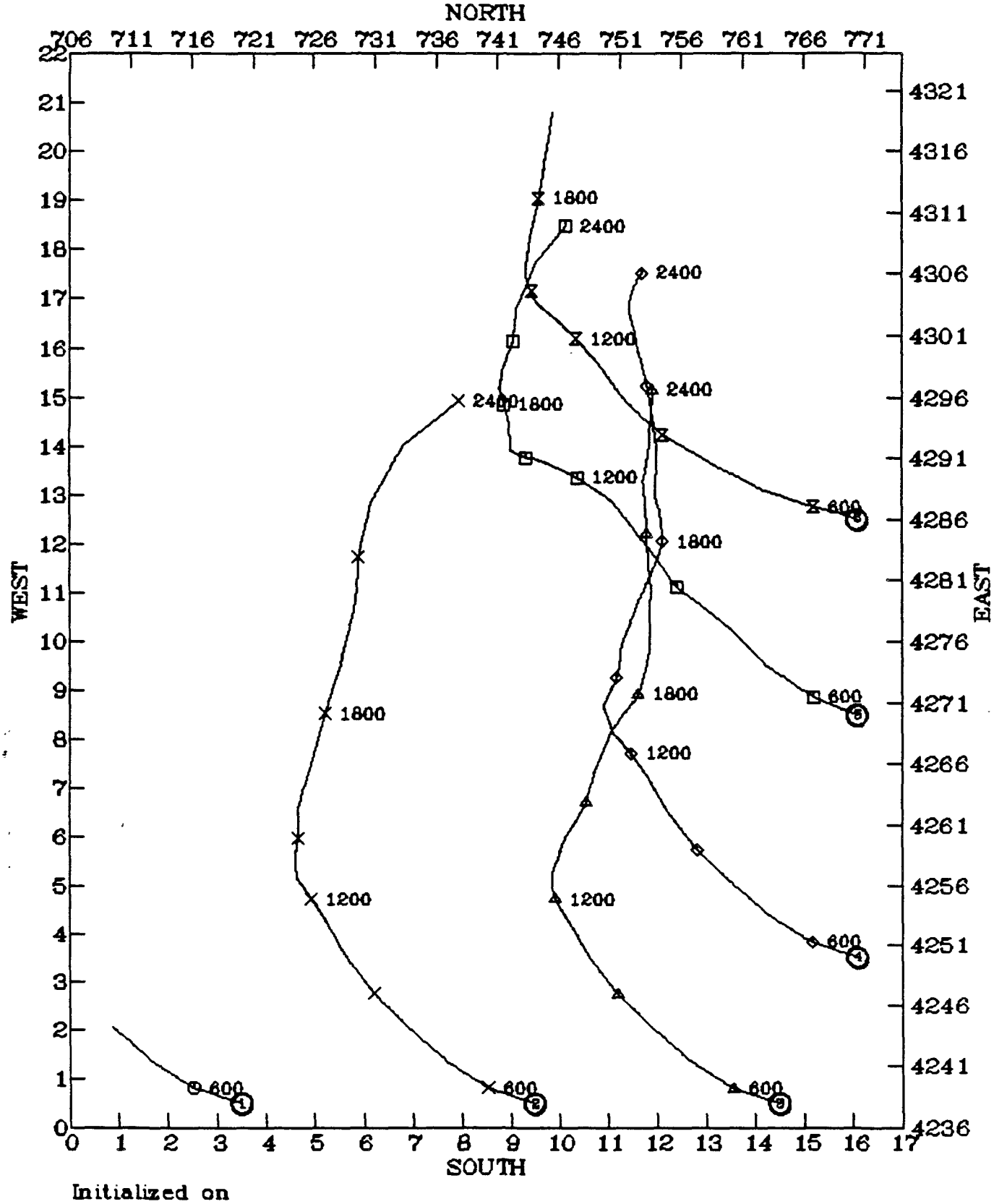

Initialized on

① 500 ON 7/13/76
② 500 ON 7/13/76
③ 500 ON 7/13/76
④ 500 ON 7/13/76
⑤ 500 ON 7/13/76
⑥ 500 ON 7/13/76

ST. LOUIS REGIONAL OZONE ANALYSIS
Forward Trajectories

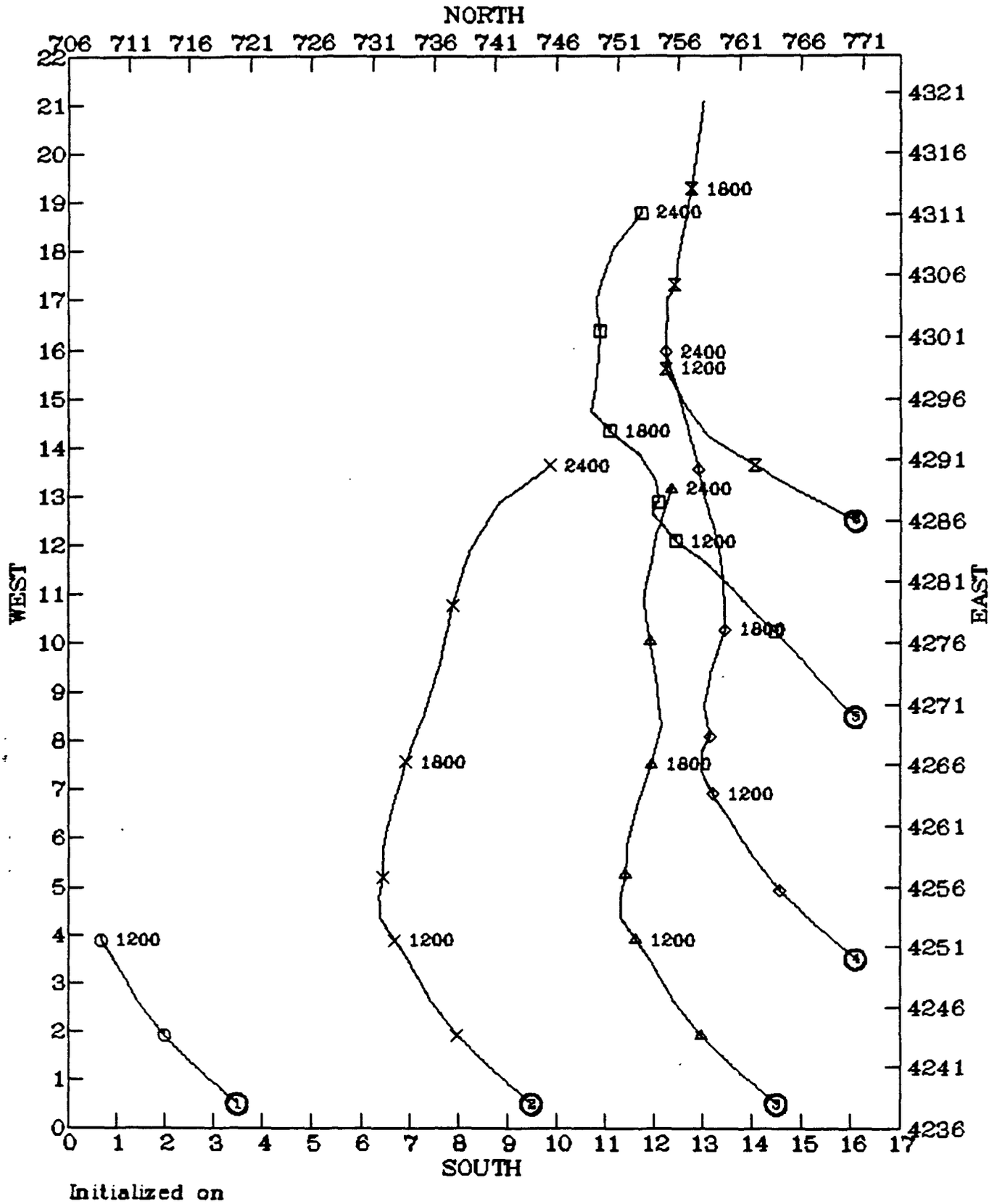

Initialized on

① 700 ON 7/13/76
② 700 ON 7/13/76
③ 700 ON 7/13/76
④ 700 ON 7/13/76
⑤ 700 ON 7/13/76
⑥ 700 ON 7/13/76

ST. LOUIS REGIONAL OZONE ANALYSIS
Forward Trajectories

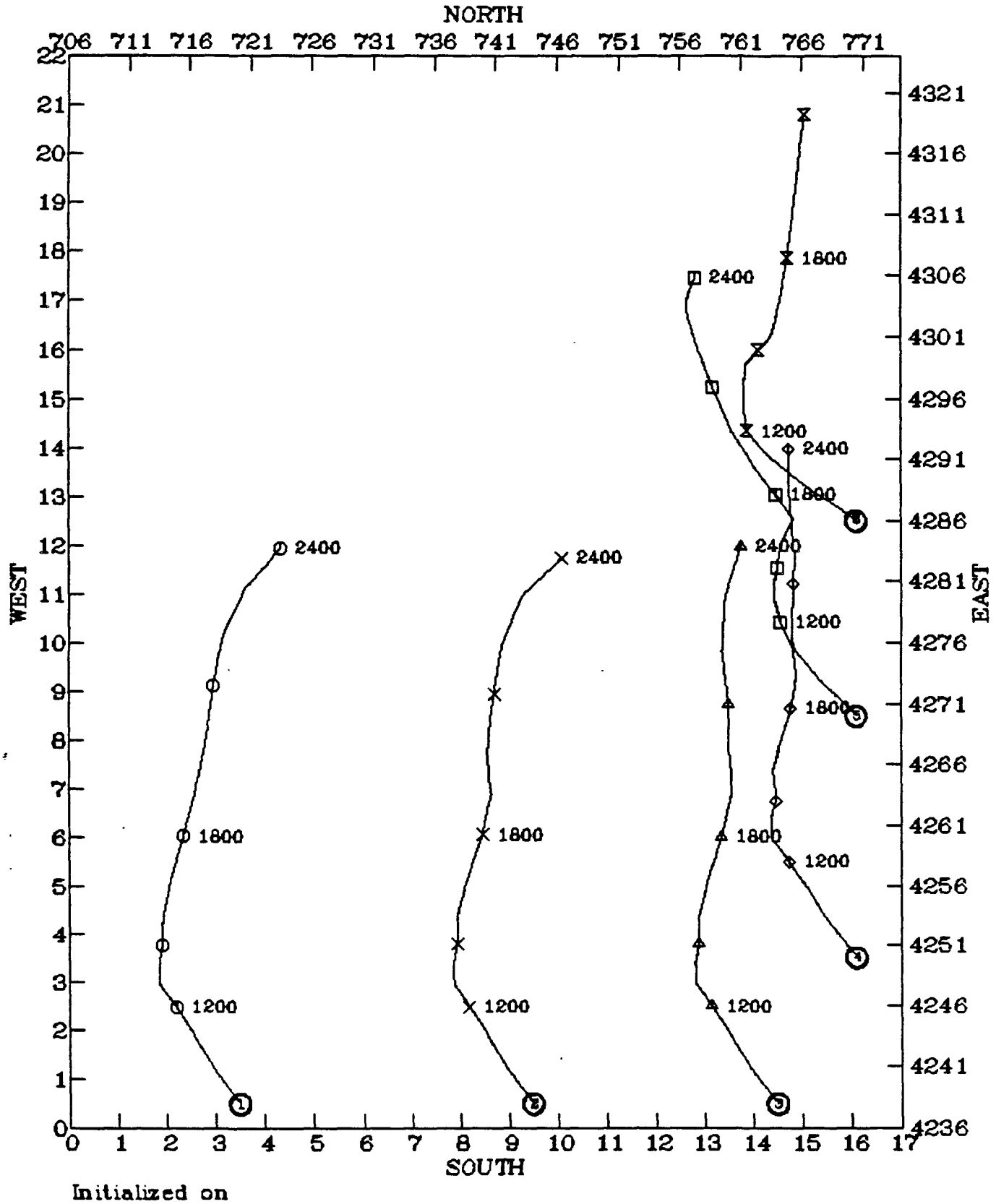

Initialized on

① 900 ON 7/13/76
② 900 ON 7/13/76
③ 900 ON 7/13/76
④ 900 ON 7/13/76
⑤ 900 ON 7/13/76
⑥ 900 ON 7/13/76

ST. LOUIS REGIONAL OZONE ANALYSIS
Forward Trajectories

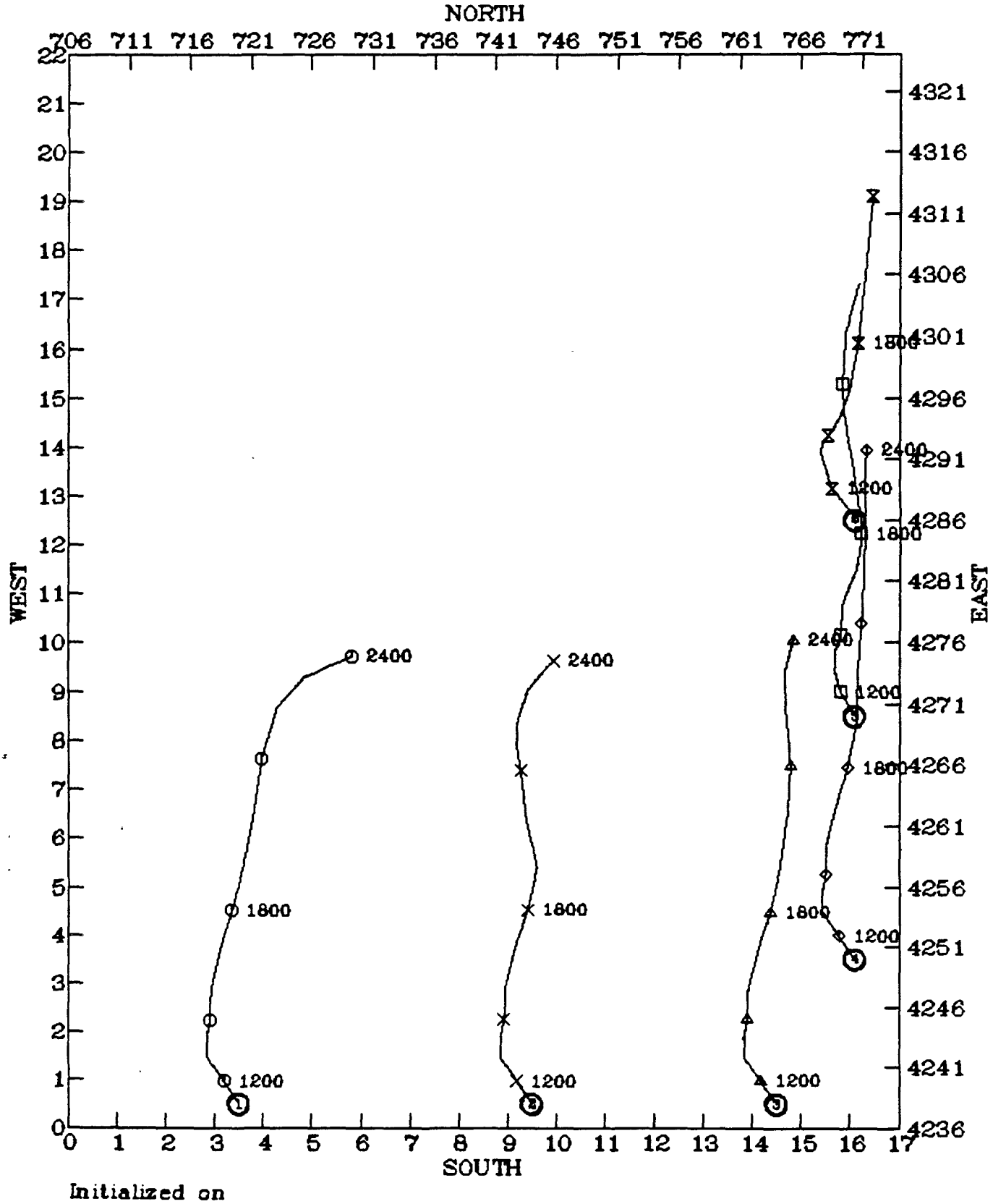

Initialized on

① 1100 ON 7/13/76
② 1100 ON 7/13/76
③ 1100 ON 7/13/76
④ 1100 ON 7/13/76
⑤ 1100 ON 7/13/76
⑥ 1100 ON 7/13/76

ST. LOUIS REGIONAL OZONE ANALYSIS
Forward Trajectories

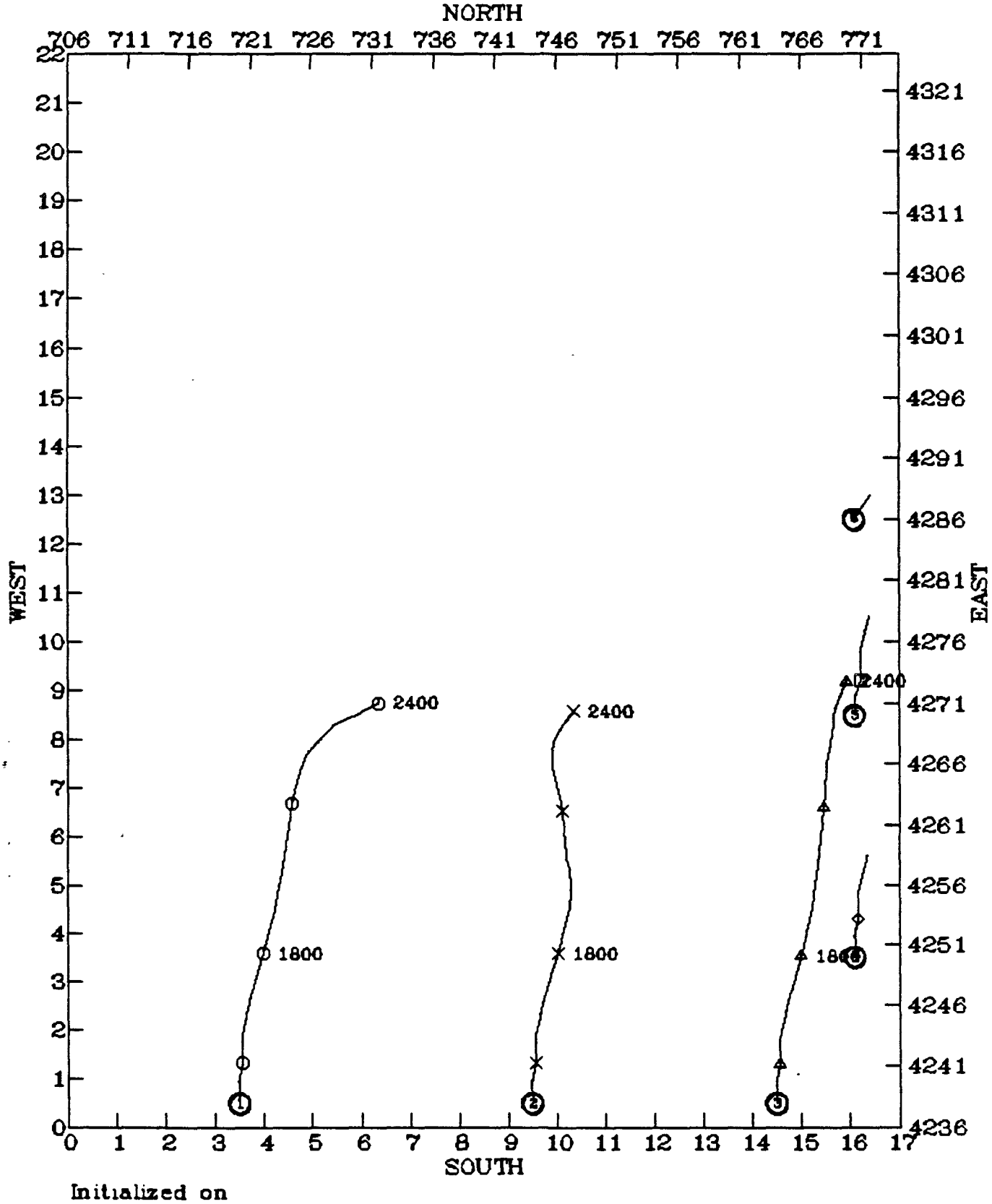

Initialized on

① 1300 ON 7/13/76
② 1300 ON 7/13/76
③ 1300 ON 7/13/76
④ 1300 ON 7/13/76
⑤ 1300 ON 7/13/76
⑥ 1300 ON 7/13/76

ST. LOUIS REGIONAL OZONE ANALYSIS
Forward Trajectories

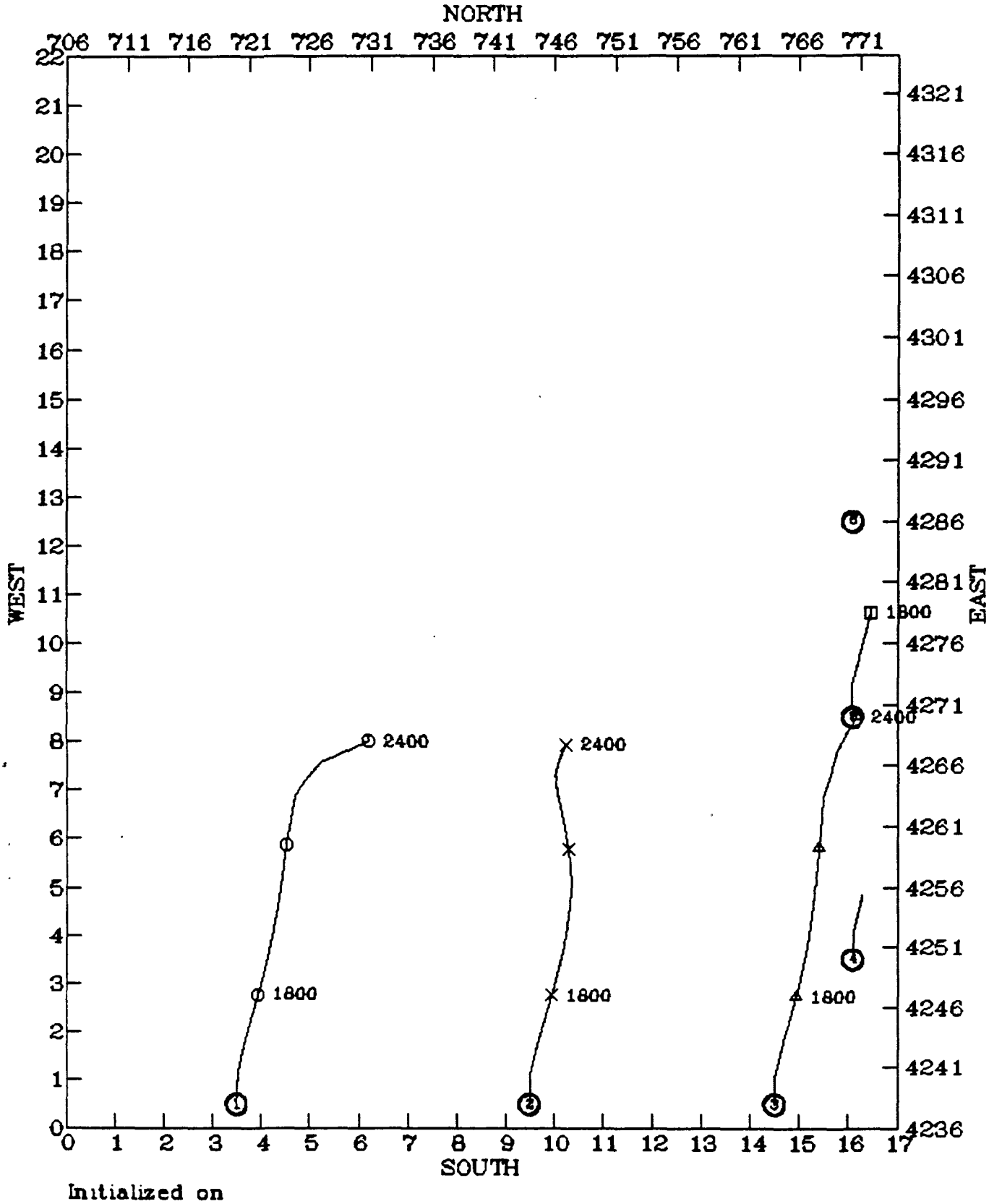

Initialized on

① 1500 ON 7/13/76
② 1500 ON 7/13/76
③ 1500 ON 7/13/76
④ 1500 ON 7/13/76
⑤ 1500 ON 7/13/76
⑥ 1500 ON 7/13/76

ST. LOUIS REGIONAL OZONE ANALYSIS
Forward Trajectories

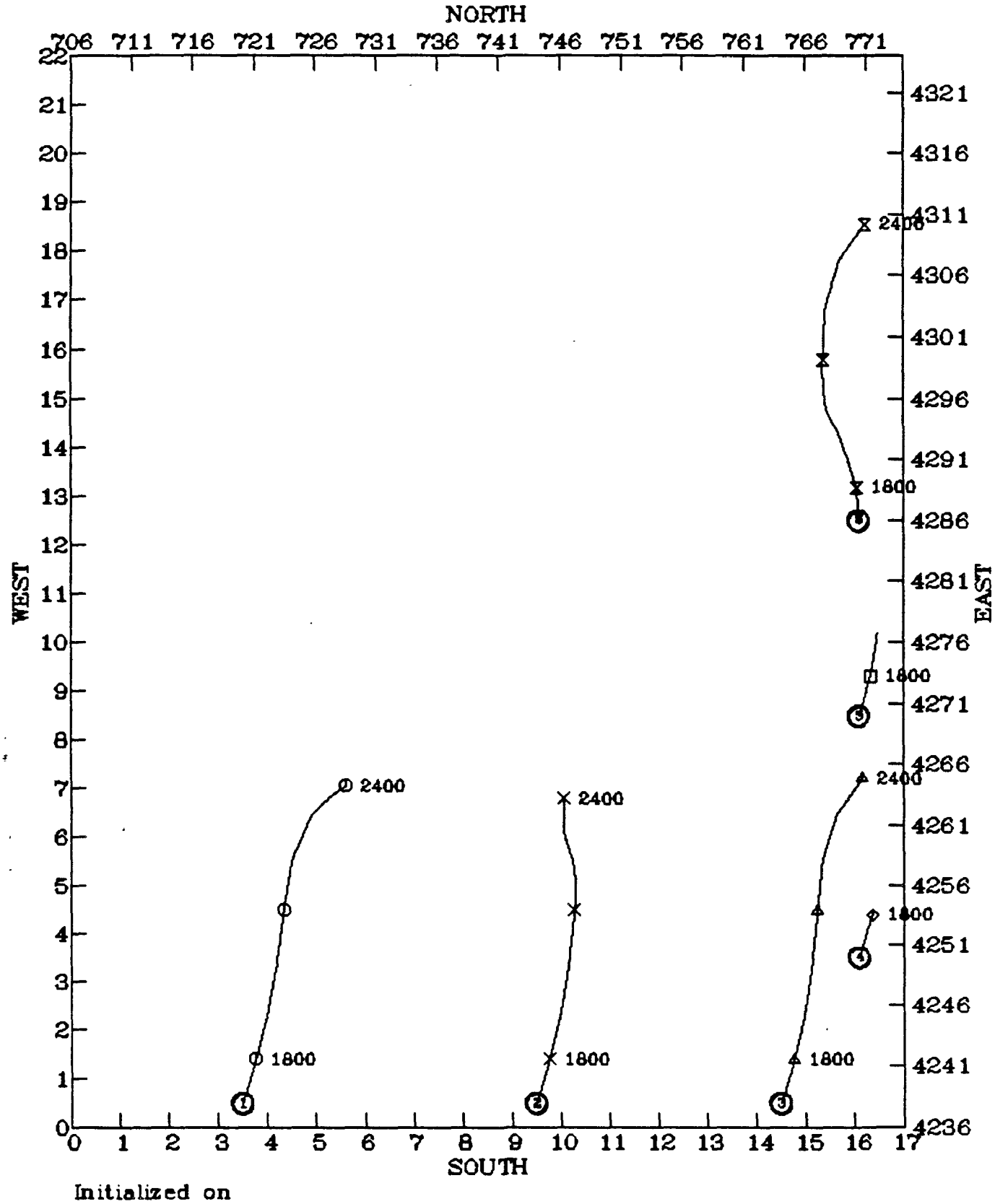

Initialized on

① 1700 ON 7/13/76
② 1700 ON 7/13/76
③ 1700 ON 7/13/76
④ 1700 ON 7/13/76
⑤ 1700 ON 7/13/76
⑥ 1700 ON 7/13/76

ST. LOUIS REGIONAL OZONE ANALYSIS
Forward Trajectories

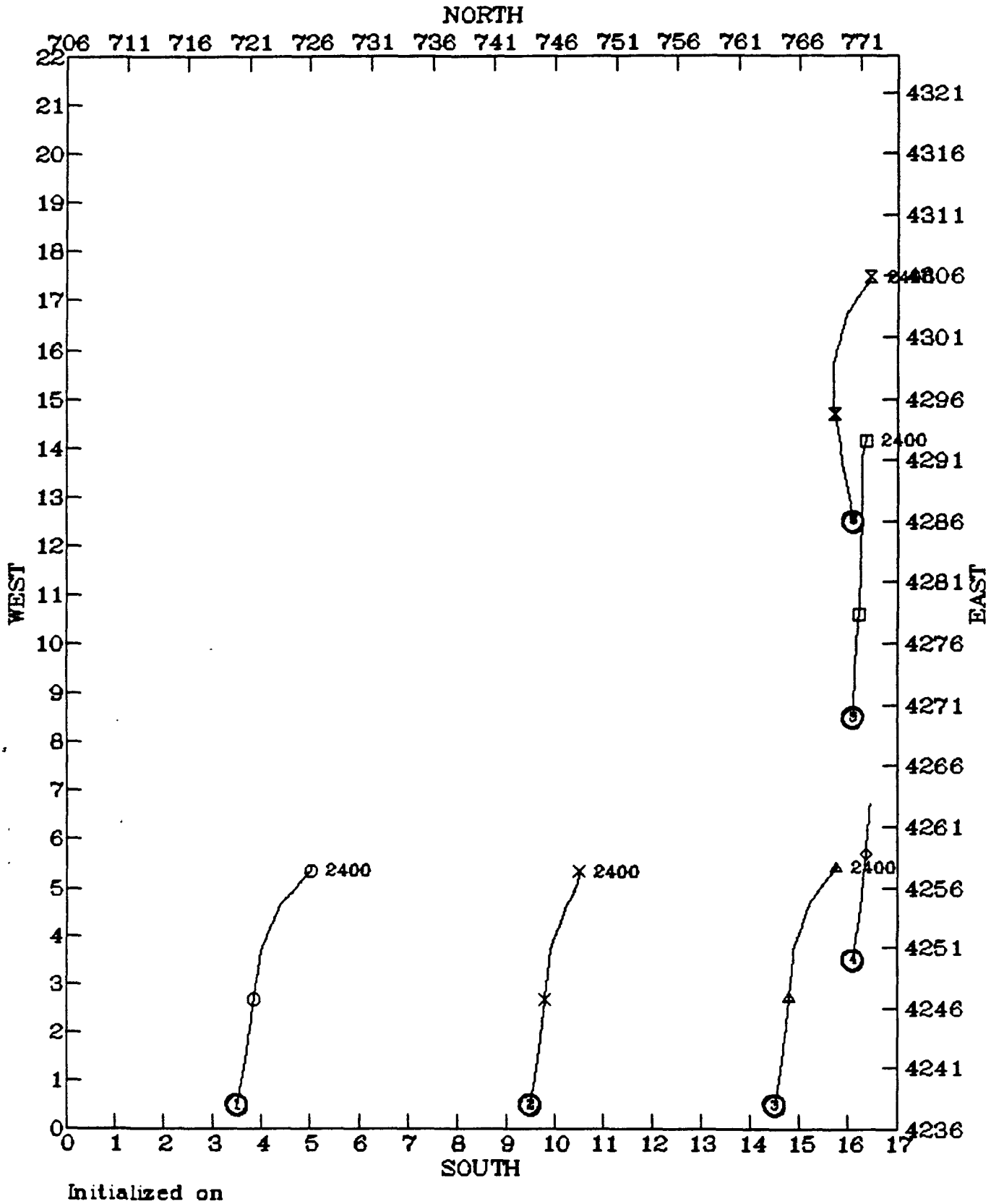

Initialized on

① 1900 ON 7/13/76
② 1900 ON 7/13/76
③ 1900 ON 7/13/76
④ 1900 ON 7/13/76
⑤ 1900 ON 7/13/76
⑥ 1900 ON 7/13/76

ST. LOUIS REGIONAL OZONE ANALYSIS
Forward Trajectories

Appendix D

ISOPLETHS OF HOURLY OZONE CONCENTRATIONS (PPHM) AND HOURLY OZONE CONCENTRATION DIFFERENCES (PPB) BETWEEN SCENARIOS FOR THE NEW YORK APPLICATION OF THE UAM ON THE AFTERNOON OF 8 AUGUST 1980

FIGURE D-1: Scenario 1

FIGURE D-2: Scenario 2

FIGURE D-3: Differences between Scenario 1 and Scenario 2

FIGURE D-4: Scenario 3

FIGURE D-5: Differences between Scenario 2 and Scenario 3

FIGURE D-6: Scenario 4

FIGURE D-7: Differences between Scenario 4 and Scenario 1

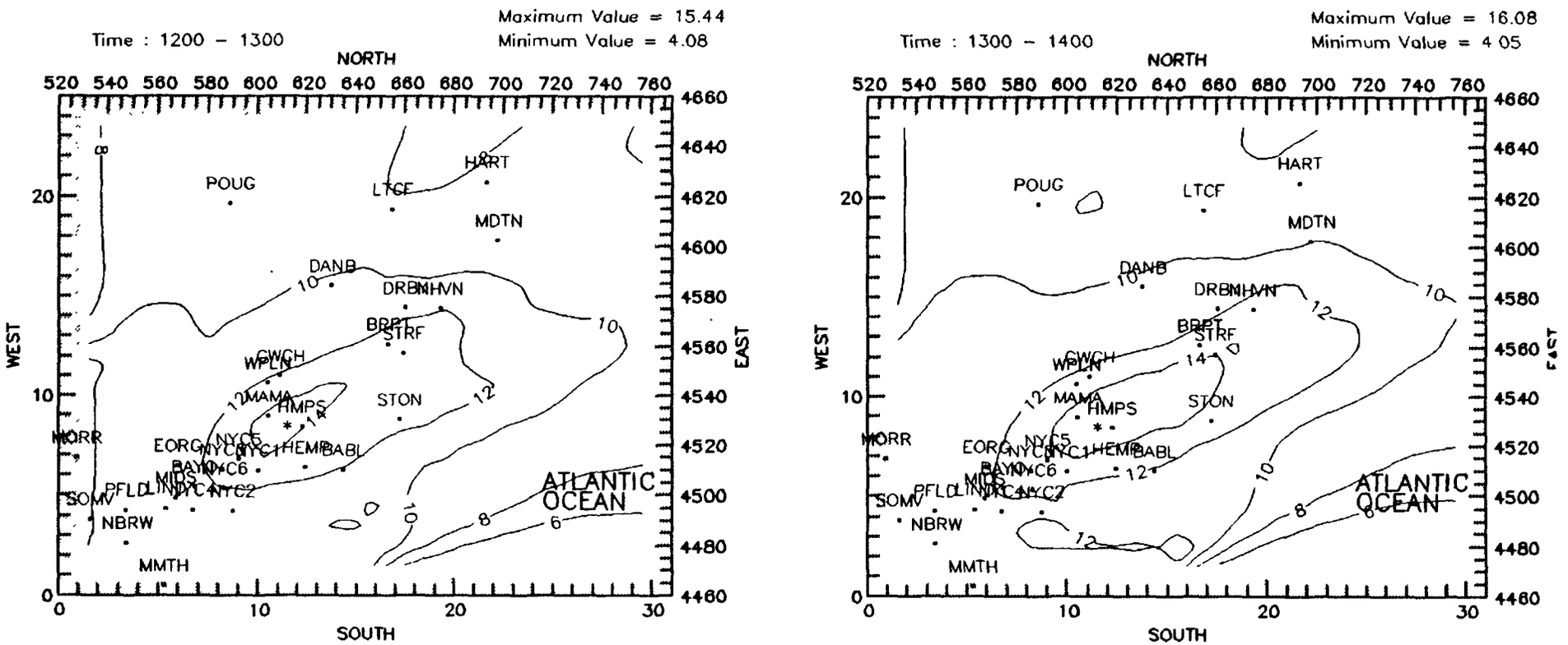

FIGURE D-1a. Ozone concentration Scenario 1, 8 August 1980 (pphm).

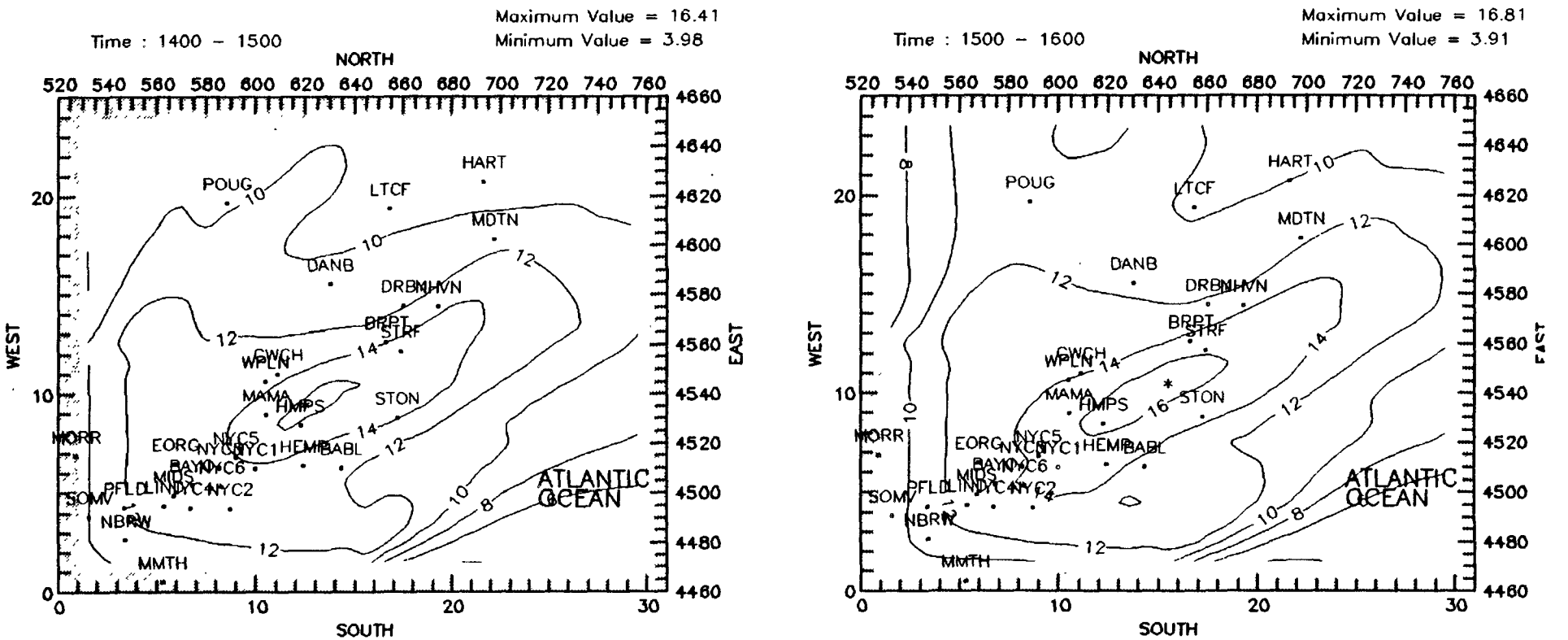

FIGURE D-1b. Ozone concentration Scenario 1, 8 August 1980 (pphm).

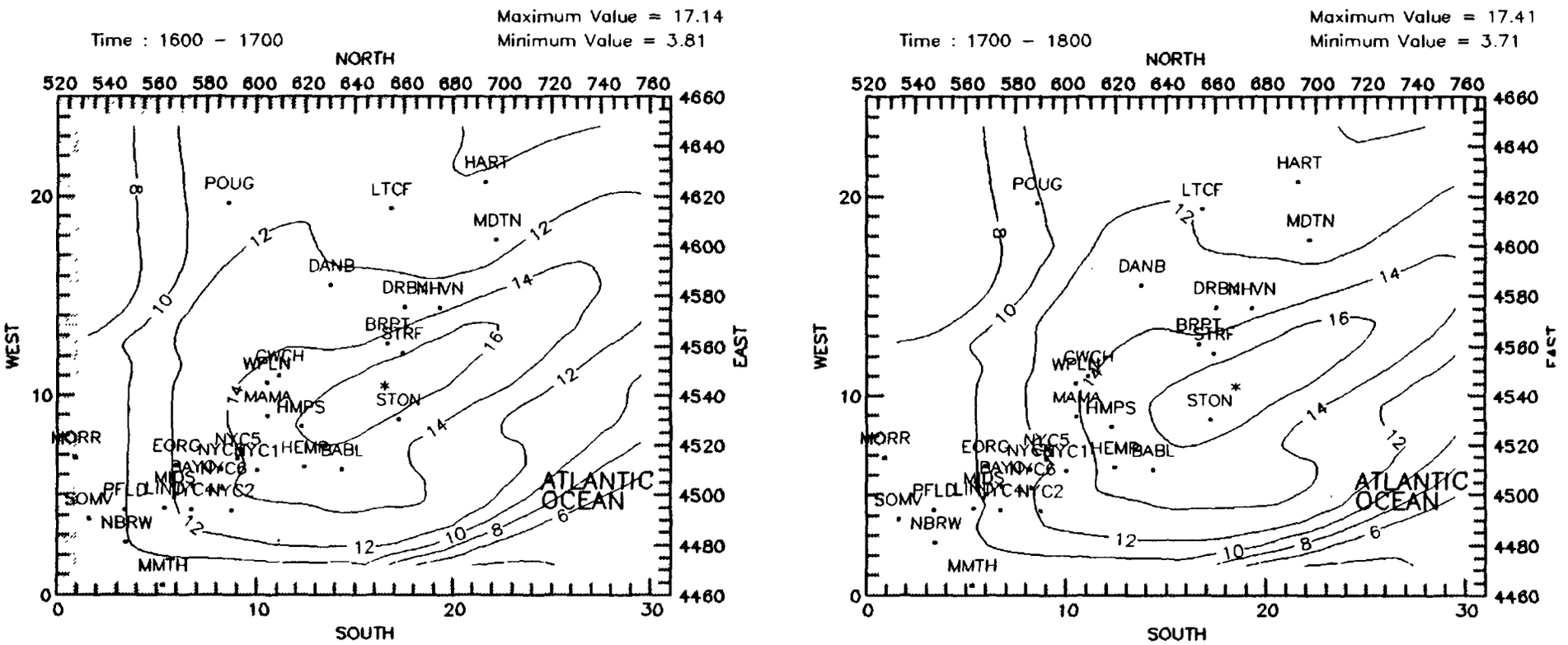

FIGURE D-1c. Ozone concentration Scenario 1, 8 August 1980 (pphm).

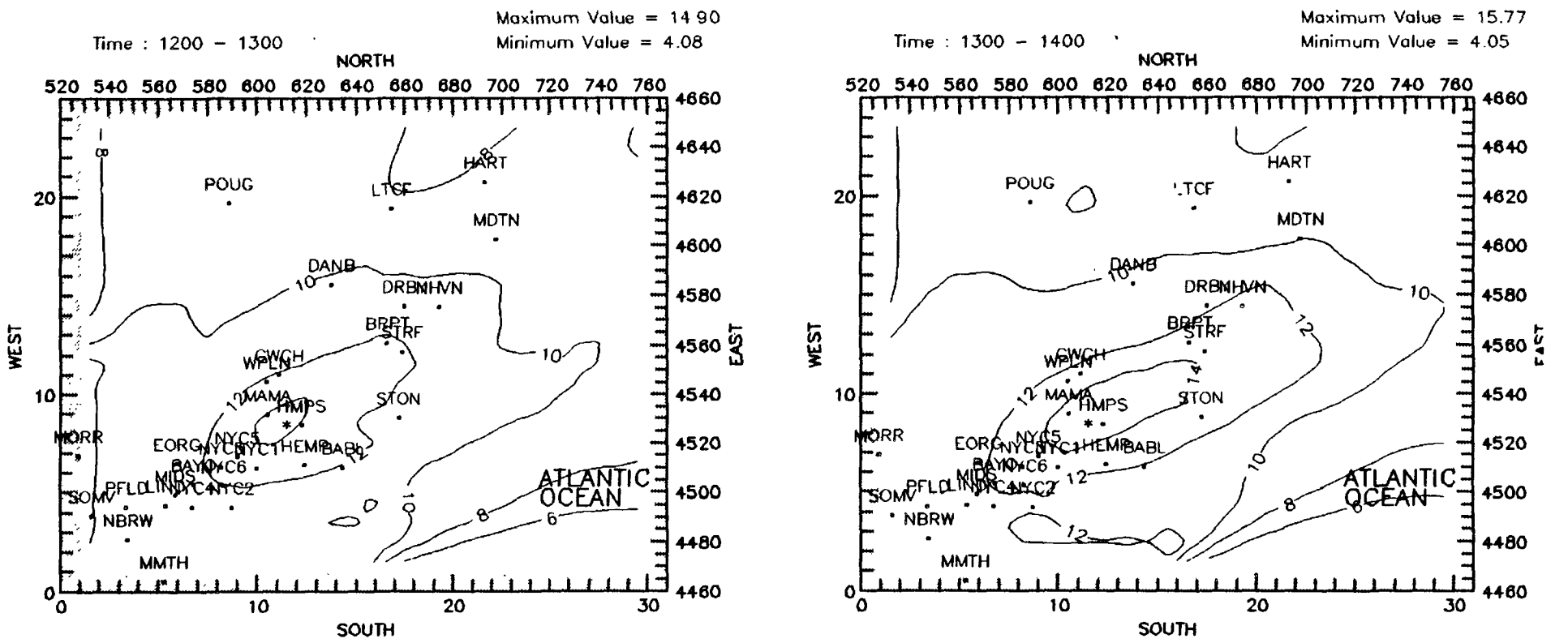

FIGURE D-2a. Ozone concentration Scenario 2, 8 August 1980 (pphm).

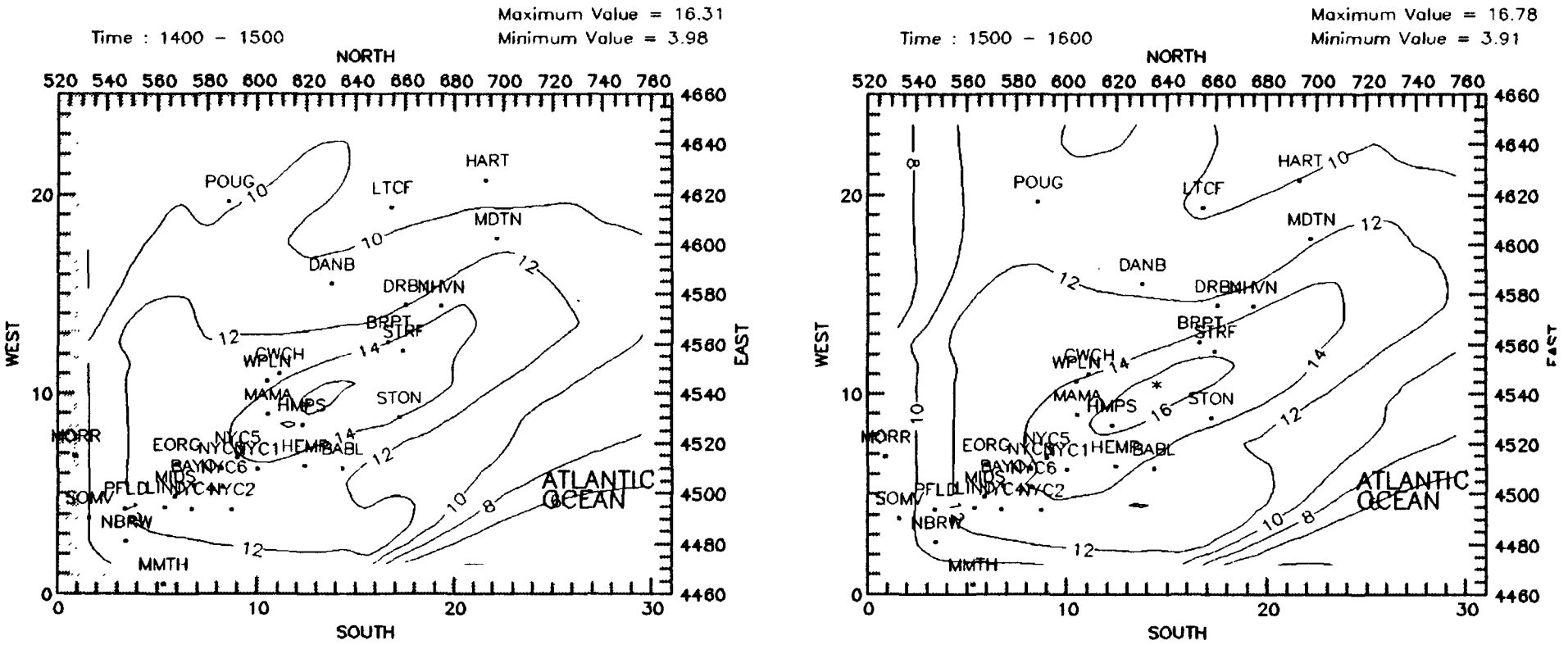

FIGURE D-2b. Ozone concentration Scenario 2, 8 August 1980 (pphm).

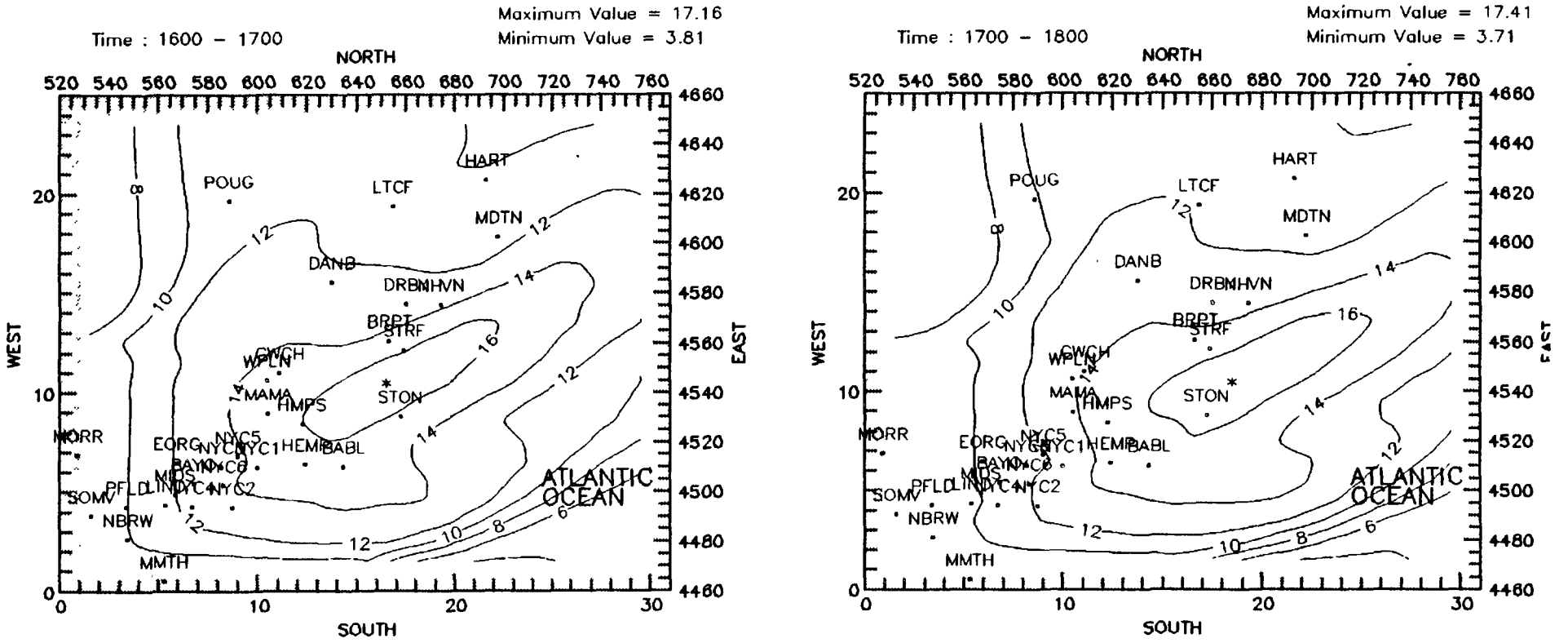

FIGURE D-2c. Ozone concentration Scenario 2, 8 August 1980 (pphm).

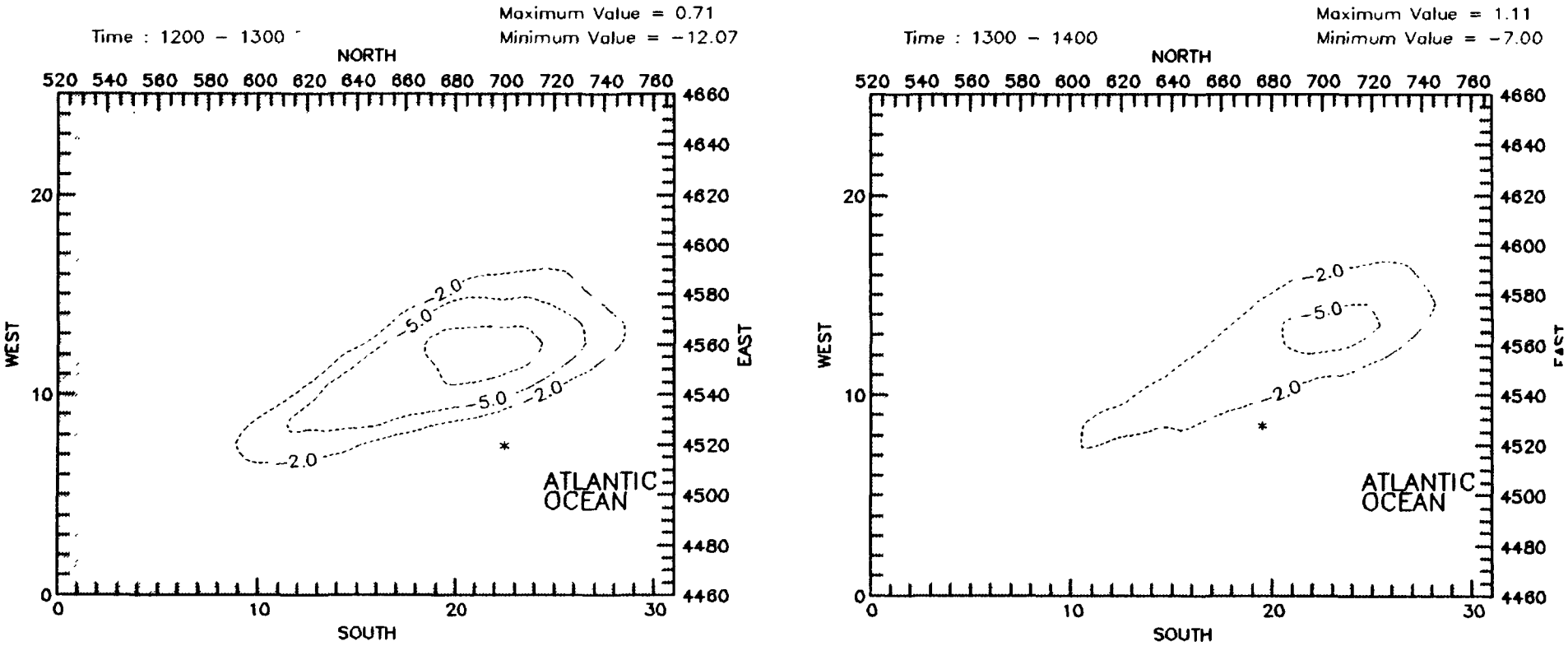

FIGURE D-3a. Ozone concentration difference between Scenario 1 and Scenario 2, 8 August 1980 (ppb).

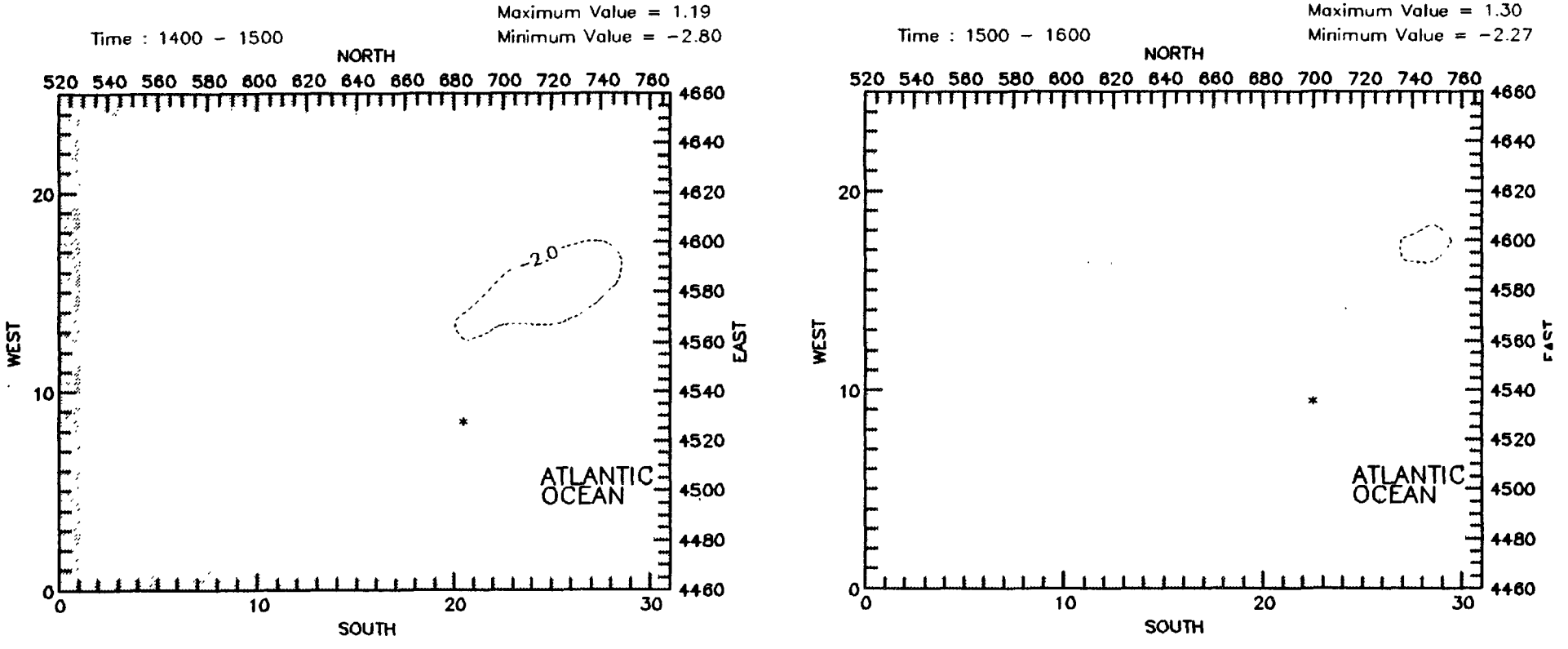

FIGURE D-3b. Ozone concentration difference between Scenario 1 and Scenario 2, 8 August 1980 (ppb).

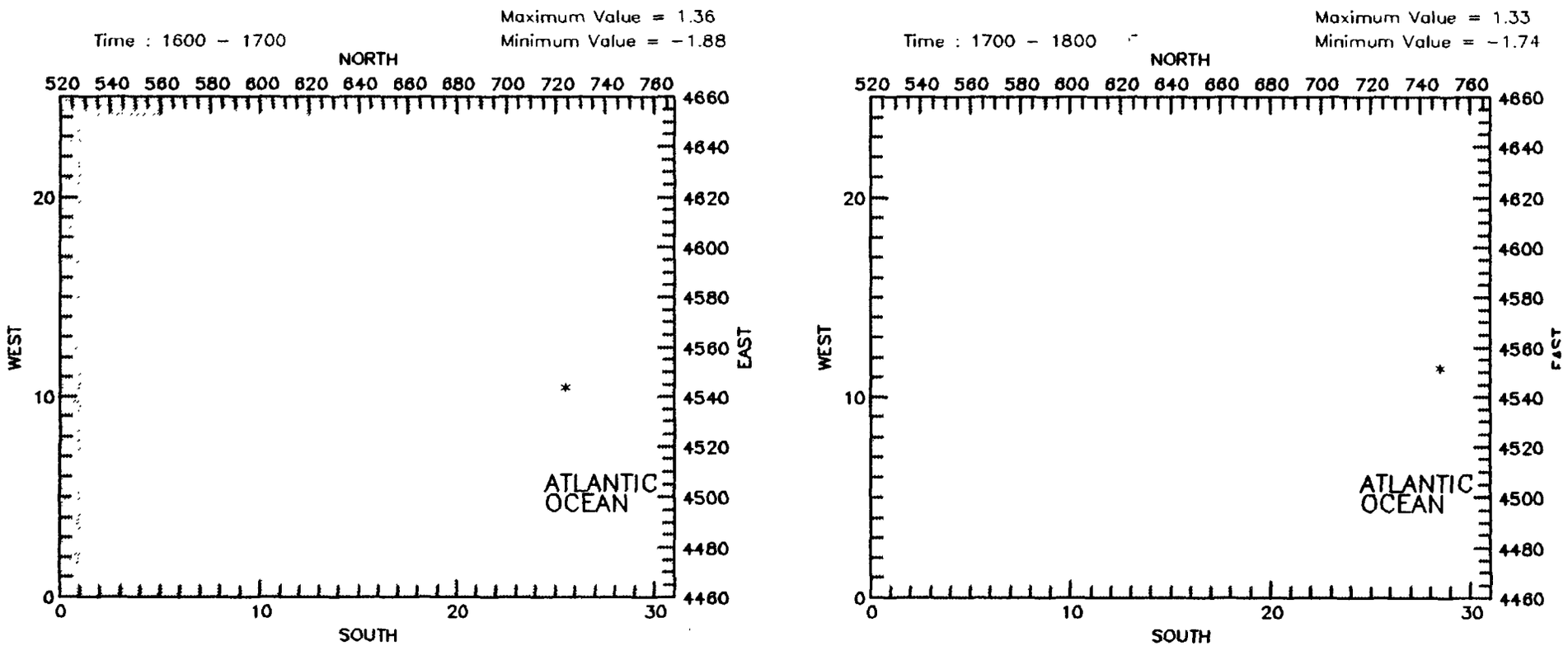

FIGURE D-3c. Ozone concentration difference between Scenario 1 and Scenario 2, 8 August 1980 (ppb).

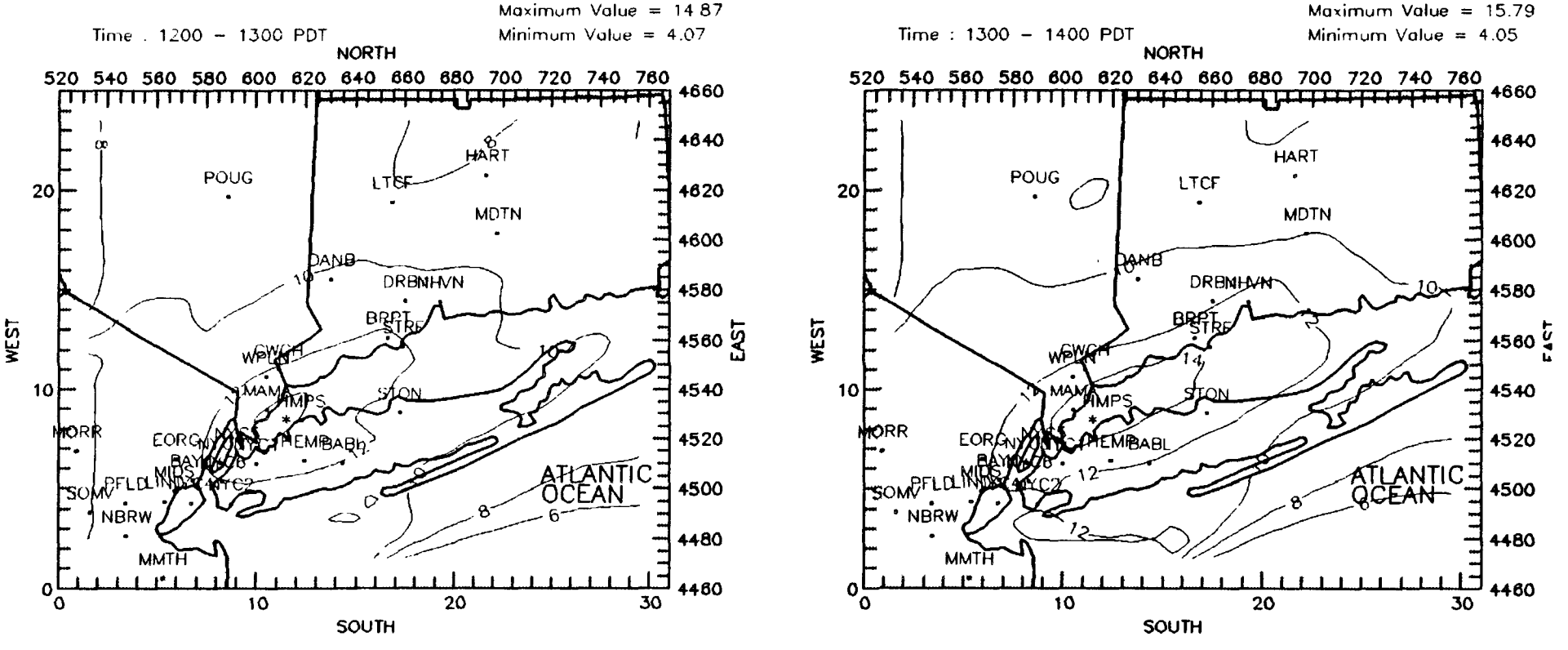

FIGURE D-4a. Ozone Concentration Scenario 3, Aug 8, 1980 (pphm).

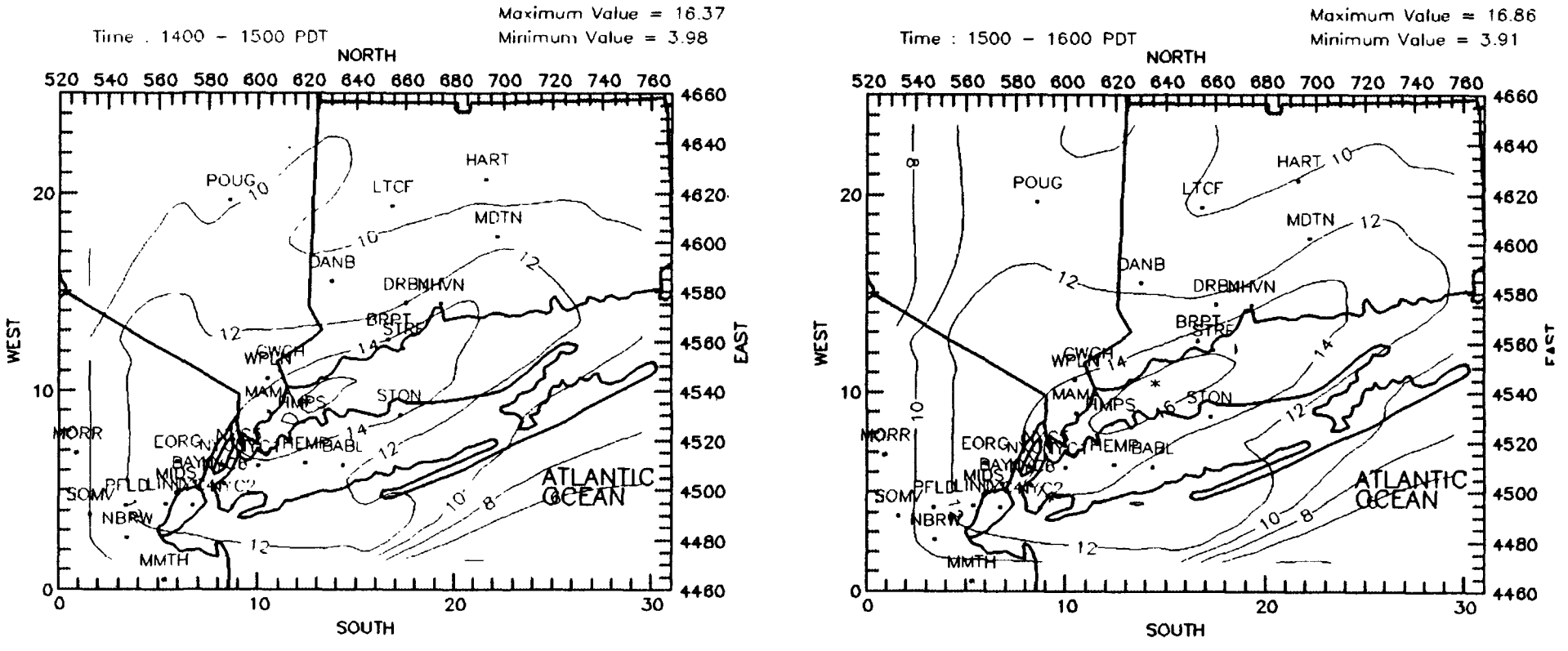

FIGURE D-4b. Ozone Concentration Scenario 3, Aug 8, 1980 (pphm).

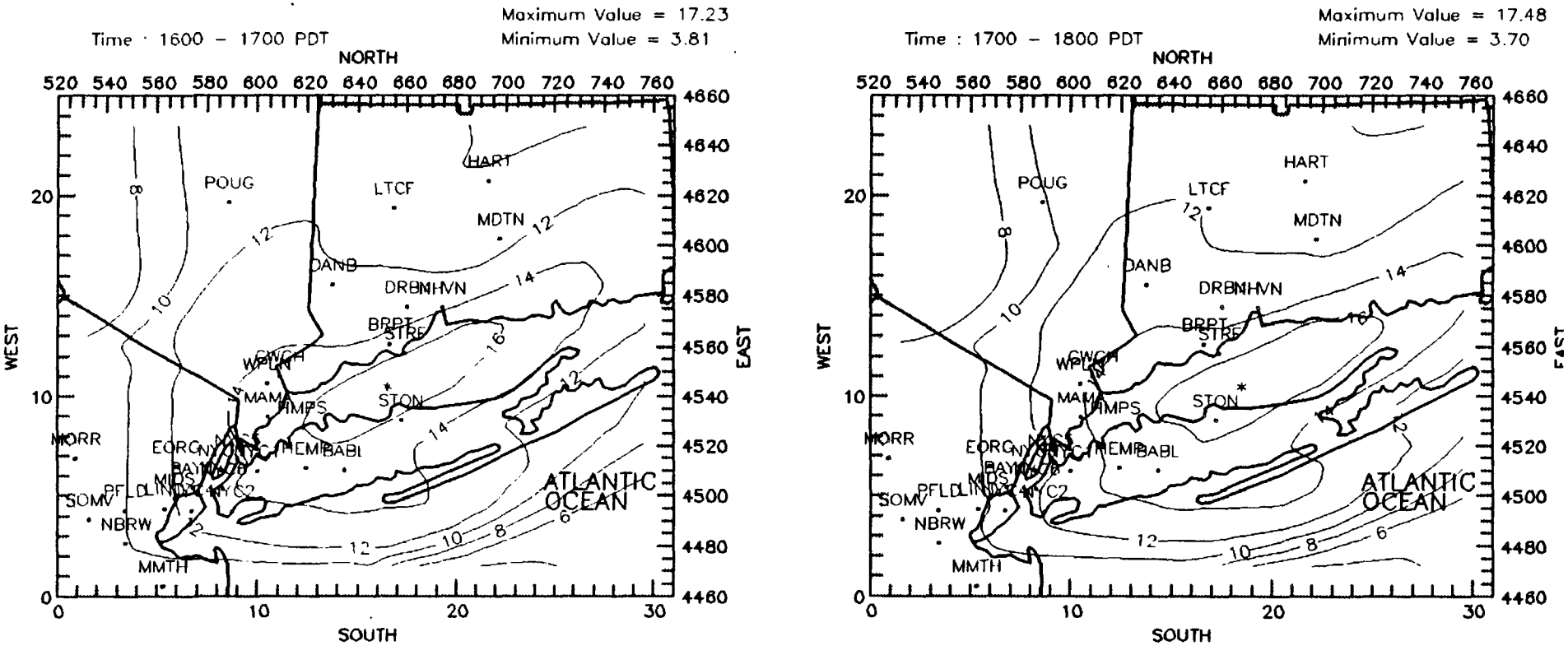

FIGURE D-4c. Ozone Concentration Scenario 3, Aug 8, 1980 (pphm).

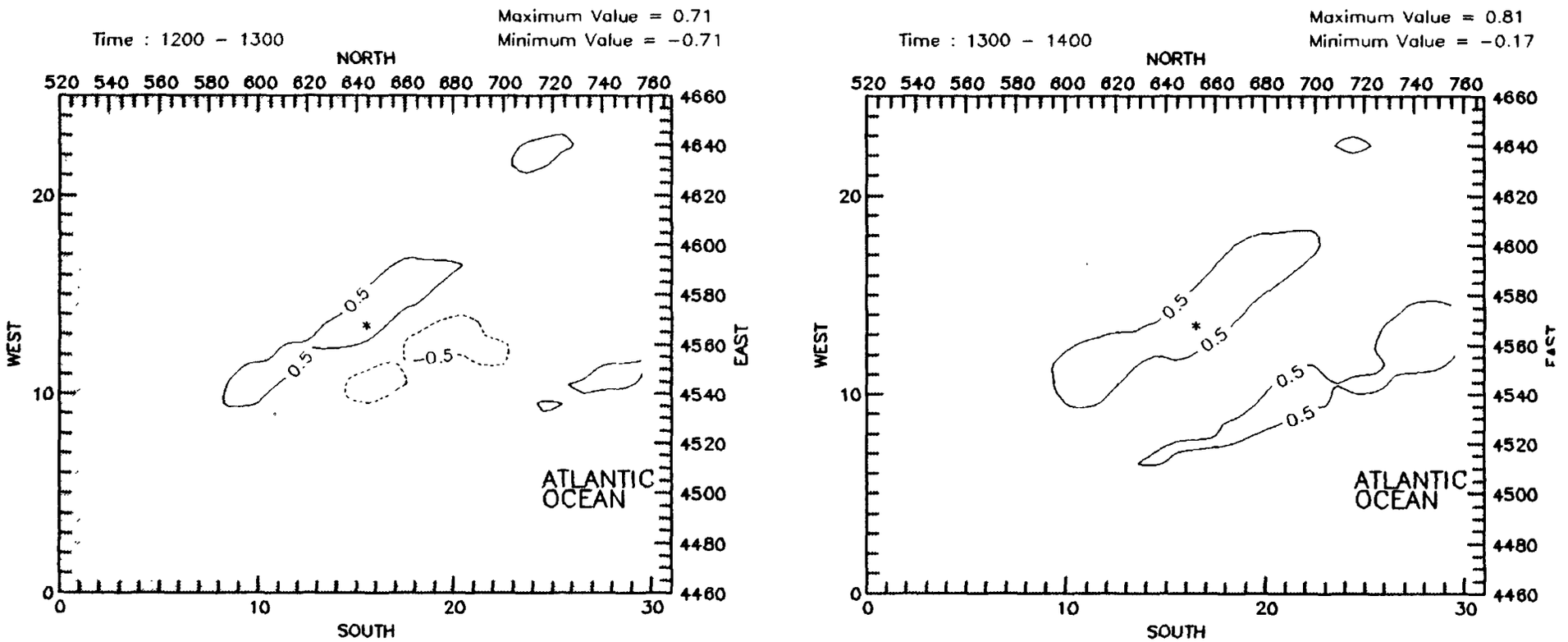

FIGURE D-5a. Ozone concentration difference between Scenario 2 and Scenario 3, 8 August 1980 (ppb).

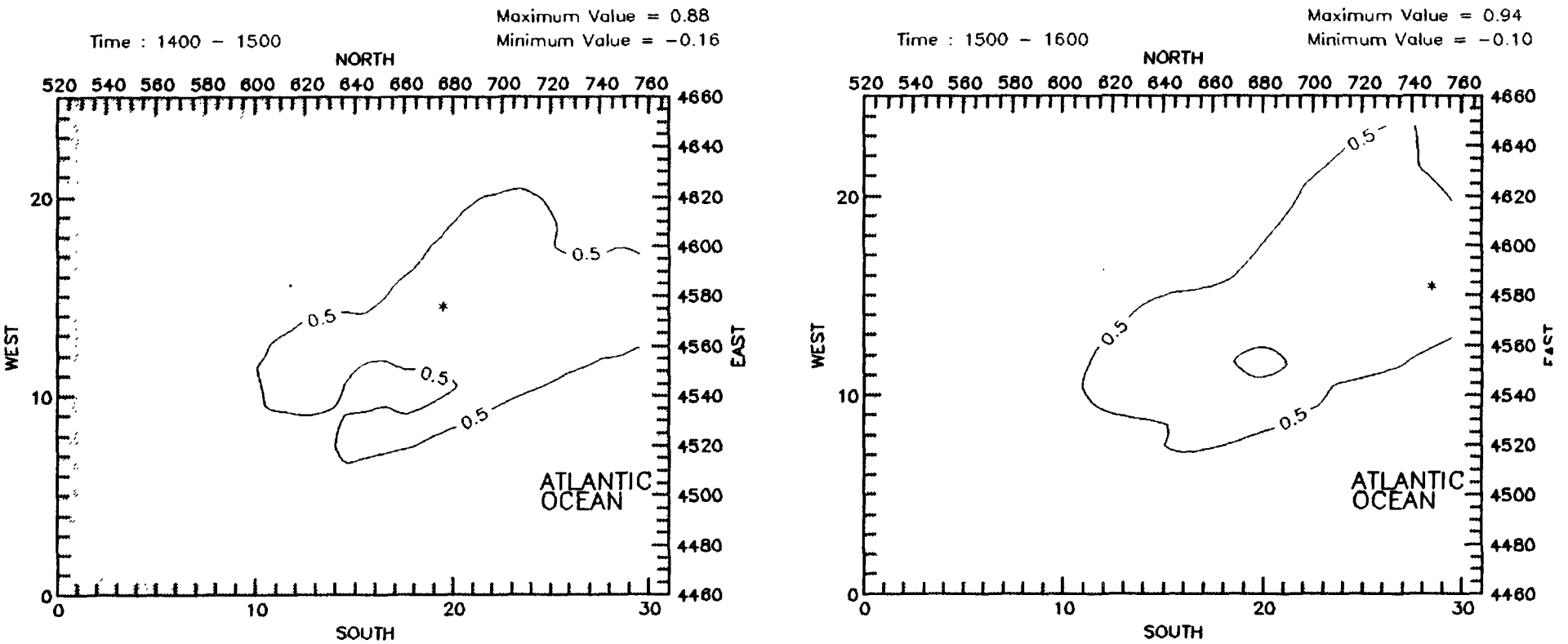

FIGURE D-5b. Ozone concentration difference between Scenario 2 and Scenario 3, 8 August 1980 (ppb).

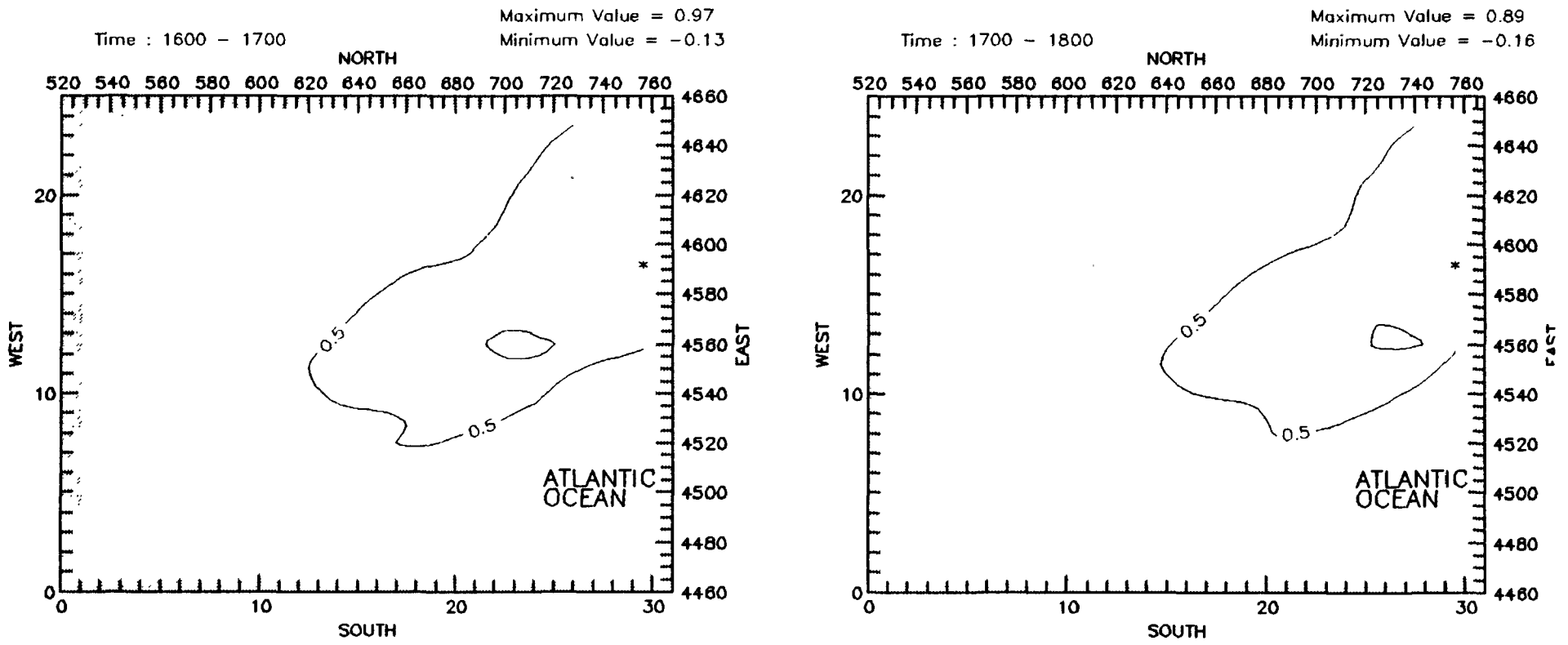

FIGURE D-5c. Ozone concentration difference between Scenario 2 and Scenario 3, 8 August 1980 (ppb).

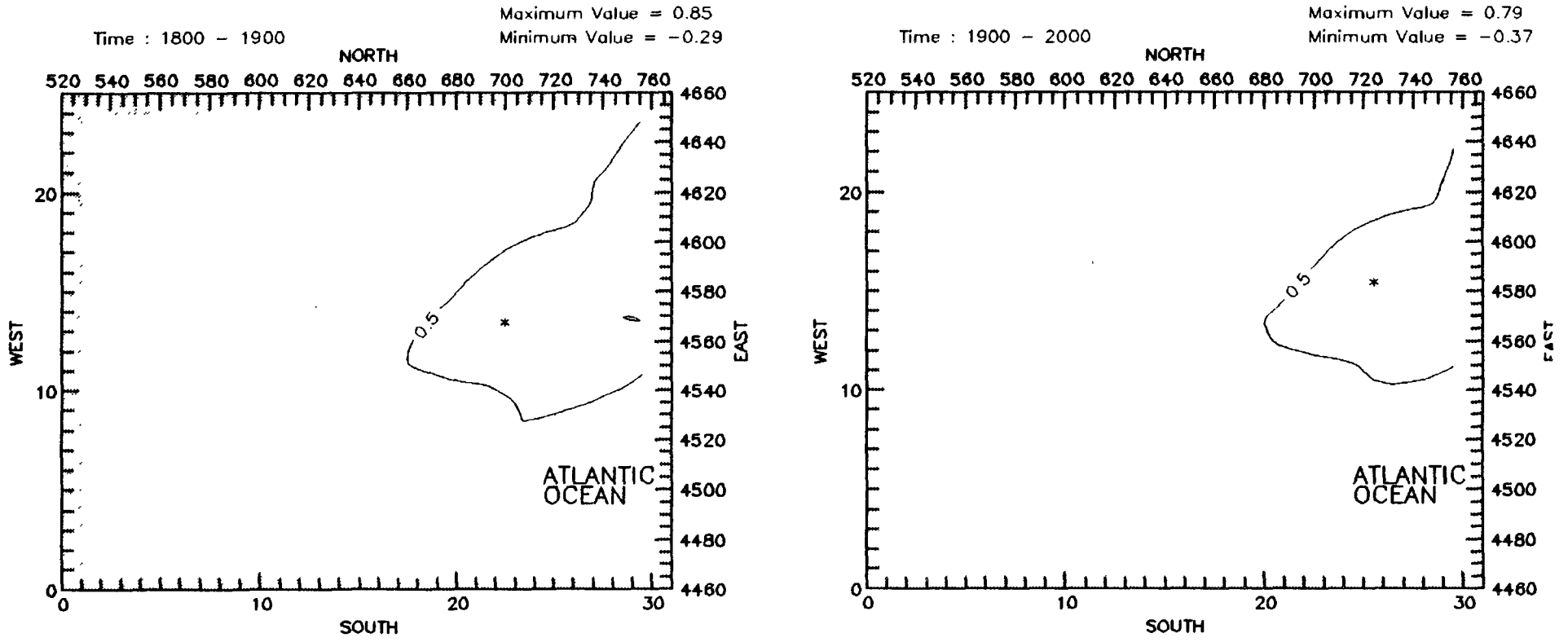

FIGURE D-5d. Ozone concentration difference between Scenario 2 and Scenario 3, 8 August 1980 (ppb).

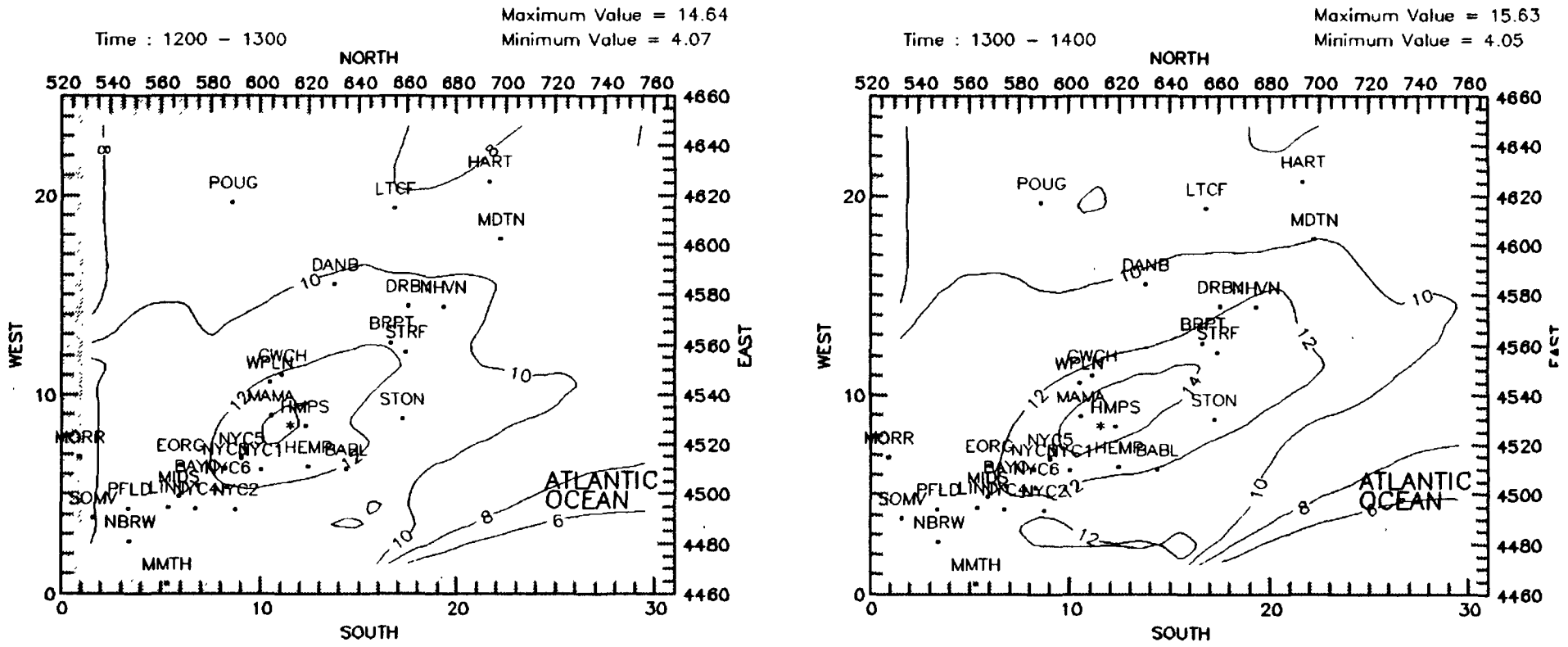

FIGURE D-6a. Ozone concentration Scenario 4, 8 August 1980 (pphm).

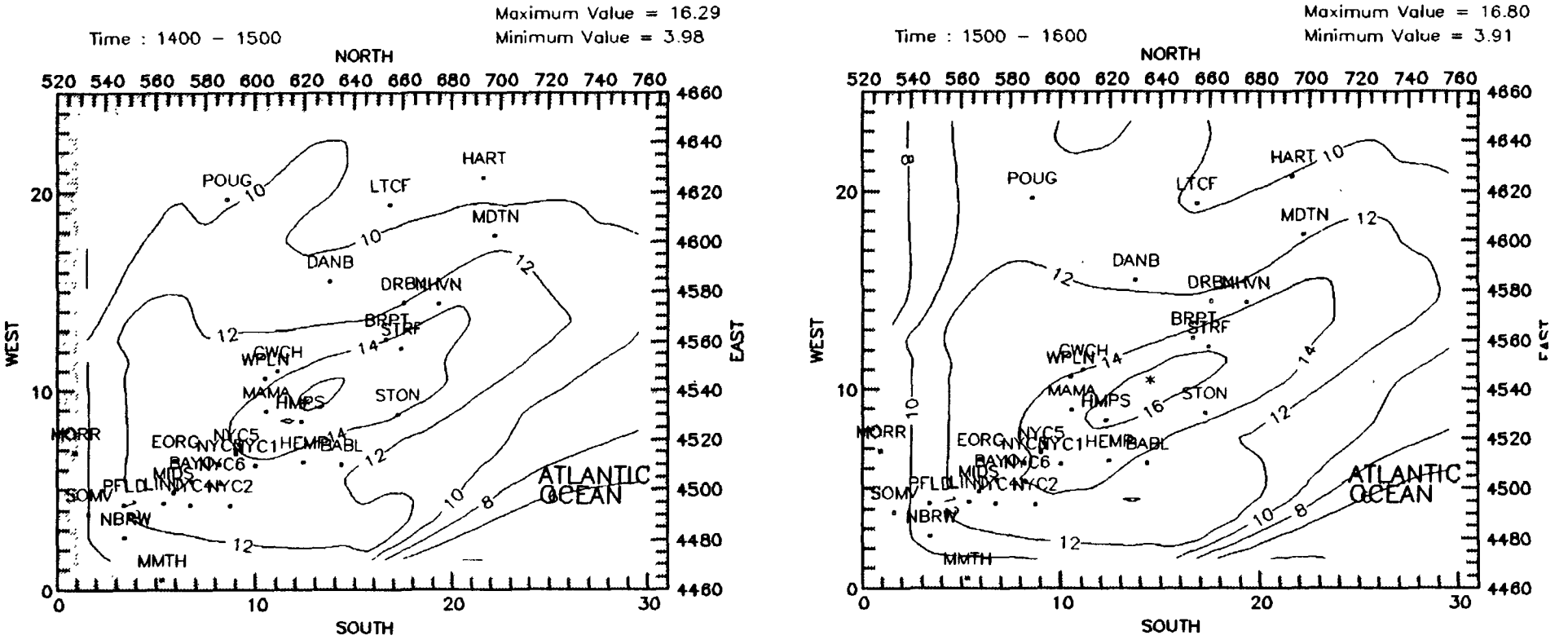

FIGURE D-6b. Ozone concentration Scenario 4, 8 August 1980 (pphm).

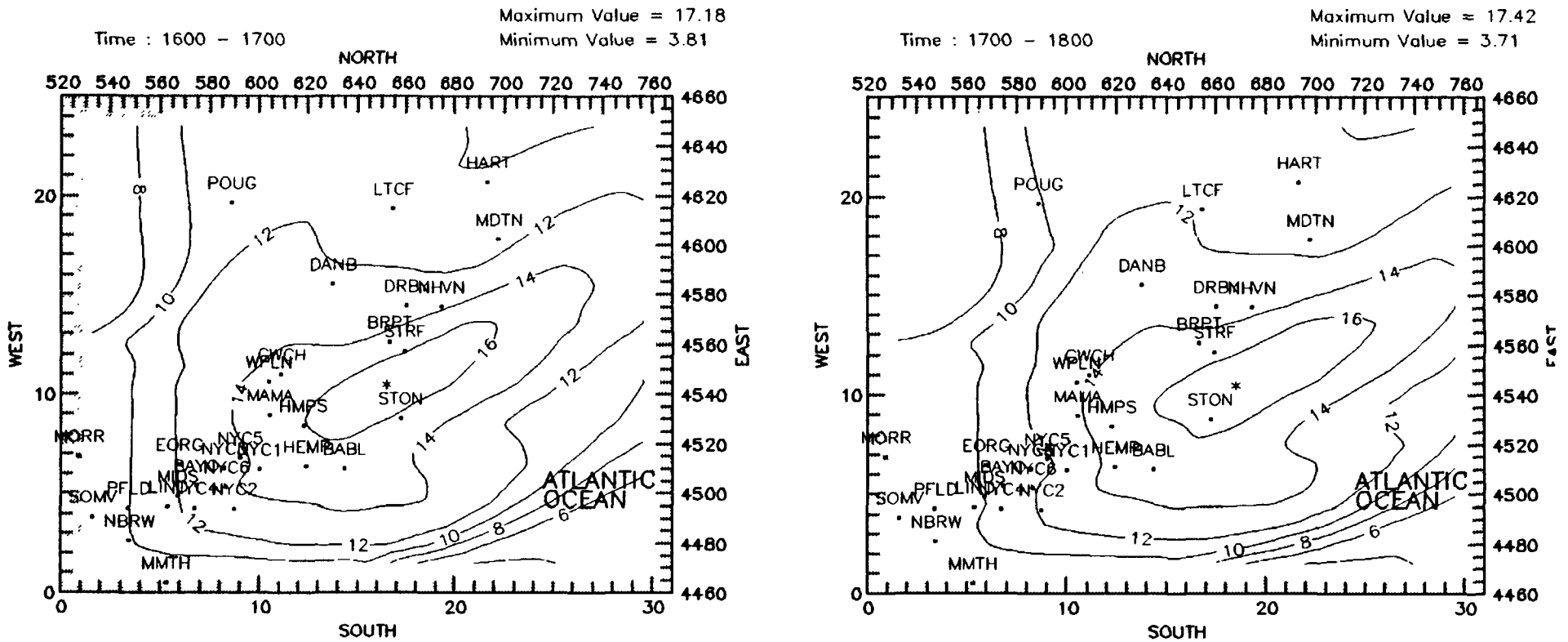

FIGURE D-6c. Ozone concentration Scenario 4, 8 August 1980 (pphm).

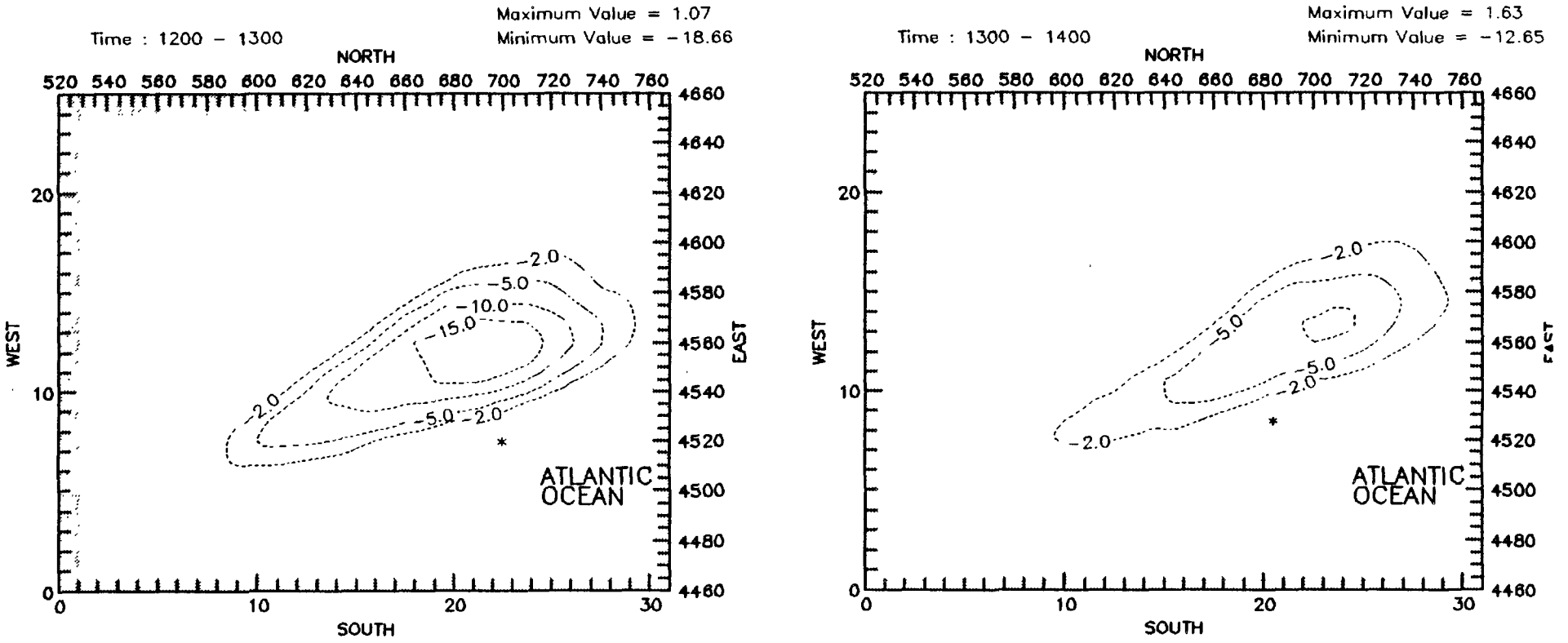

FIGURE D-7a. Ozone concentration difference between Scenario 1 and Scenario 4, 8 August 1980 (ppb).

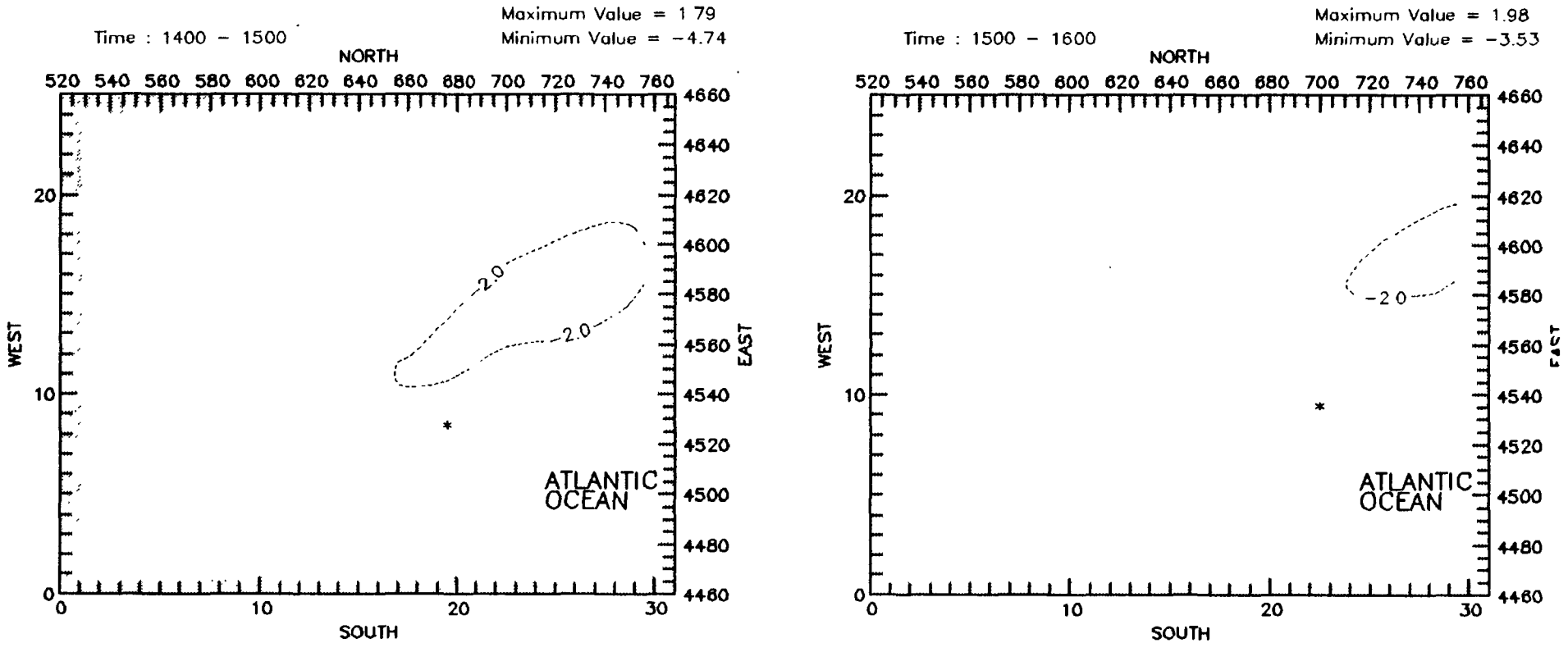

FIGURE D-7b. Ozone concentration difference between Scenario 1 and Scenario 4, 8 August 1980 (ppb).

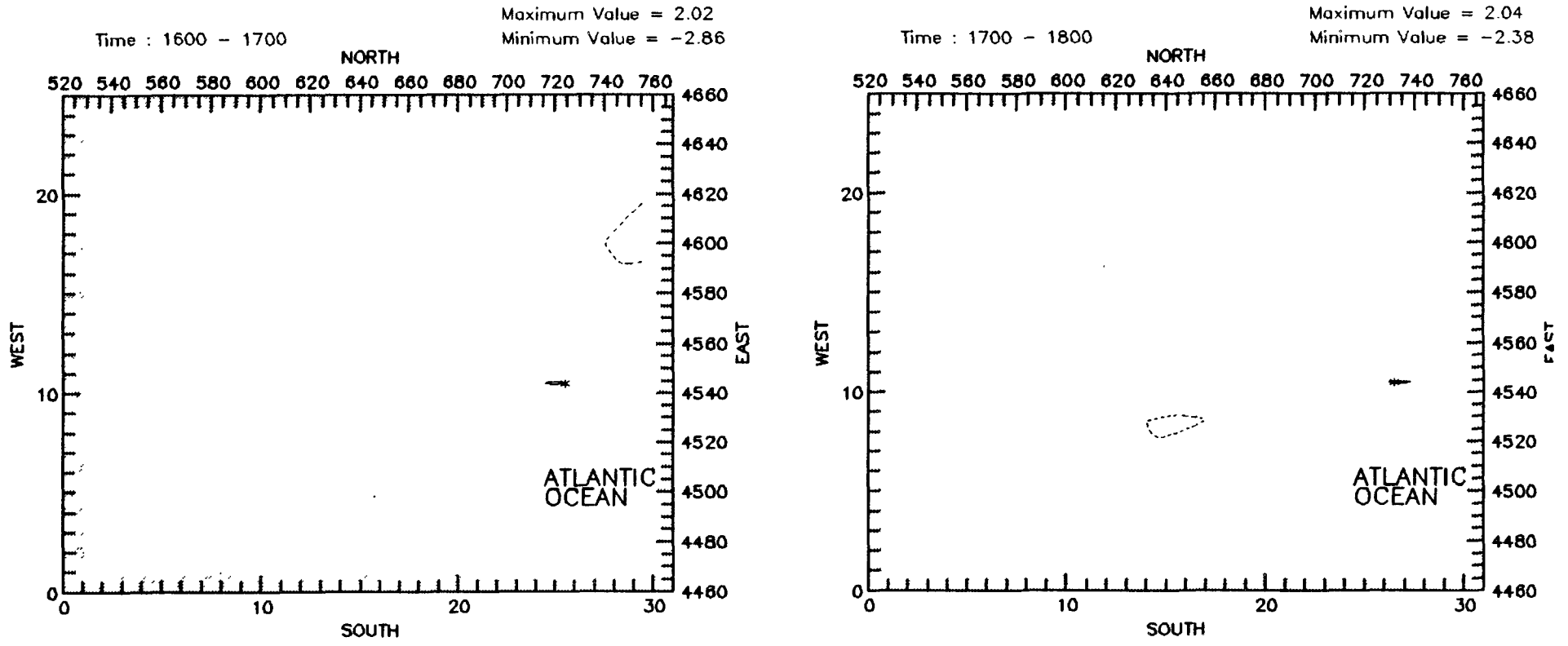

FIGURE D-7c. Ozone concentration difference between Scenario 1 and Scenario 4, 8 August 1980 (ppb).

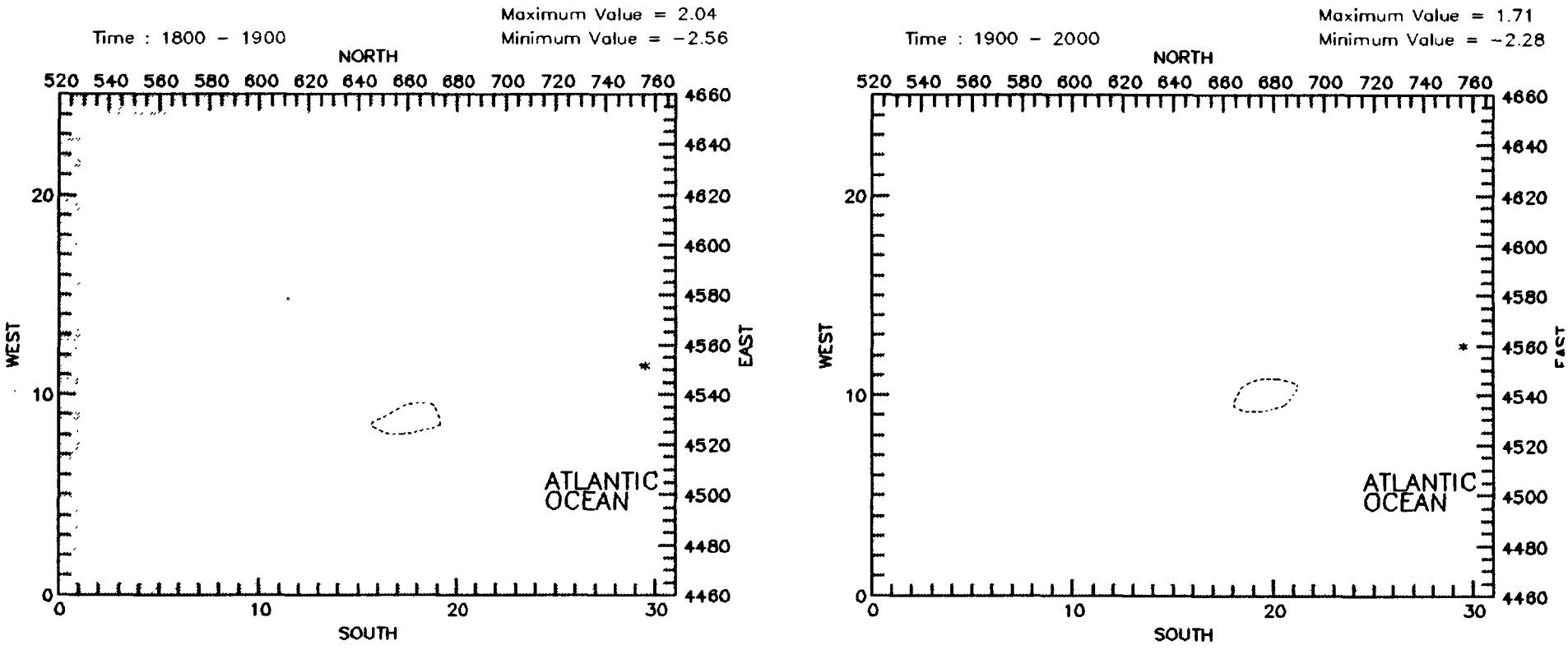

FIGURE D-7d. Ozone concentration difference between Scenario 1 and Scenario 4, 8 August 1980 (ppb).

Appendix E

ISOPLETHS OF HOURLY OZONE CONCENTRATIONS (PPHM)
AND HOURLY OZONE CONCENTRATION DIFFERENCES (PPB)
BETWEEN SCENARIOS FOR THE ST. LOUIS APPLICATION OF THE
UAM ON THE AFTERNOON OF 13 JULY 1976

FIGURE E-1: Scenario 1
FIGURE E-2: Scenario 2
FIGURE E-3: Differences between Scenario 1 and Scenario 2
FIGURE E-4: Scenario 5
FIGURE E-5: Scenario 6
FIGURE E-6: Differences between Scenario 2 and Scenario 5
FIGURE E-7: Differences between Scenario 2 and Scenario 6
FIGURE E-8: Scenario 7
FIGURE E-9: Differences between Scenario 1 and Scenario 8
FIGURE E-10: SIP Scenario A
FIGURE E-11: SIP Scenario B
FIGURE E-12: Differences between Scenario 1 and SIP Scenario A
FIGURE E-13: Differences between Scenario 1 and SIP Scenario B

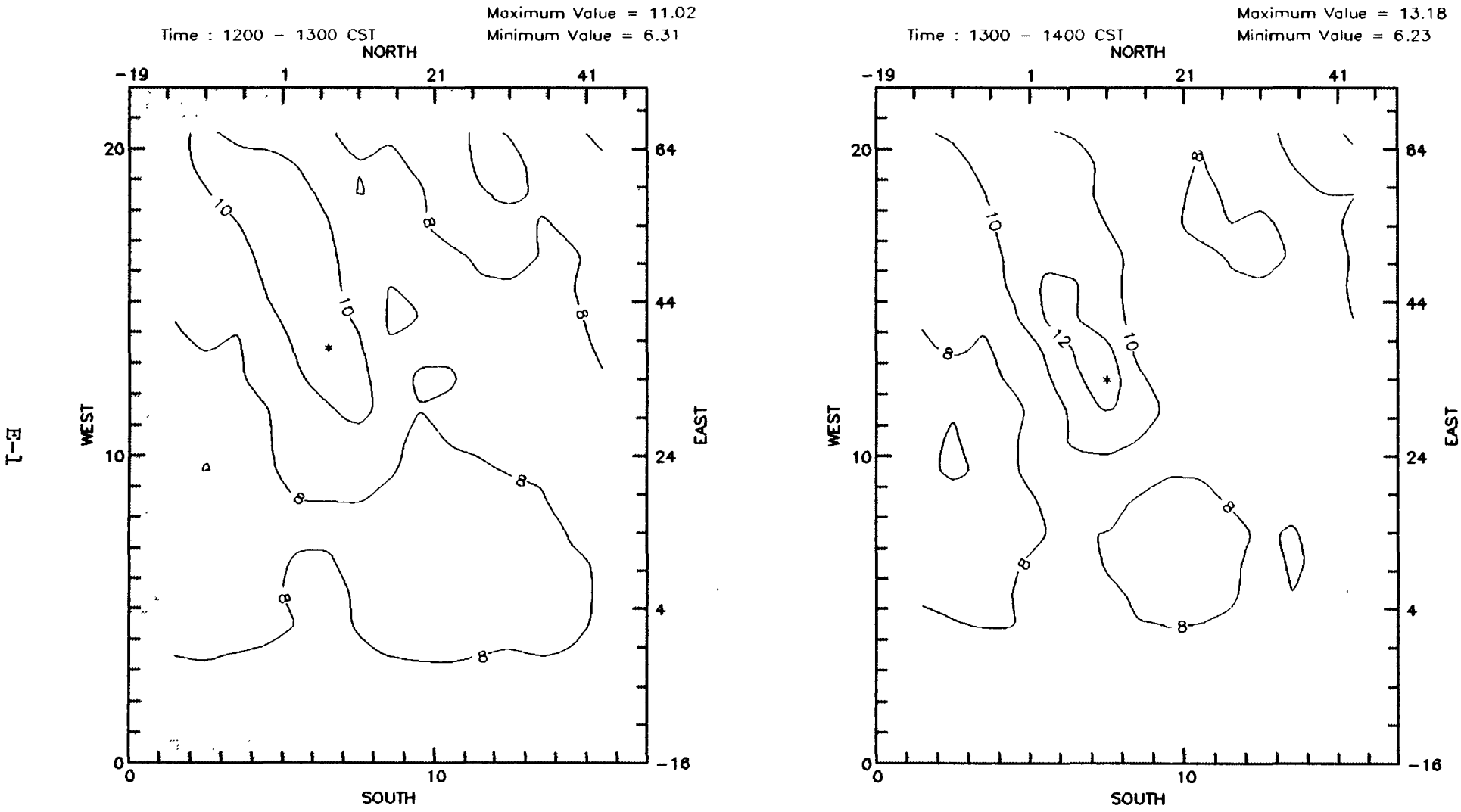

FIGURE E-1a. Ozone concentration Scenario 1, 13 July 1976 (pphm).

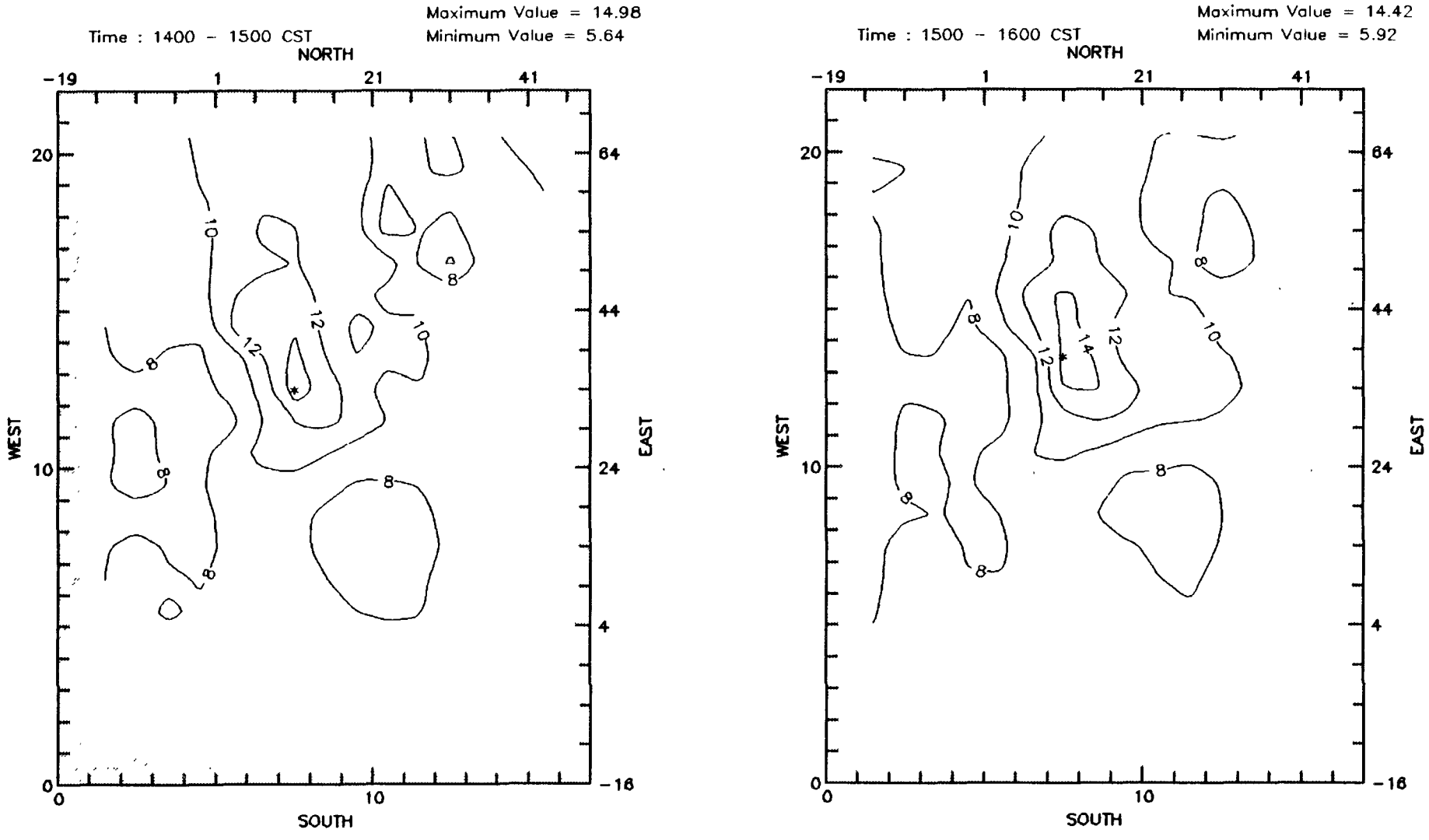

FIGURE E-1b. Ozone concentration Scenario 1, 13 July 1976 (pphm).

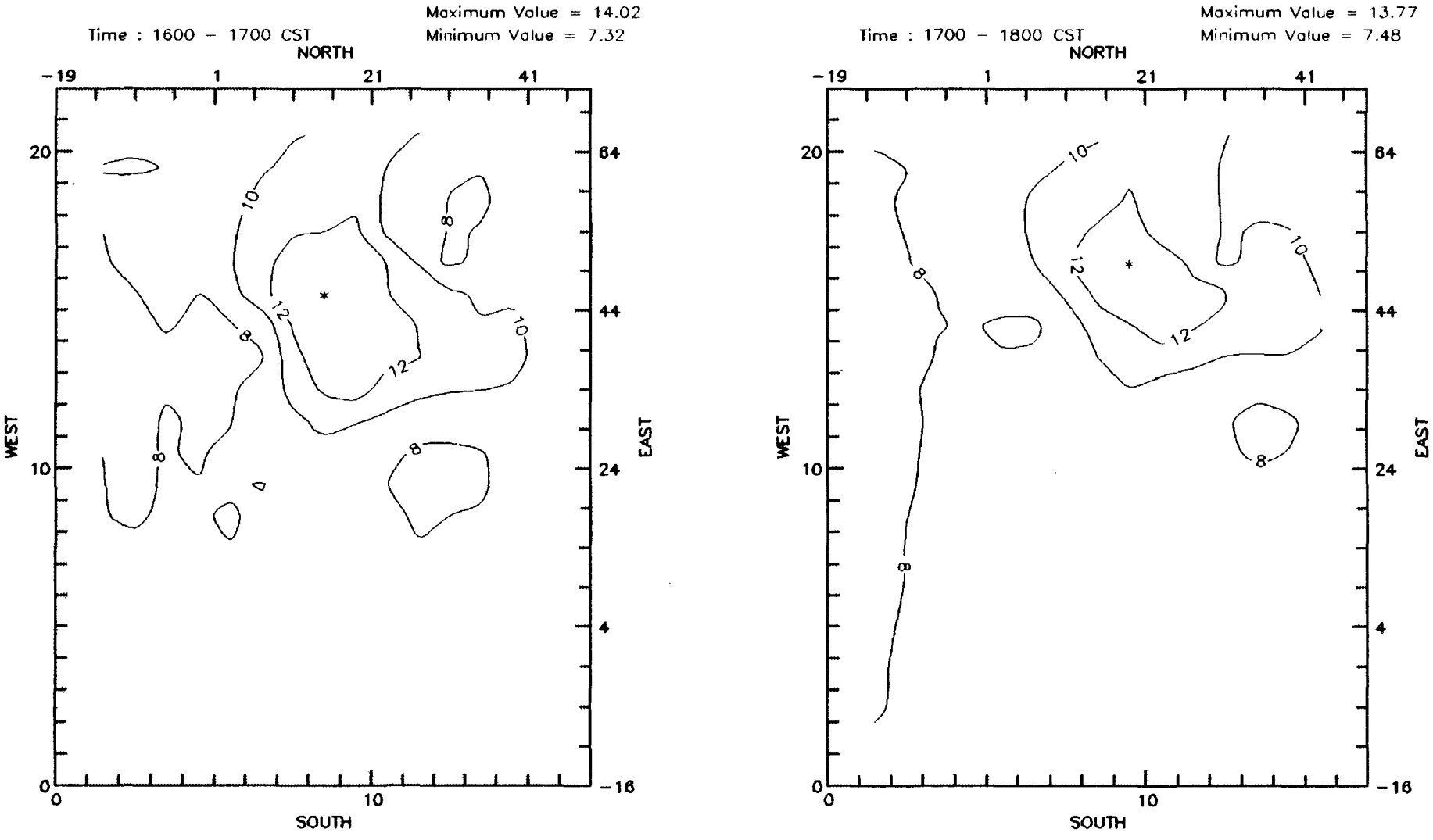

FIGURE E-1c. Ozone concentration Scenario 1, 13 July 1976 (pphm).

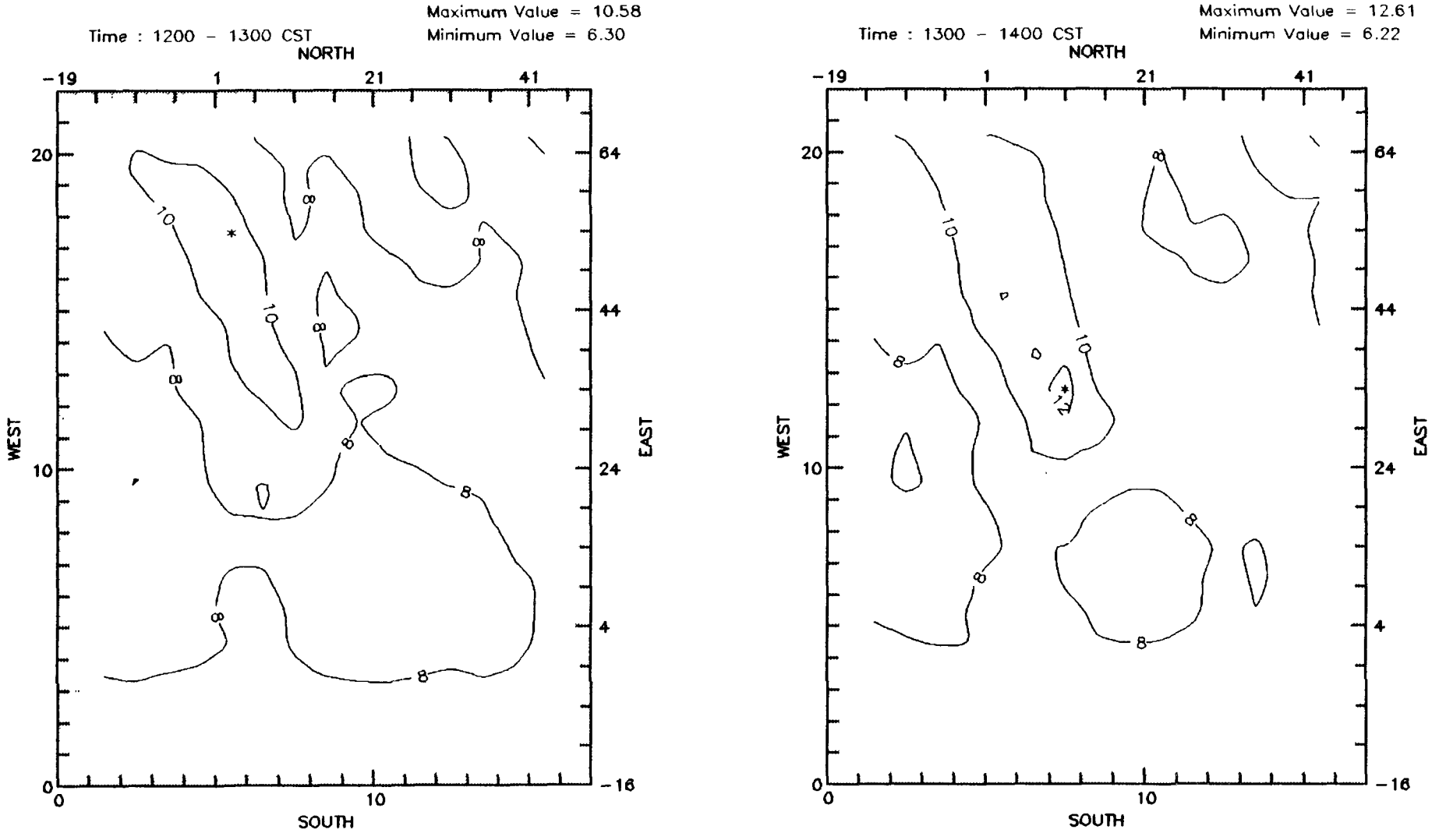

FIGURE E-2a. Ozone concentration Scenario 2, 13 July 1976 (pphm).

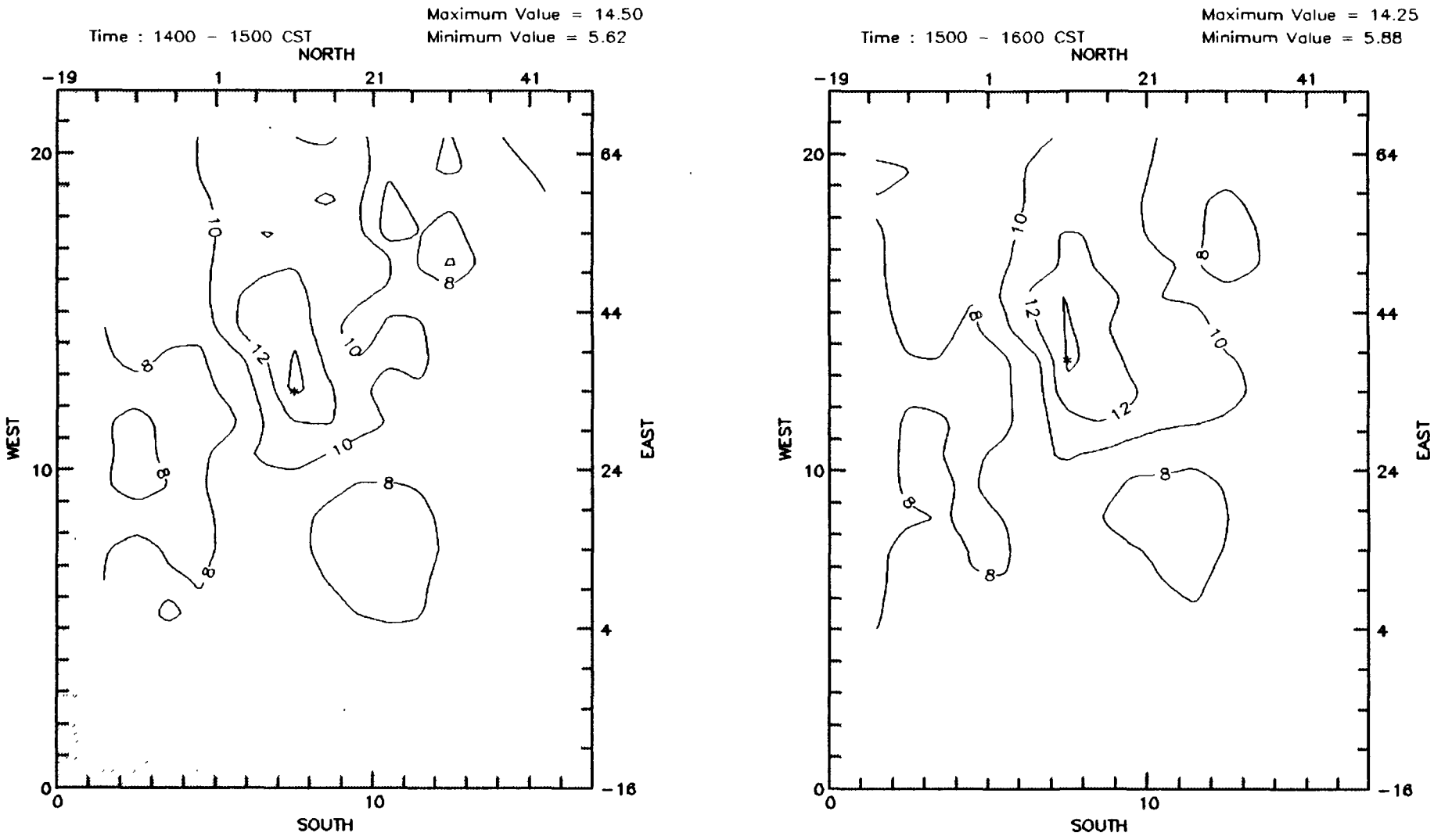

FIGURE E-2b. Ozone concentration Scenario 2, 13 July 1976 (pphm).

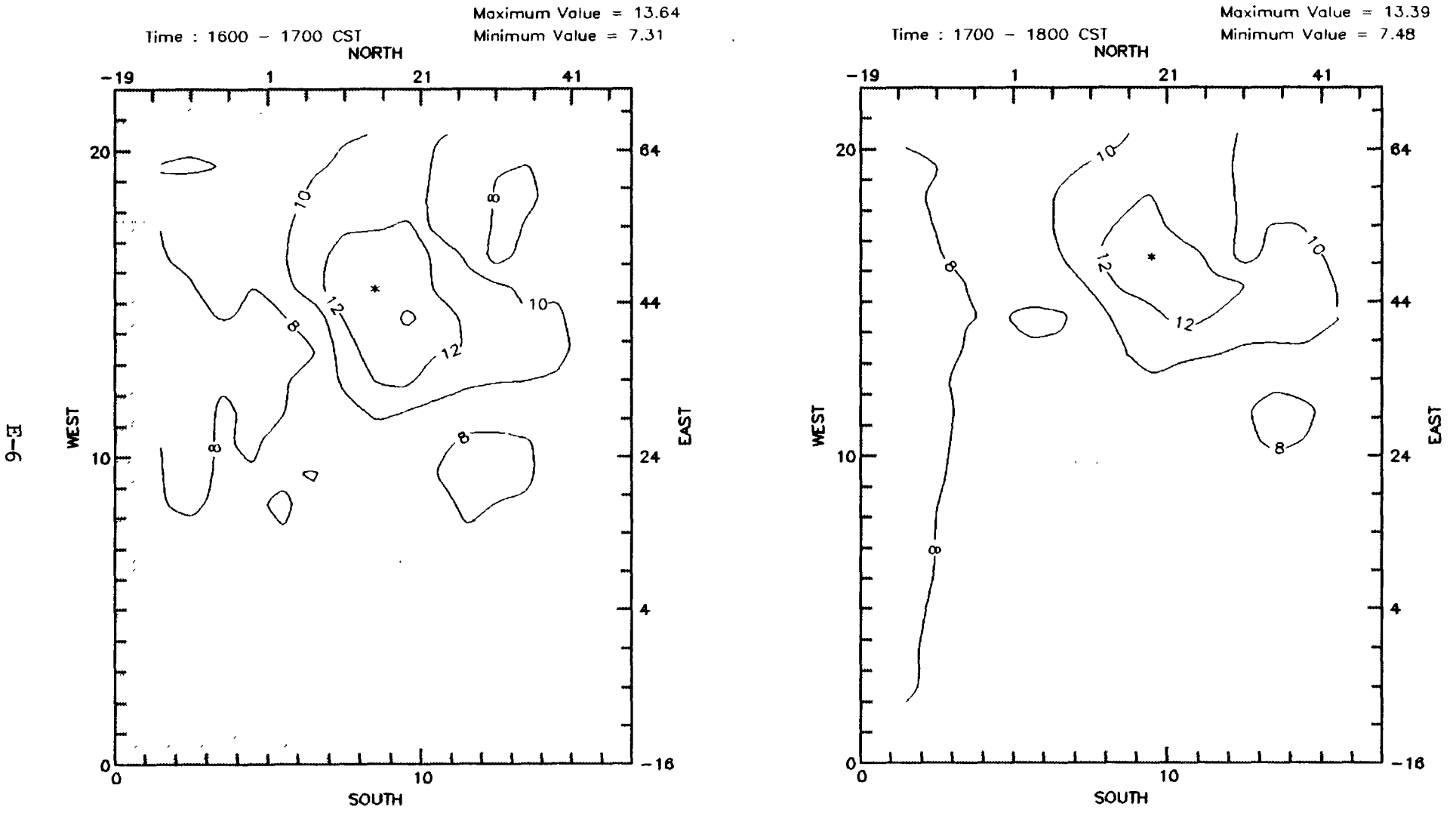

FIGURE E-2c. Ozone concentration Scenario 2, 13 July 1976 (pphm).

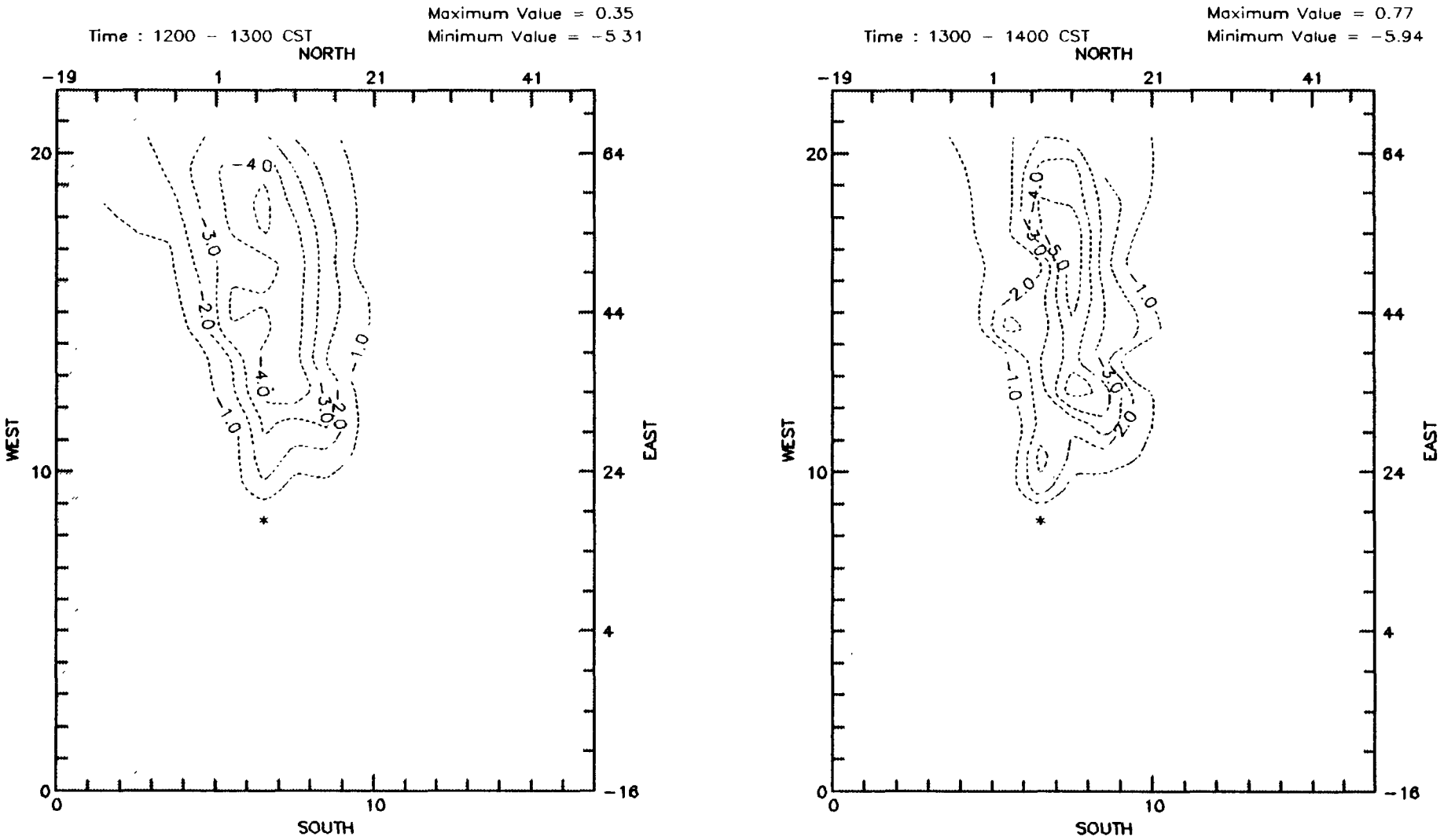

FIGURE E-3a. Ozone concentration difference between Scenario 1 and Scenario 2, 13 July 1976 (ppb).

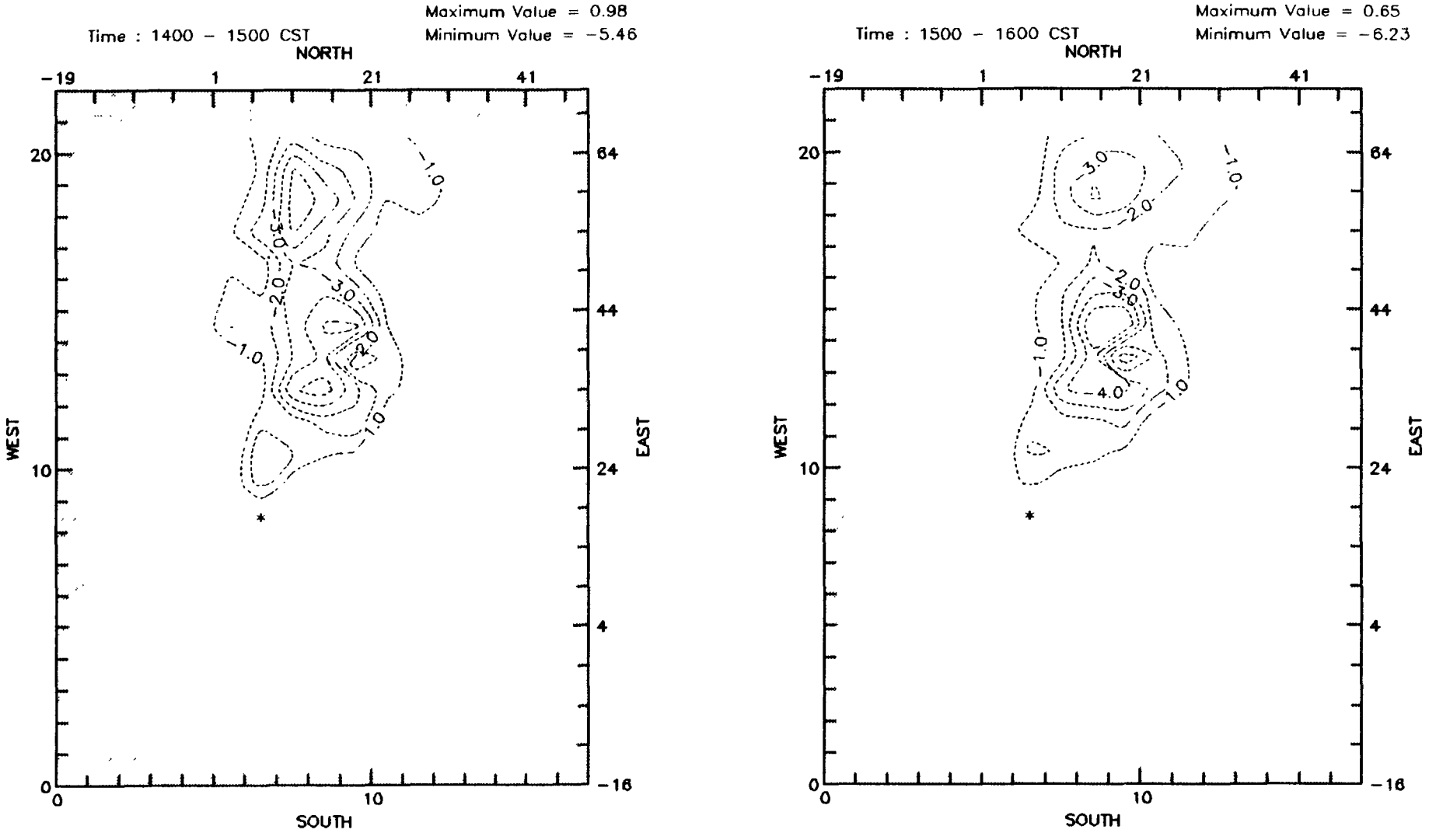

FIGURE E-3b. Ozone concentration difference between Scenario 1 and Scenario 2, 13 July 1976 (ppb).

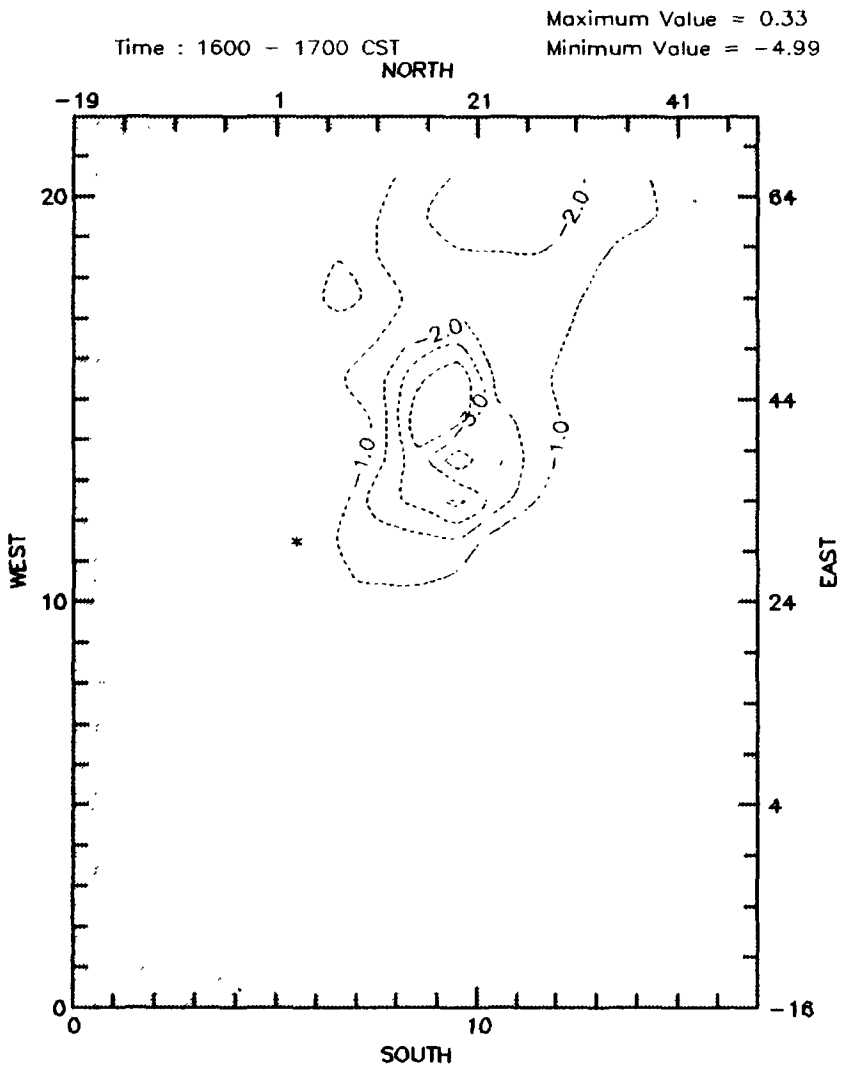

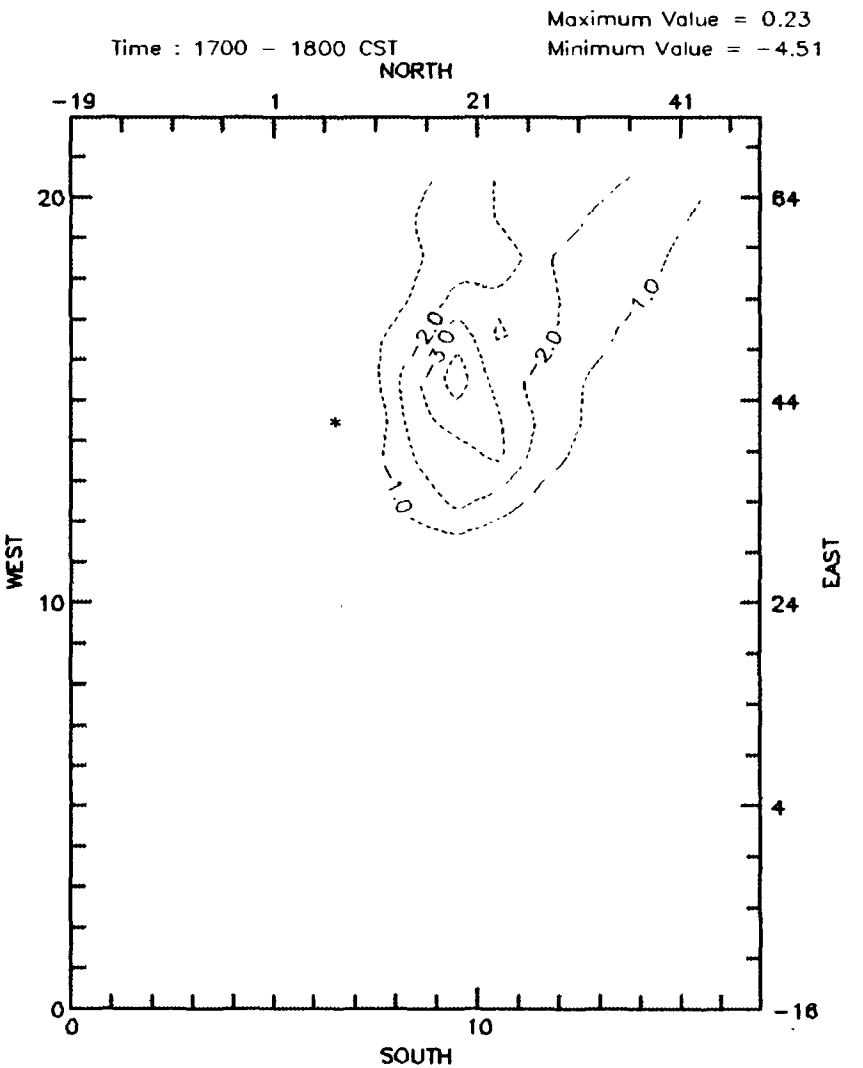

FIGURE E-3c. Ozone concentration difference between Scenario 1 and Scenario 2, 13 July 1976 (ppb).

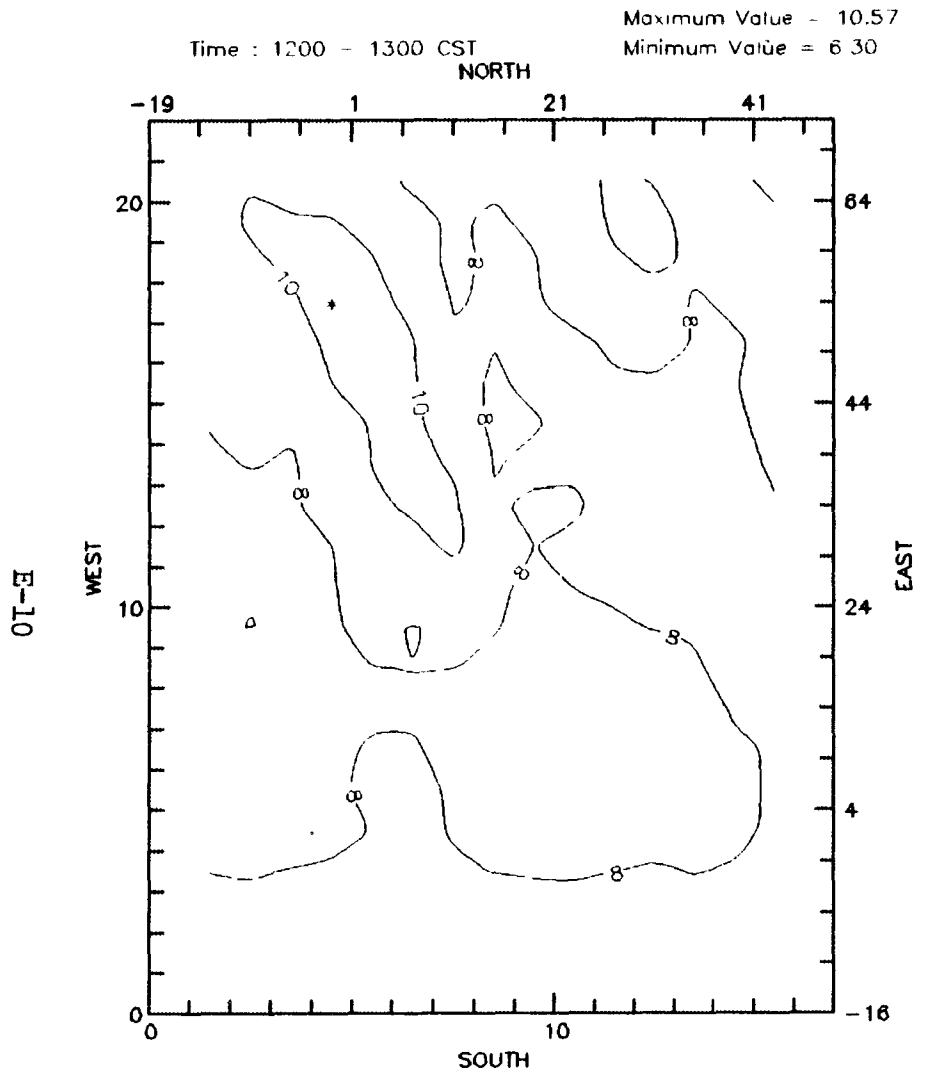

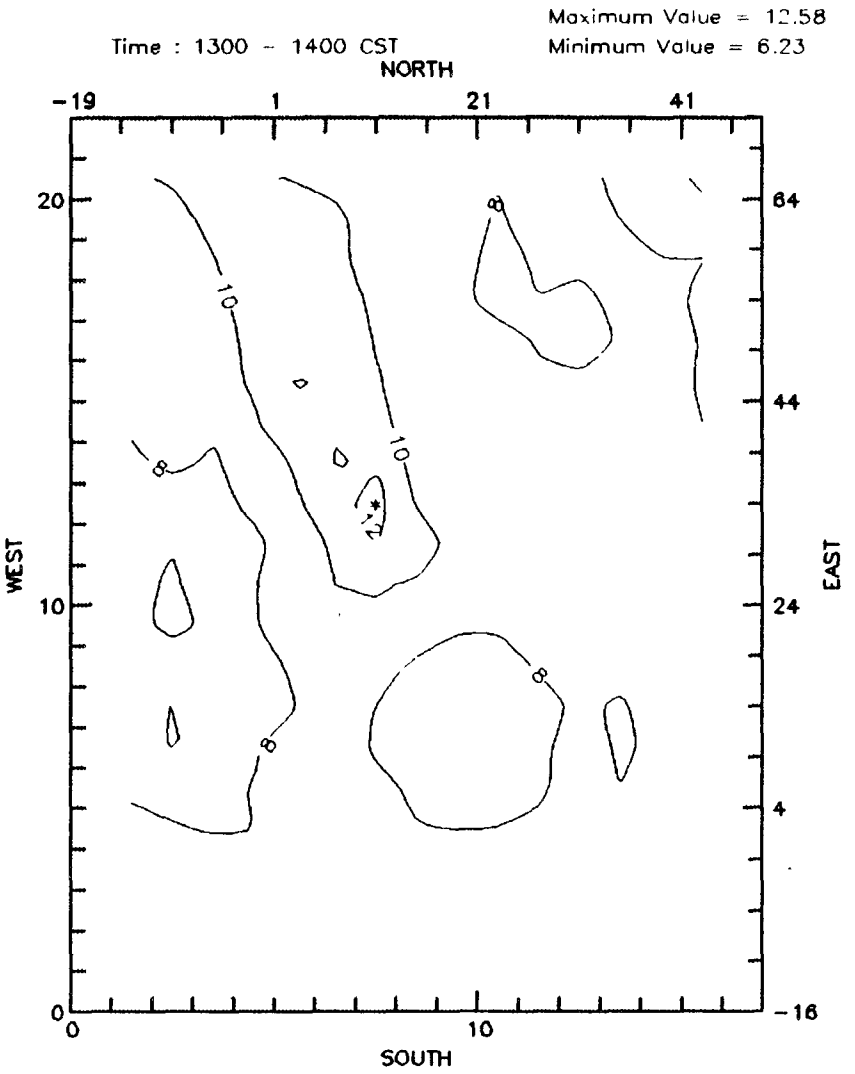

FIGURE E-4a. Ozone Concentration Scenario 5, July 13,1976 (pphm)

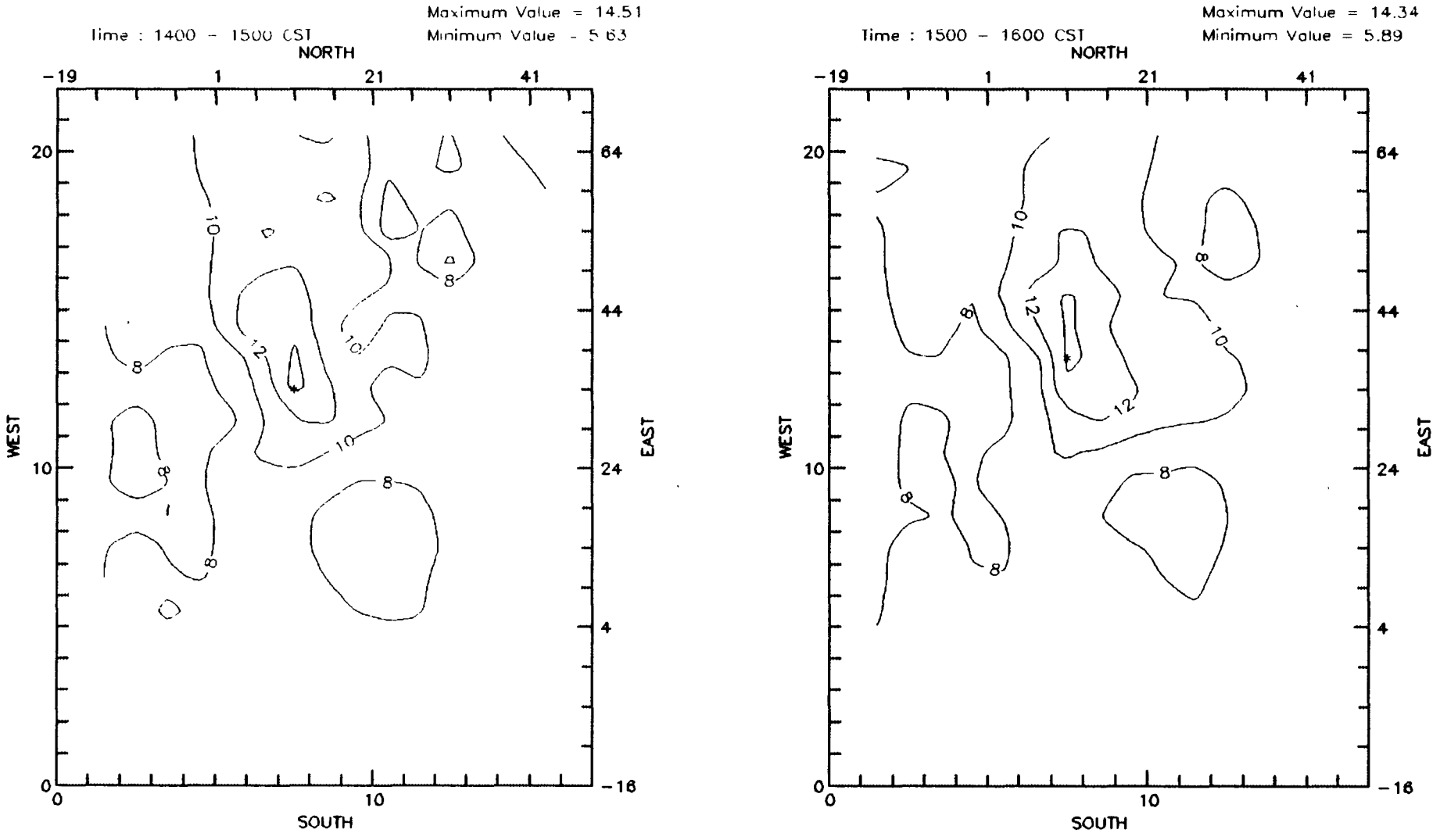

FIGURE E-4b. Ozone Concentration Scenario 5, July 13,1976 (pphm)

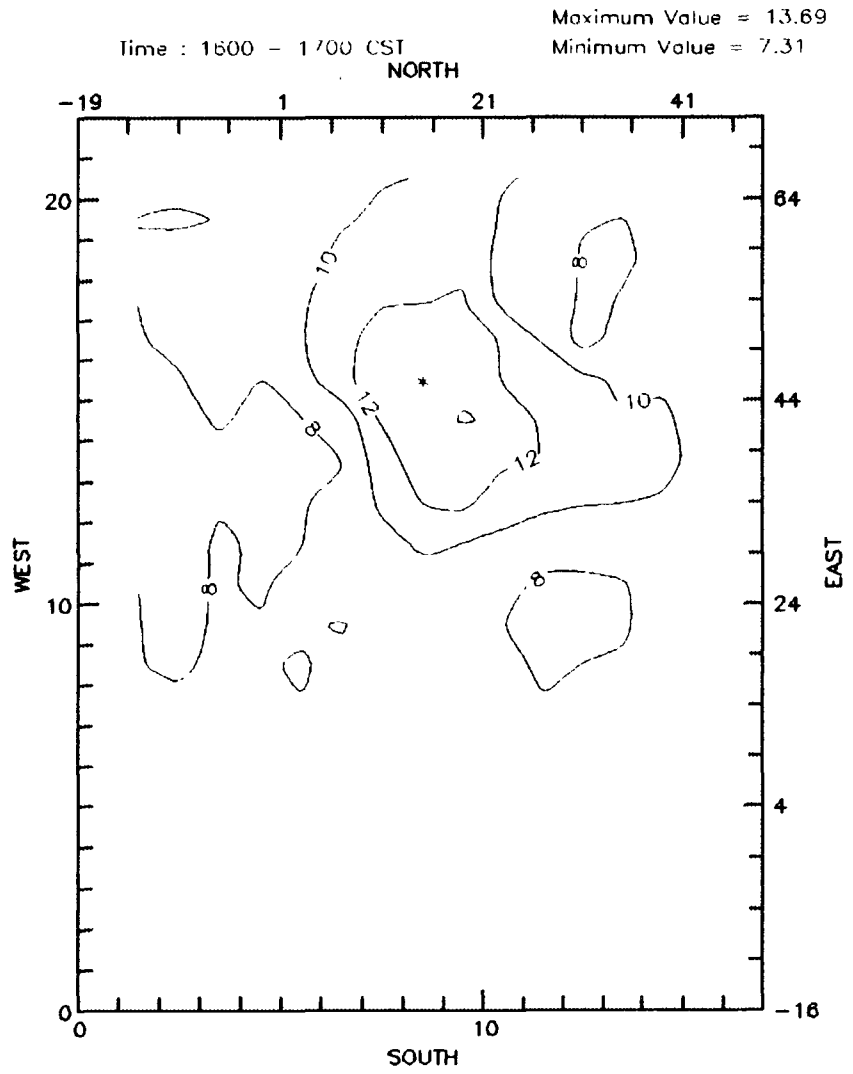

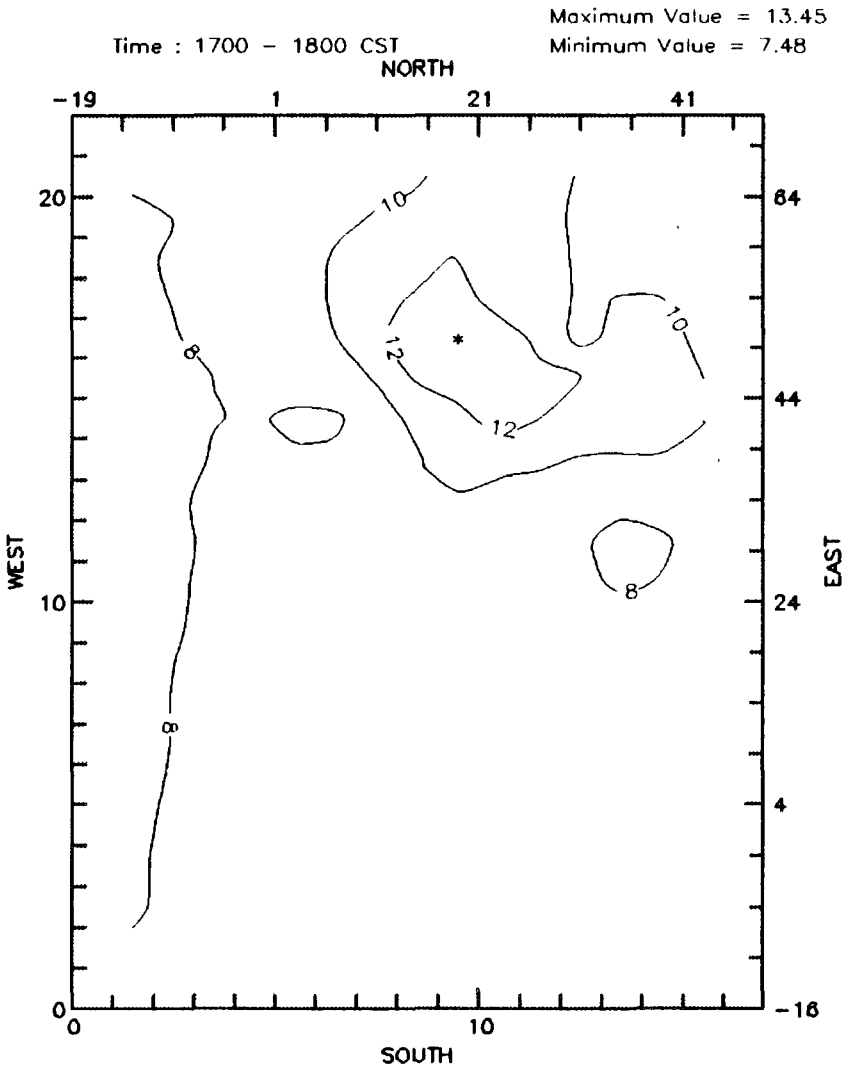

FIGURE E-4c. Ozone Concentration Scenario 5, July 13, 1976 (pphm)

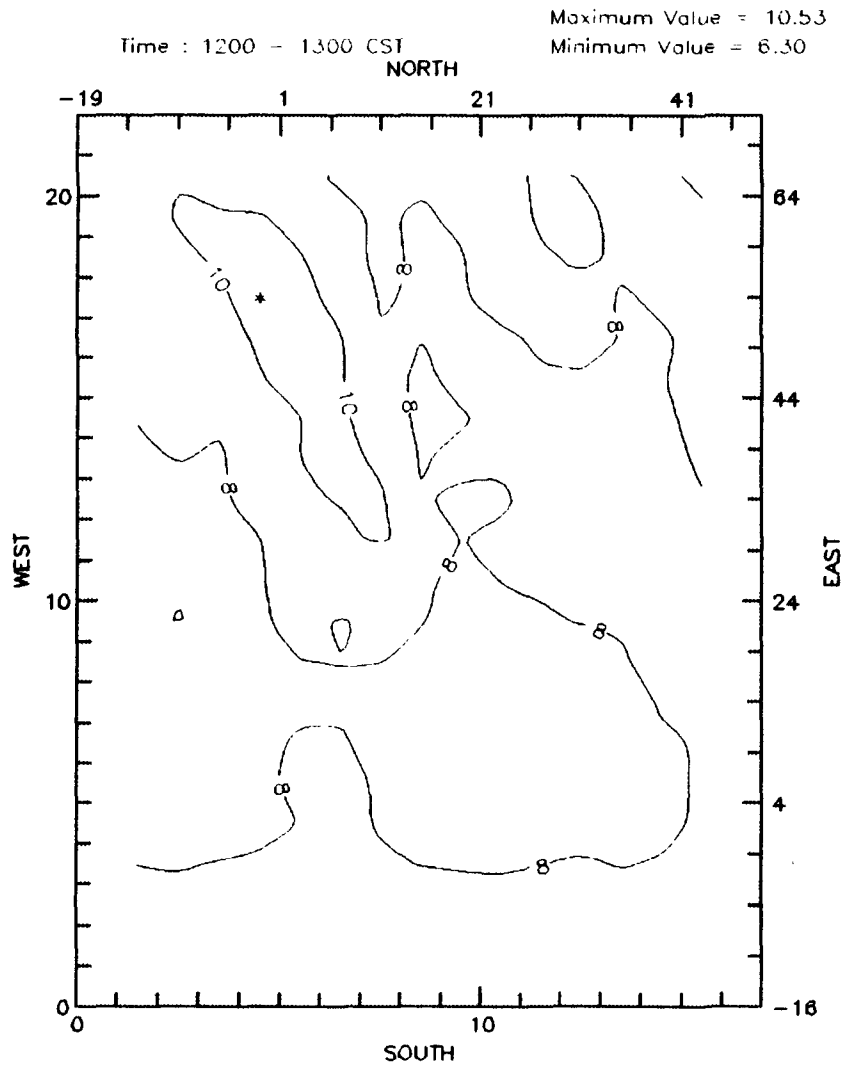

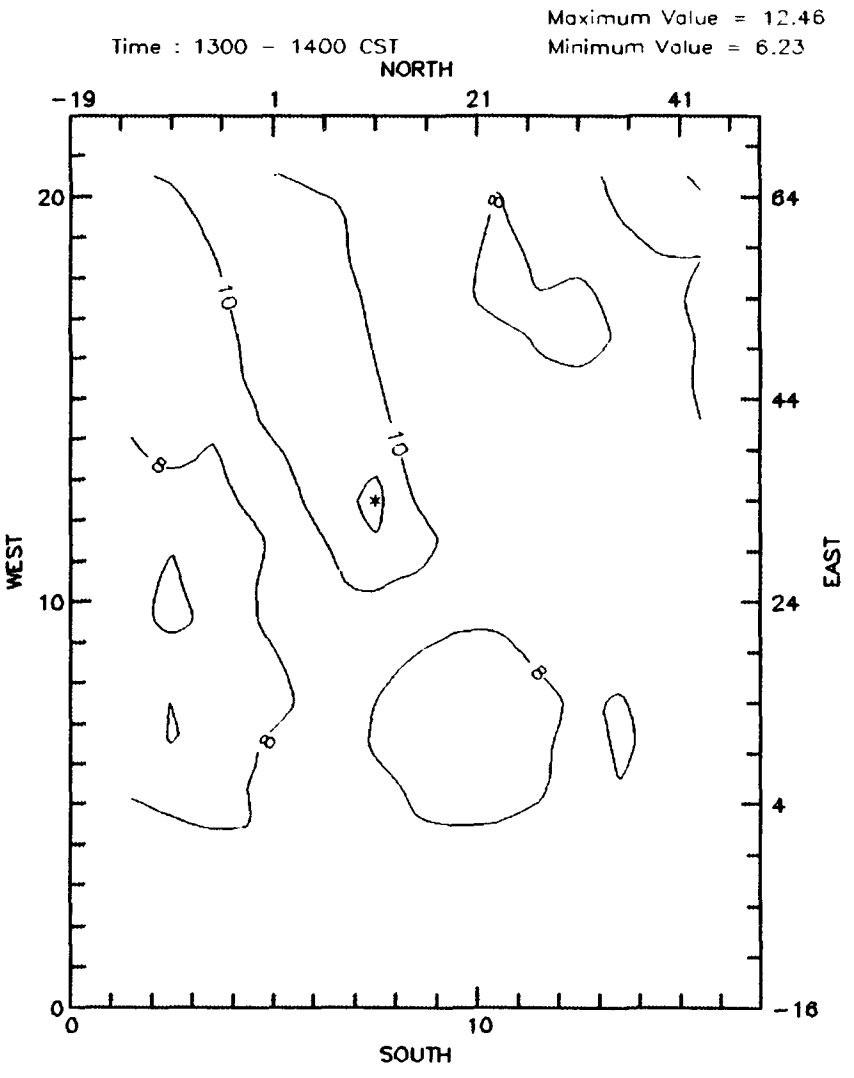

FIGURE E-5a. Ozone Concentration Scenario 6, July 13,1976 (pphm)

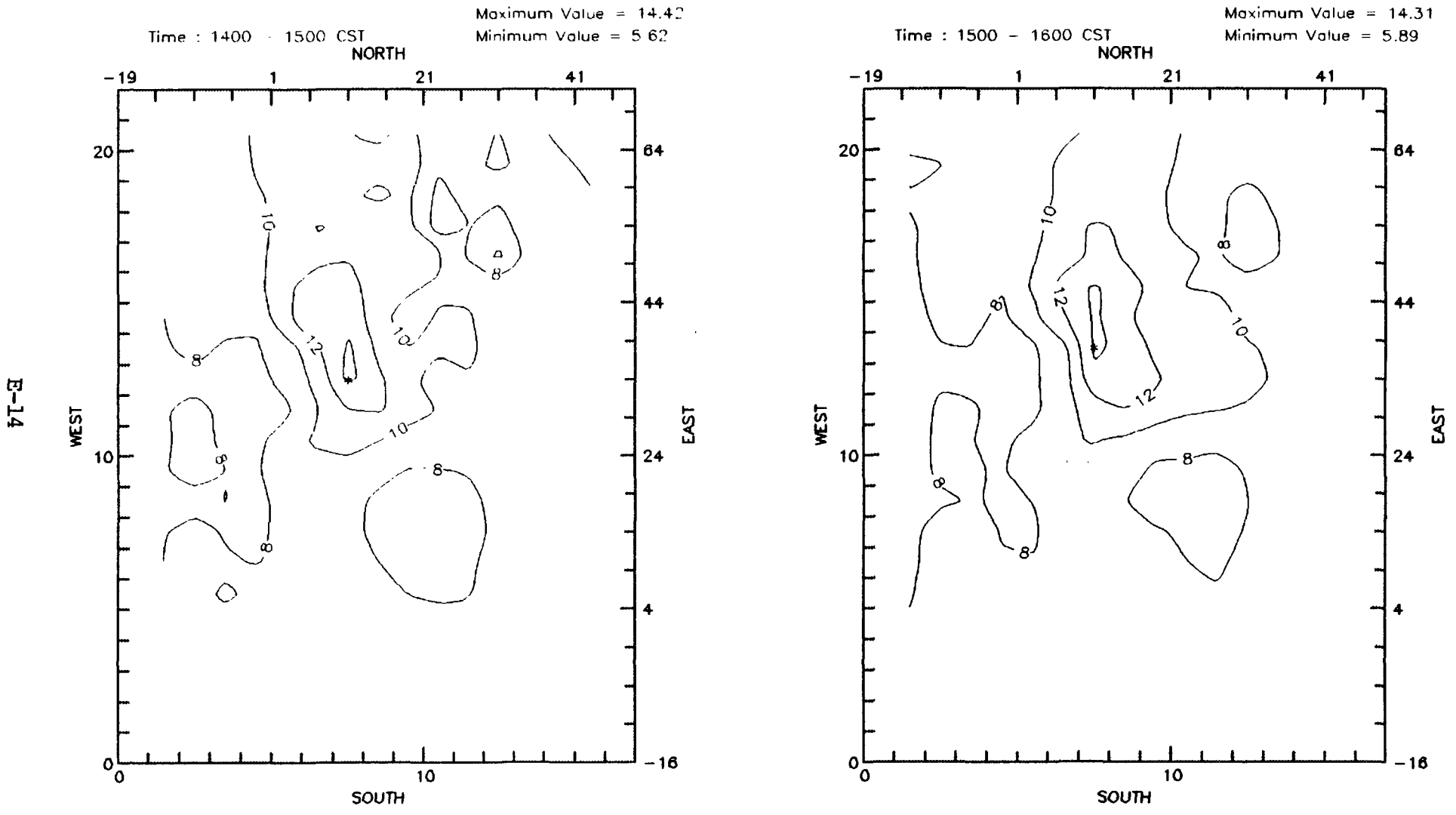

FIGURE E-5b. Ozone Concentration Scenario 6, July 13,1976 (pphm)

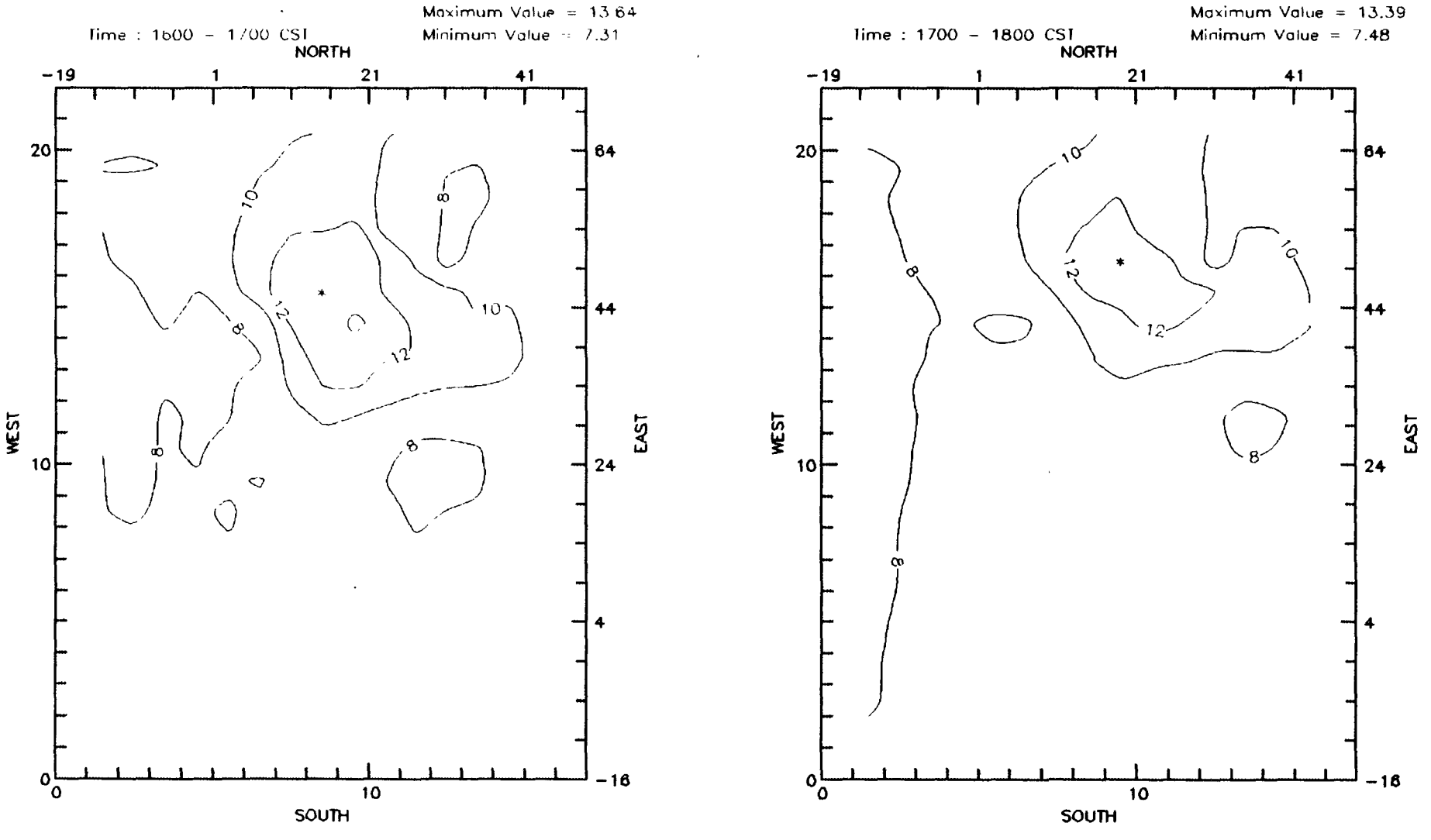

FIGURE E-5c. Ozone Concentration Scenario 6, July 13,1976 (pphm)

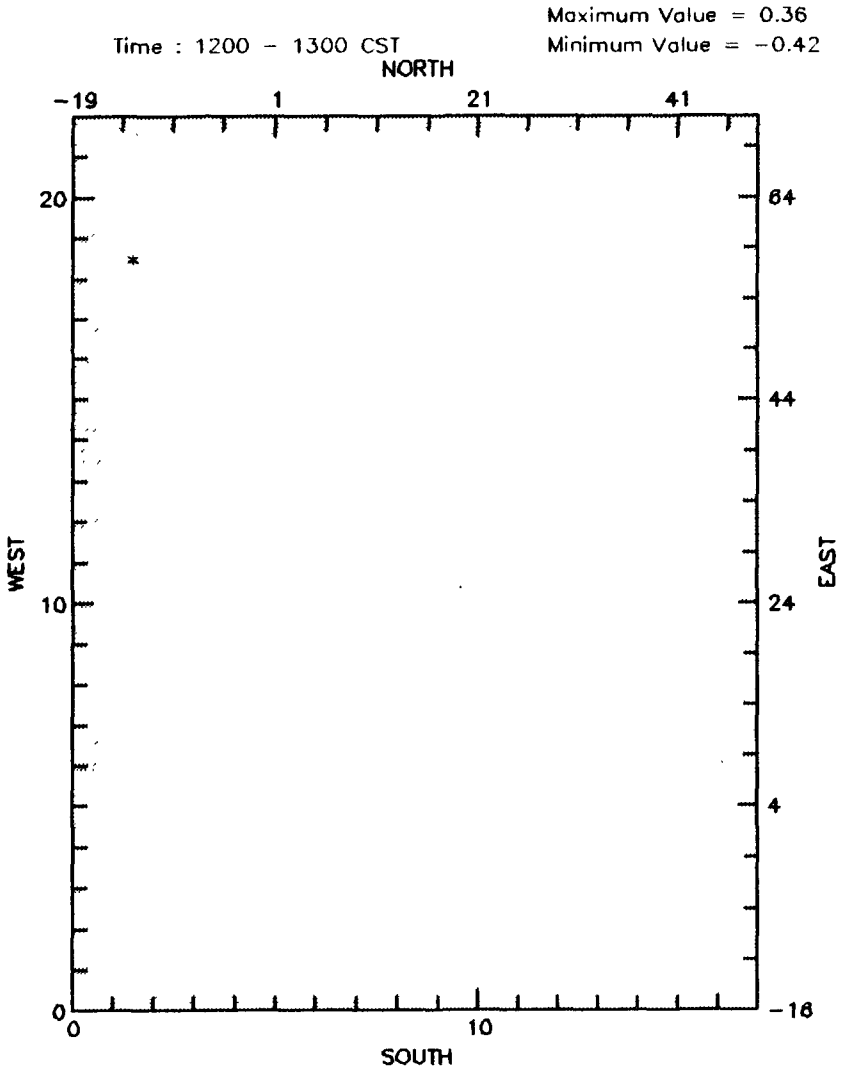

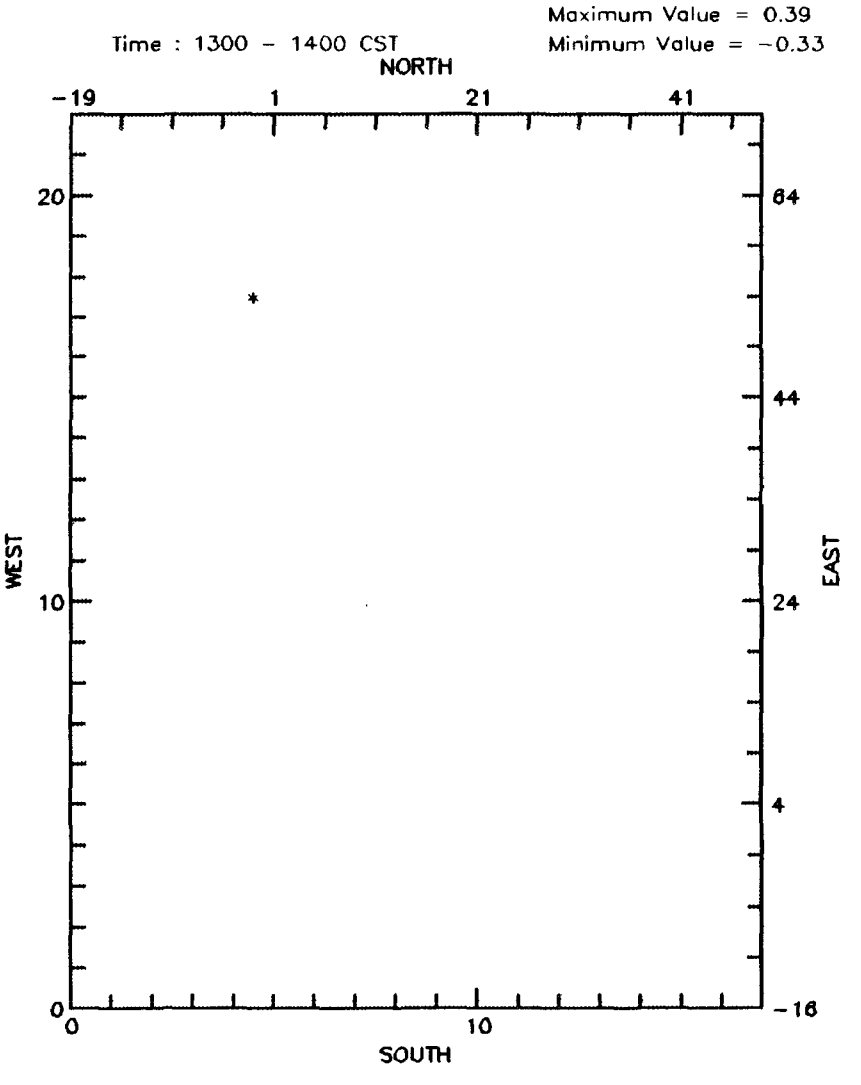

FIGURE E-6a. Ozone concentration difference between Scenario 2 and Scenario 5, 13 July 1976 (ppb).

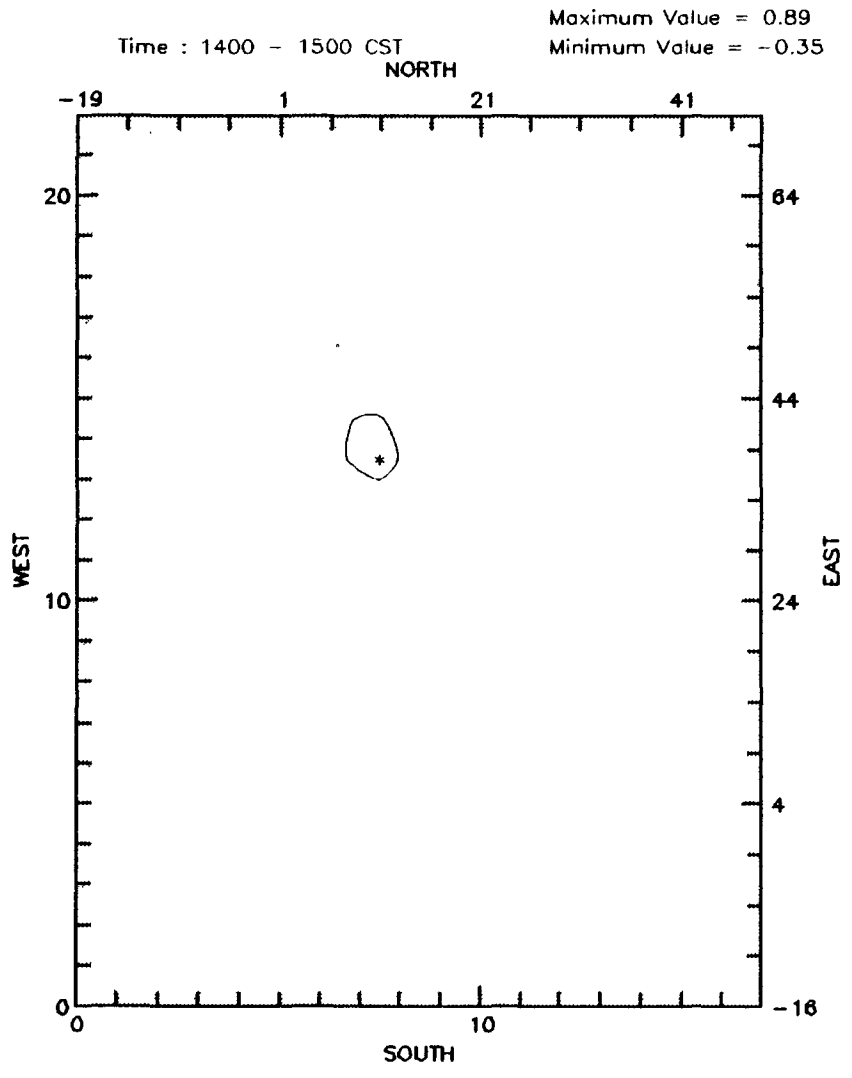

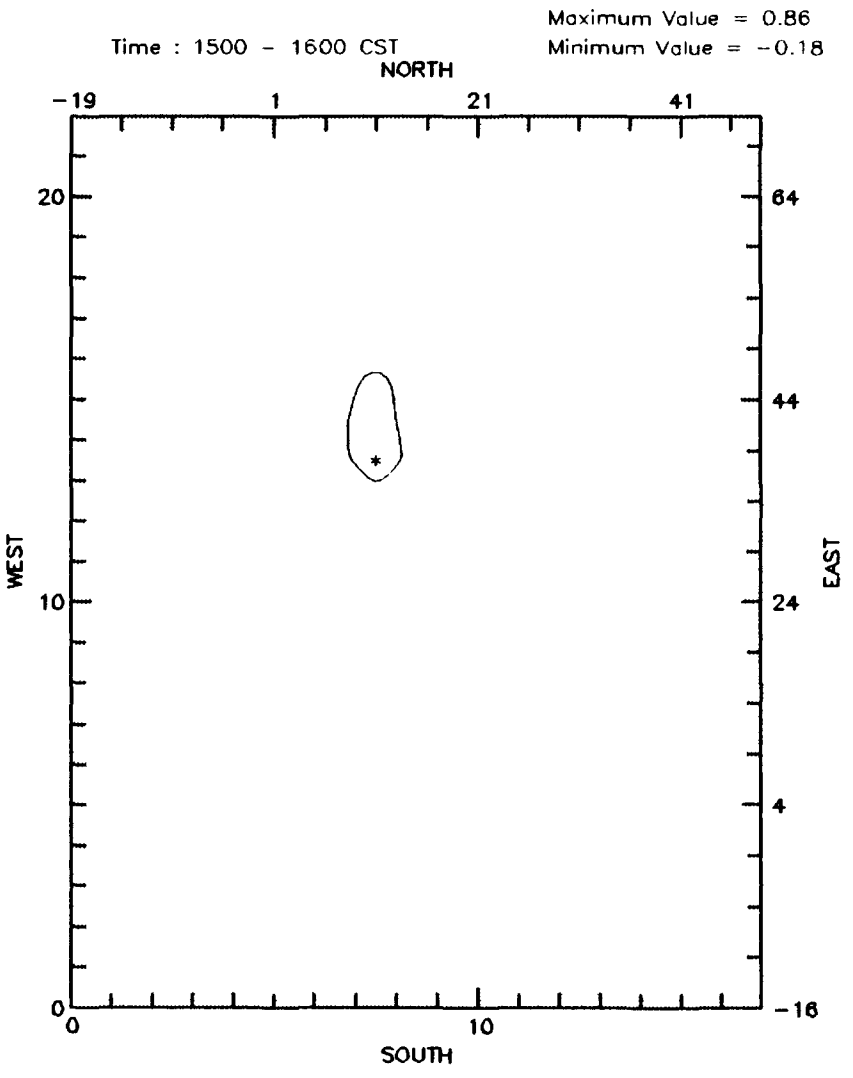

FIGURE E-6b. Ozone concentration difference between Scenario 2 and Scenario 5, 13 July 1976 (ppb).

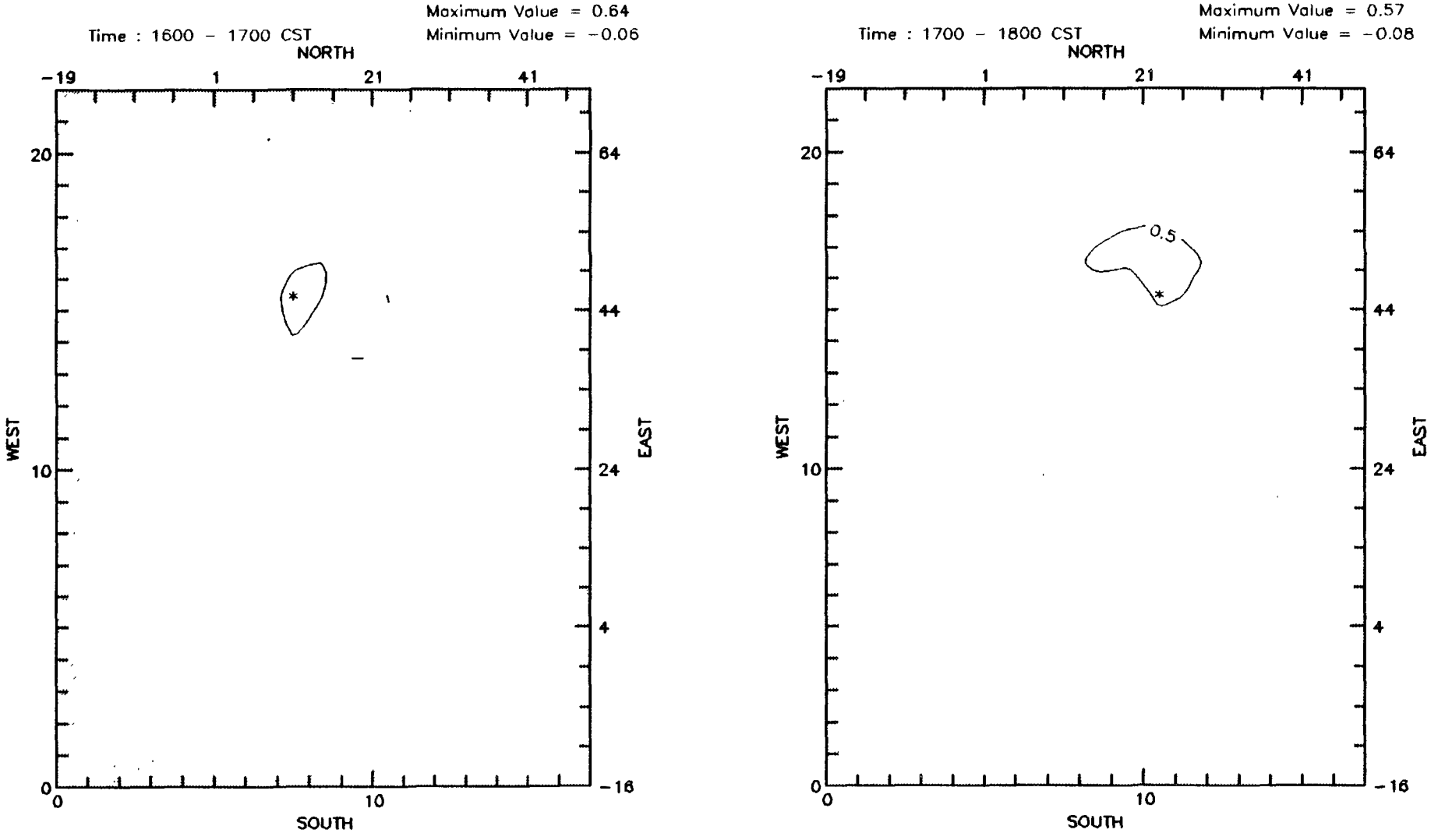

FIGURE E-6c. Ozone concentration difference between Scenario 2 and Scenario 5, 13 July 1976 (ppb).

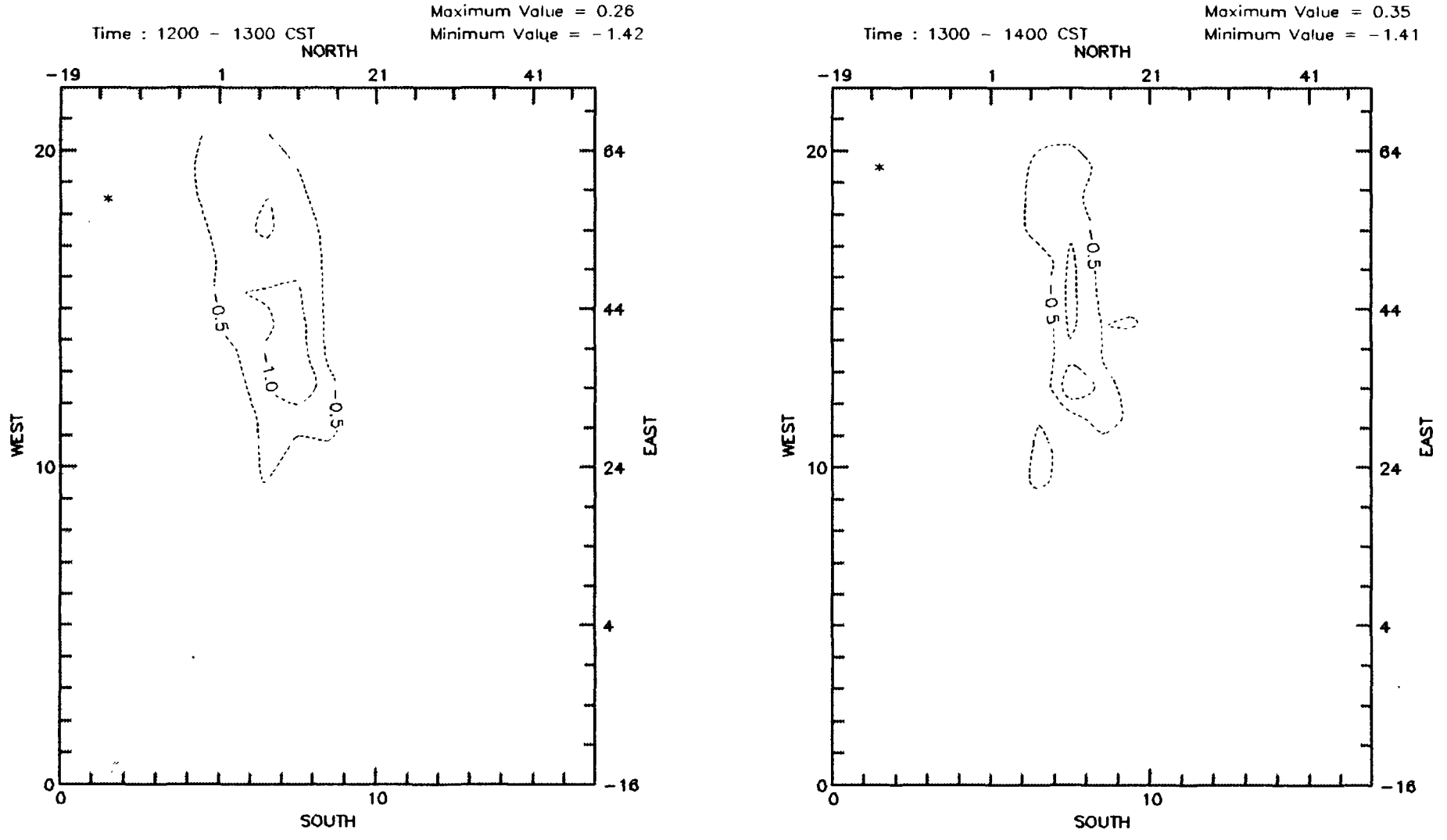

FIGURE E-7a. Ozone concentration difference between Scenario 2 and Scenario 6, 13 July 1976 (ppb).

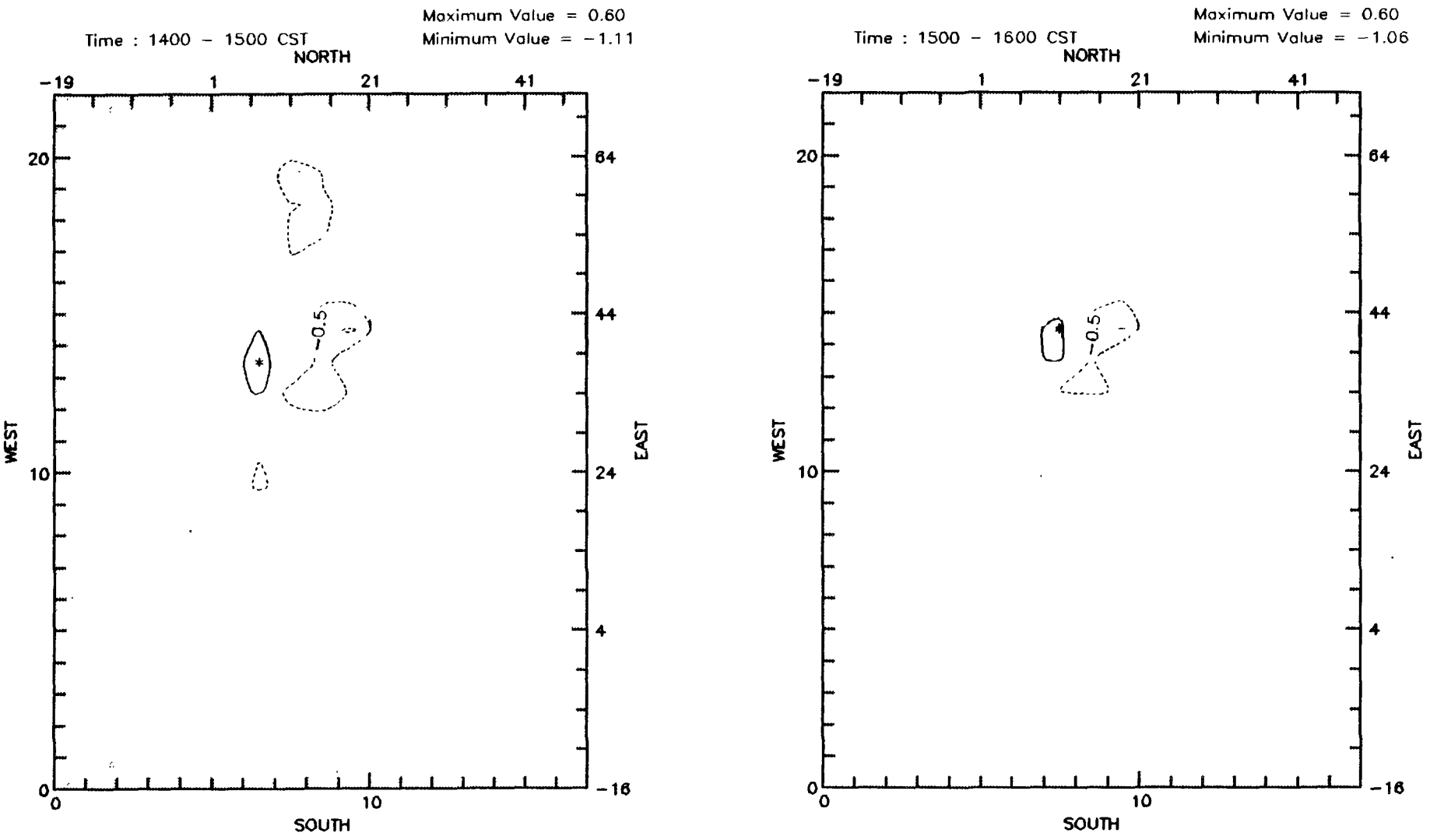

FIGURE E-7b. Ozone concentration difference between Scenario 2 and Scenario 6, 13 July 1976 (ppb).

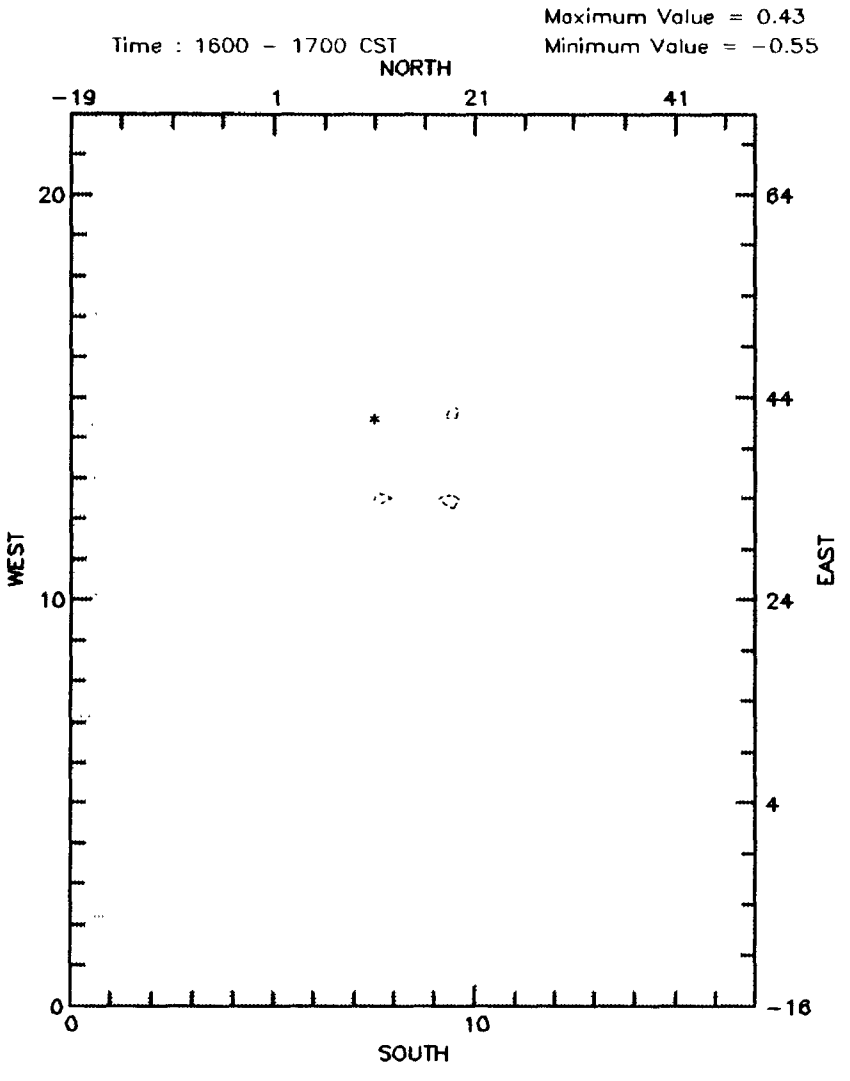

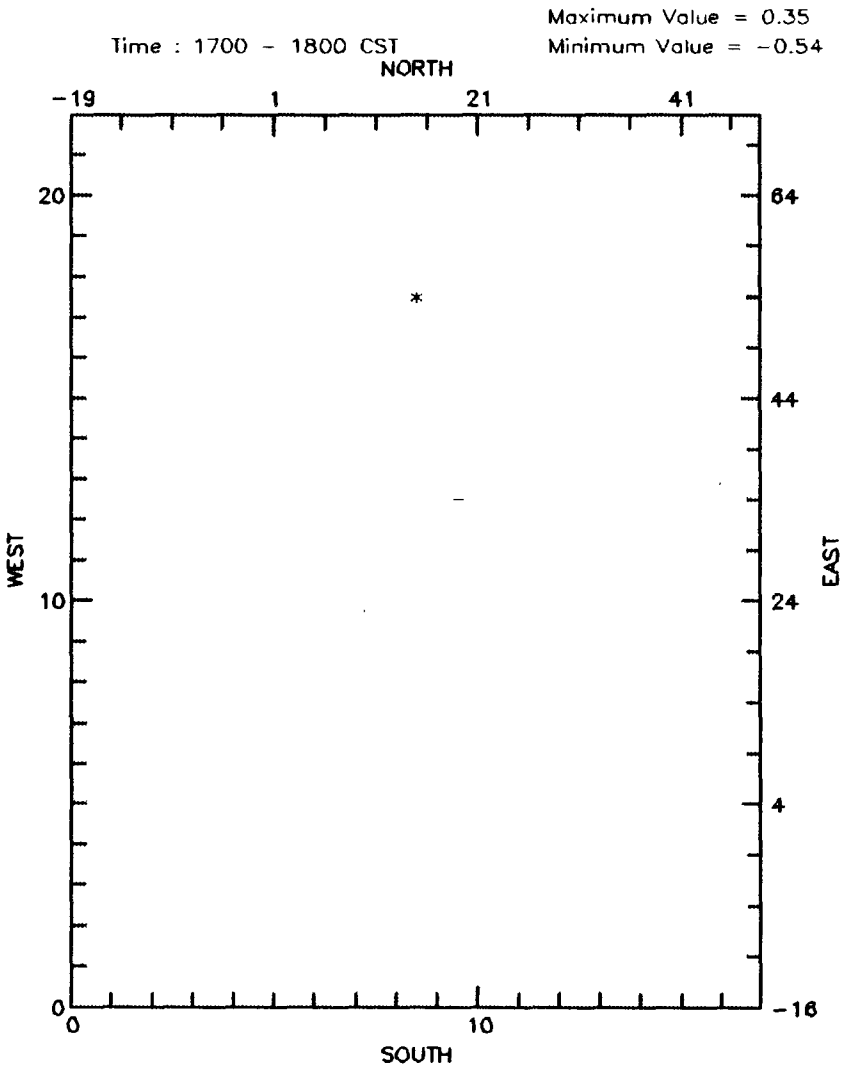

FIGURE E-7c. Ozone concentration difference between Scenario 2 and Scenario 6, 13 July 1976 (ppb).

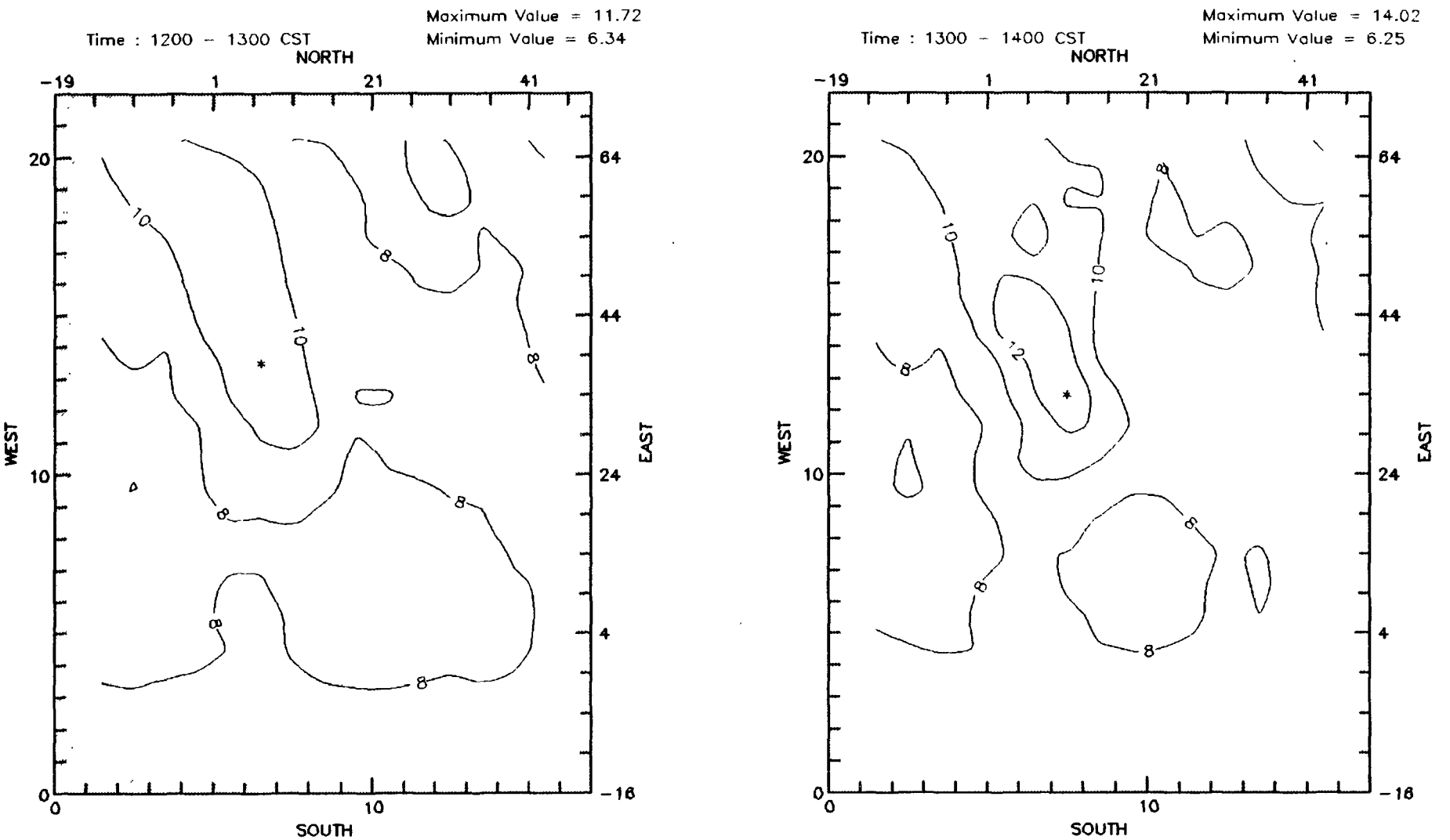

FIGURE E-8a. Ozone concentration Scenario 7, 13 July 1976 (pphm).

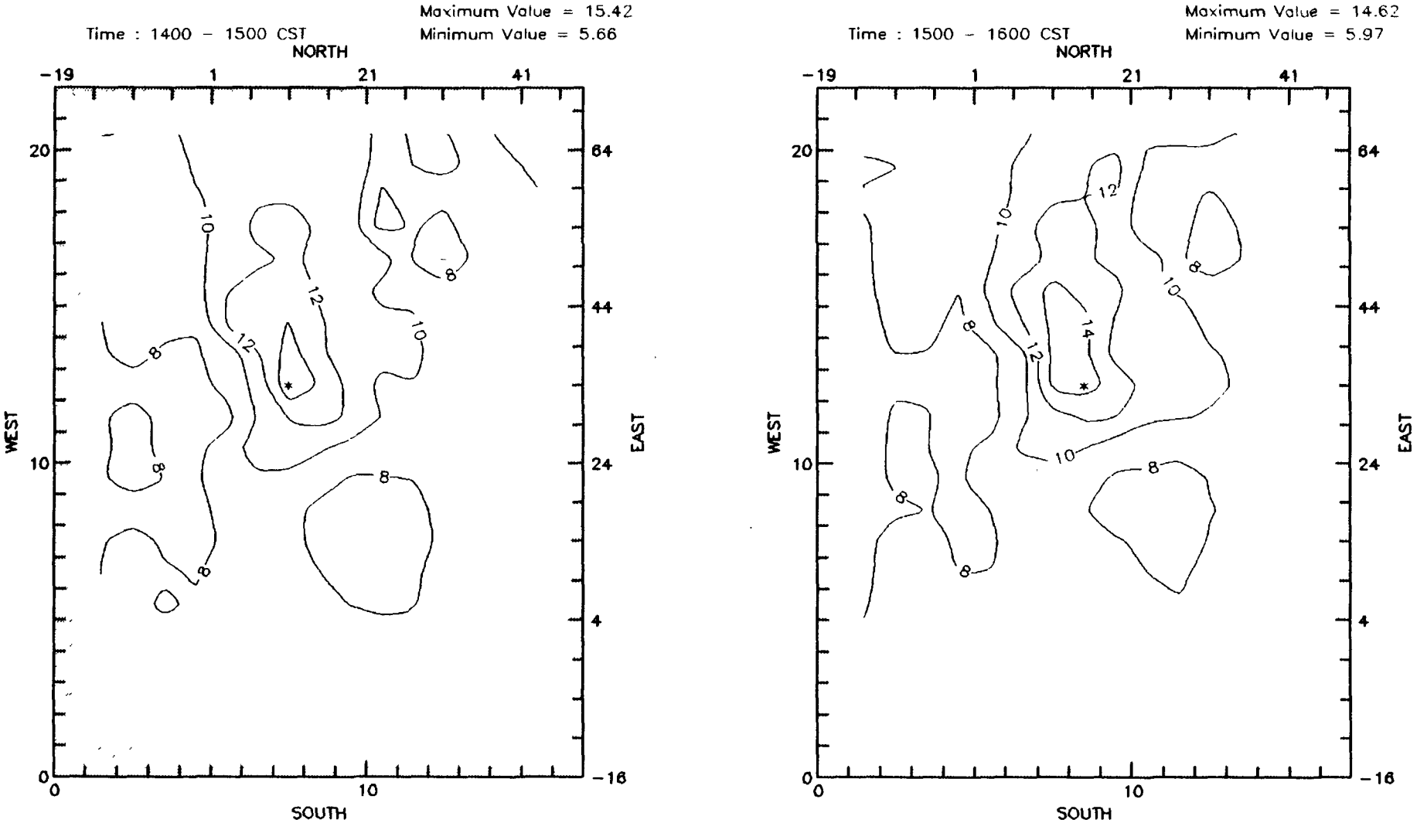

FIGURE E-8b. Ozone concentration Scenario 7, 13 July 1976 (pphm).

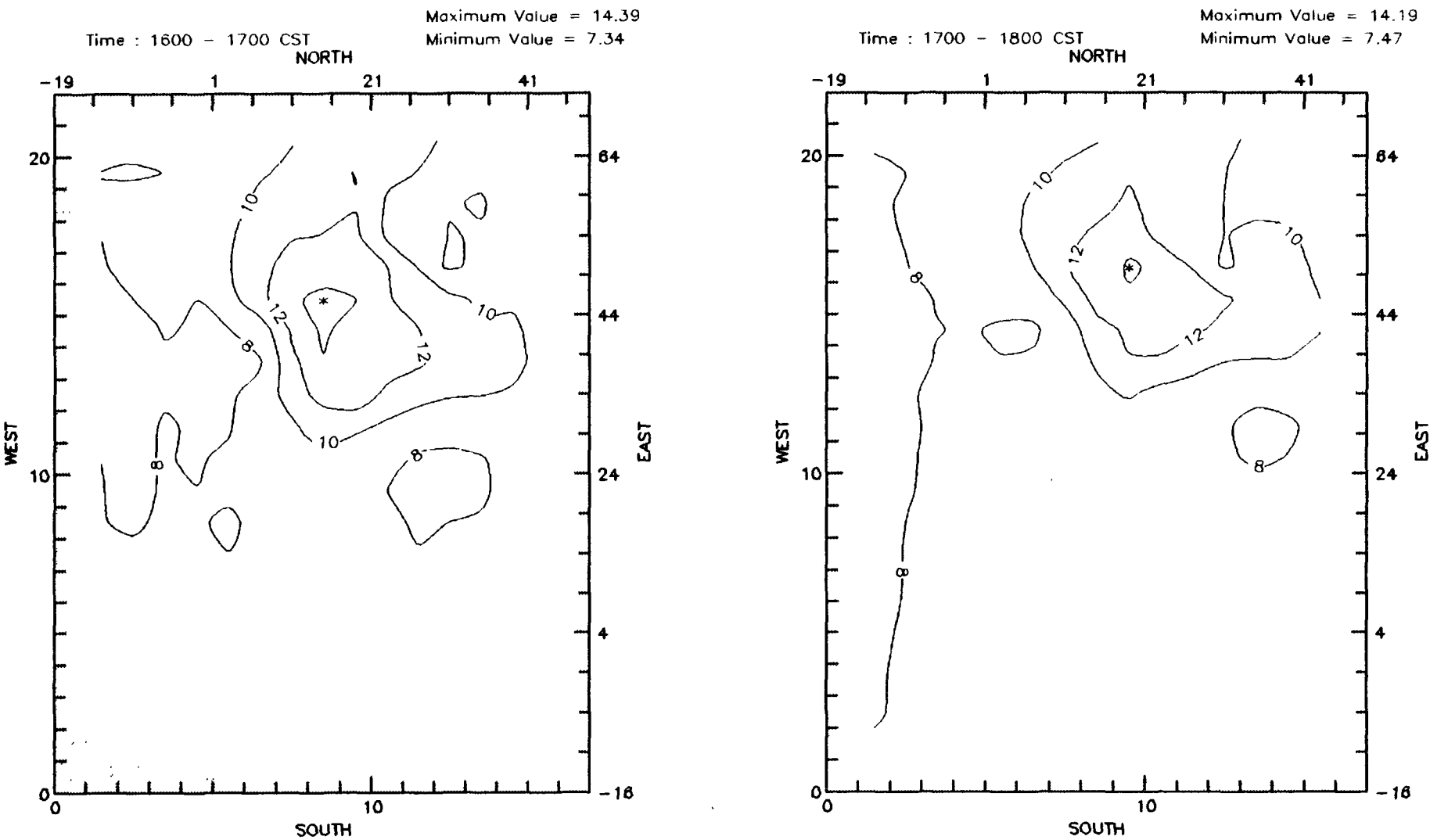

FIGURE E-8c. Ozone concentration Scenario 7, 13 July 1976 (pphm).

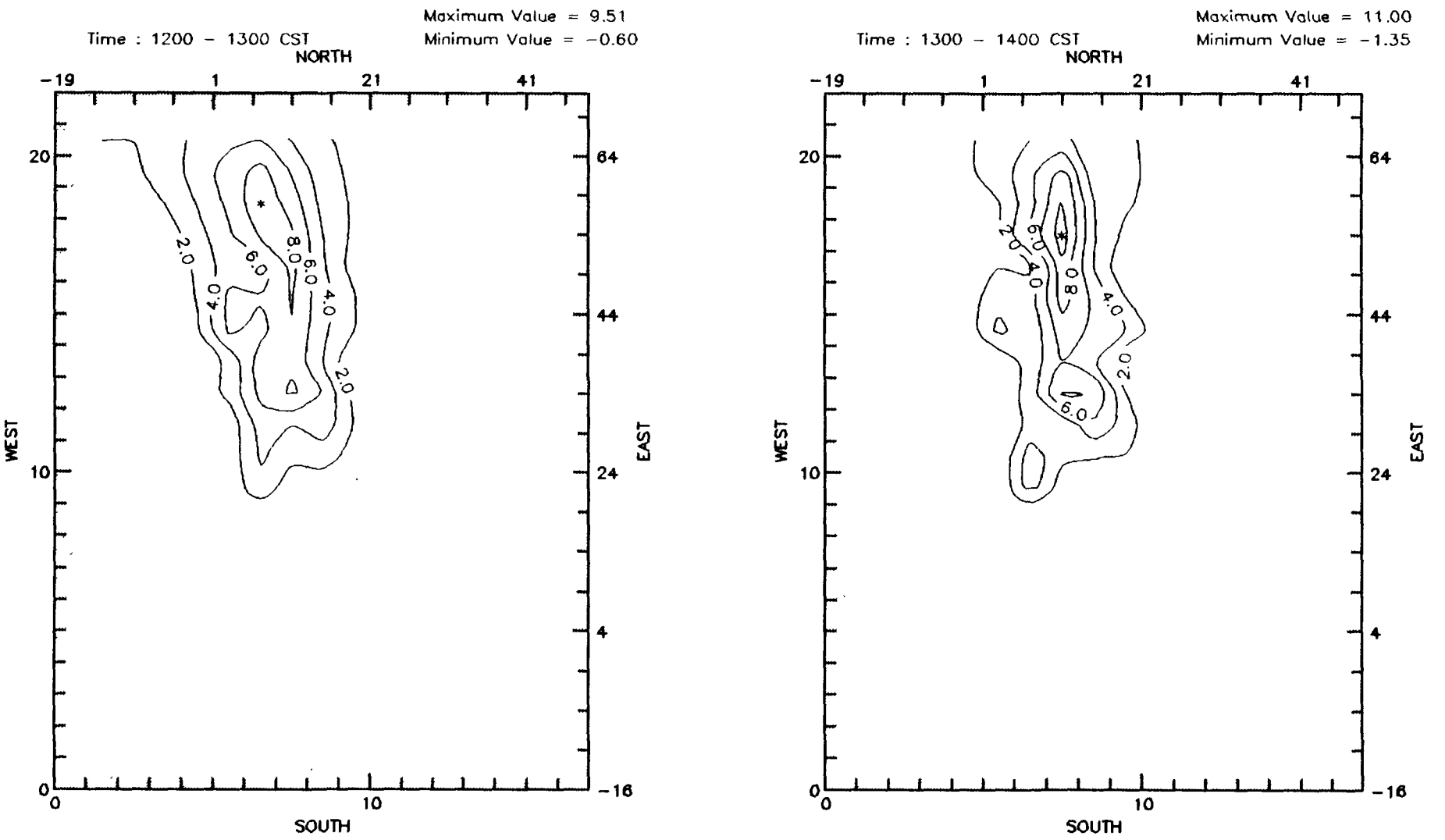

FIGURE E-9a. Ozone concentration difference between Scenario 1 and Scenario 8, 13 July 1976 (ppb).

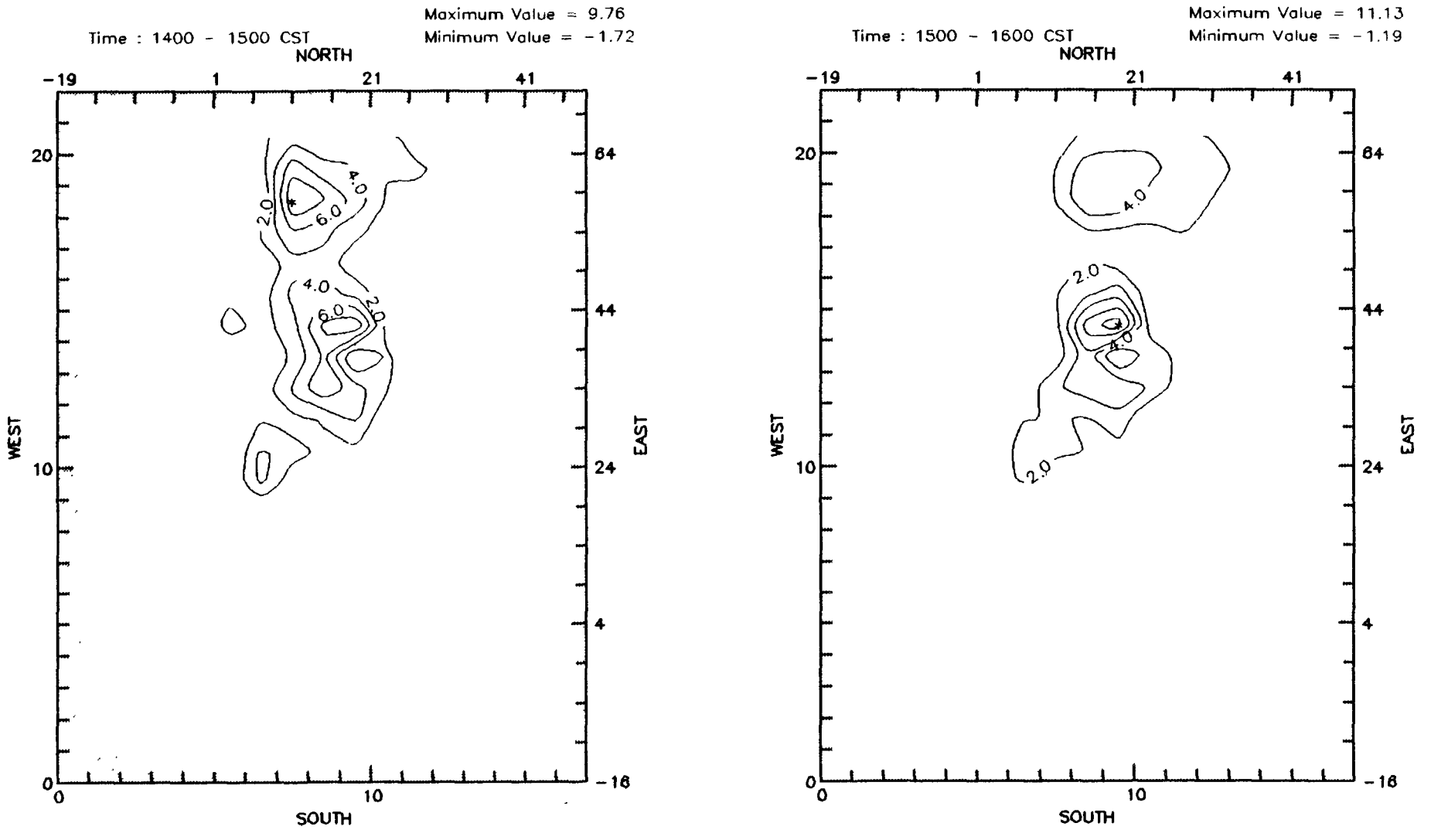

FIGURE E-9b. Ozone concentration difference between Scenario 1 and Scenario 7, 13 July 1976 (ppb).

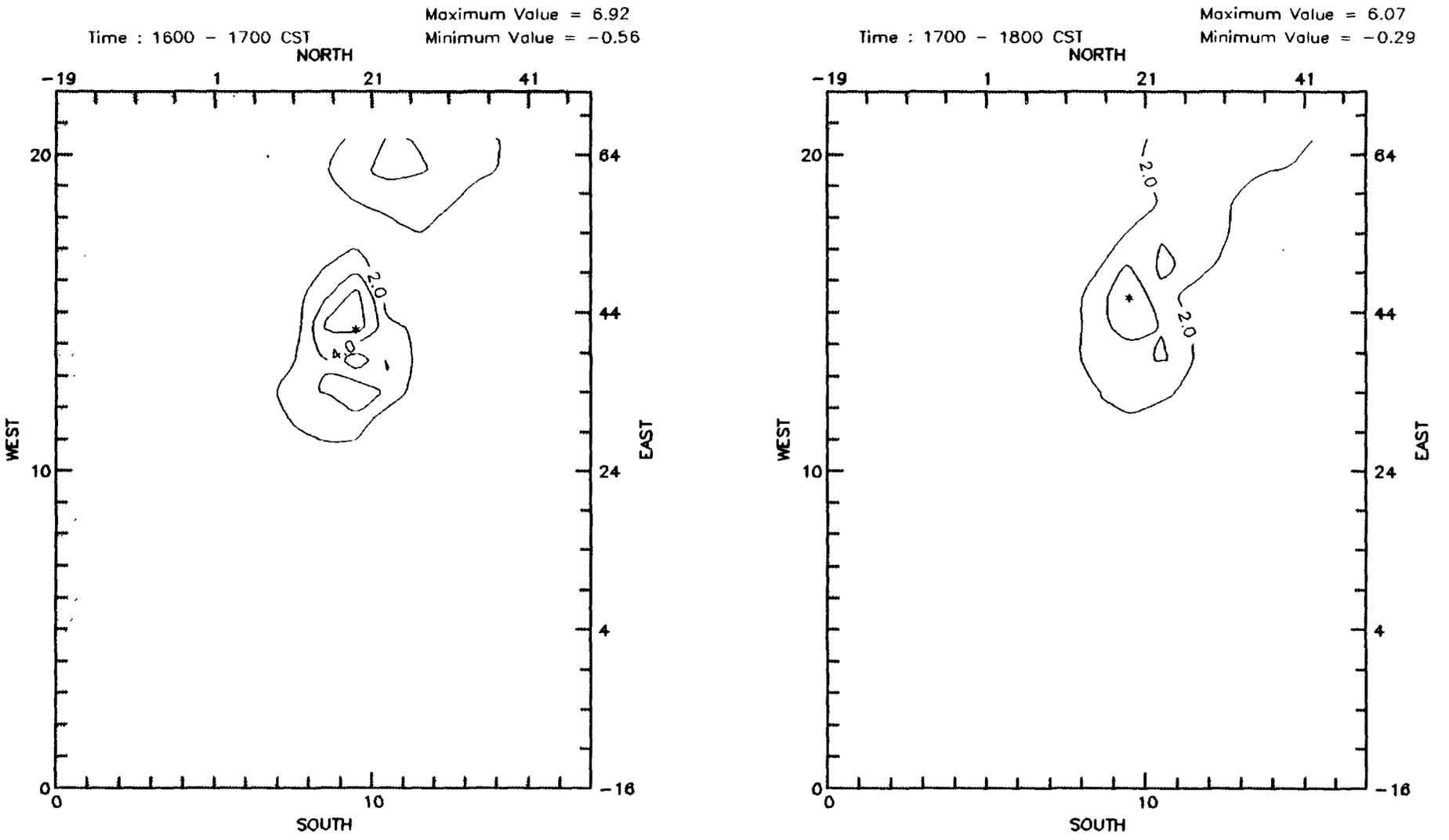

FIGURE E-9c. Ozone concentration difference between Scenario 1 and Scenario 7, 13 July 1976 (ppb).

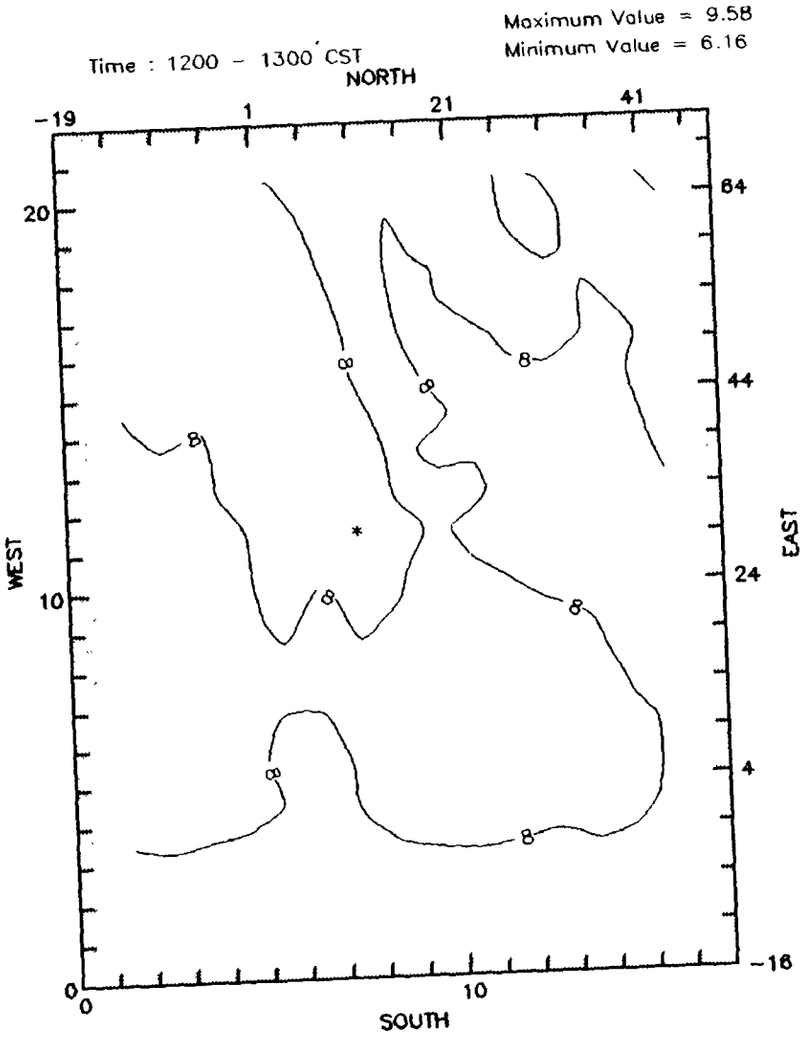

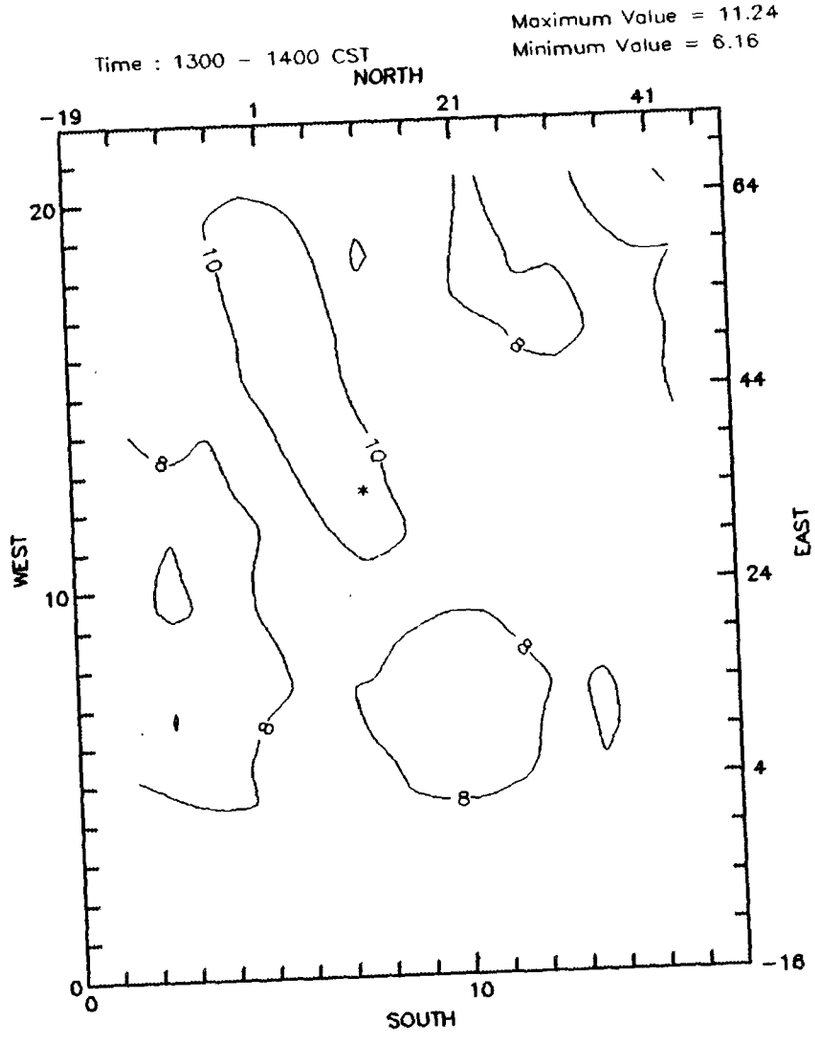

FIGURE E-10a. Ozone concentration SIP Scenario A, 13 July 1976 (pphm).

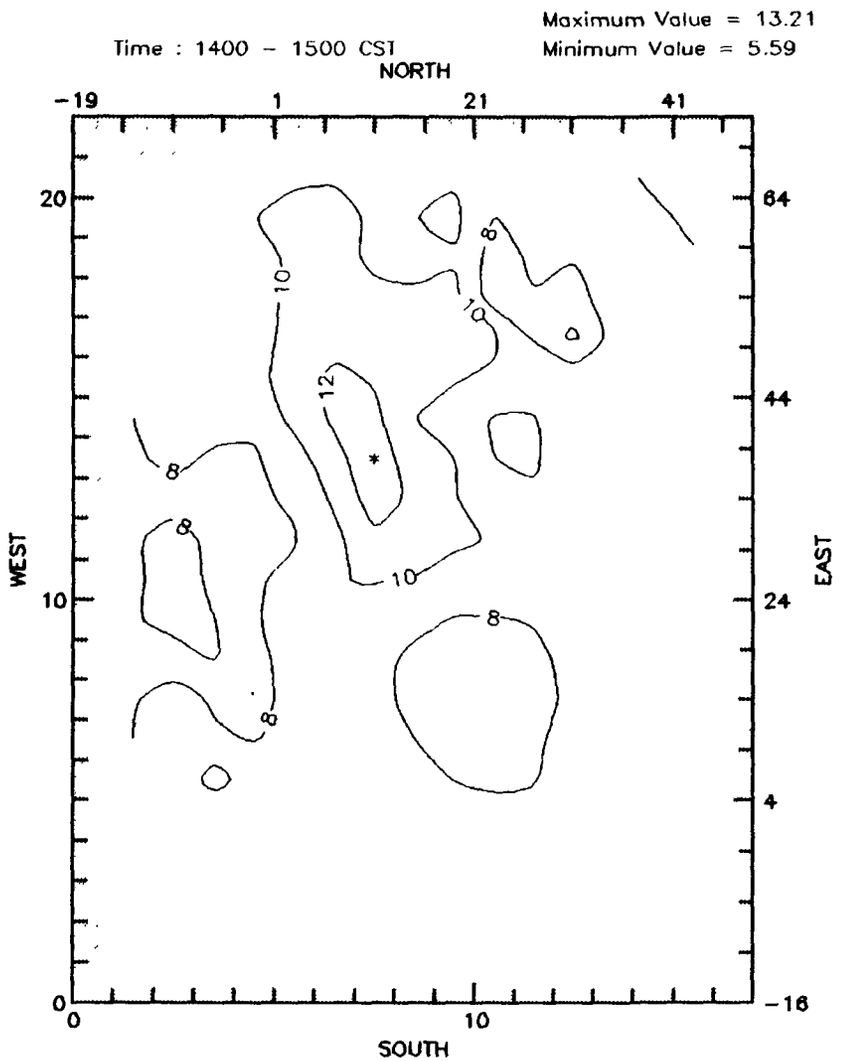

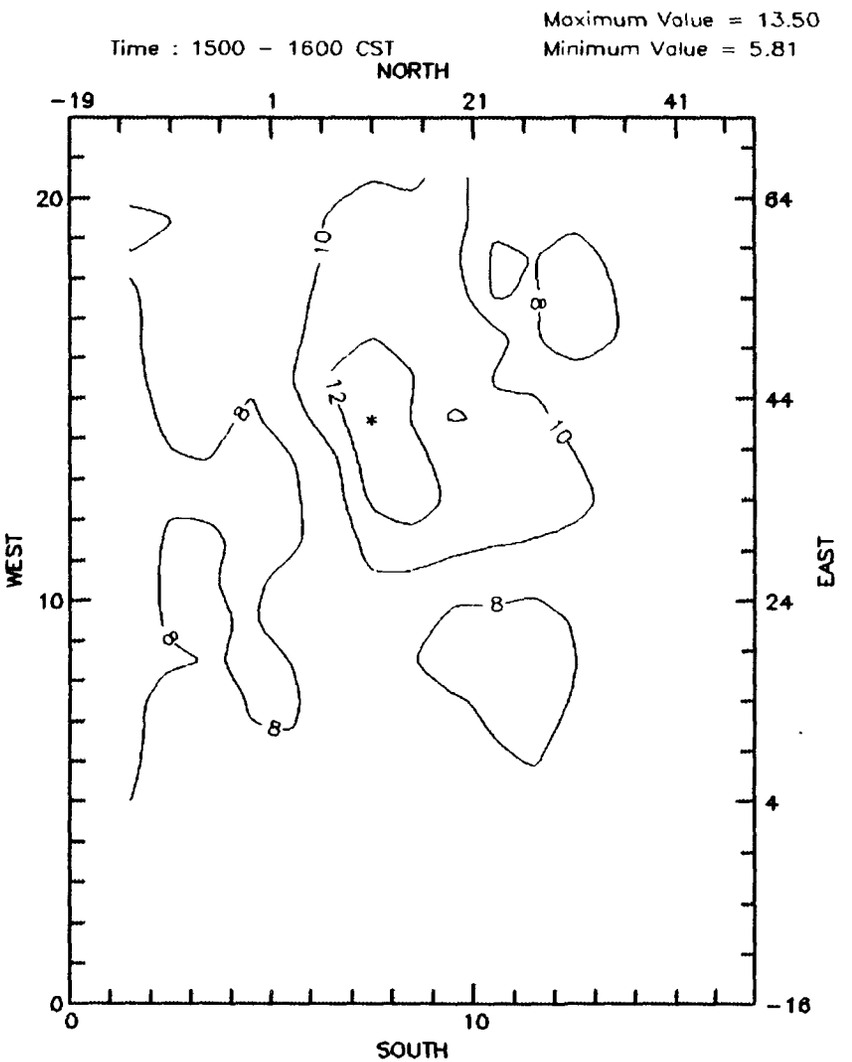

FIGURE E-10b. Ozone concentration SIP Scenario A, 13 July 1976 (pphm).

88151

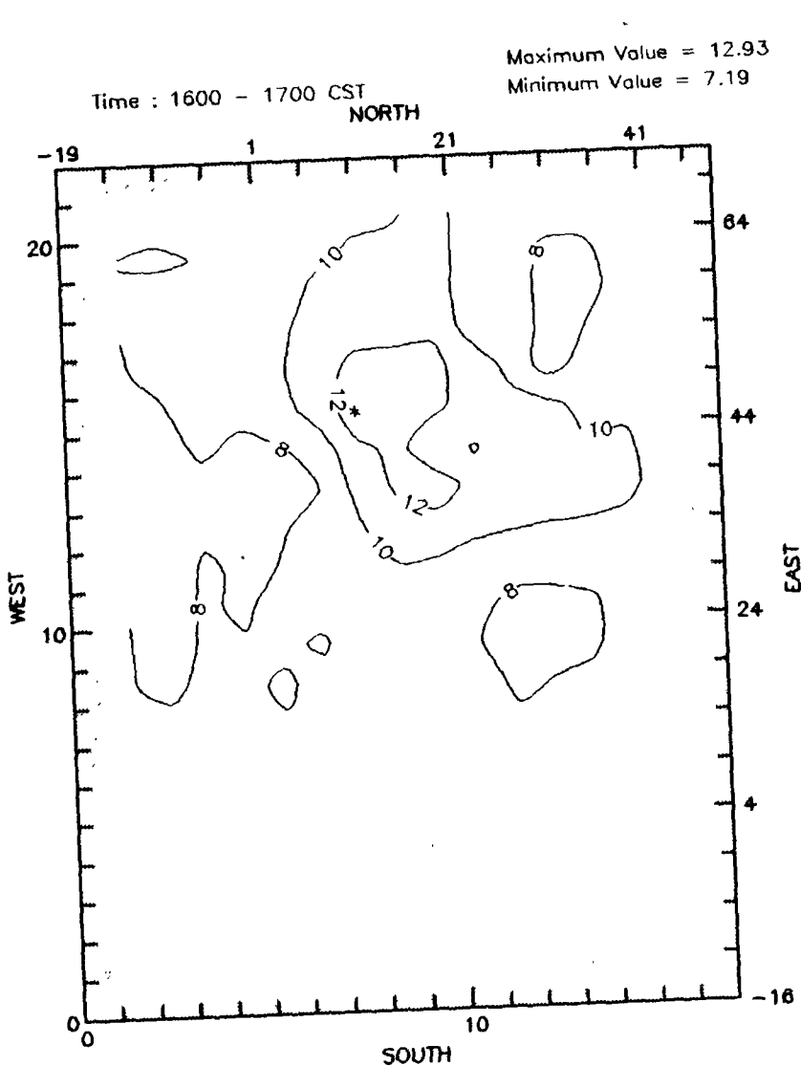

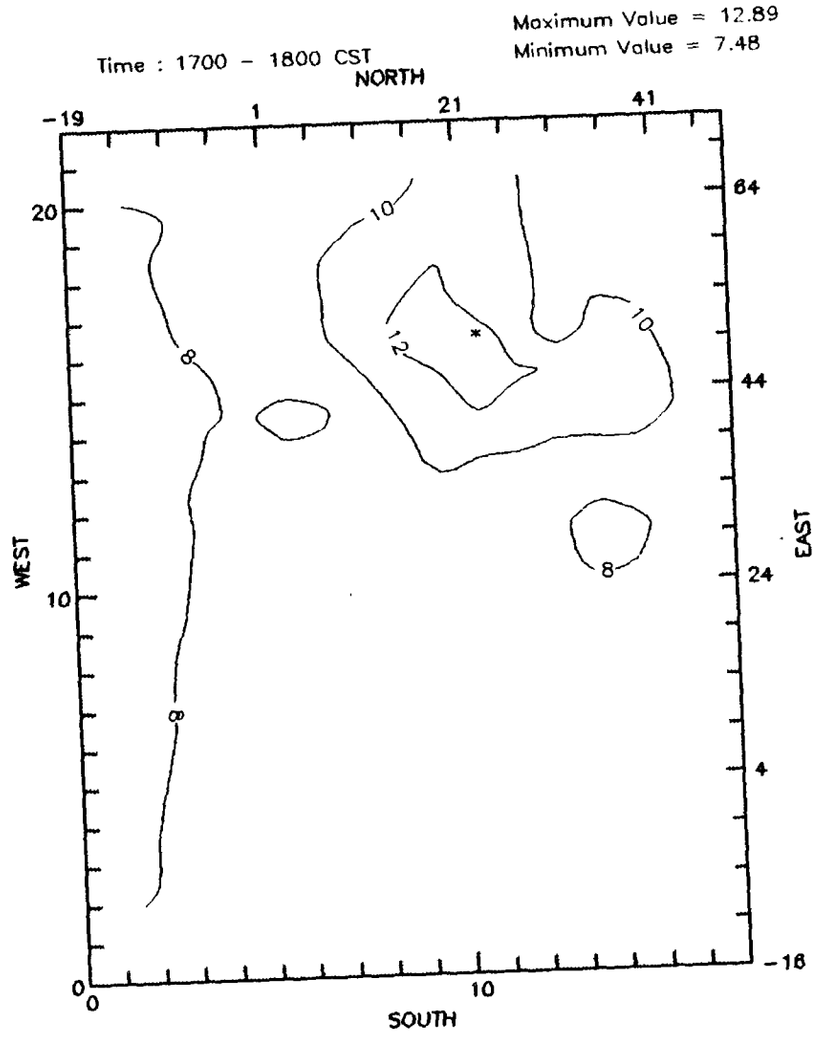

FIGURE E-10c. Ozone concentration SIP Scenario A, 13 July 1976 (pphm).

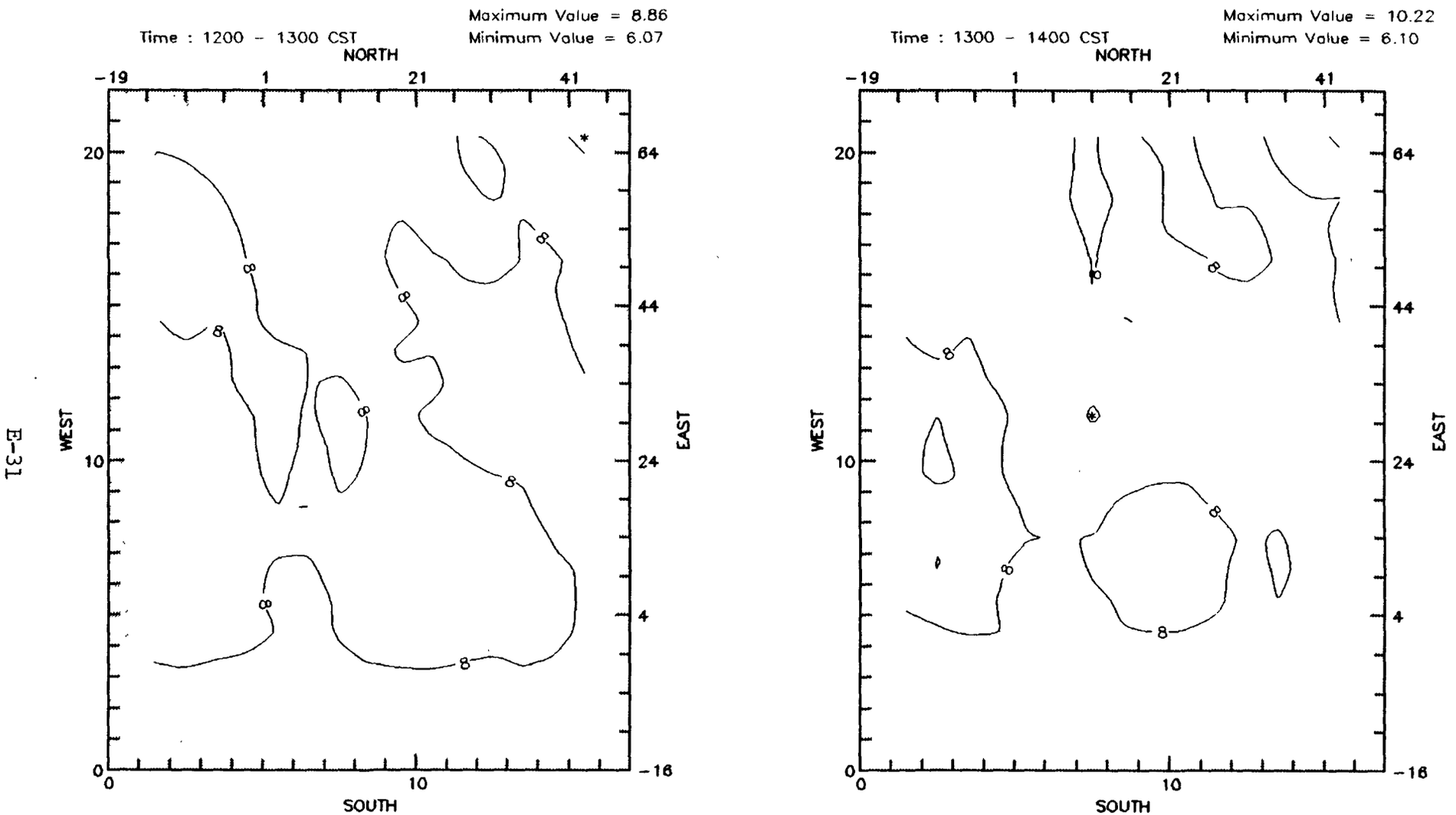

FIGURE E-11a. Ozone concentration SIP Scenario B, 13 July 1976 (pphm).

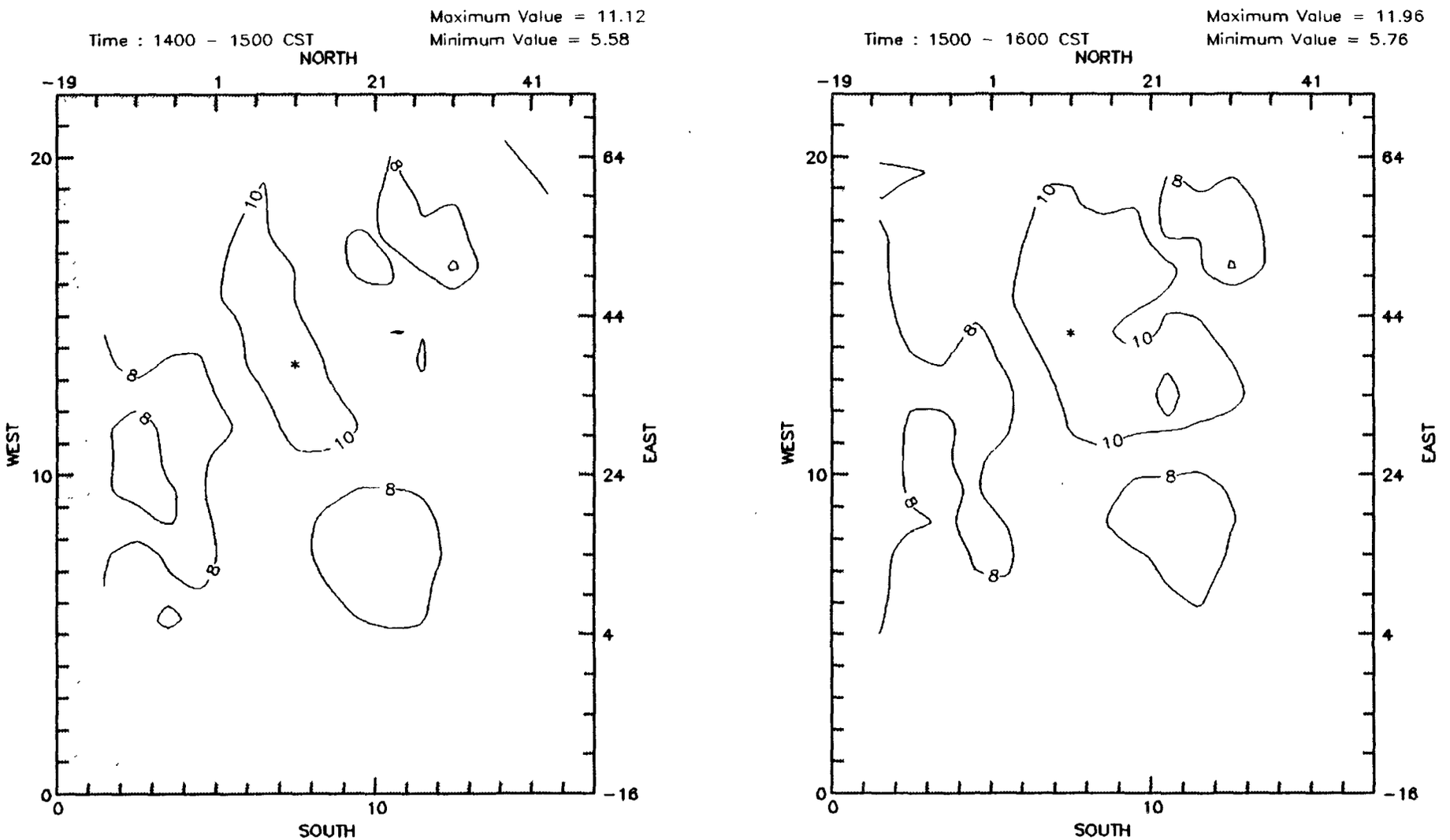

FIGURE E-11b. Ozone concentration SIP Scenario B, 13 July 1976 (pphm).

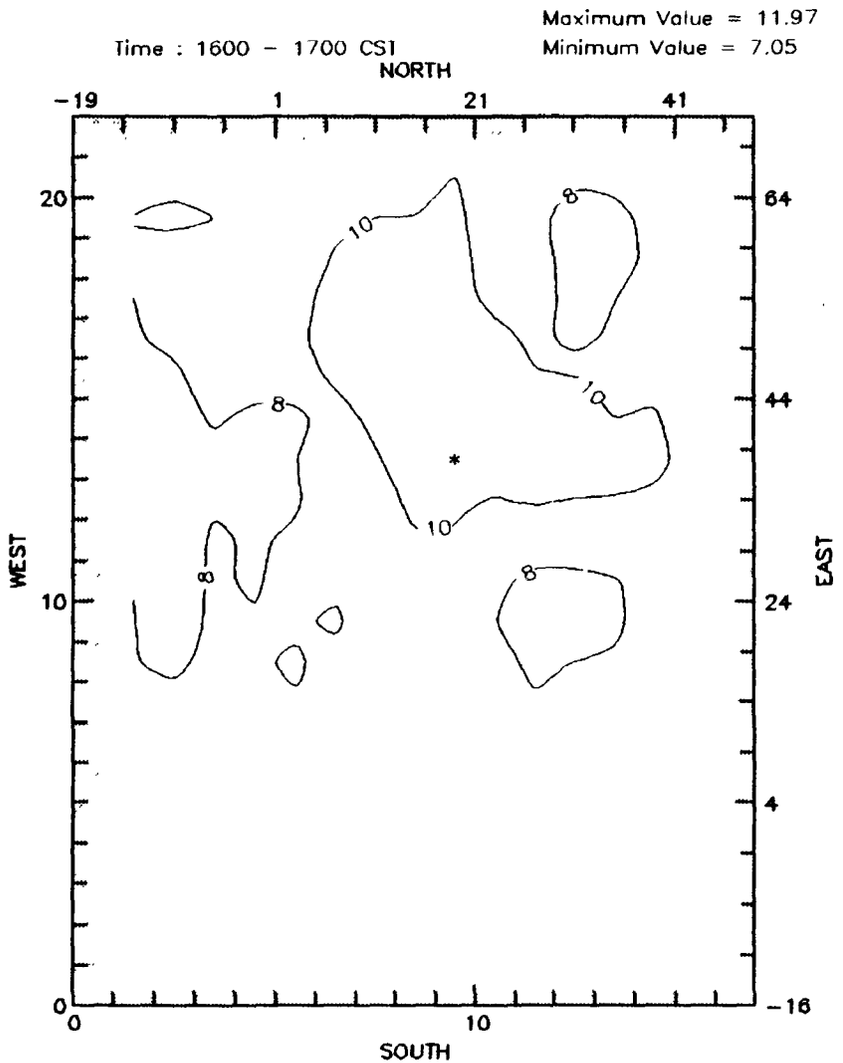

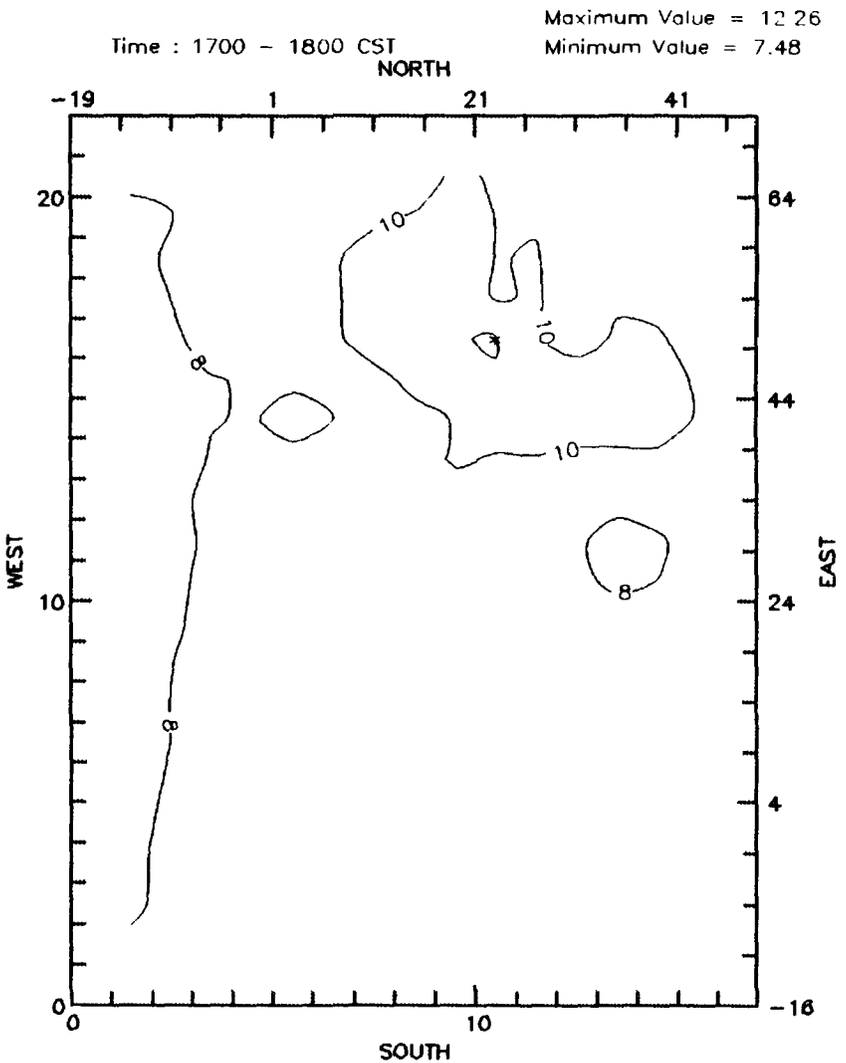

FIGURE E-11c. Ozone concentration SIP Scenario B, 13 July 1976 (pphm).

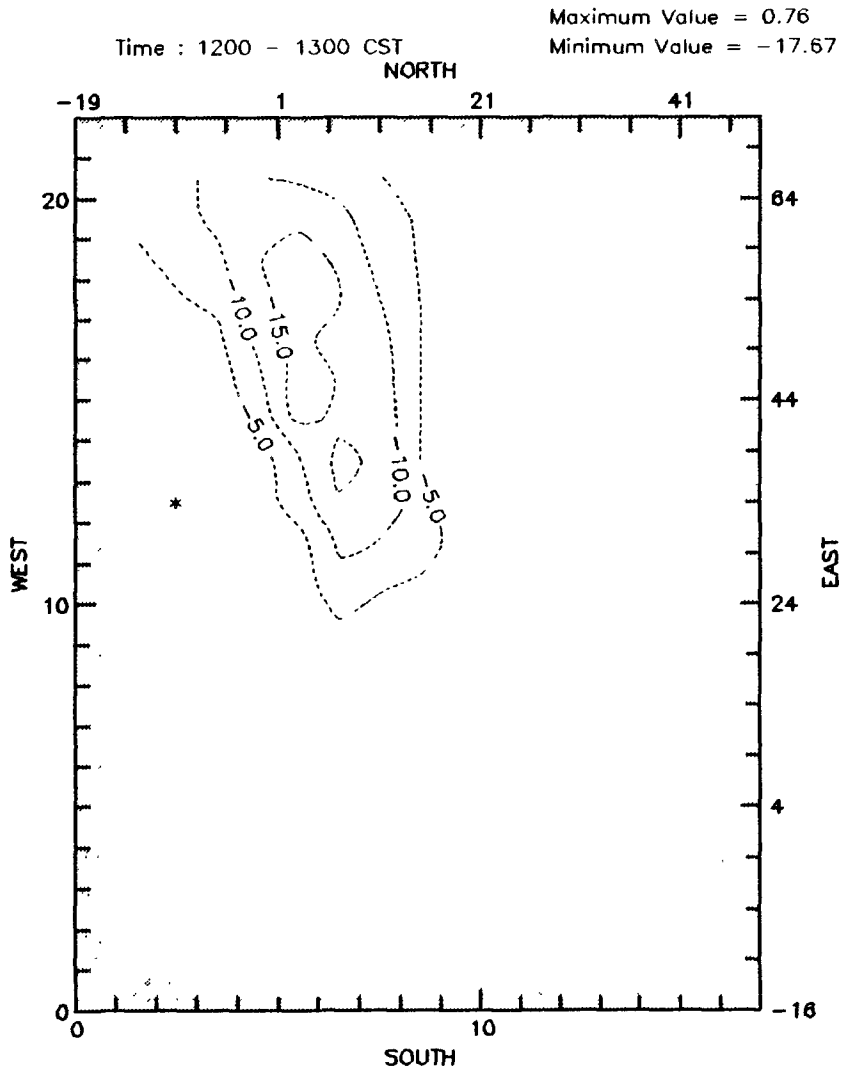

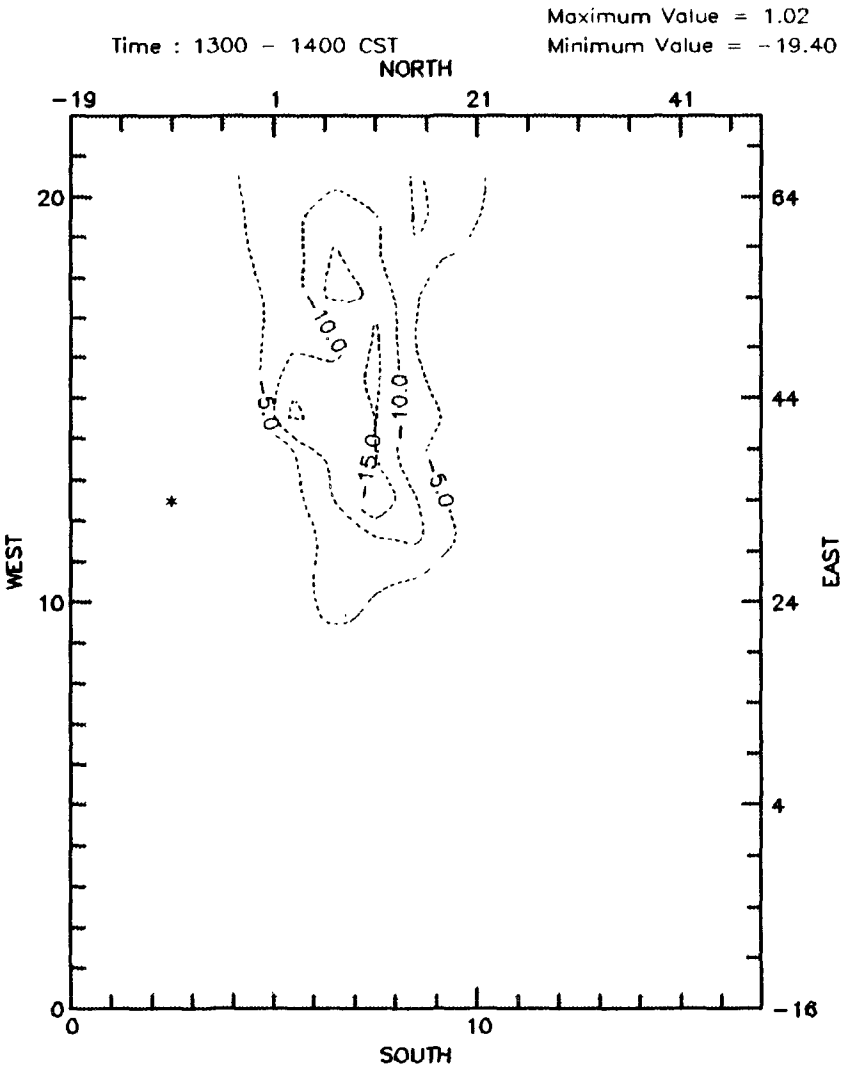

FIGURE E-12a. Ozone concentration difference between Scenario 1 and SIP A, 13 July 1976 (ppb).

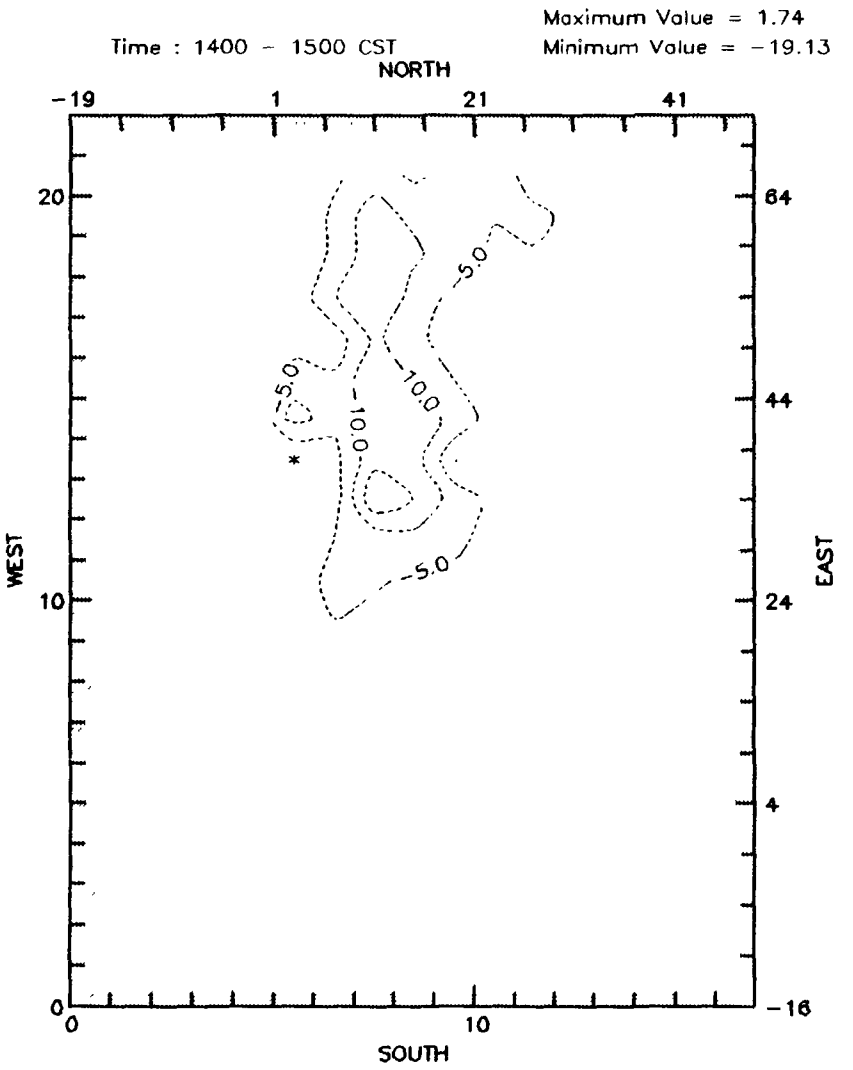

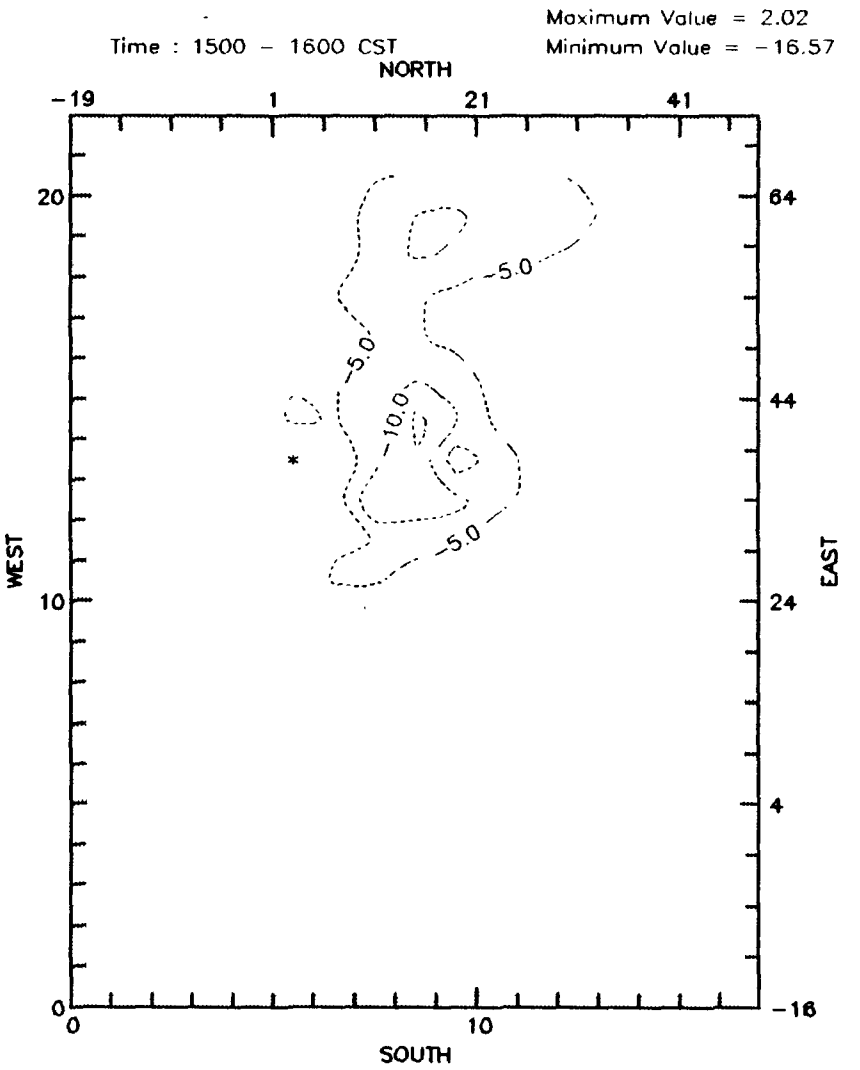

FIGURE E-12b. Ozone concentration difference between Scenario 1 and SIP A, 13 July 1976 (ppb).

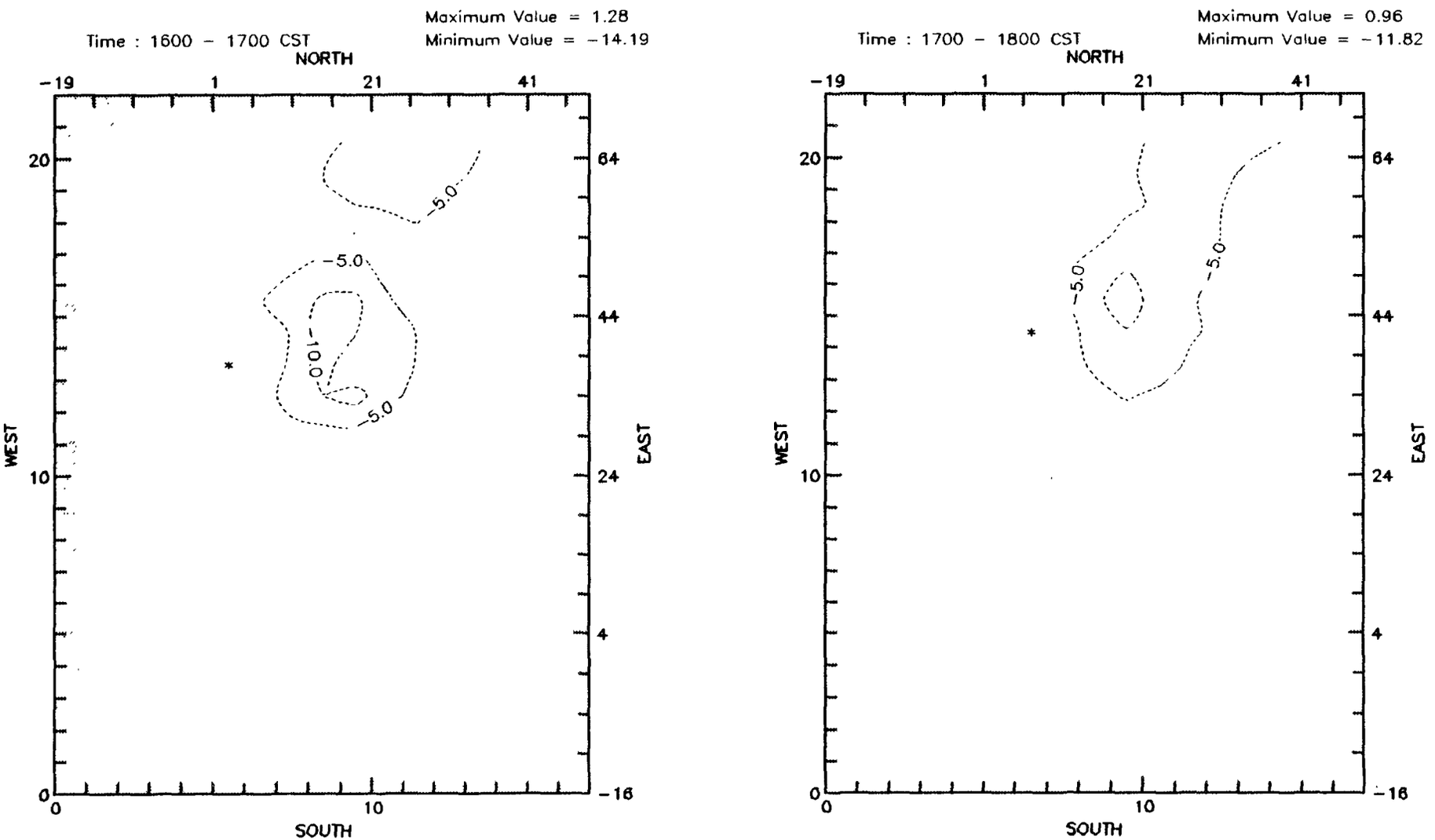

FIGURE E-12c. Ozone concentration difference between Scenario 1 and SIP A, 13 July 1976 (ppb).

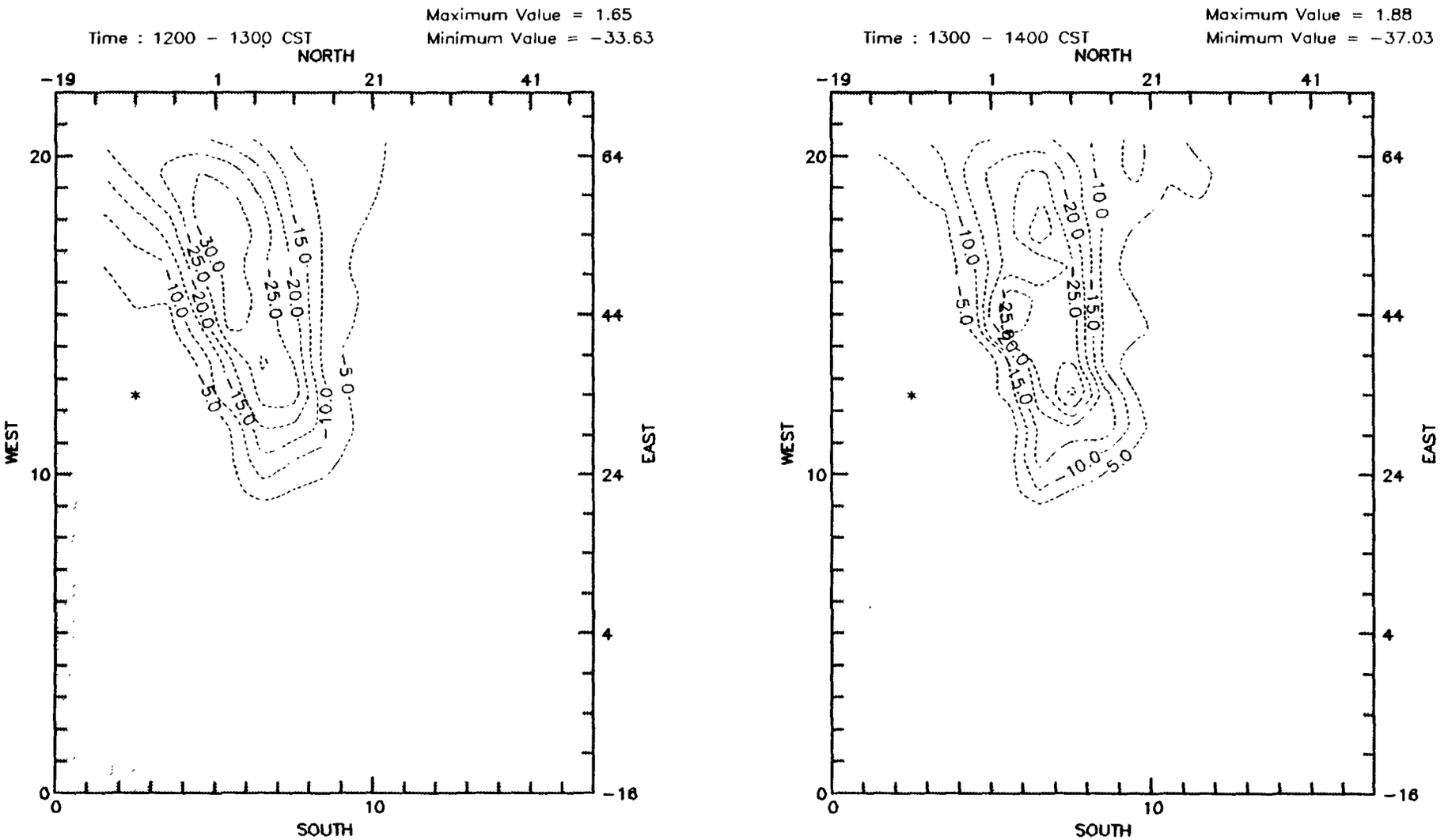

FIGURE E-13a. Ozone concentration difference between Scenario 1 and SIP B, 13 July 1976 (ppb).

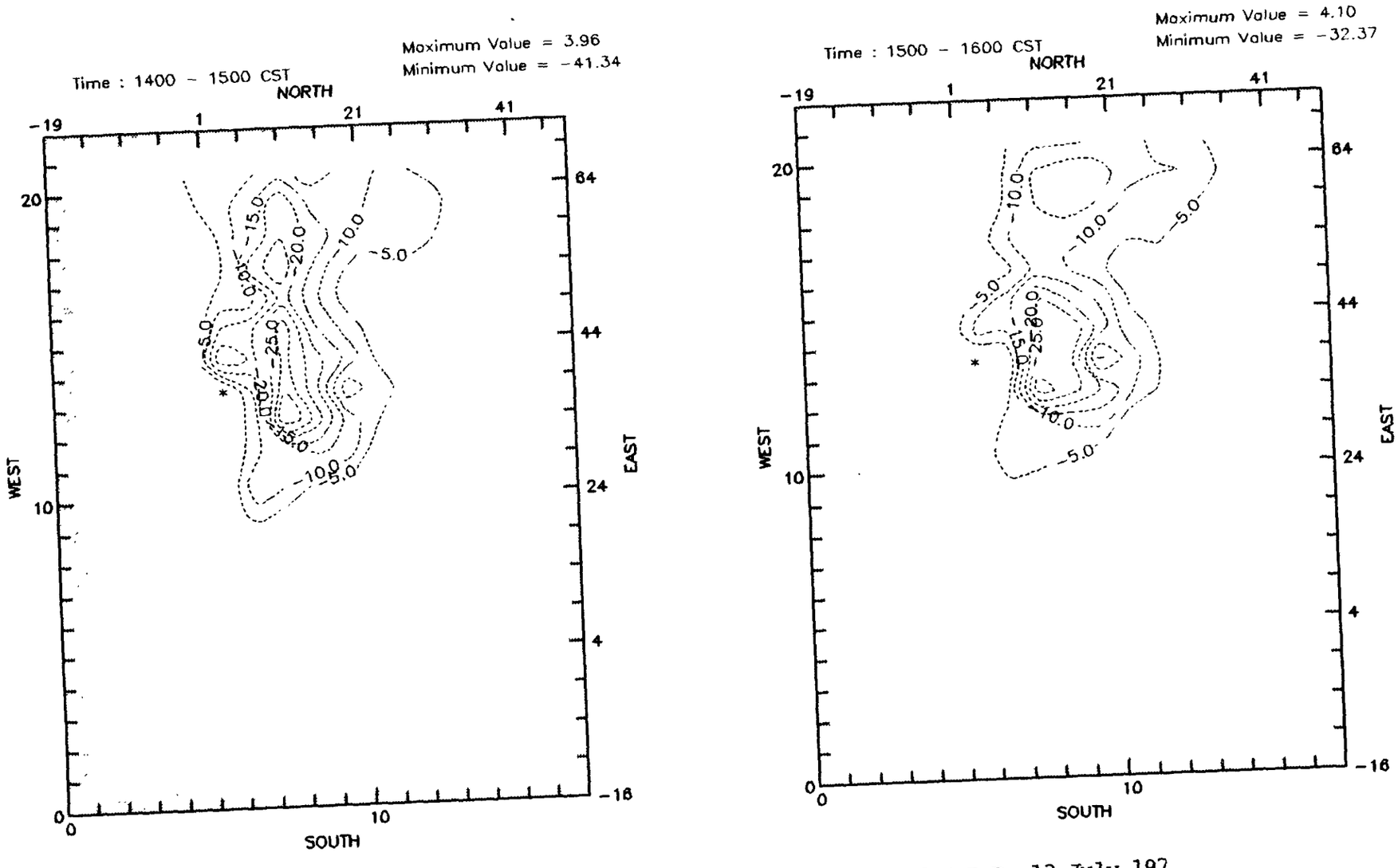

FIGURE E-13b. Ozone concentration difference between Scenario 1 and SIP B, 13 July 197

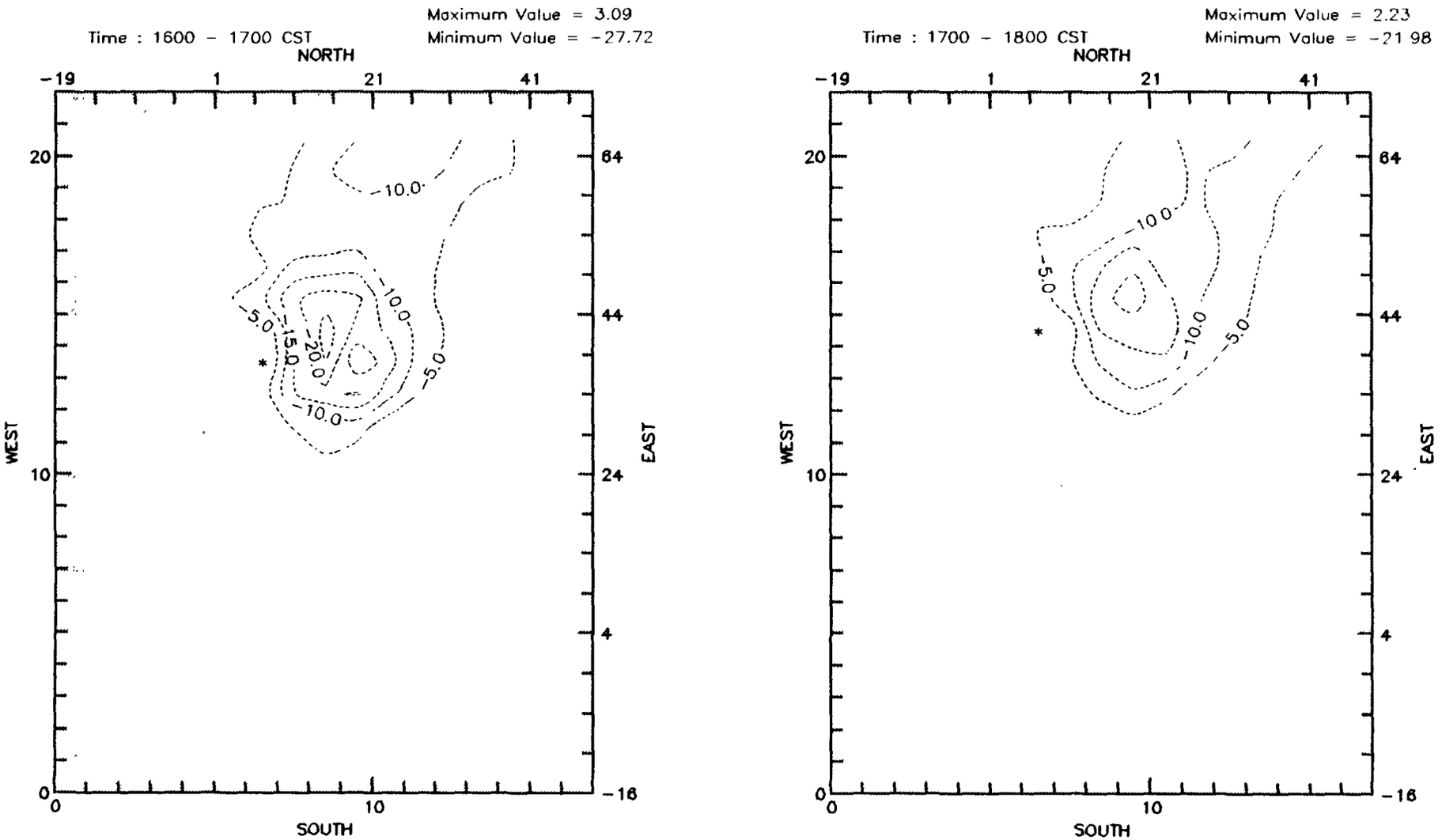

FIGURE E-13c. Ozone concentration difference between Scenario 1 and SIP B, 13 July 1976 (ppb).

TECHNICAL REPORT DATA
(Please read Instructions on the reverse before completing)

1. REPORT NO.	2.	3. RECIPIENT'S ACCESSION NO.
EPA 450/4-90-006E		

4. TITLE AND SUBTITLE	5. REPORT DATE
URBAN AIRSHED MODEL STUDY OF FIVE CITIES - A Low Cost Application of the Urban Airshed Model to the New York Metropolitan Area and the City of St. Louis EPA 450/4-90-006E	April 1990
	6. PERFORMING ORGANIZATION CODE

7. AUTHOR(S)	8. PERFORMING ORGANIZATION REPORT NO.
Ralph E. Morris, Thomas C. Myers, Henry Hogo, Lyle R. Chinkin, LuAnn Gardner, Robert G. Johnson	

9. PERFORMING ORGANIZATION NAME AND ADDRESS	10. PROGRAM ELEMENT NO.
Systems Applications, Inc. 101 Lucas Valley Road San Rafael, CA 94903	11. CONTRACT/GRANT NO.

12. SPONSORING AGENCY NAME AND ADDRESS	13. TYPE OF REPORT AND PERIOD COVERED
U.S. Environmental Protection Agency Office of Air Quality Planning and Standards Research Triangle Park, NC 27711	14. SPONSORING AGENCY CODE

15. SUPPLEMENTARY NOTES

16. ABSTRACT

This document presents Urban Airshed Modeling results for New York and St. Louis. Included are a series of emissions strategies based on Reid Vapor Pressure (RVP) reduction and alcohol/gasoline blended fuels.

17. KEY WORDS AND DOCUMENT ANALYSIS

a. DESCRIPTORS	b. IDENTIFIERS/OPEN ENDED TERMS	c. COSATI Field/Group
Ozone Urban Airshed Model Photochemistry Ethanol		

18. DISTRIBUTION STATEMENT	19. SECURITY CLASS *(This Report)*	21. NO. OF PAGES
		319
	20. SECURITY CLASS *(This page)*	22. PRICE

INSTRUCTIONS

1. **REPORT NUMBER**
   Insert the EPA report number as it appears on the cover of the publication.

2. **LEAVE BLANK**

3. **RECIPIENTS ACCESSION NUMBER**
   Reserved for use by each report recipient.

4. **TITLE AND SUBTITLE**
   Title should indicate clearly and briefly the subject coverage of the report, and be displayed prominently. Set subtitle, if used, in smaller type or otherwise subordinate it to main title. When a report is prepared in more than one volume, repeat the primary title, add volume number and include subtitle for the specific title.

5. **REPORT DATE**
   Each report shall carry a date indicating at least month and year. Indicate the basis on which it was selected *(e.g., date of issue, date of approval, date of preparation, etc.)*.

6. **PERFORMING ORGANIZATION CODE**
   Leave blank.

7. **AUTHOR(S)**
   Give name(s) in conventional order *(John R. Doe, J. Robert Doe, etc.)*. List author's affiliation if it differs from the performing organization.

8. **PERFORMING ORGANIZATION REPORT NUMBER**
   Insert if performing organization wishes to assign this number.

9. **PERFORMING ORGANIZATION NAME AND ADDRESS**
   Give name, street, city, state, and ZIP code. List no more than two levels of an organizational hirearchy.

10. **PROGRAM ELEMENT NUMBER**
    Use the program element number under which the report was prepared. Subordinate numbers may be included in parentheses.

11. **CONTRACT/GRANT NUMBER**
    Insert contract or grant number under which report was prepared.

12. **SPONSORING AGENCY NAME AND ADDRESS**
    Include ZIP code.

13. **TYPE OF REPORT AND PERIOD COVERED**
    Indicate interim final, etc., and if applicable, dates covered.

14. **SPONSORING AGENCY CODE**
    Insert appropriate code.

15. **SUPPLEMENTARY NOTES**
    Enter information not included elsewhere but useful, such as: Prepared in cooperation with, Translation of, Presented at conference of, To be published in, Supersedes, Supplements, etc.

16. **ABSTRACT**
    Include a brief *(200 words or less)* factual summary of the most significant information contained in the report. If the report contains a significant bibliography or literature survey, mention it here.

17. **KEY WORDS AND DOCUMENT ANALYSIS**
    (a) DESCRIPTORS - Select from the Thesaurus of Engineering and Scientific Terms the proper authorized terms that identify the major concept of the research and are sufficiently specific and precise to be used as index entries for cataloging.

    (b) IDENTIFIERS AND OPEN-ENDED TERMS - Use identifiers for project names, code names, equipment designators, etc. Use open-ended terms written in descriptor form for those subjects for which no descriptor exists.

    (c) COSATI FIELD GROUP - Field and group assignments are to be taken from the 1965 COSATI Subject Category List. Since the majority of documents are multidisciplinary in nature, the Primary Field/Group assignment(s) will be specific discipline, area of human endeavor, or type of physical object. The application(s) will be cross-referenced with secondary Field/Group assignments that will follow the primary posting(s).

18. **DISTRIBUTION STATEMENT**
    Denote releasability to the public or limitation for reasons other than security for example "Release Unlimited." Cite any availability to the public, with address and price.

19. & 20. **SECURITY CLASSIFICATION**
    DO NOT submit classified reports to the National Technical Information service.

21. **NUMBER OF PAGES**
    Insert the total number of pages, including this one and unnumbered pages, but exclude distribution list, if any.

22. **PRICE**
    Insert the price set by the National Technical Information Service or the Government Printing Office, if known.